FUNCTIONAL ANALYSIS OF GENES ENCODING HYDROLYTIC ENZYMES IN THE INTERACTION OF *EPICHLOË FESTUCAE* WITH PERENNIAL RYEGRASS

A thesis presented in partial fulfilment of the
requirements for the degree of

Doctor of Philosophy
in
Molecular Genetics

at Massey University, Palmerston North, New Zealand

Michelle Kay Bryant

2005

ABSTRACT

Hydrolytic enzymes degrade macromolecules into smaller components. These enzymes are important in fungal nutrition and have been implicated in the pathogenicity and virulence of pathogenic fungi towards their hosts. However, it is unknown if hydrolytic enzymes play important roles in mutualistic symbioses. In this study, the function of two different classes of hydrolytic enzymes was examined in the mutualistic symbiosis between the fungal endophyte *Epichloë festucae* and perennial ryegrass (*Lolium perenne* cv. Nui).

Nine members of a gene family encoding subtilisin-like proteases were identified in *E. festucae*. The *prt2, prt3* and *prt5* genes encode putative extracellular proteins belonging to the proteinase K subfamily 1, and *prt1* and *prt6* encode putative extracellular proteins belonging proteinase K subfamily 2. The *prt7* and *prt8* genes encoded pyrolysin-like enzymes from subfamilies 1 and 2. The *prt4* gene encodes a putative vacuolar protease, while the *kex2* gene encodes a putative proprotein convertase. Expression analysis showed that the *prt1, prt3, prt5, prt4* and *kex2* genes, but not the *prt2* gene, were expressed in culture. The *prt1* and *prt3* genes appeared to be up-regulated *in planta* compared to culture.

The function of *prt1* and *prt2* in the symbiotum between *E. festucae* and perennial ryegrass was characterised by expressing these genes under the control of the *Aspergillus nidulans gpdA* or the *E. festucae* Fl1 *ltmM* promoters. No major differences in hyphal or plant morphology were observed between symbioses containing wild type *E. festucae* or endophyte strains containing the *prt1* or *prt2* transgenes.

The *gcn1* gene, which encodes a β-1,6-glucanase, was identified immediately downstream of the *prt2* gene. The function of the *gcn1* gene was characterised by gene replacement and testing the phenotype during growth in culture and *in planta*. *E. festucae* Δ*gcn1* strains grew normally on glucose-containing media. On media containing the β-1,6-glucan pustulan, Δ*gcn1* strains did not form aerial hyphae or hydrolyse pustulan, which the wild type strain did. This phenotype was partially

complemented by growth of the Δ*gcn1* mutant in close proximity to wild type strains, and fully complemented by insertion of the *gcn1* gene. This suggests that the *gcn1* gene encodes the major β-1,6-glucanase activity of *E. festucae*.

ACKNOWLEGDEMENTS

Firstly, I would like to thank my chief supervisor, Barry Scott, for his supervision throughout my project. Your knowledge, support and tact have been deeply appreciated. To my other supervisor, Greg Bryan, thanks for your involvement and the fresh perspective you brought to our discussions. I would also like to thank AGMARDT for the Doctoral scholarship that supported me throughout the first three years of this degree.

To my lab mates, past and present: thank you also for the support, discussions and helpful suggestions throughout, especially to Carolyn Young and Xiuwen Zhang. To Andrea Bryant and Carla Eaton, thanks for your friendship and support, especially when it all felt too hard. Thanks also to Kim, Sanjay, Aiko, Shuguang, Heike, Damien, Brendon and Simon for helpful suggestions, Ruth for technical assistance, and Glenda for her support. I'd also like to thank other people in the institute who have been very supportive. To Paul Stock and Cynthia Charron, thanks for supporting me and listening when I got stressed and things weren't going right. Also to our institute secretaries Ann and Cynthia, who have been so helpful during the many draft printings of this thesis. Special thanks must also go to my "PhD support group" – Xiuwen and Carolyn during the first part of my degree, and Vikki Weake and Andrew Clarke in more recent times.

Thanks also to everyone at AgResearch Grasslands who has been so helpful. To Mike Christensen, thank you for our many discussions and to Wayne and Anouk, thanks for your help with the plants (special thanks for the immunoblotting). Thanks to Richard Johnson for providing the *N. lolii* Lp19 kexin sequence that enabled me to clone the *E. festucae kex2* gene, and also Linda Johnson for helpful discussions.

Andrea, I really owe you double amounts of thanks. Not only do I thank you for your help in the lab, I also have to thank you for introducing me to your brother! To my husband Jeremy, you've been my tower of strength. Without your love and support I could not have completed this task. I know at times it's been hard with the two of us doing our doctorates at the same time – it's my fault for convincing you to do a PhD too! To my parents Pat and Teresa, and my brothers Des and Steve, thanks for your support throughout this degree. To my sister Roslyn, thanks for being there, listening and understanding – and for the many visits with Ari. To Ralph and Raewyn, thanks for your unceasing support. To Nikki and Scott, Kayley, Zoe, and Joel, thanks for the fun family times. Thanks also to the friends and relatives who have helped cheer me up and provided diversions along the way, especially Kelly, Blair, Greg and Heather.

TABLE OF CONTENTS

CHAPTER 1: Introduction

CHAPTER 2: Materials and methods

CHAPTER 3: Gene family

CHAPTER 4: Functional analysis of *prt1* and *prt2*

CHAPTER 5: Functional analysis of *gcn1*

CHAPTER 6: Discussion

APPENDIX

BIBLIOGRAPHY

TABLE OF FIGURES

TABLE OF TABLES

TABLE OF ABBREVIATIONS

ABBREVIATION	IN FULL
ACM	*Aspergillus* complete medium
BcAPs	*Botrytis cinerea* Aspartic Proteases
bp	base pair
BSA	bovine serum albumin
cAMP	cyclic adenosine monophosphate
CAP	calf alkaline phosphatase
CDK	cyclin-dependent kinase
cDNA	complementary cDNA
CHEF	contour-clamped homogeneous electric field
CTAB	hexadecyltrimethylammonium bromide
CTD	carboxy-terminal domain
cv.	cultivar
dCTP	deoxycytosine
DEPC	Dierucoyl phosphatidylcholine
DMAT	dimethylallyltryptophan
DNA	deoxyribonucleic acid
DNase	deoxyribonuclease
dNTP	deoxynucleotide
DTT	dithiothreitol
EDTA	ethylenediamine tetraacetic acid
ER	Endoplasmic Reticulum
EST	Expressed Sequence Tag
FAD	Flavin-adenine dinucleotide
GPI	Glycophosphoinositidol
GUS	β-glucuronidase
HMP	hydroxymethylpyrimidine
HR	Hypersensitive Response
IEF	isoelectric focusing
IP	imaging plate
IWF	Intercellular Wash Fluid
kb	kilobase
LB	Luria-Bertani
LMP	low melting point
MEME	Multiple EM for Motif Elicitation
mRNA	messenger RNA
NJ	Neighbour joining
NRPS	Non-Ribosomal Peptide Synthetase
PA	Protease-associated
PCD	Programmed Cell Death
PCR	polymerase chain reaction
PD	Potato dextrose
PDA	potato dextrose agar
PDB	Potato dextrose broth
PEG	polyethylene glycol
PFU	plaque forming units
PIP3	phosphatidylinositol 3,4,5-triphosphate
Pir	Protein with Internal Repeat
PTEN	phosphatase and tensin
PTP	protein tyrosine phosphatase
RG	regeneration medium
RNA	ribonucleic acid
RNAi	Ribonucleic Acid Interference
RNase	ribonuclease
RO	reverse osmosis
RT-PCR	reverse transcriptase polymerase chain reaction
SAPs	Secreted Aspartic Proteases
SDS	sodium dodecyl sulfate
SLS	sodium lauryl sarcosine
TGN	Trans Golgi Network
UTR	untranslated region
X-Gal	5-bromo-4-chloro-3-idolyl beta-D-galactoside

CHAPTER 1

Introduction

1.1 FUNGAL LIFESTYLES

Fungi play important roles in natural ecosystems, agriculture, horticulture, medicine and industry. In ecosystems, fungi act as nutrient recyclers by decomposing components of dead plants and other organisms. Fungi cause disease in many plants and animals, and are important as opportunistic pathogens of immunocompromised individuals. Many industrial, food and pharmaceutical products use the metabolic abilities of fungi.

As heterotrophs, fungi cannot fix their own carbon and nitrogen, so they obtain these elements by breaking down molecules from other organisms. Fungi obtain nutrients by three different means: by growing as saprotrophs, parasites or mutualists. Saprotrophic fungi decompose dead and decaying matter by growing through the substrate, then secreting hydrolytic enzymes to degrade the substrate into smaller soluble molecules that the fungus can absorb. These molecules enter hyphae by diffusion or specific high-affinity transport systems (Jennings, 1995).

Parasitic fungi obtain nutrients from living organisms by growing as necrotrophs or biotrophs. Necrotrophic fungi invade their host, secreting enzymes and/or toxins that cause host cell death (Govrin and Levine, 2002). The fungus degrades the dead cells, providing nutrients to support fungal growth. Biotrophic fungi live in their host, obtaining nutrients without causing host cell death (Schulze-Lefert and Panstruga, 2003). Parasitic fungi may use hydrolytic enzymes degrade host macromolecules to provide nutrients or to break down physical and chemical barriers to infection of their host.

Mutualistic fungi form a symbiosis, or "common life", with their host. Mutualistic symbiota benefit both the fungal species and their hosts. Common examples of fungi in mutualistic symbiota include mycorrhizal fungi (Buscot et al., 2000), lichen fungi (Nash III, 1996) and some fungal endophytes (Carroll, 1988). Mutualistic symbiota all share a common factor: the host provides nutrients (in the form of carbon) to the fungus, while the fungus benefits the host through improved nutrient absorption and/or bioprotective metabolites.

1.2 *EPICHLOË* AND *NEOTYPHODIUM* ENDOPHYTES

1.2.1 Relationships between *Epichloë* and *Neotyphodium* endophytes and their hosts

Epichloë and *Neotyphodium* spp. fungi grow as endophytes in the intercellular spaces of cool season grasses (Siegel and Schardl, 1991). *Epichloë* spp. are part of tribe Balansiae from the family Clavicipitaceae (Clay, 1988; Siegel and Schardl, 1991). Tribe Balansiae includes grass pathogens that are epibiotic, forming reproductive stromata on leaves or inflorescences, or endophytic, forming systemic infections in the host as well as external stromata, which are masses of fungal tissue on which reproductive structures such as perithecia form.

Epichloë species grow systemically during host vegetative growth. However, fungal stromata can develop when the sexual stage of the *Epichloë* life cycle initiates (Figure 1.1). *Neotyphodium* species, which do not form external stromata, appear to be asexual derivatives of *Epichloë* species. Similarities in morphology, secondary metabolites, host ranges, nuclear DNA sequences, isozymes and serology studies support a relationship between the two genera (Glenn et al., 1996; Leuchtmann and Clay, 1990; Schardl et al., 1991; Tsai et al., 1994). Some *Neotyphodium* species may have arisen by loss of the sexual cycle, potentially after infecting a host with which the endophyte has not co-evolved (Moon et al., 2004). Other asexual *Neotyphodium* endophytes have complex evolutionary histories, often with one or two interspecific hybridisations. For instance, *Lolium perenne* taxonomic group 2 (LpTG-2) is the result of a hybridisation between *E. typhina* and *N. lolii* (Schardl et al., 1994).

The association of *Epichloë* and *Neotyphodium* spp. with their grass hosts can benefit both partners (Schardl et al., 2004). The fungus gains nutrients from its host, protection from the external environment, and a means of dissemination through the seed, which is particularly important for the asexual *Neotyphodium* species. The grass host benefits through improved drought tolerance and field persistence, resistance to nematodes and

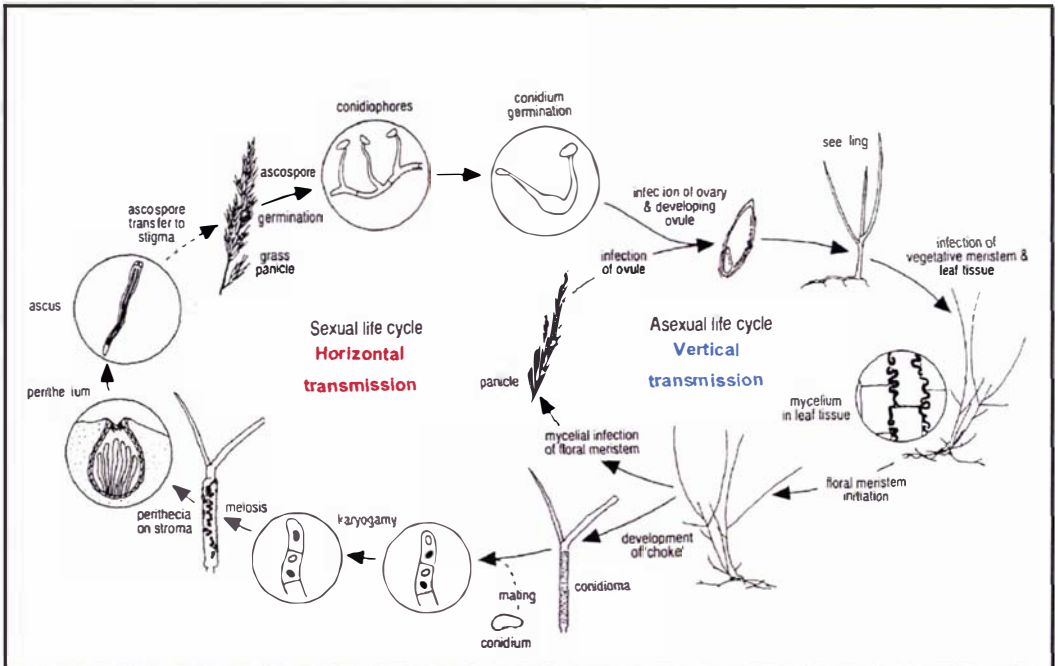

Figure 1.1 Life cycles of *Epichloë* and *Neotyphodium* species within their grass hosts

The lifecycles represented show the sexual and asexual stages of the life cycles of *Epichloë* and *Neotyphodium* spp. endophytes. The sexual life cycle initiates when mycelia emerge from the leaf intercellular spaces. Conidioma develop on the surface of flag leaves, causing choke disease on immature inflorescences. This prevents the host from flowering, and renders the grass tiller infertile. *Epichloë* species are heterothallic, meaning mating can only take place between conidia of two different mating types. Female flies (*Botanophila* sp.) mediate transfer of conidia between infected plants (Bultman *et al*, 1998). After mating has taken place, sexual stromata are formed. The stromata contain perithecia, which bear ascospores. The ascospores are transferred to the stigma of a grass flower, where they germinate. Conidiophores are formed, releasing conidia, which germinate and infect the ovary and developing ovule of the grass flower.

During the asexual phase of the endophyte life cycle, growth within the grass is asymptomatic. The endophyte is initially found within the apical meristem of vegetative plants. After the floral meristem develops, mycelia invade the ovaries and ovules, before eventual incorporation into the seed. If seeds from the infected plant germinate, they will almost certainly be infected with the same endophyte as the maternal parent plant. The asexual phase of the life cycle is also known as vertical transmission. Vertical transmission is a highly efficient means of endophyte transmission, with nearly all the seeds of a host plant infected.

Dashed lines indicate spore transfer. Diagram prepared by Liz Grant, Department of Ecology, Massey University.

some fungal pathogens, and fungal secondary metabolites that act as feeding deterrents to mammalian and insect herbivores.

1.2.2 Endophyte secondary metabolites

Epichloë and *Neotyphodium* species produce a wide range of secondary metabolites (Lane et al., 2000). The four major classes of metabolites produced are lolitrems (indole diterpenes), ergot alkaloids, lolines (pyrrolizidines) and peramine (a pyrrolopyrazine). Lolitrems act as potent neurotoxins in a syndrome called ryegrass staggers, which causes loss of co-ordination due to tetanic muscle spasms in livestock (Siegel and Bush, 1997). Lolitrems also act as feeding deterrents for some insect species (Dymock et al., 1989). Three linked gene clusters appear to contain the genes involved in lolitrem biosynthesis (Young, 2005; Young et al., 2005). The *ltmM* gene, encoding a putative FAD-dependent mono-oxygenase, is necessary for lolitrem biosynthesis (Young et al., 2005).

Ergot alkaloids are highly toxic to mammalian herbivores. These alkaloids cause tall fescue toxicosis, a syndrome associated with poor weight gain, hormonal imbalances, reduced levels of fertility and milk production, vasoconstriction and gangrene of limbs (Strickland et al., 1993). The activity of ergot alkaloids may be due to their high affinity for amine receptors such as dopamine, epinephrine and serotonin receptors. Three endophyte genes essential for ergot alkaloid biosynthesis have been identified. The *dmaW* gene from *Neotyphodium* sp. Lp1 encodes a dimethylallyltryptophan (DMAT) synthetase thought to act at an early, rate-limiting step in ergot alkaloid biosynthesis (Wang et al., 2004a). Two non-ribosomal peptide synthetase (NRPS) genes, *lpsA* (Panaccione et al., 2001) and *lpsB* (D. Fleetwood, personal communication) are also essential for ergot alkaloid biosynthesis. Deletion of the *dmaW*, *lpsA* or *lpsB* genes blocks ergovaline production, but does not affect the symbiosis between the fungus and its host.

Peramine is a pyrrolpyrazine alkaloid that may be derived from a precursor of proline, 1-pyrroline-5-carboxylate, and arginine (Tanaka et al., 2005). Peramine promotes grass persistence in the presence of the Argentine stem weevil, which is a major grass parasite

in New Zealand pastures (Rowan and Gaynor, 1986). Tanaka et al. (2005) identified a two-module non-ribosomal peptide synthetase gene, *perA*, which is essential for peramine biosynthesis *in planta*. Deletion of *perA* increases grass susceptibility to herbivory by the Argentine stem weevil.

Lolines are pyrrolizidine alkaloids that act against insects as feeding deterrents or toxins depending on the insect species (Bush et al., 1997). Lolines may be allelopathic towards competing dicotyledonous and monocotyledonous species, thus improving competitiveness of their host grass (Bush et al., 1993). Loline production has been demonstrated in *Neotyphodium uncinatum*, where the fungus produces lolines in culture under certain conditions (Blankenship et al., 2001; Wilkinson et al., 1997). *N. uncinatum* contains two related gene clusters LOL-1 and LOL-2, each of which contain nine genes putatively associated with loline biosynthesis (Spiering et al., 2005). RNA knockdown (RNAi) of one of these nine genes, *lolC*, which encodes a putative *O*-acetylhomoserine-(thiol) lyase, reduces *lolC* mRNA levels and loline production.

1.2.3 Endophyte growth and colonisation within their hosts

The *Epichloë* and *Neotyphodium* spp. endophytes grow exclusively within the intercellular spaces of grass aerial tissues. Unlike other fungal species, the *Epichloë/Neotyphodium* species do not penetrate or destroy host cells or produce specialised feeding structures such as haustoria or arbuscles. The endophytes grow mainly in the leaf sheath, seeds and crown of the host, all of which are sink tissues that tend to import carbohydrates.

The symbiota between *Epichloë/Neotyphodium* spp. and their hosts cover a continuum ranging from antagonism to mutualism (Schardl et al., 2004). In type I associations where the fungus is antagonistic towards its host, most host inflorescences abort development due to production of stromata that allow the endophyte to reproduce sexually (horizontal transmission; Figure 1.1). In type II associations, some host inflorescences abort due to stromata production (horizontal transmission), while other inflorescences fully develop and seeds are colonised by the endophyte, allowing clonal

propagation of the fungus (vertical transmission). Fungi are vertically transmitted through the seed in the type III mutualistic associations that are typical of the asexual *Neotyphodium* species.

During growth in vegetative host tissues, the association is usually asymptomatic (Koga et al., 1993). The endophyte grows near the apical meristem during vegetative growth. After the grass switches to reproductive growth, the apical meristem becomes a floral meristem and produces floral structures. At this point, the endophyte is in position to infect the developing ovaries and ovules (Philipson and Christey, 1986). Although the endophyte heavily infects the diploid nucellus (megasporangium), it does not grow in the ovule integuments or in the haploid embryo sac (gametophyte) (Majewska-Sawka and Nakashima, 2004; Philipson and Christey, 1986). After the grass floret is fertilised, endophyte hyphae are most abundant in an area that Majewska-Sawka and Nakashima (2004) describe as the "infection layer". This area contains the remains of the nucellus with numerous hyphae. During early stages of seed development, the embryo contains no endophyte hyphae. At the notch stage of embryo development when organs begin to differentiate, the endophyte begins to colonise the embryo.

During horizontal transmission of the *Epichloë* species, the endophyte aborts host reproduction and flowering. During grass reproduction, the fungus begins to proliferate when the grass forms inflorescence primordia. Just before the inflorescence emerges from within the flag leaf surrounding it, hyphal proliferation increases in the inflorescence and hyphae emerge and grow epiphytically to cover the exterior of the leaf sheath. The mass of fungal tissue surrounding the inflorescence, described as a stroma (plural stromata), is covered by conidia.

Epichloë species are heterothallic, with two different mating types. Once stromata form, female anthomyiid flies (*Botanophila* spp.) can transfer conidia from the opposite mating type to the stroma while laying eggs on the stroma surface (Bultman et al., 1998). Fly eggs then hatch, and the larva feed on the stroma before dropping to pupate in the soil. After fertilisation of the stroma by conidia from the other mating type, ascospore-containing fruiting bodies called perithecia form. Ascospores can be ejected

from perithecia and colonise new host plants either by infecting seeds or neighbouring plants. Chung and Schardl (1997) suggested ascospores may colonise grass hosts through a mechanism similar to that used by the closely related fungus *Claviceps purpurea* during grass floret infection, where ascospores germinate to produce conidia, and hyphae from germinated conidia invade the ovule.

1.2.4 Endophyte-host compatibility

Grasses resist infection by most potential endophytes through non-specific resistance mechanisms that protect the plant from potential pathogens. Plants achieve non-specific resistance to infection through constitutive mechanisms, such as physical or chemical barriers to infection (Osbourn, 1995; Park et al., 2004), or by induced mechanisms, such as production of antimicrobial proteins and metabolites (Broekaert et al., 1997; Maor and Shirasu, 2005).

Natural associations show no obvious response by the grass host to the endophyte's presence, suggesting the endophyte has developed means of overcoming host non-specific resistance. However, artificial inoculations of some endophytes into new grass hosts produce incompatible interactions characterised by either fungal or plant cell death (Christensen, 1995; Koga et al., 1993). In associations causing fungal cell death, the hyphae collapse and become distorted, with degenerated cytoplasm and electron-dense cell walls. This phenotype resembles hyphae from plant pathogenic fungi that have penetrated resistant hosts (Koga et al., 1993). In artificial inoculations resulting in host cell death, stunted tillers form. Stunted tillers are associated with necrosis resembling a hypersensitive response (HR) in the cells of the apical meristem. Healthy tillers produced by the grass are uninfected, suggesting these associations are incompatible (Christensen, 1995).

Endophyte-host compatibility is affected by both endophyte and grass genotypes. Chung et al. (1997) showed that in *E. typhina* multiple genes that act additively or synergistically to determine host specificity during seedling infection. Host and endophyte genotypes also affect the persistence of associations. Christensen et al. (1997)

showed that in artificial inoculations, some genotypes of *E. festucae* cause stunting and chlorotic lesions in a non-host grass. These artificial associations did not show any of the host cell death observed by Christensen (1995). Instead, hyphae were located in the vascular bundles, often in direct contact with the sieve tube elements (Christensen et al., 1997). Endophyte and host genotypes also control secondary metabolite production by the endophyte, which may affect the field persistence of endophyte-infected plants under herbivore grazing (Easton et al., 2002).

1.2.5 Endophyte nutrition within its host grass

Epichloë and *Neotyphodium* spp. endophytes grow within the intercellular spaces of their hosts without penetrating the cell wall or cytoplasm. Therefore, the endophyte must obtain amino acids, simple sugars, vitamins and vitamin precursors required for growth from within the intercellular spaces. In culture, *Epichloë* and *Neotyphodium* species utilise a range of different carbon and nitrogen sources (Naffaa et al., 1998). Carbon sources used by endophytes include pentoses, hexoses, disaccharides and polysaccharides. Ammonium, nitrate, asparagine, glutamine, glycine and alanine, as well as complex nitrogen sources such as peptone and soytone provide nitrogen sources to support fungal growth. Some endophyte strains can use tryptophan and methionine as nitrogen sources, but most strains were unable to use these amino acids.

Endophyte hyphae are normally restricted to basal parts of plant aerial tissues, typically in the host leaf sheath and meristematic zones, but occasionally are found in the leaf blade (Neill, 1940). The leaf sheaths and meristematic zones are sink tissues within plants, where carbohydrates are unloaded from the phloem (Allard and Nelson, 1991). As the major sugar transported in the phloem, sucrose and its derivatives glucose and fructose are the most common carbohydrates available to the endophyte (Amiard et al., 2004).

The endophyte has two different mechanisms for sucrose uptake (Lam et al., 1995). The first involves direct uptake by a sucrose carrier, while the second mechanism involves an invertase activity that breaks down sucrose into glucose and fructose before uptake by

separate glucose and fructose carriers. Accumulation of mannitol, other sugar alcohols and trehalose produced by the fungus may affect uptake of sucrose and other carbohydrates (Bacon and White, 2000). The plant cannot utilise fungal carbohydrates such as mannitol, so the concentration gradient between plant sources and sinks needed to promote carbohydrate movement in the phloem increases. Sugar alcohols lower water potential in the endophyte, promoting water diffusion into the fungus. Mannitol & other polyols may also act as drought protective osmolytes within infected plants (Richardson et al., 1992).

Host amino acids are important sources of carbon and nitrogen for endophyte nutrition. Endophyte infection significantly affects host nitrogen metabolism (Bacon and White, 2000). Large increases in carbon assimilation into amino acids in the leaf blade were associated with significantly higher glutamine synthetase activity within the leaf blade. Ammonium, a key precursor in amino acid biosynthesis, is present at double the concentration in the leaf sheaths (but not in leaf blades) of endophyte-infected plants compared to uninfected plants. Amino acids are also important precursors for alkaloid biosynthesis, so variation in nitrogen metabolism could influence the types and levels of alkaloids in endophyte-grass associations (Clay, 1988).

Various *Epichloë* and *Neotyphodium* endophytes require vitamins such as thiamine for growth (Kulkarni and Nielsen, 1986; Zhang, 2004). Thiamine is a cofactor for many enzymes involved in fungal metabolism. When the *thi1* gene (the orthologue of *Saccharomyces cerevisiae THI4*) in a thiamine-autotrophic *E. typhina* strain was deleted, hyphal density and branching were reduced in thiamine-free media (Zhang, 2004). Thiamine and its precursor thiazole complemented these growth defects. The mutant strain can still colonise and infect the host, and still form stromata. However, the Δ*thi1* mutant did not cause as many detrimental effects, branching less within the host and not containing the abundant glycogen deposits found in the wild-type *E. typhina* strain.

Hydrolytic enzymes may also be involved in endophyte growth within their host. In the association between a *Neotyphodium* sp. endophyte and its *Poa ampla* host, subtilisin-like protease, β-1,6-glucanase, chitinase and *N*-acetylglucosaminidase activities have

been identified (Li et al., 2005; Li et al., 2004; Lindstrom et al., 1993; Moy et al., 2002). The activities of all of these hydrolytic enzymes could affect the growth of the endophyte in both culture and *in planta,* possibly through autolysis, the self-digestion of old hyphae through the activity of hydrolytic enzymes (White et al., 2002). The protease, glucanase and chitinase activities detected in endophytes are also similar to the hydrolytic enzyme system produced by *Trichoderma* species to lyse fungal cell walls (Section 1.5.2) (Moy et al., 2002). Loosening of the rigid structure of the fungal cell wall is required to enable fungal branching, so enzymes degrading structural components (e.g. chitin) and cross-links (β-1,6-glucans) in the wall may be important for fungal growth. The endophyte *N*-acetylglucosaminidase may enable the endophyte to circumvent host defence responses by degrading chitin oligomers that induce hypersensitive responses to phytopathogenic fungi in some plant species (Li et al., 2005).

1.2.6 *Epichloë* and *Neotyphodium* sp. endophytes as experimental systems

Epichloë and *Neotyphodium* spp. fungi are extremely well adapted to growth within their hosts. However, compared to the model fungal systems such as *Neurospora crassa* and *Aspergillus nidulans*, *Epichloë* and *Neotyphodium* spp. fungi grow much more slowly in culture. Some endophyte species such as *Neotyphodium occultans* do grow out of their host plant after lengthy incubations, but cannot be sub-cultured (Moon et al., 2000). Generally, the sexual *Epichloë* endophytes grow more quickly than the asexual *Neotyphodium* endophytes (M. Christensen, personal communication), which are often interspecific hybrids (Section 1.2.1). Consequently, *Epichloë* endophytes recover and grow more quickly from processes such as genetic transformation.

Differences between *Epichloë* and *Neotyphodium* endophytes are also seen when these fungi are artificially inoculated into grasses. A higher infection rate is usually obtained with the more quickly growing *Epichloë* endophytes compared to the *Neotyphodium* endophytes (Zhang and Christensen, personal communication). This means that in experiments where genetically modified endophytes are introduced into grasses by

artificial inoculation, a higher infection rate will be obtained when the modified strains are *Epichloë* spp..

Using *E. festucae* as a model endophyte system was first suggested by Schardl (2001). *E. festucae* strains form stable associations with *Festuca* and *Lolium* spp. grasses, where the fungus can either be efficiently vertically transmitted through the seed, or produce reproductive structures such as stromata (Section 1.2.3). As a sexual species, *E. festucae* is amenable to Mendelian and molecular genetic analysis. Many asexual interspecific *Neotyphodium* hybrids appear to be derived from *E. festucae*. Strains of *E. festucae* produce different combinations of the four major anti-herbivore secondary metabolites (Section 1.2.2), making them suitable for analysis of endophyte toxin production. *E. festucae* infection of grasses has also been associated with enhanced host fitness. All of these characteristics, along with the relatively quick growth in culture and high rate of infection in artificial inoculations, make *E. festucae* ideal as a model endophyte system.

1.3 HYDROLYTIC ENZYMES

Hydrolytic enzymes break down large macromolecules into smaller compounds that can be reutilised by other organisms. These proteins catalyse the splitting of covalent bonds between building blocks of macromolecules by adding a water molecule. As described in Section 1.1, hydrolytic enzymes allow fungi to recycle macromolecules found in their environment. Table 1.1 shows a list of common hydrolytic enzymes and the product of the reactions they catalyse. Pathogenic fungi can potentially break down physical or chemical barriers to host infection using hydrolytic enzymes (Osbourn, 1995; St Leger et al., 1987).

Hydrolytic enzymes have two possible modes of action: an endo- action, resulting in internal cleavage of macromolecules, or an exo- action, resulting in sequential cleavage from the end of the macromolecule (Figure 1.2). Exohydrolytic enzymes can completely degrade macromolecules (Figure 1.2A), but endohydrolytic enzymes cannot (Figure 1.2B). The fastest means of degrading a macromolecule involves endo- and

Table 1.1 Degradation of macromolecules by hydrolytic enzymes

Macromolecule	Subunit	Enzyme
Starch	Glucose	Amylase
Cellulose	Glucose	Cellulase
ß-1,3-glucan (callose)	Glucose	ß-1,3-glucanase
ß -1,6-glucan	Glucose	ß-1,6-glucanase
Lipid	Fatty acids	Lipase
Protein	Amino acids	Protease
DNA RNA	Deoxyribonucleotides Ribonucleotides	Deoxyribonuclease Ribonuclease
Ester		Esterase
Cutin (polymer)	Cutin (monomer) Mainly C16 and C18 interesterified hydroxy, and epoxy-hydroxy fatty acids	Cutinase
Chitin	N-acetylglucosamine	Chitinase
Chitosan	Glucosamine	Chitosanase
Avenacin (phytoanticipin) Toxin	mono- and bis-deglucosylated avenacin (non-toxic derivative)	Avenacinase

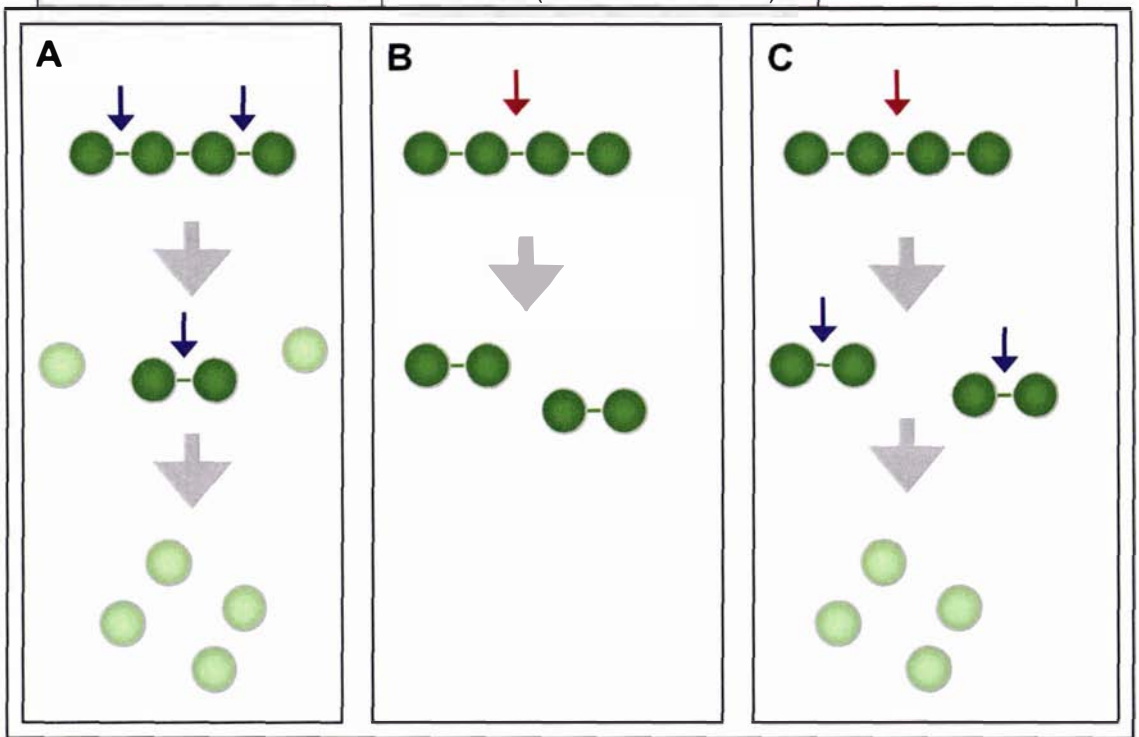

Figure 1.2 Exo- and endohydrolytic cleavage of molecules

Hydrolytic enzymes cleave molecules by exo- or endo-acting mechanisms. Polymers and oligomers are indicated by dark green circles joined by a dark green line. Monomers are indicated by a light green circle. Sites of exohydrolytic cleavage are indicated by dark blue arrows, while endohydrolytic cleavage sites are indicated by dark red arrows. (**A**) An exo-action cleaves individual monomers sequentially from the end of polymers. (**B**) An endo-action cleaves within polymers, but does not cleave monomers from the ends of polymers. (**C**) Exo- and endo- actions can act together to fully degrade a polymer.

exohydrolytic enzymes working together, with the endohydrolytic enzymes breaking down the macromolecule into smaller pieces, then the exohydrolytic enzyme breaking down each of these smaller pieces into their individual building blocks (Figure 1.2C).

1.4 SUBTILISIN-LIKE PROTEASES

Proteases catalyse the cleavage of polypeptides (proteins) to oligopeptides or amino acids. In fungi, there are six major classes of proteases, grouped as aspartic, cysteine, metallo-, serine, threonine or unknown proteases according to the amino acid residues required for enzyme activity (Rawlings et al., 2004). As hydrolytic enzymes, proteases break the covalent bond between amino acid residues in polypeptides by adding a water molecule (Figure 1.3). Proteases can act as endopeptidases, which cleave within a polypeptide to produce oligopeptides, or exopeptidases, which cleave from the end of polypeptide or oligopeptide to release amino acids.

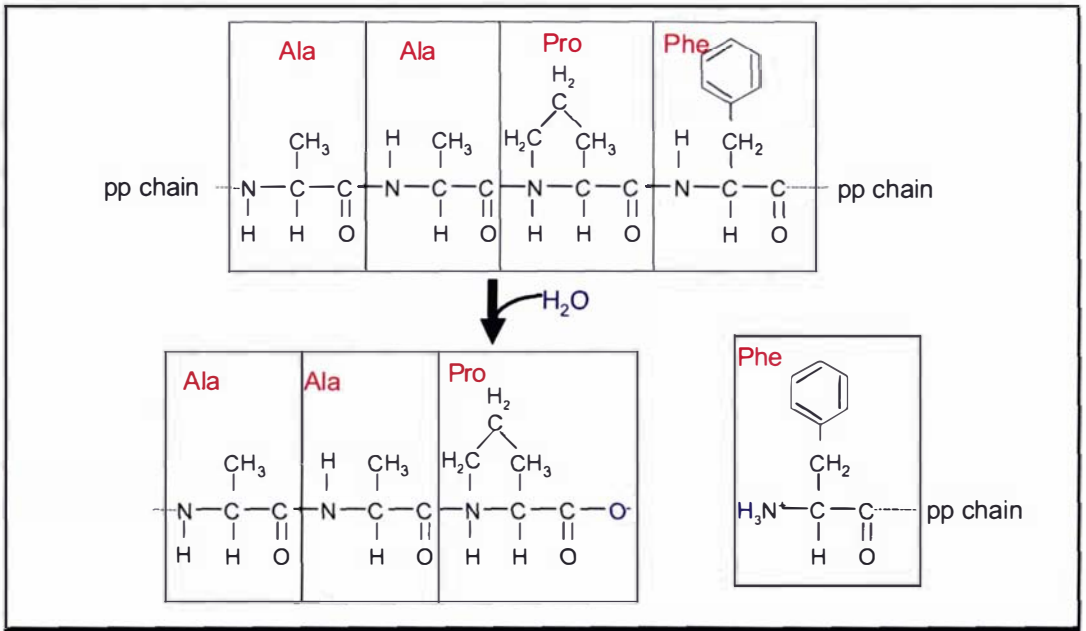

Figure 1.3 Hydrolytic reaction catalysed by subtilisin-like proteases

Endoproteolytic cleavage of polypeptides is catalysed by subtilisin-like proteases. The names of amino acid residues are shown in red, with each amino acid residue surrounded by a black box. The remainder of the polypeptide chain is designated by pp chain. Groups added during hydrolytic cleavage are shown in blue.

Experimental evidence implicates the subtilisin-like proteases, a class of serine proteases, in fungal-host interactions (Section 1.5). Figure 1.3 shows an example of the hydrolytic cleavage of a polypeptide chain catalysed by subtilisin-like proteases. Phylogenomic analysis suggests three families of subtilisin-like proteases are present in fungi (Hu and St Leger, 2004). The first family, known as the pyrolysins, encodes relatively large proteins whose function is currently unknown. The second family, named for its similarity to the widely known *Tritirachium album* proteinase K, consists of three subfamilies. Two of these subfamilies (subfamilies 1 and 2) contain secreted proteases, while the remaining subfamily (subfamily 3) contains intracellular proteases normally localised to the vacuole. The third family, kexins (proprotein convertases), are involved in post-translational protein processing.

1.4.1 Family I of the fungal subtilisin-like proteases: pyrolysin-type proteases

The pyrolysin family encodes relatively large proteases in comparison to other subtilisin-like proteases, generally of 700-1000 amino acid residues in size. A characteristic feature of the pyrolysins is a protease-associated (PA) domain, found in some proteases and receptors. Mahon and Bateman (2000) suggested the PA domain could be a protein-protein interaction domain involved in protease binding to their substrates and in determining substrate specificity.

Very few members of the pyrolysin family have been described in fungi, although multiple copies of genes encoding these proteases have been found in the genomes of *Magnaporthe grisea* and *Fusarium graminearum* (*Gibberella zeae*) (Hu and St Leger, 2004). The only characterised family I subtilisin-like protease is PoS1 from the basidiomycete *Pleurotus ostreatus*, a fungus that causes white rot in woody trees (Faraco et al., 2005). PoS1 activates a proteolytic cascade regulating degradation of laccase isoenzymes, which are involved in lignin degradation.

1.4.2 Family II of the fungal subtilisin-like proteases: proteinase K-type proteases

Family II of the fungal subtilisin-like proteases contain the well-known proteinase K from *T. album*. Phylogenetic analysis shows family II forms three subfamilies (Hu and St Leger, 2004). Subfamilies 1 and 2 both contain extracellular enzymes that have broad substrate specificities, acting as both proteases and esterases (Ebeling et al., 1974; Lim et al., 2005; Velasco et al., 2001). Proteases in subfamilies 1 and 2 play roles in the interactions of fungal pathogens of insects, nematodes and other fungi with their hosts (Section 1.5) (Hu and St Leger, 2004). As extracellular enzymes, enzymes in subfamilies 1 and 2 may break down proteins to provide nutrients to support fungal growth, and to break down physical and chemical barriers to host infection (Reddy et al., 1996).

Subfamily 3 contains a group of closely related proteases that are localised to the vacuole. Proteinase B (encoded by the *PRB1* gene) from the yeast *S. cerevisiae* was the first identified protease in this subfamily (Zubenko et al., 1979; Zubenko et al., 1980). Deletion of *PRB1* causes autophagic bodies to accumulate in the yeast vacuole during nitrogen starvation (Zubenko and Jones, 1981). Autophagic bodies are the product of autophagy, a membrane-trafficking process that leads to breakdown and recycling of cytoplasmic components in the vacuole. This suggests that *S. cerevisiae* proteinase B plays a role in degrading autophagic bodies within the vacuole and recycling macromolecules.

In *S. cerevisiae*, nitrogen starvation induces sporulation and autophagy. When the Δ*PRB1* mutant grows under nitrogen starvation conditions, developmental defects are observed (Zubenko and Jones, 1981). Δ*PRB1* cells do not complete sporulation or produce normal asci. Δ*PRB1* sporulative cells, which are much smaller than asci produced by wild-type cells, are embedded in a thick matrix. Nitrogen starvation also induces sexual differentiation and expression of the *isp6* gene (the homologue of the *S. cerevisiae PRB1* gene) in *Schizosaccharomyces pombe*. Deletion of *isp6* results in cell cycle arrest prior to conjugation and drastically blocks sporulation (Sato et al., 1994).

Protein degradation during nitrogen starvation-induced autophagy may be necessary to provide nitrogen sources for the manufacture of new proteins needed for sporulation.

The *Podospora anserina PRB1* homologue, *pspA* (also known as *idi6*), was identified during a screen for genes up regulated during vegetative incompatibility (Paoletti et al., 2001). Sequence comparisons suggested the PspA protease might have similar functions as *S. cerevisiae* proteinase B, with roles in autophagy and developmental processes. Autophagic bodies accumulated in the Δ*pspA* mutant during nitrogen starvation, just as they did in the *S. cerevisiae* Δ*PRB1* mutant. Nitrogen starvation, vegetative incompatibility and cellular development induce autophagy in *P. anserina* (Paoletti et al., 2001; Pinan-Lucarre et al., 2003). Δ*pspA* mutants have reduced hyphal density, aerial hyphae and pigmentation, very few protoperithecia and female sterility compared to wild-type *P. anserina*.

Deletion of the *Aspergillus fumigatus PRB1* homologue, *alp2,* also caused developmental defects (Reichard et al., 2000). The *A. fumigatus* colony changed colour from greyish-green in wild-type colonies to white or light green in the Δ*alp2* strain. While conidial numbers were greatly reduced, conidial size was unchanged. The conidiophore in the Δ*alp2* strain was much smaller than in the wild-type strain, largely due to a reduction in the diameter of conidiophore vesicles. In addition, the rate of vegetative growth was slightly slower in the *alp2* deletion strain.

Vacuolar subtilisin-like proteases play roles in the recycling of proteins during autophagy, a type of programmed cell death (PCD) conserved across all eukaryotes that is induced in response to cellular stress (Wang and Klionsky, 2003). In the fungal vacuole, this particular type of subtilisin-like protease breaks down the autophagosomes. This enables the cell to recycle cytoplasmic components to provide nutrients to support survival during growth under stressful conditions like nutrient limitation.

1.4.3 Fungal subtilisin-like protease family III: kexin-type proteases

Kexins are a conserved group of calcium-dependent subtilisin-like proteases also known as prohormone or proprotein convertases (Fuller et al., 1989; Henrich et al., 2005). Kexin-like enzymes contain a subtilisin-like catalytic domain, a P domain important for protein stability and substrate specificity, a transmembrane domain, and sometimes a cytoplasmic carboxyl terminal domain (Henrich et al., 2005). Kexins hydrolyse the covalent bond of the carboxyl-terminal side of a dibasic sequence, generally KR or a RR motif.

Eukaryotes often produce secreted proteins as preproproteins or zymogens. At least two proteolytic cleavage events are required for processing of preproproteins to their mature forms. The first proteolytic step takes place in the endoplasmic reticulum (ER), where a signal peptidase cleaves the signal peptide (prepeptide) directing the preproprotein to enter the secretory pathway (Conesa et al., 2001). Once proteins have entered the ER, they fold and undergo modifications such as phosphorylation and glycosylation before correctly folded proteins move to the Golgi body in transport vesicles. The second proteolytic event takes place in the Golgi body, where kexins cleave the propeptide from the proprotein to give the active, fully processed protein. After other modifications such as further glycosylation have taken place, proteins either are secreted to the exterior of the cell, remain in the membrane or become targeted to the vacuole.

Kexins cycle between the *trans* Golgi network (TGN) and the endosome, but are returned to the Golgi body due to a Golgi retention motif within the cytoplasmic carboxyl-terminal domain (Redding et al., 1991; Wilcox et al., 1992). As kexins are localised to the TGN, any potential target proteins cleaved by kexin must pass through the Golgi network with their amino terminus within the Golgi lumen. Membrane, vacuolar, cell wall and secreted proteins are all potential targets of kexins, while cytoplasmic proteins are not. Kexins process a large number of proteins; thus, mutations in kexin-like genes are pleiotropic, resulting in a large number of potential changes in protein secretion and activity.

The *S. cerevisiae KEX2* gene was identified during a screen for genes interfering with proteolytic processing of the K1 killer toxin (Leibowitz and Wickner, 1976). Mutants in *KEX2* incorrectly processed the K1 killer toxin and had mating defects. In α-mating type Δ*KEX2* strains, incorrect processing of the α-mating factor propeptide results in poor secretion of α-factor. This means the α-mating type Δ*KEX2* strain cannot successfully mate with a-mating type cells not carrying a *KEX2* deletion. However, deletion of *KEX2* in a-mating type strains does not affect the ability to mate with wild type α mating type strains. This suggests Kex2 activity is required for correct processing and secretion of α-mating type, but not a-mating type, pheromones. Experimental evidence suggests the α mating pheromone of *Candida albicans*, the B-type mating pheromone of *Yarrowia lipolytica* and the Map2 pheromone of *S. pombe* are processed by kexin-like proteins in a similar manner (Davey et al., 1994; Enderlin and Ogrydziak, 1994; Newport and Agabian, 1997).

Deletion of *KEX2* homologues causes phenotypic changes in yeast and filamentous fungal species. In the dimorphic yeasts *C. albicans* and Y. *lipolytica*, deletion of the kexin-like genes *KEX2* and *XPR6* resulted in strains unable to switch to hyphal growth (Enderlin and Ogrydziak, 1994; Newport and Agabian, 1997). Deletion of *KEX2* homologues resulted in abnormal yeast cell morphology in *S. cerevisiae, C. albicans, Y. lipolytica* and *Candida glabrata* (Bader et al., 2001; Enderlin and Ogrydziak, 1994; Komano and Fuller, 1995; Leibowitz and Wickner, 1976; Newport and Agabian, 1997; Newport et al., 2003). In these species, large cell aggregates formed after cells did not separate after budding. In *S. pombe*, a temperature-sensitive mutation in the *KEX2* homologue, *krp1,* caused cell division to cease, non-polarised cell growth and lemon-shaped cells (Davey et al., 1994). Deletion of the *KEX2* homologue *kexB* in *Aspergillus oryzae* resulted in shrunken colonies with no conidiophores or conidia (Mizutani et al., 2004). However, conidiophore and conidia production took place in *Aspergillus nidulans* and *Aspergillus niger* Δ*kexB* deletion strains (Jalving, 2005; Jalving et al., 2000; Kwon et al., 2001). *A. oryzae* and *A. niger* Δ*kexB* deletion strains have a hyper-branching phenotype resulting in increased hyphal density in colonies.

Some of these phenotypic changes after loss of kexin activity are associated with cell surface changes. The cell walls of *C. albicans* Δ*KEX2* deletion strains have an abnormal chitin distribution (Newport and Agabian, 1997). *C. glabrata KEX2* mutants were hypersensitive to any treatment that affected the surface of hyphae, suggesting changes in the cell surface had made the yeast more sensitive to these agents (Bader et al., 2001).

Disruptions in the cell wall or membrane activate cell integrity signalling, which regulates gene expression by signalling through a MAP kinase cascade containing the Mpk1 MAP kinase (Levin, 2005). In *S. cerevisiae*, hypo-osmotic stress, heat shock, exposure to mating pheromone and treatments perturbing the cell wall activate this signalling cascade. Deletion of *KEX2* and the MAP kinase gene *MPK1* in *S. cerevisiae* is lethal. This suggests Mpk1 normally signals through the cell integrity pathway in response to cell surface changes caused by the *KEX2* deletion, allowing the cell to compensate for these changes (Roelants et al., 2002). In *A. oryzae*, *kexB* deletion results in increased expression of the *MPK1* homologue, *mpkA* (Mizutani et al., 2004). Activation of the cell integrity-signalling pathway may lead to increased expression of the cell wall biosynthesis genes *chsB*, *chsC* and *gelB* in Δ*kexB A. oryzae*.

Loss of kexin activity results in incorrect processing of other secreted proteins. Deletion of *KEX2* homologues lead to defects in processing and secretion of members of the SAP family of aspartic proteases in *C. albicans* (Newport and Agabian, 1997) and the AEP alkaline extracellular protease of *Y. lipolytica* (Enderlin and Ogrydziak, 1994). Loss of kexin activity is also associated with pathogenicity changes in *C. albicans* and *C. glabrata* (Bader et al., 2001; Newport et al., 2003). In *C. albicans*, the SAP aspartic proteases act as pathogenicity/virulence factors (Naglik et al., 2003), so any change in the distribution or activity of these proteases could compromise *C. albicans* pathogenicity or virulence.

1.4.4 Distribution of subtilisin-like proteases in fungal genomes

The distribution of genes encoding subtilisin-like proteases differs between fungal lineages (Table 1.2). The distribution pattern of the protease genes is consistent with a

model where genes have been lost in some lineages, but have diversified in others (Hu and St Leger, 2004). Genes encoding pyrolysin family and proteinase K subfamilies 1 and 2 enzymes were the most commonly duplicated. Multiple vacuolar protease-encoding genes may be present in yeast lineages, or filamentous ascomycetes may have subsequently lost a vacuolar protease gene copy. The only fungus known to contain duplications of the kexin gene family is *Pneumocystis carinii* f. sp. carinii, where the kexin gene is part of a duplicated sub-telomeric region (Lugli et al., 1997). Higher numbers of genes encoding subtilisin-like proteases are found in pathogenic fungi, such as the phytopathogens *M. grisea* and *F. graminearum*, compared to saprotrophs such as *A. nidulans*. Phylogenetic relationships of fungi discussed in this paper are shown in Figure 1.4

Table 1.2 Distribution of subtilisin-like protease encoding genes in fungal genomes

SPECIES	OTHER	PYROLYSIN (CLASS 1)		PROTEINASE K (CLASS 2)				KEXIN
		Subfam 1	Subfam 2	Subfam 1	Subfam 2	Subfam 3 (vacuolar)	Other	
Aspergillus nidulans[1]				-	1	1		1
Magnaporthe grisea[1]	1	6	8	2	3	1		1
Neurospora crassa[1]		1		1	2	1		1
Fusarium graminearum[1]	5	2	1	2	7	1	2	1
Stagonospora nodorum[1]	1	2		4	1	1		1
Chaetomium globosum[1]		1		3	1	1		1
Metarhizium anisopliae[2]	?	1	?	5	4	1	?	?
Sclerotinia sclerotiorum[1]		1		-	1	1		1
Botrytis cinerea[1]		1		-	1	1		1
S.cerevisiae[3]				1	-	2		1
S. pombe[4]	1			-	-	2		1
Ustilago maydis[1]	1	1		-	-	1		1

[1] Gene numbers were derived from analysis of the peptidase S8 family identified during HMMR analysis of these genomes at http://www.broad.mit.edu/annotation/fgi/

[2] These sequences were derived during analysis of ESTs from *M. anisopliae* grown on cockroach cuticle. The numbers for this organism are shaded in grey because they do not represent a full genomic analysis of genes encoding subtilisin-like proteases. There may be more subtilisin-like protease-encoding genes in the *M. anisopliae* genome.

[3] *S. cerevisiae* sequences were obtained from http://www.yeastgenome.org

[4] *S. pombe* sequences were obtained from http://www.genedb.org/genedb/pombe/index.jsp

Phylogenomic analysis by Hu and St Leger (2004) suggests that members of the pyrolysin gene family of *M. grisea* have been duplicated many times. The large number of members of this gene family in the *M. grisea* genome suggests that these genes offer some benefit in terms of pathogenicity or virulence towards the host. However, the role of these genes in *M. grisea* remains to be determined. *F. graminearum* appears to

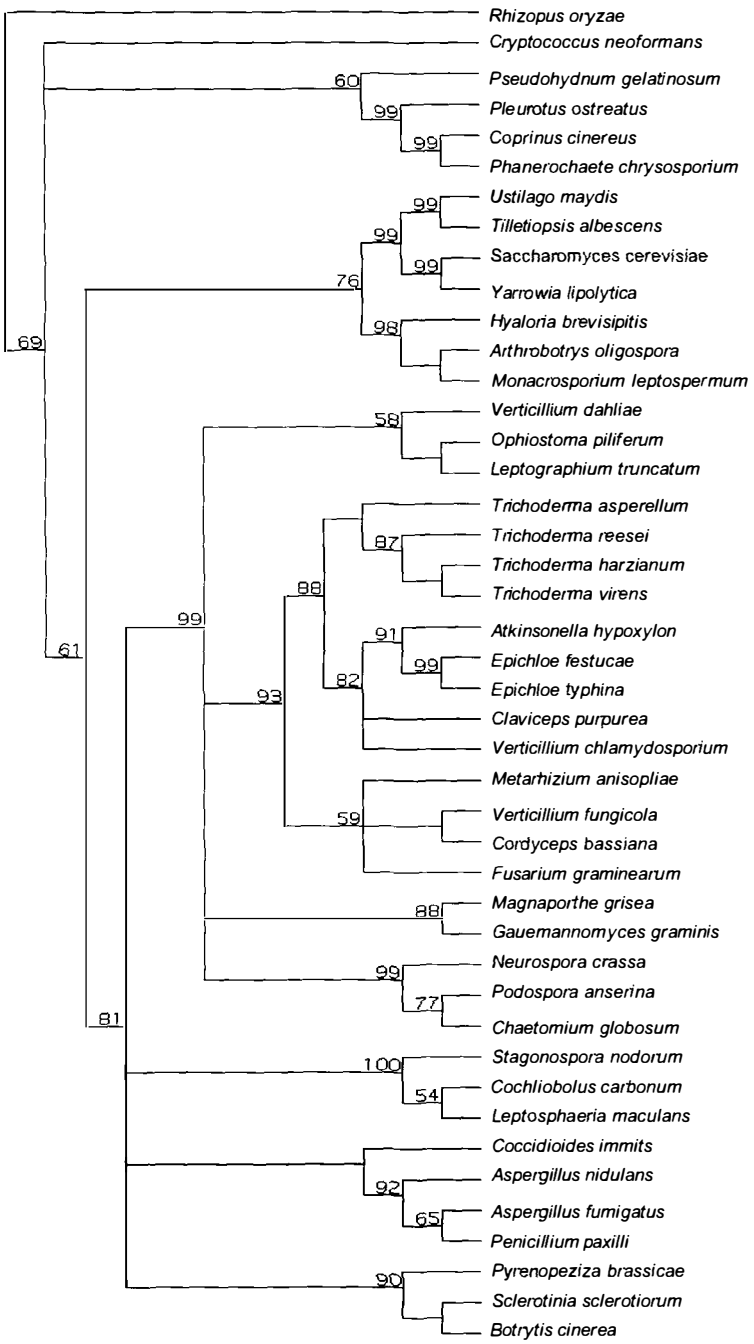

Figure 1.4 Phylogenetic relationships of fungal species

Phylogenetic relationships between fungi used for comparisons in this study based on ITS1, 5.8S rRNA and ITS2. The phylogenetic tree was prepared in the MacVector 7.2.3 program, using Neighbour Joining and bootstrapping (1000 replicates) of sequences aligned using the ClustalW module of MacVector to form the tree. For details of sequences used in this alignment, see Appendix A13.1.

contain duplications of the proteinase K subfamily 2, which may benefit the fungus in colonisation or virulence towards its host.

1.5 ROLE OF PROTEASES IN INTERACTIONS WITH THEIR HOSTS

1.5.1 Insect pathogenic fungi

Metarhizium anisopliae var. anisopliae infects a broad range of insect hosts (Freimoser et al., 2005). The fungus enters the insect by using enzymatic degradation and physical forces to break through the cuticle, which consists of approximately 70% protein and 30% chitin (Griesch, 1998). A cocktail of hydrolytic enzymes secreted by *M. anisopliae*, which include subtilisin-like proteases, trypsin-like proteases, carboxypeptidases and chitinases, acts to degrade the insect cuticle (da Silva et al., 2005; Goettel et al., 1989; Joshi and St Leger, 1999; Joshi et al., 1997; St Leger et al., 1994; St Leger et al., 1996b). Proteases produced by *M. anisopliae* act together with secondary metabolites such as destruxins to suppress the host immune system by suppressing the phagocytic activity, attachment, spreading and cytoskeleton formation of host plasmatocytes (Griesch, 1998).

The hydrolytic enzyme best characterised in host colonisation by *M. anisopliae* is the subtilisin-like protease Prl A. The surface of the insect cuticle is low in available nitrogen, which triggers appressorium formation. Prl A in the appressorium breaks down proteins in the cuticle and enables hyphae to penetrate through the cuticle (Goettel et al., 1989). Once hyphae are in the insect haemolymph, a circulatory fluid surrounding the cells of the insect exoskeleton, Prl A expression is down regulated (Freimoser et al., 2005). When nutrients in the haemolymph are exhausted, Prl A expression is up-regulated, with the Prl A protease degrading the cuticle to allow hyphae to emerge from the insect and conidiate (Small and Bidochka, 2005).

Constitutive expression of Prl A by *M. anisopliae* increases fungal virulence and host melanisation but decreases host food intake (St Leger et al., 1996c). Prl A protein is not

present in the haemolymph of insects infected with wild type *M. anisopliae*. In transformants with constitutive *prl A* expression, the presence of the Prl A protease in the haemolymph was associated with degradation of haemolymph proteins. Pure Prl A activates a trypsin cascade in the host haemolymph that activates prophenol oxidase, an enzyme involved in melanin production that is an important part of the insect immune response. Prl A over expression also reduces fungal sporulation. As the host dies more quickly when infected with Prl A-over expressing strains, the fungus will have fewer nutrients available to complete sporulation and less time to complete its life cycle.

Expressed sequence tag (EST) analysis identified eleven subtilisin-like protease genes expressed during host infection by *M. anisopliae* var. anisopliae (Freimoser et al., 2003). Phylogenetic studies confirm the Prl A, Prl B, Prl G, Prl I and Prl K genes belong to subfamily 1 of the proteinase K family of subtilisin-like proteases, while Prl D, Prl E, Prl F and Prl J belong to subfamily 2 (Hu and St Leger, 2004). The Prl H gene encodes a vacuolar type protease from proteinase K subfamily 3, while the Prl C gene encodes a member of the pyrolysin family.

The Prl subtilisin-like protease genes differ in their response to nutrient limitation, different host insect cuticles, insect haemolymph and saprotrophic growth (Freimoser et al., 2005; Wang et al., 2005). The Prl genes are temporally regulated during growth on insect cuticle, with a subset of the genes (Prl A, C, D and J) induced early in response to *Manduca sexta* cuticle, while another subset of genes (Prl E and K) are expressed at later stages. Other genes (Prl B, F and I) are induced at particular time points, suggesting these proteases could act at certain stages to break down particular protein substrates. Expression of genes encoding subtilisin-like proteases in *M. anisopliae* also differed in response to *M. sexta* haemolymph. Expression of Prl B, Prl C, Prl F, Prl G, Prl I and Prl K genes is repressed in response to haemolymph, while expression of the other Prl genes is unaffected.

Homology modelling suggests different members of the Prl gene family have different substrate specificities. Gron and Breddam (1992) suggested that the S1 and S4 active site pockets determine the substrate specificities of subtilisin-like proteases. Based on

this and sequence comparisons with a closely related subtilisin like protease with known structure (proteinase K from *Tritirachium album*), differences in amino acid sequence between Pr1 proteases were identified that could potentially change the substrate specificity and catalytic ability of these enzymes. The differences in substrate specificity may also affect the inhibition of these proteases by protease inhibitors found in the host haemolymph (Frobius et al., 2000; Samuels and Reynolds, 2000).

The Pr2 gene family encodes trypsin-like proteases (St Leger et al., 1996a). Unlike the Pr1 proteases, the Pr2 gene(s) are almost inactive against insoluble proteins in the cuticle. However, they are highly active against soluble proteins released from the cuticle by the action of the Pr1 proteases. The Pr2 trypsin activity appears to be complementary to Pr1 enzyme activity in degrading host proteins. In *M. anisopliae*, trypsin activity is associated with appressoria produced by the fungus to enable penetration of the host during the early stages of colonisation. Like the subtilisin-like proteases, trypsins are up regulated during growth in cuticle (Freimoser et al., 2005). Carboxypeptidase, metalloprotease, chymotrypsin and aspartic protease genes are also expressed during host infection. Like the subtilisin and trypsin-like protease genes, expression of these genes is also up regulated during growth on cuticle (Freimoser et al., 2005).

While the subtilisin-like protease genes and one of the two trypsin-encoding genes are down regulated in the insect haemolymph, the expression of the chymotrypsin, carboxypeptidase, metalloprotease and aspartic protease genes was unchanged (Freimoser et al., 2005). Repressing expression of some protease genes may prolong the life of the fungus within the host by preventing the triggering of the host trypsin cascade activating prophenol oxidase. If these subtilisin-like protease-encoding genes were expressed in the haemolymph, their products could potentially trigger melanisation in the same manner as over expression of Pr1A. This would result in premature death of the host, complicating the completion of the fungal life cycle.

1.5.2 *Trichoderma* species

Trichoderma species are saprophytic fungi that grow in the rhizosphere. In some situations, they can act as symbionts of plants and as pathogens towards phytopathogenic fungi and nematodes (Harman et al., 2004; Suarez et al., 2004). Species of *Trichoderma* positively influence plant growth and induce plant resistance towards some phytopathogenic fungi. During antagonism, *Trichoderma* spp. hyphae grow towards phytopathogenic fungi (Lu et al., 2004). *Trichoderma* hyphae form coils around the host fungus, then penetrate the host mycelium after partially degrading the host cell wall (Cortes et al., 1998).

Several varieties of hydrolytic enzymes have been associated with the lytic activity of *Trichoderma* species towards the cell walls of other fungi. Extracellular enzymes such as β-1,3-glucanases, β-1,6-glucanases, chitinases, and proteases act either additively or synergistically together to promote cell wall degradation (De la Cruz et al., 1995; El-Katatny et al., 2001; Suarez et al., 2004). The expression of many of the hydrolytic enzymes appear to be co-ordinately regulated (Geremia et al., 1993; Montero et al., 2005).

Proteases are required to lyse fungal cells (Scott and Schekman, 1980). Proteases may degrade the external protein matrix of the cell wall, allowing access to the glucan and chitin structural polysaccharides below. Three protease families are associated with antagonism by *Trichoderma* species: subtilisin-like proteases (Prb1 from *T. harzianum* and Tvsp1 from *T. virens*), trypsin-like proteases (Pra1 from *T. harzianum*) and aspartic proteases (Geremia et al., 1993; Suarez et al., 2004; Viterbo et al., 2004).

Subtilisin-like proteases play roles in antagonism towards soil and phytopathogenic fungi (Flores et al., 1997) and towards nematodes (Sharon et al., 2001). Over expression of *prb1* or *tvsp1* improves the ability of *Trichoderma* spp. fungi to acts as biocontrol agents towards phytopathogenic fungi on plants, suggesting both these proteases are involved in mycoparasitism (Flores et al., 1997; Pozo et al., 2004).

T. harzianum coils around nematodes, and can penetrate second-stage juvenile (J2) nematodes and free nematode eggs. Treatment of nematode-infested soils with *T. harzianum* resulted in a reduction in root galling caused by the root nematode fungus *Meloidogyne javanica,* and an increase in plant fresh weight (Sharon et al., 2001). *T. harzianum* strains over expressing *prb1* (Flores et al., 1997) caused even larger reductions in galling and increases in plant fresh weight, and were even able to penetrate nematode egg masses, unlike wild-type strains.

Trypsin-like proteases produced by *T. harzianum* may be involved in mycoparasitic and nematicidal activity (Suarez et al., 2004). Like Prb1 and other lytic enzymes produced by *T. harzianum*, the trypsin-like protease Pra1 is induced by fungal cell walls and chitin, suggesting that these proteases may play a role in degrading fungal cell walls during the lytic process. Pra1 is also directly toxic to nematodes, dramatically reducing the hatching rate of nematode eggs.

The aspartic proteases PapA and PapB from *T. asperellum* are induced in response to hyphal attachment to plant roots, and both *papA* and *papB* are expressed in *planta* (Viterbo et al., 2004). The *papA* gene is up regulated prior to contact in direct plate confrontation assays with the phytopathogenic fungus *Rhizoctonia solani*, suggesting this protease may play a role in lysing fungal hyphae. Another aspartic protease, P6821, is induced during growth of *T. harzianum* on fungal cell walls (Suarez et al., 2005). P6821 is not an orthologue of PapA or PapB, due to its differences in sequence and biochemical properties. P6821 has a similar expression profile to Prb1 and Pra1, with expression within four hours of growth on cell walls.

1.5.3 Nematode pathogenic fungi

1.5.3.1 *Arthrobotrys oligospora*

Arthrobotrys oligospora lives in the rhizosphere, where it forms special structures called traps to capture and parasitize nematodes. The nematode cuticle consists mainly of protein. In culture, *A. oligospora* produces serine, metallo-, aspartic and cysteine proteases (Tunlid and Jansson, 1991). Hyphal treatment with inhibitors active against

each of these protease classes does not affect hyphal adhesion to the nematode. However, treatment with serine protease and metalloprotease inhibitors does affect nematode immobilisation, suggesting serine and metalloproteases are important in virulence of *A. oligospora*.

Two orthologous protease genes, *PII* and *aoz1*, which share 97% identity at the nucleotide level, play a role in this parasitism (Åhman et al., 1996; Zhao et al., 2004). The PII protease was first identified in *A. oligospora* as an abundant protease found when the fungus was cultured in conditions that induce the formation of fungal traps (Åhman et al., 1996), while Aozl was isolated as the major protease activity in a different *A. oligospora* strain (Zhao et al., 2004). The PII and Aozl subtilisin-like proteases immobilize nematodes and degrade proteinaceous components of the nematode cuticle. The *PII* gene may also influence trap development. Although *PII* deletion mutants had reduced proteolytic activity and a lower number of traps than wild type *A. oligospora*, there was little difference in the numbers of trapped nematodes or in the immobilisation of nematodes (Åhman et al., 2002). When *PII* was over expressed, not only were a higher number of traps formed, but a higher percentage of nematodes were immobilised compared to wild type.

Recombinant PII itself is directly toxic to nematodes, as it could immobilise nematodes. Hybridisation results obtained by Åhman et al. (1996) and PCR results obtained by Zhao et al. (2004) suggest more *PII*-related sequences are present in the *A. oligospora* genome, some of which could partially compensate for the loss of PII activity in strains where the *PII* gene has been replaced.

1.5.3.2 *Verticillium chlamydosporium*

The nematode pathogen *Verticillium chlamydosporium* produces a subtilisin-like protease, VCP1, which degrades the protein components of the nematode eggshell. VCP1 hydrolyses proteins in the outer layer of the nematode eggshell to expose the inner chitin layer (Segers et al., 1994), which is degraded by a chitinase that acts synergistically with VCP1 (Tikhonov et al., 2002).

1.5.3.3 *Paecilomyces lilacinus*

P. lilacinus, a fungus pathogenic towards nematode eggs, produces a protease activity (P32) induced by chitin, vitellin and intact eggs of root-knot nematode (Bonants et al., 1995). While immature eggs are very sensitive to the subtilisin-like protease activity, older eggs are more resistant and hatched larvae appear to be unaffected. The purified P32 protease binds to nematode eggs, suggesting the P32 protease may play a role in *P. lilacinus* penetration of the egg. Purified P32 can also degrade vitellin, a component of the nematode egg yolk.

1.5.4 Candida albicans

Candida albicans is the most common fungal pathogen of humans (Naglik et al., 2003). Under normal conditions, *C. albicans* is present in the body as part of the normal microflora; however, if microflora is disturbed or the immune system compromised, systemic infection can occur, leading to disease. Extracellular hydrolytic enzymes such as phospholipase B, lipases and secreted aspartic proteinases (SAPs) produced by *C. albicans* have been identified as potential virulence factors (Naglik et al., 2003).

Ten *SAP* encoding genes are present in the genome of *C. albicans* (Naglik et al., 2004). SAP proteinases may provide nutrients, to facilitate invasion and penetration of the host, and to help *C. albicans* evade host immune responses. The *SAP1* to *SAP8* genes encode secreted enzymes, while the SAP9 and SAP10 proteins contain glycophosphoinositidol (GPI) anchors that localise SAP9 and SAP10 to the cell membrane.

Members of the SAP gene family are differentially expressed (Staib et al., 2000). *SAP1*, *SAP2* and *SAP3* are expressed throughout yeast and hyphal forms of the dimorphic *C. albicans*, and are associated with virulence in superficial infections. Deletion of the *SAP1*, *SAP2* or *SAP3* genes results in attenuated virulence towards the host (Hube et al., 1997). The *SAP4*, *SAP5* and *SAP6* gene subfamily are expressed only in hyphal cells closely attached to host cells, and are associated with systemic infections resulting in organ damage in animals. Triple deletions of the *SAP4*, *SAP5* and *SAP6* genes resulted in reduced virulence (Sanglard et al., 1997). Single, double and triple mutants lacking

functional SAP6 showed significantly reduced tissue damage compared to wild-type *C. albicans* (Felk et al., 2002; Kretschmar et al., 2002). SAP9 and SAP10 are required for cell surface integrity in the same manner as *S. cerevisiae* yapsins (Albrecht et al., 2005; Krysan et al., 2005). Deletion of *SAP9* and *SAP10* decreased *C. albicans* adhesion and virulence towards their host.

The SAP aspartic proteases also have different pH optimums and substrate specificities (Naglik et al., 2003). SAP1, SAP2 and SAP3 are most active at lower pH values of 3-5, SAP4, SAP5 and SAP6 have optimal activity at pH 5-7. SAP1, SAP2, SAP3 and SAP6 cleave peptide bonds between larger hydrophobic amino acids. SAP1, SAP2 and SAP6 prefer to cleave after phenylalanine, while SAP3 prefers to cleave after leucine. The SAP9 and SAP10 proteases, which appear to contain GPI anchor sequences, cleave distinct substrates in a similar manner to kexins and yapsins (Albrecht et al., 2005).

1.5.5 Dermatophytic fungi

Dermatophytic fungi are the most common agents of superficial mycoses in animals (Weitzman and Summerbell, 1995). These fungi grow between keratinised cells in hair, nails and the stratum corneum, the outermost layer of the epidermis. All of these structures contain keratin, a structural protein found in the skin epidermis, hair, wool, horns, hoofs, nails/claws, beaks, feathers and scales. Secreted protease activity has been associated with virulence of dermatophytic fungi, with a strong correlation observed between high keratinase activity and development of mycosis symptoms (Viani et al., 2001). Families of metalloprotease (Brouta et al., 2002; Jousson et al., 2004a), subtilisin-like protease (Descamps et al., 2002; Jousson et al., 2004b), aminopeptidase and dipeptidylpeptidase (Monod et al., 2005) encoding genes have been identified in dermatophytic fungi.

Five secreted fungalysin-type metalloproteases that form a single gene family are present in each of the dermatophyte species *Trichophyton rubrum*, *Tricophyton mentagrophytes* and *Microsporum canis* (Jousson et al., 2004a). At least two of these metalloprotease genes, *MEP2* and *MEP3*, are expressed during infection of the host (Brouta et al., 2002). Monod et al. (2005) also identified expression of genes encoding

two aminopeptidases and two dipeptidylpeptidases during growth on keratin as the sole carbon and nitrogen source, suggesting the enzymes encoded by these genes may degrade keratin during infection by dermatophytic fungi.

Seven subtilisin-like protease genes were identified in *T. rubrum*. With the exception of *SUB2* (a member of proteinase K subfamily 2), all appear to have arisen by recent gene duplication events. Of these seven genes, *SUB1*, *SUB2* and *SUB3* are expressed during dermatophyte infection. *SUB3* is the major polypeptide secreted by fungus in minimal keratin-enriched medium. Activity studies have shown that at least SUB3 and SUB4 are highly active against a keratin substrate (Jousson et al., 2004b). However, the closely related SUB5 protein is not active against either keratin or casein, suggesting this protease has different substrate specificity. The SUB6 protein (previously identified as Tri r 2; (Woodfolk et al., 1998)) induces immediate and delayed skin hypersensitive reactions, as does the SUB3 protein (Descamps et al., 2002)

1.5.6 *Plant pathogenic fungi*

1.5.6.1 *Magnaporthe grisea*

Sequencing of the *M. grisea* genome revealed many protease-encoding genes (Table 1.2; http://www.broad.mit.edu/annotation/fungi/magnaporthe/). To date, only two subtilisin-like proteases from this organism have been characterised. The *Mp1* gene, encoding an enzyme of the proteinase K subfamily 1, is present in *M. grisea* as a multigene family, as shown by Southern blot analysis. The *Mp1* gene is expressed during infection of Kentucky bluegrass (*Poa pratensis*) roots, with immunoblot analysis showing correlation of Mp1 levels with the increasing severity of disease symptoms (Sreedhar et al., 1999). However, this result is likely to be due to increased biomass of the phytopathogen within the plant.

The *Spm1* gene encodes a protease that shares significant sequence homology with PspA (Section 1.4.2). Like PspA, the Spm1 protease is probably localised to the fungal vacuole (Fukiya et al., 2002). In *M. grisea*, the vacuole is important in fungal pathogenicity as it is involved in the lytic system of the developing appressorium (Weber et al., 2001). The lytic system is involved in degrading lipid droplets in the

vacuole of the appressorium. As vacuolar proteases are involved in degrading autophagosomes in the vacuole, they may play a role in releasing the lipid droplets from autophagosomes in the appressorium.

1.5.6.2 *Botrytis cinerea*

Aspartic proteases have been implicated in the virulence of the necrotrophic *B. cinerea* towards their plant hosts, with the aspartic protease inhibitor pepstatin drastically reducing infection caused by *B. cinerea* (Movahedi and Heale, 1990). A gene family of at least five aspartic protease-encoding genes (BcAPs) has been identified in *B. cinerea*, all of which were expressed in all host tissues studied (ten Have et al., 2004). The BcAP1 protein is unusual compared to the other members of the family in that it does not have a signal peptide. Like the *C. albicans* SAP9 and SAP10 and *S. cerevisiae* yapsins, BcAP3 and BcAP4 have GPI anchors. None of the *BcAP* genes is temporally regulated during host infection. Like the SAP proteases, the BcAP proteases differ in expression levels in different host tissues. Consequently, differential expression of members of this gene family may help *B. cinerea* adapt to different host niches.

1.5.6.3 *Sclerotinia sclerotiorum*

S. sclerotiorum is a necrotrophic pathogen that causes tissue maceration and cell death in its host. Polygalacturonase (pectin-degrading) enzymes produced by *S. sclerotiorum* are associated with the extensive damage caused to the host tissue (Fraissinet-Tachet et al., 1995; Kasza et al., 2004). However, proteases may still play a role in degrading host antifungal, cell wall and membrane proteins released during pathogenesis. Two acid proteases are produced during growth on sunflower cell walls. *acp1* is an acid non-aspartic protease-encoding gene expressed at low levels during the initial stages of infection (Poussereau et al., 2001a). At later stages of infection, when fungal-induced necrosis begins to spread, the *acp1* gene is expressed at higher levels. The *aspS* gene encodes an aspartic protease expressed throughout infection of sunflowers (Poussereau et al., 2001b). The expression of the *aspS* gene increases during the stage where mycelia begin to colonise the sunflower's cotyledons. When the cotyledons are completely colonised and degraded, *aspS* expression decreases.

1.5.6.4 *Fusarium* species

A single subtilisin-like protease gene has been identified in *F. oxysporum* f. sp. lycopersici, a fungus that causes vascular wilt disease in tomatoes (Di Pietro et al., 2001). This subtilisin-like protease gene, *prt1*, is expressed constitutively at low levels both in culture and in *planta*. Deletion of the *prt1* gene did not alter total protease production or alter fungal pathogenicity, virulence or colonisation of the host.

Fusarium solani f. sp. eumartii is a potato pathogen that enters the potato tuber through wounds, and colonises intercellular spaces. This fungus produces a subtilisin-like protease that degrades at least three proteins from intercellular wash fluid (IWF) (Olivieri et al., 2002). Two proteins degraded by the protease were basic chitinase and β-1,3-glucanase, antifungal proteins produced by the potato plant. If the protease degrades the same proteins during potato infection, it would allow *F. solani* f. sp. eumartii to nullify some of the host's natural defences against fungal infections.

A large number of protease-encoding genes are present in the genome of *F. graminearum* (Section 1.4.4, Table 1.2), although the role of these proteases has not been identified. *F. graminearum* shows high levels of synteny with *Epichloë* and *Neotyphodium* spp. (S. Foster, A. Tanaka and G. Bryan, personal communication) to which it is closely related. This could suggest large numbers of protease genes are also present in the genomes of *Epichloë* and *Neotyphodium* spp. fungi.

1.5.6.5 *Verticillium dahliae*

Verticillium dahliae, a fungal pathogen that causes vascular wilt in a wide range of plant species, produces a VTP1 trypsin-like activity (Dobinson et al., 2004). Deletion of the *vtp1* gene did not change either fungal pathogenicity towards its host or growth in culture. Significant protease activity remained in the Δ*vtp1* strain, which may be due to the presence of at least two subtilisin-like protease genes, *vsp1* and *vsp2*, also identified in *V. dahliae* (Neumann and Dobinson, 2003). Two other proteases encoding a pyrolysin subtilisin-like protease and an aspartic protease have been identified in *V. dahliae* (Wang et al., 2004b).

1.5.6.6 *Stagonospora nodorum*

S. nodorum, a fungal pathogen of wheat, expresses the trypsin-like protease gene *snp1* during early stages of hyphal growth on host leaf surface and during leaf penetration (Carlile et al., 2000). The proteolytic action of SNP1 releases hydroxyproline from wheat cell walls. However, deletion of *snp1* does not affect the pathogenicity of *S. nodorum* towards its host (Bindschedler et al., 2003). Like the *V. dahliae* Δ*vtp1* mutant, the *S. nodorum* Δ*snp1* mutant still maintained significant levels of protease activity, with a residual subtilisin-like protease activity possibly compensating for loss of the trypsin activity.

1.5.6.7 *Cochliobolus carbonum*

Murphy and Walton (1996) detected three different protease activities in *C. carbonum*, a pathogen of maize. Two of these activities were trypsin-like, while the third was subtilisin-like. Deletion of the *ALP1* gene, which encoded both the two trypsin-like protease activities, reduced protease activity by 35-40%. However, the *in vitro* growth of the Δ*ALP1* strain and its disease phenotype were very similar to wild-type *C. carbonum*. Again, the subtilisin-like protease activity identified in *C. carbonum* may have partially compensated for the loss of the *ALP1* gene.

1.5.6.8 *Glomerella cingulata*

Glomerella cingulata causes bitter rot disease in pip fruit such as apples and pears. *G. cingulata* contains a single gene encoding an aspartic protease, not a family of related genes as seen in *B. cinerea* and *C. albicans*. The *gcsap* gene, which encodes the only aspartic protease detected in culture, is expressed by *G. cingulata* during appressorium formation, but not in germinated conida (Plummer et al., 2004). When the *gcsap* gene was disrupted, mutant strains were still able to infect undamaged apples. This indicates GcSAP is not required for pathogenicity on apple hosts or for penetration of the apple epidermis. GcSAP was also not required for appressorium formation *in vitro*. The growth rate of the *gcsap* disruption strain on defined media containing protein was not affected, suggesting the mutant still had residual protease activity. Subsequent studies showed that GcSAP contained residual serine protease activity.

1.5.6.9 *Ophiostoma piliferum*

O. piliferum is a wood sap-staining fungus that produces proteases that hydrolyse wood proteins. Deletion of the *albinl* gene, which encodes the major subtilisin-like protease activity from *O. piliferum*, caused significant loss of protease activity that correlated with much slower growth in BSA media, and significantly reduced growth in wood (Hoffman and Breuil, 2004b). This suggests the *albinl*-encoded subtilisin-like protease activity is important in the ability of *O. piliferum* to acquire nitrogen from wood proteins.

1.5.6.10 *Epichloë* sp. protease

An *Epichloë* sp. endophyte infecting big bluegrass (*Poa ampla*) produces a subtilisin-like protease, Atl, which forms up to 2% of the total protein in infected leaf sheaths (Lindstrom and Belanger, 1994). The Atl-encoding gene is highly expressed in the association between *Poa* spp. grasses and their *Epichloë/Neotyphodium* spp. endophytes, but the corresponding gene is expressed at much lower levels in the interaction between *Epichloë festucae* and *Festuca rubra* subsp. rubra and the interaction between *N. lolii* and *Lolium perenne.* It is unclear whether the difference in *Atl* expression is due to higher expression in the *Poa* spp.-endophyte associations, or if this difference is due to differences in fungal biomass (Reddy et al., 1996). The potential role of the Atl protease during endophyte growth within its host is unclear, but like most hydrolytic enzymes it may play a role in degrading host macromolecules (in this case, proteins) to provide nutrients to support fungal growth.

1.6 β-1,6-GLUCANASES

1.6.1 β-1,6-glucans: role in the fungal cell wall

The cell wall is critical to the survival of fungal cells. Fungal cell walls provide structural rigidity, protecting cells from lysis during osmotic stress. The cell wall is also critical in the interaction of the fungus with its environment, with factors affecting fungal adhesion and host recognition often located in the wall. The porosity of the cell wall also determines the access of compounds present in the external environment to the

fungal cell. The cell wall also provides a surface matrix for fungal proteins that may be involved in fungal growth or nutrition.

The fungal cell wall is a complex array of biological polymers. Chitin, a fibrous polymer of *N*-acetyl-D-glucosamine, is at the innermost part of the fungal cell wall. Chitin is linked to β-1,3-linked glucans, which are linked to mannoproteins in the outer cell wall by β-1,6-glucans (Odds et al., 2003). Mannoproteins may be linked covalently to the wall through glycophosphoinositidyl (GPI) anchors or Pir linkages, or be held at the wall through electrostatic interactions (Kapteyn et al., 1999). As extracellular proteins, cell wall proteins are often glycosylated during passage through the secretory pathway (Conesa et al., 2001).

β-1,6-glucans act as anchor or branch points within the cell wall. In the yeast *S. cerevisiae*, β-1,6-glucan has been described as the "glue" that holds all the components of the cell wall together (Kollar et al., 1997). Chitin and β-1,3-glucan are directly attached to β-1,6-glucan, while mannoproteins are attached to β-1,6-glucan through part of a GPI anchor. In filamentous fungi such as *Aspergillus niger*, *Penicillium roqueforti* and *F. oxysporum*, β-1,6-glucans are also implicated in attaching GPI-anchored mannoproteins to the β-1,3-glucan backbone of the cell wall (Brul et al., 1997; Schoffelmeer et al., 1999).

Hydrolytic enzymes may be involved in maintaining wall plasticity or remodelling the wall during development. Selective degradation of cell wall components could permit hyphal branching. Hydrolytic enzymes may also influence wall porosity, thus affecting the interaction of the hyphae with its external environment. As β-1,6-glucans are implicated as branch points within the wall, the action of enzymes that hydrolyse this compound, such as β-1,3-1,6-glucanases and β-1,6-glucanases, may play important roles in wall plasticity and wall porosity.

1.6.2 β-1,6-glucanases: enzymatic activity and roles in pathogenicity

Enzymes with β-1,6-glucanase activity catalyse the hydrolytic cleavage between two molecules of glucose linked together by a β-1,6-glucan linkage (Figure 1.5).

Filamentous fungi have at least two different types of enzymes with β-1,6-glucanase activity. The first group, members of glycosyl hydrolase family 30, are closely related to glucosylceramidases (Oyama et al., 2002). Little information is available regarding the biological role of these enzymes in fungi. Some fungal species also contain a second endo-β-1,6-glucanase activity, associated with glycosyl hydrolase family 5 (Lora et al., 1995). β-1,6-glucanases from this family are related to enzymes with exo- β-1,3-glucanase activity.

Three different β-1,6-glucanase activities have been identified in the mycoparasitic fungus *Trichoderma harzianum* (de la Cruz and Llobell, 1999; De la Cruz et al., 1995; Montero et al., 2005). All three classes, BGN16.1, BGN16.2 and BGN16.3, are potentially involved in mycoparasitism through their ability to break down β-1,6-glucan linkages in in the cell wall

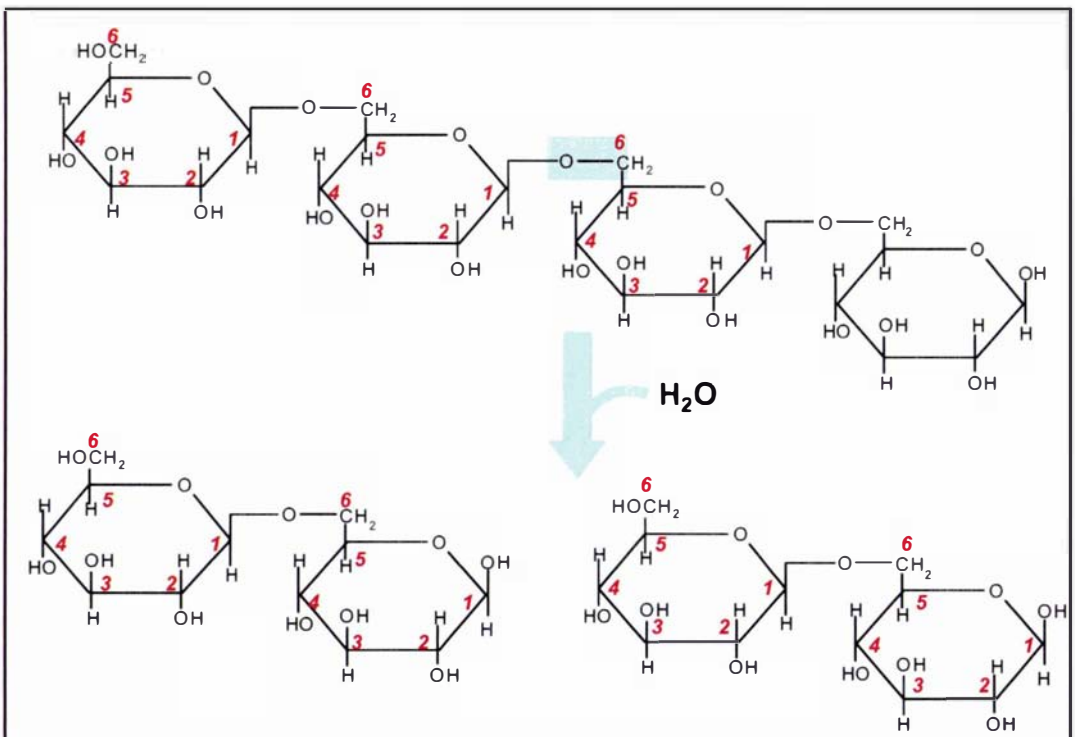

Figure 1.5 Reaction catalysed by endo-ß-1,6-glucanases

Endo-hydrolytic cleavage of ß-1,6-glucan catalysed by ß-1,6-glucanases. Numbering of the glucose units comprising the ß-1,6-glucan is shown in red. The bond between position 1 of the first glucose unit and position 6 of the second glucose unit that gives ß-1,6-glucan its name.

While all three activities act as endo- β-1,6-glucanases, they differ in their substrate specificities towards glucans with mixed β-1,3-β-1,6-linkages. BGN16.1 and BGN16.3 can both degrade yeast glucan (β-1,3: β-1,6 4:1) and laminarin (β-1,3: β-1,6 7:1).

BGN16.2 can degrade yeast glucan, but not laminarin. The enzymes also differ in their catalytic rate constants for pustulan, which contains only β-1,6-linkages. BGN16.2 had the highest catalytic rate constant towards pustulan, followed by BGN16.3 and BGN16.1. The proteins also differ in their regulation, with both BGN16.1 and BGN16.2 induced by chitin, but BGN16.3 is induced by pustulan and fungal cell walls.

The role of β-1,6-glucanases in the interaction between a mycoparasite and its host has been characterised in the *Verticillium fungicola - Agaricus bisporus* interaction (Amey et al., 2003). Disruption of the *BGN16.2* homologue of *V. fungicola*, *VfGlu1*, reduced virulence of *V. fungicola* towards *A. bisporus*. This reduction was associated with the reduced growth rate of Δ*VfGlu1* strains on chitin, suggesting disruption of the *VfGlu1* gene reduces virulence of *V. fungicola* by impairing its ability to degrade components of the fungal cell wall.

β-1,6-glucanase activity of the glycosyl hydrolase 5 family is present in the interaction between a fungal endophyte and its grass host. The endophyte *Neotyphodium* sp. FCB2002 produces a β-1,6-glucanase enzyme that it secretes into the plant apoplast in and on its host, *Poa ampla* (Moy et al., 2002). As this fungus forms epiphyllous nets on the surface of grass leaves, Moy et al. (2002) suggested this enzyme activity might be involved in niche exclusion. The antifungal activity of the β-1,6-glucanase could potentially lyse cell walls of competing fungi in co-operation with proteases and chitinases produced by the *Neotyphodium* endophyte.

1.7 FUNCTIONAL CHARACTERISATION OF HYDROLYTIC ENZYMES IN HOST/FUNGAL INTERACTIONS

The function of hydrolytic enzymes in interactions with their hosts have been analysed in various ways. The most common way of determining the function of these enzymes

has been gene replacement, where a selectable marker replaces the gene of interest. While this approach has worked well for analysing the roles of some hydrolytic enzymes in pathogenicity and/or virulence (Amey et al., 2003), the presence of hydrolytic enzyme-encoding genes in gene families can complicate these analyses. Often, this means that single gene replacements do not show a detectable phenotype, while double, triple or quadruple replacements may show a phenotype.

An example of this is the *THI5* gene family from *S. cerevisiae*, which consists of the *THI5*, *THI11*, *THI12* and *THI13* genes (Wightman and Meacock, 2003). The members of the *THI5* gene family are functionally redundant in biosynthesis of hydroxymethylpyrimidine (HMP), a precursor of thiamine. Deletion of one, two or three members of the gene family resulted in strains that were prototrophic for thiamine. When all four *THI5* family members were disrupted, the resulting strain was auxotrophic for thiamine. This suggested that all four members were involved, but functionally redundant, in HMP (and thus thiamine) biosynthesis.

In filamentous fungi, which are less genetically tractable than the yeast *S. cerevisiae*, deletion of multiple members of the same gene family may prove difficult due to the large numbers of genes involved and the limited availability of suitable selectable markers. For example, in *M. anisopliae, M. grisea* and *F. graminearum*, the gene family of subtilisin-like proteases can consist of up to 22 genes (Table 1.2).

Another means used to analyse the function of genes is gene knockdown, or an RNAi strategy. Gene knockdown using a construct driving expression of an antisense RNA can reduce mRNA levels for a gene, generally giving a similar phenotype to a gene replacement. Potentially, the formation of double stranded RNAs produced by the annealing of the antisense RNA to the mRNA could also reduce RNA levels from multiple genes with similar sequences (for an example, see Spiering et al. (2005)). However, in gene families, genes do not necessarily share the high degree of sequence similarity necessary for silencing multiple genes with a single antisense RNA. It may be necessary to again introduce multiple constructs, each with a different selectable marker (as for gene replacements), or make single constructs with expressing multiple antisense RNAs. While this approach may be less time-consuming than constructing and

analysing gene replacements, the limited availability of suitable selectable markers could make this strategy difficult to use in many fungal systems.

Gene function is often demonstrated by complementation in another organism. This mechanism may be useful for showing the function of hydrolytic enzymes with a particular well-known action conserved amongst most fungi, such as kexins and vacuolar subtilisin-like proteases. However, expression of a hydrolytic enzyme-encoding gene in a different organism may not reflect the substrate specificity of the enzyme towards specific components found in the environment. For instance, the Prl A enzyme of *M. anisopliae* has a particular substrate specificity favouring the hydrophobic proteinaceous components of the insect cuticle, which it digests much more rapidly than proteinase K from *T. album* does (St Leger et al., 1992).

Biochemical characterisation is another means of identifying the possible role of a hydrolytic enzyme within its host. These analyses allow the determination of the substrate specificity, subunit arrangement, kinetic parameters and stability of an enzyme, along with cofactors that may be required for enzyme activity. Two approaches can be used to biochemically characterise an enzyme: the enzyme can be purified directly from the organism, or obtained through heterologous expression in another organism. Purification of the enzyme where the organism was originally identified can be time consuming and labour intensive, especially in the case of large multigene families where some enzymes may be produced at low levels. When enzymes are heterologously expressed in another organism, they can be easier to purify, especially if expressed with a tag to facilitate purification such as the His tag. However, enzymes may be abnormally processed or distributed in the new organism compared to their normal cellular background, which could affect the enzyme activity. Addition of a tag for purification may also change some of the characteristics of the enzyme.

Gene over-expression is also a means of examining the function of genes encoding hydrolytic enzymes. This technique circumvents the difficulties of determining gene function in large gene families, because the observed phenotype is not necessarily affected by the presence of other similar genes. Over expression has been used to

successfully determine the function of subtilisin-like protease genes in *M. anisopliae*, *T. harzianum* and *A. oligospora* in the interactions of these fungi with their hosts (Åhman et al., 2002; Flores et al., 1997; Pozo et al., 2004; St Leger et al., 1996c), despite these fungi containing other related subtilisin-like protease genes.

1.8 AIMS OF THIS PROJECT

Hydrolytic enzymes are often important in the interaction between pathogenic fungi and their plant, insect, nematode or fungal hosts. While several hydrolytic enzymes have been identified in the interaction between *Epichloë* endophytes and their grass hosts, the role of these enzymes in the symbiotic relationship between endophyte and host is unknown. While the function of hydrolytic enzymes in pathogenic fungi has been extensively studied, the function of hydrolytic enzymes in mutualistic associations between fungi and their hosts is poorly understood.

Subtilisin-like proteases have been identified as pathogenicity or virulence factors in several fungi. The first aim of this study was to confirm the presence and determine the identity of subtilisin-like proteases in the genome of the endophytic fungus, *E. festucae*. The second aim was to examine the role of subtilisin-like proteases in the symbiotic interaction between *E. festucae* and perennial ryegrass (*Lolium perenne* cv. Nui). In order to do this, the hypothesis was tested that over expression of fungal subtilisin-like protease genes would alter the interaction of an endophyte with its host grass. Two subtilisin-like genes were overexpressed under the control of the constitutive *gpdA* (glyceraldehyde-3-phosphate dehydrogenase) promoter from *A. nidulans* or the plant-induced *ltmM* (FAD-dependent monooxygenase for lolitrem biosynthesis) promoter from *E. festucae* Fl1. The phenotypes of symbiota containing strains with altered expression of the *prt1* and *prt2* genes were examined.

The third aim of this study was to examine the role of a β-1,6-glucanase in the symbiotic interaction between *E. festucae* and perennial ryegrass (*Lolium perenne* cv. Nui). The hypothesis was tested that a loss of endophyte β-1,6-glucanase activity would affect

endophyte growth within the host plant. The *gcn1* gene encoding a β-1,6-glucanase enzyme was disrupted, and the phenotype of the Δ*gcn1* strain was examined in culture and *in planta.*

CHAPTER 2

Materials and methods

2.1 BIOLOGICAL MATERIAL

Fungal, bacterial and plant strains, λ clones and plasmids used in this study are listed in Table 2.1.

Table 2.1 Biological material

Strains	Relevant Characteristics	References
	Fungal strains	
E. festucae Fl1	Host grass *Festuca longifolia*	Christensen et al. (1993)
E.festucae Frr1	Host grass *Festuca rubra* subspecies rubra	Christensen et al. (1993)
E. typhina PN2311	Host grass *Poa ampla*	Lindstrom and Belanger (1994)
N. lolii Lp19	Host grass *Lolium perenne*	Christensen et al. (1993)
N. lolii AR1	Host grass *L. perenne*	-
N. lolii Lp5	Host grass *L. perenne*	Christensen et al. (1993)
MM4.1, MM4.2, MM4.3, MM4.4, MM4.5, MM4.6, MM4.7, MM4.8, MM4.9, MM4.10, MM4.11, MM4.12	*E. festucae* Fl1/pMM26, Hyg^R	This study
MM5.1, MM5.2, MM5.3, MM5.4, MM5.5, MM5.6, MM5.7, MM5.8, MM5.9, MM5.10, MM5.11, MM5.12	*E. festucae* Fl1/pMM27; Hyg^R	This study
MM8.1, MM8.2, MM8.3, MM8.4, MM8.5, MM8.6, MM8.7, MM8.8	*E. festucae* Fl1/pMM32; Hyg^R	This study
MM9.1, MM9.2, MM9.3, MM9.4, MM9.5	*E. festucae* Fl1/pMM33; Hyg^R	This study
MM18.3	*E. festucae* Fl1/ pAN7-1; Hyg^R	This study
MM19.1	*E. festucae* Fl1 regenerated after protoplasting	This study
MM20.1, MM20.3	*E. festucae* Fl1/5' *gcn1-hph*-3' *gcn1*; Hyg^R, ectopic	This study
MM20.2, MM20.15	*E. festucae* Fl1/Δ*gcn1*::P*trpC-hph*; Hyg^R	This study
MM22.1, MM22.2, MM22.3, MM22.4, MM22.5, MM22.6, MM22.7, MM22.8, MM22.9, MM22.10, MM22.11, MM22.12, MM22.13, MM22.14, MM22.15, MM22.16, MM22.17, MM22.18, MM22.19, MM22.20	MM20.15/pII99, pMM44; Hyg^R Gen^R	This study
	Escherichia coli strains	
KW251	F⁻*sup*E44 *galK gal*T22 *met*B1 *hsd*R2 *mcr*B1 *mcr*A [*arg*A81:Tn10]*rec*D1014	Promega Corp.
XL-1	*sup*E44 *hsd*R17 *rec*A1 *end*A1 *gyr*A46 *thi rel*A1 *lac*⁻ F'[*pro*AB⁺ *lacI*^{q} *lacZ*ΔM15 Tn10(Tet^R)]	Bullock et al. (1987)
PN1671	XL-1/pMM2	This study

PN1672	XL-1/pMM3	This study
PN1673	XL-1/pMM4	This study
PN1674	XL-1/pMM7	This study
PN1806	XL-1/pMM26	This study
PN1807	XL-1/pMM27	This study
PN1821	XL-1/pMM32	This study
PN1812	XL-1/pMM33	This study
PN1824	XL-1/pMM44	This study
PN1825	XL-1/pMM45	This study
PN1900	XL-1/pMM46	This study
PN1889	XL-1/pMM61	This study
PN1890	XL-1/pMM62	This study
PN1891	XL-1/pMM65	This study
Plant symbiota		
MF-Fl1	*Festuca pratensis/E. festucae* Fl1	Young (2005)
G1056	*L. perenne* cv. Nui/*N. lolii* Lp19	Young (2005)
G1057	*L. perenne* cv. Nui	Young (2005)
G1206, G1207, G1209	*L. perenne cv.* Nui/MM4.2	This study
G1210, G1213	*L. perenne* cv. Nui/MM5.2	This study
G1214, G1215	*L. perenne* cv. Nui/MM8.1	This study
G1217, G1218	*L. perenne* cv. Nui/MM9.1	This study
G1220, G1222	*L. perenne* cv. Nui/MM4.3	This study
G1227, G1229	*L. perenne* cv. Nui/MM5.6	This study
G1233	*L. perenne* cv. Nui/MM8.3	This study
G1245, G1248	*L. perenne* cv. Nui/MM9.2	This study
G1250, G1251	*L. perenne* cv. Nui/*E. festucae* Fl1	This study
G1255, G1256	*L. perenne* cv. Nui/MM4.5	This study
G1264, G1268	*L. perenne* cv. Nui/MM5.7	This study
G1274, G1277	*L. perenne* cv. Nui/MM8.4	This study
G1284, G1286	*L. perenne* cv. Nui/MM9.3	This study
G1291. G1297	*L. perenne* cv. Nui/MM4.9	This study
G1300, G1301	*L. perenne* cv. Nui/MM5.9	This study
G1312, G1314	*L. perenne* cv. Nui/MM8.5	This study
G1317, G1318	*L. perenne* cv. Nui/MM9.4	This study
G1326, G1327	*L. perenne* cv. Nui/MM4.10	This study
G1331, 1332	*L. perenne* cv. Nui/MM5.11	This study
G1335, G13367	*L. perenne* cv. Nui/MM8.8	This study
G1339, G1340	*L. perenne* cv. Nui/MM9.5	This study
G1444	*L. perenne* cv. Nui/*E. typhina* PN2311	This study
Plasmids		
pUC118	3.2 kb Amp^R	Vieira and Messing (1987)
pGEM-T Easy	3.0 kb Amp^R	Promega Corp.
pPN1688	pUC118 +P*trpC-hph* fragment from pCB1004	Young et al. (2005)
pAN7-1	6.8 kb Hyg^R Amp^R	Punt et al. (1987)
pLM1	9.2 kb P*gpdA-uidA* Hyg^R Amp^R	L. McMillan, unpublished
pXZ56	8.2 kb P*ltmM-uidA* Hyg^R Amp^R	X. Zhang, unpublished
phGFP2	sGFP-Tyg-Nos; Hyg^R Amp^R	X. Zhang, unpublished
pFunGus	5 kb, *uidA* Amp^R	McGowan (1996)
phFunGus	pFunGus + 1.3 kb *Hin*dIII fragment from phGFP2, Hyg^R Amp^R	This study
pII99	*nptII*, Amp^R	Namiki et al. (2001)
pMM2	pUC19 + 3.3 kb *Eco*RI fragment ex λMM30.4, Amp^R	McGill (2000)
pMM3	pUC19 + 1.8 kb *Eco*RI fragment ex λMM30.4, Amp^R	McGill (2000)
pMM4	pUC19 + 1.4 kb *Eco*RI fragment ex λMM30.4, Amp^R	McGill (2000)

pMM7	pUC19 + 2.0 kb *Bam*HI fragment ex λMM3.3, Amp^R	McGill (2000)
pMM26	8.2 kb P*gpdA-prt2* Hyg^R Amp^R	This study
pMM27	7.2 kb P*ltmM-prt2* Hyg^R Amp^R	This study
pMM32	8.2 kb P*gpdA-prt1* Hyg^R Amp^R	This study
pMM33	7.3 kb P*ltmM-prt1* Hyg^R Amp^R	This study
pMM38	pGEM-T Easy + 0.5 kb Lp19 MM75-MM76 PCR product	This study
pMM44	pUC118 + 4.0 kb *Bam*HI fragment ex 13B2 cosmid	This study
pMM45	pUC118 + 4.6 kb *Bam*HI fragment ex 13B2 cosmid	This study
pMM46	pGEM T Easy + MM93-MM94 degenerate PCR product from *E. festucae*	This study
pMM47	pUC118 + 2.6 kb *Sal*I fragment ex 46F6 cosmid	This study
pMM48	pUC118 + 4.6 kb *Pst*I fragment ex 13B2 cosmid	This study
pMM49	pUC118 + 4.0 kb *Pst*I fragment ex 13B2 cosmid	This study
pMM51	pUC118 + 4.6 kb PstI fragment ex 3F7 cosmid	This study
pMM52	pUC118 + 2.8 kb *Eco*RI-*Sst*I fragment from *E. festucae* MM96-MM97 PCR product	This study
pMM53	pUC118 + 2.8 kb *Xba*I-*Hin*dIII fragment from *E. festucae* MM98-MM99 PCR product	This study
pMM54	10.2 kb *gcn1::hph* Hyg^R Amp^R	This study
pMM61	pUC118 + 3.8 kb *Hin*dIII fragment ex 38H10 cosmid	This study
pMM62	pUC118 + 5.6 kb *Xho*I fragment ex 1A1 cosmid	This study
pMM65	pUC118 +7.7 kb *Sph*I fragment ex1D6 cosmid	This study
pMM66	pGEM-T Easy + MM5-MM8 cDNA product	This study
pMM67	pGEM-T Easy + MM70-MM25 cDNA product	This study
pMM68	pGEM-T Easy + MM141-MM192 cDNA product	This study
pMM69	pGEM-T Easy + MM141-MM192 cDNA product	This study
pMM71	pGEM-T Easy + MM141-MM192 cDNA product	This study
λ clones		
λMM30.2	λGEM-12 clone from *N. lolii* Lp19 genomic library	McGill (2000)
λMM30.4	λGEM-12 clone from *N. lolii* Lp19 genomic library	McGill (2000)
λMM3.3	λGEM-12 clone from *N. lolii* Lp19 genomic library	McGill (2000)
Cosmids		
1A1	pMO-cosX clone Fl1 genomic DNA cosmid library containing the *prt5* and *prt1* genes	This study
3F7	pMO-cosX clone Fl1 genomic DNA cosmid library containing the *prt5* and *prt1* genes	This study
13B2	pMO-cosX clone Fl1 genomic DNA cosmid library containing the *prt2, gcn1, cyc1* and *ptn1* genes	This study
32E4	pMO-cosX clone Fl1 genomic DNA cosmid library containing the *prt4* gene	This study
38H10	pMO-cosX clone Fl1 genomic DNA cosmid library containing the *prt4* gene	This study
46F6	pMO-cosX clone Fl1 genomic DNA cosmid library containing the *prt3* and *gao1* genes	This study
1D6	pMO-cosX clone Fl1 genomic DNA cosmid library containing the *kex2* gene	This study

2.2 GROWTH OF BACTERIAL AND FUNGAL CULTURES

2.2.1 Bacterial cultures

Escherichia coli cultures were grown at 37°C overnight in LB broth or on LB agar. When *E. coli* was grown in broth, cultures were incubated with shaking at 150-200 rpm.

2.2.2 Fungal cultures

Neotyphodium and *Epichloë* spp. endophytes were grown at 22°C on PD agar or in PD broth with shaking at 150 rpm. Cultures used for DNA or RNA extraction were ground in 500 μL of PD broth, and the homogenised mycelia were used to inoculate either 25 or 50 mL of PD broth in a 125 mL flask. Liquid cultures were incubated at 22°C with shaking at 150 rpm for 5-14 days. After harvesting, mycelia were washed twice in double-distilled water, then snap frozen in liquid nitrogen.

2.3 MEDIA

All media were prepared using distilled water and sterilized by autoclaving at 121°C and 15 psi for 15 min before use. Liquid media were cooled to room temperature before inoculation or addition of supplements. Solid media were cooled to 50°C before antibiotics were added and plates poured. Uninoculated plates were stored at 4°C.

2.3.1 Aspergillus complete medium (ACM)

ACM broth contained (per litre): 20 g malt extract (Difco), 10 g mycological peptone and 20 g glucose. To make solid medium, agar was added to ACM broth at 15 g/L.

2.3.2 Luria-Bertani medium (LB)

LB broth contained (per litre): 10 g tryptone, 5 g yeast extract and 5 g NaCl. The pH was adjusted to between 7 and 7.5 prior to autoclaving. For solid medium, agar or agarose was added to LB broth at 15 g/L.

2.3.3 Potato dextrose medium (PD)

Potato dextrose broth (PDB) contained (per litre): 24 g dehydrated potato dextrose broth (Difco). The pH was adjusted to 6.5 prior to autoclaving. For solid medium (PD agar), agar was added to PD broth at 15 g/L.

2.3.4 Pustulan or glucose media

Pustulan medium contained 1% (w/v) pustulan (Calbiochem), 0.1% (w/v) yeast extract and 20 mM NH_4Cl. Solid media was made by adding Noble agar to 15 g/L. Glucose media contained the same reagents except that 1% pustulan was ecxchanged for 1% glucose.

2.3.5 Regeneration medium (RG)

Regeneration (RG) medium contained (per litre): 24 g dehydrated potato dextrose broth and 273.8 g sucrose. The pH was adjusted to 6.5 prior to autoclaving. To make solid media, agar was added at 15 g/L to make agar suitable for plates, or at 8 g/L to make an overlay.

2.3.6 SOC medium

SOC medium contained 20 g tryptone, 5 g yeast extract, 0.6 g NaCl, 0.2 g KCl, 0.95 g $MgCl_2$, 2.5 g $MgSO_4.7H_2O$ and 3.6 g glucose per litre of water.

2.3.7 TOP agarose medium

TOP agarose contained 10 g tryptone, 5 g NaCl and 8 g agarose 15 per litre of water. The media was cooled to 45-50°C after autoclaving, and supplemented with $MgSO_4.7H_2O$ to a concentration of 10 mM before use.

2.3.8 Water agar medium

Water agar contained distilled water (RO water) with agar added to 30 g/L.

2.3.9 Media additions

Table 2.2 Supplements added to media

Supplement	Stock concentration	Final concentration
Ampicillin	100 mg/mL	100 µg/mL
Geneticin		200 µg/mL
Hygromycin	50 mg/mL	150 µg/mL, 50 µg/mL
IPTG	24 mg/mL	
Tetracycline	10 mg/mL	10-15 µg/mL
X-Gal (in dimethylformamide)	20 mg/mL	

2.4 BUFFERS AND SOLUTIONS

2.4.1 Buffers

2.4.1.1 Byrd extraction buffer

Byrd extraction buffer contained 150 mM EDTA, 50 mM Tris HCl (pH 8.0) and 1% (w/v) sodium lauryl sarcosine (SLS).

2.4.1.2 20% PEG solution

20% PEG solution contained 20% PEG 8000 and 2 M NaCl dissolved in SM buffer (Section 2.4.1.3) containing no gelatin.

2.4.1.3 SM buffer

SM buffer contained 0.1 M NaCl, 8 mM $MgSO_4.7H_2O$, 50 mM Tris-HCl (pH 7.5) and 0.01% gelatin.

2.4.1.4 20x SSPE buffer

20x SSPE buffer contained 3 M NaCl, 200 mM $NaH_2PO_4.H_2O$ and 25 mM Na_2EDTA.

2.4.1.5 STE (100/10/1) buffer

STE (100/10/1) buffer contained 100 mM NaCl, 10 mM Tris-HCl (pH 8.0) and 1 mM Na_2EDTA.

2.4.1.6 STET buffer

STET buffer contained 8% sucrose (w/v), 5% (v/v) Triton X-100, 50 mM Na_2EDTA and 50 mM Tris-HCl (pH 8.0).

2.4.1.7 Taha lysis buffer

Taha lysis buffer contained 40 mM of Tris Acetate buffer (Section 2.4.1.10), 20 mM sodium acetate, 1 mM Na_2EDTA and 1% SDS.

2.4.1.8 TE (10/0.1) buffer

TE (10/0.1) buffer contained 10 mM Tris-HCl (pH 8.0) and 0.1 mM Na_2EDTA.

2.4.1.9 TES buffer

TES buffer contained 100 mM Tris (pH 8.0), 10 mM Na_2EDTA and 2% SDS.

2.4.1.10 Tris acetate buffer

Tris acetate buffer contained 0.4 M Tris, with acetic acid added to adjust the pH to 7.8.

2.4.2 Enzymes

2.4.2.1 DNase I

DNase I (Sigma) was prepared at 10 mg/mL in double-distilled water.

2.4.2.2 Lysozyme

Lysozyme was prepared at 50 mg/mL in alkaline lysis solution I. (Section 2.5.6.1).

2.4.2.3 Proteinase K

Proteinase K (Roche) was prepared at 10 mg/mL in TES buffer (Section 2.4.1.9).

2.4.2.4 RNase A (DNase free)

DNase-free RNase was prepared using RNase A (Sigma) at 10 mg/mL in double-distilled water. The solution was heated to 100°C for 15 min, then allowed to cool to room temperature, dispensed into aliquots and stored at -20°C.

2.4.3 Commonly used stock solutions

Table 2.3 Stock solutions

Stock	Concentration	pH
Ammonium acetate	5 M	
Cetyltrimethylammonium bromide (CTAB, Sigma)	10% (w/v)	
Ethanol	70%, 95%, 100% (v/v)	
Ethidium bromide	10 mg/mL	
Heparin	5 mM	
Maltose	20% (w/v)	
$MgSO_4.7H_2O$	1 M	
Na_2EDTA	250 mM	8.0
PEG solution	20% (w/v)	
Sodium acetate	3 M	7.0
Sodium chloride	5 M	
Sodium dodecyl sulphate (SDS)	10% (w/v)	
Spermidine	50 mM	
Tris-HCl	1 M	7.5, 8.0

2.4.4 Stains

2.4.4.1 Aniline Blue stain

Aniline blue stain contained 22% (w/v) lactic acid, 50% glycerol and 0.1% aniline blue.

2.4.4.2 Congo Red stain

Congo Red stain contained 0.1% Congo Red.

2.5 DNA ISOLATION AND PURIFICATION

2.5.1 Phenol-chloroform purification

Equal volumes of Tris-equilibrated phenol (Invitrogen) and chloroform were added to DNA samples and mixed before centrifugation for 5 min in a microcentrifuge at 16,060 × g. Two volumes of chloroform were added to the aqueous phase of the phenol/chloroform extraction. The tube was mixed before centrifugation for 3 min at 16,060 × g. The DNA in the aqueous phase from the chloroform extraction was precipitated with either ethanol or isopropanol (Section 2.5.2).

2.5.2 Precipitation of DNA with ethanol or isopropanol

DNA samples were precipitated by adding $^{1}/_{10}$ volume of 3 M sodium acetate (Section 2.4.3) and either 2.5 volumes of 95% ethanol or 0.6 volumes of isopropanol. Samples were mixed gently and left at -20°C for 30 min to 2 h. The DNA was pelleted by centrifugation at 16,060 × g for 10 min, then washed in 70% (v/v) ethanol. The pellet was left to dry at 37°C for 15 to 30 min before resuspension in an appropriate volume of double-distilled water or 10mM Tris HCl (pH 8.0).

2.5.3 Gel purification

2.5.3.1 Freeze-thaw extraction

DNA was recovered from 0.7% to 2% Seaplaque agarose gels by the phenol-freeze-thaw method (Thuring et al., 1975). The agarose was prepared using 1 × TAE (Section 2.8.1.1) and 1x TAE was also used as the electrophoresis buffer. Gels were viewed under long-wave UV light and fragments of the appropriate size were excised. Each fragment was placed into a 1.5 mL Eppendorf tube, and melted at

65°C in a heating block. An equal volume of Tris-equilibrated phenol (Invitrogen) was added before the tube was vortexed and left at -20°C for at least 2 h. The tube was centrifuged for 10 min in a microcentrifuge at 16,060 × g and the aqueous phase was phenol/chloroform extracted (Section 2.5.1) and ethanol precipitated (Section 2.5.2) to purify the DNA.

2.5.3.2 Extraction from agarose using the QiaQuick™ gel extraction kit (Qiagen)

DNA was recovered from 0.7% to 2% Seaplaque agarose gels. The gels were prepared and run, and the fragment of the desired size was excised from the gel as described in Section 2.5.3.1. Three volumes of QG buffer (where the weight of the fragment in mg is equivalent to one volume in mL) were added to the agarose, and the mixture was incubated at 50°C for 10 min. One volume of isopropanol was added to the sample and mixed. To bind DNA, the sample was applied to a QiaQuick™ spin column and centrifuged at 16,060 × g for 1 min. The column was washed with 0.75 mL of PE buffer and centrifuged at 16,060 × g for 1 min. DNA was eluted using 30-50 μL of elution buffer or double-distilled water.

2.5.4 PCR product purification

PCR products were purified using the MinElute™ PCR purification kit (Qiagen). Five volumes of PB buffer were added to the amplified PCR product. The mixture was added to a MinElute™ column, and DNA was bound during centrifugation at 16,060 × g for 1 min. The DNA bound to the column was washed with 750 μL of PE buffer. DNA was eluted with 10 μL of either EB buffer or double-distilled water.

2.5.5 Plasmid DNA isolation

2.5.5.1 Rapid boil plasmid isolation

E. coli cells were grown overnight at 37°C in LB broth (Section 2.3.2) supplemented with antibiotic (Section 2.3.9). The cells were pelleted by centrifugation and resuspended in STET buffer (Section 2.4.1.6). Lysozyme (Section 2.4.2.2) was added and the solution was boiled for 40 s. The pellet was removed after centrifugation in a microcentrifuge for 10 min. An equal volume of isopropanol was added to the supernatant, mixed and left at -20°C for 10 to 20 min. The plasmid DNA was

pelleted by centrifugation for 10 min, and washed once with 70% ethanol. The pellet was left to dry at 37°C for approximately 20 min, and resuspended in 50 μL of double-distilled water. This method is based on that of Holmes and Quigley (1981).

2.5.5.2 High Pure™ plasmid isolation kit (Roche)

E. coli cells containing the plasmid of interest were grown overnight at 37°C in 5 mL of LB broth (Section 2.3.2) supplemented with antibiotic (Section 2.3.9). Half a mL of cells in culture was pelleted by centrifugation for 30 s. The pelleted cells were resuspended in 250 μL of cell resuspension buffer (containing RNase). Cells were lysed by the addition of 250 μL of lysis buffer, mixed by inversion, then incubated at room temperature for 5 min. The mixture was neutralised by the addition of 350 μL of binding buffer, mixed by inversion, and incubated on ice for 5 min. Tubes were centrifuged at 16,060 × g to pellet cellular debris. The supernatant was placed in a spin filter, and centrifuged at 16,060 × *g* for 1 min. The filter was washed with 700 μL of wash solution II and centrifugation at 16,060 × *g* for 1 min. DNA was eluted from the filter with 100 μL of elution buffer and centrifugation at 16,060 × *g* for 1 min. DNA concentration was measured as described in Section 2.6.

2.5.5.3 Quantum™ plasmid miniprep kit (Bio-Rad)

E. coli cells containing the plasmid of interest were grown overnight at 37°C in 5 mL of LB broth (Section 2.3.2) supplemented with antibiotic (Section 2.3.9). Two to five mL of culture was pelleted by centrifugation for 30 s, and the supernatant was discarded. The pelleted cells were resuspended in cell resuspension buffer. Cell lysis solution was added to the tube, followed by neutralisation solution. The tube was spun for 5 min, and the supernatant mixed with Quantum preparation matrix. The supernatant was washed through a spin filter, and the matrix washed twice in wash solution. DNA was eluted from the matrix using double-distilled water and the DNA concentration was measured as described in Section 2.6.

2.5.5.4 Quantum™ plasmid midiprep kit (Bio-Rad)

E. coli cells containing the plasmid of interest were grown overnight at 37°C in 50 mL of LB broth (Section 2.3.2) supplemented with antibiotic (Section 2.3.9). Forty mL of culture was pelleted by centrifugation at 3000 × *g* for 5 min. The pelleted cells were resuspended in 5 mL of cell resuspension buffer. Cells were lysed by adding 5 mL of cell lysis solution, followed by 5 mL of neutralisation solution. The tube was

centrifuged at 7500 × *g* for 10 min, and the supernatant mixed with 1 mL of Quantum preparation matrix. The tube was then centrifuged at 7500 × *g* for 2 min. The pelleted matrix was mixed with 10 mL of wash buffer, and centrifuged at 7500 × *g* for 2 min. At this stage, the pelleted matrix was resuspended in 0.6 mL of wash buffer and transferred to a spin filter, and centrifuged at 16,060 × *g* for 30 s. The matrix was then washed with 0.5 mL of wash buffer, and centrifuged at 16,060 × *g* for 2 min. DNA was eluted from the matrix using double-distilled water and the DNA concentration was measured as described in Section 2.6.

2.5.6 Alkaline lysis purification of plasmids and cosmids

2.5.6.1 Alkaline lysis solutions

2.5.6.1.1 Alkaline lysis solution I

Alkaline lysis solution I contained 50 mM glucose, 25 mM Tris-HCl (pH 8.0) and 10 mM Na_2EDTA.

2.5.6.1.2 Alkaline lysis solution II

Alkaline lysis solution II contained 0.2 N NaOH and 1% SDS.

2.5.6.1.3 Alkaline lysis solution III

Alkaline lysis solution III contained 3 M potassium acetate and 2 M acetic acid.

2.5.6.2 Alkaline lysis preparation of plasmid and cosmid DNA for sequencing

E. coli cells containing the plasmid or cosmid of interest were grown overnight at 37°C in 5 mL of LB broth (Section 2.3.2) supplemented with an appropriate antibiotic (Section 2.3.9). Cells were pelleted by centrifugation at 16,060 × *g* for 1 min, and resuspended in 200 µL of Solution I (Section 2.5.6.1.1). Cells were treated with 10 µL of lysozyme (Section 2.4.2.2) at room temperature for 5 min. In order to lyse the cells, 300 µL of alkaline lysis Solution II (Section 2.5.6.1.2) was added, and tubes were incubated on ice for 5 min. To neutralise the solution, 300 µL of Solution III (Section 2.5.6.1.3) was added, and the tubes were incubated on ice for a further 5 min. Samples were centrifuged at 16,060 × *g* for 10 min to pellet cellular debris. The supernatant was treated with 1.6 µL of RNase (10 mg/mL; Section 2.4.2.4) at 37°C

for 20 min. The supernatant was chloroform extracted twice, then DNA was precipitated by adding an equal volume of isopropanol. The tubes were centrifuged at 16,060 × *g* for 10 min to pellet the DNA, which was then washed with 70% ethanol. The DNA pellet was resuspended in water, and the DNA concentration was measured as described in Section 2.6.

2.5.6.3 Large scale cosmid DNA isolation by alkaline lysis

E. coli cells containing the cosmid of interest were grown overnight at 37°C in 50 mL of LB broth (Section 2.3.2) supplemented with an appropriate antibiotic (Section 2.3.9). Bacterial cells were harvested by centrifugation at 20201 *g* for 5 min, and resuspended in 1.5 mL of alkaline lysis solution I (Section 2.5.6.1.1). One hundred and fifty µL of lysozyme were added, and the tubes were incubated at room temperature for 5 min. Three mL of Alkaline lysis solution II (Section 2.5.6.1.2) were added, then samples were mixed and incubated on ice for 5 min. To neutralise the mixture, 2.5 mL of alkaline lysis solution III was added, samples were mixed, then incubated on ice for 5 min. Samples were centrifuged at 20201 *g* for 10 min to remove cellular debris and genomic DNA. Cosmid DNA was precipitated with 8 mL of 95% ethanol and 600 µL of 3 M NaOAc, and incubated at -20°C for 10-20 min. To pellet the DNA, samples were centrifuged at 16060 *g* for 30 min. The pellet was washed with 70% ethanol during centrifugation at 20201 *g* for 2 min. The dried pellet was resuspended in 500 µL of double-distilled water or 10 mM Tris pH 8.0.

2.5.7 λ DNA isolation

2.5.7.1 Plating λ phage

E. coli strain KW251 was used as a host for phage λ. Fifty µL of the λ population to be screened, diluted to approximately 10^6 plaque forming units (PFU) per plate, was diluted in 50 µL of SM buffer (Section 2.4.1.3). The diluted phage was combined with 100 µL of *E. coli* KW251 cells grown overnight in LB broth (Section 2.3.2) supplemented with 10 mM $MgSO_4$ and 0.2% (w/v) maltose. The phage-*E. coli* mixture was incubated at 37°C for 30 min. The mixture was combined with 3 mL of supplemented TOP agarose (Section 2.3.7) and overlaid on a LB agarose plate (Section 2.3.2). The plates were incubated at 37°C until confluent lysis of the *E. coli* cells was obtained.

2.5.7.2 Isolation of λ phage DNA

Phage was plated as described in Section 2.5.7.1. Once confluent lysis had been obtained, 5mL of SM buffer (Section 2.4.1.3) was added to each plate. The plates were left at 4°C overnight. The lysate was collected and centrifuged at 3,020 *g* for 10 min at 4°C. DNase (Section 2.4.2.1) and RNase (Section 2.4.2.4) were added to the supematant at a concentration of 1 μg/mL each. Reactions were incubated at 37°C for 30 min. Five mL of 20% PEG solution (Section 2.4.1.2) was added and the tubes were left to stand on ice for 1 hour. The phage was pelleted by centrifugation at 7,710 *g* for 15 min at 4°C and resuspended in 0.4 mL of SM buffer, 5 μL of 10% SDS and 10 μL of 250 mM Na_2EDTA (pH 8.0). The tubes were incubated at 68°C for 15 min, then briefly vortexed. An equal volume of phenol was added, vortexed for 10 s, and left to stand at room temperature for 5 min. Samples were vortexed for another 10 s and the aqueous phase was phenol-chloroform extracted (Section 2.5.1) and ethanol precipitated (Section 2.5.2). The DNA was resuspended in 50 μL of double-distilled water and 10 μg of RNase (Section 2.4.2.4) was added. The DNA concentration was measured as described in Section 2.6.

2.5.8 Fungal and plant genomic DNA isolation

2.5.8.1 Isolation of genomic DNA from fungal protoplasts

Fungal protoplasts were prepared as described in Section 2.15.2. Protoplasts were resuspended in 5 mL of Byrd extraction buffer (Section 2.4.1.1), and treated with 50 μL of RNase (Section 2.4.2.4) before being incubated at 37°C for 2-5 min. An equal volume (5 mL) of Tris-equilibrated phenol (Invitrogen) was added, and the sample was mixed well. The sample was centrifuged at 11953 *g* for 15 min. The aqueous phase was transferred to a new tube and 3 mL each of Tris-equilibrated phenol and chloroform were added. The sample was mixed well, then centrifuged at 11953 *g* for 15 min. The aqueous phase was then extracted with 5 mL of chloroform by centrifugation at 11953 *g* for 15 min. The aqueous phase from this stage was transferred to a new tube, the precipitated with 0.1 volumes of 3 M sodium acetate (pH 7.0) and an equal volume of isopropanol. The mixture was incubated at -20°C for at least 2 h. Samples were centrifuged at 11953 *g* for 30 min to pellet the DNA. The DNA pellet was washed in 70% ethanol and air dried before being resuspended in 10mM Tris HCl (pH 8.0). The DNA concentration was measured as described in Section 2.6.

2.5.8.2 Isolation of fungal or plant genomic DNA using modified Taha method

This method is based on that of Al-Samarrai and Schmid (2000). Freeze dried mycelia (30 mg) or grass tissue (15 mg) was ground to a powder in liquid nitrogen. The powder was resuspended in 500 µL of Taha lysis buffer (Section 2.4.1.7), and mixed by vigourous pipetting that caused the solution to froth. NaCl was added to a final concentration of 1.24 M, and samples were centrifuged at 16,060 × *g* for 10 min to pellet cellular debris and polysaccharides. The supernatant was transferred to a fresh tube and mixed with an equal volume of chloroform by pipetting. Samples were centrifuged at 16,060 × *g* for 5 min, and the aqueous phase was transferred to a new tube. The chloroform extraction step was repeated twice in total. Ammonium acetate was added to the aqueous phase at a final concentration of 1.2 M. Samples were spun at 16,060 × *g* for 10 min, and the supernatant transferred to a fresh tube. DNA was precipitated with an equal volume of isopropanol, and centrifuged at 16,060 × *g* for 15 min. DNA pellets were washed with 1 mL of 70% ethanol during centrifugation at 16,060 × *g* for 3 min. The dried pellet was resuspended in 50 µL of double-distilled water for fungal samples, or 25 µL double-distilled water for plant samples. The DNA concentration was measured as described in Section 2.6.

2.5.8.3 Isolation of genomic DNA using the plant-fungal method

This method is based on that of Moller et al. (1992). Freeze-dried fungal tissue (50 mg) was ground to a powder in liquid nitrogen, then resuspended in 10 mL of TES buffer (Section 2.4.1.9). Two mg of proteinase K (Section 2.4.2.3) was added, and samples were incubated at 60°C for 30 min to 1 h. NaCl and CTAB (Section 2.4.3) were added to final concentrations of 1.4 M and 1% respectively. Samples were incubated at 65°C for 10 min to allow polysaccharides to precipitate in the presence of CTAB and the high salt concentration. The sample was then mixed with an equal volume of chloroform and incubated on ice for 30 min. Samples were centrifuged at 11953 *g* for 10 min, and the aqueous phase transferred to a new tube. NH_4Ac was added to the aqueous phase to a final concentration of 1.2 M. Samples were incubated on ice for 30 min, then centrifuged at 11953 *g* for 10 min. The supernatant was transferred to a new tube, and DNA precipitated with 0.6 volumes of isopropanol. Samples were mixed and left of ice for 15 to 30 min. DNA was pelleted by centrifugation at 11953 *g* for 10 min. The pellet was washed twice in 70%

ethanol, then air dried. The DNA pellet was resuspended in double-distilled water or 10 mM Tris pH 8.0. The DNA concentration was measured as described in Section 2.6.

2.5.8.4 Isolation of fungal genomic DNA using modified Byrd method

Fungal cultures were grown as described in PD broth that was not pH adjusted. Mycelia was harvested by filtration through nappy liner, washed in sterile double-distilled water and blotted dry. Approximately 0.3 g of mycelia was ground to a powder in liquid nitrogen, then resuspended in 800 µL of Byrd extraction buffer (Section 2.4.1.1). Proteinase K (Roche) was added to a concentration of 2 mg/mL, and the sample was incubated at 37°C for 20 min. The samples were centrifuged at 16,060 × *g* for 10 min to pellet cellular debris. The supernatant was phenol-chloroform extracted three times with half volumes each of both phenol and chloroform, then chloroform extracted once (Section 2.5.1). DNA was precipitated with an equal volume of isopropanol (Section 2.5.2). DNA was pelleted by centrifugation at 16,060 × *g* for 10 min. The DNA pellet was washed in 70% ethanol, then airdried at 37°C. The DNA was resuspended in approximately 100 µL of sterile double-distilled water.

2.6 DNA QUANTIFICATION

2.6.1 Fluorometric quantitation with Hoescht dye

2.6.1.1 Solutions for fluorometric quantitation

2.6.1.1.1 Hoescht dye solution

Hoescht dye solution contained 1 mg/ml of Hoechst 33258 dye (Sigma).

2.6.1.1.2 10 × TNE buffer

TNE buffer (10×) contained 0.1 M Tris base, 10 mM Na_2EDTA and 1 M NaCl.

2.6.1.1.3 Calf thymus DNA stock

For low concentration assays, calf thymus DNA was resuspended at 100 ng/µL in 1 × TNE buffer (Section 2.6.1.1.2). For high concentration assays, calf thymus DNA was resuspended at 1000 ng/µL in 1 × TNE buffer.

2.6.1.1.4 Assay solution A (for low range assays)

Assay solution A used for low range assays (*i.e.* concentrations of 10-500 ng/μL) contained 1 × TNE buffer (Section 2.6.1.1.2) and 0.01% Hoescht dye solution (Section 2.6.1.1.1).

2.6.1.1.5 Assay solution B (for high range assays)

Assay solution B used for high range assays (*i.e.* concentrations of 100-5000 ng/μL) contained 1 × TNE buffer (Section 2.6.1.1.2) and 0.1% Hoescht dye solution (Section 2.6.1.1.1).

2.6.1.2 Quantitation using the fluorometer

2.6.1.2.1 Low concentration assays of DNA concentration

To measure lower DNA concentrations, the fluorometer was blanked against solution A (Section 2.6.1.1.4). To calibrate the instrument, calf thymus DNA (100 ng/μL) (Section 2.6.1.1.3) was diluted 1000 fold in assay solution A, and the fluorometer was calibrated to 100 ng/mL. To measure DNA concentrations in other samples, the sample was diluted 1000 fold in assay solution A, and measured on the fluorometer, which showed the concentration of the sample in ng/mL. Allowing for the 1000 fold dilution of the sample for quantitation, the concentration of DNA in the sample was then determined in ng/μL.

2.6.1.2.2 High concentration assays of DNA concentration

To measure higher DNA concentrations, the fluorometer was blanked against solution B (Section 2.6.1.1.5). To calibrate the instrument, calf thymus DNA (1000 ng/μL) (Section 2.6.1.1.3) was diluted 1000 fold in assay solution B, and the fluorometer was calibrated to 1000 ng/mL. To measure DNA concentrations in other samples, the sample was diluted 1000 fold in assay solution B, and measured on the fluorometer, which showed the concentration of the sample in ng/mL. Allowing for the 1000 fold dilution of the sample for quantitation, the concentration of DNA in the sample was then determined in ng/μL.

2.6.2 Quantitation by ethidium bromide staining

A sample of the DNA solution was separated by agarose gel electrophoresis (Section 2.8.2) with a series of standard DNA solutions. This method was used for plasmid DNA and λ DNA. Smaller DNA fragments were quantitated against a low DNA mass ladder (Invitrogen) that consisted of a ladder of fragments, each of a different known concentration. Once the SDS loading dye front had migrated at least two-thirds of the way down the gel, the gel was stained with ethidium bromide and then photographed (Section 2.8.3). The intensity of ethidium bromide staining from the unknown DNA sample was compared to that of the known standards.

2.7 RESTRICTION ENDONUCLEASE DIGESTION OF DNA

Restriction digests were carried out using the manufacturer's recommended buffer supplied the restriction endonuclease. An excess of enzyme was used to cut the DNA. Digestions of plasmid and λ DNA were performed at 37°C for 2 h and stored at 4 °C until an aliquot was checked by agarose electrophoresis (Section 2.8). Digestions of cosmid and genomic DNA were performed in the presence of 0.1 mg/mL BSA, and incubated at 37 °C for 3-12 h.

2.8 AGAROSE GEL ELECTROPHORESIS

2.8.1 Agarose gel electrophoresis solutions

2.8.1.1 1 × TAE electrophoresis buffer

1 × TAE buffer contained 40 mM Tris-acetate (pH8.5) and 2 mM Na_2EDTA.

2.8.1.2 1 × TBE electrophoresis buffer

1 × TBE buffer contained 89 mM Tris (pH8.2), 89 mM boric acid and 2.5 mM Na_2EDTA.

2.8.1.3 SDS loading dye

SDS loading dye contained 1% (w/v) SDS, 0.02% (w/v) bromophenol blue, 20% (w/v) sucrose and 5 mM Na_2EDTA (pH8.0).

2.8.1.4 Ethidium bromide staining solution

Ethidium bromide staining solution contained 1 μg/mL ethidium bromide dissolved in double-distilled water.

2.8.2 Agarose gel electrophoresis

Agarose electrophoresis was performed either in a minigel apparatus for 1-2 h, or in a Bio-Rad Sub-Cell apparatus for several h to overnight. Agarose gels were made of agarose (Roche) or Seaplaque agarose (FMC) at either 0.7%, 1%, 1.2%, 1.5% or 2% (v/v) in either 1 × TAE (Section 2.8.1.1) or 1 × TBE buffer (Section 2.8.1.2). Agarose was melted in either a pressure cooker or microwave and allowed to equilibrate to 50°C before the gel was poured. SDS loading dye (Section 2.8.1.3) was added to samples before loading. Electrophoresis was performed at 80-120 V for minigels and Bio-Rad subcell short runs, or at 30-40V overnight in the Bio-Rad subcell.

2.8.3 Staining and photographing gels

Once the loading dye had moved at least half way down the gel, it was stained with ethidium bromide (Section 2.8.1.4) before destaining in double-distilled water. Bands on the gel were visualised using an UV transilluminator and photographed using either an gel documentation system from Alpha Innotech or Bio-Rad.

2.8.4 Sizing DNA bands

DNA fragment sizes were determined after electrophoresis by using Alpha Innotech gel documentation system software or through a semi-logarithmic graph of mobility (distance travelled in cm) vs. fragment size (in kb). The program compares the distance travelled by molecular markers of known size, such as the λ/*Hin*dIII ladder, with fragments of unknown size.

2.9 SOUTHERN BLOTTING

2.9.1 Southern blotting solutions

2.9.1.1 Solution 1
Solution 1 contained 0.25 M HCl.

2.9.1.2 Solution 2
Solution 2 contained 0.5 M NaOH and 0.5 M NaCl.

2.9.1.3 Solution 3
Solution 3 contained 2.0 M NaCl and 0.5 M Tris-HCl (pH 7.4).

2.9.1.4 20 × SSC
20 × SSC contained 5 M NaCl and 0.3 M sodium citrate.

2.9.1.5 2 × SSC
2 × SSC contained 0.5 M NaCl and 0.03 M sodium citrate.

2.9.1.6 10 × Denhardt's Solution
10 × Denhardt's solution contained (per litre): 50 mL of 1 M Hepes (Sigma) (pH 7.0), 150 mL 20 × SSC, 18 mg phenol-extracted herring sperm DNA (Sigma), 1.0 g SDS, 20 mg *Escherichia coli* tRNA, 2 g Ficoll (Sigma), 2 g bovine serum albumin (Sigma) and 2 g polyvinylpyrrolidone (Sigma PVP-10).

2.9.1.7 Library hybridisation solution
Library hybridisation solution contained 360 mM Na_2HPO_4, 50 mM NaH_2PO_4, 7% SDS (w/v), 1% BSA (w/v) and 1 mM EDTA pH 8.0.

2.9.1.8 Alkaline stripping solution
Alkaline stripping solution contained 0.1 M NaOH, 10 mM Na_2EDTA pH 8.0 and 0.1% SDS (w/v).

2.9.2 Southern (capillary) blotting

Overnight gel electrophoresis was used to separate the DNA to be transferred to the membrane, and the gel was stained, visualised and photographed as described in Section 2.8.3. The gel was placed in a tray containing Solution 1 (Section 2.9.1.1)

and gently agitated for 15 min. The solution was poured off and replaced with Solution 2 (Section 2.9.1.2) and gently agitated for 30 min. This solution was replaced with Solution 3 (Section 2.9.1.3) and agitated for 30 to 60 min. The gel was then washed for 2 min in 2x SSC (Section 2.9.1.5).

Before the blotting apparatus was set up, a plastic trough with wells at both ends was prepared so two sheets of Whatman 3MM chromatography paper soaked in 20 × SSC (Section 2.9.1.4) protruded into the wells, which were then filled with 20 × SSC. Plastic wrap was placed over the trough and pressed flat. A grid 2 mm smaller than the gel size was removed from the plastic wrap and the treated gel was placed so it overlapped the edges of the grid. A piece of positively charged nylon membrane (Roche) was cut to 2 mm greater than the gel size, pre-soaked in 2 × SSC (Section 2.9.1.5) and laid on the gel. Four sheets of Whatman 3MM chromatography paper were cut to 2 mm less than the gel size. Two of these sheets were pre-soaked in 2 × SSC and then laid on the membrane, followed by the other two dry sheets. A pile of paper towels was placed at the top of the blotting apparatus and weighed down. The apparatus was left to blot overnight. On the next day, the blot apparatus was disassembled and the DNA was crosslinked to the membrane using 120,000 $\mu J/cm^2$ of energy in an ultraviolet crosslinker (Ultra-Lum, Claremont, CA, USA).

2.9.3 Radiolabelling of DNA probes

DNA to be labelled (30 ng) was diluted to an 11 μL volume, denatured by boiling for 3 min, then placed immediately on ice to cool. Four μL of High Prime solution (Roche) and 5 μL of [α^{32}P]-dCTP (3000 Ci/mmol, Amersham) was added. Reactions were incubated at 37°C for 30 min-1 hour before the reaction was stopped by adding 30 μL of STE buffer (Section 2.4.1.5) or 10 × TNE buffer (Section 2.6.1.1.2). Unincorporated nucleotides were removed from the mixture using a Sephadex G-50 column (ProbeQuant). The vortexed column was prespun at 735 *g* for 1 min to remove the void volume from the column. The probe sample was applied to the column, and the column was spun for 2 min at 735 *g*. Before use, the purified probe was boiled for 3 min to denature the probe, then left on ice to cool.

2.9.4 Hybridisation of radiolabelled DNA probes

A Southern blot (Section 2.9.2) membrane was prehybridised for at least 2 h in 10 × Denhardt's solution (Section 2.9.1.6) at 65°C. The denatured [α^{32}P]-dCTP labelled probe (Section 2.10.3) was added and left to hybridise at 65°C overnight. Following removal from the tube, the blot was washed with 2 × SSC, 0.1 % SDS at 65°C for at least 15 min. Two subsequent washes of 15 min were performed with either the 2 × SSC, 0.1 % SDS wash solution or more stringent wash solutions (1 × SSC, 0.1 % SDS or 0.5 × SSC, 0.1 % SDS).

2.9.5 Autoradiography

The hybridised blot was wrapped in plastic and exposed to a sheet of Fuji Medical X-ray film in the presence of a Cronex intensifying screen in an X-ray cassette at -80°C for an appropriate period of time, which varied according to the incorporated radioactivity in the probe and the type of DNA on the blot. The film was developed using a 100 Plus Automatic X-ray film processor (All-Pro Imaging Group) using 100 Plus developer and fixative solutions.

If the blot was to be visualised using a phosphoimager, the hybridised blot was incubated overnight at room temperature with the imaging plate (IP). The imaging plate was read using the Fujifilm FLA-5000 scanner with Image Reader FLA-5000 v2.1 software. The Profile/MW mode of Science Lab 2001 Image Gauge v4.0 software was used to assess signal intensity.

2.9.6 Stripping of Southern blots

Southern blots were stripped either by the use of boiling sodium dodecyl sulphate (SDS) or alkaline hydrolysis. For gels stripped by boiling SDS, a solution of boiling 0.1% (w/v) SDS was poured over the hybridised membrane and gently agitated until the solution had cooled to room temperature. This process was repeated several times to ensure all probe DNA was removed from the filter. Alkaline stripping of blots was performed using washing the filter twice in alkaline stripping solution (Section 2.9.1.8) for 10 min with shaking. The filter was then washed twice in 5x SSPE

(prepared by 4 fold dilution of 20x SSPE described in Section 2.4.1.4) for 10 min with shaking.

For both methods, the stripped membranes were checked by autoradiography (Section 2.9.5) to ensure no signal from the probe remained. If stripping was incomplete, the stripping process was repeated.

2.10 LIBRARY SCREENING

An *E. festucae* Fl1 genomic DNA cosmid library was prepared as described previously (Tanaka et al., 2005). DNA from a selection of clones from this cosmid library were arrayed onto a membrane filter at a six-by-six density with double off-set by the Australian Genome Research Facility (AGRF), Melbourne, Australia. The library was prehybridised in library hybridisation solution (Section 2.9.1.7) at 65°C for a minimum of 2 h. Denatured radiolabelled probe prepared as described in Section 2.9.3 was hybridised to the library filter at 65°C overnight. The filter was rinsed with 2 × SSC, 0.1% SDS wash buffer, then incubated with the same wash buffer for 30 min at 65 °C. Successive washes were performed with increased stringency using 1 × SSC, 0.1% SDS buffer then 0.1 × SSC, 0.1% SDS buffer each at 65°C for 30 min. Autoradiography was performed as described in Section 2.9.5. Filters were stripped by alkaline lysis as described in Section 2.9.6. After library screening was complete, bacterial clones containing the cosmid of interest were isolated by streaking for single colonies from the bacterial stocks stored in 96 well plates at -70°C. Cosmid DNA was isolated from bacterial strains as described in Section 2.5.6.2.

2.11 DNA SEQUENCING

DNA sequencing was performed using BigDye™ fluorescent dye-labelled terminators based on the dideoxy chain termination method (Sanger et al., 1977) by the Allan Wilson Centre Genome Service at Massey University, Palmerston North. Primers used for sequencing were synthesised by Invitrogen or Sigma Genosys. DNA intended for sequencing was purified either by the use of a commericial plasmid kit (as described in Section 2.5.5), through λ DNA isolation as described in

Section 2.5.7.2, or through alkaline lysis/PEG precipitation (as described in Section 2.5.6.2). Products were labelled using the BigDye™ terminator Version 3.1 Ready Reaction cycle sequencing kit (Applied Biosystems). For sequencing of plasmids, 300 ng of DNA was mixed with 3.2 pmol of primer in a volume of 20 μL reaction. For λ and cosmid sequencing, 500 ng of DNA was mixed with 5 pmol of primer in a 20 μL reaction. For PCR products, 2ng/100 bp of PCR product was mixed with 3.2 pmol of primer in a volume of 20 μL. For detection, fluorescently labelled sequencing reactions were run on the capillary ABI3730 Genetic Analyzer (Applied Biosystems). DNA sequence was analysed as described in Section 2.21.

2.12 DNA LIGATION

2.12.1 CAP treatment of vector DNA

Approximately 5 μg of vector DNA was digested with an excess of restriction enzyme. Where possible, the restriction enzyme was inactivated by heat. A small DNA sample was removed as a pre-treatment control. Half a unit of calf intestine alkaline phosphatase (CAP, Roche) and 1/10 volume of 10 × phosphorylation buffer were added and the reaction was incubated at 37°C for 30 min. At this stage, the samples were purified using one of two different means.

The first purification method used proteinase K to remove residual CAP activity, followed by phenol-chloroform extraction and ethanol precipitation. Na_2EDTA and SDS were added to concentrations of 5 mM and 0.5% (w/v) respectively. Proteinase K (Section 2.4.2.3) was added to a final concentration of 50 μg/mL and the reaction mixture was incubated at 56°C for 30 min. The reaction mix was phenol-chloroform extracted (Section 2.5.1) and ethanol precipitated (Section 2.5.2). The second purification method used QiaQuick gel extraction kit (Qiagen, Section 2.5.3.2) to purify the reactions. After purification, control ligations were performed using before and after ligation samples of vector from pre-CAP treatment and after CAP treatments to determine the degree of vector self-ligation.

2.12.2 DNA ligation

Ligations were performed in two different ways. The first way involved ligation mixtures that contained 1 × T4 DNA ligation buffer (diluted from 10x stock, NE Biolabs), 10-20 ng of plasmid DNA, insert DNA (if appropriate) and 160 U of T4 DNA ligase (NE Biolabs). The second method involved using I × T4 DNA ligase buffer (diluted from 2 × or 10 × stocks, Promega), 10 ng of plasmid DNA, insert DNA (where appropriate) and 3 Weiss units of T4 DNA ligase (Promega).

Ligation of PCR products into the pGEM-T Easy™ vector (Promega) was performed using the pGEM-T Easy kit (Promega). The 10 μL reaction mix contained 10 to 50 ng PCR products, 25 ng of the pGEM-T Easy vector, 1 × ligation buffer supplied with the kit and 3 Weiss units of T4 DNA ligase (Promega). Reactions were incubated at 4 °C overnight.

For three or four-way ligations, 1:1:1or 1:1:1:1 molar ratios of vector to insert fragments were used to promote ligation. Three and four way ligations were performed in reaction mixtures containing 1 × T4 DNA ligation buffer (diluted from 10x stock, NE Biolabs), 10-20 ng of plasmid DNA, equimolar amounts of each insert DNA fragment and 160 U of T4 DNA ligase (400 U/μL, NE Biolabs).

2.12.3 Shot gun cloning of λ and cosmid DNA fragments

In order to perform "shotgun" cloning of DNA fragments, λ or cosmid DNA was digested with the appropriate restriction endonuclease. The products of this digestion were purified by phenol-chloroform extraction (Section 2.5.1) and ethanol precipitation (Section 2.5.2). The resulting DNA was ligated into a vector cut with the same restriction enzyme (or an enzyme that produces compatible ends), using standard ligation protocols as described in Section 2.12.2. The resulting colonies were screened by blue-white selection, restriction endonuclease digestion of resulting vectors or colony PCR screening (Section 2.14.3.3).

2.13 VECTOR CONSTRUCTION

2.13.1 Construction of vectors to give heterologous prt1 or prt2 expression

2.13.1.1 Construction of the phFunGus vector

The phFunGus vector (Figure 2.1) was constructed by cloning an *Nco*I-free *hph* fragment (from the vector phGFP2) into the *Hin*dIII site of the pFunGus vector (Appendix A1.1.1; McGowan, 1996). The phFunGus vector was used as a backbone for vectors created to transform *E. festucae* Fl1 with heterologous copies of *prt1* or *prt2*.

2.13.1.2 Construction of vectors to give heterologous *prt1* expression

The pMM32 and pMM33 vectors direct expression of *E. festucae* Fl1 *prt1* under the control of the *A. nidulans gpdA* or *E. festucae* Fl1 *ltmM* genes respectively. Two independent PCR amplifications were used to amplify the *E. festucae* Fl1 *prt1* coding region (Figure 2.2). The 5' region of the *prt1* gene (amplified with the MM63Nco-MM74 primers) was digested with *Nco*I and *Sal*I, while the 3' region of the *prt1* gene (amplified with the MM1-MM67Pst primers) was digested with *Sal*I and *Pst*I. The *Nco*I/*Sal*I and *Sal*I/*Pst*I digested fragments were purified by PCR product purification as described in Section 2.5.4 before being used in ligations.

The pMM32 vector contained the *E. festucae* Fl1 *prt1* coding region fused to the promoter and 5' untranslated region (UTR) of the *A. nidulans gpdA* gene at the translation start codon. The vector backbone was a 4.2 kb *Eco*RI/*Pst*I fragment from phFunGus (Figure 2.1) containing the *hph* gene, which confers hygromycin resistance. The *gpdA* promoter and 5' UTR were derived from the pLM1 vector (Appendix 1) as a 2.3 kb *Eco*RI/*Nco*I fragment. The phFunGus *Eco*RI/*Pst*I and pLM1 *Eco*RI/*Nco*I fragments were gel purified before use (Section 2.5.3.2). The pMM32 vector was constructed by means of a four way ligation, ligating the phFunGus *Eco*RI/*Pst*I, pLM1 *Eco*RI/*Nco*I, and *prt1* *Nco*I/*Sal*I and *Sal*I/*Pst*I fragments together in a single reaction. PCR screening was performed to ensure that pMM32 contained the fragments in the expected order. The *prt1* fragments in pMM32 were sequenced to check for PCR misincorporation errors in the *prt1* coding sequence.

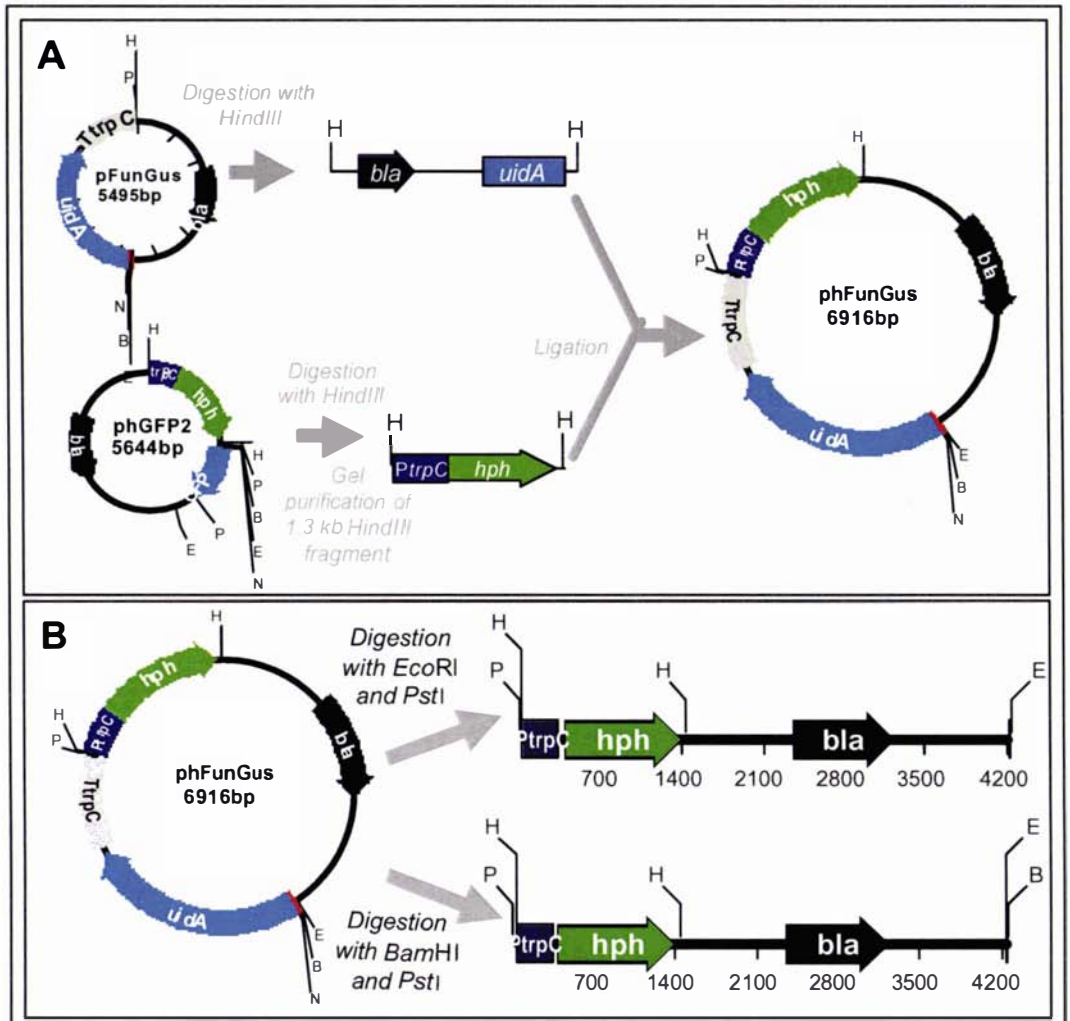

Figure 2.1 Construction of the phFunGus vector

A schematic showing how the phFunGus vector was constructed. **(A)** The phFunGus vector was created by ligation of a 1.3 kb *Hin*dIII fragment from the phGFP2 vector into the *Hin*dIII site of the pFunGus vector. Restriction sites are designated as follows: *Bam*HI (B), *Eco*RI (E), *Hin*dIII (H), *Nco*I (N) and *Pst*I (P). **(B)** The phFunGus vector was digested with *Eco*RI/*Pst*I or *Bam*HI/*Pst*I to create the backbone of the *prt1* or *prt2* heterologous expression vectors. The 4.2 kb *Eco*RI/*Pst*I or *Bam*HI/*Pst*I fragments were gel purified before use in DNA ligations.

The pMM33 vector contained the *E. festucae* Fl1 *prt1* coding region fused to the promoter and 5' untranslated region (UTR) of the *E. festucae* Fl1 *ltmM* gene at the translation start codon. The vector backbone was a 4.2 kb *Bam*HI/*Pst*I fragment from phFunGus (Figure 2.1) containing the *hph* gene, which confers hygromycin resistance. The *ltmM* promoter and 5' UTR were derived from pXZ56 (Appendix A1.1.7) as a 1.3 kb *Bam*HI/*Nco*I fragment. The phFunGus *Bam*HI/*Pst*I and pXZ56 *Bam*HI/*Nco*I fragments were gel purified before use (Section 2.5.3.2). The pMM33 vector was constructed by means of a four way ligation, ligating the phFunGus

*Bam*HI/*Pst*I, pXZ56 *Bam*HI/*Nco*I, and *prt1* *Nco*I/*Sal*I and *Sal*I/*Pst*I fragments together in a single reaction. PCR screening was used to ensure that pMM33 contained the fragments in the expected order. The *prt1* fragments in pMM33 were sequenced to check for PCR misincorporation errors in the *prt1* coding sequence.

2.13.2 Construction of vectors to give heterologous *prt2* expression

The pMM26 and pMM27 vectors direct expression of *E. festucae* Fl1 *prt2* under the control of the *A. nidulans gpdA* or *E. festucae* Fl1 *ltmM* promoters respectively. The *E. festucae* Fl1 *prt2* coding region was amplified from *E. festucae* Fl1 genomic DNA using the MM65Rca and MM67Pst primers (Figure 2.3A and B). The resulting PCR product was digested with *Rca*I and *Pst*I. Restriction digestion by the *Rca*I enzyme (recognition site T↓CATGA) produces overhanging ends that are cohesive to those produced by *Nco*I (recognition site C↓CATGG).

The pMM26 vector contained the *E. festucae* Fl1 *prt2* coding region was fused to the promoter and 5' untranslated region (UTR) of the *A. nidulans gpdA* gene at the position of the translation start codon. The backbone of the vector was a 4.2 kb *Eco*RI/*Pst*I fragment from phFunGus (Figure 2.1) containing the *hph* gene, which confers hygromycin resistance. The *gpdA* promoter and 5' UTR were derived from the pLM1 vector (Appendix 1) as a 2.3 kb *Eco*RI/*Nco*I fragment. The phFunGus *Eco*RI/*Pst*I and pLM1 *Eco*RI/*Nco*I fragments were gel purified before use (Section2.5.3.2). The pMM26 vector was constructed by means of a three way ligation, ligating the phFunGus *Eco*RI/*Pst*I, pLM1 *Eco*RI/*Nco*I, and *prt2* *Rca*I/*Pst*I fragments together in a single reaction. The expected fragment order was confirmed by PCR screening. pMM26 was sequenced to check for PCR misincorporation errors in the *prt2* coding sequence.

The pMM27 vector contained the *E. festucae* Fl1 *prt1* coding region was fused to the promoter and 5' untranslated region (UTR) of the *E. festucae* Fl1 *ltmM* gene at the position of the translation start codon. The backbone of the vector was a 4.2 kb *Bam*HI/*Pst*I fragment from phFunGus (Figure 2.1) containing the *hph* gene, which confers hygromycin resistance. The *ltmM* promoter and 5' UTR were derived from the pXZ56 vector (Appendix 1) as a 1.3 kb *Bam*HI/*Nco*I fragment. Both the phFunGus *Bam*HI/*Pst*I and pXZ56 *Bam*HI/*Nco*I fragments were gel purified before

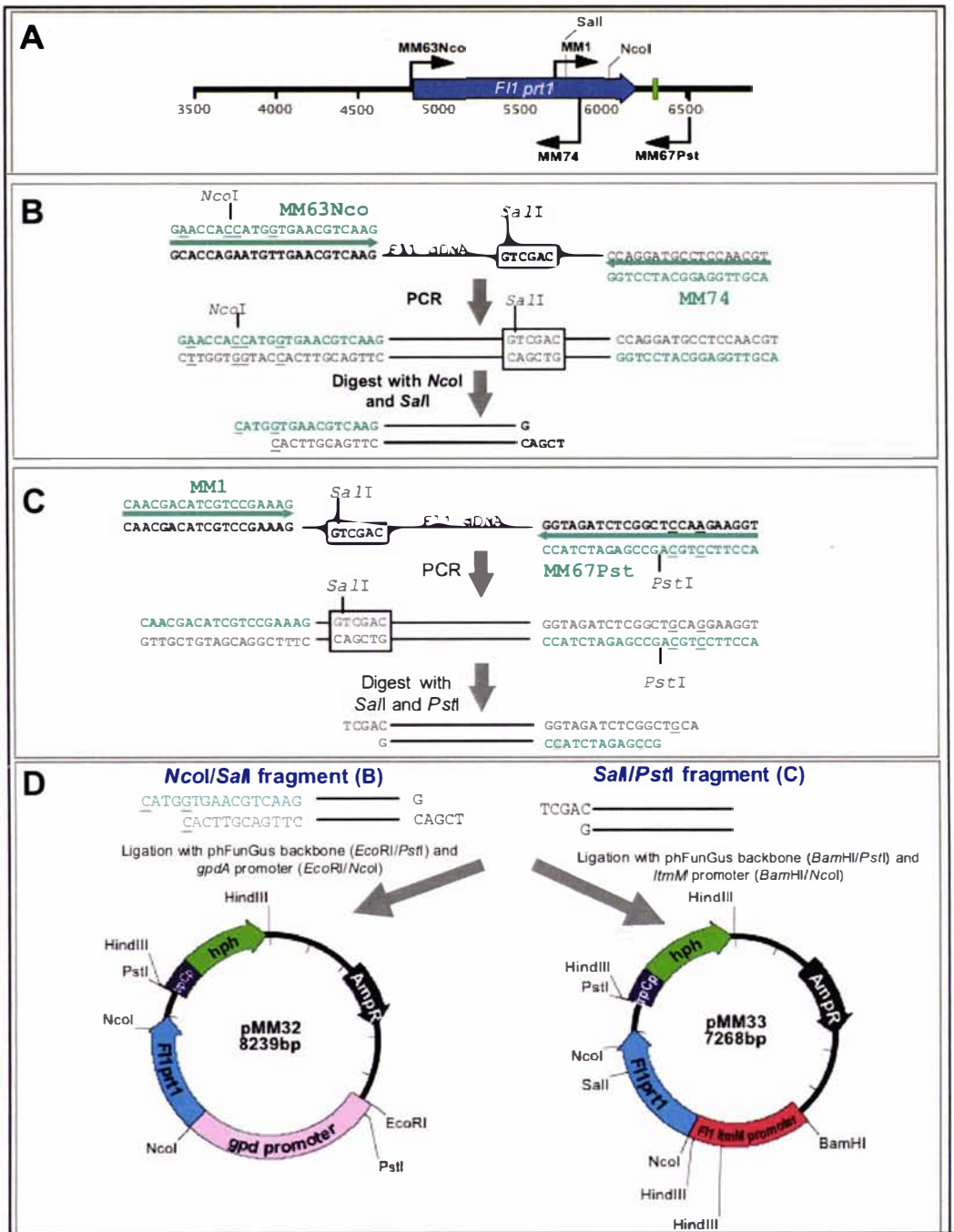

Figure 2.2 Construction of vectors directing heterologous expression of *prt1*

Schematic diagrams showing how the pMM32 (P*gpdA-prt1*) and pMM33 (P*ltmM-prt1*) vectors were created. **(A)** The *E. festucae* Fl1 *prt1* gene. The coding sequence is indicated by a blue arrow. Positions of the primers used to amplify the *prt1* coding region are indicated by heavy black arrows with primer names in bold black text. *Sal*I and *Nco*I restriction sites within the coding region are indicated by light black lines with names above. The green box indicates a microsatellite sequence in the 3' UTR of the *prt1* gene. **(B,C)** Strategies used to amplify the 5' and 3' regions respectively of the *prt1* coding sequence. Primers are indicated as teal arrows with the nucleotide sequence of the primer shown in teal text. Nucleotide differences between the primer and the corresponding genomic DNA sequence are indicated by underlined text. Nucleotides of the *E. festucae* Fl1 genomic DNA are shown in black text. Sequences complementary to the primers that were amplified during PCR are shown in grey text, with nucleotide differences from the corresponding genomic DNA sequences indicated by underlined text. Restriction sites are indicated by a black line positioned at the recognition site. **(D)** Schematic diagram showing how the four way ligations used to create the pMM32 (P*gpdA-prt1*) and pMM33 (P*ltmM-prt1*) vectors were performed. Maps of the resulting pMM32 and pMM33 vectors are shown.

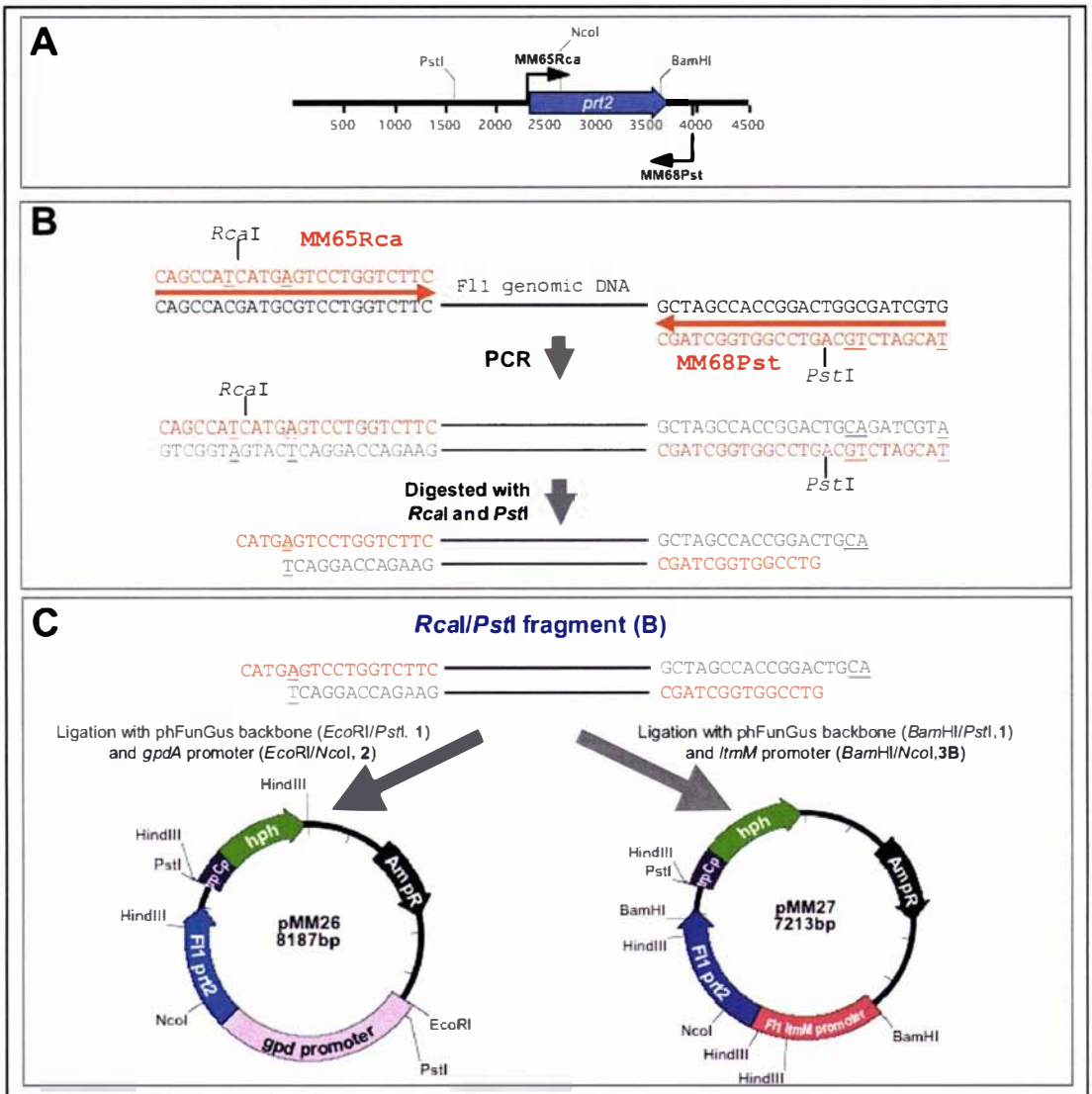

Figure 2.3 Construction of vectors directing heterologous expression of *prt2*

Schematic diagrams showing how the pMM26 (P*gpdA-prt2*) and pMM27 (P*ltmM-prt2*) vectors were created. **(A)** The *E. festucae* Fl1 *prt2* gene. The coding sequence is indicated by a blue arrow. Positions of the primers used to amplify the *prt1* coding region are indicated by heavy black arrows with primer names in bold black text. *Sal*I and *Nco*I restriction sites within the coding region are indicated by light black lines with names above. **(B)** Strategy used to amplify the *prt2* coding sequence. Primers are indicated as orange arrows with the nucleotide sequence of the primer shown in orange text. Nucleotide differences between the primer and the corresponding genomic DNA sequence are indicated by underlined text. Nucleotides of the *E. festucae* Fl1 genomic DNA are shown in black text. Sequences complementary to the primers that were amplified during PCR are shown in grey text, with nucleotide differences from the corresponding genomic DNA sequences indicated by underlined text. Restriction sites are indicated by a black line positioned at the recognition site. **(C)** Schematic diagram showing how the four way ligations used to create the pMM26 (P*gpdA-prt2*) and pMM27 (P*ltmM-prt2*) vectors were performed. Maps of the resulting pMM26 and pMM27 vectors are shown.

use (Section 2.5.3.2). Construction of the pMM27 vector was performed by means of a three-way ligation, ligating the phFunGus *Bam*HI/*Pst*I, pXZ56 *Bam*HI/*Nco*I, and *prt2* *Rca*I/*Pst*I fragments together in a single ligation reaction. The expected fragment order was confirmed by PCR screening. pMM33 was sequenced to check for PCR misincorporation errors in the *prt1* coding sequence.

2.13.3 Construction of the gcn1 gene replacement vector

The *gcn1* replacement vector consisted of 2.8 kb 5' and 3' fragments flanking the *gcn1* gene separated by a hygromycin cassette derived from the vector pPN1688 (Figure 2.4). The flanking sequences were amplified by long-template PCR (Section 2.17.4) from the cosmid 13B2 using the MM96-MM97 and MM98-MM99 primer pairs. The MM96, MM97, MM98 and MM99 primers introduce *Eco*RI, *Sst*I, *Xba*I and *Hin*dIII sites respectively. The MM96-MM97 PCR product was digested with *Eco*RI and *Sst*I, then subcloned into pUC118 to give the vector pMM52. The plasmid was sequenced to ensure the fragment contained no PCR misincorporation errors. The pMM53 vector was created by subcloning of the MM98-MM99 PCR product digested with *Xba*I/*Hin*dIII into pUC118. Again, the MM98-MM99 PCR product was sequenced to check for misincorporation errors. Error-free versions of the 5' *Eco*RI/*Sst*I and 3' *Xba*I/*Hin*dIII flanking fragments were ligated together with a 3.2 kb *Eco*RI/*Hin*dIII pUC118 fragment and a 1.3 kb *Sst*I/*Xba*I fragment from pPN1688 containing the *hph* cassette in a four-way ligation. PCR screening confirmed the resulting vector, pMM54, contained all of the desired fragments in the correct order. The linear DNA fragment containing the *gcn1*::*hph* used for transformation of *E. festucae* Fl1 was amplified from pMM54 with the M13F and M13R primers (Table 2.4) using long template PCR (Section 2.17.4).

2.14 BACTERIAL TRANSFORMATION

2.14.1 Preparation of electro-competent E. coli cells

One litre of LB broth (Section 2.3.2) was inoculated with *E. coli* XL-1 cells and grown with shaking at 37°C until an optical density (A_{600}) of the culture was between 0.5 and 1.0. The cells were chilled on ice for 20 min, then harvested by centrifugation at 4000 *g* for 10 min at 4°C. The cells were washed in ice cold water, firstly in 1000 mL, then 500 mL), then in 20 mL of ice cold 10% glycerol. The

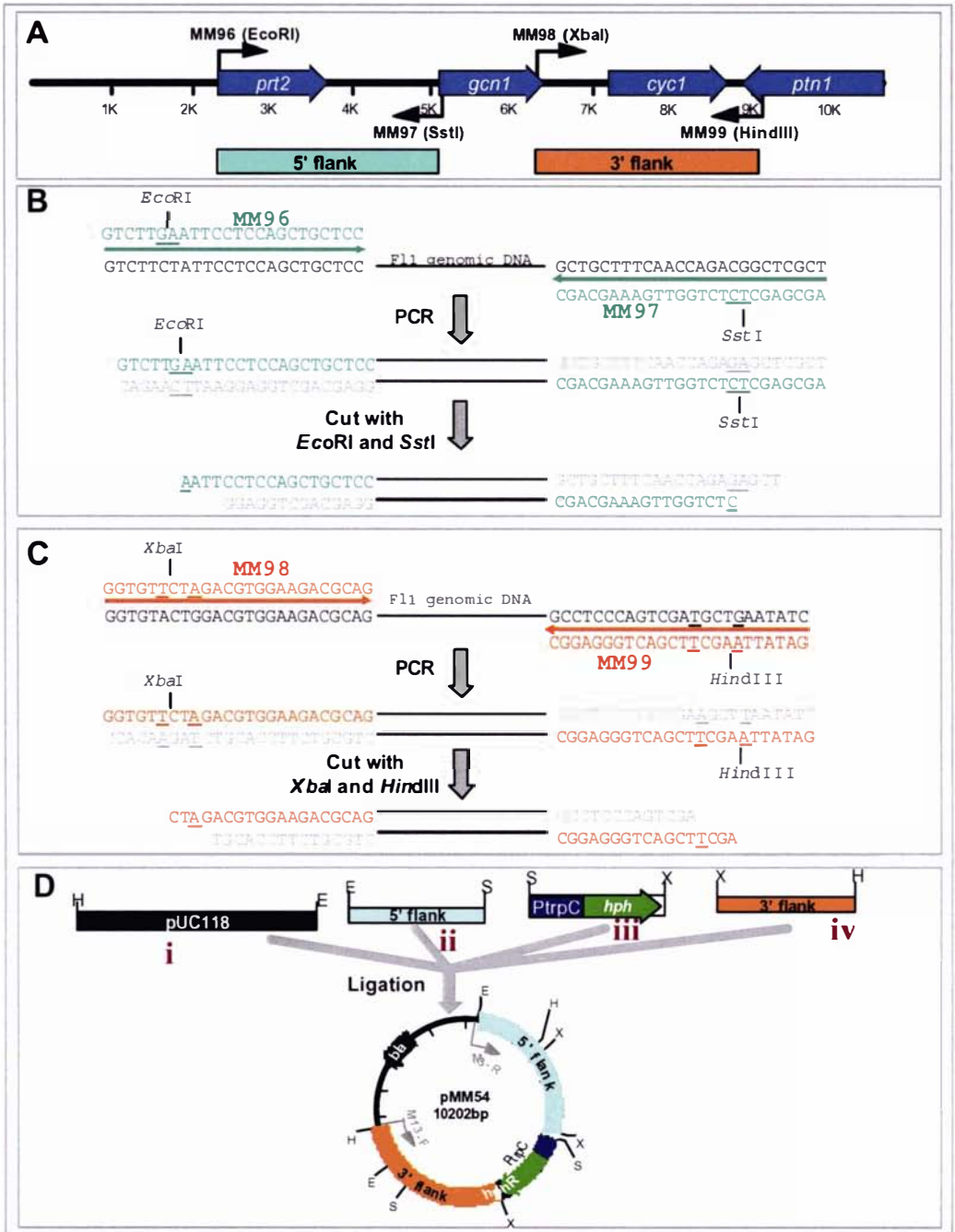

Figure 2.4 Construction of the *gcn1*::*hph* vector pMM54

Construction of the pMM54 vector. **(A)** Map of the *gcn1* locus. The primers used to amplify the 5' and 3' flanking sequences (represented by teal and orange boxes respectively) are indicated by thick black arrows, with primer names in bold text. Each of the four primers introduces a different enzyme restriction site, which is listed in brackets next to the primer name. The *prt2*, *gcn1*, *cyc1* and *ptn1* coding sequences are indicated by blue arrows. The ruler underneath the sequences is shown in kb. **(B, C)** Amplification of the 5' flanking sequence with the MM96 and MM97 primers and the 3' flanking sequences with the MM98 and MM99 primers. For the 5' flanking sequence, primer sequences are shown in teal, while for the 3' flanking sequence, primer sequences are indicated in orange. The genomic sequence is shown in black text and sequence amplified during PCR in grey text. Nucleotides that differ to the corresponding genomic sequence at the same position are indicated by underlined text. The recognition sites introduced in the primers used to amplify these fragments are indicated by a line corresponding to the position where these enzymes cut the DNA. **(D)** Strategy used to used to create the pMM54 vector. A 3.2 kb *Hin*dIII/*Eco*RI fragment was used to create the backbone of the vector (indicated by **i**). The *Eco*RI/*Sst*I 5' flanking sequence (**ii**) was amplified from *E. festucae* Fl1 genomic DNA as described in **B**. The PtrpC-hph cassette (**iii**) was derived from pPN1688 as a 1.4 kb *Sst*I/*Xba*I cassette. The *Xba*I/*Hin*dIII 3' flanking sequence (**iv**) was amplified from *E. festucae* Fl1 genomic DNA as described in **C**. All four fragments were ligated together in a single ligation reaction to create the pMM54 vector.

pelleted cells were resuspended in 4 mL of ice cold 10% glycerol and stored in 40 µL aliquots at -80°C.

2.14.2 Transformation of DNA by electroporation

Electrocompetent *E. coli* XL-1 cells prepared as described in Section 2.14.1 were gently thawed, then left on ice. The Gene Pulser (Bio-Rad) was set at 25 µF and 2.5 kV, and the pulse controller to 200 Ω resistance. One to 2 µL of DNA ligation (Section 2.12.2) was mixed with the electrocompetent cells, which were then incubated on ice for 1 min. The cell-DNA mixture was transferred and shaken to the bottom of an ice cold 0.2 cm cuvette, then pulsed at the settings described above. If the time constant for the electroporation pulse was between 4 and 5 ms, the electroporated cells were resuspended in 1 mL of SOC medium (Section 2.3.6). For each set of electroporation experiments, a cells only control (which contained no DNA) and a positive control (which contained 20 ng of pUC118 DNA) were included. Electroporated cells were incubated at 37°C for one hour, and then suitably diluted before being plated on LB agar plates (Section 2.3.2) containing ampicillin (Section 2.3.9).

2.14.3 Screening of transformants

2.14.3.1 Blue-white selection

Transformants where DNA was inserted into the *lacZ* gene of pUC118 or derived vectors were identified by screening using blue-white selection. One hundred µL of transformed cells were aliquoted onto the agar surface and mixed with 40 µL each of 24 mg/mL IPTG and 20 mg/mL X-Gal (Section 2.3.9). The cell mixture was spread over the agar surface with a glass spreader and incubated overnight at 37°C. White colonies, which contain a plasmid where the *lacZ* α gene was disrupted by insertion of a DNA fragment, were selected for further analysis.

2.14.3.2 Clone Checker™ analysis (Invitrogen)

CloneChecker™ analysis was performed in one of two ways. For both procedures, a colony of transformed bacteria were picked from freshly grown agar plate and resuspended in 6 µL of LB broth (Section 2.3.2). For restriction endonuclease analysis, 3 µL of the resuspended colony was mixed with 8 µL of Green solution.

The sample was incubated at 100°C for 30 s, then cooled to room temperature. A mix containing 1 μL of 10× restriction endonuclease buffer and 10 U (1 μL) of restriction endonuclease was added to each sample. The samples were incubated at 37°C for 10 min. Two μL of loading dye was added to the sample before electrophoresis on a 0.7% agarose in 1 × TBE gel (Section 2.8.2).

For supercoiled DNA analysis, 3 μL of the resuspended colony were mixed with 5 μL of red solution. Five μL of yellow solution was added to each sample, and mixed by vortexing. Four μL of loading buffer was added to each sample, and samples were vortexed immediately before electrophoresis on a 0.7% agarose in 1 × TBE gel (Section 2.8.2).

2.14.3.3 Colony PCR

Reactions for colony PCR contained 1 × *Taq* polymerase buffer (2.5 mM $MgCl_2$, Roche), 50 μM of each dNTP, 200 nM each of both forward and reverse primers and 0.5 U *Taq* polymerase (Roche). A very small amount of cells directly from bacterial colonies were introduced into the PCR reaction as a template. The following PCR program was used: 95°C for 3 min, 30 cycles of 95°C for 30 s, 55-60°C for 30 s, 72°C for *x* min (where 1 kb = 1 min, *x* is dependent on the size of the fragment being amplified), followed by 5 min at 72°C.

2.15 FUNGAL PROTOPLAST PREPARATION AND CHEF ELECTROPHORESIS

2.15.1 Protoplasting solutions

All protoplasting solutions were sterilised by autoclaving before use.

2.15.1.1 OM buffer

OM buffer contained 1.2 M $MgSO_4.7H_2O$ and 10 mM Na_2HPO_4. The pH was adjusted to 5.8 with 100 mM $NaH_2PO_4.2H_2O$.

2.15.1.2 Glucanex

Glucanex (Novo Nordisk) was dissolved in OM buffer (Section 2.15.1.1) at a concentration of 10 mg/mL and filter sterilised before use.

2.15.1.3 ST buffer
ST buffer contained 0.6 M sorbitol and 100 mM Tris-HCl (pH 8.0).

2.15.1.4 STC buffer
STC buffer contained 1 M sorbitol, 50 mM $CaCl_2$, 50 mM Tris-HCl (pH8.0).

2.15.1.5 40% PEG buffer
PEG buffer contained 40% (w/v) PEG 4000, 50 mM $CaCl_2$, 1 M sorbitol, 40 mM Tris-HCl (pH8.0).

2.15.1.6 GMB buffer
GMB buffer contained 0.9 M sorbitol and 125 mM Na_2EDTA (pH7.5).

2.15.1.7 LMP in GMB
LMP in GMB contained 1.4% (w/v) low melting point agarose (Sigma) in GMB buffer (Section 2.15.1.6).

2.15.1.8 SE buffer
SE buffer contained 2% (w/v) SDS and 250 mM Na_2EDTA (pH 8.0).

2.15.1.9 10 × ET buffer with SLS
10 × ET buffer contained 10 mM Tris and 500 mM Na_2EDTA (pH 8.0), along with 1% SLS.

2.15.1.10 1 × ET buffer
1x ET buffer contained 1 mM Tris and 50 mM Na_2EDTA (pH 8.0).

2.15.2 Protoplast preparation

Fungi were inoculated into PD broth (Section 2.3.3) as described in Section 2.2.2, and grown at 22°C with shaking at 150 rpm for varying lengths of time. *E. typhina* PN2311 was grown for five days and *E. festucae* Fl1 for seven days, while *N. lolii* strain Lp19 was grown for twelve days. Four 50 mL cultures were pooled for each protoplast preparation. Mycelia were harvested from cultures by filtering through a nappy liner, and washed three times in sterile double-distilled water. Mycelia were rinsed with OM buffer (Section 2.15.1.1) and resuspended in 30 mL of Glucanex (Section 2.15.1.2). Hyphae were incubated overnight at 30°C with shaking at 80-100

rpm. At this stage, the numbers of protoplasts generated were checked by viewing a small sample under the microscope.

Protoplasts were collected by filtering the treated mycelia through a nappy liner into sterile centrifuge tubes, with each tube containing approximately 5 mL. Each sample was overlaid with 2 mL of ST buffer (Section 2.15.1.3), and tubes were centrifuged at 2210 *g* for 5 min at 4°C. Protoplasts, which collect at the interface between the Glucanex and ST buffer solutions, were removed and transferred to a fresh tube. Protoplasts were resuspended in 5 mL of STC buffer (Section 2.15.1.4) and centrifuged at 2210 *g* for 5 min at 4°C. This process was repeated three times to wash protoplasts. Protoplasts were resuspended in 0.5 mL of STC buffer, then the concentration of protoplasts was assessed using a haemocytometer. At this point, protoplasts were either used for the isolation of fungal genomic DNA (Section 2.5.8.1), used for fungal transformation (Section 2.16) or to make protoplast plugs for CHEF (Section 2.15.3).

2.15.3 Preparation of protoplast plugs for CHEF

Protoplasts were resuspended at a concentration of 1×10^9 protoplasts/mL in GMB buffer (Section 2.15.1.6). Protoplasts were mixed with an equal volume of low melting point (LMP) agarose (Invitrogen) in GMB buffer (Section 2.15.1.7) to give a final concentration of 5×10^8 protoplasts/mL into plug moulds, and left to set at 4°C for 10 min. The set plugs were incubated in 10 mL of SE buffer (Section 2.15.1.8) and incubated at 55°C for 16-20 h. Plugs were transferred into 10 × ET buffer with SLS (Section 2.15.1.9) and 20 mg proteinase K (Roche) and incubated at 50°C for 24 h. Plugs were washed three times in 1 × ET buffer (Section 2.15.1.10) to remove SLS, with changes over several hours. Protoplasts were stored at 4°C in 1 × ET buffer.

2.15.4 CHEF electrophoresis

CHEF gels were made of 0.6% chromosomal grade agarose (Bio-Rad) in 0.5 × TBE buffer (diluted 2 fold from 1 × TBE buffer, Section 2.8.1.2). The running buffer was used was also 0.5 × TBE buffer. The apparatus pump was set to 75, and the buffer

temperature was set to 14°C. Electrophoresis took place at 60V with a run program of 100 s for 15 h, 450 s for 13 h, 1600 s for 35 h and 2000 s for 35 h. After electrophoresis, the gel was stained in ethidium bromide (Section 2.8.1.4, Section 2.8.3). The gel was Southern blotted as described in Section 2.9.

2.16 FUNGAL TRANSFORMATION

2.16.1 Transformation of fungal protoplasts

Protoplasts (prepared as described in Section 2.15.2) were diluted to 1.25×10^8 protoplasts/mL in STC buffer (Section 2.15.1.4). Eighty μL of the diluted protoplast stock was added to 20 μL of 40% PEG buffer (Section 2.15.1.5). Two μL of spermidine (Section 2.4.3), 5 μL of heparin (Section 2.4.3) and 5 μg of DNA were added to the samples, which were then mixed by gentle vortexing. For each transformation, a "protoplast only" control to which no DNA was added, and a positive control with a known plasmid such as pAN7-1 or pII99. Samples were incubated on ice for 30 min. Nine hundred μL of 40% PEG buffer (Section 2.15.1.5) were added, and samples were mixed and incubated on ice for 15-20 min. One hundred μL of the sample was mixed by vortexing with 0.8% RG agar (Section 2.3.5) equilibrated to 50°C. The sample-agar mix was overlaid onto a regeneration medium agar (Section 2.3.5) plate.

For the protoplasts only control (where no DNA was added), two plates were prepared with the undiluted protoplast mix, and one plate each prepared for 10, 100 and 1000 fold dilutions. Four plates were prepared for the positive control, and ten plates for the transformed DNA sample. Plates were incubated overnight before another overlay with antibiotic selection (hygromycin to a final concentration of 150 μg/mL or geneticin to a final concentration of 200 μg/mL, Section 2.3.9). Protoplasts were regenerated by growing at 22°C for at least fourteen days. To purify transformants and ensure transformants were stable for antibiotic resistance, a small square of agar containing hyphae was subcultured onto a fresh agar plate with a hygromycin concentration of 50 μg/mL or a geneticin concentration of 75 μg/mL. Plates were incubated to allow hyphae to form a larger colony, and a new sample was subcultured. This process was repeated three times to ensure that transformants

were not heterokaryons. Transformants were then screened using the PCR-based screening approaches used in Section 2.16.2 or by Southern blot approaches (Section 2.9).

2.16.2 Screening of fungal transformants

2.16.2.1 Screening using alkaline lysis of fungal hyphae

A small amount of mycelia were scraped from the surface of a fungal colony on an agar plate and placed in lysis solution (400 mM KOH, 10 mM Na_2EDTA). Samples were incubated on ice for 10 min. One hundred µL of neutralisation solution (1 M HCl/1 M Tris-HCl pH 7.5 (4:6 v/v)) was added, and the solution was stored at 4°C. One to two µL of the sample was used in a standard PCR reaction, as described in Section 2.17.2.

2.16.2.2 Screening using the plant Extract-N-Amp™ PCR kit (Sigma)

A small scraping of mycelia from the surface of a fungal colony was placed into 50 µL of extraction solution. The sample was mixed by vortexing and incubated at 95°C for 10 min. An equal volume of dilution solution was added to the extracted hyphae. The solution was then diluted five fold with dilution solution. For screening, each 10 µL PCR reaction was contained 5µL of Extract-N-Amp™ PCR reaction mix, 40 nM of each primer, and 0.5 µL of the diluted extracted DNA. The PCR program used was as follows: 94°C for 3 min, 35 cycles of 94°C for 30 s, 60°C for 30 s, 72°C for 1 min, followed by 72°C for 10 min.

2.17 PCR

2.17.1 PCR reagents

2.17.1.1 Oligonucleotide primers

Oligonucleotide primers were synthesised by Invitrogen or Sigma Genosys. Each primer was resuspended to a final concentration of 100 pmol/µL. For PCR reactions, primer stocks were diluted to 10 pmol/µL. For sequencing reactions, primer stocks were diluted to 3.2 pmol/µL or 5 pmol/µL. Primers were stored at -20°C until needed. Primer used in this study are shown in Table 2.4.

Table 2.4 Primers used in this study			
Names	Sequences (5'-3')	Locus	Applications
M13F	GCC AGG GTT TTC CCA GTC ACG A	M13 lacZ	Sequencing
M13R	AGC GGA TAA CAA TTT CAC ACA GGA	M13 lacZ	Sequencing
T7	TAA TAC GAC TCA CTA TAG GG	pGEM T Easy	Sequencing
SP6	CCA TTT AGG TGA CAC TAT AG	pGEM T Easy	Sequencing
T1.1	GAG AAA ATG CGT GAG ATT GT	*tub2*	PCR
T1.2	TGG TCA ACC AGC TCA GCA CC	*tub2*	PCR
lol1	TGG ATC ATT CGC AGA TAC	*ltmG*	PCR
lol3	ACC GAC GCC ATT AAT GAG	*ltmG*	PCR
lol14	ATT AGA GGC ACC GAA CGC	*ltmM*	PCR
lol28	GCT CCT TGC CCA TTA TTT	*ltmM*	PCR
lol107	CTA TAA CcA CTC TCC TAT C	*ltmM*	PCR
lol148	TGC GTG AGA GAT AAA GCA AG	*ltmM*	PCR
lol238	AGG AAA GCC ACG GGA TAA CC	*ltmM*	PCR
pUC*hph*5	TCA GGC AGG TCT TGC AAC	*hph*	PCR
pUC*hph*6	ACT TCG AGC GGA GGC ATC	*hph*	PCR
MM1	CAA CGA CAT CGT CCG AAA G	*prt5-prt1*	Sequencing, PCR
MM2	GTG ATC CAG TCG AGA GTC	*prt5-prt1*	Sequencing, PCR
MM3	AAG TCT CGC CAT GAC CAC	*prt5-prt1*	Sequencing
MM4	CAG GTC GAG GTT GTT GAG	*prt5-prt1*	Sequencing, PCR
MM5	TGA TGC CTG GAC ATG TTG	*prt5-prt1*	Sequencing, PCR
MM6	TCG TTC AGC GAC TGC GAG	*prt2-gcn1*	Sequencing, PCR
MM7	GCC TCC CAG TTA GCA TTC	*prt5-prt1*	Sequencing
MM8	CGG ACG CGT GTG ACT GAC	*prt5-prt1*	Sequencing, PCR
MM9	CCA AAC CAA CAT GTC CAG	*prt5-prt1*	Sequencing
MM10	TGG GCA ACG ACA AGG ATG	*prt5-prt1*	Sequencing
MM12	AGC AGC GCG ATG CTC CTC	*prt2-gcn1*	Sequencing
MM13	ATC AAG GTA CTC AGC GAC	*prt2-gcn1*	Sequencing
MM14	GAC TTC TTT GAG CCC GAG	*prt5-prt1*	Sequencing
MM15	GTG ACA TTG GTG GCT ACG	*prt2-gcn1*	Sequencing, PCR
MM16	GAT CGA ACA TCA CCT CTG	*prt5-prt1*	Sequencing
MM20	GTG ATC GAG AAC AAG TAC	*prt2-gcn1*	Sequencing, PCR
MM21	CTC GAT GTA GTC AAC CTG	*prt2-gcn1*	Sequencing
MM22	TGG AAC CGA CAC GGC AGG	*prt2-gcn1*	Sequencing
MM25	TGC GAG ACC AAC AAT GTG	*prt2-gcn1*	Sequencing, PCR
MM26	CCA CAT TGT TGG TCT CGC	*prt2-gcn1*	Sequencing, PCR
MM27	CGC ATC TCT TCA AAG TGC	*prt5-prt1*	Sequencing
MM28	GCA CTT TGA AGA GAT GCG	*prt5-prt1*	Sequencing
MM29	GAT GGG TCT TCA GAT GAC	*prt2-gcn1*	Sequencing, PCR
MM30	GTC ATC TGA AGA CCC ATC	*prt2-gcn1*	Sequencing, PCR
MM32	TAG CAT GAG GAA ATG ACG	*prt5-prt1*	Sequencing
MM33	GGT GTA ACG GTT CTT TGC	*prt2-gcn1*	Sequencing
MM34	CGT TAC GCA CAA GAT GAG	*prt2-gcn1*	Sequencing
MM37	TGT AGA GTC TGC TCT GCC	*prt2-gcn1*	Sequencing
MM38	TAG GGC ACC AAG GCT GGC	*prt2-gcn1*	Sequencing
MM39	CTC TGA ATG CTA ACT GGG	*prt5-prt1*	Sequencing
MM40	TCG TGA CAA GGT TGG CAG	*prt2-gcn1*	Sequencing
MM41	TGA ATC AGT CCG TCC CAC	*prt2-gcn1*	Sequencing
MM42	TGG GAC GGA CTG ATT CAC	*prt2-gcn1*	Sequencing
MM43	GCC ATT TGG TGG TCA TGG	*prt5-prt1*	Sequencing
MM44	CGA ACC AAG ATG TAT GCC	*prt2-gcn1*	Sequencing
MM45	GCA AAT CGG GAA GGT GTC	*prt2-gcn1*	Sequencing
MM48	GCT GCA GCC TTC ATA ACG	*prt5-prt1*	Sequencing
MM51	TTG AGT CGA CAA GTC TGC	*prt2-gcn1*	Sequencing
MM52	AGA TCA AAG CTC ATC CTG	*prt5-prt1*	Sequencing
MM53	TCT GCA AAC CTT GTC ACG	*prt2-gcn1*	Sequencing
MM54	ATC TGT GAG CCG TGG ATG	*prt2-gcn1*	Sequencing
MM55	AAC GTC GTG GGC TGA CTG	*prt2-gcn1*	Sequencing, PCR
MM56	TCA CTC CAT CCT TGT CCC	*prt2-gcn1*	Sequencing, PCR
MM61	GGC ATG ATT GAG GTT CTC	*prt2-gcn1*	Sequencing
MM63Nco	GAA CCA CCA TGG TGA ACG TCA AG	*prt5-prt1*	Cloning
MM65Rca	CAG CCA TCA TGA GTC CTG GTC TTC	*prt2-gcn1*	Cloning

MM67Pst	ACC TTC CTG CAG CCG AGA TCT ACC	*prt5-prt1*	Cloning
MM68Pst	TAC GAT CTG CAG TCC GGT GGC TAG C	*prt2-gcn1*	Cloning
MM69	GGA TCT TAA CCA GAT TCG	PgpdA	PCR
MM70	TTC ATC TTC CCA TCC AAG	PgpdA	PCR
MM71	CGT ATC AAT AGA CCT CAT C	*prt2-gcn1*	Cloning
MM72	TCA CGT GGA GCT TCT TGC C	*prt2-gcn1*	Sequencing, PCR
MM74	ACG TTG GAG GCA TCC TGG	*prt5-prt1*	Sequencing, PCR
MM75	GGC TCG AAC GAG TAC GTC	*prt3-gao1*	Sequencing, PCR
MM76	TGG TTT GTG GCC TTG GAG	*prt3-gao1*	Sequencing, PCR
MM82	CAT GAT GCA CCT TGC TCG TC	*prt3-gao1*	Sequencing, PCR
MM83	ATG CCA GCA GAT TGA CCG	*prt3-gao1*	Sequencing, PCR
MM84	TTG GCT TGG AAA GGA ATG TG	*prt2-gcn1*	Sequencing
MM85	TAG TTG TAC TCT GCG TCG	*prt2-gcn1*	Sequencing
MM86	GTA GAG GAC ACG ATC AAG	*prt2-gcn1*	Sequencing, PCR
MM87	AAC CTG CCG TTC ATC AGC	*prt2-gcn1*	Sequencing
MM88	TGA GTC TCG AAC TTG TCG	*prt2-gcn1*	Sequencing
MM89	CGG TGG AAT TGT CGC TCG	*prt3-gao1*	Sequencing
MM90	CGA GCG ACA ATT CCA CGG	*prt3-gao1*	Sequencing, PCR
MM91	ACC AGG TTG CAG GCA CGG	*prt3-gao1*	Sequencing
MM92	ACC GTG CCT GCA ACC TGG	*prt3-gao1*	Sequencing, PCR
MM93	GAT CAY GTA GAT TTY GAR GG	*prt4*	Cloning
MM94	GCA TCA GCG TTA TCR TTN CC	*prt4*	Cloning
MM95	AGC ATC ACA AGT CGA CCA GG	*prt2-gcn1*	Sequencing
MM96	GTC TTG AAT TCC TCC AGC TGC TCC	*prt2-gcn1*	Cloning
MM97	AGC GAG CTC TCT GGT TGA AAG CAG C	*prt2-gcn1*	Cloning
MM98	GGT GTT CTA GAC GTG GAA GAC GCA G	*prt2-gcn1*	Cloning
MM99	GAT ATT AAG CTT CGA CTG GGA GGC	*prt2-gcn1*	Cloning
MM100	CGT CAG AGT AGG TCC AGC	*prt2-gcn1*	PCR
MM101	CTG ATC TTG ACG TCG ATG	*prt2-gcn1*	Sequencing, PCR
MM102	TCG TGA ATA CTG ACT AGG	*prt3-gao1*	Sequencing
MM103	TCT ACC ACA GCA TCG CTC	*prt3-gao1*	Sequencing
MM104	TCA CCA GCC AAG TCA TAC	*prt3-gao1*	Sequencing
MM105	TGG AGC CGA AAC AAT GAG	*prt2-gcn1*	Sequencing
MM106	ATG GTA CCT GAG CAA TGC	*prt4*	Sequencing, PCR
MM107	CGA ACA TGT CGC TTG GTC	*prt4*	Sequencing
MM120	TGT GAG GAG ATA TTG TGG	*prt3-gao1*	Sequencing
MM121	GCA ACG TTC ATG TCA GCC	*prt3-gao1*	Sequencing, PCR
MM122	TCT GAG GAG ATA TTG TGG	*prt5-prt1*	Sequencing, PCR
MM123	GAC AAA GAC ACC ACC AAC	*prt5-prt1*	Sequencing
MM124	TAT CTC GAC AAT CTC AAT C	*prt2-gcn1*	Sequencing, PCR
MM125	AGC TTC AGG TGT CAA CAG	*prt2-gcn1*	PCR
MM126	TCC GAA ATC AAG ATC CAG	*prt2-gcn1*	Sequencing, PCR
MM127	GAT CGC CTC GGT CTC TGT AAC	*prt2-gcn1*	Sequencing, PCR
MM128	CTT GAT CTG TGC TAC GTG AC	*prt2-gcn1*	Sequencing, PCR
MM129	TCG CAA GTG ACT TTC CAT C	*prt3-gao1*	Sequencing
MM130	TAG TCC ATG CCA GCA ATG	*prt5-prt1*	Sequencing, PCR
MM131	CCA TTG GAT TTG TGT GTC	*prt5-prt1*	Sequencing
MM135	GAA CGT TTC CGT GGA ACG	*prt2-gcn1*	PCR
MM136	GAA CCA TCA ACT CAA GAC	*prt5-prt1*	Sequencing
MM138	GAA CTT TGC TGG TGA TGG	*prt5-prt1*	Sequencing
MM139	GTA CGT CTA CGA CAA TAG	*prt3-gao1*	Sequencing
MM141	ATG TAC AGC CAC GAT TGG	*kex2*	Sequencing
MM142	CAT AGT AGT AAG ACA ACG	*kex2*	Sequencing
MM143	AAC GAC TGT GTC CTT CTC	*prt4*	Sequencing
MM144	CTG CCA AGG ATG GAA AGC	*prt4*	Sequencing
MM145	GTC GAA AGC AGG ACT TCC	*prt5-prt1*	Sequencing
MM146	GCA AAC TTG GAT CAA GGC	*prt5-prt1*	Sequencing
MM149	GGN CAY GGN ACN CAY GTN GC	*other*	Degenerate PCR
MM150	GGN SWN GCC ATN GAN GTN CC	*other*	Degenerate PCR
MM151	AGG TGC ATT GCT GAT TGG	*prt5-prt1*	Sequencing
MM152	TTC TGC AAC GGA CGC TAG	*prt5-prt1*	Sequencing
MM155	TAC AGC CAC TCC TTC AAC	*prt5-prt1*	Sequencing, PCR
MM156	CCA TCA CCA GCA AAG TTC	*prt5-prt1*	Sequencing
MM157	GAC CAG AGC ATA GGC ATC	*kex2*	Sequencing

MM158	TCG TCG TAT GTG GCT TGG	*kex2*	Sequencing
MM159	TGT CGA GAT ACA CGT CTG	*prt2-gcn1*	Sequencing
MM160	GAA AGT CAC TTG CGA CAG	*prt3-gao1*	Sequencing, PCR
MM161	GGT TAC ATT GGG ATT CTC GC	*prt3-gao1*	Sequencing
MM164	CGT GAT TGA GAA AGT CCG	*prt4*	Sequencing, PCR
MM165	TCC TCT CCA TCT CAC AAC	*prt4*	Sequencing
MM166	ATC AAA CGA GGT CGT AGC	*prt4*	Sequencing
MM167	GAT GCG AAG ACA CTC AG	*prt4*	Sequencing
MM168	AAG CTC CGA CAA GTC AAC	*prt4*	Sequencing
MM170	TGG AAT AGT GGC TAC GAC	*prt4*	Sequencing
MM171	CTG AAC ATG AAC GCT CTC	*prt4*	Sequencing
MM172	TAG GAC TTG AGC TGG TGG	*prt3-gao1*	Sequencing
MM175	ACA TGT TGG CGA CGC TGC	*prt5-prt1*	PCR
MM176	GGA CAA GTT CGA CAA TCG	*prt3-gao1*	Sequencing
MM177	AGA ACT CAT CCT TCG TCC	*prt2-gcn1*	Sequencing
MM178	AAG GGG ACA AAC ACT GTG C	*prt4*	Sequencing
MM179	GAG AGC ATT CGG ATT CCC	*kex2*	Sequencing
MM180	GAA TAC ACG AGG GAA CTG	*kex2*	Sequencing
MM181	TGG AGA ATC ATT GTC AAG	*kex2*	Sequencing
MM183	GCT TAC TGC TGG TAT TTC	*prt3-gao1*	Sequencing
MM184	AAG AAT GGT TGG GGT TGG	*prt5-prt1*	Sequencing
MM185	GTG AAC TCG TGA GAA CAG	*prt5-prt1*	Sequencing
MM186	GCA CTA TCG TCG TAG ATG	*prt5-prt1*	Sequencing
MM187	AAG TTC CAG ATG GTG CAG	*kex2*	Sequencing
MM188	CAA CGA CCT CAA TGT ATC	*kex2*	Sequencing
MM189	TAC TGC ACC ATC TGG AAC	*kex2*	Sequencing
MM190	TAC TGC ACC ATC TGG AAC	*kex2*	Sequencing
MM191	AGA GCA AAG CAC ATG CAG	*kex2*	Sequencing
MM192	CAA GCC ACA TAC GAC GAC	*kex2*	Sequencing, PCR
MM199	GTG ACC GAT TTT CCT TCC TC	*kex2*	Sequencing
MM200	CAC TTG GTA CGA CGC TAA TC	*kex2*	Sequencing
MM201	ATG GTG TTG GAA GTT GGG	*kex2*	Sequencing
MM205	ACG TTC ACC ATG CAG TTC	*kex2*	Sequencing, PCR
MM206	TGT GAA GCG TTA TTG GAG	*kex2*	Sequencing, PCR
MM207	GAA CTC TGA GAT AAC AAG	*kex2*	Sequencing
MM208	GAT GAT GAG GGA ATG AAC	*kex2*	Sequencing, PCR
MM209	CGC AAG TAT CGG CAT TCC	*kex2*	Sequencing, PCR
MM212	CAG AGT CAT CAA AAT GCC	*prt5-prt1*	Sequencing, PCR
MM213	AGG TTG AGG CTT GTT TCC	*prt3-gao1*	PCR
MM214	CCA GAA CTA ATC CAC AAG	*kex2*	PCR
MM215	GTG GCG AGC AAG GCG TCC	*kex2*	PCR

2.17.1.2 dNTPs

dNTPs (Roche) were prepared at concentrations of either 1.25 mM or 10 mM each dNTP.

2.17.2 Standard PCR

Standard PCR reactions were performed using reactions containing approximately 1.25 ng of plasmid or 5-10 ng of genomic DNA template, 1 × *Taq* polymerase buffer (2.5 mM $MgCl_2$, Roche), 50 μM of each dNTP, 200 nM each of both forward and reverse primers and 0.5 U *Taq* polymerase (Roche). The following PCR program was used: 94°C for 2 min, 30-35 cycles of 94°C for 30 s, 55-60°C for 30 s, 72°C for

x min (where 1 kb = 1 min, x is dependent on the size of the fragment being amplified), followed by 5 min at 72°C.

2.17.3 Gradient PCR

Gradient PCR was performed using the same reaction components as standard PCR (Section 2.17.2). During the annealing phase of the PCR program, the PCR machine (PC960G gradient thermal cycler, Corbett Research) introduced a temperature gradient across the PCR block, generally varying from a low of 49-51°C to a high of 60°C.

2.17.4 PCR using Expand™ Long Template (Roche)

Long-template PCR was performed using PCR reactions containing approximately 1.25 ng of template plasmid, 1 × Expand™ Long Template buffer 1 (1.75 mM $MgCl_2$), 350 µM each dNTP, 300 nM each of both forward and reverse primers and 3.75 U of Expand™ Long Template enzyme mix. The following PCR program was used: 93°C for 2 min, 10 cycles of 93°C for 10 s, 60°C for 30 s, 68°C for x min (where 1 kb = 1 min, x is dependent on the fragment size being amplified), 17 cycles of 93°C for 10 s, 60°C for 30 s, 68°C for x min + 20 s per cycle, followed by 10 min at 68°C.

2.17.5 PCR using Expand™ High Fidelity (Roche)

High-fidelity PCR was performed using PCR reactions containing either 1.25 ng of plasmid or 5-10 ng of genomic DNA template, 1 × Expand™ High Fidelity buffer (1.5 mM $MgCl_2$), 200 µM of each dNTP, 300 nM each of both forward and reverse primers, and 2.6 U of Expand™ High Fidelity enzyme mix. The following PCR program was used: 94°C for 2 min, 28 cycles of 94°C for 15 s, 60°C for 30 s, 72°C for x min (where 1 kb = 1 min, x is dependent on the fragment size being amplified), followed by 5 min at 72°C.

2.17.6 Inverse PCR

Inverse PCR was performed to obtain the 5' region of the *N. lolii* Lp19 *prt2* promoter. Genomic DNA from *N. lolii* Lp19 was digested with *Bam*HI and a small aliquot was ligated as described in Section 2.12. Circular DNA molecules that are formed by intrAmolecular ligation of *Bam*HI-digested ends act as a template during inverse PCR. The ligation mix was amplified by the primers MM26 and MM38 to obtain the unknown DNA sequence that was contained on the 4 kb *Bam*HI fragment. The sequence was amplified by *Taq* polymerase as for a standard PCR reaction (Section 2.17.2).

2.17.7 TripleMaster® PCR

TripleMaster® PCR reactions were performed using reactions containing approximately 50 ng of genomic DNA template, 1 × high fidelity buffer (2.5 mM $MgCl_2$, Eppendorf), 200 μM of each dNTP, 300 nM each of both forward and reverse primers and 0.05 U TripleMaster® polymerase mix (Eppendorf). The following PCR program was used: 94°C for 2 min, 30 cycles of 94°C for 20 s, 60°C for 20 s, 72°C for *x* min (where 1 kb = 1 min, *x* is dependent on the size of the fragment being amplified), followed by 5 min at 72°C.

2.17.8 RT-PCR

RT-PCR reactions were performed as for standard PCR reactions using cDNA (Section 2.18.5) as a template.

2.18 RNA ISOLATION AND PURIFICATION

Standard precautions were taken before experiments involving RNA were started. All glassware was washed in chromic acid overnight and oven baked at 180°C for 2 h. Solutions were made with reagents used only for RNA work only with DEPC-treated water, and placed in acid-washed oven-baked glassware. Mortars and pestles were soaked in 0.3% hydrogen peroxide overnight before use. DNase and RNase free barrier tips were used to reduce the potential for RNase contamination of RNA samples. Gloves were worn while experiments involving RNA were performed.

2.18.1 Purification of total RNA using Trizol

A sample of grass or fungal tissue (1-2 g) in liquid nitrogen was ground to a powder using a mortar and pestle. The powdered tissue was mixed to a paste with 10 mL of Trizol (Invitrogen), and left to thaw. The Trizol-tissue mixture was transferred to a 14 mL Falcon tube, and centrifuged at 9682 *g* at 4°C for 10 min to pellet cellular debris. The supernatant was mixed with 2 mL of chloroform, and left to sit at room temperature for 3 min. The mixture was centrifuged at 9682 *g* at 4°C for 15 min. The aqueous phase was mixed with 2.5 mL each of isopropanol and sodium citrate/sodium chloride solution to precipitate the RNA. The mixture was incubated at 10 min, then centrifuged at 9682 *g* at 4°C for 10 min. The RNA pellet was washed with 10 mL of 70% ethanol and centrifuged at 5365 *g* at 4°C for 5 min. The pellet was air dried, then resuspended in 100-300 μL of DEPC-treated water.

2.18.2 Purification of polyA RNA from total RNA

One hundred to two hundred μg of total RNA isolated using Trizol (Section 2.18.1) was taken up to a volume of 250 μL of DEPC-treated water, mixed with 250 μL of 2 × binding solution and vortexed to mix. 15 μL of oligo dT beads were added to the total RNA, and mixed by vortexing. The sample was incubated at 70°C for 3 min to allow RNA to denature, then incubated at room temperature for 10 min to allow polyA RNA to bind to the oligo dT beads. The beads were then collected by centrifugation at 16,060 × g for 1 min. The supernatant was discarded, and the pellet resuspended in 500 μL of wash buffer. The mixture was transferred to a spin filter, and centrifuged for 1 min to remove the wash buffer. The filtrate was discarded, and an additional 500 μL of wash buffer added to the spin filter. The wash buffer was removed by centrifugation at 16,060 × g for 2 min. The spin filter was transferred to a new tube. Fifty μL of elution buffer preheated to 70°C was added to the spin filter, and the sample was incubated at 70°C for 3 min, before poly A RNA was eluted by centrifugation at 16,060 × g for 1 min. The elution process was repeated twice.

2.18.3 RNA quantitation by measuring absorbance and A_{260}/A_{280} nm

The concentration and purity of the isolated RNA was assessed by measuring the absorbance of the RNA at 260 and 280 nm. The concentration of RNA was assessed

by measuring the absorbance of a 100-fold dilution of the RNA in TE buffer (Section 2.4.1.8, prepared with DEPC-treated double-distilled water). For RNA, an absorbance of 1 at 260 nm is equivalent to a concentration of 40 μg/mL. To calculate the RNA concentration, the absorbance at 260 nm was multiplied by the dilution factor and by 40 μg/mL. The purity of the RNA was assessed by measuring the ratio between the absorbances at 260 and 280 nm, with a ratio of 1.8 to 2.2 indicating pure RNA had been obtained.

2.18.4 DNase I treatment of RNA

Before cDNA synthesis, RNA was treated with Amplification grade DNase I (Invitrogen). Each 10 μL reaction contained 1 μg of RNA (or 100 ng of mRNA), 1 × DNase I reaction buffer (Invitrogen) and one unit of DNase I, amplification grade (Invitrogen). Reactions were scaled up as necessary, and incubated at room temperature for 15 min. The DNase I was inactivated by the addition of 1 μL of 25 mM EDTA solution followed by treatment at 65°C for 10 min.

2.18.5 cDNA synthesis

cDNA was prepared using either 1 μg of total RNA or 100 ng of poly A RNA along with 0.09 OD units of random hexamer primer (Roche) per 20 μL cDNA reaction. The RNA/primer mix was incubated at 65°C for 10 min to denature the RNA. After this step, components were added so the final 20 μL reaction volume contained 1 × Expand™ RT buffer (Roche), 10 mM DTT, 1 mM dNTPs and 8 U RNaseOUT™ RNase inhibitor (Invitrogen). For a reactions to make cDNA, 50 U of Expand™ reverse transcriptase (Roche) was added. If reactions were to be used as no RT controls, the reverse transcriptase was omitted. Reactions were incubated at 30°C for 10 min to allow the random hexamer primers to anneal, then incubated at 42°C for 45 min to allow primer extension. cDNA was normally diluted before use.

2.19 PLANT-ENDOPHYTE SYMBIOTA GROWTH AND MAINTENANCE

2.19.1 Plant maintenance

Plant symbiota created in this study were maintained at the GMO grass glasshouse at AgResearch Grasslands, Palmerston North. Plants were grown in potting mix containing the slow release fertiliser Osmacote™. Plants were maintained by regularly cutting the plants back to several cm above the leaf base. Plants were treated for fungal infections by spraying with antifungal agents and insect infestations by spraying with insecticides. Plants were occasionally repotted to reduce the root mass of grass plants.

2.19.2 Inoculation of grass seedlings with endophyte hyphae

2.19.2.1 Surface sterilisation of grass seeds

Grass seeds were soaked in 50% H_2SO_4 for 30 min to remove traces of fungicide on the seeds, then washed three times in water. The seeds were then soaked in 50% chlorine bleach for 30 min and washed three times in sterile double-distilled water. The seeds were air-dried on sterlised filter paper before use.

2.19.2.2 Inoculation of grass seedlings with endophytes

Grass seeds were germinated on water agar (Section 2.3.8) at 22°C for seven days. Seedlings were grown in the dark to ensure the seedling was etiolated, making the location of the meristematic zone (which appears as a slight bulge in the pseudostem) easier to find. Looking at the seedlings under a dissecting microscope, a small incision was cut in the meristematic zone. A small square of agar containing fungal hyphae was then placed over the incision. The inoculated grass seedlings were then incubated for a further seven days in the dark, followed by at least two days under bright light before the seedlings were transferred into root trainers.

2.19.2.3 Root training of inoculated seedlings

Seedlings were placed in potting mix containing fertiliser in root training pots in the GMO glasshouse at AgResearch. Seedlings were grown for approximately one month before being assessed for the presence of endophyte by aniline blue staining (Section 2.19.3.1) or immunoblot detection (Section 2.19.3.2).

2.19.3 Detection of infected seedlings after endophyte inoculation

2.19.3.1 Aniline blue staining

The outermost leaf sheath was removed from a grass tiller and epidermal strips were scraped off using a scalpel blade and placed into a drop of aniline blue stain (Section 2.4.4.1) on a slide and covered by a coverslip. The slide was heated to remove air bubbles and hasten staining. The slides were examined by microscopy as described in Section 2.20.

2.19.3.2 Immunodetection by immunoblotting

2.19.3.2.1 Immunoblotting blocking solution

Blocking solution contained 20 mM Tris (hydroxymethyl) methylamine, 50 mM NaCl, 0.5% non fat milk powder and 10 mM HCl in distilled water at pH 7.5.

2.19.3.2.2 Immunoblotting Tris buffer

Tris buffer contained 200 mM Tris (hydroxymethyl) methylamine in distilled water at pH 8.2.

2.19.3.2.3 Fast Red chromogen

Fast Red was dissolved at 0.6% (w/v) in immunoblotting Tris buffer (Section 2.19.3.2.2) and naphthol AS-MX phosphate was dissolved at 1 mg/mL in immunoblotting Tris buffer. The Fast Red and naphthol AS-MX phosphate solutions were then combined at a 1:1 ratio.

2.19.3.2.4 Immunoblot detection of endophyte in grass tissues

This method is based on that of Gwinn et al. (1991). Freshly cut grass tillers were pressed onto 0.45 μM Electran Nitocellulose membrane (BDH). The membrane was incubated in immunoblotting blocking buffer (Section 2.19.3.2.1) for at least 2 h at room temperature. Fresh blocking solution containing 1000 fold dilution of primary antibody (a rabbit polyclonal antibody prepared against homogenised endophyte mycelia) was added, and incubated with shaking overnight at 4°C. The primary antibody/blocking solution was removed, and a 2000 fold dilution of anti-rabbit

enzyme-conjugated secondary antibody was added to the membrane. The membrane was then incubated at room temperature for 2 h. The secondary antibody-blocking solution was removed, and the membrane was rinsed in fresh blocking solution. The membrane was incubated in Fast Red chromogen (Section 2.19.3.2.3)

2.20 MICROSCOPY AND PHOTOGRAPHY

Microscopic analysis was performed at the Confocal Microscope facility, IMBS, Massey University using bright field microscopy on an upright fluorescent microscope with DIC optics and bright field with image capture using an attached digital camera. Photos of fungal hyphae in culture were taken by a digital camera using bright field microscopy on a stereo dissecting microscope. All other plate photos were taken using a Olympus OM camera.

2.21 BIOINFORMATICS

DNA sequences were assembled into contigs using Sequencher™ 4.5 (Genetic Codes Corporation). Sequences were annotated and diagrammatically represented using the MacVector™ 4.2.3 program (Accelrys). Sequences were analysed for similarities to other nucleotide or peptide sequences by BlastN, BlastX and BlastP (Altschul et al., 1997). Open reading frames were identified by similarity to other fungal sequences detected by BlastX or by FGENESH HMM-based gene structure prediction using the *F. graminearum* model at http://www.softberry.com (Salamov and Solovyev, 2000). Sequences from fungal genomes were obtained as follows: *A. nidulans, C. globosum, F. graminearum, M. grisea, N. crassa, S. nodorum, U. maydis*, *Coprinus cinereus* and *Cryptococcus neoformans* serotype A were obtained from http://www.broad.mit.edu/annotation/fgi/. *P. anserina* sequences were obtained from http://podospora.igmors.u-psud.fr/facts.html, and *Phanerochaete chrysosporum* sequences from http://genome.jgi-psf.org/whiterot1/whiterot1.home.html.

Alignments of nucleotide and peptide sequences were performed using the ClustalW module of MacVector ™ 4.2.3. Phylogenetic analyses were performed using Neighbour Joining (with tie breaking resolved randomly) with Poisson distribution of

distances with gaps distributed proportionally, with bootstrapping analysis performed with 1000 repetitions.

MEME (Multiple EM for Motif Elicitation) analysis of promoter DNA sequences to search for frequently occurring motifs was performed as described in Bailey and Elkan (1994) at the website http://meme.sdsc.edu/meme/meme.html. SignalP analysis of peptide sequences was performed at http://www.cbs.dtu.dk/services/SignalP/ using the SignalP3.0 server, which is optimised for the detection of eukaryotic signal peptides and signal anchors typically found in secreted and membrane proteins (Bendtsen et al., 2004).

CHAPTER 3

Results:

E. festucae subtilsin-like protease gene family

3.1 *E. FESTUCAE* AND *N. LOLII* PROTEINASE K FAMILY GENES (SUBFAMILIES 1 AND 2)

The first aim of this study was to characterise members of the subtilisin-like protease gene family in *E. festucae* Fl1. Previous studies identified three different subtilisin-like protease genes from *Epichloë* and *Neotyphodium* spp. closely related to *E. festucae* Fl1 (McGill, 2000; Reddy et al., 1996). The *prt1* and *prt2* genes were identified in *N. lolii* Lp19 by library screening using PCR products amplified using primers based on the *At1* gene from *E. typhina*. The *prt1*, *prt2* and *At1* genes all encoded distinct subtilisin-like proteases. The characterisation of homologues of these three genes, along with additional subtilisin-like protease genes, is reported.

3.1.1 The prt1 and prt5 genes

The *N. lolii* Lp19 *prt1* gene was previously identified within a λGEM-12 *N. lolii* Lp19 genomic DNA library (McGill, 2000) using the *prt1* probe described in McGill (2000). The corresponding *prt1* gene was identified within a *E. festucae* Fl1 genomic DNA cosmid library described in Tanaka et al. (2005) using a [^{32}P]-dCTP-labelled PCR product amplified from *N. lolii* Lp19 *prt1* with the primer pair MM5-MM2 as a probe (Section 2.10). Six independent cosmids from the library hybridised to this probe. Cosmids 1A1 and 3F7 were used for subcloning and sequencing.

Comparison of Southern hybridisation and sequence data for the *N. lolii* Lp19 and *E. festucae* Fl1 *prt1* genes showed differences in restriction fragment lengths between the two genes at the 3' end, but not at the 5' end (Figures 3.1, 3.2 and 3.3; Table 3.1). Based on the Southern hybridisation, a 4.6 kb *Pst*I fragment from Fl1, chosen because it contained the complete *prt1* gene (Figures 3.1 and 3.3, isolated from cosmid 3F7), was subcloned into pUC118 to create the pMM51 plasmid and then sequenced. Sequencing of pMM51 and direct sequencing of the cosmids 1A1 and 3F7 showed another subtilisin-like protease gene, *prt5*, was directly upstream of *prt1* in the *E. festucae* Fl1 genome (Figure 3.3). Southern blotting demonstrated that the *E. festucae* Fl1 *prt5* and *prt1* genes were on a common 3 kb *Rca*I band (Figures 3.1 and 3.4; Tables 3.1 and 3.2).

Further sequencing upstream of the *N. lolii* Lp19 *prt1* gene was performed using the plasmids pMM3 and pMM4, which contained *Eco*RI fragments from λMM30.4 (previously identified within a λGEM-12 *N. lolii* Lp19 genomic DNA library, as described in McGill (2000). pMM3 contained a 1.9 kb *Eco*RI fragment, which was identified by PCR screening with the primer pair MM131-MM48 as containing part of the *prt5* gene. pMM4 contained a 1.5 kb *Eco*RI fragment, which may have been truncated in comparison to the genomic band as some λ vector sequence was found in this insert (data not shown). Sequencing from the pMM3 and pMM4 plasmids demonstrated that *N. lolii* also contained a gene with strong identity to the *E. festucae* Fl1 *prt5* gene directly upstream of the *N. lolii prt1* gene.

The *N. lolii* Lp19 and *E. festucae* Fl1 *prt1* genes contain two exons, separated by a single intron at a conserved position (confirmed by sequencing of a cDNA product). Both *prt1* genes encode 434 amino acid residue-preproproteins with high levels of similarity to the *Metarhizium anisopliae* proteases Pr1D, Pr1E and Pr1F (Bagga *et*

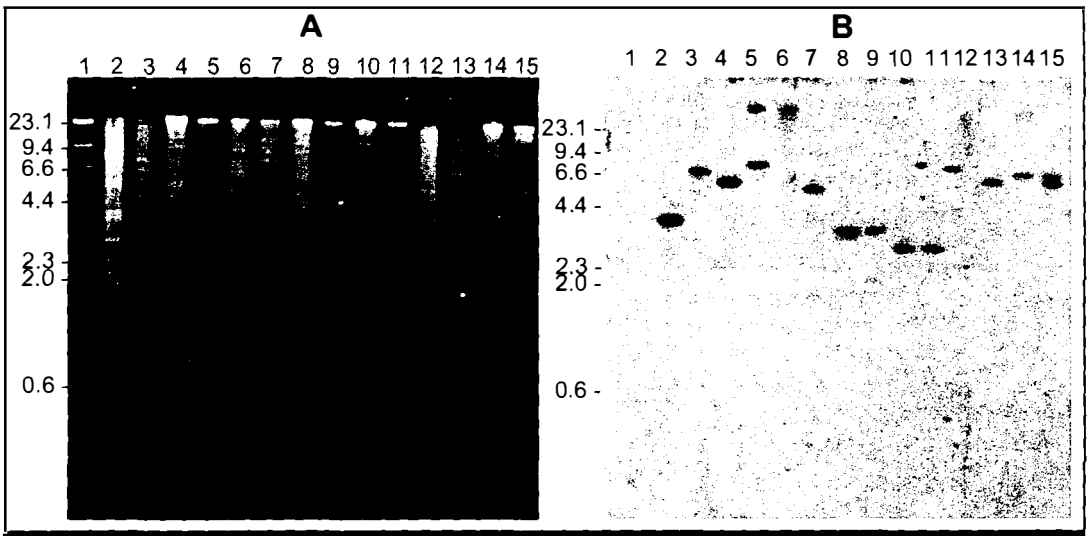

Figure 3.1 Southern analysis of *N. lolii* Lp19 and *E. festucae* Fl1 *prt1*

Southern analysis of *N. lolii* Lp19 and *E. festucae* Fl1 *prt1*. **(A)** *N. lolii* Lp19 (lanes 2, 4, 6, 8, 10, 12 and 14) and *E. festucae* Fl1(lanes 3, 5, 7, 9, 11, 13 and 15) genomic DNA (1 µg) digested with *Eco*RI (lanes 2 and 3), *Nco*I (lane 4 and 5), *Pst*I (lanes 6 and 7), *Rca*I (lanes 8 and 9), *Sal*I (lanes 10 and 11), *Sst*I (lanes 12 and 13) and *Xho*I (lanes 14 and 15). Lane 1 contains λ *Hin*dIII ladder. Sizes of marker fragments are shown in kb. **(B)** Autoradiograph of the gel from **A** hybridised with a [^{32}P]-labelled *N. lolii* Lp19 *prt1* fragment amplifed with primers MM5 and MM2.

Table 3.1 Fragments homologous to *N. lolii* Lp19 and *E. festucae* Fl1 *prt1*

Endophyte strain	*Eco*RI	*Nco*I	*Pst*I	*Rca*I	*Sal*I	*Sst*I	*Xho*I
N. lolii Lp19	3.3 kb	4.8 kb	>23 kb	3.0 kb	2.6 kb	22.0 kb	20.6 kb 5.6 kb
E. festucae Fl1	5.6 kb	6.0 kb	4.6 kb	3.0 kb	2.6 kb	5.0 kb	4.9 kb 5.6 kb

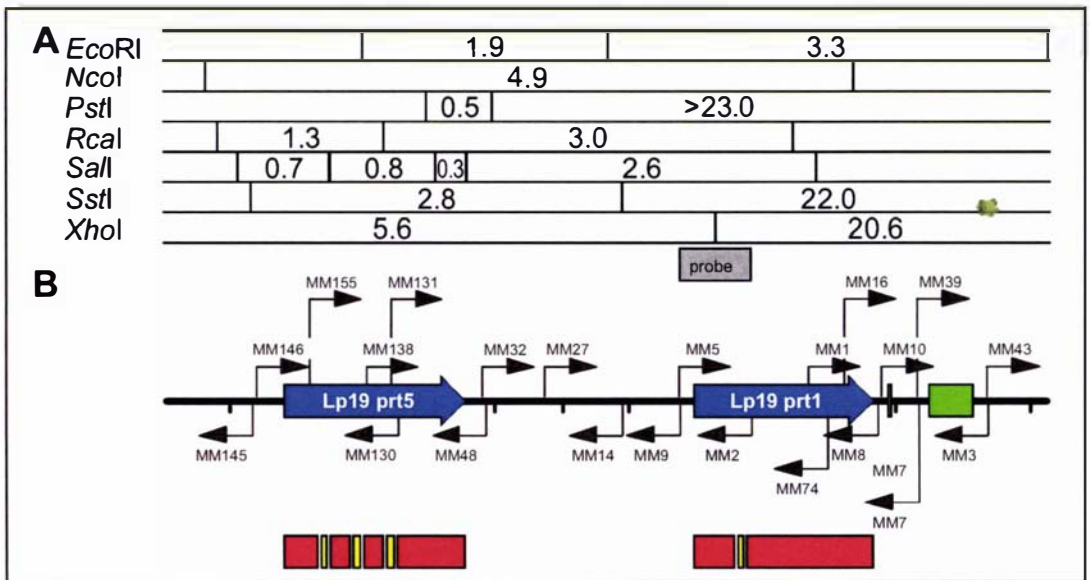

Figure 3.2 Structure of the *N. lolii* Lp19 *prt5* and *prt1* genes

Structure and restriction map of the *N. lolii* Lp19 *prt5* and *prt1* genomic region. **(A)** Restriction map of *N. lolii* Lp19 *prt5* and *prt1* genomic region. Sizes of restriction fragments are shown in kb. **(B)** Structure of the *N. lolii* Lp19 *prt5* and *prt1* genomic region. The *N. lolii* Lp19 *prt5* and *prt1* coding regions are shown in blue. Primers are shown by arrows (5' to 3'). The exon-intron structure of the genes is shown beneath, with exons and introns indicated by red and yellow boxes respectively. Microsatellite regions downstream of *N. lolii* Lp19 *prt1* are indicated by green boxes. The position that the probe used in Figure 3.1 would hybridise to is indicated by a grey box.

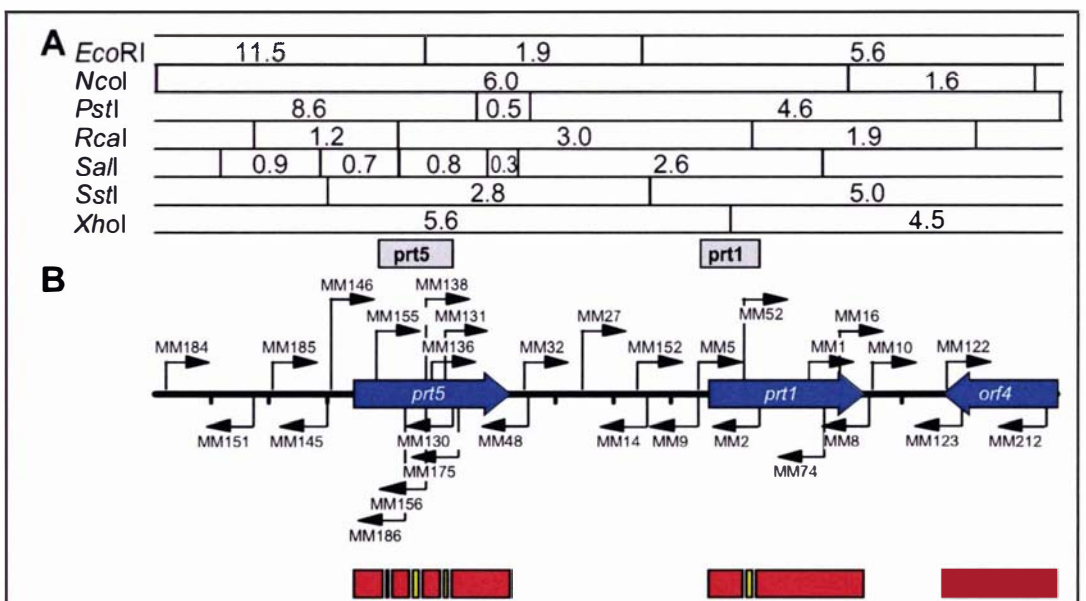

Figure 3.3 Structure of the *E. festucae* Fl1 *prt5* and *prt1* genes

Structure and restriction map of the *E. festucae* Fl1 *prt5* and *prt1* genomic region. **(A)** Restriction map of *E. festucae* Fl1 *prt5* and *prt1* genomic region. Sizes of restriction fragments are shown in kb. **(B)** Structure of the *E. festucae* Fl1 *prt5* and *prt1* genomic region. The *E. festucae* Fl1 *prt5* and *prt1* coding regions are shown in blue. Primers are shown by arrows (indicating direction of amplification from the primers). The exon-intron structure of the genes is shown beneath, with exons and introns indicated by red and yellow boxes respectively. The positions where the probes used in Figures 3.1 and 3.4 would hybridise are indicated by grey boxes labelled prt1 and prt5 respectively.

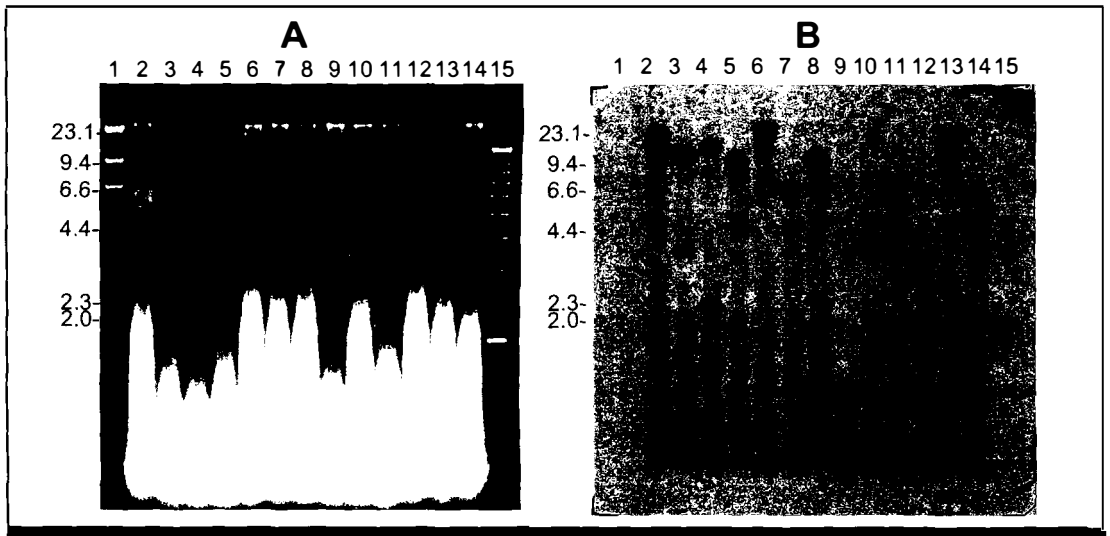

Figure 3.4 Southern analysis of *E. festucae* Fl1 *prt5*

Southern analysis of *E. festucae* Fl1 *prt5*. **(A)** *E. festucae* Fl1 genomic DNA (1 µg) digested with *Bam*HI (lane 2), *Bgl*II (lane 3), *Eco*RI (lane 4), *Hin*dIII (lane 5), *Kpn*I (lane 6), *Nco*I (lane 7), *Pst*I (lane 8), *Sal*I (lane 9), *Rca*I (lane 10), *Sph*I (lane 11), *Sst*I (lane 12), *Xba*I (lane 13) and *Xho*I (lane 14). Lanes 1 and 15 contain λ *Hin*dIII and 1 kb plus ladder (Invitrogen) respectively. Sizes of marker fragments are shown in kb. **(B)** Autoradiograph of the gel from **A** hybridised with a [^{32}P]-labelled *E. festucae* Fl1 *prt5* fragment amplifed with primers MM155 and MM130.

Table 3.2 Fragments homologous to *E. festucae* Fl1 *prt5*

Enzyme	Hybridising fragment size (kb)
*Bam*HI	>23.0
*Bgl*II	9.0, 2.8
*Eco*RI	11.5, 1.8
*Hin*dIII	8.4
*Kpn*I	20.0
*Nco*I	5.5
*Pst*I	8.6
*Sal*I	0.8, 0.7
*Rca*I	3.0, 1.2
*Sph*I	5.1
*Sst*I	2.5
*Xba*I	12.0
*Xho*I	5.0

al., 2004), and *Fusarium graminearum* hypothetical proteins FG00806.1, FG11405.1 and FG08464.1 (http://www.broad.mit.edu) (Figure 3.18). However, the bootstrap value for this clade is relatively low (Figure 3.18). Analysis of the *N. lolii* Lp19 and *E. festucae* Fl1 Prt1 preproprotein sequences showed a putative signal peptide cleaved between amino acid residues 21 and 22 (Section 2.21, SignalP3.0 prediction, Bendtsen *et al.,* 2004; Appendix 17). The *N. lolii* Lp19 and *E. festucae* Fl1 Prt1 preproproteins are 99% identical, differing only at amino acid residues 164 (*N. lolii* Lp19 I > *E. festucae* Fl1 V) and 431 (*N. lolii* Lp19 S > *E. festucae* Fl1 P).

The *N. lolii* Lp19 and *E. festucae* Fl1 *prt5* genes contain four exons. The intervening introns, which were confirmed by direct sequencing of cDNA, are 64 bp in

E. festucae Fl1 (63 bp in *N. lolii* Lp19), 78 bp in *E. festucae* Fl1 (81 bp in *N. lolii* Lp19) and 74 bp in *E. festucae* Fl1 and *N. lolii* Lp19 in length respectively. Both the *N. lolii* Lp19 and *E. festucae* Fl1 *prt5* genes encode identical preproproteins of 395 amino acid residues in length. Again, both the *N. lolii* Lp19 and *E. festucae* Fl1 Prt5 preproproteins appeared to contain a signal peptide cleaved between amino acid residues 18 and 19 (Section 2.21, SignalP 3.0 prediction, Bendtsen *et al.*, 2004).

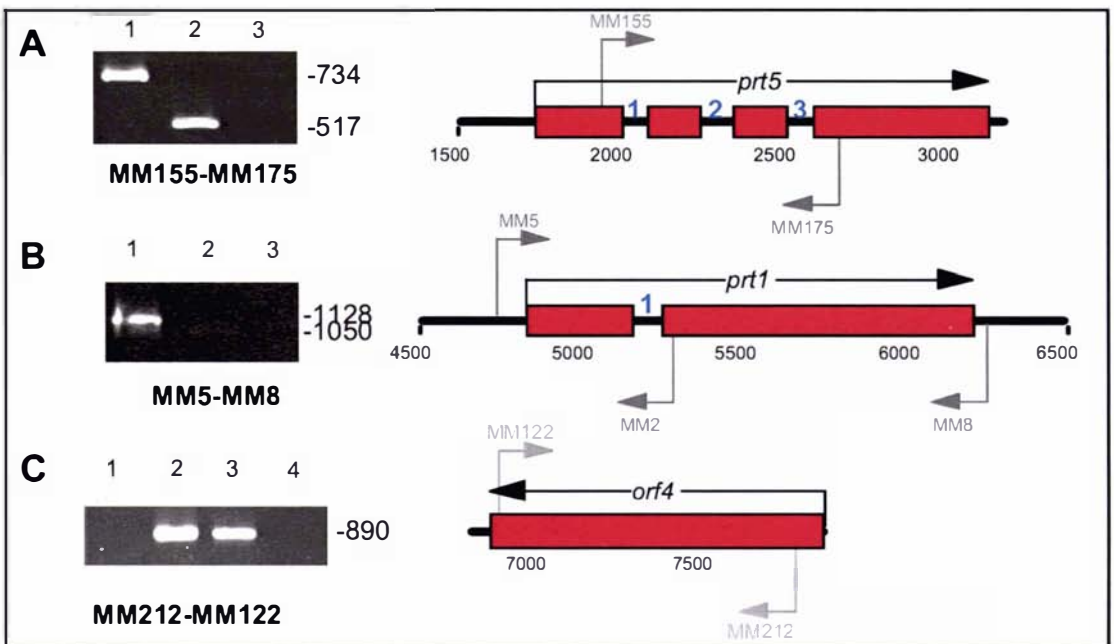

Figure 3.5 Gene structure of the *E. festucae* Fl1 *prt5* and *prt1* genes

Gene structure of the *E. festucae* Fl1 *prt5*, *prt1* and *orf4* genes. RT-PCR analysis for the *prt5* and *prt1* genes was performed with total RNA isolated from *E. festucae* Fl1 cultures grown in PD broth for 7 days, while poly A RNA was used for *orf4*. cDNA was reverse transcribed from DNase I-treated total RNA or poly-A RNA using the Expand RT enzyme (Roche) (Section 2.18.5). All fragment sizes shown adjacent to gels are indicated in bp. On the schematic diagram of each gene, the position within the *prt5-prt1* locus is indicated in bp. Exons (confirmed by sequencing of cDNA products) are indicated by red boxes. Primers are positioned above or below the sequence for forward or reverse direction respectively. Introns are numbered in blue text between exons. The position within the *prt5-prt1* locus is indicated below the sequence schematic in bp. (A) The *E. festucae* Fl1 *prt5* gene. Lane 1: *E. festucae* Fl1 genomic DNA, lane 2: 10 fold dilution of *E. festucae* Fl1 cDNA, lane 3: negative control. B) The *E. festucae* Fl1 *prt1* gene. Lane 1: *E. festucae* Fl1 genomic DNA, lane 2: 10 fold dilution of *E. festucae* Fl1 cDNA, lane 3: negative control. C) The 3' region of the *E. festucae* Fl1 *orf4* coding region. Lane 1: no RT control, lane 2: *E. festucae* Fl1 genomic DNA, lane 3: 10 fold dilution of *E. festucae* Fl1 cDNA, lane 4: negative control.

The following PCR conditions were used: 5 ng genomic DNA or 5 µL 20 fold diluted cDNA, 1x Taq polymerase buffer (Roche), 50 µM each dNTP, 200 nM of each primer, and 0.5 U Taq polymerase in a volume of 25 µL. The PCR amplification conditions were as follows: 94°C for 2 min, followed by 35 cycles of 94°C for 30 s, 60°C for 30 s, 72°C for 1 min, then one cycle of 72°C for 5 min.

FGENESH analysis also identified another incomplete open reading frame, *orf4*, directly downstream of *E. festucae* Fl1 *prt1*. The *orf4* gene encodes a protein that shares some identity with a small gene family of unknown function from *F. graminearum,* consisting of the FG10477, FG02198 and FG10456 genes. Related sequences are present in the genome of the closely related *Trichoderma reesei*, but not in the genomes of the more distantly related species M. *grisea, N. crassa or A. nidulans* (Appendix A3). The *orf4* gene is expressed in culture (Figure 3.5).

The promoter regions of both the *E. festucae* Fl1 *prt5* and *prt1* genes were analysed for the presence of sequences known to bind the fungal global transcription factors CreA, AreA/Nit2/AreA, PacC and Seb1. CreA represses gene expression in response to the presence of glucose (Dowser and Kelly, 1989), while AreA/Nit2/AreA activates gene expression in the absence of a preferred nitrogen source such as glutamine or ammonium (Marzluf, 1997). PacC regulates the expression of genes in response to pH (Mingot et al., 2001), while the role of Seb1 in gene regulation is unclear (Peterbauer et al., 2002).

The 1688 bp intergenic region between the *E. festucae* Fl1 *prt5* and *prt1* coding regions (containing the promoter for the *E. festucae* Fl1 *prt1* gene) contained seven putative CreA binding sites, while only two putative binding sites were found within the gene itself. Within this region, there were two closely spaced putative CreA binding sites. However, the 1655 bp region downstream of *prt1* contained 10 putative binding sites. This is in contrast with the *E. festucae* Fl1 *prt5*, which contained 10 putative CreA binding sites in its promoter, but also contained 12 putative CreA binding sites in the *prt5* coding region (Figure 3.6A).

The *E. festucae* Fl1 *prt1* promoter contained no strong affinity sites for the AreA/Nit2/AreA transcription factor, but did contain six weaker affinity sites (Figure 3.6B). Again, only two weak affinity binding sites were present in the *E. festucae* Fl1 *prt1* coding region. However, the *E. festucae* Fl1 *prt5* promoter contained seven high affinity binding sites for ArcA/Nit2/AreA (HGATAR), with three weak affinity binding sites (GATA). The *E. festucae* Fl1 *prt5* coding region, however, only contained one strong and one weaker affinity AreA/Nit2/AreA binding sites. These

results could suggest that *E. festucae* Fl1 *prt5* may be regulated by availability of a preferred nitrogen source.

Both *E. festucae* Fl1 *prt5* and *prt1* promoters contained 4 putative PacC binding sites, while the coding regions contained 6 and 7 putative binding sites for *prt5* and *prt1* respectively (Figure 3.6C). The distribution of Seb1 binding sites was most interesting for the Fl1 *prt5* gene, which contained 5 putative Seb1 binding sites

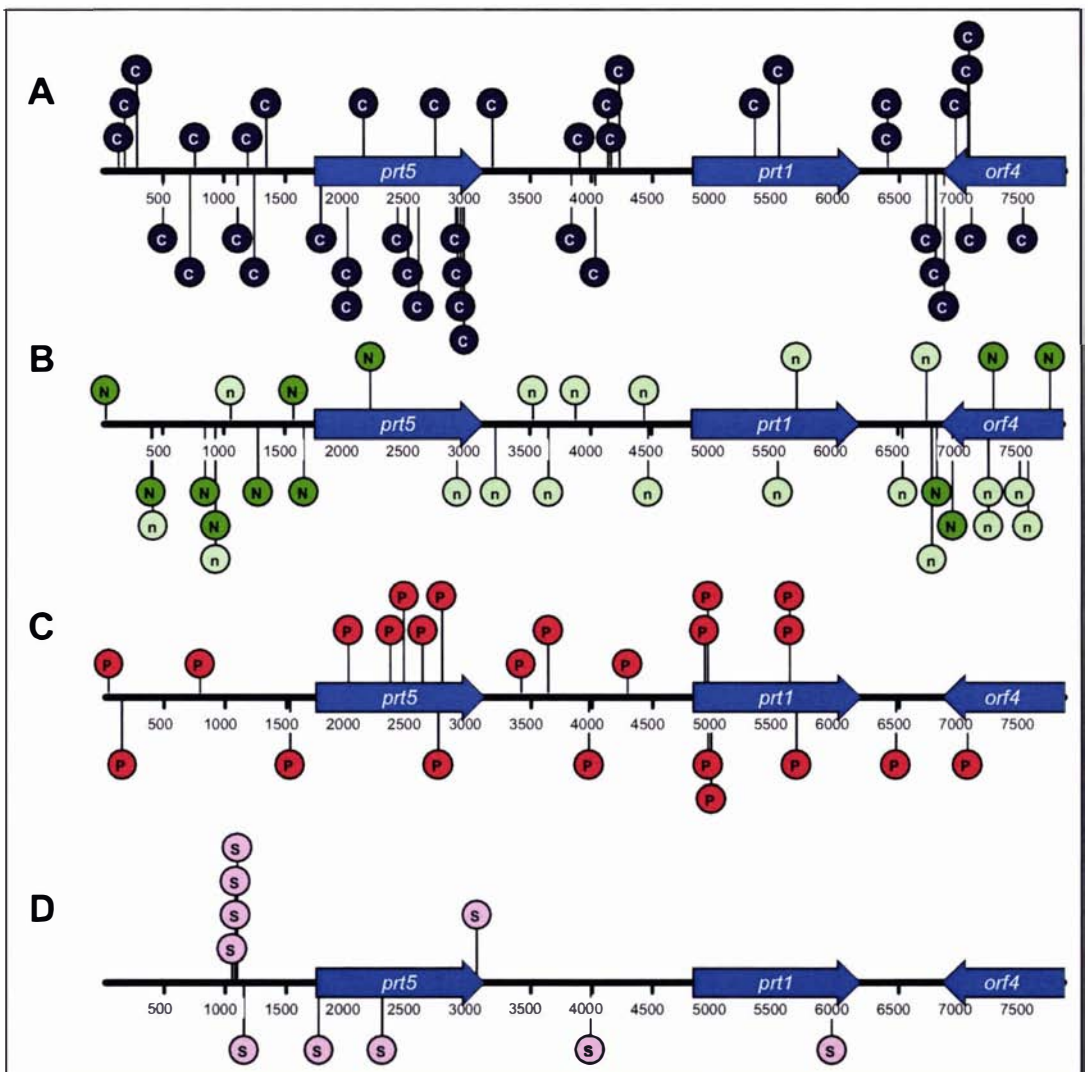

Figure 3.6 Potential binding sites for fungal global transcription regulators in *E. festucae* Fl1 *prt5* and *prt1*

Analysis for putative binding sites for the fungal transcription factors CreA (carbon regulation), Nit2/AreA (nitrogen regulation), PacC (pH regulation) and Seb1 (transcriptional regulator) in the *E. festucae* Fl1 *prt5* and *prt1* genes.(A) Putative binding sites for CreA (SYGGRG) are indicated by blue lollipops containing the letter C. (B) Putative binding sites for Nit2/AreA (HGATAR) are indicated by green lollipops containing the letter N. Weaker binding sites (GATA) are indicated by light green lollipops containing the letter n. (C) Putative binding sites for PacC (GCCARG) are indicated by red lollipops containing the letter P. (D) Putative binding sites for Seb1 (AGGGG) are indicated by purple lollipops containing the letter S.

within a very small region of the promoter, but three putative binding sites spread throughout the *E. festucae* Fl1 *prt5* coding region. This could indicate some role for Seb1 (or other transcription factors binding to this sequence) in regulating expression of the *E. festucae* Fl1 *prt5* gene. Meanwhile, the *E. festucae* Fl1 *prt5* promoter and coding region both contained only a single putative binding site for Seb1.

The *prt1* promoter contained more CreA, strong affinity AreA/Nit2, PacC and Seb1 binding sites, but less weak affinity AreA/Nit2 binding sites, than expected if the binding site sequences occurred randomly throughout the promoter[1]. The *prt1* promoter contained approximately the same number of CreA binding sites if the sequence occurred at random through the promoter. However, less of both the strong and weaker affinity AreA/Nit2 binding sites and the Seb1 binding sites were seen than expected in this promoter sequence. Slightly more PacC binding sites were observed than expected for a random occurrence through the promoter.

MEME (Multiple EM for Motif Elicitation) analysis was also carried out on the promoter to look for any sequences over-represented in the promoter sequence (Section 2.21, Figure 3.7). All of the resulting MEME motifs are listed in Appendix A11). The most common sequence identified in the *E. festucae* Fl1 *prt1* promoter was a poly A sequence (MEME motif 1). However, the *prt5* promoter did not contain this motif. Both the *prt5* and *prt1* promoters contained MEME motifs 2, 12 and 18. The *prt5* promoter also contained multiple copies of MEME motifs 4, 6, 10 and 15, which were also found as motifs in the promoters of the *prt2* and *prt3* genes (Figure 3.7, Section 3.1.2 and 3.1.3).

3.1.2 The prt2 gene

The *prt2* gene from *N. lolii* Lp19 was also identified and partially sequenced in a previous study (McGill, 2000). The gene was identified within a λGEM-12 *N. lolii* Lp19 genomic DNA library using the *prt2* probe described in McGill (2000). In this

---

[1] Probability of 5 bp sequence Seb1 binding sequence AGGGG assuming bases distributed randomly:
Probability of having a particular base at nucleotide position (assuming random distribution of nucleotides)= 0.25 (1 of 4 possible nucleotides)
Therefore: the probability of having AGGGG sequence $=(0.25)^5 = 9.77 \times 10^{-4}$
The probability of having AGGGG sequence in 2.3 kb of promoter sequence
$= 9.77 \times 10^{-4}$ x number of bases (2300) x 2 (to account for double stranded DNA)
= **4.5** expected instances of AGGGG sequence in 2300 base pairs of promoter

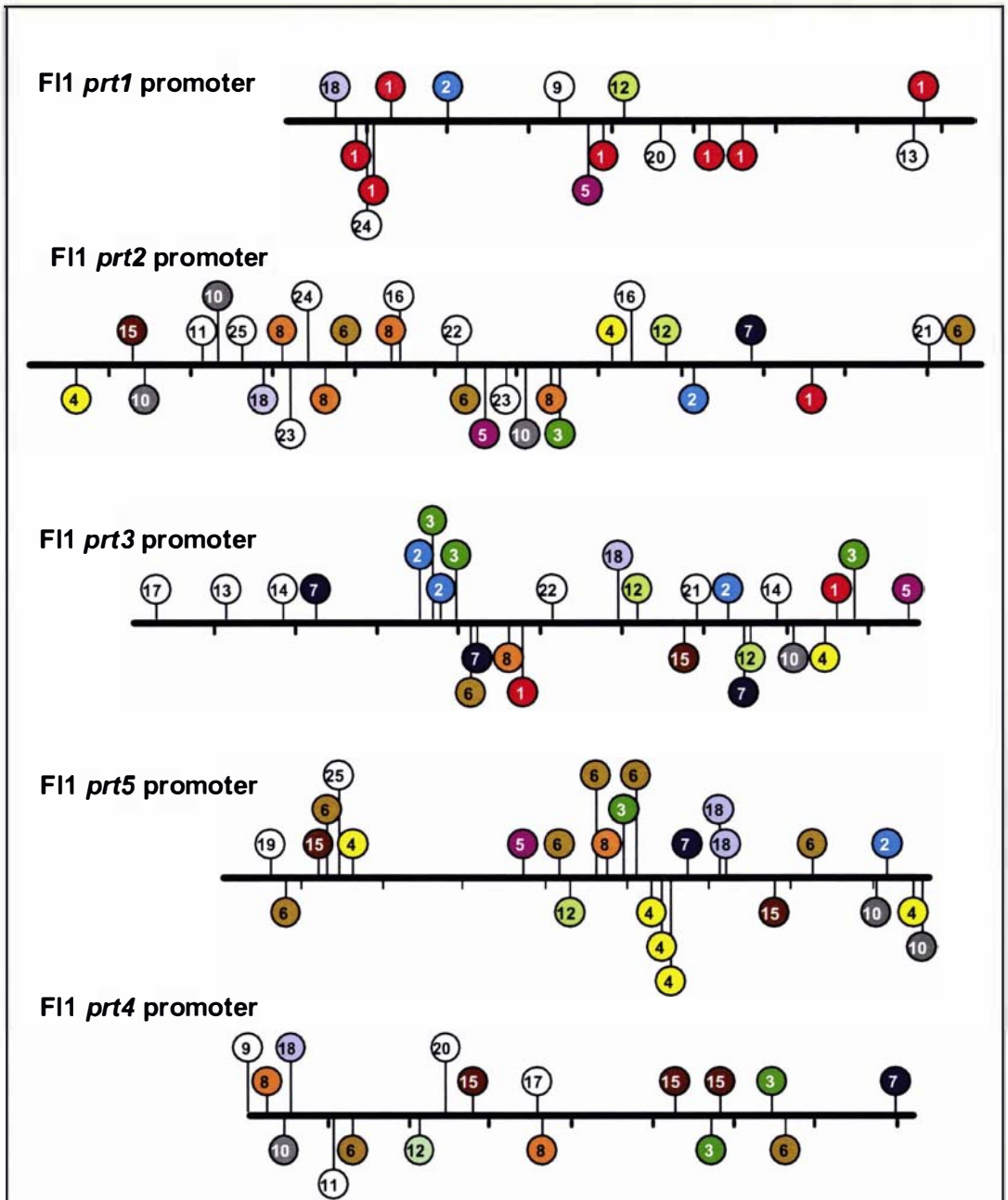

Figure 3.7 MEME analysis of repeated sequence elements found in the *prt* promoters

MEME analysis of the *E. festucae* Fl1 *prt* promoters (performed as described in Appendix A11)

previous study, a 2 kb truncated *Bam*HI fragment (from λMM3.3) had been subcloned into pUC118 (to give the vector pMM7) and sequenced. In this study, the remainder of the coding region of *N. lolii prt2* along with further downstream sequence was obtained by directly sequencing λMM3.3.

Southern blotting of *N. lolii* Lp19 (with related strains *N. lolii* AR1 and *E. typhina* x *N. lolii* hybrid Lp1) was performed in order to develop a restriction map of the *N. lolii* Lp19 *prt2* locus (Figure 3.8, Table 3.3). This showed that pMM7 did indeed contain a truncated *Bam*HI fragment, with the genomic *Bam*HI digest giving a fragment of 3.6 kb (Figure 3.8D). Direct sequencing of λMM3.3 using the MM14

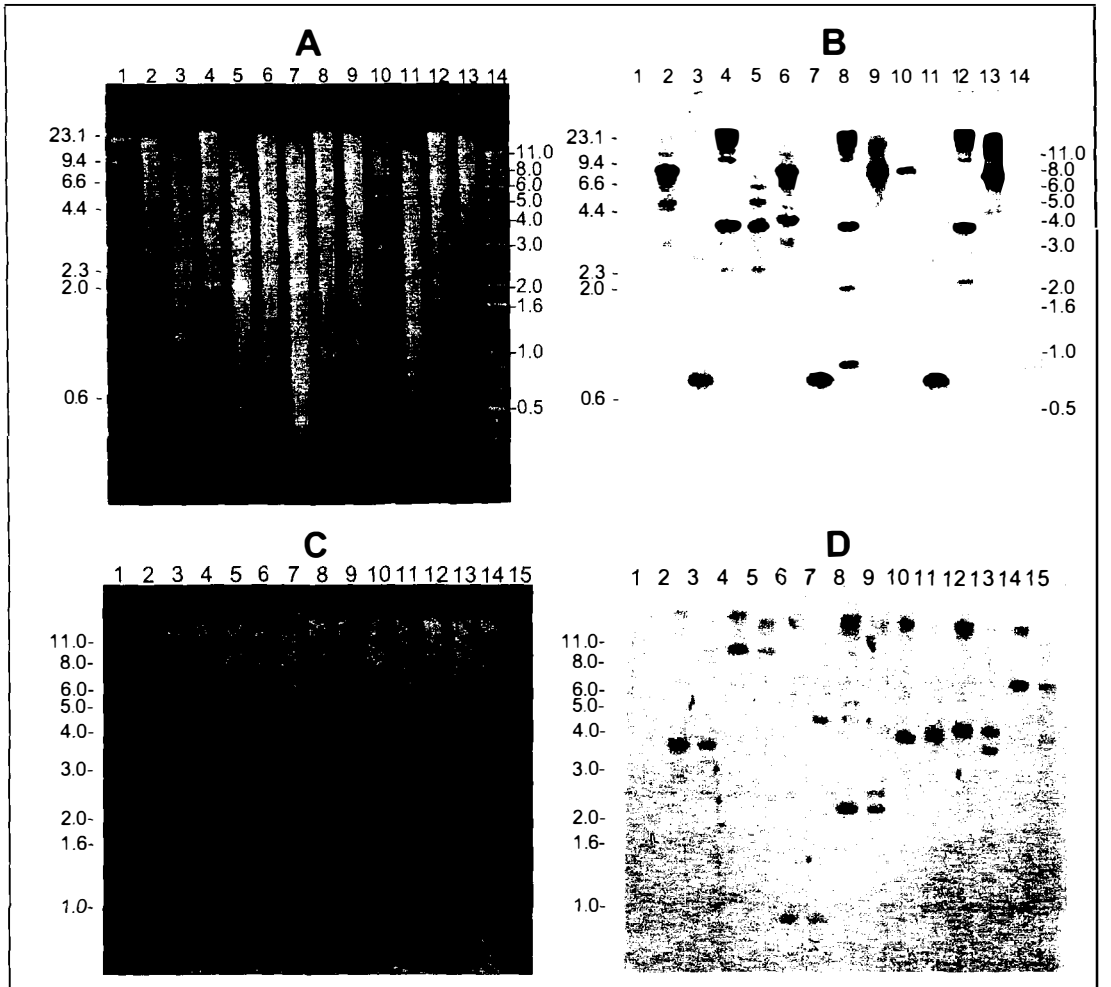

Figure 3.8 Southern analysis of *prt2*

Southern analysis of *prt2*. **(A)** Endophyte genomic DNA (2 µg) from *N. lolii* Lp19 (lanes 2-5) digested with *Eco*RI (lane 2), *Hin*dIII (lane 3), *Sal*I (lane 4) and *Sal*I/*Sst*I (lane 5); *N. lolii* x *E. typhina* strain Lp1 (lanes 6-19) digested with *Eco*RI (lane 6), *Hin*dIII (lane 7), *Sal*I (lane 8) and *Sst*I (lane 9); *N. lolii* strain AR1 (lanes 10-13) digested with *Eco*RI (lane 10), *Hin*dIII (lane 11), *Sal*I (lane 12) and *Sst*I (lane 13); Lanes 1 and 15 contain λ *Hin*dIII and 1 kb plus (Invitrogen) ladders respectively. Sizes of marker fragments are shown in kb. **(B)** Autoradiograph of the gel from **A** hybridised with a [^{32}P]-labelled *Eco*RI-*Sst*I fragment from the vector pGH3, containing the larger PCR product shown in Appendix 1. **(C)** Endophyte genomic DNA (2 µg) from *N. lolii* Lp19 (lanes 2, 4, 6, 8, 10, 12 and 14) and *N. lolii* x *E. typhina* strain Lp1 (lanes 3, 5, 7, 9, 11, 13 and 15) digested with *Bam*HI (lanes 2 and 3), *Cla*I (lanes 4 and 5), *Eco*RV (lanes 6 and 7), *Nco*I (lanes 8 and 9), *Pst*I (lanes 10 and 11), *Sma*I (lanes 12 and 13) and *Xho*I (lanes 14 and 15). Lanes 1 and 15 contain λ *Hin*dIII and 1 kb (Invitrogen) plus ladders respectively. Sizes of marker fragments are shown in kb. **(D)** Autoradiograph of the gel from **C** hybridised with a [^{32}P]-labelled *Eco*RI-*Sst*I fragment from the vector pGH3 (McGill, 2000).

Table 3.3 Fragments homologous to *N. lolii* Lp19 *prt2*			
Enzyme	**Lp19**	**Lp1**	**AR1**
EcoRI	8.5 kb	8.5 kb, 4.0 kb	8.5 kb
HindIII	0.8 kb	0.8 kb	0.8 kb
SalI	3.8 kb	3.8 kb, 0.9 kb	3.8 kb
SstI	3.8 kb*	8.2 kb, 7.8 kb	7.8 kb
Enzyme	**Lp19**	**Lp1**	
BamHI	3.6 kb	3.6 kb, 10.0 kb	
ClaI	10.0 kb	10.0 kb	
EcoRV	0.8 kb	0.8 kb	
NcoI	2.3 kb	2.6 kb, 2.3 kb	
PstI	3.10 kb	4.0 kb, 3.10 kb	
SmaI	4.2 kb	4.2 kb, 3.4 kb	
XhoI	6.4 kb	6.4 kb	

primer showed that the only lambda sequence was upstream of 2.0 kb *Bam*HI fragment containing the *prt2* gene, so it was necessary to perform inverse PCR to obtain sequence upstream of *prt2* (as described in Section 2.17.6). A *Bam*HI digest of *N. lolii* Lp19 genomic DNA was self-ligated, then amplified with the primer pair MM38 and MM26 (Table 2.4, Figure 3.9). The inverse PCR product was subcloned into pGEM-T Easy (Promega) (to give the vector pMM12), then sequenced. This region was also sequenced by direct sequencing from a PCR product amplified from *N. lolii* Lp19 genomic DNA with the primers MM119 and MM38.

Sequencing downstream of the *prt2* coding region (i.e. in the *gcn1* region) was carried out by designing primers based on a closely related sequence from the endophyte *Neotyphodium* sp. FCB2002 (Moy *et al.*, 2002). This region was amplified with the primer pair MM56 and MM71, and the PCR product sequenced. The *N. lolii* Lp19 *gcn1* gene encodes a putative β-1,6-glucanase, with high similarities to the *Neotyphodium* sp. FCB2002 glucanase, and also to related β-1,6-glucanases from *Trichoderma harzianum* and *Verticillium fungicola*.

The *E. festucae* Fl1 *prt2* gene was identified in the same *E. festucae* Fl1 genomic DNA cosmid library described in Section 3.1.1 by probing with a MM15-MM6 PCR product amplified from *N. lolii* Lp19. Library screening identified fifteen cosmids that contained the *prt2* gene. Cosmid 13B2 was digested with *Bam*HI, and then shotgun cloned into pUC118. PCR screening using primer pairs MM15-MM6 (*prt2*) and MM56-MM55 (*gcn1*) identified transformants containing the 4 kb *Bam*HI

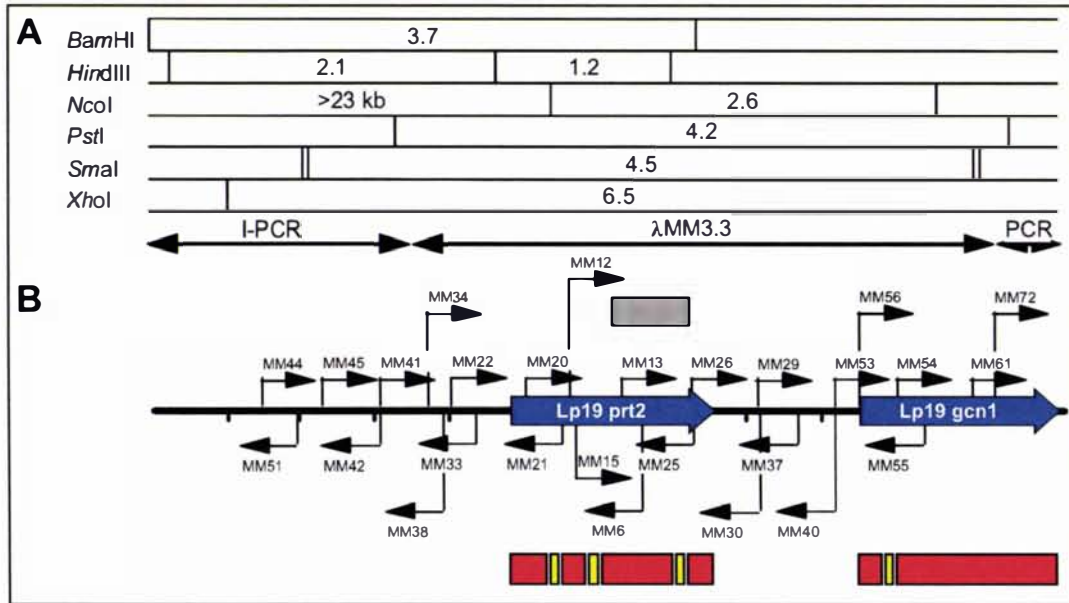

Figure 3.9 Structure of the *N. lolii* Lp19 *prt2* locus

Structure and restriction map of the *N. lolii* Lp19 *prt2* genomic region. **(A)** Restriction map of *N. lolii* Lp19 *prt2* genomic region. Sizes of restriction fragments are shown in kb. **(B)** Structure of the *N. lolii* Lp19 *prt2* genomic region. The *N. lolii* Lp19 *prt2* and *gcn1* coding regions are shown in blue. Primers are shown by black arrows (5' to 3'). The exon-intron structure of the genes is shown beneath, with exons and introns indicated by red and yellow boxes respectively. The probe used in Figure 3.7 is indicated by a grey box. The origin of each fragment is indicated by black double arrows above the sequence. The inverse PCR (I-PCR) fragment was amplified from a *Bam*HI digested genomic DNA ligation, amplified with primers MM38 and MM26. The PCR fragment at the end of the *gcn1* gene was amplified using the primers MM56 and MM71. Sequence of the MM71 primer was based on the *Neotyphodium* sp. FCB2002 ß-1,6-glucanase mRNA (accession AF535131). The annealing site of MM71 primer is not shown as it is not present in the sequence obtained.

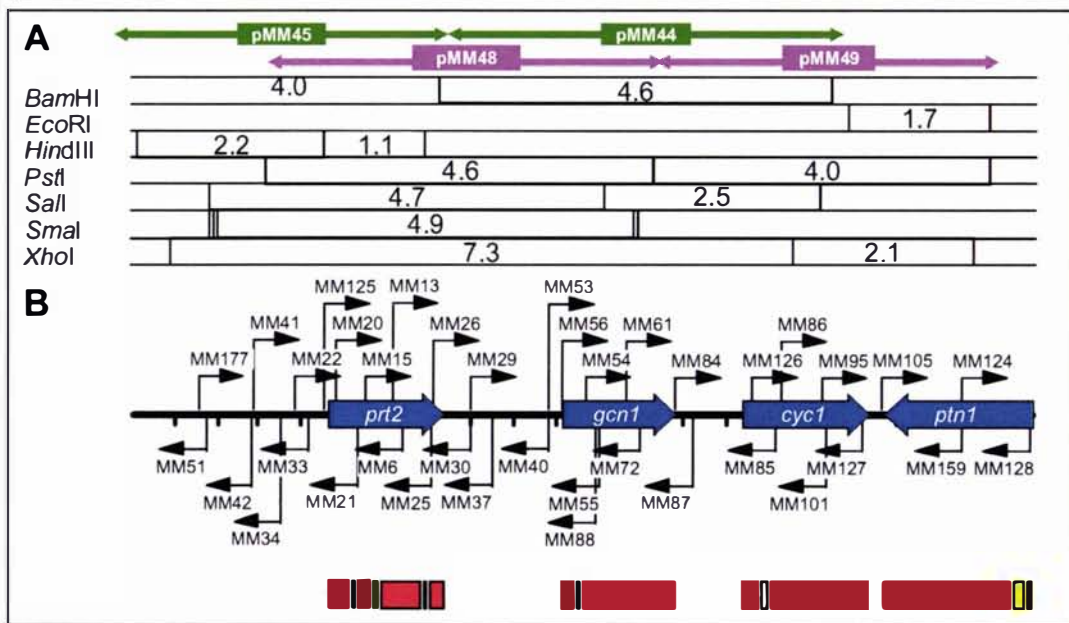

Figure 3.10 Structure of the *E. festucae* Fl1 *prt2* locus

Structure and restriction map of the *E. festucae* Fl1 *prt2* genomic region. **(A)** Restriction map of the *E. festucae* Fl1 *prt2* genomic region. Sizes of restriction fragments are shown in kb. The positions of the inserts in pMM44 and pMM45 (*Bam*HI inserts), and pMM48 and pMM49 (*Pst*I inserts) plasmids are shown above the restriction map. **(B)** Structure of the *E. festucae* Fl1 *prt2* genomic region. The *E. festucae* Fl1 *prt2*, *gcn1*, *cyc1* and *ptn1* coding regions are shown in blue. Primers are shown by black arrows (5' to 3'). The exon-intron structure of the genes is shown beneath, with exons and introns indicated by red and yellow boxes respectively.

(pMM45) or 4.6 kb *Bam*HI (pMM44) fragments respectively (Figure 3.10). In order to obtain overlapping clones giving further sequence downstream of the *prt2* and *gcn1* genes, the 13B2 cosmid was also digested with *Pst*I, then shotgun cloned into pUC118. PCR screening of transformants was performed to identify clones containing the *prt2*, *gcn1* and *cyc1* genes using the MM15-MM6, MM56-MM55 and MM86-MM101 primer pairs respectively (Table 2.4, Figure 3.10).

Through sequencing of pMM44, pMM49 and direct sequencing of cosmid 13B2, two further genes were identified downstream of the *E. festucae* Fl1 *prt2* and *gcn1* genes. These genes were named *cyc1* and *ptn1*. The *cyc1* gene encodes a putative C-type cyclin similar to the product of the *S. cerevisiae ctk2* gene (Appendix A4). Based on sequence identity, the *cyc1* gene is predicted to contain one intron (Figure 3.11C). However, this gene is expressed at low levels in culture, so the presence of this intron has not been experimentally confirmed. In *S. cerevisiae*, Ctk2 forms a divergent cyclin-CDK (cyclin dependent kinase) complex (CTDK-I) with two other subunits (Hautbergue and Goguel, 2001; Sterner et al., 1995), which regulates RNA polymerase I and II by phosphorylating a serine residue in the carboxy-terminal domain (CTD).

The *ptn1* gene encodes a putative phosphoinositide 3-phosphatase, a homologue of the *Schizosaccharomyces pombe ptn1* gene and the vertebrate PTEN gene (Maehama et al., 2001; Mitra et al., 2004). The *ptn1* gene appears to contain one intron based on sequence identitity with related fungal sequences; however, due to low expression levels introns have not been experimentally confirmed (Figure 3.11D). The Ptn1 protein contains the protein tyrosine phosphatase (PTP) superfamily catalytic motif of HCxxGxxR found in PTEN homologues. All of the catalytic residues required for phosphoinositide 3-phosphatase activity are conserved in Ptn1 (Appendix A5), suggesting that the *ptn1* gene could encode a functional phosphoinositide 3-phosphatase.

The *N. lolii* Lp19 and *E. festucae* Fl1 *prt2* genes both appear to consist of four exons (Figure 3.11, experimentally confirmed in Section 4.3.1). This exon-intron arrangement is identical to that of the *prt5* gene in intron number. Putative introns 1, 2 and 3 are 72 bp in *E. festucae* Fl1 (72 bp in *N. lolii* Lp19), 83 bp in *E. festucae* Fl1

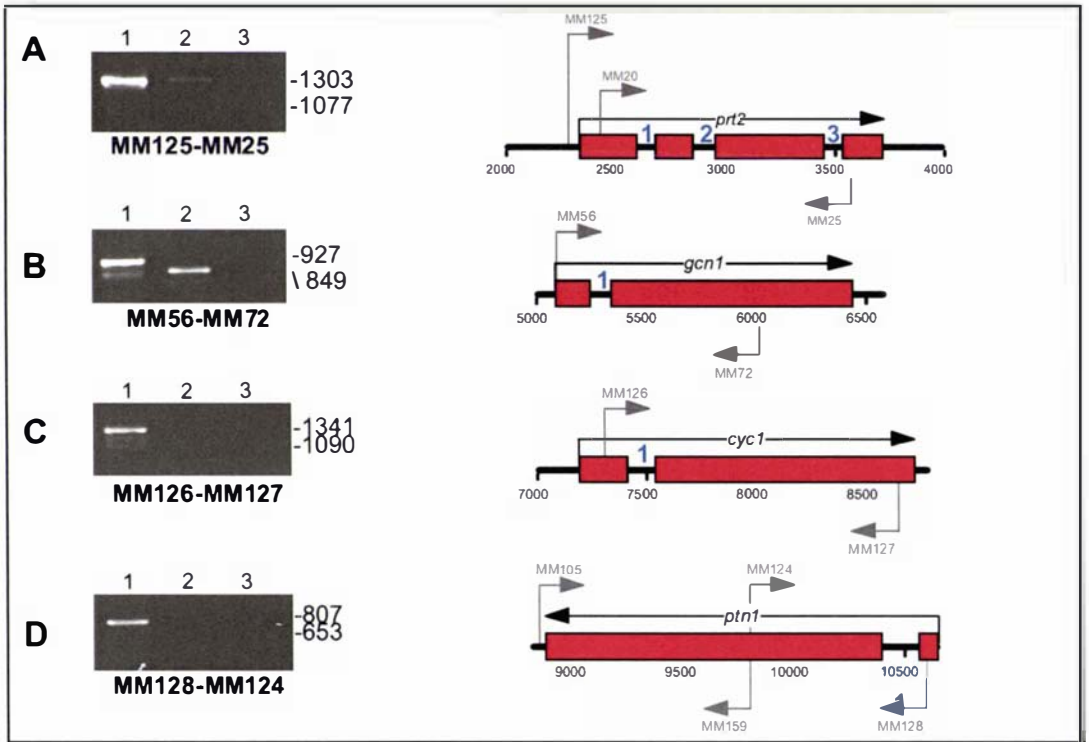

Figure 3.11 Gene structure of the *E. festucae* Fl1 *prt2*, *gcn1*, *cyc1* and *ptn1* genes

Gene structure of the *E. festucae* Fl1 *prt2*, *gcn1*, *cyc1* and *ptn1* genes. RT-PCR analysis was performed with RNA isolated from *E. festucae* Fl1 cultures grown in PD broth for 7 days. cDNA was reverse transcribed from poly-A RNA using the Expand RT enzyme (Roche) (Section 2.18.5). All fragment sizes shown adjacent to gels are indicated in bp. On the schematic diagram of each gene, the position within the *prt2* locus is indicated in bp. Exons (confirmed by sequencing of cDNA products) are indicated by red boxes. Primers are positioned above or below the sequence for forward or reverse direction respectively. Introns are numbered in blue text between exons. The position within the *prt5-prt1* locus is indicated below the sequence schematic in bp. (A) The *E. festucae* Fl1 *prt2* gene. Lane 1: *E. festucae* Fl1 genomic DNA, lane 2: 10 fold dilution of *E. festucae* Fl1 cDNA, lane 3: negative control. B) The *E. festucae* Fl1 *gcn1* gene. Lane 1: *E. festucae* Fl1 genomic DNA, lane 2: 10 fold dilution of *E. festucae* Fl1 cDNA, lane 3: negative control. C) The *E. festucae* Fl1 *cyc1* gene. Lane 1: *E. festucae* Fl1 genomic DNA, lane 2: 10 fold dilution of *E. festucae* Fl1 cDNA, lane 3: negative control. D) The *E. festucae* Fl1 *ptn1* gene. Lane 1: *E. festucae* Fl1 genomic DNA, lane 2: 10 fold dilution of *E. festucae* Fl1 cDNA, lane 3: negative control.

The following PCR conditions were used: 5 ng genomic DNA or 5 µL diluted cDNA, 1x Taq polymerase buffer (Roche), 50 µM each dNTP, 200 nM of each primer, and 0.5 U Taq polymerase in a volume of 25 µL. The PCR amplification conditions for the primer pairs MM125-MM25, MM56-MM72, MM126-MM127, MM159-MM105 and MM128-MM124 were as follows: 94°C for 2 min, followed by 30 cycles of 94°C for 30 s, 60°C for 30 s, 72°C for 1 min, then one cycle of 72°C for 5 min.

(85 bp in *N. lolii* Lp19) and 71 bp in *E. festucae* Fl1 (73 bp in *N. lolii* Lp19) respectively. Putative introns were determined based on homology with closely related fungal subtilisin-like protease genes, as no expression of this gene has been detected in culture or *in planta* (Section 3.5, Section 4.3). Exon-intron boundaries for

the *prt2* gene were confirmed by sequencing a *prt2* cDNA expressed under the control of the *A. nidulans gpdA* promoter as described in Section 4.3.

The *E. festucae* Fl1 and *N. lolii* Lp19 *prt2* genes encode highly similar preproproteins of 389 amino acid residues in length. The only differences between the *N. lolii* Lp19 and *E. festucae* Fl1 Prt2 proteins arise at positions 124 (*N. lolii* Lp19 Q > *E. festucae* Fl1 K) and 134 (*N. lolii* Lp19 A > *E. festucae* Fl1 E). Like the Prt5 and Prt1 preproproteins, the Prt2 preproprotein also contains a signal peptide probably cleaved between residues 16 and 17 (Section 2.21, SignalP 3.0 prediction, Bendtsen *et al.,* 2004), indicating that the *prt2* genes encode putative extracellular proteins. Comparisons between the *E. festucae* Fl1 and *N. lolii* Lp19 *gcn1* genes and their encoded proteins are shown in Figures 5.1 and 5.2 (Section 5.1).

The *prt2* promoter contained multiple binding sites for both CreA and AreA/Nit2 (Figure 3.12). The distribution of the CreA binding sites was noteworthy, as there were two pairs, each containing two very closely spaced CreA sites. However, less CreA sites were observed than expected by chance for this region. The number of AreA/Nit2, PacC and Seb1 binding sites was similar to that expected for a random occurrence of these sequences within the 2340 bp promoter region.

MEME analysis was also carried out on the *E. festucae* Fl1 *prt2* promoter to look for any sites over-represented in the promoter sequence (Figure 3.7, Section 2.21, Appendix A11). The *prt2* promoter contained MEME motifs 2, 12 and 18 found in both the *prt1* and *prt5* promoters, MEME motif 1 found in the *prt1* promoter, and MEME motifs 3, 4, 5, 6, 7, 8, 10, 15 and 25 found in the *prt5* promoter. The *prt2* promoter contains multiple copies of MEME motifs 4, 6, 8, 10 and 23.

3.1.3 The prt3 gene

3.1.3.1 Isolation of the *N. lolii* Lp19 and *E. festucae* Fl1 *prt3* genes

None of the *N. lolii* or *E. festucae prt5*, *prt1* or *prt2* gene products is similar enough to the *E. typhina Atl* gene product to suggest these genes are the Atl homologues. Based on this, the primer pair MM75-MM76 (Table 2.4) was designed based on the

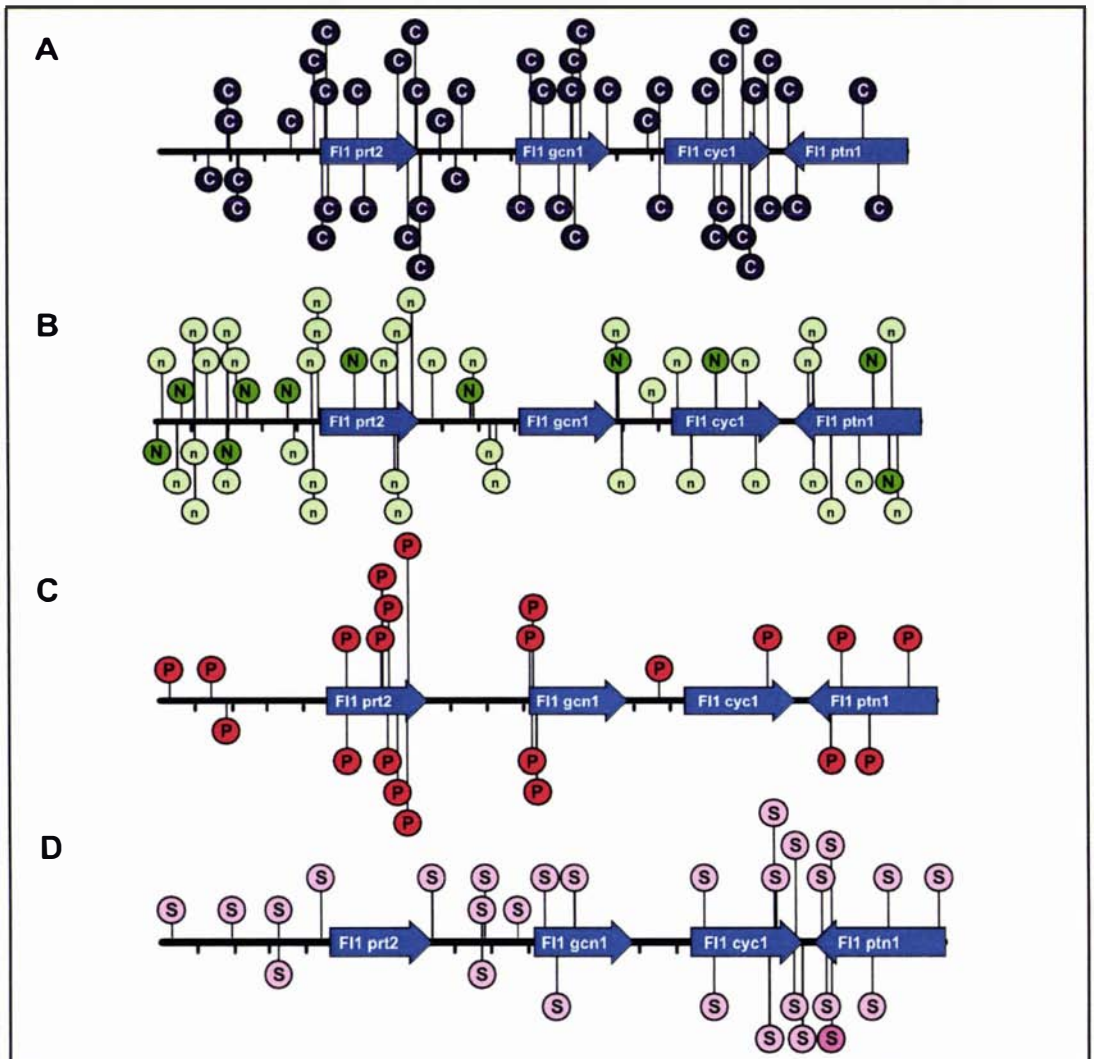

Figure 3.12 Potential binding sites for fungal global transcription regulators at the *E. festucae* Fl1 *prt2* locus

Analysis for putative binding sites for the fungal transcription factors CreA (carbon regulation), Nit2/AreA (nitrogen regulation), PacC (pH regulation) and Seb1 (transcriptional regulator) at the *E. festucae* Fl1 *prt2* locus.(A) Putative binding sites for CreA (SYGGRG) are indicated by blue lollipops containing the letter C. (B) Putative binding sites for Nit2/AreA (HGATAR) are indicated by green lollipops containing the letter N. Weaker binding sites (GATA) are indicated by lighter green lollipops containing the letter n. (C) Putative binding sites for PacC (GCCARG) are indicated by red lollipops containing the letter P. (D) Putative binding sites for Seb1 (AGGGG) are indicated by purple lollipops containing the letter S.

Atl nucleotide sequence. A 463 bp product was amplified from *N. lolii* Lp19 genomic DNA (Figure 3.13), and subcloned into pGEM-T Easy (Promega) to give the plasmid pMM38. Sequencing demonstrated that the MM75-MM76 PCR product in pMM38 was 90% identical to *Atl* at the nucleotide level (compared to *prt1*, *prt2* and *prt5* with nucleotide identities with Atl of 46%, 58% and 59% respectively over the same region). This suggested this product, designated *prt3,* is the *N. lolii* Lp19 homologue of the *E. typhina Atl* gene.

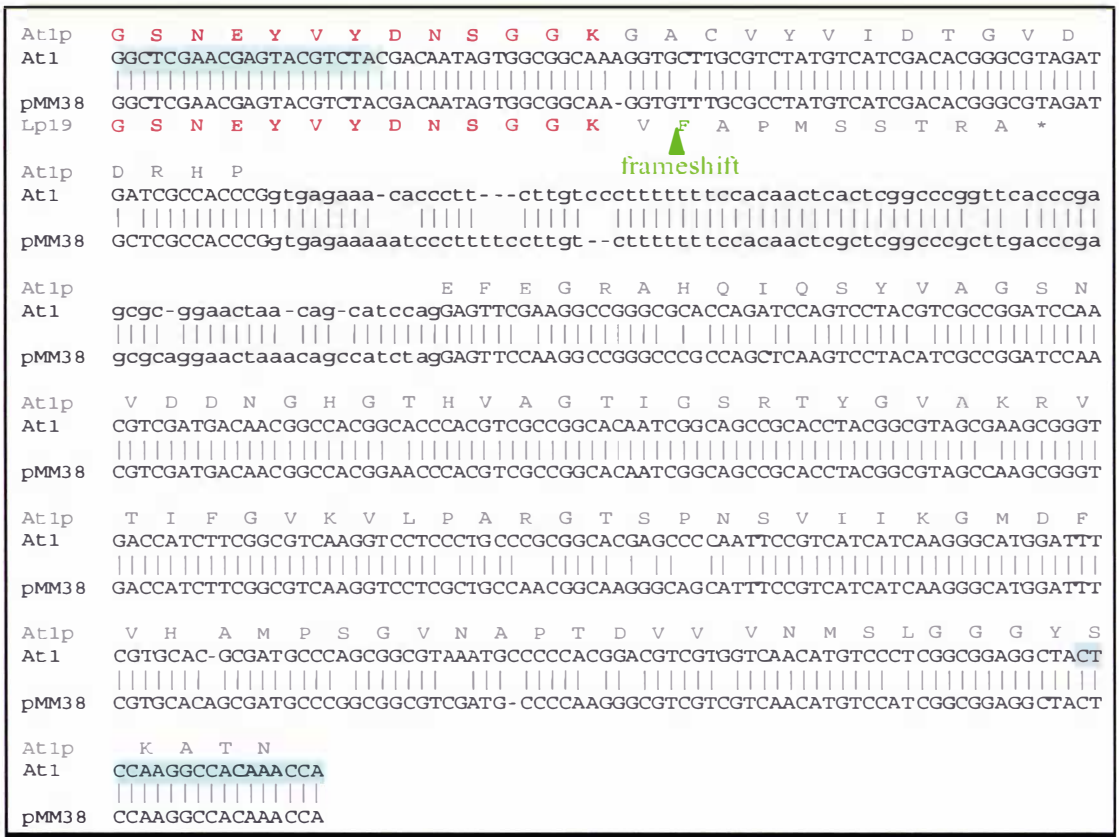

Figure 3.13 Sequence of the At1 homologue from *N. lolii* Lp19

The *N. lolii* Lp19 homologue of the *At1* gene was identified by PCR amplification with primers MM75 and MM76 (indicated in blue shading), which were designed based on the At1 nucleotide sequence. The *N. lolii* Lp19 MM75-MM76 PCR product was subcloned into pGEM-T Easy to give the vector pMM38. Identity between the two DNA sequences is shown by a grey line connecting the two nucleotide residues. Sequence identity between the amino acid residues is indicated in red. Exon sequences are shown in uppercase and intron sequences in lowercase text.

The pMM38 insert was reamplified with the MM75-MM76 primer pair, and used to screen a *E. festucae* Fl1 genomic DNA Southern blot (Figure 3.14; Table 3.4) and an. *festucae* Fl1 genomic DNA cosmid library (Sections 3.1.1 and 3.1.2). Twelve independent cosmids with homology to the *prt3* gene, including 46F6, were identified. pMM47 contained a 4.3 kb *Sal*I fragment with homology to *prt3* from the cosmid 46F6 subcloned into pUC118. Sequencing of pMM47 and the 46F6 cosmid gave the complete sequence of the *E. festucae* Fl1 *prt3* gene (Figure 3.15).

The *E. festucae* Fl1 *prt3* gene exon-intron structure is identical to that of the *prt2* gene, consisting of 4 exons with introns at conserved postions (Figures 3.11, 3.15, and 3.16). At the nucleotide level, the *E. festucae* Fl1 *prt3* gene had 87% identity at the nucleotide level with the *E. typhina At1* gene. The *prt3* gene encodes a putative preproprotein of 388 amino acid residues in length, with a predicted signal peptide of

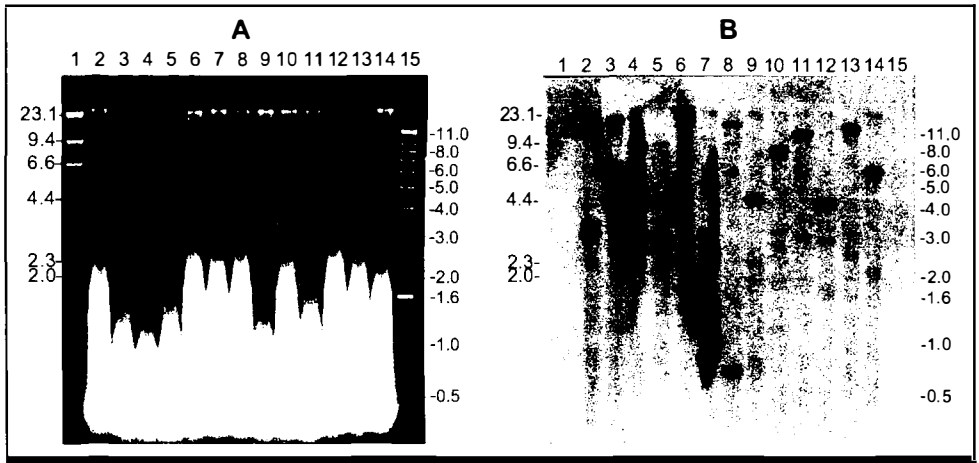

Figure 3.14 Southern analysis of *E. festucae* Fl1 *prt3*

Southern analysis of *E. festucae* Fl1 *prt3*. **(A)** *E. festucae* Fl1 genomic DNA (1 µg) digested with *Bam*HI (lane 2), *Bgl*II (lane 3), *Eco*RI (lane 4), *Hin*dIII (lane 5), *Kpn*I (lane 6), *N*coI (lane 7), *Pst*I (lane 8), *Sal*I (lane 9), *Rca*I (lane 10), *Sph*I (lane 11), *Sst*I (lane 12), *Xba*I (lane 13) and *Xho*I (lane 14). Lanes 1 and 15 contain λ *Hin*dIII and 1 kb plus (Invitrogen) ladders respectively. Sizes of marker fragments are shown in kb. **(B)** Autoradiograph of the gel from A hybridised with a [^{32}P]-labelled *N. lolii* Lp19 *prt3* fragment amplifed with primers MM75 and MM76.

Table 3.4 Fragments homologous to *E. festucae* Fl1 *prt3*

Enzyme	Hybridising fragment length (kb)
*Bam*HI	3.4, 3.0
*Bgl*II	15.0
*Eco*RI	8.6
*Hin*dIII	2.9
*Kpn*I	18.0
*N*coI	6.0, 0.8
*Pst*I	13.0, 0.6
*Sal*I	4.3
*Rca*I	8.0
*Sph*I	10.5
*Sst*I	4.0
*Xba*I	12.0
*Xho*I	4.3

19 amino acid residues (SignalP 3.0 prediction, Bendtsen *et al.,* 2004). The *E. festucae* Fl1 Prt3 protein is most similar to the At1 protease, with 83% identity at the amino acid level.

The promoter of *E. festucae* Fl1 *prt3* contained 8 putative CreA binding sites, with 5 putative binding sites found in the coding region (Figure 3.17). For the global nitrogen regulator AreA/Nit2/AreA, 5 strong affinity binding sites and 2 weak affinity binding sites were found in the *prt3* promoter. However, only 5 weak affinity binding sites were found in the coding region. This raises the possibility that the *E. festucae* Fl1 *prt3* gene may be subject to regulation by AreA/Nit2/AreA. Six PacC binding sites were found in the *E. festucae* Fl1 *prt3* promoter, compared to 3 in the

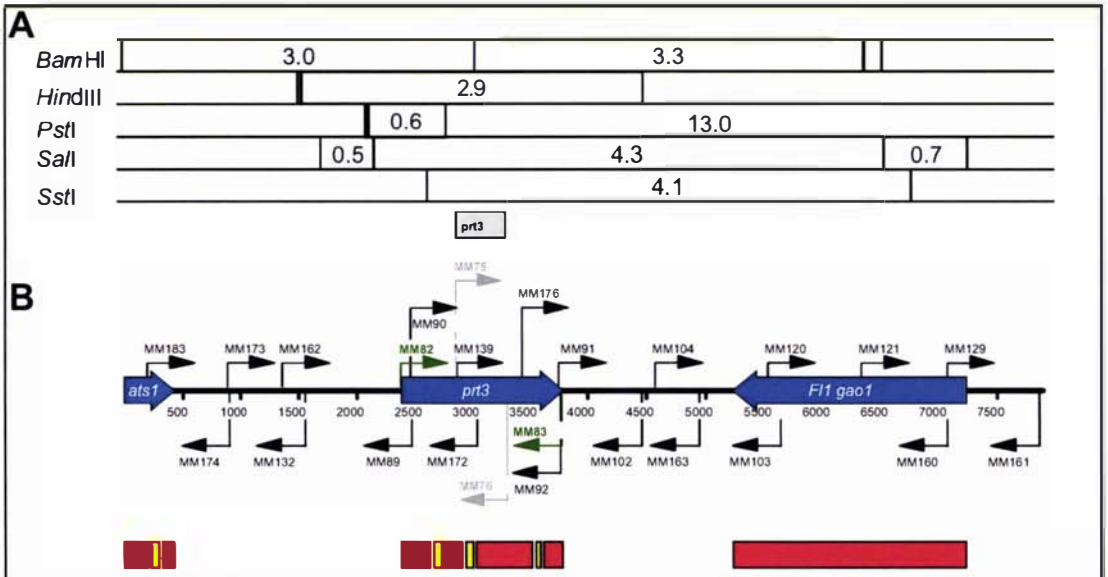

Figure 3.15 Structure of the *E. festucae* Fl1 *prt3* genomic region

Structure and restriction map of the *E. festucae* Fl1 *prt3* genomic region. **(A)** Restriction map of the *E. festucae* Fl1 *prt3* genomic region. Sizes of restriction fragments are shown in kb. **(B)** Structure of the *E. festucae* Fl1 *prt3* genomic region. The *E. festucae* Fl1 *prt3* coding regions are shown in blue. Primers are shown by arrows (indicating direction of amplification from the primers). The exon-intron structure of the genes is shown beneath, with exons and introns indicated by red and yellow boxes respectively. The position where the probe used in Figure 3.11 would hybridise is indicated by a grey box just below the restriction map.

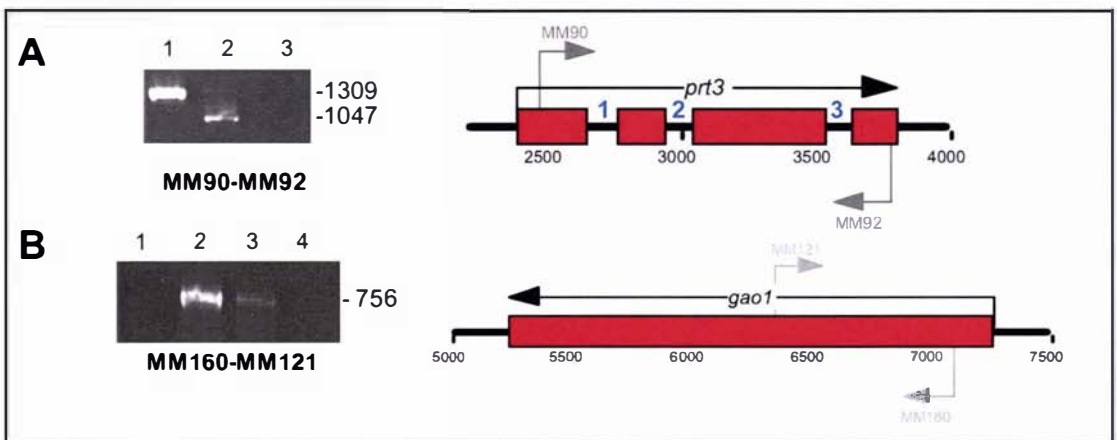

Figure 3.16 Gene structure of the *E. festucae* Fl1 *prt3* and *gao1* genes

Gene structure of the *E. festucae* Fl1 *prt3* and *gao1* genes. RT-PCR analysis was performed with RNA isolated from *E. festucae* Fl1 cultures grown in PD broth for 7 days. cDNA was reverse transcribed from poly-A RNA using the Expand RT enzyme (Roche) (Section 2.18.5). All fragment sizes shown adjacent to gels are indicated in bp. On the schematic diagram of each gene, the position within the *prt3* locus is indicated in bp. Exons (confirmed by sequencing of cDNA products) are indicated by red boxes. Primers are positioned above or below the sequence for forward or reverse direction respectively. Introns are numbered in blue text between exons. The position within the *prt3* locus is indicated below the sequence schematic in bp. (A) The *E. festucae* Fl1 *prt3* gene. Lane 1: *E. festucae* Fl1 genomic DNA, lane 2: 10 fold dilution of *E. festucae* Fl1 cDNA, lane 3: negative control. B) The *E. festucae* Fl1 *gao1* gene. Lane 1: no RT control, lane 2: *E. festucae* Fl1 genomic DNA, lane 3: 10 fold dilution of *E. festucae* Fl1 cDNA, lane 4: negative control.

The following PCR conditions were used: 5 ng genomic DNA or 5 µL diluted cDNA, 1 x Taq polymerase buffer (Roche), 50 µM each dNTP, 200 nM of each primer, and 0.5 U Taq polymerase in a volume of 25 µL. The PCR amplification conditions for the primer pairs MM90-MM92 and MM160-MM121 were as follows: 94°C for 2 min, followed by 30 cycles of 94°C for 30 s, 60°C for 30 s, 72°C for 1 min, then one cycle of 72°C for 5 min.

coding sequence, while 3 Seb1 binding sites were found in each of the promoter and coding region. The *prt3*promoter contained numbers of CreA, strong affomotu AreA/Nit2, and Seb1 binding sites similar to those expected if the binding sites occurred randomly throughout the promoter. However, more PacC sites were observed than would be expected by random occurrence through the promoter. Less weak affinity AreA/Nit2 binding sites were observed than expected throughout the *prt3* promoter region.

MEME analysis was also carried out on the promoter to look for any sites over-represented in the *prt3* promoter sequence (Appendix A11). The *prt3* promoter contained MEME motifs 1, 2, 12 and 18, which were also found in the *prt1*, *prt5* and *prt2* promoters. MEME motifs 3, 4, 5, 6, 7, 8 and 10, which are found in the *prt5* and *prt2* promoters, were also present in the *prt3* promoter (Figure 3.7). MEME motifs 2, 3 and 7 were present in multiple copies.

Putative genes were found both upstream and downstream of *E. festucae* Fl1 *prt3*. Part of a open reading frame for a gene designated *ats1* was found directly upstream of *E. festucae* Fl1 *prt3*. The *ats1* gene encodes a protein similar to those of yeast asparaginyl-tRNA synthetases. The gene downstream of Fl1 *prt3*, named *gao1*, encodes a putative galactose oxidase. The protein encoded by *gao1* is similar to the galactose oxidase from *Fusarium* spp. (McPherson et al., 1992; Ögel et al., 1994), which has been extensively studied in terms of its interesting catalytic mechanism, its use in industry and research, and its ability to generate free radicals. Galactose oxidase converts a primary alcohol (e.g. D-galactose) to the corresponding aldehyde (e.g. galactohexodialdose), in the process converting oxygen to hydrogen peroxide, thus generating free radicals (Machado and Kemmelmeier, 2001). Genes encoding similar proteins are also found in other fungal species (Appendix A6).

3.1.3.2 The *N. lolii* Lp19 and Lp5 *prt3* genes encode non-functional proteins

During sequencing of the *N. lolii* Lp19 *prt3* gene PCR product, the PCR product was noted to contain a single base pair deletion relative to the At1 gene (Figure 3.13). However, the *E. festucae* Fl1 *prt3* sequence did not contain this deletion. To confirm

that *N. lolii* Lp19 *prt3* did have this deletion, the primer pair MM82-MM83 was used to amplify most of the *prt3* coding region from several related endophyte strains. Three *N. lolii* strains (Lp19, Lp5 and AR1) and two *E. festucae* strains (Fl1 and Fr1) were amplified with the primer pair MM82-MM83, and the PCR products were directly sequenced. *N. lolii* strains Lp19 and Lp5 both had a single base deletion

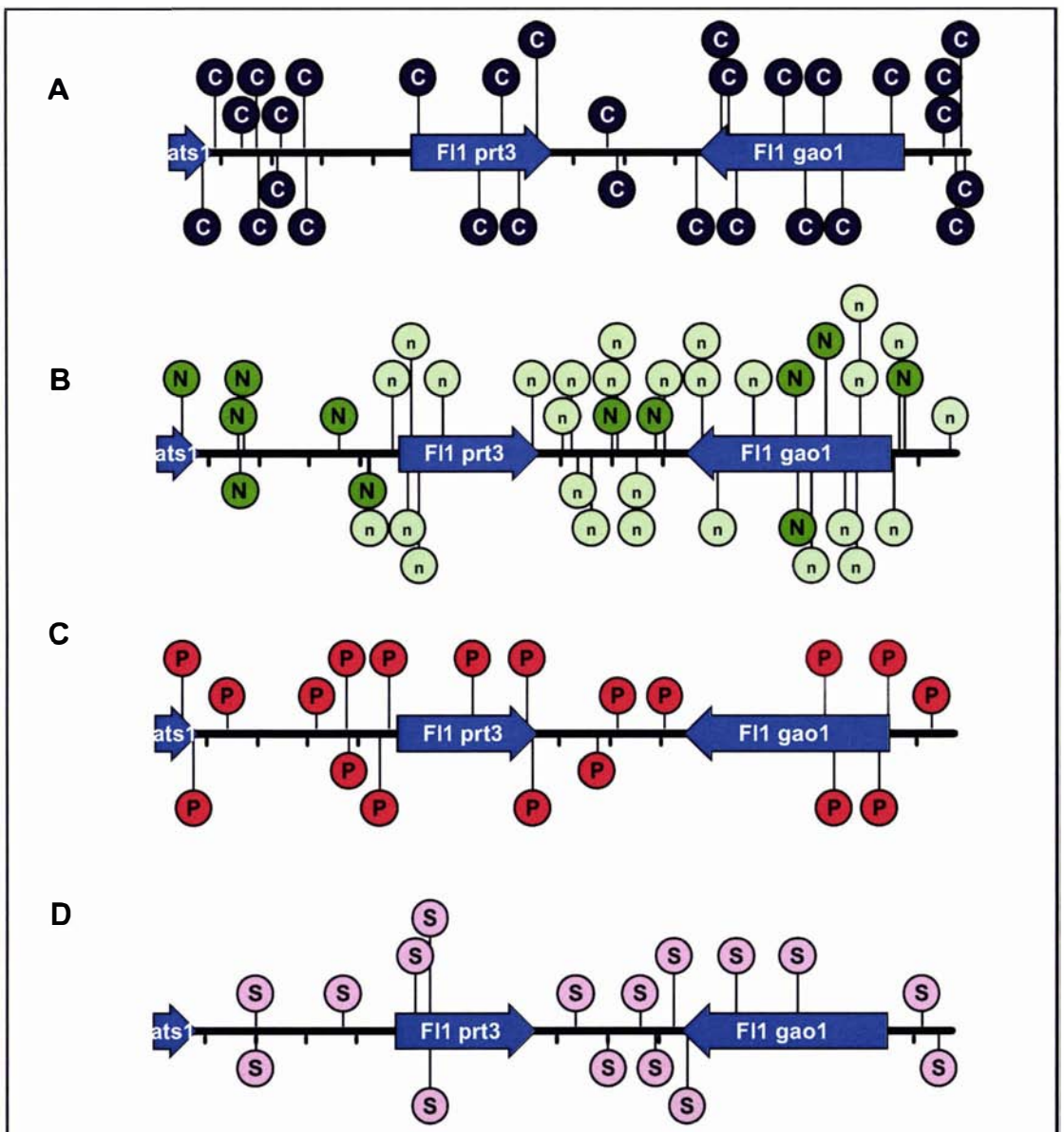

Figure 3.17 Potential binding sites for fungal global transcription regulators at the *E. festucae* Fl1 *prt3* locus

Analysis for putative binding sites for the fungal transcription factors CreA (carbon regulation), Nit2/AreA (nitrogen regulation), PacC (pH regulation) and Seb1 (transcriptional regulator) at the *E. festucae* Fl1 *prt3* locus.(A) Putative binding sites for CreA (SYGGRG) are indicated by blue lollipops containing the letter C. (B) Putative binding sites for Nit2/AreA (HGATAR) are indicated by green lollipops containing the letter N. Weaker binding sites (GATA) are indicated by lighter green lollipops containing the letter n. (C) Putative binding sites for PacC (GCCARG) are indicated by red lollipops containing the letter P. (D) Putative binding sites for Seb1 (AGGGG) are indicated by purple lollipops containing the letter S.

shortly before intron 2, while *N. lolii* AR1, *E. festucae* Fl1 and *E. festucae* Fr1 did not (Appendix A2.3).

The consequence of this single base pair deletion in *N. lolii* strains Lp19 and Lp5 is a frame shift (at amino acid residue 140 relative to At1), which results in premature truncation of the protein (Figure 3.13). As the *N. lolii* Lp19 and Lp5 truncated Prt3 protein does not contain any of the conserved catalytic residues (D147, H178 or S332 numbered relative to At1; Reddy et al, 1996), they will be non-functional.

3.1.4 Phylogenetic analysis of *E. festucae* Fl1 and *N. lolii* Lp19 *prt1, prt2, prt3 and prt5* genes

The relationship between the *E. festucae* Fl1 and *N. lolii* Lp19 *prt1, prt2, prt3* and *prt5* genes and their relationships to other fungal proteases was studied using a phylogenetic approach (source of sequences listed in Appendix A13.1). Polypeptide sequences encoded by these genes were aligned using the ClustalW module of MacVector 7.2.3 as described in Section 2.21. The alignment was then subjected to Neighbour Joining (NJ) analysis (with ties being resolved randomly), with Poisson correction. Trees were also bootstrapped to give an indication of the reliability of individual branches of the tree. The resulting tree (with bootstrap identities) is shown in Figure 3.18.

As expected, the *E. festucae* Fl1 and *N. lolii* Lp19 copies of each of the proteins cluster together in the tree, normally with 100% bootstrap support (except in the case of *N. lolii* Lp19 Prt3, due to the truncated nature of this protein). In accordance with the nomenclature suggested by St Leger and Hu (2004), the Prt2, Prt3 and Prt5 proteins group with subfamily 1 of the proteinase K family, while Prt1 groups with subfamily 2 of the proteinase K family. These results indicate Prt1, Prt2, Prt3 and Prt5 are putative extracellular enzymes that are secreted, and are related to enzymes involved in fungal-host interactions (references listed in Appendix A13.1).

The exon structure of these genes also suggests how these genes may have evolved. The *prt1, 2, 3* and *5* genes contained a conserved intron at the first position (Appendix A14.1). However, *prt1* (the sole member of subfamily 2 isolated in this

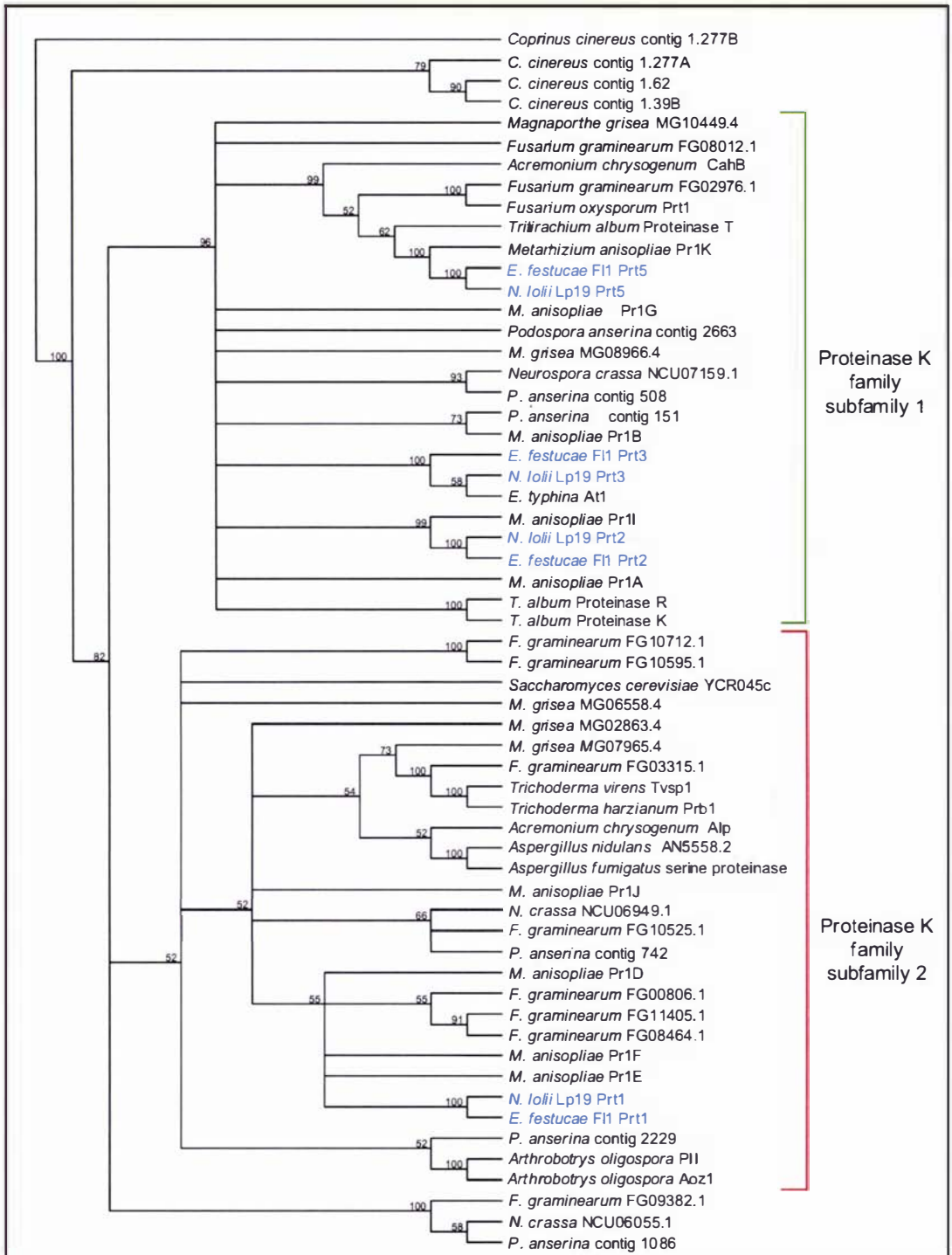

Figure 3.18 Phylogenetic relationships of Prt1, Prt2, Prt3 and Prt5

Phylogenetic relationships of the *N. lolii* Lp19 and *E. festucae* Fl1 Prt1, Prt2, Prt3 and Prt5 proteins with other related fungal proteins. The phylogenetic tree in this figure was prepared in the MacVector 7.2.3 program, using Neighbour joining and bootstrapping (1000 replicates) of sequences aligned using the ClustalW module of MacVector to form the tree. For details of the sequences used in this alignment, see Appendix A13.2. In this phylogenetic tree, endophyte protein names are shown in blue text, with all other protein names in black text. Proteinase K protease subfamily 1 and 2 (Hu and St Leger 2004) are indicated by green and red lines respectively.

study) did not contain a conserved intron at position 2 found in *prt2*, *prt3* and *prt5*. The presence of these two shared introns in the subfamily 1 genes supports the phylogenetic data. However, the *prt5* gene differed from the *prt2* and *prt3* genes in the position of its final intron. The *prt5* gene had its third intron at position 3, while *prt2* and *prt3* both had an intron at a common site, position 4. Conserved intron positions suggest *prt2* and *prt3* are more closely related to each other than to *prt5*.

3.2 *E. FESTUCAE* FL1 PROTEINASE K FAMILY GENE (SUBFAMILY 3)

3.2.1 The prt4 gene

Degenerate PCR was used to identify the *E. festucae* Fl1 vacuolar protease gene. The degenerate primers MM93 and MM94 were designed based of an alignment of fungal vacuolar proteases (Appendix A7.1; Figure 3.19A). When these primers were used to amplify *E. festucae* Fl1 genomic DNA at an annealing temperature of 55°C, a single product of 398 bp was detected (Figure 3.19B). This product was subcloned into pGEM-T Easy (Promega) to create the vector pMM46 and subsequently sequenced.

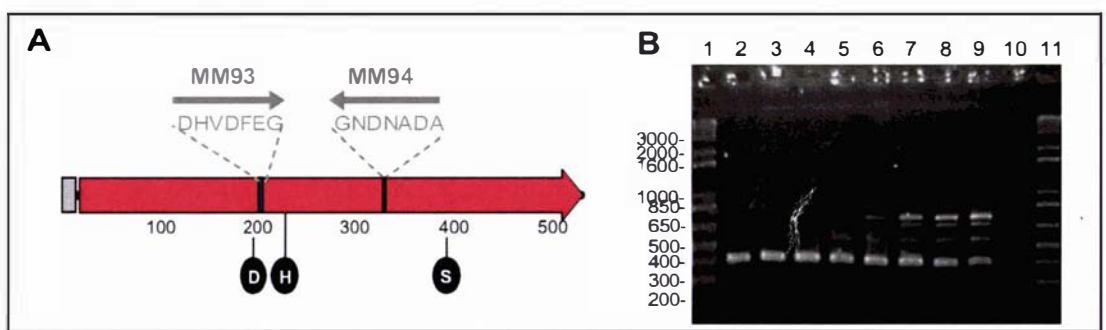

Figure 3.19 Strategy for identifying a vacuolar protease homologue

(A) The degenerate primers MM93 and MM94 were designed based on conserved regions of vacuolar subtilisin-like proteases. The structure of the closely-related *Metarhizium anisopliae* Pr1H protein is shown, with the signal peptide indicated in grey and the proprotein (consisting of the propeptide and mature protein) shown in red. Conserved catalytic residues are indicated by black circles. The regions the primers MM93 and MM94 bind to are shown in blue. Amino acid residues used for degenerate primer design are shown in grey, with an arrow indicating direction of primer amplification. **(B)** Gradient PCR was used to identify the optimum annealing temperature for the degenerate primer set. Lanes 2- 9 contain *E. festucae* Fl1 genomic DNA amplified at 55°C, 53.6°C, 52.1°C, 50.7°C, 49.3°C, 47.9°C, 46.4°C and 45°C respectively. Lane 10 contains a negative control. Lanes 1 and 11 both contain 1kb + ladder (Invitrogen). Fragment sizes are indicated in bp.

The sequence of the degenerate PCR product was highly similar to the Prl H vacuolar protease gene from *M. anisopliae*, with 83% identity at the nucleotide level and 90% identity at the amino acid level (Figure 3.20). This suggested that the *E. festucae* Fl1 degenerate PCR product was amplified from a gene encoding a vacuolar protease with strong similarities to related vacuolar protease-encoding genes from other fungal species.

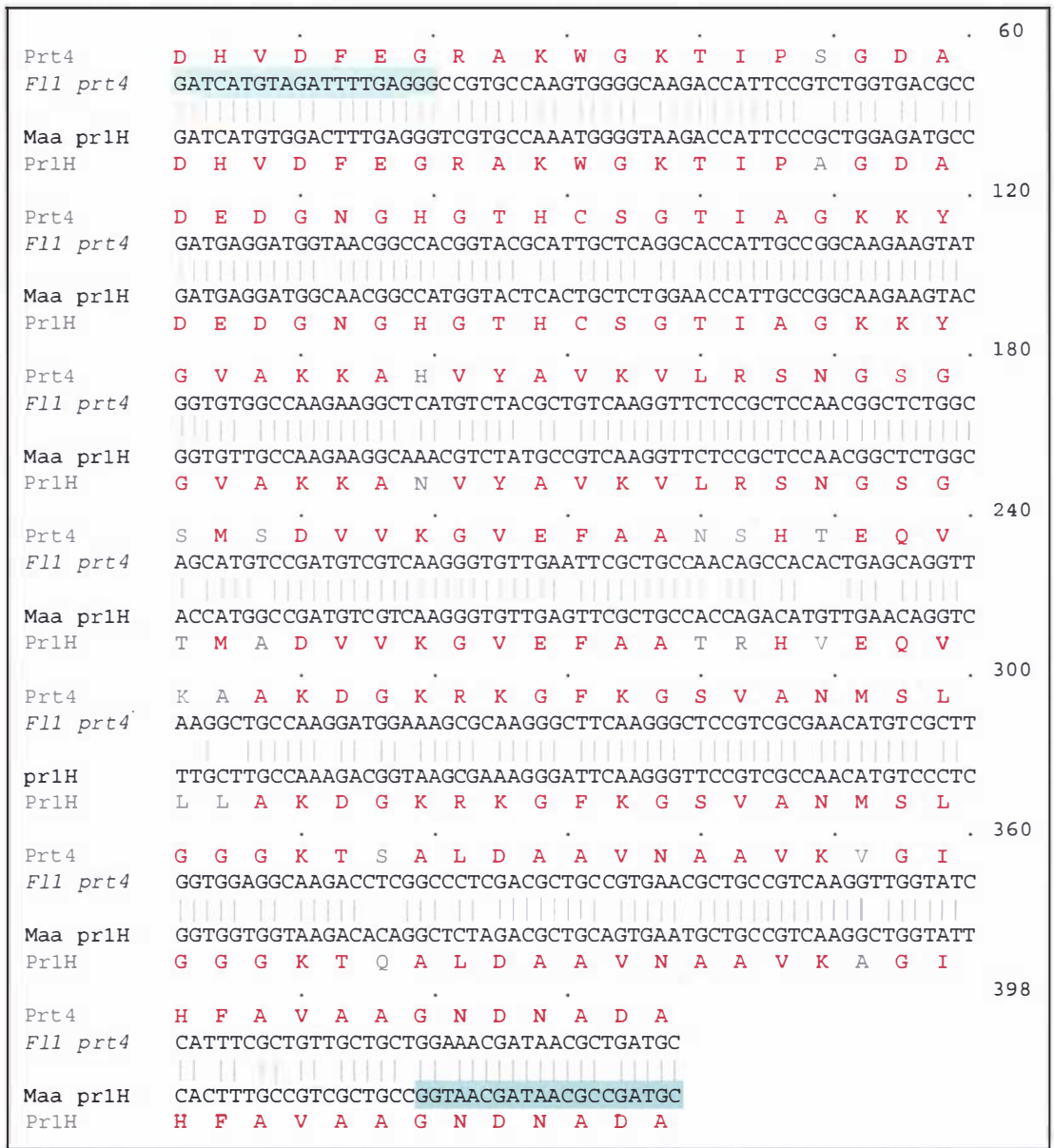

Figure 3.20 Sequence of the *prt4* degenerate PCR product

The *prt4* fragment was amplified from *E. festucae* Fl1 genomic DNA with the degenerate PCR primers MM93 and MM94. The annealing sites of the primers are highlighted in blue. The sequence of the *prt4* fragment is shown aligned to the gene pr1H from *Metarhizium anisopliae* var. *anisopliae* (nucleotide accession AJ421473, protein accession CAD13274). Identity between the two DNA sequences is shown by a grey line connecting the two nucleotide residues. Sequence identity between the amino acid residues is indicated in red.

In order to isolate the vacuolar protease gene (designated as *prt4)* from *E. festucae* Fl1, the degenerate PCR product described above was used to probe an *E. festucae* Fl1 genomic cosmid library (Section 2.10). Eight independent cosmids that contained the *prt4* gene were identified.

Southern blotting was performed to develop a restriction map of the *E. festucae* Fl1 *prt4* locus (Figure 3.21, Table 3.5). In order to sequence the *prt4* gene, a 3.9 kb *Hin*dIII fragment was subcloned into pUC118 to give the vector pMM61. Sequencing revealed this *Hin*dIII fragment contained the complete sequence of the *prt4* gene.

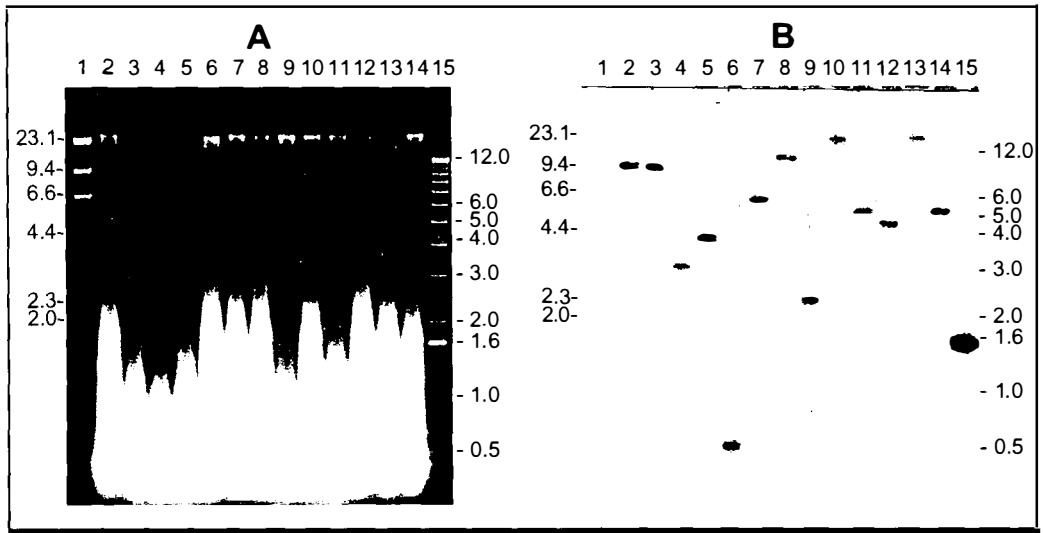

Figure 3.21 Southern analysis of the *E. festucae* Fl1 *prt4*

Southern analysis of *E. festucae* Fl1 *prt4*. **(A)** *E. festucae* Fl1 genomic DNA (1 µg) digested with *Bam*HI (lane 2), *Bgl*II (lane 3), *Eco*RI (lane 4), *Hin*dIII (lane 5), *Kpn*I (lane 6), *N*coI (lane 7), *Pst*I (lane 8), *Sal*I (lane 9), *Rca*I (lane 10), *Sph*I (lane 11), *Sst*I (lane 12), *Xba*I (lane 13) and *Xho*I (lane 14). Lanes 1 and 15 contain λ *Hin*dIII and 1 kb plus (Invitrogen) ladders respectively. Size standards are shown in kb. **(B)** Autoradiograph of the gel from **A** hybridised with a [^{32}P]-labelled *prt4* fragment amplifed with primers MM93 and MM94.

Table 3.5 Fragments homologous to *E. festucae* Fl1 *prt4*

Enzyme	Hybridising fragment length (kb)
*Bam*HI	9.4
*Bgl*II	9.4
*Eco*RI	12.5, 2.9
*Hin*dIII	3.9
*Kpn*I	4.5, 0.5
*N*coI	5.8
*Pst*I	9.5
*Sal*I	2.2
*Rca*I	15.0
*Sph*I	5.0
*Sst*I	4.5
*Xba*I	14.5
*Xho*I	5.1

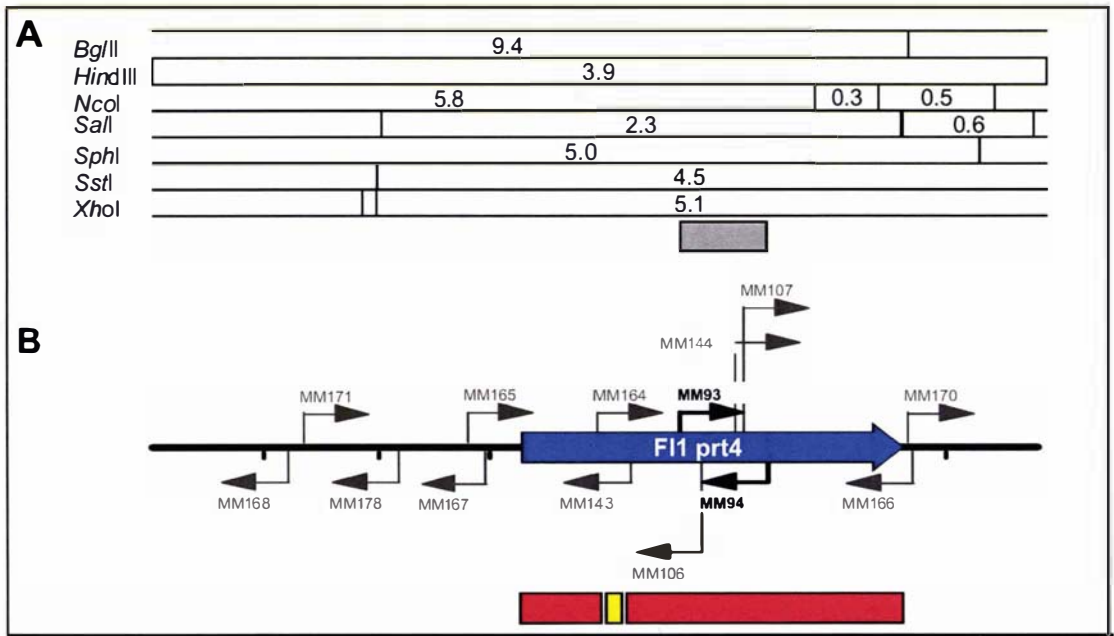

Figure 3.22 Structure of the *E. festucae* Fl1 *prt4* gene

Structure and restriction map of the *E. festucae* Fl1 *prt4* gene. **(A)** Restriction map of the *E. festucae* Fl1 *prt4* gene. Sizes of restriction fragments are shown in kb. **(B)** Structure of the *E. festucae* Fl1 *prt4* genomic region. The *E. festucae* Fl1 *prt4* coding region is shown in blue. Primers are shown by arrows (indicating direction of amplification from the primers). The exon-intron structure of the genes is shown beneath, with exons and introns indicated by red and black boxes respectively. The position of the probe used in Figure 3.17 (corresponding to the degenerate PCR product amplified with the MM93-MM94 primer set) is indicated by a black box just below the restriction map.

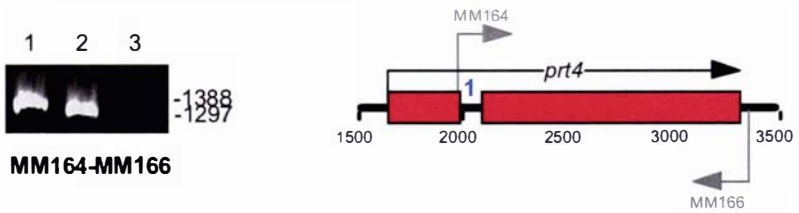

Figure 3.23 Gene structure of the *E. festucae* Fl1 *prt4* gene

Gene structure of *E. festucae* Fl1 *prt4*. RT-PCR analysis was performed with RNA isolated from *E. festucae* Fl1 cultures grown in PD broth for 7 days. cDNA was reverse transcribed from poly-A RNA using the Expand RT enzyme (Roche) (Section 2.18.5). Fragment sizes are shown adjacent to gels in bp. The position within the *prt4* locus is indicated in bp. Exons (confirmed by sequencing of cDNA products) are indicated by red boxes. Primers are positioned above or below the sequence for forward or reverse direction respectively. Introns are numbered in blue text between exons. The position within the *prt4* locus is indicated below the sequence schematic in bp. Lane 1: *E. festucae* Fl1 genomic DNA, lane 2: 10 fold dilution of *E. festucae* Fl1 cDNA, lane 3: negative control.
The following PCR conditions were used: 5 ng genomic DNA or 5 µL diluted cDNA, 1x Taq polymerase buffer (Roche), 50 µM each dNTP, 200 nM each primer, and 0.5 U Taq polymerase in a volume of 25 µL. PCR amplification conditions for the primer pair MM164-MM166 were as follows: 94°C for 2 min, followed by 30 cycles of 94°C for 30 s, 60°C for 30 s, 72°C for 1 min 30 s, then one cycle of 72°C for 5 min.

The *E. festucae* Fl1 *prt4* gene consists of two exons separated by a single intron, which is in a conserved position with other fungal vacuolar protease genes (Figures 3.22 and 3.23, Appendix A14.2). The *prt4* gene is most similar to the *prlH* gene from the entomopathogenic fungus *Metarhizium anisopliae*, which like *E. festucae* Fl1 is a member of the Clavicipitaceae. The *prt4* gene shares 74% identity with PrlH at the nucleotide level, and 78% identity at the amino acid level.

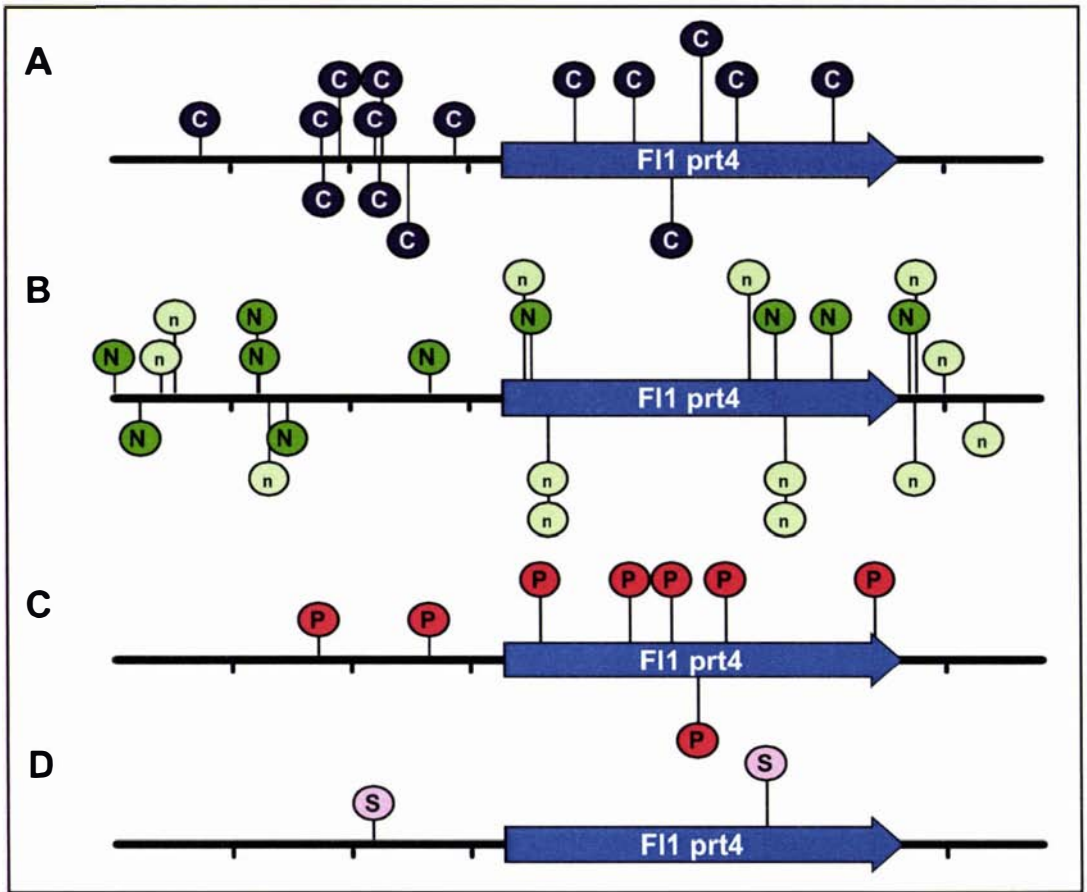

Figure 3.24 Potential binding sites for fungal global transcription regulators in the *E. festucae* Fl1 *prt4* gene

Analysis for putative binding sites for the fungal transcription factors CreA (carbon regulation), Nit2/AreA (nitrogen regulation), PacC (pH regulation) and Seb1 (transcriptional regulator) at the *E. festucae* Fl1 *prt4* locus.(A) Putative binding sites for CreA (SYGGRG) are indicated by blue lollipops containing the letter C. (B) Putative binding sites for Nit2/AreA (HGATAR) are indicated by green lollipops containing the letter N. Weaker binding sites (GATA) are indicated by lighter green lollipops containing the letter n.(C) Putative binding sites for PacC (GCCARG) are indicated by red lollipops containing the letter P. (D) Putative binding sites for Seb1 (AGGGG) are indicated by purple lollipops containing the letter S.

The promoter of the *E. festucae* Fl1 *prt4* gene was analysed for the presence of putative binding sites for fungal global transcriptional regulators as described in Section 3.1 (Figure 3.24). Nine putative binding sites were found for the CreA transcription factor. For the AreA/Nit2/AreA transcription factor, six strong affinity and three weak affinity binding sites were found. Only two and one binding sites were found for the PacC and Seb1 transcription factors respectively. Analysis showed the promoter contained higher numbers of CreA and strong AreA/Nit2 binding sites than expected if these sites occurred at random in the promoter sequence. The number of PacC binding sites was similar to that expected if the sequence occurred randomly, while less binding sites than expected were observed for weak affinity AreA/Nit2 sites and for Seb1 sites.

MEME analysis showed the *E. festucae* Fl1 *prt4* promoter contained MEME motif 18, found in the *prt1*, *prt2*, *prt3* and *prt5* promoters (Figure 3.7). The *prt4* promoter also contained the MEME motifs 3, 6, 7, 8, 10 and 15, also found in the *prt2*, *prt3* and *prt5* promoters. MEME motifs 3, 6, 8 and 15 were present in multiple copies.

3.2.2 Phylogenetic analysis of proteinase K subfamily 3 genes

The relationship between the *E. festucae* Fl1 Prt4 protein and other fungal vacuolar proteases was studied using a phylogenetic approach (sequences listed in Appendix A13). Polypeptide sequences were aligned as described in Section 2.21. The alignment was then subjected to Neighbour Joining (NJ) analysis (with ties being resolved randomly), with Poisson correction. The reliability of individual branches of the tree was analysed by bootstrapping (1000 repetitions). The resulting tree (with bootstrap identities) is shown in Figure 3.25. As expected for a protein encoded by a gene present in a single copy in the genomes of filamentous ascomycetes, the

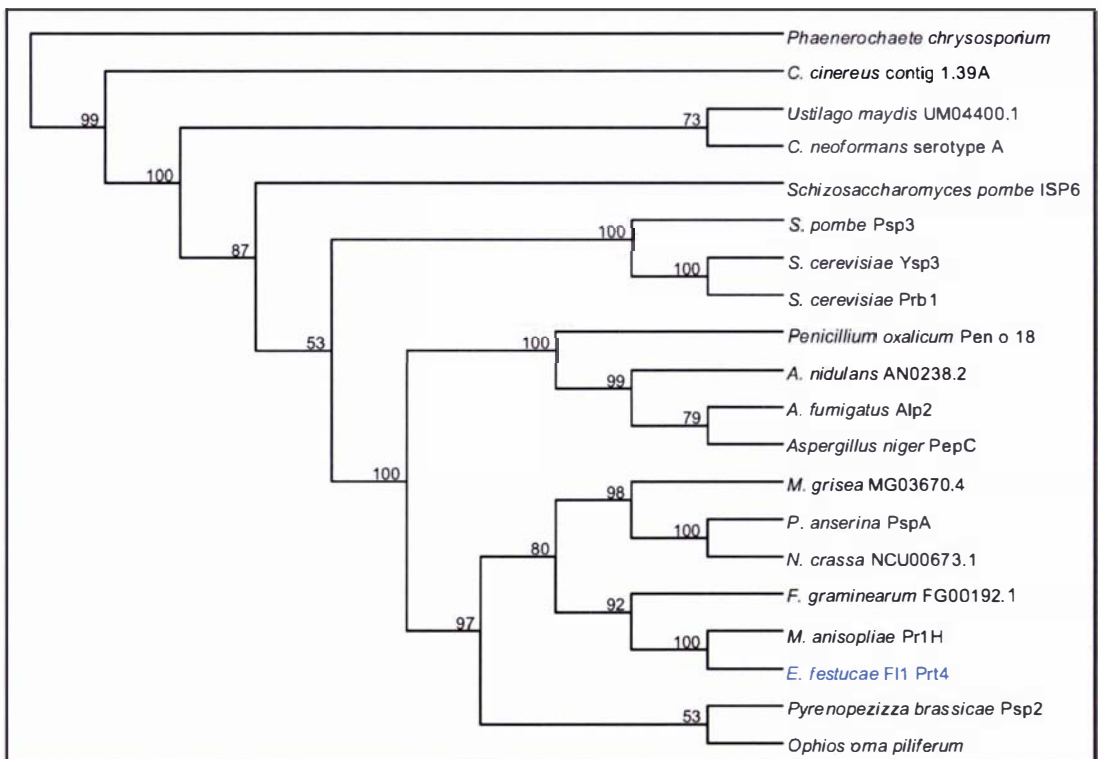

Figure 3.25 Phylogenetic relationship of *E. festucae* Fl1 Prt4 to fungal vacuolar proteases

Phylogenetic relationships of the *E. festucae* Fl1 Prt4 proteins with other related fungal proteins. The phylogenetic tree in this figure was prepared in the MacVector 7.2.3 program, using Neighbour joining and bootstrapping (1000 replicates) of sequences aligned using the ClustalW module of MacVector to form the tree. For details of the sequences used in this alignment, see Appendix A13.3. In this phylogenetic tree, the endophyte protein name are shown in blue text, with all other protein names in black text.

Prt4 protein shows strongest similarity to homologues from the most closely related fungal species, *M. anisopliae* and *F. graminearum*. The position of the *prt4* intron was conserved across all the filamentous ascomycete genomes examined. The single intron observed in *prt4* was also conserved in position in *prt1*, and with the first introns of *prt2*, *prt3* and *prt5* (Appendix A13).

3.3 THE *E. FESTUCAE KEX2* GENE

A kexin homologue sequence was isolated based on a partial sequence from *N. lolii* Lp19 with homology to fungal kexins from R. Johnson (AgResearch Grasslands). The primer pair MM141/MM142 (Figure 3.27) was designed to this sequence and used to amplify a PCR product from *N. lolii* Lp19 genomic DNA. The *N. lolii* Lp19 MM141-MM142 PCR product was used as a probe for an *E. festucae* Fl1 genomic DNA blot (Figure 3.26, Table 3.6) and for screening the *E. festucae* Fl1 cosmid genomic DNA library described in Sections 3.1 and 3.2 (Section 2.10).

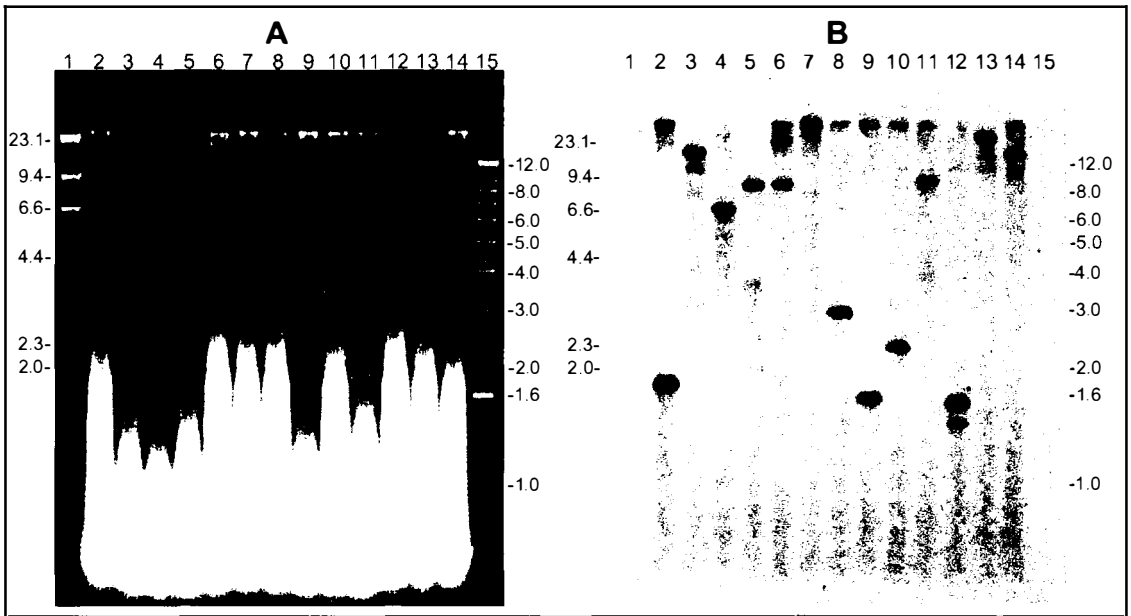

Figure 3.26 Southern analysis of *E. festucae* Fl1 *kex2*

Southern analysis of *E. festucae* Fl1 *kex2*. **(A)** *E. festucae* Fl1 genomic DNA (1 µg) digested with *Bam*HI (lane 2), *Bgl*II (lane 3), *Eco*RI (lane 4), *Hin*dIII (lane 5), *Kpn*I (lane 6), *Nco*I (lane 7), *Pst*I (lane 8), *Sal*I (lane 9), *Rca*I (lane 10), *Sph*I (lane 11), *Sst*I (lane 12), *Xba*I (lane 13) and *Xho*I (lane 14). Lanes 1 and 15 contain λ *Hin*dIII and 1 kb plus (Invitrogen) ladders respectively. Size standards are shown in kb. **(B)** Autoradiograph of the gel from **A** hybridised with a [^{32}P]-labelled *N. lolii* Lp19 *kex2* fragment amplifed with primers MM141 and MM142.

Table 3.6 Fragments homologous to *E. festucae* Fl1 *kex2*	
Enzyme	**Hybridising fragment size (kb)**
*Bam*HI	1.7
*Bgl*II	9.6
*Eco*RI	5.2
*Hin*dIII	6.6
*Kpn*I	6.6, 12.0
*Nco*I	19.0
*Pst*I	2.4
*Sal*I	1.4
*Rca*I	1.9
*Sph*I	8.6
*Sst*I	1.3, 1.8
*Xba*I	13.0
*Xho*I	9.8

Library screening identified eight cosmids containing homology to the *kex2* gene. Of these, cosmid 1D6 was selected for further analysis. An 8.6 kb *Sph*I fragment containing the *kex2* gene (Figures 3.26 and 3.27) was isolated and subcloned into pUC118, giving the plasmid pMM65. Double stranded sequencing of this fragment revealed there were four putative open reading frames on this *Sph*I fragment, including the *kex2* gene (Figure 3.27). Gene structures for the four putative open reading frames are shown in Figure 3.28.

The first open reading frame on this fragment, *orf2*, showed homology to part of the 5' region of the *F. graminearum* FG07967.1 gene and several bacterial genes encoding products of unknown function. The second open reading frame, *orf3*, contained some homology to the *N. crassa* NCU01050.1. The third open reading frame, Nc25, is 87% identical at the amino acid level to a *Neotyphodium coenophialum* protein (accession AAO92022) differentially expressed when associated with its host grass (Johnson et al., 2003).The kexin gene, *kex2*, is the last gene found on the *Sph*I fragment. The *kex2* gene encodes a putative preproprotein of 742 amino acid residues in length. The Kex2 protein is most similar to kexins from *A. niger*, (46%), *A. fumigatus* (46%), *A. nidulans* and *A. oryzae* (both 45%) at the amino acid level.

The intron position within the *kex2* gene was highly conserved with other fungal kexin genes (Appendix A14.3). The position of the intron in the *E. festucae* Fl1 gene was conserved with the only introns in the *Aspergillus* spp. and *N. crassa* kexins, and also with the second intron of the *F. graminearum* kexin gene. However,

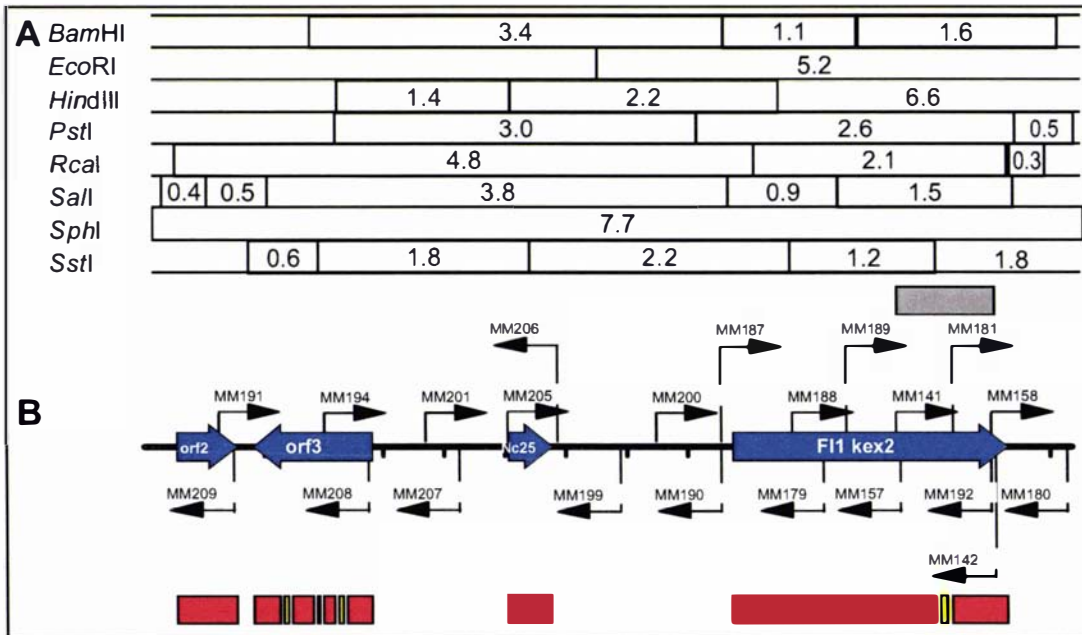

Figure 3.27 Structure of the *E. festucae* Fl1 *kex2* gene

Structure and restriction map of the *E. festucae* Fl1 *kex2* genomic region. **(A)** Restriction map of *E. festucae* Fl1 *kex2* genomic region. Sizes of restriction fragments are shown in kb. **(B)** Structure of the *E. festucae* Fl1 *kex2* genomic region. Coding regions are shown in blue. Primers are shown by arrows (indicating direction of amplification from the primers). The exon-intron structure of the genes is shown beneath, with exons and introns indicated by red and yellow boxes respectively. The position the *N. lolii* Lp19 probe used in Figure 3.25 would anneal is indicated by a grey boxes just below the restriction map.

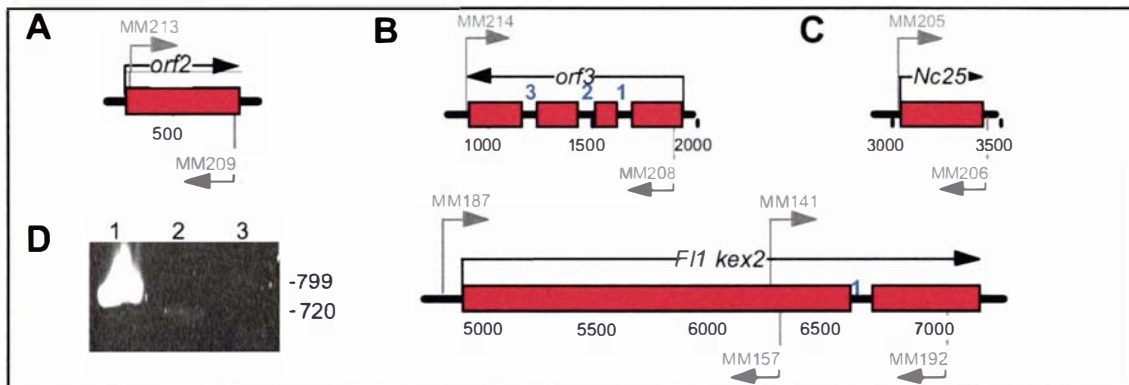

Figure 3.28 Gene structure of *E. festucae* Fl1 *orf2, orf3, Nc25* and *kex2*

Structure of the *E. festucae* Fl1 *orf2, orf3, Nc25* and *kex2* genes. RT-PCR analysis was performed with RNA isolated from *E. festucae* Fl1 cultures grown in PD broth for 7 days. cDNA was reverse transcribed from poly-A RNA using the Expand RT enzyme (Roche) (Section 2.18.5). Fragment sizes are shown adjacent to the gel in bp. On the schematic diagram of each gene, the position within the *kex2* locus is indicated in bp. Exons (confirmed by sequencing of cDNA products) are indicated by red boxes. Primers are positioned above or below the sequence for forward or reverse direction respectively. Introns are numbered in blue text between exons. (A) Proposed structure of the *orf2* gene. (B) Proposed structure of the *orf3* gene. (C) Proposed structure of the *Nc25* gene. (D) The *kex2* gene. Lane 1: *E. festucae* Fl1 genomic DNA, lane 2: 10 fold dilution of *E. festucae* Fl1 cDNA, lane 3: negative control.
The following PCR conditions were used: 5 ng genomic DNA or 5 µL diluted cDNA, 1x Taq polymerase buffer (Roche), 50 µM each dNTP, 200 nM of each primer, and 0.5 U Taq polymerase in a volume of 25 µL. The PCR amplification conditions for the primer pair MM141-MM192 were as follows: 94°C for 2 min, followed by 30 cycles of 94°C for 30 s, 60°C for 30 s, 72°C for 1 min 30 s, then one cycle of 72°C for 5 min.

while the *M. grisea* and *F. graminearum* shared a common first intron, no conservation was observed in the second intron in *M. grisea*. This suggests the intron position in the *kex2* gene is conserved in most, but not all, fungal kexin genes.

Many CreA, AreA and Seb1 binding sites were found in the *kex2* promoter (Figure 3.29A, B and D). In contrast, there were very few binding sites for PacC within the *kex2* promoter (Figure 3.29C). In the *kex2* promoter, more binding sites were observed than expected for a random distribution for CreA and Scb1, whereas lower

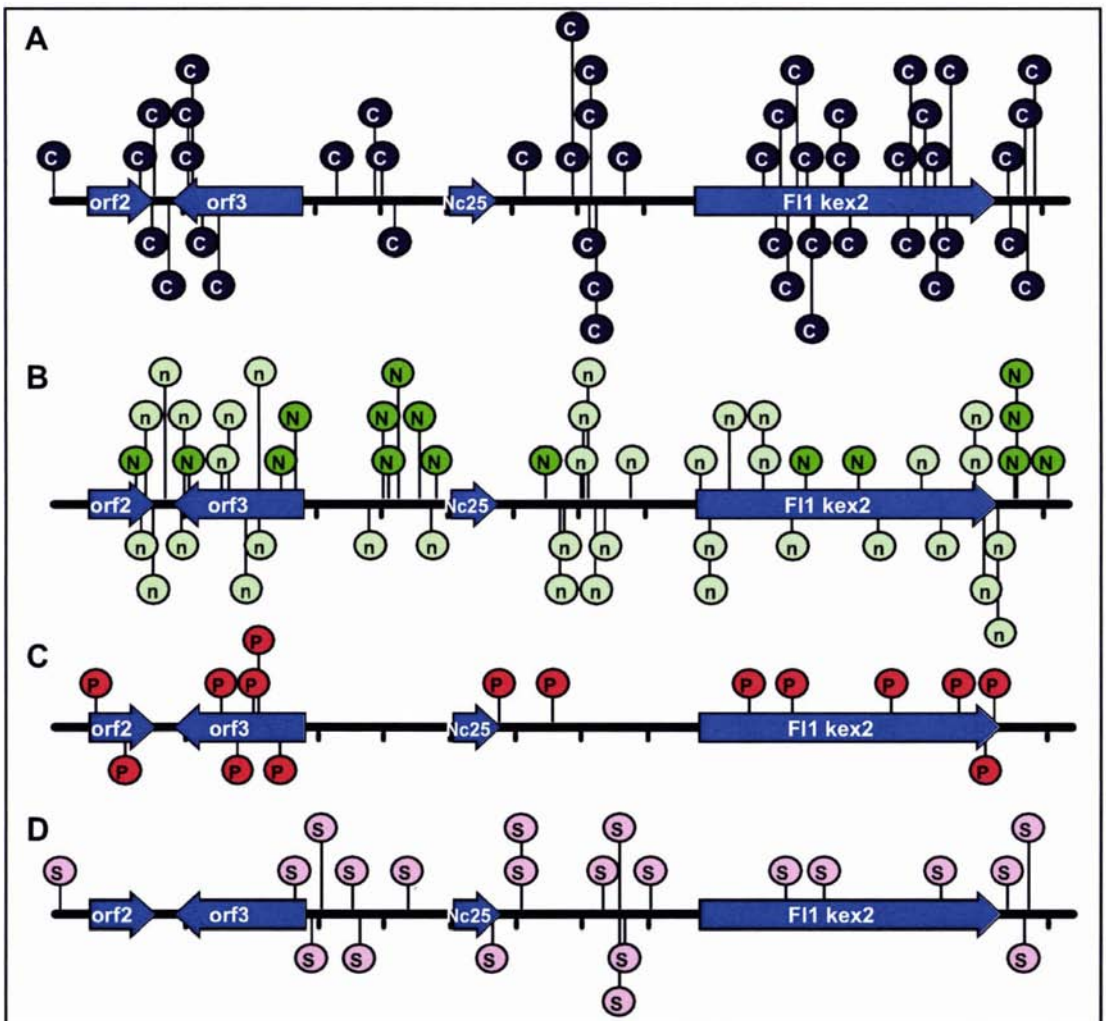

Figure 3.29 Potential binding sites for fungal global transcription factors at the *E. festucae* Fl1 *kex2* locus

Analysis for putative binding sites for the fungal transcription factors CreA (carbon regulation), Nit2/AreA (nitrogen regulation), PacC (pH regulation) and Seb1 (transcriptional regulator) at the *E. festucae* Fl1 *kex2* locus.(A) Putative binding sites for CreA (SYGGRG) are indicated by blue lollipops containing the letter C. (B) Putative binding sites for Nit2/AreA (HGATAR) are indicated by green lollipops containing the letter N. Weaker binding sites (GATA) are indicated by lighter green lollipops containing the letter n. (C) Putative binding sites for PacC (GCCARG) are indicated by red lollipops containing the letter P. (D) Putative binding sites for Seb1 (AGGGG) are indicated by purple lollipops containing the letter S.

than expected numbers were observed for AreA/Nit2. The number of PacC binding sites in the promoter was consistent with the number expected for a random distribution. These observations suggest *kex2* expression could be regulated by carbon availability.

Phylogenetic analysis of the *E. festucae* Fl1 Kex2 protein showed this protein grouped with kexins from other filamentous ascomycete fungi (Figure 3.30). As a single gene in most fungal genome, the Kex2 protein would be expected to group with its closest phylogenetic relative, FG09156.1. However, Kex2 did not group with sequences from the most closely related species. It is unclear if this is due to gene duplication and subsequent loss, or divergent evolution.

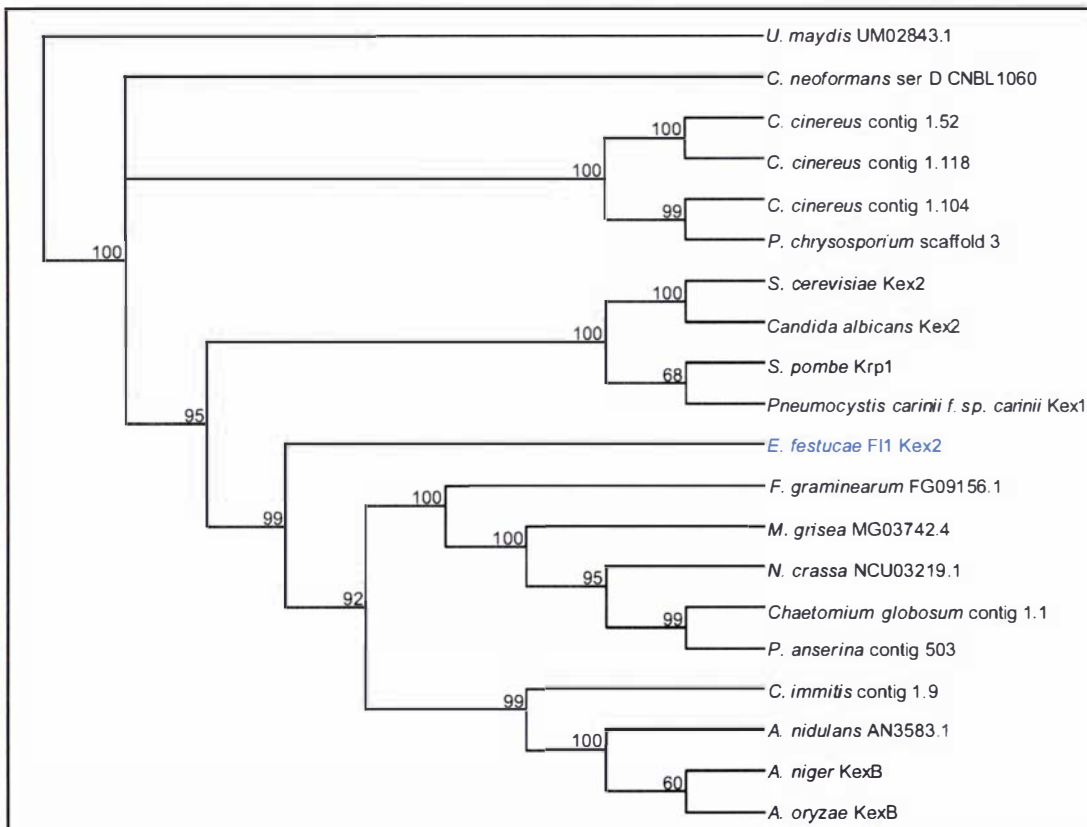

Figure 3.30 Phylogenetic relationships of the *E. festucae* Fl1 Kex2 protein with fungal kexins

Phylogenetic relationships of the *E. festucae* Fl1 Kex2 protein (shown in blue) with other related fungal proteins. The phylogenetic tree in this figure was prepared in the MacVector 7.2.3 program, using Neighbour joining and bootstrapping (1000 replicates) of sequences aligned using the ClustalW module of MacVector to form the tree. For details of the sequences used in this alignment, see Appendix A13.4.

3.4 *E. FESTUCAE* FL1 CONTAINS OTHER GENES ENCODING SUBTILISIN-LIKE PROTEASES

A degenerate PCR approach was used to identify other subtilisin-like protease genes in the *E. festucae* Fl1 genome. The degenerate primers MM149 and MM150 were designed based on highly conserved polypeptide sequences flanking histidine and serine residues required for catalytic activity (Figure 3.31A, Appendix A7.2). Degenerate PCR gave at least eight distinct products (Figure 3.31B), four of which were characterised (Table 3.8). Three of these products shared identity with subtilisin-like protease-encoding genes.

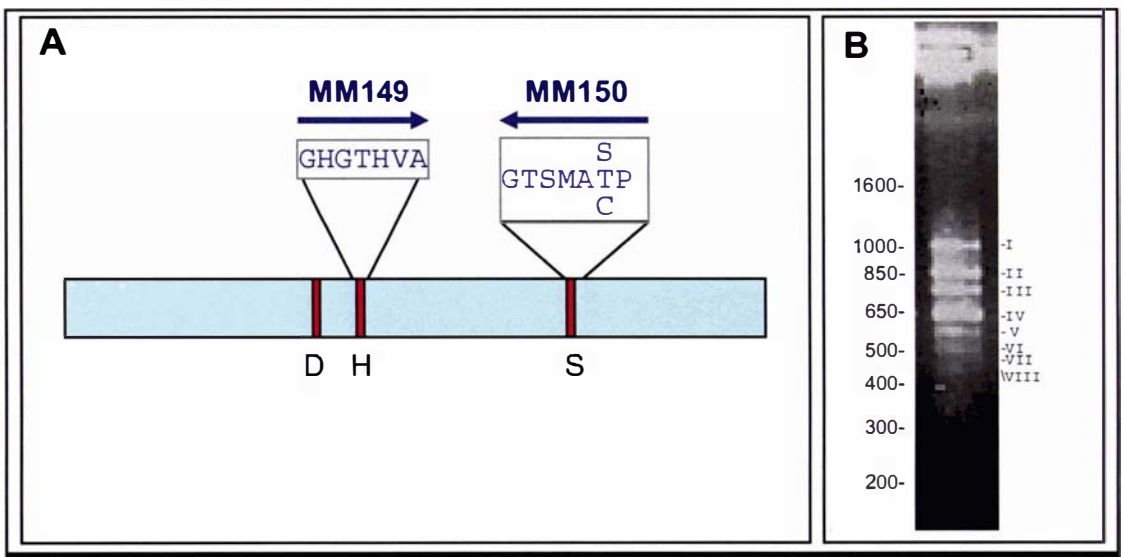

Figure 3.31 Degenerate PCR amplification of subtilisin-like protease-encoding sequences from *E. festucae* Fl1

Amplification of subtilisin-like protease-encoding sequences from *E. festucae* Fl1 by degenerate PCR. **(A)** The degenerate primers MM149 and MM150 were designed based on conserved regions surrounding the histidine and serine catalytic site residues of subtilisin-like proteases. The alignment used to design these primers is shown in Appendix A7.2. **(B)** Degenerate PCR products amplified with the MM149 and MM150 primers. Sizes are indicated in bp. Amplified fragments of different sizes are indicated by roman numerals.

The following PCR conditions were used: 50 ng genomic DNA, 1x Taq polymerase buffer (Roche), 50 µM each dNTP, 400 nM of each primer, and 0.5 U Taq polymerase in a volume of 25 µL. The PCR amplification conditions for the primer pairs MM149-MM150 were as follows: 94°C for 2 min, followed by 30 cycles of 94°C for 30 s, 47°C for 30 s, 72°C for 1 min, then one cycle of 72°C for 5 min.

Table 3.7 Characterised products from degenerate PCR with theMM149- MM150 primers

Fragment	Size (bp)	Named	Highest similarity	Family
I*	~1000	*prt8*	Pr1C (*M. anisopliae*)	Pyrolysin subfamily 1
II	~850	*orf5*	FG09135.1 *F. graminearum*)	WD40 repeat
III*	718	*prt7*	FG06332.1 *F. graminearum*)	Pyrolysin subfamily 2
IV*	611	*prt6*	Pr1J (*M. anisopliae*)	Proteinase K subfamily 2

*Rows shaded in grey correspond to fragments amplified from genes encoding subtilisin- like proteases

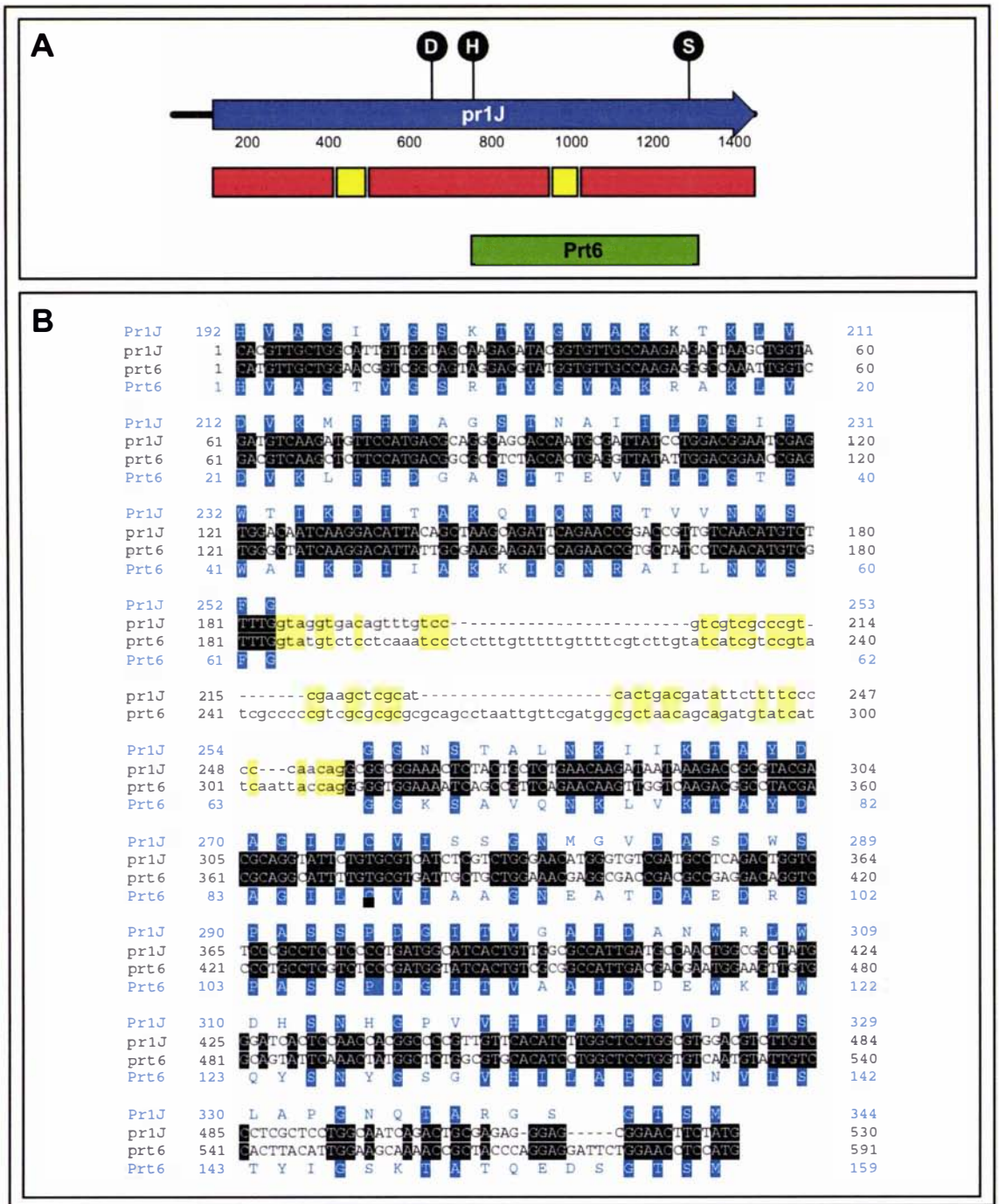

Figure 3.32 The *E. festucae* Fl1 *prt6* gene

(A) Schematic diagram showing the most similar sequence to *prt6*, the *pr1J* gene from *M. anisopliae*. The *pr1J* open reading frame is shown by a blue arrow, with the exons and intron indicated by red and yellow boxes respectively. The sequences encoding conserved catalytic residues are indicated by black circles. The position of the amplified *prt6* product relative to *pr1J* is indicated by a green box. **(B)** Alignment of the *pr1J* and *prt6* nucleotide sequences (shown in black text) and the Pr1J and Prt6 polypeptide sequences (shown in blue text). For the nucleotide sequence, exons are shown in uppercase text, with the intron sequence in lower case text. Sequence identity at the nucleotide level is indicated by black or yellow shading in exons or introns respectively. Sequence identity at the amino acid level is indicated by blue shading.

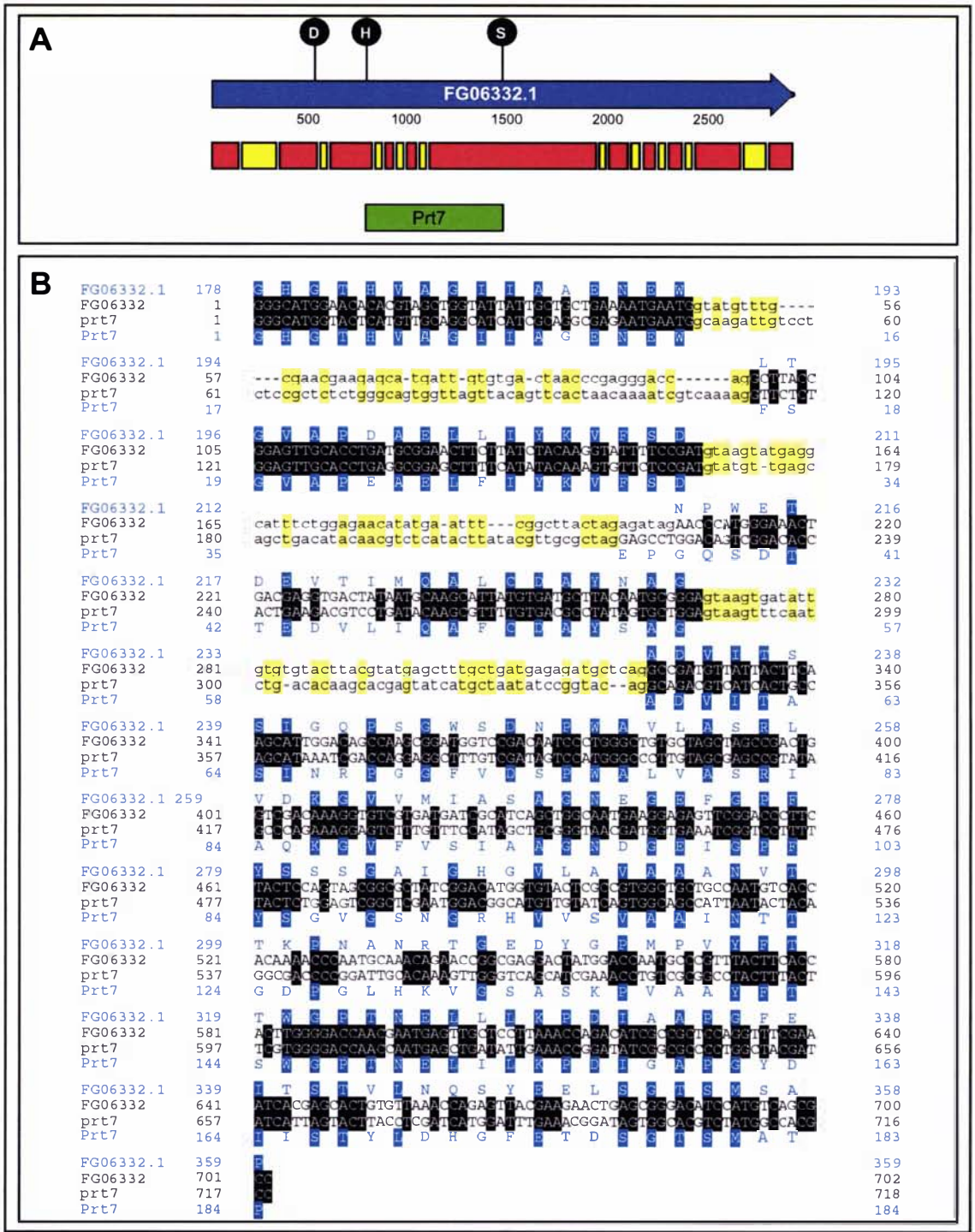

Figure 3.33 The *E. festucae* Fl1 *prt7* gene

(A) Schematic diagram showing the most similar sequence to *prt7*, the *FG06332.1* gene from *F. graminearum*. The *FG06332.1* open reading frame is shown by a blue arrow, with the exons and intron indicated by red and yellow boxes respectively. The sequences encoding conserved catalytic residues are indicated by black circles. The position of the amplified *prt7* product relative to *FG06332.1* is indicated by a green box. **(B)** Alignment of the *FG06332.1* and *prt7* nucleotide sequences (shown in black text) and the FG06332.1 and Prt7 polypeptide sequences (shown in blue text). For the nucleotide sequence, exons are shown in uppercase text, with the intron sequence in lower case text. Sequence identity at the nucleotide level is indicated by black or yellow shading in exons or introns respectively. Sequence identity at the amino acid level is indicated by blue shading.

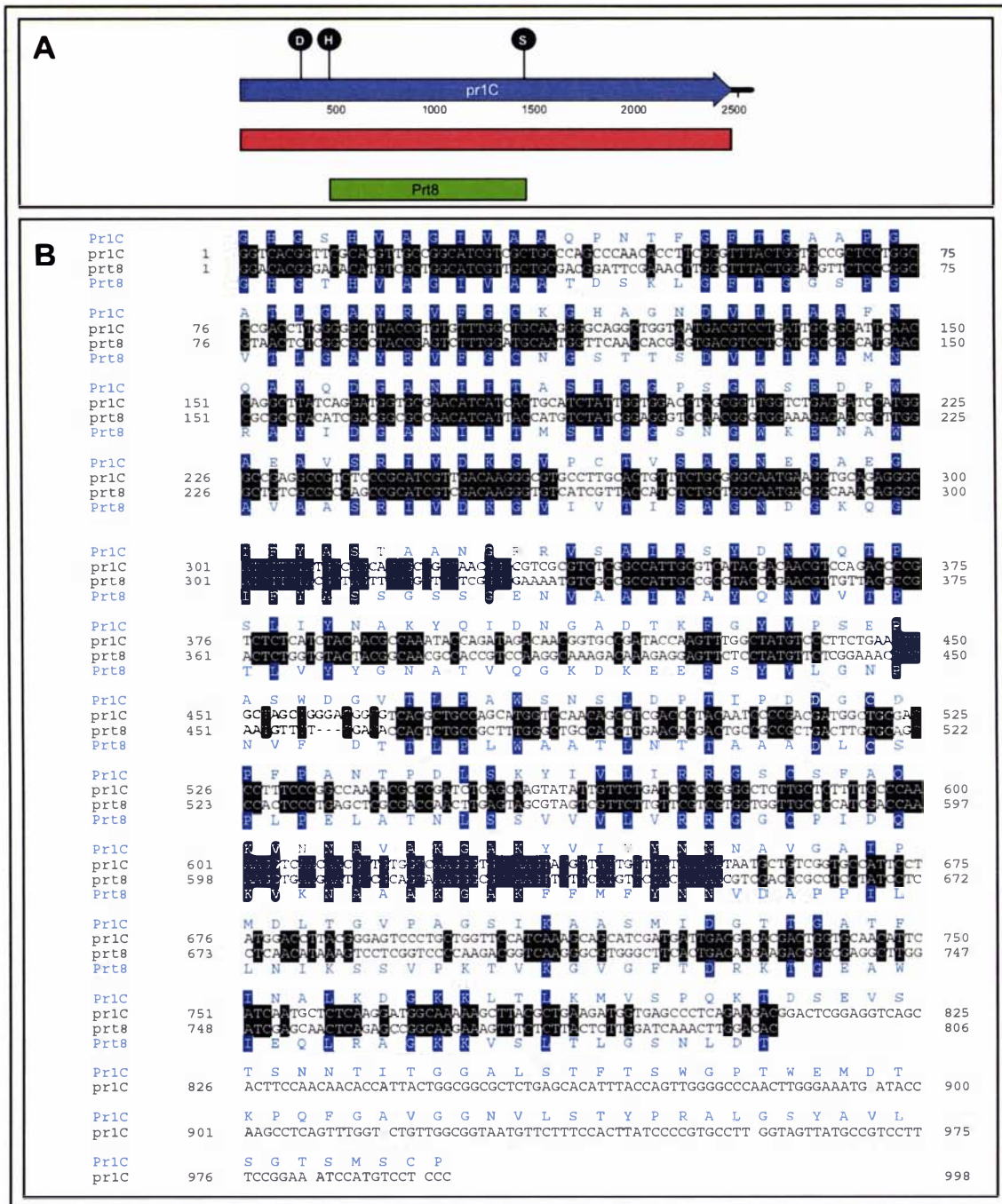

Figure 3.34 The *E. festucae* Fl1 *prt8* gene

(A) Schematic diagram showing the most similar sequence to *prt8*, the *pr1C* gene from *M. anisopliae*. The *pr1C* open reading frame is shown by a blue arrow, with the single exon indicated by a red box. The sequences encoding conserved catalytic residues are indicated by black circles. The position of the amplified *prt8* product relative to *pr1C* is indicated by a green box. **(B)** Alignment of the *pr1C* and *prt8* nucleotide sequences (shown in black text) and the Pr1C and Prt8 polypeptide sequences (shown in blue text). Sequence identity at the nucleotide level is indicated by black or yellow shading in exons or introns respectively. Sequence identity at the amino acid level is indicated by blue shading.

The largest product, I (Figure 3.31B), was designated *prt8*, and was most similar to the *prlC* gene from *M. anisopliae* (Figure 3.34A,B). This suggests the *prt8* gene encodes a subtilisin-like protease from pyrolysin subfamily 1. Product II (Figure 3.31B), designated *orf5*, appears to encode a protein similar to FG09135.1 from *F. graminearum*, a protein that contains a WD40 repeat domain. Product III (Figure 3.31B), designated *prt7*, was most similar to FG06332.1, a pyrolysin subfamily 2 subtilisin-like protease (Figure 3.33A,B). Product IV, which was designated *prt6*, was most similar to *prlJ* from *M. anisopliae* (Figure 3.32A,B). The Prl J protease belongs to proteinase K subfamily 2, suggesting that the protease encoded by *prt6* also belongs to this group.

The smaller uncharacterised fragments amplified by degenerate PCR may have been amplified from genes that have already been characterised, such as the *prtl*, 2, 3, or 5 genes. Fragment V is the size expected for the *prt2*, *prt3* and *prt5* products, while fragment VII is the expected size for the *prtl* gene.

3.5 CHROMOSOMAL LOCALISATION OF THE *PRT* AND *KEX2* GENES

The chromosomal location of the *prtl*, *prt2*, *prt3*, *prt4*, *prt5* and *kex2* genes was assessed using Southern blotting of chromosomal DNA. Protoplast plugs were prepared for endophyte strains *N. lolii* Lp19, *E. festucae* Fl1 and *E. typhina* PN2311 as described in Section 2.15.3. The *N. lolii* Lp19 and *E. festucae* Fl1 strains were selected as they were strains used throughout this study, while the *E. typhina* PN2311 strain was selected as it is the *Poa ampla*-infecting endophyte strain from which the Atl protease was first characterised. Protoplast plugs from *S. cerevisiae* and *S. pombe* were used as molecular weight standards, as they contained chromosomal DNA of known size. Chromosomal DNA was separated by contour-clamped homogeneous electrical field (CHEF) electrophoresis as described in Section 2.15.4 (Figures 3.35A and 3.36A).

Hybridisation of chromosomal DNA with *prtl* and *prt5* probes (Figure 3.35B and C) showed that the *prt5* and *prtl* genes were both located on the same chromosome in each of the three endophyte strains. The *prt2* gene (Figure 3.35D) in *N. lolii* Lp19

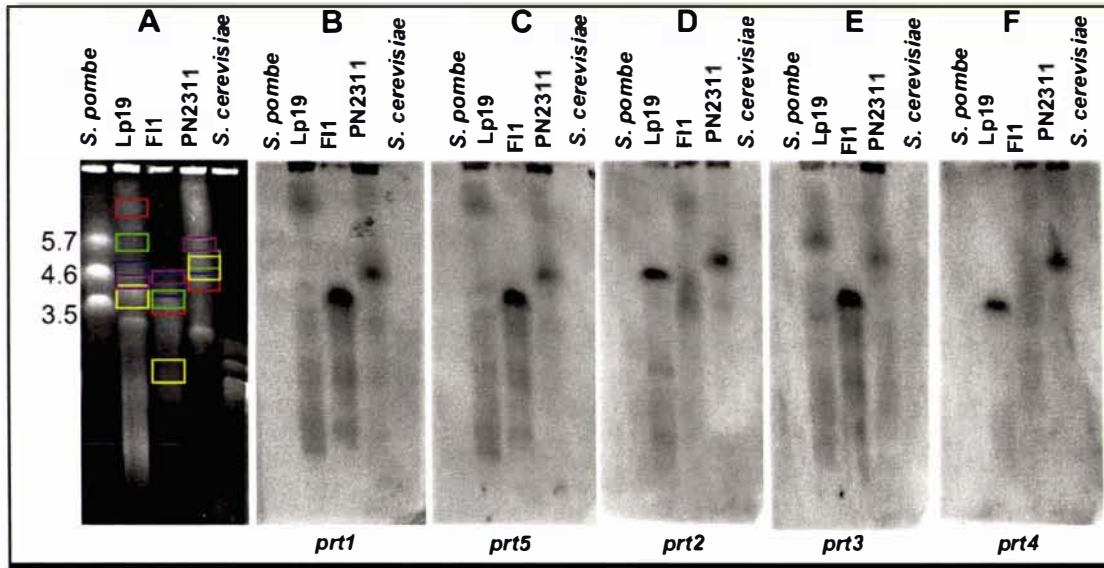

Figure 3.35 Chromosomal location of the *prt* genes

(**A**) Separation of chromosomal DNA from *N. lolii* Lp19, *E. festucae* Fl1 and *E. typhina* PN2311 by CHEF electrophoresis as described in Section 2.15.4. The size standards are indicated in Mb. Red boxes represent *prt1* and *prt5*, blue boxes *prt2*, green boxes *prt3*, and yellow boxes represent *prt4* hybridising fragments. The purple boxes indicate the chromosomal DNA band that hybridises to the *kex2* probe (as shown in Figure 3.35). (**B**) Autoradiograph of a Southern blot from the gel in **A** hybridised with a [^{32}P]-labelled *prt1* fragment amplifed with primers MM5 and MM2. Hybridising chromosomal DNA is surrounded by a red box in panel A. (**C**) Autoradiograph of a Southern blot from the gel in **A** hybridised with a [^{32}P]-labelled *prt5* fragment amplifed with primers MM15 and MM6. Hybridising chromosomal DNA is surrounded by a red box in panel A. (**D**) Autoradiograph of a Southern blot from the gel in **A** hybridised with a [^{32}P]-labelled *prt2* fragment amplifed with primers MM75 and MM76. Hybridising chromosomal DNA is surrounded by a blue box in panel A. (**E**) Autoradiograph of a Southern blot from the gel in **A** hybridised with a [^{32}P]-labelled *prt3* fragment amplifed with primers MM93 and MM94. Hybridising chromosomal DNA is surrounded by a green box in panel A. (**F**) Autoradiograph of a Southern blot from the gel in **A** hybridised with a [^{32}P]-labelled *prt4* fragment amplifed with primers MM155 and MM130. Hybridising chromosomal DNA is surrounded by a yellow box in panel A.

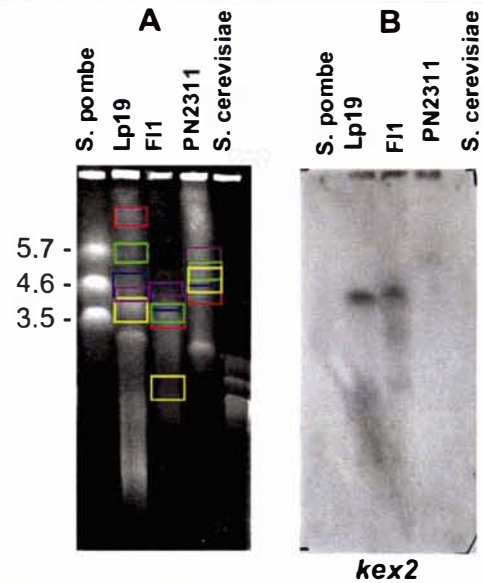

Figure 3.36 Chromosomal location of the *kex2* gene

(**A**) Separation of chromosomal of *N. lolii* Lp19, *E. festucae* Fl1 and *E. typhina* PN2311 by CHEF electrophoresis as described in Section 2.15.4. The size standards are indicated in Mb. Purple boxes indicate chromosomal DNA bands that hybridise to the kex2 probe. Bands that hybridise to *prt1* and *prt5* (red boxes), *prt2* (blue boxes), *prt3* (green boxes), and *prt4* (yellow boxes) are also shown (see Figure 3.30). The purple boxes indicate the chromosomal DNA band that hybridise to the *kex2* probe (as shown in Figure 3.31). (**B**) Autoradiograph of a Southern blot from the gel in **A** hybridised with a [^{32}P]-labelled *kex2* fragment amplifed with primers MM141 and MM192. Hybridising chromosomal DNA is surrounded by a purple box in panel A.

and *E. typhina* PN2311 strains was located on a different chromosome to that containing *prt5* and *prt1* genes (Figure 3.35D). In *E. festucae* Fl1, the *prt2* and *prt3* genes appeared to be on the same chromosome as *prt5* and *prt1*, or on a chromosome of the same size. The *E. festucae* Fl1 *prt4* gene is located on a different chromosome to the *prt1, prt5, prt2* and *prt3* genes. In *E. typhina* PN2311, the *prt3* and *prt4* genes appeared to be on the same chromosome as *prt2*, or on a chromosome of a similar size. In *N. lolii* Lp19, the *prt2, prt3* and *prt4* genes were located on independent chromosomes to each other and distinct to that containing the *prt1* and *prt5* genes. The *kex2* gene is located on chromosomes that do not contain any of the *prt* genes in all of the three endophyte strains tested (Figure 3.36B).

3.6 EXPRESSION OF THE PRT AND *KEX2* GENES IN CULTURE AND *IN PLANTA*

The *kex2* gene and all of the *prt* genes with the exception of *prt2* were previously shown to be expressed in culture (Figures 3.5A and B, 3.11A, 3.16A, 3.23 and 3.28D). To examine whether expression of these genes were differed during endophyte growth *in planta* when compared to rich culture conditions (in PDB medium; Section 2.3.3), a cDNA equalisation approach was used. cDNA pools were synthesised from polyA mRNA extracted from either the symbiotum G1251 (*L. perenne* cv. Nui infected with *E. festucae* Fl1) or from *E. festucae* Fl1 grown in PD broth for seven days. Expression levels of the constitutively expressed *tub2* gene in the plant and culture samples were analysed by comparing a 10-fold dilution of G1251 cDNA (hereafter called P10, Figure 3.37) with various dilutions of the cDNA pool from *E. festucae* Fl1 grown in culture where amplification of the product is similar (Figure 3.34). In this equalisation experiment, the amount of the *tub2* cDNA product in the G1251 10-fold dilution was approximately equal to that from the 200-fold cDNA dilution from *E. festucae* Fl1 grown in culture. No DNA contamination was observed in no RT cDNA controls for either the symbiotum or culture samples.

After the two cDNA pools were equalised for *tub2* expression, the expression of other genes could be compared in culture and *in planta*. The G1251 symbiotum 10-fold cDNA dilution was amplified together with the equalised culture 200-fold cDNA dilution and a 10-fold more concentrated culture 20-fold cDNA dilution

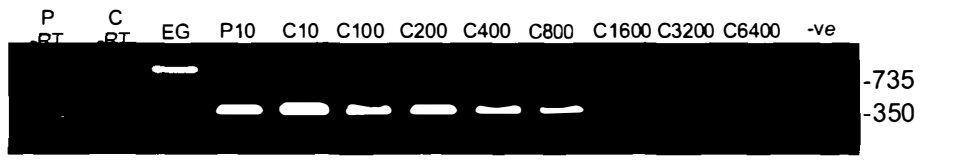

Figure 3.37 Equalisation between in culture and *in planta tub2* expression

Equalisation of *E. festucae* FI1 *tub2* expression between culture and symbiotum samples. The G1251 symbiotum (*L. perenne* cv. Nui infected with *E. festucae* FI1) was used as the plant sample (P), while *E. festucae* FI1 grown for 7 days in PD broth was used the culture sample (C). –RT reactions prepared during cDNA synthesis (P –RT for G1251 and C –RT for *E. festucae* FI1 respectively) were included as controls, along with the negative control (-ve) to which no DNA was added. *E. festucae* FI1 genomic DNA (EG) was included as a positive control. Lanes contained G1251 cDNA 10 fold cDNA dilution (P10), *E. festucae* FI1 10 fold (C10), 100 fold (C100), 200 fold (C200), 400 fold (C400), 800 fold (C800), 1600 fold (C1600), 3200 fold (C3200) and 6400 fold (C6400) cDNA dilutions.
PCR was performed with the T1.1-T1.2 primer pair. PCR reactions contained diluted cDNA no RT reaction mixes or 5 ng of genomic DNA as the template, along with 1 x *Taq* polymerase buffer (2.5 mM $MgCl_2$, Roche) , 50 µM of each dNTP, 200 nM of both T1.1 and T1.2 primers and 0.5 U *Taq* polymerase (Roche). The following PCR program was used: 94°C for 2 min, 30 cycles of 94°C for 30 s, 60°C for 30 s, 72°C for 1 min, followed by 72°C for 5 mins.

(Figure 3.38). *prt1* expression was detected in the G1251 10-fold cDNA dilution, but not in the equalised 200-fold cDNA dilution from *E. festucae* Fl1 grown in culture. However, *prt1* expression was detected in the 20-fold cDNA dilution from culture. This suggests that *prt1* expression is up regulated *in planta.* As expected based on the results of previous experiments, *prt2* expression was not detected either in culture or *in planta. prt3* expression was detected in the G1251 10 fold dilution, but not in either the 200-fold or 20-fold cDNA dilutions from *E. festucae* Fl1 grown in culture. This suggests that under the conditions assayed, *prt3* expression in culture was below the limit of detection of the RT-PCR conditions used. It also suggests that expression of the *prt3* gene, like *prt1*, is up regulated *in planta.* The *prt4* gene was strongly expressed both in culture and *in planta*. Like *prt1* and *prt3*, *prt4* expression also appeared to be up regulated *in planta.*

Expression of *prt5* and *kex2* was not detected in either the symbiotum or culture samples, suggesting that the expression of these two genes is below the detection level of the RT-PCR system used in this experiment. However, unlike the *prt2* gene, expression of these two genes has previously been detected in culture (Figures 3.28D and 3.5A). The *gcn1* gene appeared to be expressed at similar levels in culture and *in planta.* Expression of the lolitrem biosynthetic gene *ltmM* has previously been shown to be upregulated during endophyte growth *in planta* (Young, 2005). In this

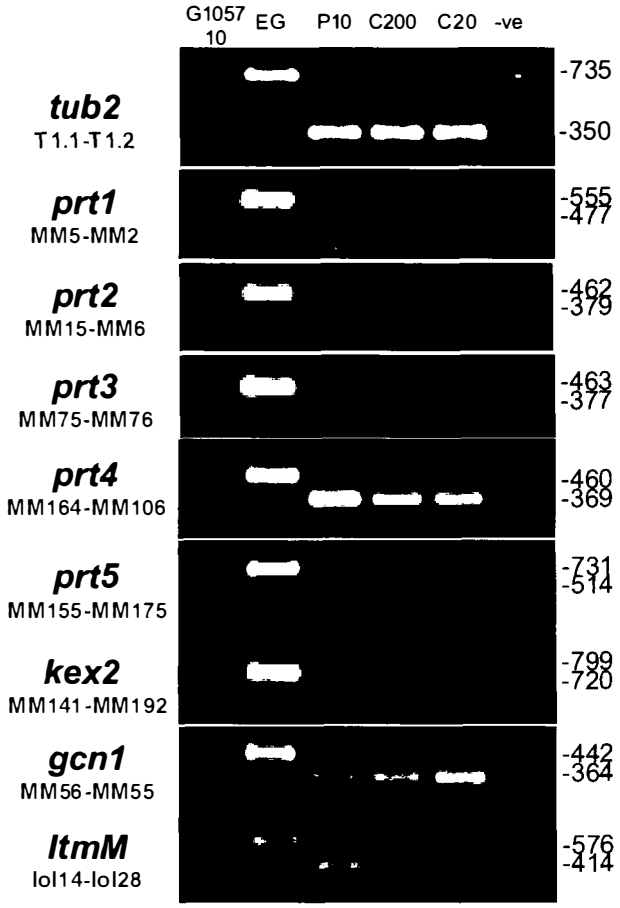

Figure 3.38 Comparison of hydrolytic enzyme gene expression in culture and *in planta*

RT-PCR using the equalised symbiotum and culture cDNA dilutions (P10 and C200) identified in Figure 3.33. A 20 fold dilution of cDNA from *E. festucae* Fl1 grown in culture (C20), which contains 10 fold more cDNA than the equalised culture cDNA dilution (C200), was included, along with a 10 fold dilution of cDNA from the G1057 sample (uninfected *L. perenne* cv. Nui), labelled as G1057 10, was also included. *E. festucae* Fl1 genomic DNA (EG) and water only controls (-ve) were included as positive and negative controls respectively. Genes analysed and the primer pairs used to amplify them are indicated on the left. Expected sizes of genomic and cDNA PCR products are shown on the right.

PCR reactions contained diluted cDNA or 5 ng of genomic DNA as the template, along with 1 x *Taq* polymerase buffer (2.5 mM $MgCl_2$, Roche) , 50 µM of each dNTP, 200 nM of both primers and 0.5 U *Taq* polymerase (Roche). The following PCR program was used for most samples was: 94°C for 2 min, 30 cycles of 94°C for 30 s, 60°C for 30 s, 72°C for 1 min, followed by 72°C for 5 mins. The exception to this was for the MM75-MM76 primer pair, where the annealing temperature was dropped from 60°C to 55°C

experiment, *ltmM* expression was detected in the G1251 symbiotum, but not in either the 200-fold or 20-fold cDNA dilutions from *E. festucae* Fl1 grown in culture.

This equalisation experiment was also repeated using cDNA from four different grass-endophyte associations (Figure 3.39). *tub2* expression from *E. festucae* Fl1 grown in culture for seven days was equalised with *tub2* expression from symbiota of

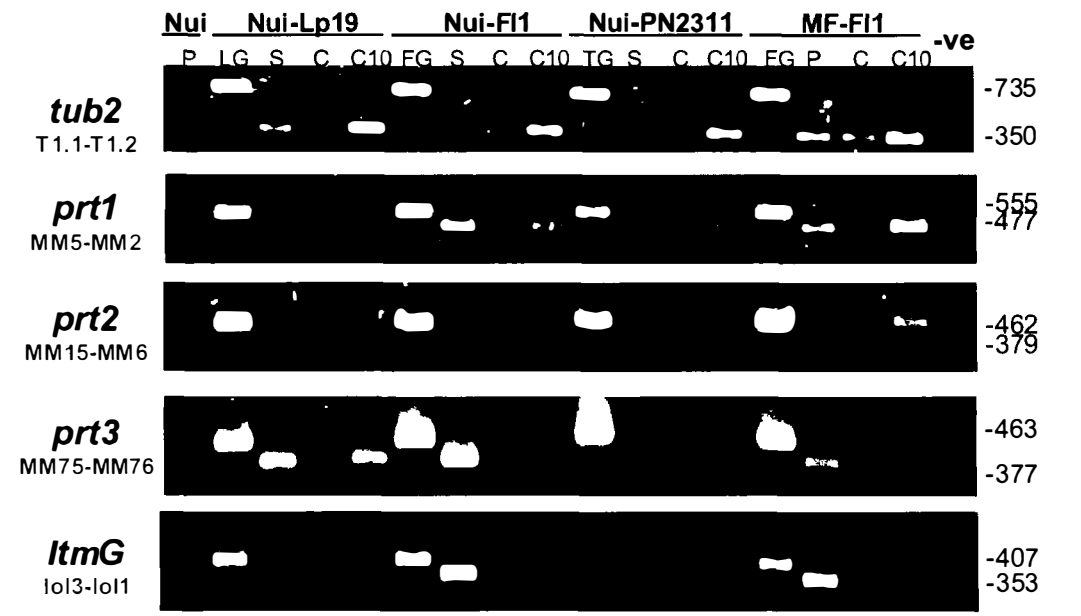

Figure 3.39 Comparison of *prt* gene regulation in different grass-endophyte symbiota

RT-PCR using equalised symbiotum (S) and culture (C) cDNA dilutions. A culture cDNA dilution 10-fold more concentrated (C10) than the equalised culture cDNA (C) dilution was included, along with cDNA dilution from uninfected *L. perenne* cv. Nui (P). Endophyte genomic DNA from *N. lolii* Lp19 (LG), *E. festucae* Fl1 (FG) and *E. typhina* PN2311 (TG) were used as positive controls. The symbiota were uninfected *L. perenne* cv. Nui (G1057), *L. perenne* cv. Nui infected with *N. lolii* Lp19 (G1056), *L. perenne* cv. Nui infected with *E. festucae* Fl1 (G1251), *L. perenne* cv. Nui infected with *E. typhina* PN2311 (G1444) and *Festuca pratensis* infected with *E. festucae* Fl1. The expected fragment sizes amplified from *E. festucae* Fl1 genomic DNA and cDNA are shown on the right in bp.
polyA mRNA was isolated from cultures grown for 5, 7 or 12 days for *E. typhina* PN2311, *E. festucae* Fl1 and *N. lolii* Lp19 respectively.PCR reactions contained diluted cDNA or 5 ng of genomic DNA as the template, along with 1 x *Taq* polymerase buffer (2.5 mM $MgCl_2$, Roche) , 50 µM of each dNTP, 200 nM of both primers and 0.5 U *Taq* polymerase (Roche). The following PCR program was used for most samples was: 94°C for 2 min, 30 cycles of 94°C for 30 s, 60°C for 30 s, 72°C for 1 min, followed by 72°C for 5 mins. The exception to this was for the MM75-MM76 primer pair, with an annealing temperature 55°C.

E. festucae Fl1 with *L. perenne* cv. Nui or meadow fescue (*F. pratensis*). *tub2* expression was also equalised between *N. lolii* grown in culture for twelve days and a symbiotum of *L. perenne* cv. Nui infected with *N. lolii* Lp19, and for *E. typhina* PN2311 grown for five days compared to a symbiotum of *L. perenne* cv. Nui infected with *E. typhina* PN2311. The different incubation periods for the fungal strains in culture were selected based on different growth rates in an attempt to harvest equivalent fungal biomass for each culture. While *E. typhina* PN2311 grows very quickly in culture, *E. festucae* Fl1 grows slightly more slowly. *N. lolii* Lp19 grows very slowly in culture: if cultures of this fungus are harvested after five or seven days growth, there will not be enough fungal tissue for RNA isolation.

The analysis of the *prt1*, *prt2*, *prt3* and *gcn1* genes was repeated using the equalised symbiota and culture cDNA dilutions. For *N. lolii* and *E. festucae*, *prt1* and *prt3* expression was up-regulated *in planta* (Figure 3.39) as seen in the previous experiment (Figure 3.38). The up-regulation of *prt1* and *prt3* was also seen in *E. festucae* Fl1 infecting meadow fescue. However, the homologue of the *prt1* gene in *E. typhina* PN2311 was expressed at the same level in culture and *in planta*.

Expression of the *E. typhina* PN2311 homologue of *prt3*, *Atl*, was not detected either in culture or *in planta*. The *prt2* gene was not expressed by any of the fungal strains either in culture or *in planta*. As a control, expression of the lolitrem biosynthetic gene *ltmG*, which is induced *in planta*, was included. As expected, the *ltmG* gene was induced *in planta* for *N. lolii* Lp19 and *E. festucae* Fl1. However, no expression of *ltmG* was detected in *E. typhina* PN2311. As genomic DNA from *E. typhina* PN2311 did not amplify with the *ltmG* primers, this may mean that a homologue of the *ltmG* gene is not present in the *E. typhina* genome.

CHAPTER 4

Results:

Functional characterisation of *prt1* and *prt2*

4.1 CONSTRUCTION OF VECTORS TO GIVE ALTERED EXPRESSION OF THE *PRT1* OR *PRT2* GENES

In order to investigate the function of the *E. festucae* Fl1 *prt1* and *prt2* genes, a strategy was developed to alter the expression of these two genes. Vectors were created that contained fusions at the translation initiation codon of the *prt1* or *prt2* coding region (including introns) with either the *A. nidulans gpdA* promoter and 5' UTR or the *E. festucae* Fl1 *ltmM* promoter and 5' UTR. The *A. nidulans gpdA* promoter directs constitutive expression of the *uidA* (GUS) reporter gene during growth *in planta* (Saunders, 1997), while the *E. festucae* Fl1 *ltmM* gene is highly expressed during growth *in planta* (Young, 2005). The construction of these vectors is described in Section 2.13.1. These resulting vectors, pMM32 (P*gpdA-prt1*), pMM33 (P*ltmM-prt1*), pMM26 (P*gpdA-prt2*) and pMM27 (P*ltmM-prt2*), are shown in Figure 4.1.

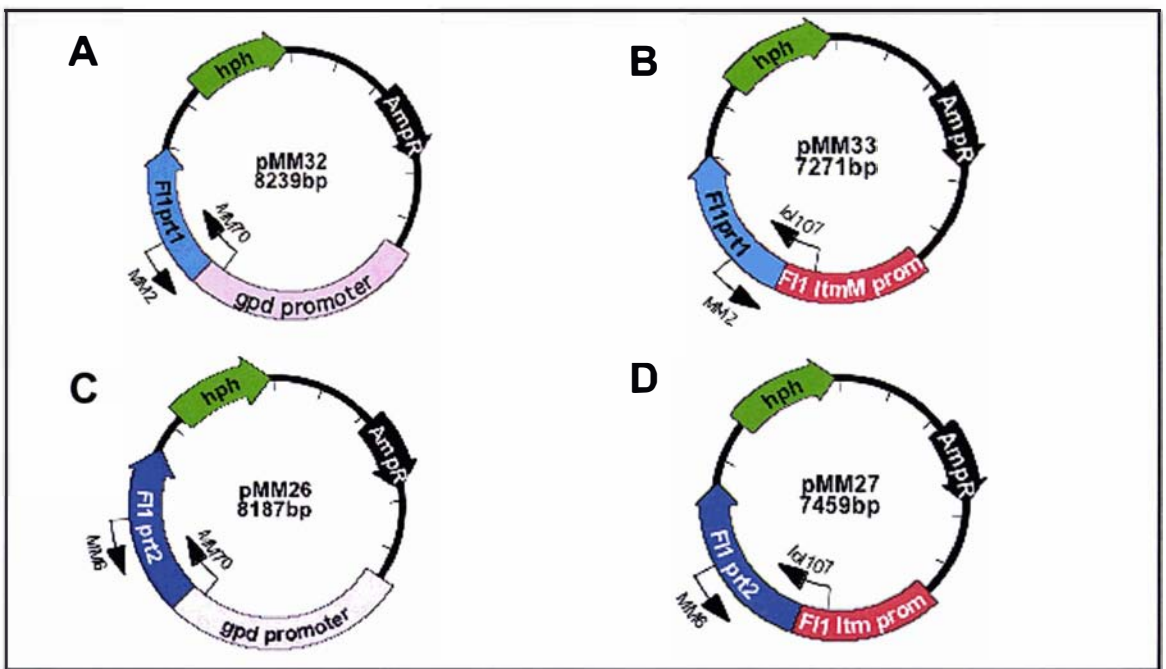

Fig 4.1 Constructs for altered expression of *prt1* and *prt2*

Constructs for altered expression of the *prt1* and *prt2* genes were created as described in Section 2.13. Translational fusions were created between the *E. festucae* Fl1 *prt1* or *prt2* coding regions and the *A. nidulans gpdA* promoter or the *E. festucae* Fl1 *ltmM* promoter. **(A)** The pMM32 vector consisted of the *A. nidulans gpdA* promoter fused to the Fl1 *prt1* coding region. **(B)** The pMM22 vector consisted of the Fl1 *ltmM* promoter fused to the Fl1 *prt1* coding region. **(C)** The pMM26 vector consisted of the *A. nidulans gpdA* promoter fused to the Fl1 *prt2* coding region. **(B)** The pMM27 vector consisted of the Fl1 *ltmM* promoter fused to the Fl1 *prt2* coding region.

4.2 TRANSFORMATION OF *E. FESTUCAE* FL1 WITH THE ALTERED EXPRESSION VECTORS

Protoplasts of *E. festucae* Fl1 prepared as described in Section 2.14.2 were transformed with circular DNA corresponding to the vectors pMM32, pMM33, pMM26 or pMM27 (Section 2.15). Transformation frequencies for the four vectors are shown in Table 4.1. Transformants were nuclear purified before further analysis. As endophyte hyphae contain only single nuclei in cells toward the hyphal tips (Spiering, 1999), transformants were purified three times by successive subculturing from the edge of a fungal colony on media containing hygromycin.

Table 4.1 Transformation frequency for different plasmid constructs

Treatment	Viable protoplasts after transformation[b]	HygR transformants (colonies per 5 µg DNA)	Freq HygR transformants (freq/5 µg DNA)
Cells only	1.84×10^5	0	0
pAN7-1[a]		17[c]	9.24×10^{-5}
pMM32[a]		8[d]	4.35×10^{-5}
pMM33[a]		5[d]	2.72×10^{-5}
pMM26[a]		85[d]	4.62×10^{-4}
pMM27[a]		57[d]	3.10×10^{-4}

[a] Circular DNA used in these transformations was isolated using the Quantum plasmid midiprep kit (Section 2.5.6)
[b] Viable protoplasts per mL
[c] Extrapolated from colonies obtained for 3 plates
d Number of colonies obtained for 10 plates

Copy number of the vectors within the genome of transformants was assessed by a Southern blot approach. A schematic showing how this strategy was used is shown in Figure 4.2. Digesting genomic DNA from wild type *E. festucae* Fl1 and various transformants digested with restriction enzymes that generate different expected fragment sizes for the wild type and transgene copies of *prt1* or *prt2* makes it possible to distinguish between the two genes (Figure 4.2A, 4.2B). As the vectors were transformed into *E. festucae* Fl1 as circular DNA, they had the potential to recombine into genomic DNA at any point within the vector sequence, which potentially could result in copies of the constructs inserting in such a way as to disrupt the introduced *prt1* or *prt2* genes. If the construct inserted in a way that disrupted the *prt1* or *prt2* coding region, other sized fragments would be obtained (Figure 4.2C).

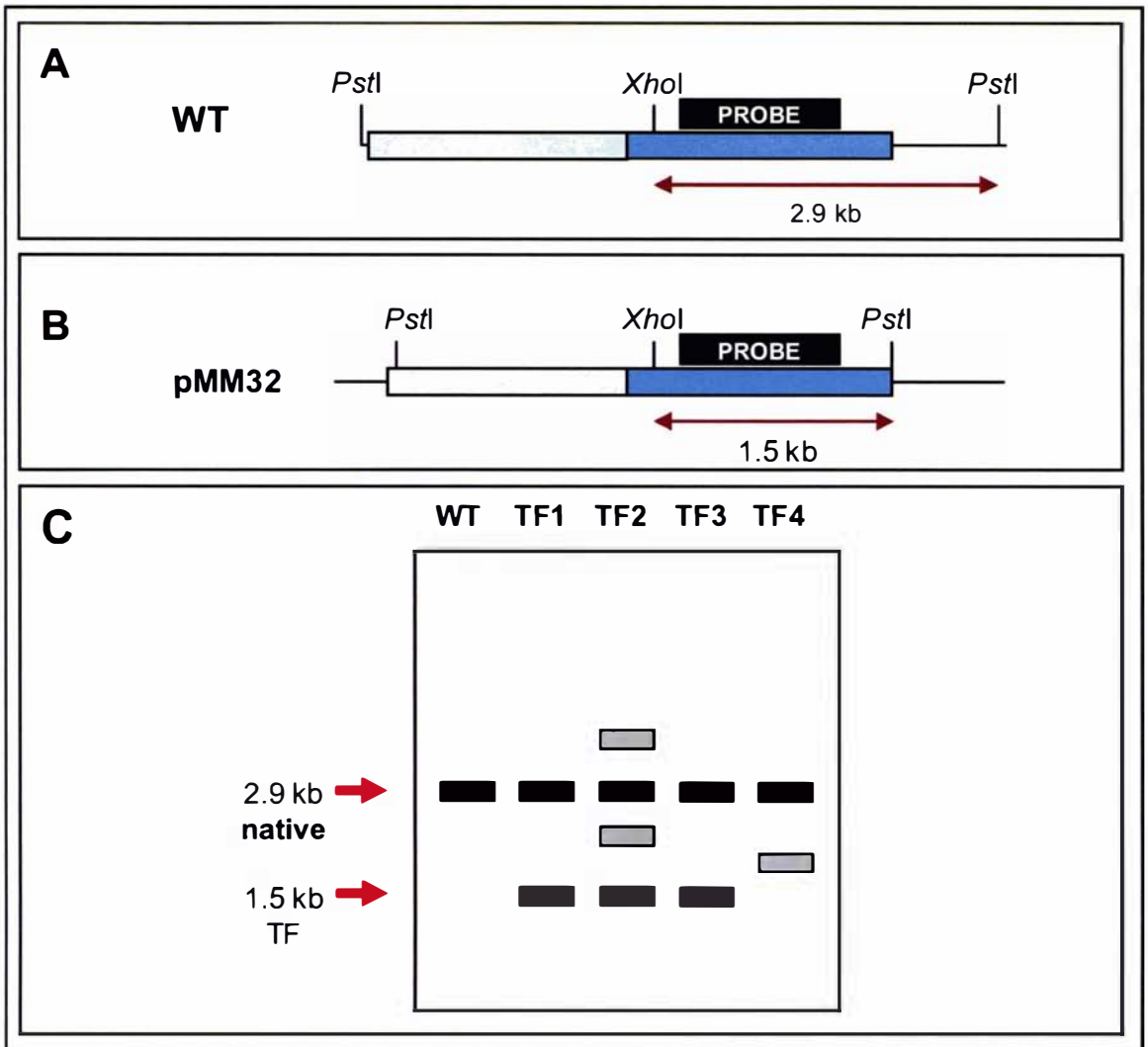

Figure 4.2 Strategy for assessing the number of intact transgene copies in transformant genomes

Diagrammatic explanation for screening functional copy number of transgenes in transformant genomes. Screening for transformants of pMM32 is shown as an example, with genomic DNA from *E. festucae* Fl1 and selected transformants digested with *Xho*I and *Pst*I. **(A)** Restriction map of the native copy of *E. festucae* Fl1 *prt1*. **(B)** Restriction map of the pMM32 vector containing the P*gpdA-prt1* fusion gene. **(C)** Schematic of a potential Southern blot for these transformants showing the position of the 2.9 kb native (black bands) and 1.5 kb intact P*gpd-prt1* (dark grey bands) copies of *prt1*. The wild type *E. festucae* Fl1 strain is indicated by WT, while various transformant strains are indicated by TF1, TF2 etc. P*gpdA-prt1* copies resulting from integration of the plasmid disrupting the *prt1* coding region are indicated by light grey bands.

In order to measure the difference in intensities between the wild type and transgene bands, Southern blots of wild type and transformant genomic DNA were prepared based on the strategy described in Figure 4.2. Southern blots were probed with [^{32}P]-labelled fragment amplified from the *prt1* or *prt2* coding regions and a

phosphoimager was used to determine intensity of each band (Section 2.9.5). Copy number of intact *prt1* or *prt2* copies was determined by measuring the relative intensity of transgene bands compared to wild type (single copy) bands. As the wild type band corresponds to a single copy gene, it acts as an internal control for each transformant. For example, the ratio of the intensity of the transgene band to wild type for transformant MM8.1 (pMM32) was 245.32% (Figure 4.3). This suggests that the transformant MM8.1 contains between 2 or 3 functional copies of the P*gpdA-prt1*gene.

Copy number analysis was completed for 8 pMM32 transformants (Figure 4.3, Table 4.2), 5 pMM33 transformants (Figure 4.4, Table 4.3), 12 pMM26 transformants (Figure 4.5, Table 4.4) and 12 pMM27 transformants (Figure 4.6, Table 4.5). Raw data for each set of transformants is shown in Appendix A.12. The results show a large range in the copy number of intact P*gpdA-prt1,* P*ltmM-prt1,* P*gpdA-prt2* or P*ltmM-prt22* introduced into the *E. festucae* Fl1 genome after transformation with the pMM32, pMM33, pMM26 or pMM27 constructs respectively. Transformants ranged from having only one intact copy of the construct (e.g. MM9.1 and MM4.1) to having more than twenty intact copies of the construct (e.g. MM8.5, MM9.2, MM4.8 and MM5.6). Five transformants for each construct with varying numbers of functional *prt1* or *prt2* copies were selected for further analysis in culture and *in planta.*

4.3 ANALYSIS OF TRANSFORMANT *PRT1* OR *PRT2* EXPRESSION

4.3.1 Expression of the transformant prt1 or prt2 genes in culture

Expression of the P*gpdA-prt1*, P*ltmM-prt1*, P*gpdA-prt2* or P*ltmM-prt2* transgenes was assessed in culture by RT-PCR analysis using primers that spanned the translation initiation site (Figure 4.1). This enabled expression of wild type and transgenes to be independently assessed. cDNA was made from DNase I-treated total RNA (Section 2.18.4) from fungal cultures grown for 8 days in PD broth (Section 2.3.3) and used for RT-PCR analysis. As controls, *E. festucae* Fl1 regenerated after protoplasting (MM19.1) and the MM18.3 transformant (*E. festucae*

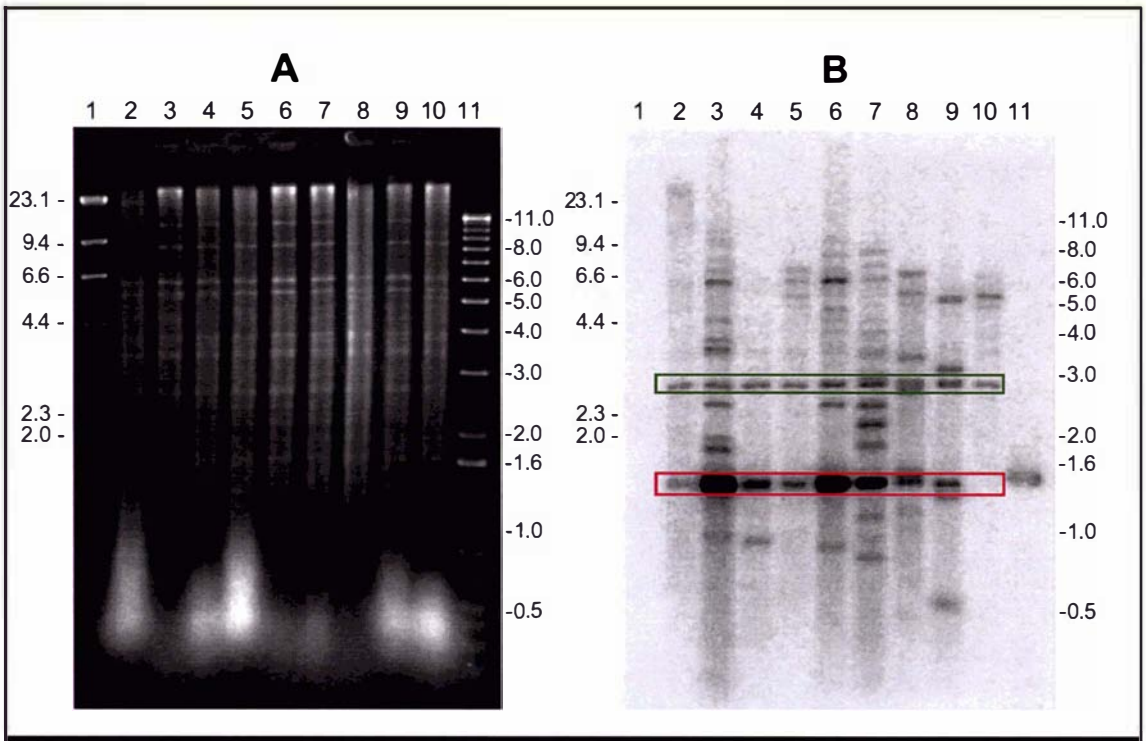

Figure 4.3 Southern blot analysis of pMM32 transformants

Southern analysis of *E. festucae* Fl1 strains transformed with pMM32. **(A)** Genomic DNA (1 µg) digested with *Xho*I and *Pst*I from the strains MM8.1 (lane 2), MM8.2 (lane 3), MM8.3 (lane 4), MM8.4 (lane 5), MM8.5 (lane 6), MM8.6 (lane 7), MM8.7 (lane 8), MM8.8 (lane 9) and *E. festucae* Fl1 (lane 10). Lanes 1 and 11 contain λ *Hin*dIII and 1 kb plus ladder (Invitrogen) respectively. Sizes of marker fragments are shown in kb. **(B)** Autoradiograph of the gel from **A** hybridised with a [^{32}P]-labelled *E. festucae* Fl1 *prt1*fragment amplifed with primers MM4 and MM74. The expected native copy of *prt1* is indicated by a green box. The expected transformant copies of the *gpd-prt1* fusion is indicated by a red box.

Table 4.2 Intact copies of pMM32[a]

Transformant	Intact construct copies[b]
MM8.1	2-3
MM8.2	>20
MM8.3	6-7
MM8.4	4
MM8.5	>20
MM8.6	>20
MM8.7	6
MM8.8	2-3

[a] copies where the P*gpdA-prt1* coding region is intact
[b] determined by the ratio of native to intact P*gpdA-prt1* copies

transformants shaded in grey were selected for inoculations into plants

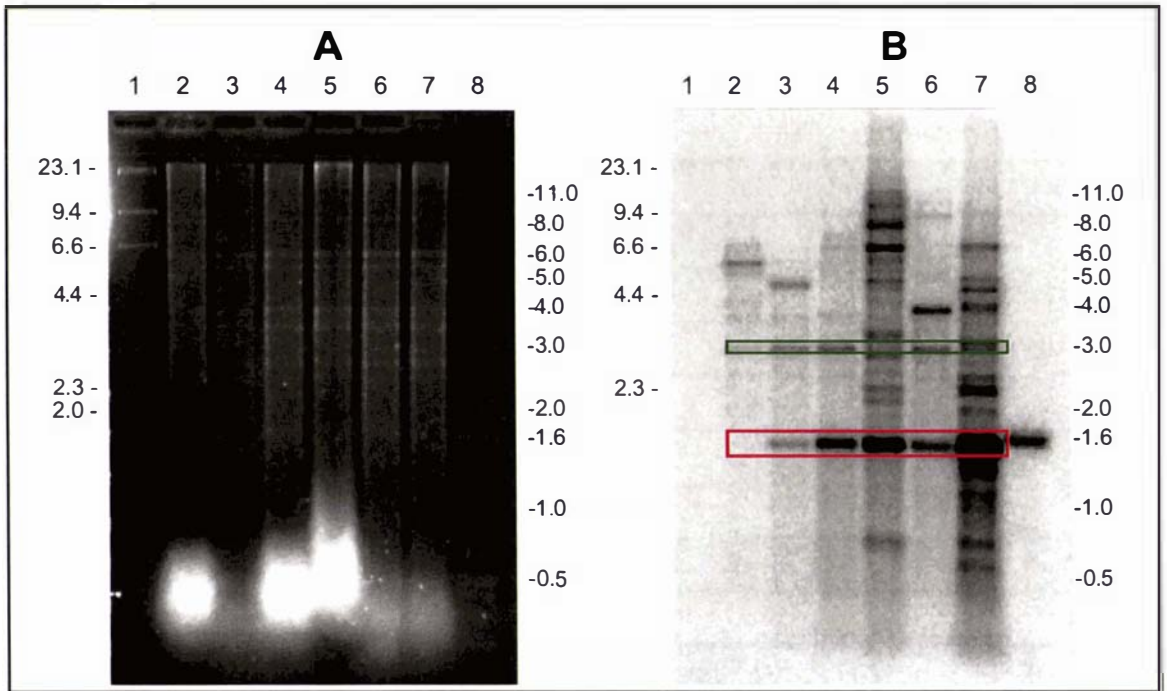

Figure 4.4 Southern blot analysis of pMM33 transformants

Southern analysis of *E. festucae* Fl1 strains transformed with pMM33. **(A)** Genomic DNA (1 µg) digested with *Xho*I and *Pst*I from the strains *E. festucae* Fl1 (lane 2), MM9.1 (lane 3), MM9.2 (lane 4), MM9.3 (lane 5), MM9.4 (lane 6) and MM9.5 (lane 7). Lanes 1 and 8 contain λ *Hin*dIII and 1 kb plus ladder (Invitrogen) respectively. Sizes of marker fragments are shown in kb. **(B)** Autoradiograph of the gel from **A** hybridised with a [^{32}P]-labelled Fl1 *prt1* fragment amplifed with primers MM4 and MM74. The expected native copy of *prt1* is indicated by a green box. The expected transformant copies of the *ltmM-prt1* fusion is indicated by a red box.

Table 4.3 Intact copies of pMM33[a]

Transformant	Intact construct copies[b]
MM9.1	1
MM9.2	5-6
MM9.3	>20
MM9.4	3-4
MM9.5	>20

[a] Copies where the P*ltmM-prt1* coding region is intact
[b] Determined by the ratio of native to intact P*ltmM-prt1* copies

Transformants shaded in grey were selected for inoculations into plants

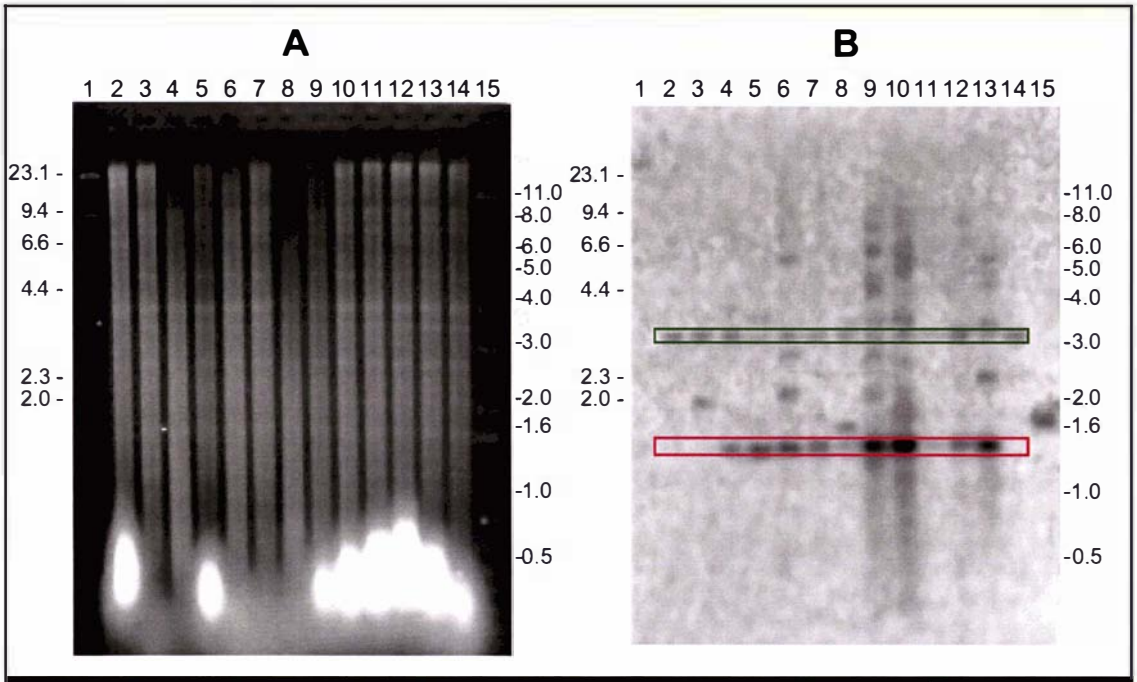

Figure 4.5 Southern blot analysis of pMM26 transformants

Southern analysis of *E. festucae* Fl1 strains transformed with pMM26. **(A)** Genomic DNA (1 µg) digested with *Nco*I and *Pst*I from the strains *E. festucae* Fl1 (lane 2), MM4.1 (lane 3), MM4.2 (lane 4), MM4.3 (lane 5), MM4.4 (lane 6), MM4.5 (lane 7), MM4.6 (lane 8), MM4.7 (lane 9), MM4.8 (lane 10), MM4.9 (lane 11), MM4.10 (lane 12), MM4.11 (lane 13) and MM4.12 (lane 14). Lanes 1 and 15 contain λ *Hin*dIII and 1 kb plus ladder (Invitrogen) respectively. Sizes of marker fragments are shown in kb. **(B)** Autoradiograph of the gel from **A** hybridised with a [^{32}P]-labelled *E. festucae* Fl1 *prt2* fragment amplifed with primers MM15 and MM6. The expected position of the native copy of *prt2* is indicated by a green box. The expected position of transformant copies of the *gpd-prt2* fusion is indicated by a red box.

Table 4.4 Intact copies of pMM26[a]

Transformant	Intact construct copies[b]
MM4.1	1
MM4.2	2
MM4.3	~15
MM4.4	9
MM4.5	4-5
MM4.6	1
MM4.7	>20
MM4.8	>20
MM4.9	3-4
MM4.10	3
MM4.11	>20
MM4.12	0

[a] **Copies where the P*gpdA-prt2* coding region is intact**
[b] **Determined by the ratio of native to intact P*gpdA-prt2* copies**

Transformants shaded in grey were selected for inoculations into plants

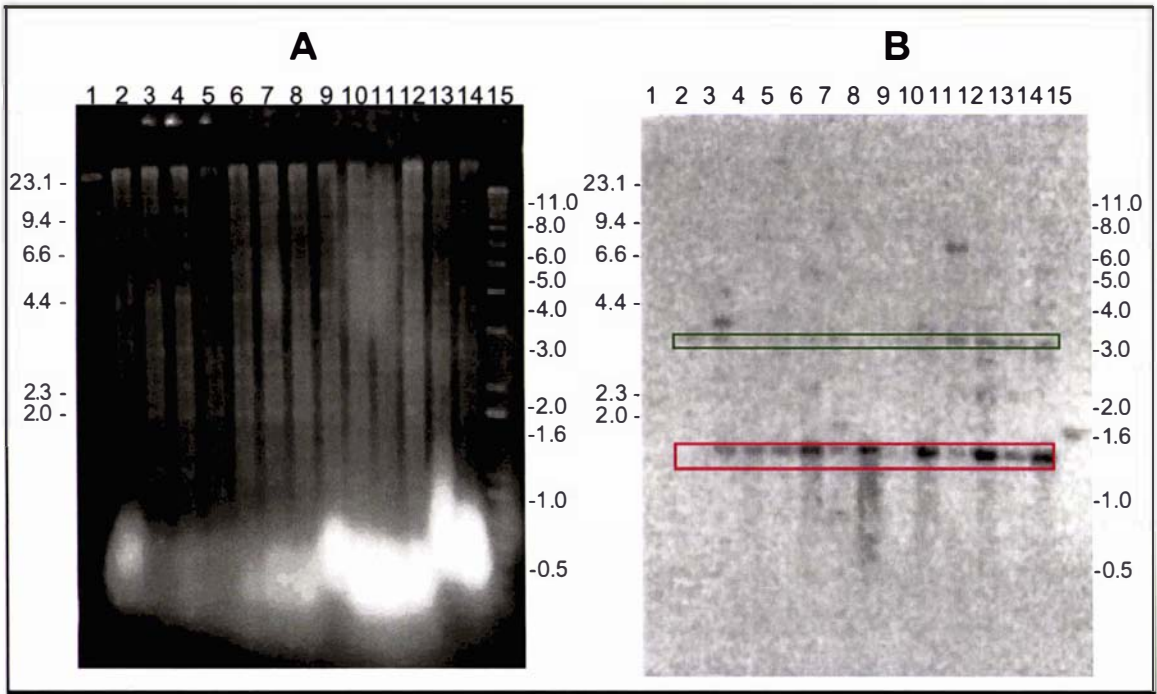

Figure 4.6 Southern blot analysis of pMM27 transformants

Southern analysis of *E. festucae* Fl1 strains transformed with pMM27. **(A)** Genomic DNA (1 µg) digested with *Nco*I and *Pst*I from the strains *E. festucae* Fl1 (lane 2), MM5.1 (lane 3), MM5.2 (lane 4), MM5.3 (lane 5), MM5.4 (lane 6), MM5.5 (lane 7), MM5.6 (lane 8), MM5.7 (lane 9), MM5.8 (lane 10), MM5.9 (lane 11), MM5.10 (lane 12), MM5.11 (lane 13) and MM5.12 (lane 14). Lanes 1 and 15 contain λ *Hin*dIII and 1 kb plus ladder (Invitrogen) respectively. Sizes of marker fragments are shown in kb. **(B)** Autoradiograph of the gel from **A** hybridised with a [^{32}P]-labelled *E. festucae* Fl1 *prt2* fragment amplifed with primers MM15 and MM6. The expected native copy of *prt2* is indicated by a green box. The expected transformant copies of the *ltmM-prt2* fusion is indicated by a red box.

Table 4.5 Intact copies of pMM27[a]

Transformant	Intact construct copies[b]
MM5.1	**4-5**
MM5.2	**7-8**
MM5.3	**6**
MM5.4	**>20**
MM5.5	**5**
MM5.6	**>20**
MM5.7	**2-3**
MM5.8	**>20**
MM5.9	**2**
MM5.10	**1-2**
MM5.11	**4-5**
MM5.12	**15-20**

[a] Copies where the P*ltmM-prt2* coding region is intact
[b] Determined by the ratio of native to intact P*ltmM-prt2* copies

Transformants shaded in grey were selected for inoculations into plants

Fl1 transformed with pAN7-1) were included in this analysis. pAN7-1 contains the hygromycin resistance gene *hph* under the control of the promoter from the constitutively expressed *A. nidulans gpdA* gene (Appendix A1.1.2). The presence of the pAN7-1 plasmid in transformed strains acts as a negative control, because the pAN7-1 vector does not contain DNA from either the *prt1* or *prt2* genes. Expression of the constitutively expressed *tub2* gene was also assessed to ensure each cDNA sample contained amplifiable cDNA.

The wild type *prt1* gene was expressed in all pMM32 and pMM33 transformant strains (Figure 4.7A). However, expression of wild type *prt1* in one pMM33 transformant strain, MM9.3, appeared to be reduced. This could be due to the position where pMM33 has inserted in this transformant. This construct may have disrupted the *prt1* promoter or inserted the P*ltmM-prt1* construct in a position that repressed *prt1* expression. Southern analysis shows that the wild type *prt1* coding region is intact in the MM9.3 transformant (Figure 4.4, lane 5). The P*gpdA-prt1* gene was expressed in culture in all of the pMM32 transformants (Figure 4.7A). The MM8.3 transformant appears to have reduced expression of the native *prt1* gene. It is unclear why *prt1* expression is reduced in this transformant, as the native gene does not appear to be disrupted in this strain. However, expression of the *ltmM-prt1* gene was not detected in the pMM33 transformants in culture. This result was expected given that *ltmM* expression is not detectable in culture (Figure 3.38) (Young, 2005).

The wild type copy of the *prt2* gene was not expressed in culture in either wild type *E. festucae* Fl1 or the transformant strains (Figure 4.7B). However, a genomic product was amplified from wild type *prt2*. This was a common observation even though RNA samples were DNase I treated prior to cDNA synthesis. However, a product was not amplified from a control prepared during cDNA manufacture without reverse

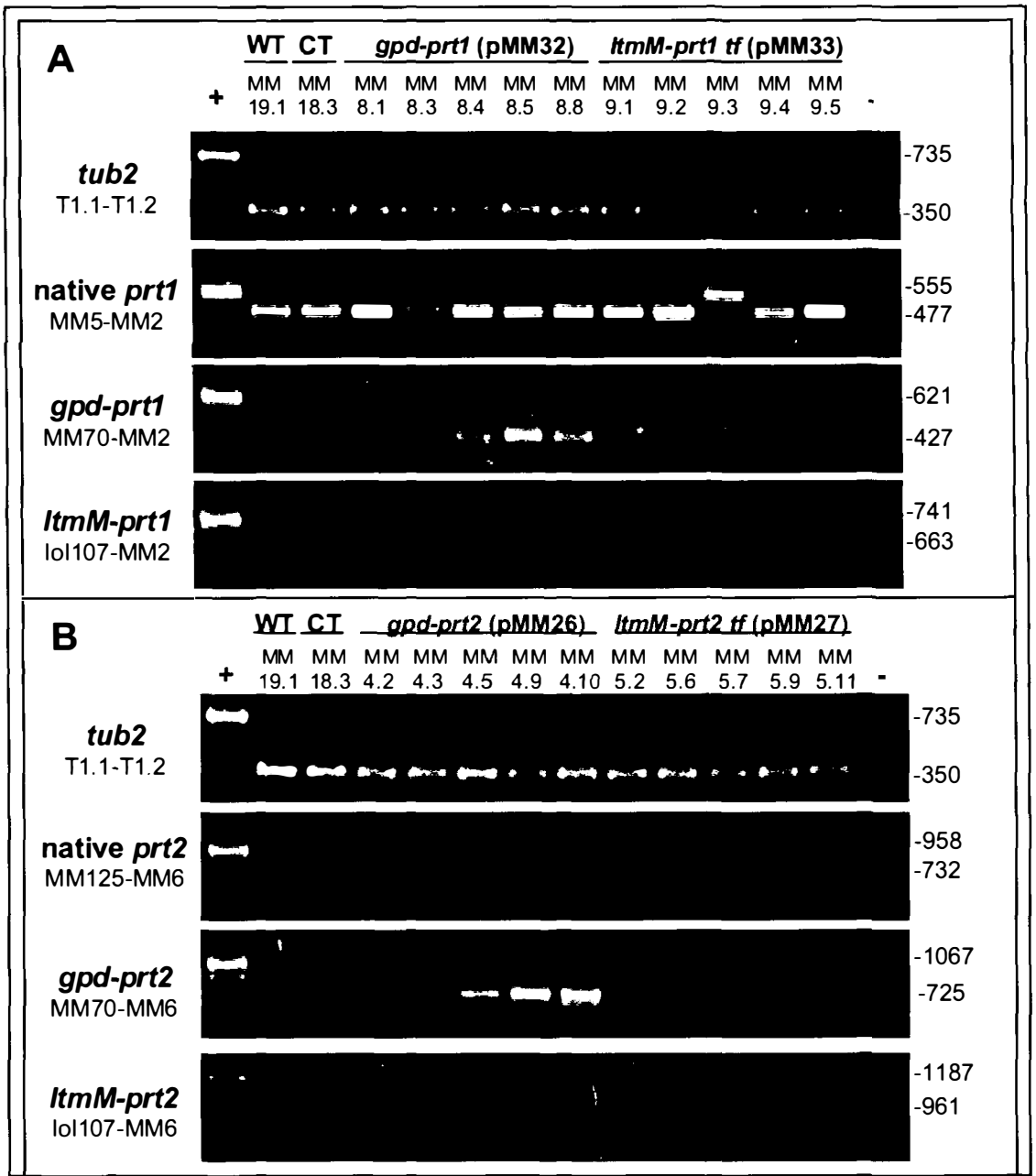

Figure 4.7 Expression of the *E. festucae* Fl1 *prt1* and *prt2* wild type genes and transgenes in culture

RT-PCR analysis of expression of the wild type and transformant *prt1* and *prt2* genes. RT-PCR was performed using cDNA made from DNase I-treated total RNA (1 µg total RNA/20 µL reaction). Wild type and pAN7-1 are listed as WT and CT respectively. Positive controls (wiild type Fl1 genomic DNA for the native genes or the transformed plasmid for transgenes) are indicated by a +. The negative control with no DNA template is indicated by -. Expected PCR product sizes are shown in bp. Names of genes and the corresponding primer pairs are shown on the left. **(A)** Expression of wild type and transformant *prt1* in pMM32 and pMM33 transformants. **(B)** Expression of wild type and transformant *prt2* in pMM26 and pMM27 transformants.

transcriptase using primers for other genes, suggesting that DNase treatment was largely, but perhaps not completely, successful. The P*gpdA-prt2* gene was expressed in all of the pMM26 transformants, but the P*ltmM-prt2* gene was not expressed in the pMM27 transformants. Sequencing of the P*gpdA-prt2* cDNA product amplified with the MM70-MM25 primer pair enabled the exon-intron structure of the *prt2* gene to be confirmed (data not shown). Three introns were confirmed in conserved positions within the *prt2* gene. The intron positions were conserved with those in the *E. festucae* Fl1 *prt3* gene, and with other closely related protease-encoding genes such as Prl1 from *M. anisopliae*. Sequencing of the PCR product also showed that an intron in the 5' untranslated region of the *gpdA* sequence was spliced out of the mRNA in the same manner as it is in *A. nidulans*.

4.3.2 Expression of the prt1 or prt2 transgenes in planta

RT-PCR analysis was also used to examine expression of the transformant copies of *prt1* or *prt2 in planta*. cDNA was prepared from DNase I-treated polyA RNA isolated from symbiota consisting of *L. perenne* cv. Nui plants infected with strains containing pMM32 (P*gpdA-prt1*), pMM33 (P*ltmM-prt1*), pMM26 (P*gpdA-prt2*) or pMM27 (P*ltmM-prt2*).

For symbiota between *L. perenne* cv. Nui and wild type *E. festucae* Fl1 or strains transformed with pMM32 (P*gpdA-prt1*), the wild type *prt1*, *tub2* and *ltmM* genes were expressed in all symbiota (Figure 4.8A). However, expression of the P*gpdA-prt1* gene was not detected in any of the five symbiota where the fungal partner had been transformed with the pMM32 plasmid. This is in contrast to the results of RT-PCR analysis in culture, where expression of the P*gpdA-prt1* gene was detected in all five strains. Expression of the P*ltmM-prt1* gene was detected *in planta* for three out of the five pMM33 transformants (Figure 4.8B).

Expression of the wild type copy of the *prt2* gene was not detected in wild type *E. festucae* Fl1 or any of the transformant strains (Figure 4.9A, 4.9B), although the *tub2*

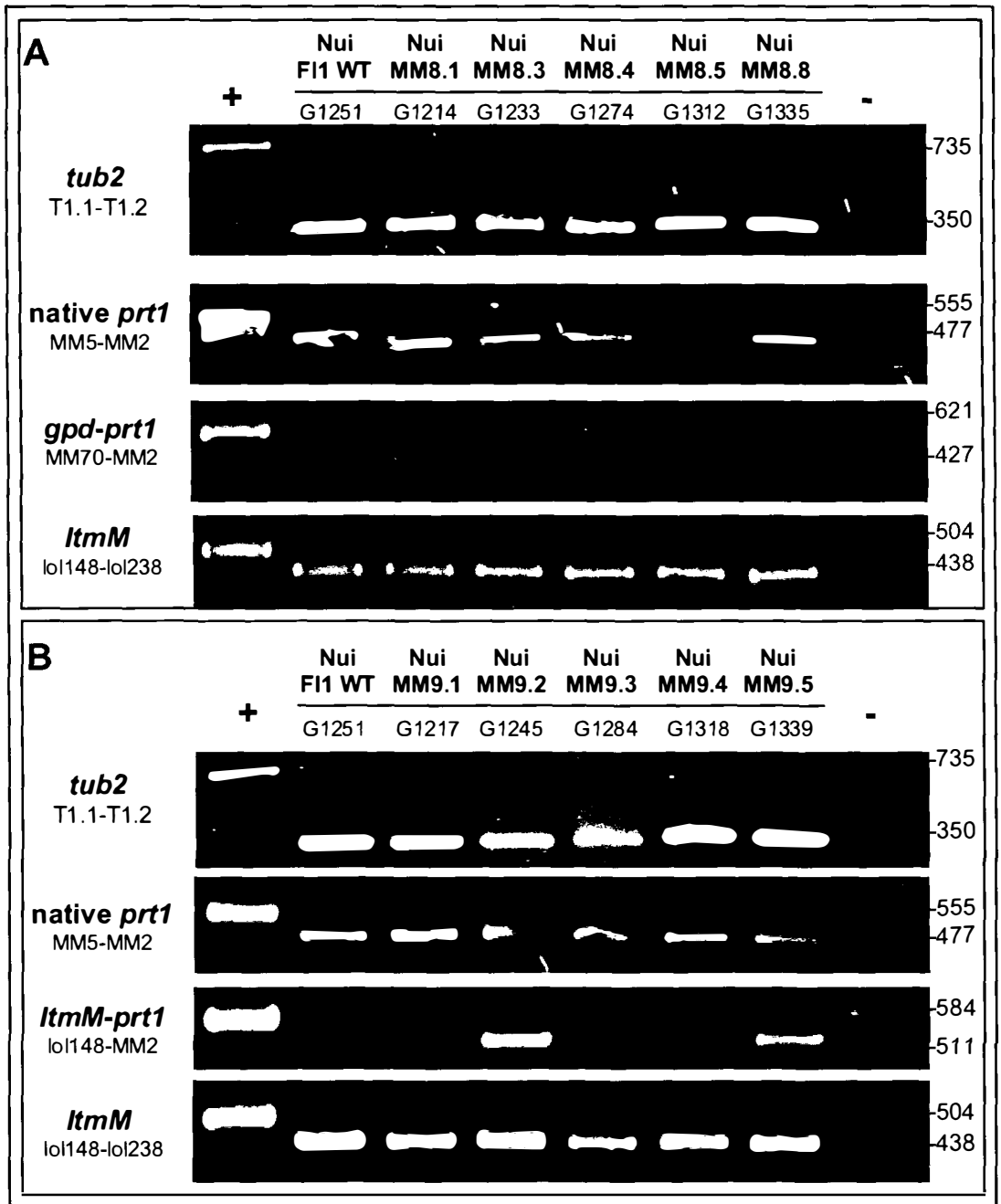

Figure 4.8 Expression of the wild type and transgene copies of *prt1 in planta*

RT-PCR analysis of expression of the native and transformant *prt1* genes *in planta*. RT-PCR was performed using cDNA made from DNase I-treated polyA RNA (~100 ng polyA RNA/20 µL reaction). RT-PCR analysis of the constitutively expressed *tub2* and plant-induced *ltmM* genes are included as a control to demonstrate that all samples contain amplifiable cDNA. Primer pairs used to amplify the genes are shown on the left. The expected sizes of genomic and cDNA bands in bp are shown on the right. G numbers eg G1251 refer to symbiota.**(A)** Expression of wild type and transformant *prt1* in pMM32 transformants *in planta*. **(B)** Expression of wild type and transformant *prt1* in pMM33 transformants.

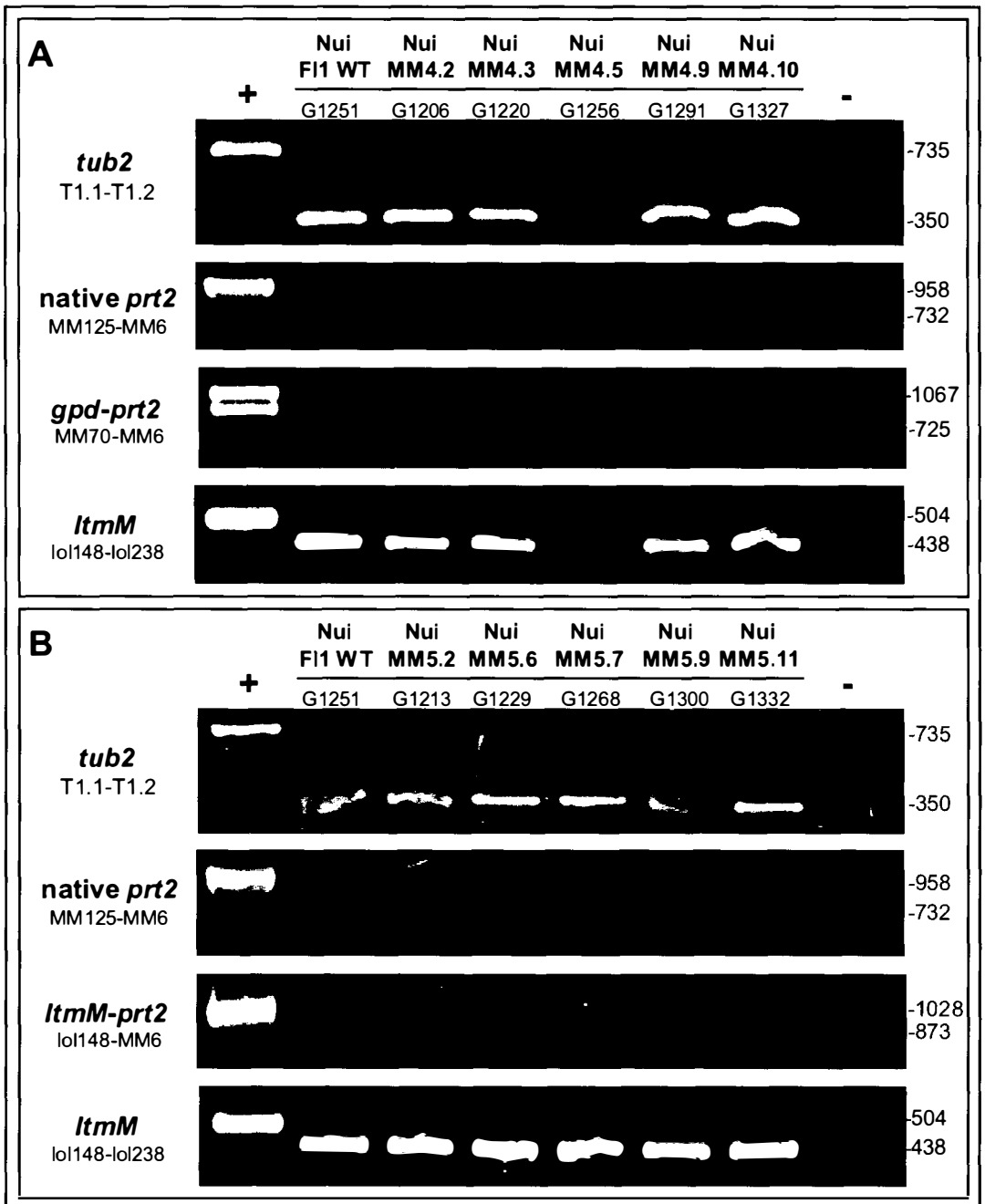

Figure 4.9 Expression of the wild type and transgene copies of *prt2 in planta*

RT-PCR analysis of expression of the native and transformant *prt2* genes *in planta*. RT-PCR was performed using cDNA made from DNase I-treated polyA RNA (~100 ng polyA RNA/20 µL reaction). RT-PCR analysis of the constitutively expressed *tub2* and plant-induced *ltmM* genes are included as a control to demonstrate that all samples contain amplifiable cDNA. Primer pairs used to amplify the genes are shown on the left. The expected sizes of genomic and cDNA bands in bp are shown on the right. G numbers eg G1251 refer to symbiota.**(A)** Expression of wild type and transformant *prt2* in pMM26 transformants *in planta*. **(B)** Expression of wild type and transformant *prt2* in pMM27 transformants.

and *ltmM* genes were expressed in all symbiota. The lack of *prt2* expression was expected given that expression has never been detected in culture or *in planta*. Expression of P*gpdA*$_p$-*prt2* was detected in three of the five symbiota containing strains transformed with pMM26, G1206 (MM4.2), G1220 (MM4.3) and G1291 (MM4.9) (Figure 4.9A). Expression of P*ltmM-prt2 in planta* was detected in one symbiotum (G1213) containing a strain transformed with pMM27 (MM5.2) (Figure 4.9B).

4.4 PHENOTYPE OF TRANSFORMANTS DURING GROWTH IN CULTURE AND *IN PLANTA*

The hyphal phenotype of the transformant strains during growth was examined during growth in culture on potato dextrose agar, and during growth on a medium containing skim milk agar. No differences were observed in colony size between any transformants and wild type strains on either of these media. Also, no difference in proteolytic activity between the wild type and transformant was observed during growth on plates containing skim milk agar.

The hyphal phenotype of transformant strains during growth *in planta* was visualised by microscopic analysis. The growth of fungal hyphae within infected tissues was visualised using aniline blue staining of infected leaf sheaths from inner, middle and outermost leaves. The growth of epiphytic hyphae on the leaf surface was also analysed by aniline blue staining and microscopy.

The pMM32 transformants with either low or high copy numbers of the P*gpdA-prt1* construct did not show any detectable differences from wild type *E. festucae* Fl1 *in planta* (Figure 4.10). The hyphae continue to grow between the plant cells largely with little hyphal branching, which is characteristic of the growth of wild type *E. festucae* Fl1 (Figure 4.10; M. Christensen, personal communication). Epiphyllous hyphae, which emerge to grow on the exterior of the leaf, were also present at similar levels and hyphal morphologies for the transformant and wild type strains. These results are not surprising when evaluated with RT-PCR analysis, showed no evidence of expression of the P*gpdA-prt1* construct *in planta* (Figure 4.8A). Although the P*ltmM-prt1* transgene was

expressed *in planta* in some strains (Figure 4.8B), few differences in hyphal morphology were observed between strains containing P*ltmM-prt1* (pMM33) and wild type *E. festucae* Fl1 (Figure 4.11). Similar results were obtained for the pMM26 P*gpdA-prt2* transformants (Figure 4.12), some of which were expressed *in planta* (Figure 4.9A), and the pMM27 P*ltmM-prt2* transformants (Figure 4.13), one of which expressed the P*ltmM-prt2* gene *in planta* (Figure 4.9B).

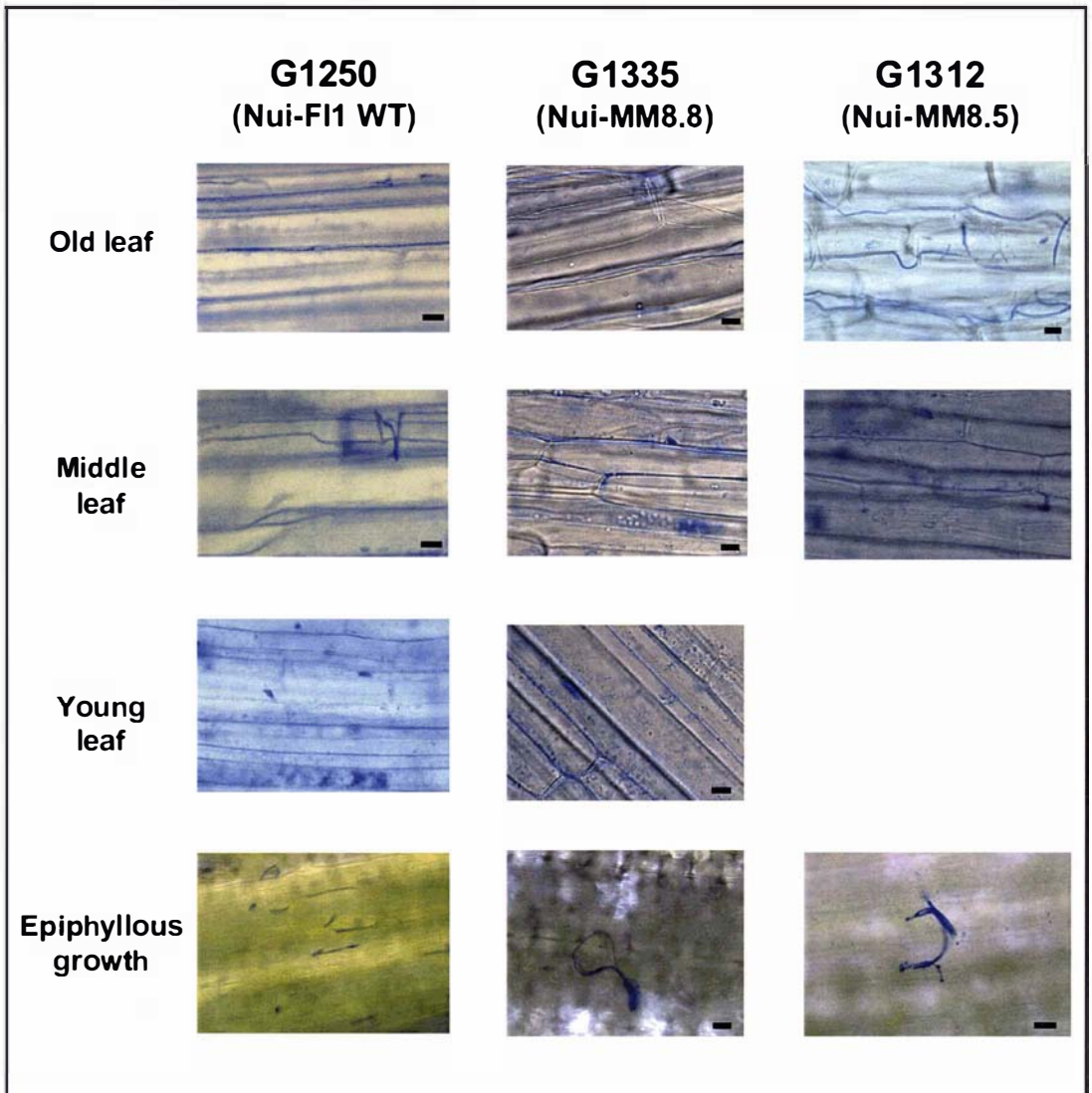

Figure 4.10 Growth of pMM32 transformants *in planta*

Growth of selected pMM32 transformants in endophyte-infected leaf sheath tissue. The growth of endophyte hyphae was assayed in the leaf sheaths of old, middle and young leaves by microscopic analysis of aniline blue-stained leaf epidermal peels. Photographs were taken at 400x magnification. The scale bar shown in the lower right hand corner of each photo is equivalent to 10 µm.

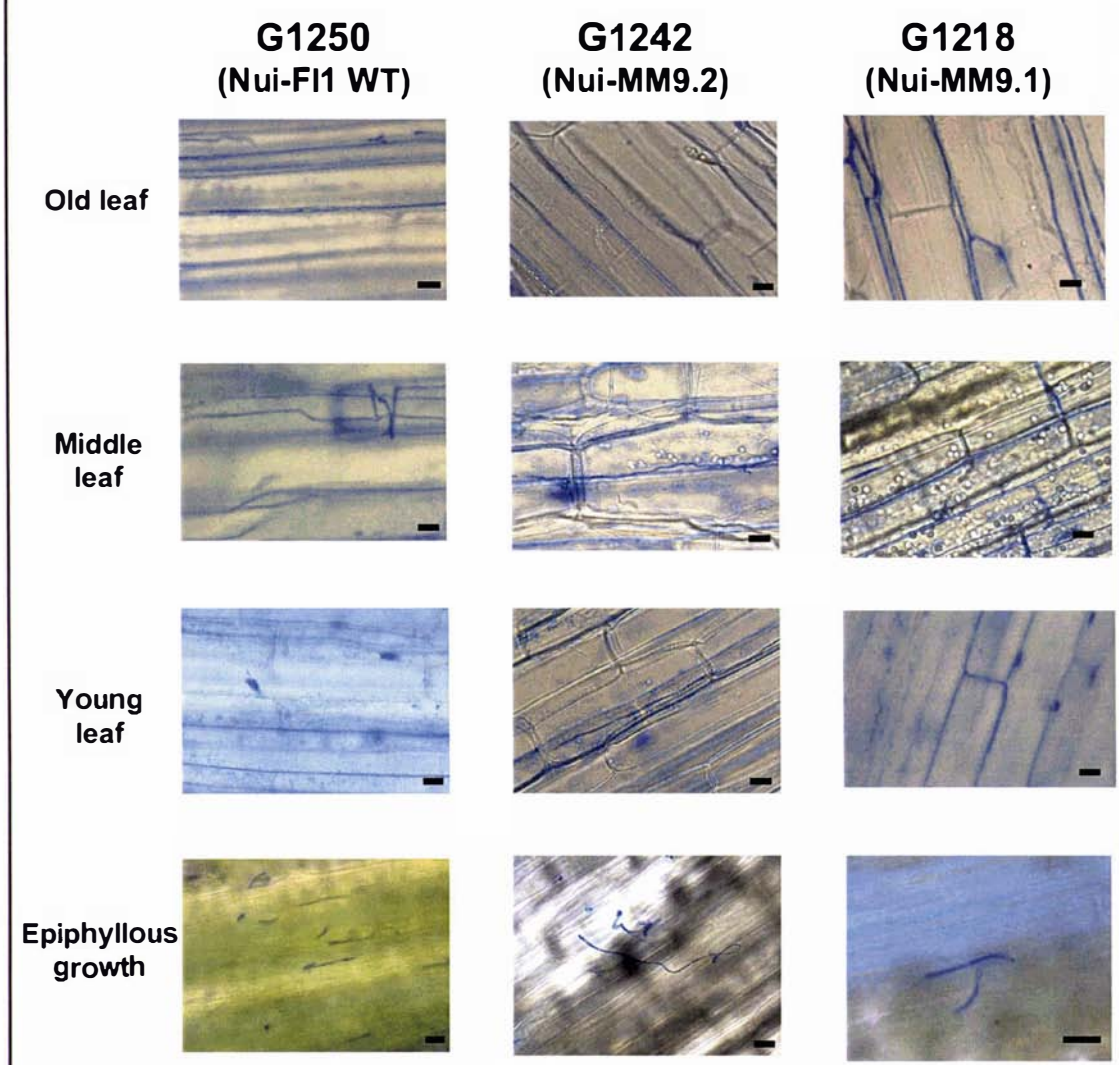

Figure 4.11 Growth of pMM33 transformants *in planta*

Growth of selected pMM33 transformants in endophyte-infected leaf sheath tissue. The growth of endophyte hyphae was assayed in the leaf sheaths of old, middle and young leaves by microscopic analysis of aniline blue-stained leaf epidermal peels. Photographs were taken at 400x magnification. The scale bar shown in the lower right hand corner of each photo is equivalent to 10 µm.

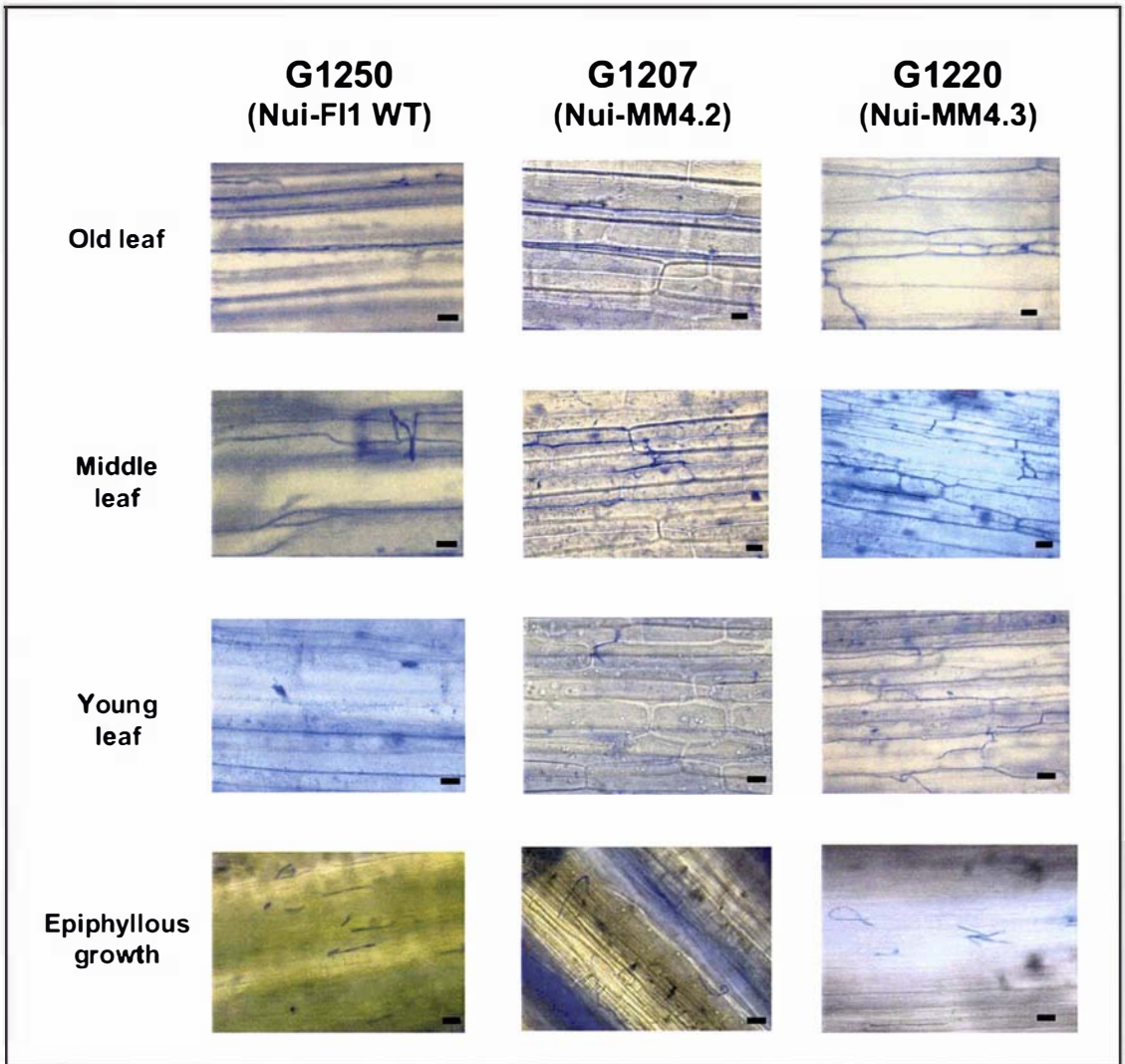

Figure 4.12 Growth of pMM26 transformants *in planta*

Growth of selected pMM26 transformants in endophyte-infected leaf sheath tissue. The growth of endophyte hyphae was assayed in the leaf sheaths of old, middle and young leaves by microscopic analysis of aniline blue-stained leaf epidermal peels. Photographs were taken at 400x magnification. The scale bar shown in the lower right hand corner of each photo is equivalent to 10 µm.

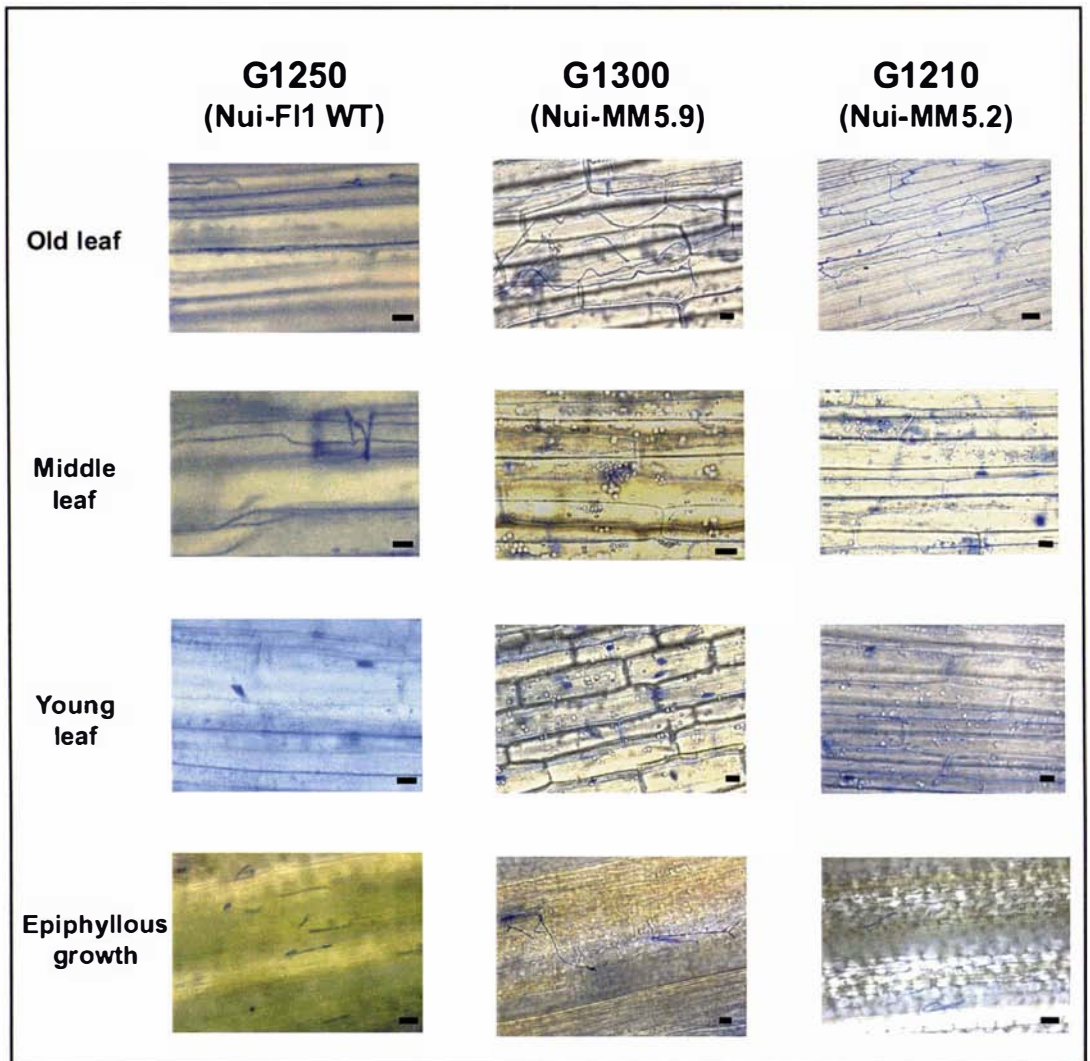

Figure 4.13 Growth of pMM27 transformants *in planta*

Growth of selected pMM27 transformants in endophyte-infected leaf sheath tissue. The growth of endophyte hyphae was assayed in the leaf sheaths of old, middle and young leaves by microscopic analysis of aniline blue-stained leaf epidermal peels. Photographs were taken at 400x magnification. The scale bar shown in the lower right hand corner of each photo is equivalent to 10 µm.

The phenotype of plants infected with various transformants strains was also assessed. Five successful-infected grasses were screened for each transformant. No gross changes in morphology were observed for any of the plants infected with the fungal strains transformed with pMM32 (P*gpdA-prt1*), pMM33 (P*ltmM-prt1*), pMM26 (P*gpdA-prt2*) or pMM27 (P*ltmM-prt2*). A characteristic phenotype of plants artificial inoculation of endophytes into grasses results in incompatible association is the stunting of grass tillers

(Zhang, 2004, A. Tanaka and M. Christensen, personal communication), where endophyte infected tillers are very small and tillers which escape endophyte infection grow to normal size. This phenotype, which is normally associated with high levels of endophyte biomass within the host, was not observed in any of the symbiota containing transformant strains.

CHAPTER 5

Results:

Functional characterisation of *gcn1*

5.1 ENDOPHYTE GENES ENCODING β-1,6-GLUCANASES

The *N. lolii* Lp19 and *E. festucae* Fl1 *gcn1* genes were identified during isolation of the *prt2* genes as described in Section 3.1. In both strains, the *gcn1* gene was directly downstream of the *prt2* gene (Figure 3.8, 3.9). Alignment of *N. lolii* Lp19 and *E. festucae* Fl1 *gcn1* regions (Appendix A2.2) showed the nucleotide sequences of the loci were very similar, with the exception of a 400 bp deletion in the *N. lolii* Lp19 *prt2-gcn1* intergenic region compared to the same region of *E. festucae* Fl1 (Figure 5.1). The polypeptide sequences of the *E. festucae* Fl1 and *N. lolii* Lp19 Gcn1 proteins were 99.7% identical, with the *E. festucae* Fl1 and *N. lolii* Lp19 Gcn1 polypeptides sharing 95.7% and 94.6% identity respectively with the β-1,6-glucanase polypeptide identified from *Neotyphodium* sp. FCB2002 (Moy et al., 2002) (Figure 5.2).

Phylogenetic analysis was performed on polypeptide sequences aligned by ClustalW as described in Section 2.21. The *E. festucae* Fl1 and *N. lolii* Lp19 Gcn1 proteins, like the *Neotyphodium* sp. FCB2002 β-1,6-glucanase, group together with the glycosyl hydrolase 5 family (Figure 5.3). The Gcn1 proteins cluster together with known

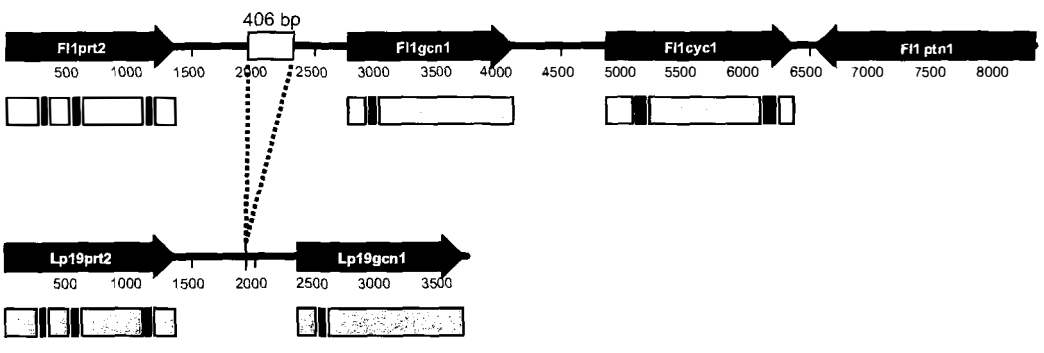

Figure 5.1 Comparison of the *E. festucae* Fl1 and *N. lolii* Lp19 *prt2-gcn1* intergenic region

Schematic diagram showing the *E. festucae* Fl1 and *N. lolii* Lp19 *prt2* and *gcn1* loci. Coding sequences are shown as dark grey arrows, with the proposed exons and introns shown beneath the line indicating the sequence. The *N. lolii* Lp19 *prt2-gcn1* intergenic region contains a deletion of 406 bp compared to the same region of *E. festucae* Fl1. This region is indicated by a white box in the *E. festucae* Fl1 sequence and a black line in the *N. lolii* Lp19 sequence with dotted lines connecting the two.

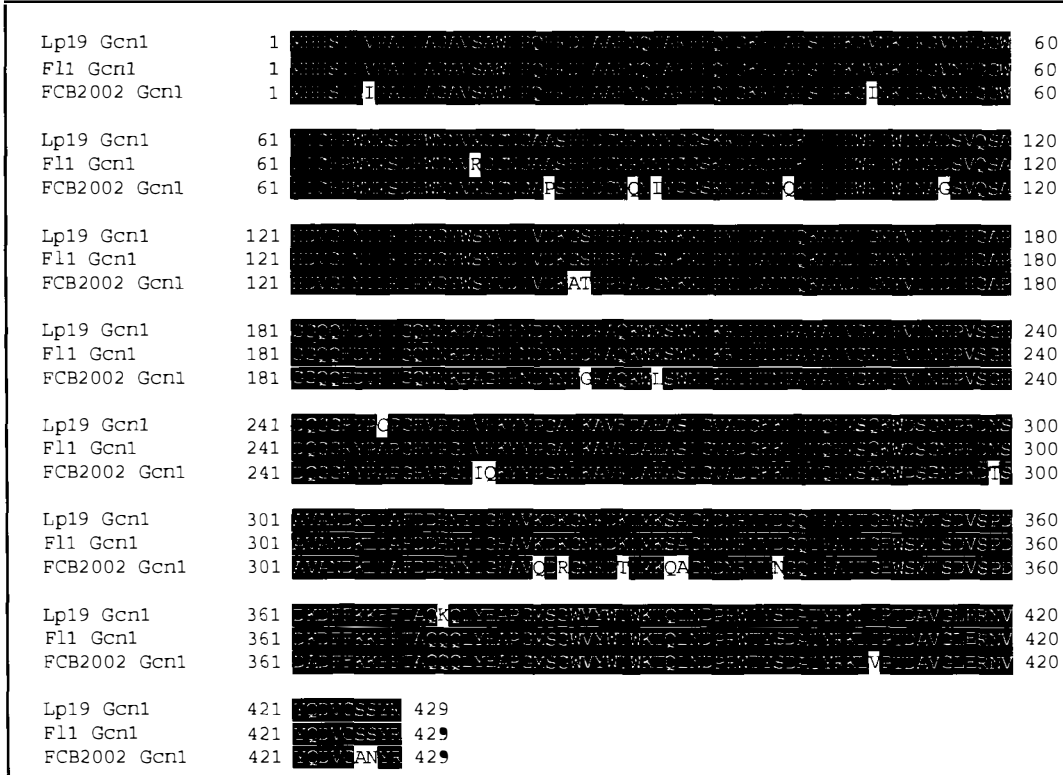

Figure 5.2 Alignment of endophyte β-1,6- glucanases

Comparison of endophyte β-1,6-glucanase polypeptide sequences from *N. lolii* strain Lp19, *E. festucae* strain Fl1 and *N. typhinum* strain FCB2002 (accession Genbank AAN04103). Amino acid identity between between two or more of the three sequences are shown in black shading with white letters. Amino acid differences at residues are shown by black text on a white background. The polypeptide sequences were aligned by the ClustalW module of MacVector™ 4.2.3.

β-1,6-glucanases within the glycosyl hydrolase 5 family such as the *T. harzianum* BGN16.2 (De la Cruz et al., 1995) and *V. fungicola* VfGlu1 (Amey et al., 2003) proteins that are involved in mycoparasitism (Section 1.6.2).

5.2 REPLACEMENT OF THE *E. FESTUCAE* FL1 *GCN1* GENE

5.2.1 Transformation of E. festucae Fl1 with a gcn1::hph construct

To determine the role of fungal β-1,6-glucanases in interactions between *E. festucae* Fl1 with perennial ryegrass (*L. perenne* cv Nui), the construct pMM54 was prepared to

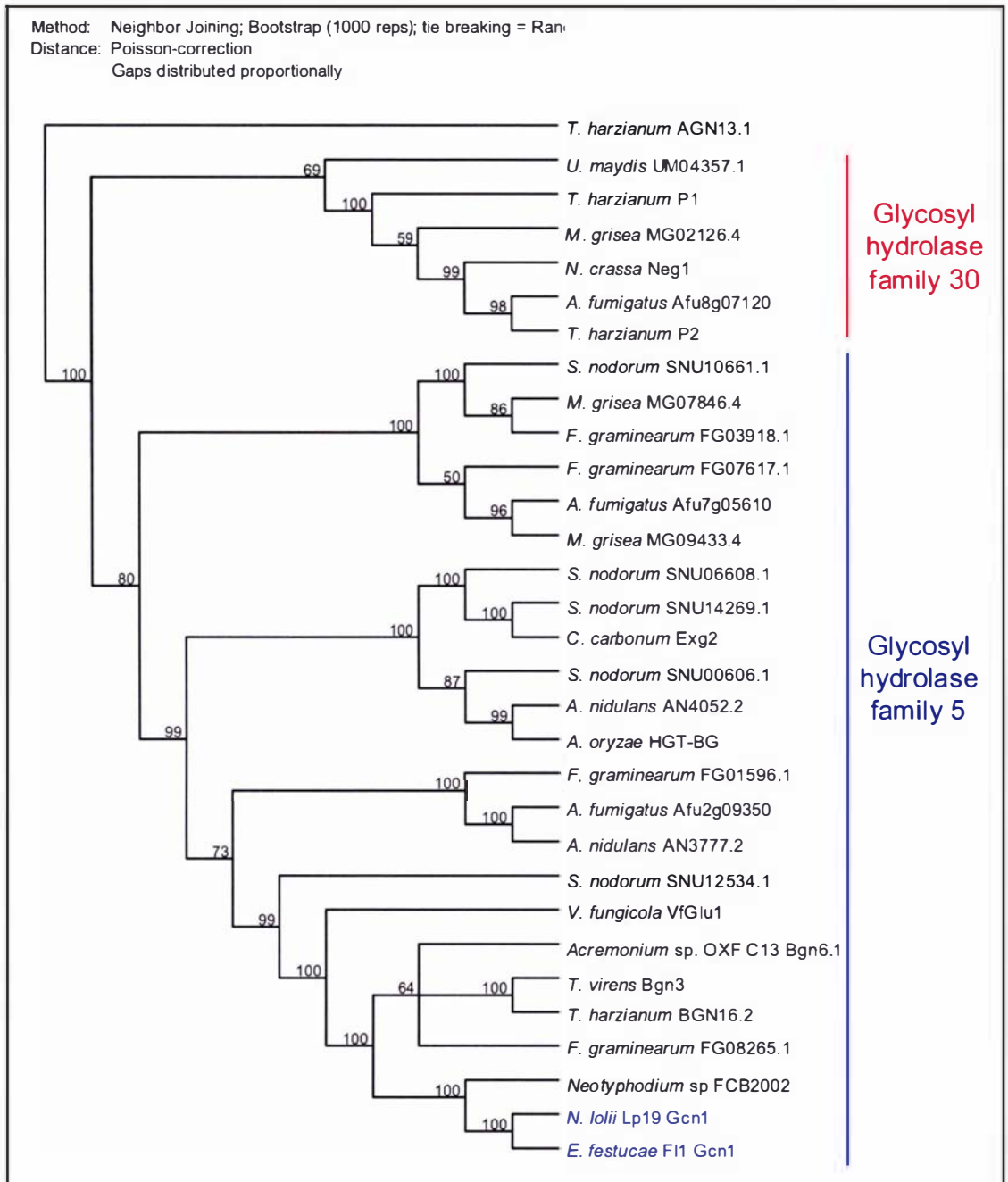

Figure 5.3 Phylogenetic analysis of fungal β-1,6-glucanases

Phylogenetic tree showing the relationship of the endophyte Gcn1 proteins with related proteins from other fungal species. Phylogenetic analysis was performed by Neighbour Joining of polypeptide sequences that were aligned by ClustalW. The *E. festucae* Fl1 and *N. lolii* Lp19 Gcn1 proteins are indicated in blue text. Members of glycosyl hydrolase family 5 are indicated by a blue line, while glycosyl hydrolase family 30 is indicated by a red line. The *T. harzianum* AGN13.1 α-1,3-glucanase was included to root the tree. Sequences used in this alignment are listed in Appendix A13.5.

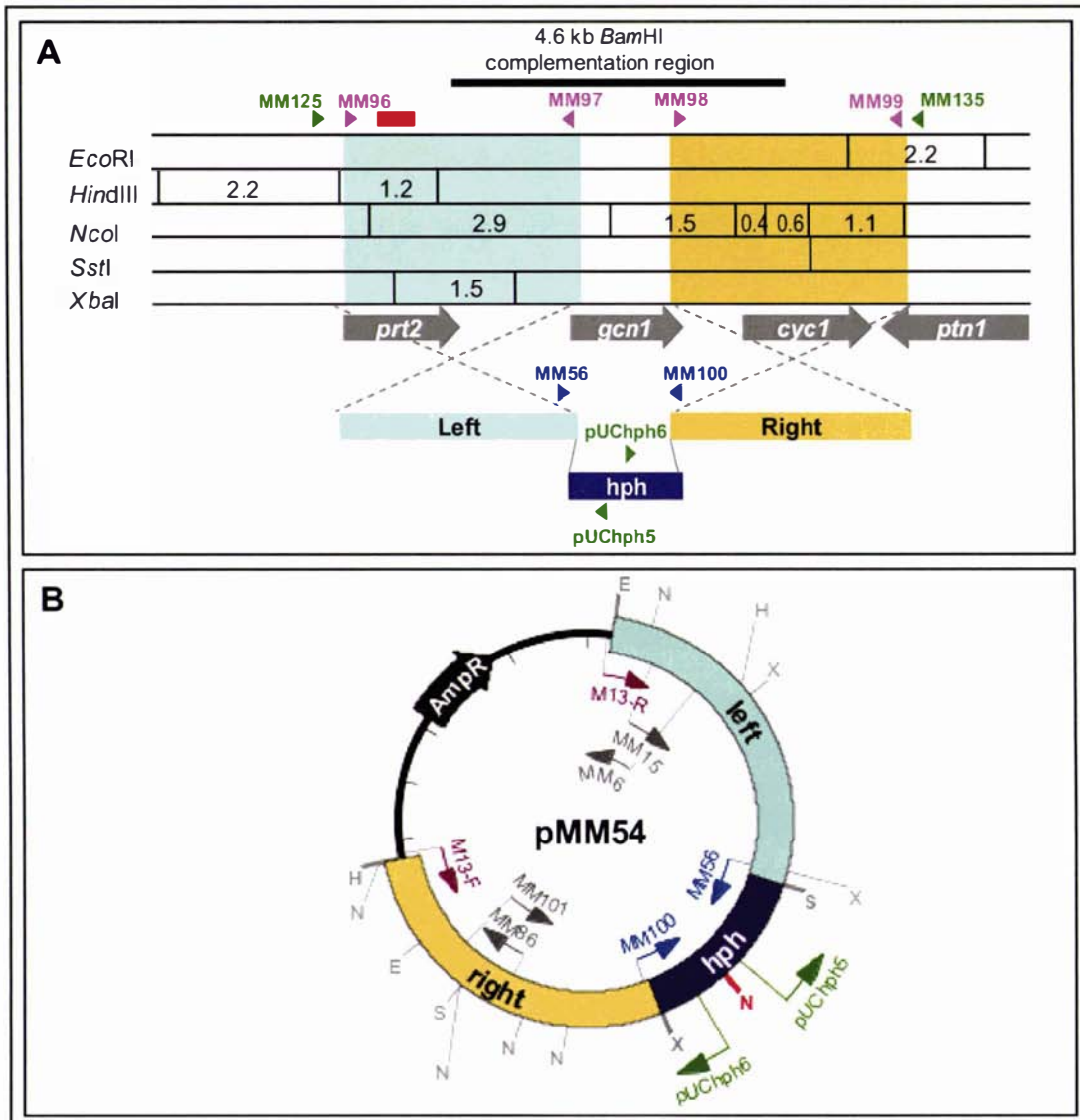

Figure 5.4 The *gcn1* deletion construct

Strategy for deleting the *E. festucae* Fl1 *gcn1* gene. Primers used for screening of transformants are shown in dark blue. Primers used to screen for replacement and deletion of flnaking sequences are shown in green. **A**. Restriction map of the Fl1 *gcn1* genomic locus. Coding regions of the genes in this region are shown in grey. The left flanking sequence (Left) chosen to make the deletion construct is shown in light blue, with the right flanking sequence (Right) shown in light orange. Primers used to amplify fragments are shown as purple triangles. The position of the probe used for Southern analysis (Figure 5.6C) is shown in red. **B**. A plasmid map of the *gcn1* deletion construct pMM54. The primers M13-F and M13-R (in maroon) were used to amplify the deletion construct used for transformation of *E. festucae* Fl1. Primers used for screening and for amplifying fragments for Southern analysis are shown in dark grey. Restriction sites, which are indicated in light grey, include *Eco*RI (E), *Hin*dIII (H), *Nco*I (N), *Sst*I (S) and *Xba*I (X). Heavy grey lines and bold grey text indicate restriction sites involved in vector construction. The heavy red line and bold red text indicate an *Nco*I site important in transformant screening by Southern analysis.

delete the wild type *gcn1* gene (Figure 5.4). The method used to construct pMM54 is described in Section 2.13.2. The linear insert from this plasmid was amplified by PCR using the M13F and M13R primers. This linear fragment was transformed into *E. festucae* Fl1 protoplasts as described in Section 2.16.1, and transformants were selected on RG media containing hygromycin at 150 ng/μL (Section 2.3.9). A total of twenty transformants were nuclear purified by sequential subculturing on media containing hygromycin.

Putative replacements were initially screened by PCR from DNA prepared by alkaline lysis of mycelia (Section 2.16.2.1) using primers MM56 and MM100 (wild type 1280 bp, replacement construct 1564 bp) that flank *hph* in the 5' and 3' flanking regions

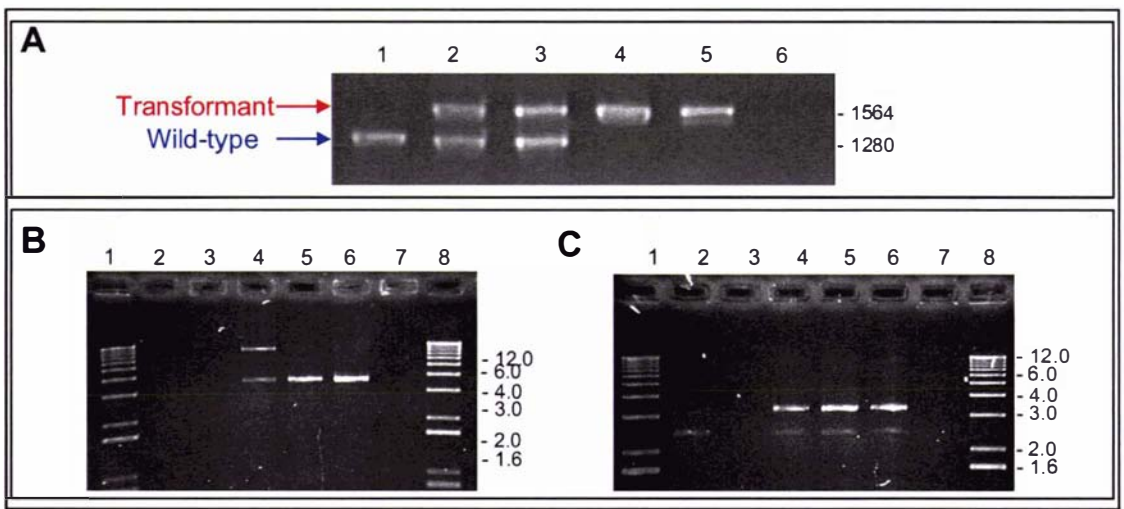

Figure 5.5 PCR analysis of selected *gcn1::hph* transformants

PCR analysis of genomic DNA from selected *E. festucae* Fl1 hygromycin-resistant transformants containing *gcn1::hph*. **(A)** Genomic DNA was amplified with the MM56-MM100 primers that flank the site where the *hph* gene is introduced during homologous recombination (Figure 5.3A). Genomic DNA from *E. festucae* Fl1 (lane 1), transformant MM20.1 (lane 2), transformant MM20.3 (lane 3), transformant MM20.2 (lane 4) and transformant MM20.15 (lane 5) were amplified. Lane 6 contains a negative control. PCR conditions were as follows: each reaction contained 1 x *Taq* polymerase buffer (Roche), 50 μM of each dNTP, 5 pmol each of the primers MM56 and MM100, 0.5 U *Taq* polymerase (Roche), and 5 ng of genomic DNA (or 5 μL water in case of the negative control). The PCR program used was as follows: 94°C 2 min, 30 cycles of 94°C for 30 s, 60°C for 30 s, 72°C for 1 min, then one 72°C for 5 min. **(B)** PCR amplification to check for an intact left end in *Δgcn1* strains. Genomic DNA from *E. festucae* Fl1 (lane 2), transformant MM20.1 (lane 3), transformant MM20.3 (lane 4), transformant MM20.2 (lane 5) and transformant MM20.15 (lane 6) were amplified with the MM125 and pUChph5 primer pair. Lane 7 contains a negative control. Lanes 1 and 8 contain 1 kb plus ladder (Invitrogen). Band sizes are shown in kb. **(C)** PCR amplification to check for an intact right end in *Δgcn1* strains. Genomic DNA from *E. festucae* Fl1 (lane 2), transformant MM20.1 (lane 3), transformant MM20.3 (lane 4), transformant MM20.2 (lane 5) and transformant MM20.15 (lane 6) were amplified with the pUChph6-MM135 primer pair (Figure 5.3A). Band sizes are shown in kb.

(Figure 5.4). Out of twenty transformants, two independent transformants MM20.2 and MM20.15 lacked the band corresponding to the wild type *gcn1* gene (Figure 5.5A lanes 4 and 5). The MM20.1 and MM20.3 transformants contained ectopic copies of the *gcn1*::*hph* construct as both the wild type *gcn1* and the *gcn1*::*hph* bands were amplified in these strains (Figure 5.5A lanes 2 and 3).

To confirm that the Δ*gcn1* strains MM20.2 and MM20.15 did not contain deletions upstream or downstream of the 5' or 3' *gcn1*::*hph* flanking sequences respectively, additional PCR screening was performed. Integration of the *gcn1*::*hph* construct through a single crossover event could potentially lead to deletion of sequences upstream of the 5' flanking sequence or downstream of the 3' flanking sequence. To test for an intact 5' region, DNA from wild type *E. festucae* Fl1, ectopic and Δ*gcn1* strains was amplified with the MM125 and pUC*hph*5 primers using TripleMaster™ PCR (Section 2.17.7). The MM125 primer anneals just outside the 5' flanking sequence used in the *gcn1*::*hph* construct, while the pUC*hph*5 primer anneals within the *hph* cassette (Figure 5.4A). A similar strategy was used to test for an intact 3' region, with the primers pUC*hph*6 and MM135 used to amplify genomic DNA from selected transformants during TripleMaster™ PCR. The pUC*hph*6 primer anneals in the *hph* region, while the MM135 primer anneals just outside of the 3' flanking region (Figure 5.4A). PCR screening confirmed that both of the Δ*gcn1* strains contained intact 5' and 3' ends (Figure 5.5B). However, the supposed ectopic strain MM20.3 also unexpectedly produced bands for both the 5' and 3' primer sets. Analysis with the MM56-MM100 primer pair had previously shown that MM20.3 contained both the native *gcn1* and the *gcn1*::*hph* products (Figure 5.5A).

Southern analysis of strains was performed using genomic DNA from wild type *E. festucae,* ectopic *gcn1*::*hph* strains and Δ*gcn1* strains digested with *Nco*I (Figure 5.6B and C). The *gcn1*::*hph* *Nco*I fragment differs in size to the fragment containing the wild type *gcn1* gene due to the replacement of a region in the wild type *gcn1* gene that contains an *Nco*I site (Figure 5.6A). There is also an *Nco*I site in the *hph* cassette from the pPN1688 vector, which gives a new *Nco*I recognition site in the *gcn1*::*hph* locus. As expected, wild type *E. festucae* Fl1 and the two ectopic strains (MM20.1 and MM20.3)

all contained the 2.9 kb *Nco*I fragment containing the wild type *gcn1* gene (Figure 5.6C, lanes 2, 3 and 4). The ectopic transformant MM20.1 also contained the 3.4 kb *Nco*I fragment found in the *gcn1*::*hph* construct (Figure 5.6D lane 3). However, the MM20.3 ectopic transformant did not contain the 3.4 kb *gcn1*::*hph* *Nco*I fragment (Figure 5.6D lane 4). This data suggests MM20.3 may have been an unstable transformant, or has

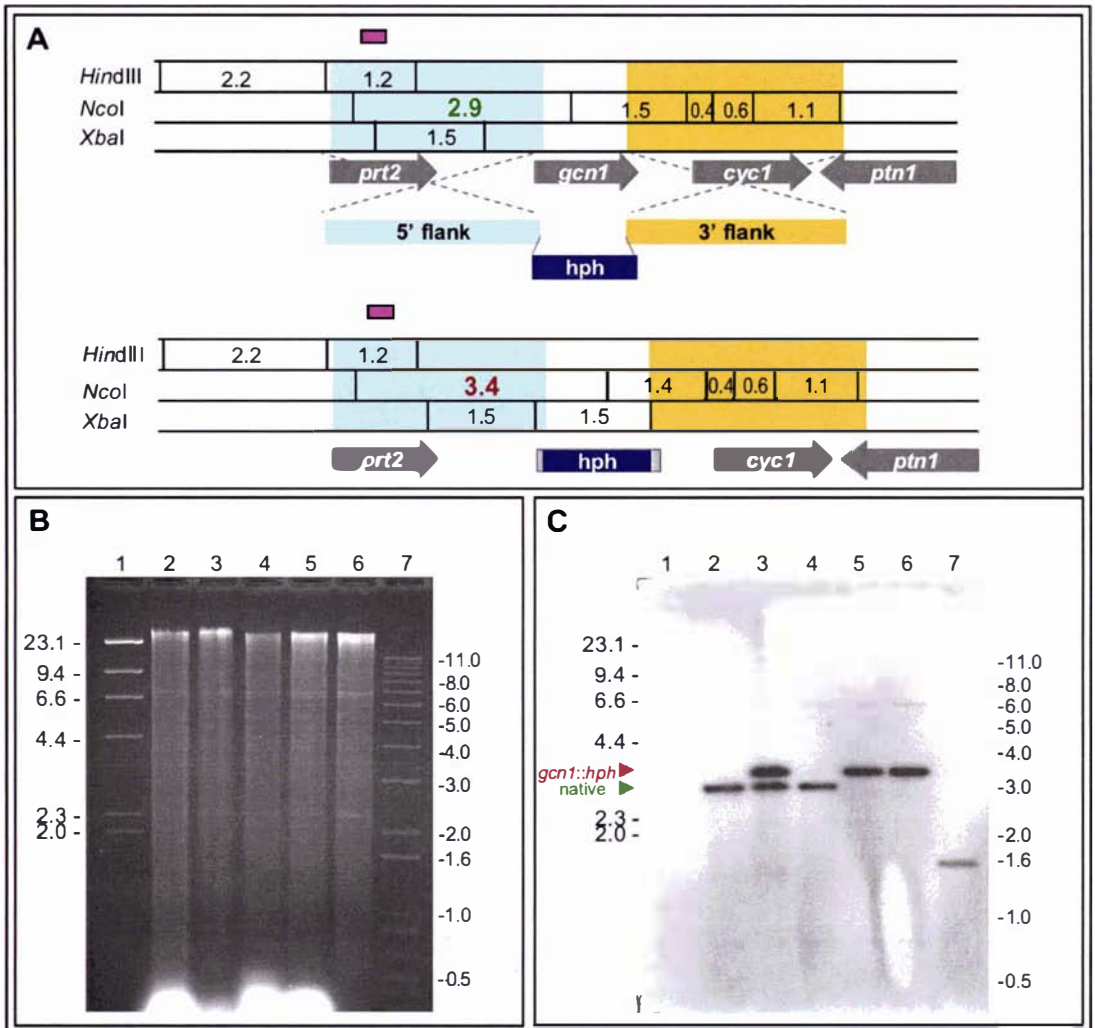

Figure 5.6 Southern analysis of selected *gcn1*::*hph* transformants

Southern analysis of *E. festucae* Fl1 hygromycin-resistant transformants containing *gcn1*::*hph*. **(A)** Restriction map of the native *gcn1* locus with the *gcn1*::*hph* construct shown below, followed by a restriction map of the *gcn1* locus after integration of the *gcn1*::*hph* construct by homologous recombination. Restriction fragment sizes are shown in kb. The wild type *gcn1* *Nco*I restriction fragment (shown in bold green text) differs in size to the *gcn1*::*hph* NcoI fragment (shown in \bold red text). The position of the probe used in **C** is indicated by a purple box. **(B)** Genomic DNA (1 µg) digested with *Nco*I from *E. festucae* Fl1 (lane 2), the ectopic transformants MM20.1 (lane 3) and MM20.3 (lane 4) and the Δ*gcn1* strains MM20.2 (lane 5) and MM20.15 (lane 6). Lanes 1 and 7 contain λ *Hin*dIII and 1 kb plus ladder (Invitrogen) respectively. Sizes of marker fragments are shown in kb. **(C)** Autoradiograph of the gel from **B** hybridised with a ^{32}P-labelled fragment amplifed with primers MM15 and MM6 (Figures 3.9 and 5.4B). Fragment sizes are indicated in kb. The native *gcn1* and *gcn1*::*hph* hybridising fragments are indicated by green and red arrows respectively.

under gone some sort of DNA rearrangement. Both of the Δ*gcn1*strains, MM20.2 and MM20.15, contained the 3.4 kb *gcn1*::*hph* but not the 2.9 kb wild type *gcn1* *Nco*I fragment (Figure 5.6C lanes 5 and 6). This confirmed that both of these strains had a *gcn1* gene that had been replaced by homologous recombination with the *gcn1*::*hph* construct.

5.2.2 Phenotype of the Δgcn1 strains during growth in culture

The phenotype of the Δ*gcn1* strains during growth in culture was examined using the preferred carbon source glucose or pustulan, a polymer of β-1,6-glucan derived from the cell walls of *Umbilicaria papullosa*. On glucose containing medium, growth of the Δ*gcn1* strains was almost identical to wild type *E. festucae* Fl1 and the MM20.1 strain carrying an ectopic integration of the *gcn1* replacement (Figure 5.7). During growth on glucose media, wild type *E. festucae*, the ectopic strain MM20.1 and the Δ*gcn1* strains MM20.2 and MM20.15 all grew with a cottony appearance, indicating that many aerial hyphae were present. All strains also produced a halo around the colony. The one difference observed was for the MM20.2 Δ*gcn1* strain, which had slightly reduced radial growth on the glucose-containing medium compared to the other three strains. However, this result must be reproduced for confirmation of this effect.

When grown on pustulan, Δ*gcn1* strains were phenotypically different to the wild type *E. festucae* Fl1 and ectopic strains (Figure 5.8). Although Δ*gcn1* strains were the same size as wild type and ectopic strains, hyphal density and the amount of aerial hyphae were greatly reduced (Figure 5.8). Some complementation of the growth defects of the Δ*gcn1* strains on pustulan by the wild type and ectopic strains was observed in older cultures (Figure 5.8A). The Δ*gcn1* strains also lacked the halo surrounding the wild type and ectopic strains during growth on pustulan. Congo red staining of the plates (Figure 5.8B) indicated that the halos corresponded to regions where pustulan was degraded, suggesting these halos correspond to zones where a β-1-6-glucanase enzyme

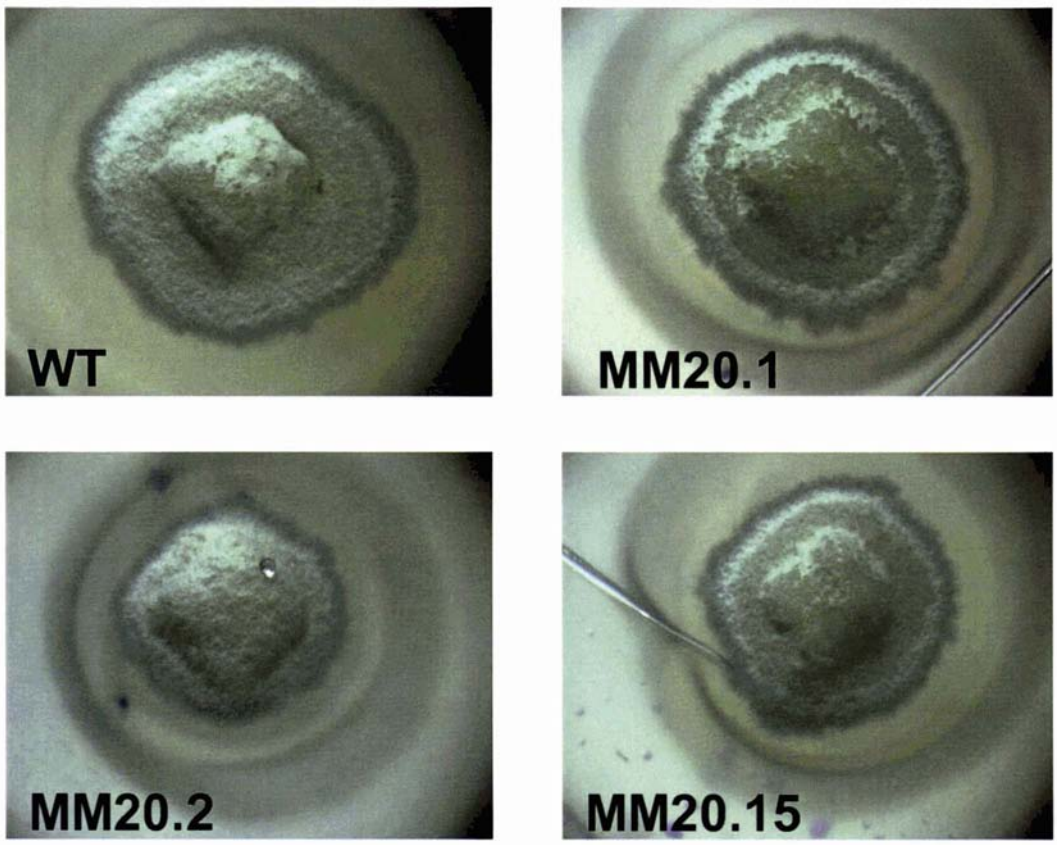

Figure 5.7 Growth of Δ*gcn1* strains on media containing glucose

Colony morphology of wild type *E. festucae* Fl1 (WT), the ectopic strain MM20.1 and the Δ*gcn1* strains MM20.2 and MM20.15 on agar plates containing 1% glucose, 20 mM NH_4Cl and 0.1% yeast extract.

is produced in wild type and ectopic strains. The absence of these halos in the Δ*gcn1* strains suggest these strains lack β-1-6-glucanase activity compared to wild type and ectopic strains.

After prolonged incubation of Δ*gcn1* strains on pustulan plates together with wild type and ectopic strains, some rescue of the Δ*gcn1* phenotype by wild type and ectopic strains was observed. Δ*gcn1* hyphae at the interface with wild type or ectopic colonies were partially rescued, showing more hyphal branching and aerial hyphae (Figure 5.8D). However, hyphae in the same colony that were not in close proximity to the wild type or

ectopic strains displayed low levels of hyphal branching and almost no aerial hyphae (Figure 5.8C) compared to wild type strains (Figure 5.8E).

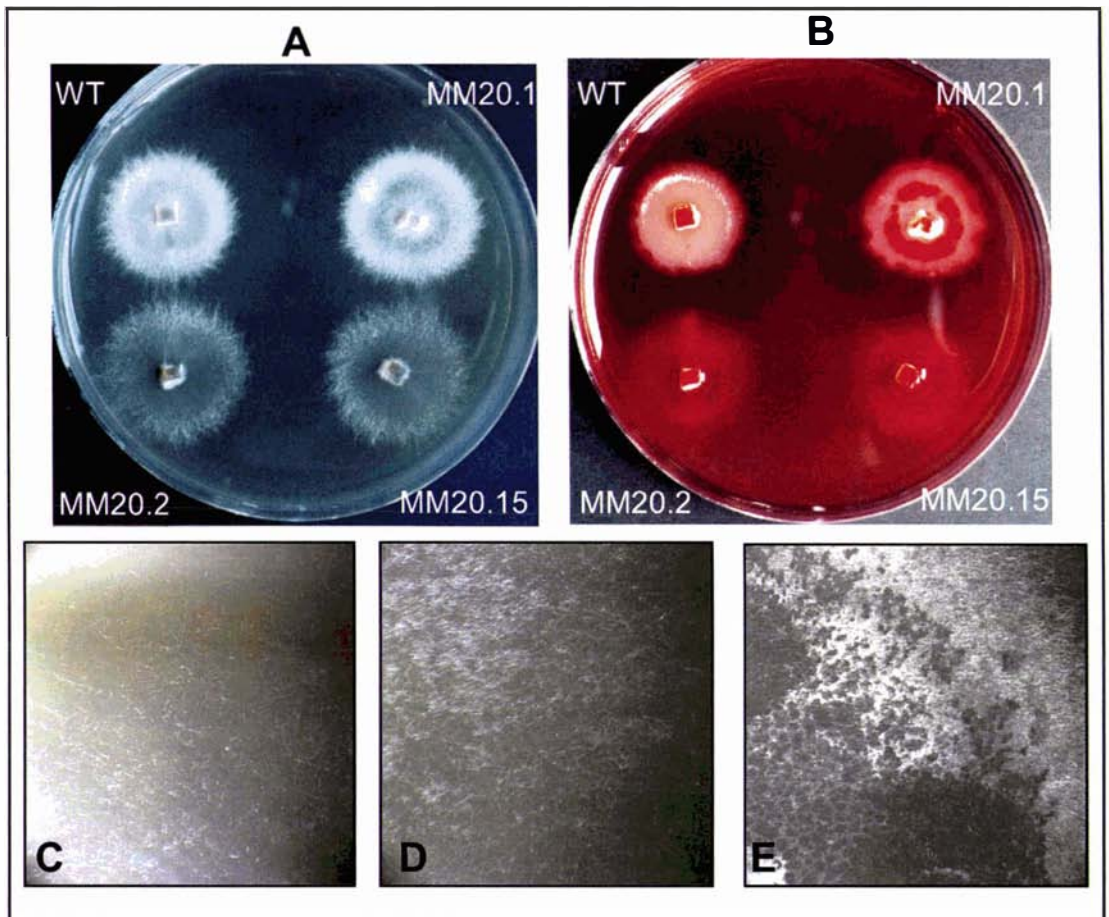

Figure 5.8 Growth of Δ*gcn1* strains on media containing pustulan, a β-1,6-glucan polymer

Growth of Δ*gcn1* strains on medium containing pustulan. **(A)** Growth of wild type *E. festucae* Fl1 (WT), the ectopic strain MM20.1 and the Δ*gcn1* strains MM20.2 and MM20.15 on pustulan medium. Colonies were approximately 2 weeks old. **(B)** Staining of pustulan media plate with Congo red. Undegraded pustulan appears red, while zones where β-1,6-glucanases have degraded the pustulan appear as dark halos. **(C)** Hyphae of the Δ*gcn1* strain MM20.15 that have not been grown in close proximity to wild type *E. festucae* Fl1 or the ectopic MM20.1 strain. **(D)** Hyphae of the Δ*gcn1* strain MM20.15 that have been grown in close proximity to wild type *E. festucae* Fl1 or the ectopic MM20.1 strain. Aerial hyphae appear as white cottony structures. **(E)** Wild type *E. festucae* Fl1 hyphae. The white cottony masses are aerial hyphae.

5.3 COMPLEMENTATION OF THE Δ*GCN1* STRAIN

Complementation of the Δ*gcn1*strain was performed by cotransformation of the Δ*gcn1* strain MM20.15 with the pII99 and pMM44 plasmids (Figure 5.9A). pMM44 contains a 4.6 kb *Bam*HI fragment containing the *gcn1* gene, including the complete *prt2-gcn1* and *gcn1-cyc1* intergenic regions, and the 5' region of the *cyc1* gene (Figure 5.4A). The pII99 vector contains the *nptII* gene, which confers resistance to the antibiotic geneticin. Twenty geneticin-resistant transformants were screened for the presence of the *gcn1* gene by PCR amplification with the MM56-MM55 primer pair that will amplify a *gcn1* PCR product in wild type *E. festucae* Fl1 and strains of MM20.15 containing the pMM44 plasmid (Figure 3.9B). A product was detected for at least eleven of the twenty strains (Figure 5.9B).

The growth of geneticin-resistant strains was analysed on medium containing the β-1,6-glucan pustulan (Figure 5.10). Out of the twenty strains tested, nineteen independent transformants out of twenty tested appeared to produce the hydrolytic halo on these plates characteristic of β-1,6-glucanase production that was lacking in the MM20.15 Δ*gcn1*strain (Figure 5.10A). This suggests that the *gcn1* deletion in the MM20.15 strain is responsible for the phenotype shown by Δ*gcn1* strains during growth on pustulan, where hyphal branching and the production of aerial hyphae were greatly reduced. A range of phenotypes was seen in the complemented strains during growth on pustulan. Some strains such as MM22.19 (Figure 5.10B), MM22.5 and MM22.6 (Figure 5.10C) produced halos during growth on pustulan media, and grew to similar diameters as the wild type *E. festucae* Fl1 strains. The MM22.20 transformant grew to a larger colony diameter with less aerial hyphae typical of the Δ*gcn1*strain MM20.15, indicating that this colony has not been genetically complemented. Other transformant strains (eg. MM22.7 and 22.8, Figure 5.10D) surrounded by large halos of β-1,6-glucanase activity grew as very dense, compact colonies with a lot of aerial hyphae. These phenotypic differences between strains were observed on media containing pustulan, but not in complex media such as potato dextrose agar. These differences in phenotype may be due to positional effects on *gcn1* gene expression or differences in gene copy number.

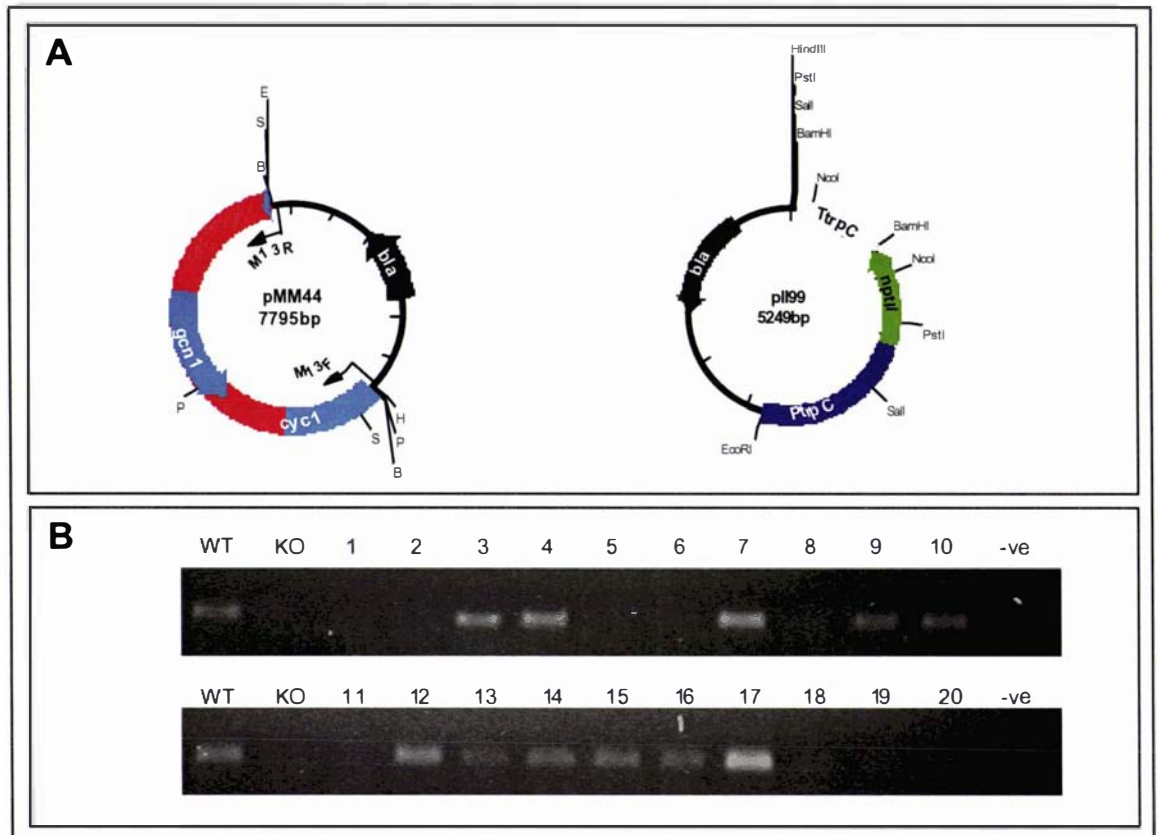

Figure 5.9 Genetic complementation of the *gcn1* deletion by co-transformation with pMM44 and pII99

(A) Plasmid maps of the pMM44 and pII99 vectors used to cotransform the ?*gcn1* strain MM20.15 to complement the lack of ß-1,6-glucanase activity and geneticin resistance. **(B)** PCR screening of selected pMM44/pII99 transformants using the Extract-N-Amp™ PCR kit. E. festucae FI1 wild type (WT), MM20.15 (KO) and various complemented strains (1-20) were screened. A DNA-free sample (-ve) was also included. PCR was performed with the MM56-MM55 primer pair. PCR conditions were as follows: The PCR program used was as follows: 94°C for 3 min, 35 cycles of 94°C for 30 s, 60°C for 30 s, 72°C for 1 min, followed by 72°C for 10 min.

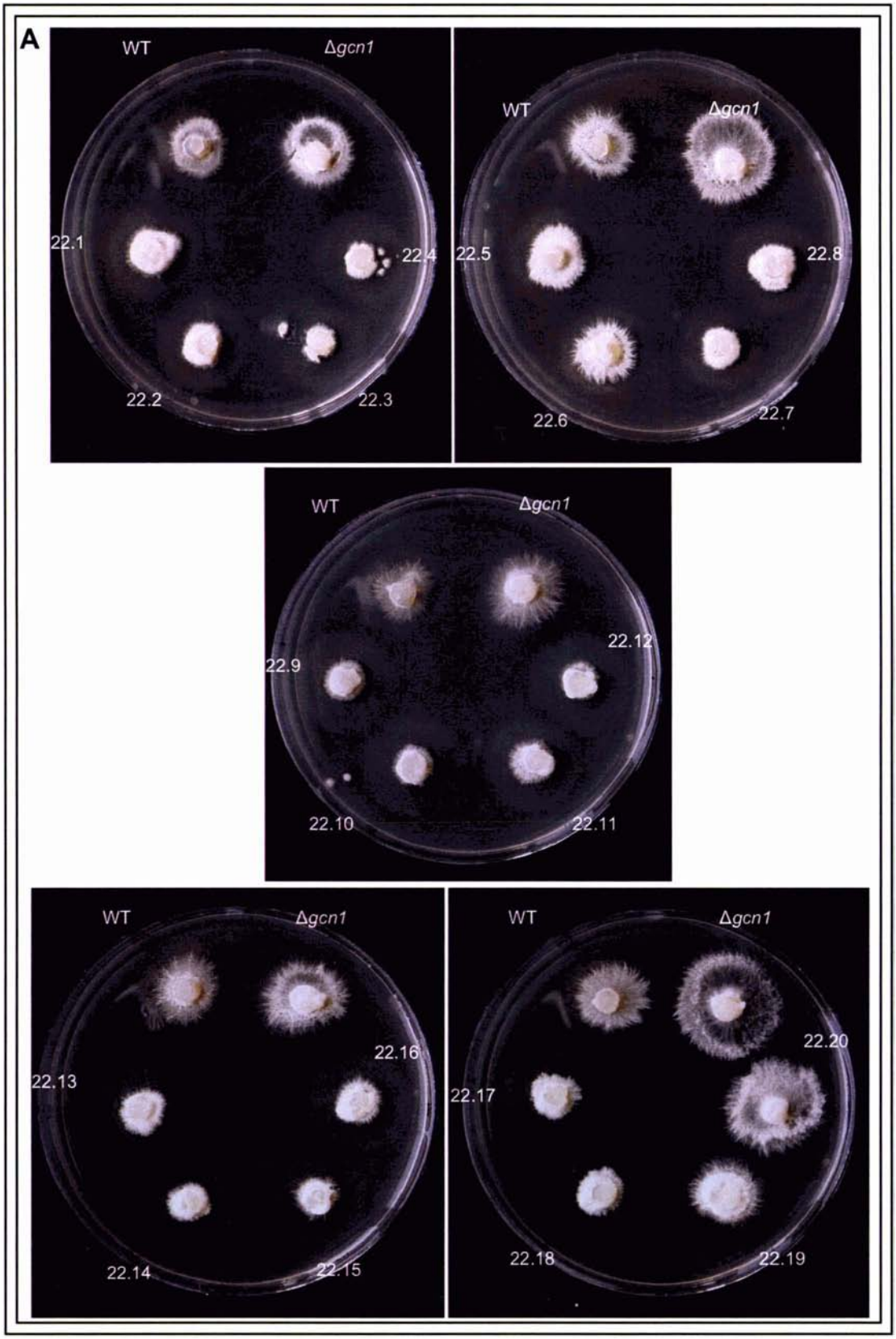
A
WT
Δgcn1
22.1
22.4
22.2
22.3
WT
Δgcn1
22.5
22.8
22.6
22.7
WT
Δgcn1
22.12
22.9
22.10
22.11
WT
Δgcn1
22.16
22.13
22.14
22.15
WT
Δgcn1
22.20
22.17
22.18
22.19

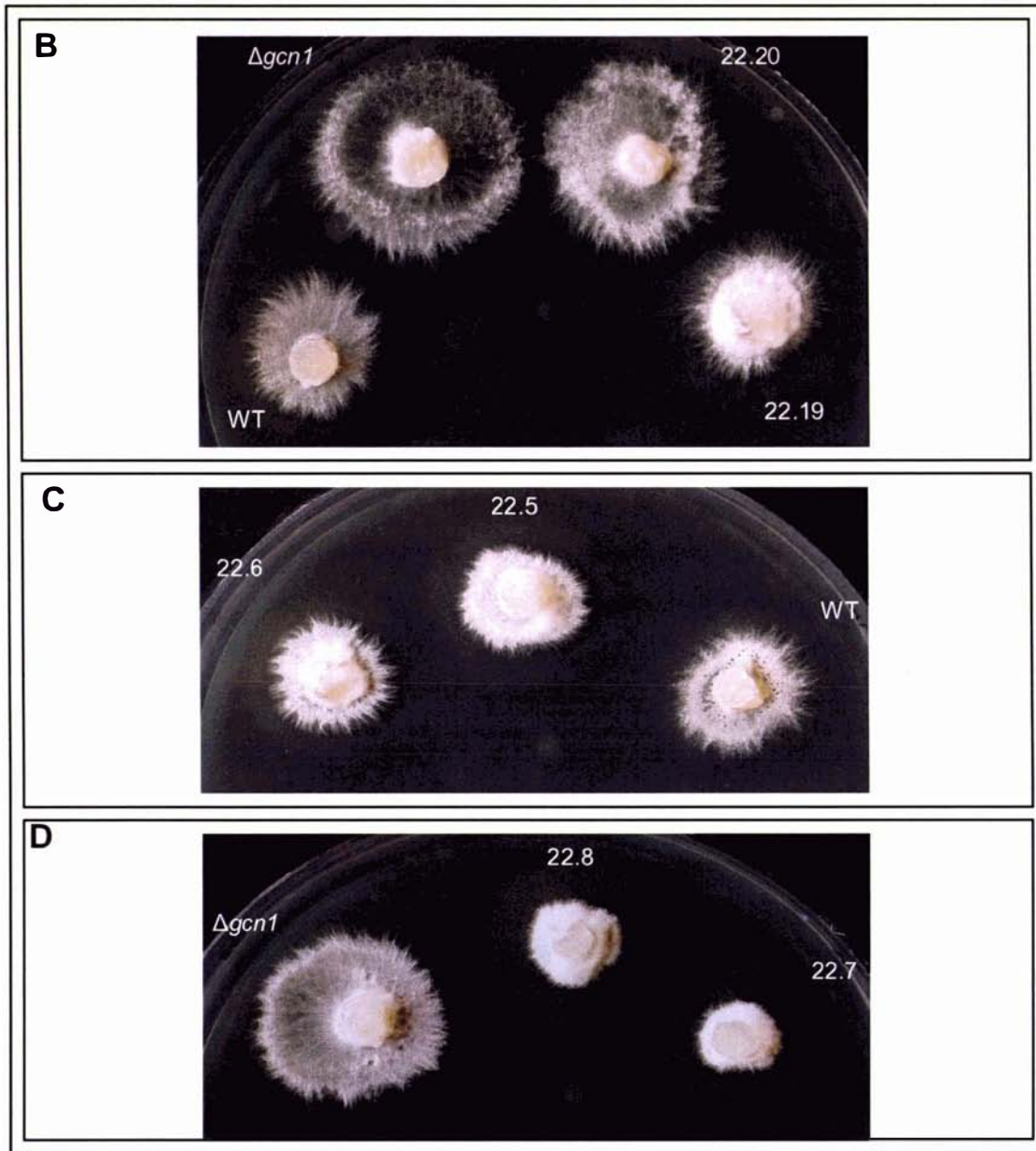

Figure 5.10 Growth screening of Δ*gcn1* strains complemented with pMM44

(A) Growth of selected geneticin resistant Δ*gcn1* strains co-transformed with the pMM44 vector and pII99 on pustulan containing media. The MM20.15 Δ*gcn1* strain that was transformed to create these strains is indicated as Δ*gcn1*, while wild type *E. festucae* FI1 is indicated as WT. **(B)** Growth of wild type *E. festucae* FI1 (WT), MM20.15 (Δ*gcn1*), MM22.20 and MM22.19 strains on pustulan media. **(C)** Growth of MM22.6, MM22.5 and wild type *E. festucae* FI1 (WT) on pustulan media. **(D)** Growth of MM20.15 (Δ*gcn1),* MM22.8 and MM22.7 strains on pustulan media.

5.4 GROWTH OF WILD TYPE, ECTOPIC AND Δ*GCN1* STRAINS DURING GROWTH *IN PLANTA*

Wild type, ectopic and Δ*gcn1* strains were inoculated into perennial ryegrass seedlings to determine if deletion of *gcn1* affected the symbiosis of the endophyte with its host. The phenotype of fungal hyphae *in planta* was examined by aniline blue staining of epidermal peels from the leaf sheaths of old and young leaves infected with wild type *E. festucae* Fl1, the ectopic strain MM20.1 and the Δ*gcn1* strain MM20.15. The appearance of epiphytic hyphae growing on the plant surface was also examined. Compared to the wild type *E. festucae* Fl1 and the ectopic MM20.1 strains, hyphae of the Δ*gcn1* strain MM20.15 appeared to grow normally in the leaf sheaths of both old (Figure 5.11A) and young (Figure 5.11B) leaves. Epiphytic hyphae also had a normal appearance in the MM20.15 Δ*gcn1* strain.

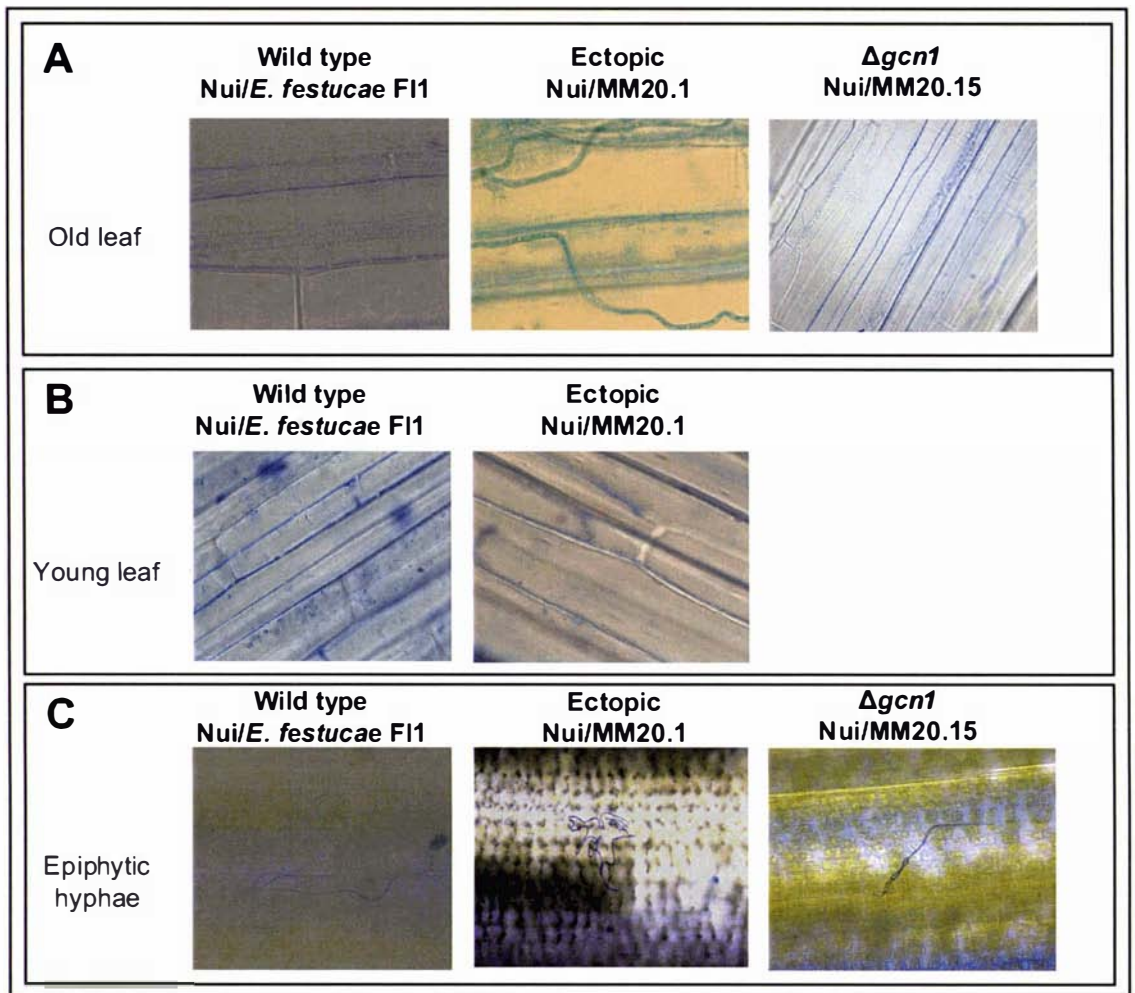

Figure 5.11 Phenotype of Δ*gcn1* hyphae during growth *in planta*

(A) Endophyte hyphae in the outermost leaf sheath as shown by aniline blue staining of epidermal peels from tillers of *L. perenne* cv Nui plants infected with either wild type *E. festucae* Fl1, the ectopic strain MM20.1 or the Δ*gcn1* strain MM20.15. **(B)** Endophyte hyphae in the young leaf sheath as shown by aniline blue staining of epidermal peels from tillers of *L. perenne* cv Nui plants infected with either wild type *E. festucae* Fl1, the ectopic strain MM20.1 or the Δ*gcn1* strain MM20.15. **(C)** Epiphytic hyphae on the leaf surface as shown by aniline blue staining of leaves from tillers of *L. perenne* cv Nui plants infected with either wild type *E. festucae* Fl1, the ectopic strain MM20.1 or the Δ*gcn1* strain MM20.15.

CHAPTER 6

Discussion

6.1 *E. FESTUCAE* CONTAINS A GENE FAMILY OF SUBTILISIN-LIKE PROTEASES

Based on the large number of genes encoding subtilisin-like proteases in other fungal genomes, it was hypothesised that *E. festucae* Fl1 contained a family of these genes. In this study, multiple subtilisin-encoding genes were identified in the *E. festucae* Fl1 genome. *prt1, prt2, prt3* and *prt5* all encode putative extracellular enzymes that belong to the proteinase K family of subtilisin-like proteases, while *prt4* encodes a vacuolar protease that also belongs to the proteinase K family. The *kex2* gene encodes a member of the kexin family of subtilisin-like proteases. Degenerate PCR also identified the presence of other genes encoding subtilisin-like proteases: one from the proteinase K family (*prt6*), and two from the pyrolysin family of subtilisin like proteases (*prt7* and *prt8*).

6.1.1 Members of the proteinase K family of subtilisin-like proteases

6.1.1.1 The *prt5-prt1* locus

Screening of an *N. lolii* Lp19 genomic DNA library identified the *prt1* gene in a previous study (McGill, 2000). In this study, the corresponding gene in the *E. festucae* Fl1 strain was identified and sequenced (Section 3.1.1). The Prt1 polypeptides of the *N. lolii* Lp19 and *E. festucae* Fl1 shared a high degree of identity at the amino acid level, with only two changes in the polypeptide sequence between the two strains. Phylogenetic analysis with related polypeptide sequences from other fungi demonstrated that the *E. festucae* Fl1 and *N. lolii* Lp19 Prt1 proteins both belong to subfamily 2 of the proteinase K family (Hu and St Leger, 2004). The Prt1 proteins were most closely related to Prl1D, Prl1E and Prl1F from *M. anisopliae*, and to FG00806.1, FG11405.1 and FG08464.1 from *F. graminearum* (Figure 3.18).

The *N. lolii* Lp19 and *E. festucae* Fl1 *prt1* genes contain repetitive DNA sequences in the 3' untranslated region (Figures 3.2 and 3.3, Appendix A2.1). In a previous study, 3' RACE of the *N. lolii* Lp19 *prt1* indicated this repetitive region, which consists of $(YTT)_4(YA)_{13}$, is associated with the polyadenylation site (McGill, 2000). This sequence

was also identified in *E. festucae* Fl1. Downstream of the *prt1* gene, the *E. festucae* Fl1 and *N. lolii* Lp19 sequences diverge. This is due to the presence of a highly repetitive mini-satellite element consisting of TTYYATYYR repeats in *N. lolii* Lp19 that is not present in the same position in *E. festucae* Fl1 (Appendix A2.1). This repetitive DNA overlaps with the 3' end of the *orf4* gene, and introduces a stop codon that results in the premature truncation of the *orf4* gene product. The presence of this mini-satellite hints at potential degeneration of the asexual *N. lolii* Lp19 genome. The mini-satellite probably arose in *N. lolii* Lp19 through slippage during DNA replication, as described for other fungal minisatellites (Giraud et al., 1998; Haber and Louis, 1998).

The *prt5* gene was identified immediately upstream of the *prt1* gene (Figures 3.2 and 3.3). The *E. festucae* Fl1 and *N. lolii* Lp19 Prt5 protein belongs to subfamily 1 of the proteinase K family (Figure 3.18). Prt5 shares strongest identity with the Prl K protease from *M. anisopliae*, and the *F. oxysporum* Prt1 protein (Di Pietro et al., 2001; Hu and St Leger, 2004). The presence of two related genes in such close proximity may suggest that the two genes could have arisen by gene duplication. However, the Prt5 and Prt1 proteins belong to different subfamilies of the proteinase K family, with the Prt5 protein belonging to subfamily 1 and the Prt1 protein belonging to subfamily 2. As these two genes encoded enzymes from different subfamilies, this suggests that these genes have not arisen recently by gene duplication at this locus. The only other known instance where two subtilisin-like protease-encoding genes were found adjacent to each other is in the genome of *M. anisopliae*, where the *prlE* and *prlF* genes are adjacent to each other. Unlike the Prt5 and Prt1 proteins, the PrlE and PrlF proteins both belong to the same subfamily, proteinase K subfamily 2. However, the sequence identity between the PrlE and PrlF proteins is relatively low, at 28% identity at the amino acid level.

6.1.1.2 The *prt2-gcn1* locus

A previous study of *prt* genes in *N. lolii* Lp19 led to the identification of *prt2* (McGill, 2000). The corresponding gene from *E. festucae* Fl1 was identified in this study (Section 3.1.2). The *N. lolii* Lp19 and *E. festucae* Fl1 Prt2 proteins, which are putative extracellular enzymes belonging to subfamily 1 of the proteinase K family (Figure 3.18),

differ at two amino acid residues. The most similar protein to the *E. festucae* Fl1 and *N. lolii* Lp19 Prt2 proteins is the Prl1 protease from *M. anisopliae* (Hu and St Leger, 2004).

The *gcn1*, *cyc1* and *ptn1* genes were identified downstream of the *prt2* gene in *E. festucae* Fl1 (Figure 3.10). The *gcn1* gene encoded a putative β-1,6-glucanase that is highly similar to β-1,6-glucanases from a *Neotyphodium* sp. endophyte and from the mycoparasitic fungus *T. harzianum* (Lora et al., 1995; Moy et al., 2002) (Figures 5.2 and 5.3). Other characteristics of the *gcn1* gene are described in Section 6.3. The *cyc1* and *ptn1* genes, which do not encode hydrolases, were syntenic with their *F. graminearum* homologues, FG04981.1 and FG04982.1 respectively. While other studies have shown large regions of synteny between *E. festucae* and *F. graminearum* genomes (Tanaka et al., 2005) (S. Foster, G. Bryan, personal communication), this was the only case of conserved synteny with another fungal genome observed in this study.

The *cyc1* gene encodes a putative C-type cyclin that may be a homologue of the *S. cerevisiae ctk2* gene (Appendix A4). In *S. cerevisiae*, Ctk2p acts with two other subunits as part of a divergent cyclin-CDK (cyclin dependent kinase) complex (CTDK-I) (Hautbergue and Goguel, 2001; Sterner et al., 1995). CTDK-I phosphorylates a serine residue in the carboxyl-terminal domain (CTD) of RNA polymerase II, a reaction that is critical for efficient transcription elongation and correct processing of mRNA 3' ends (Ostapenko and Solomon, 2005). CTDK-I also regulates activity of the RNA polymerase I CTD involved in ribosomal RNA biosynthesis (Bouchoux et al., 2004).

The *ptn1* gene encodes a putative phosphoinositide 3-phosphatase related to the PTEN (phosphatase and tensin) phosphoinositide 3-phosphatases. These related proteins are specialised protein tyrosine phosphatases that dephosphorylate phosphoinositide substrates such as phosphatidylinositol 3,4,5 triphosphate (PIP_3) (Maehama et al., 2001). These proteins act as antagonists of signalling through the PI-3-kinase pathway in *S. pombe* and in higher eukaryotes (Downes et al., 2001; Mitra et al., 2004). The putative *E. festucae* Fl1 Ptn1 protein shares all of the residues critical for the catalytic action of

PTEN homologues (Appendix A5). The catalytic signature domain (HCKAKGRSG) of *E. festucae* Ptn1 was almost identical to that of *S. pombe* ptn1p (HCKAKGRTG), which dephosphorylates PIP_3 *in vitro* and suppresses PIP_3 levels *in vivo*. This differs to the catalytic signature of the corresponding protein from *S. cerevisiae,* Tep1p (HCRMGKGRSG), which does not appear to dephosphorylate PIP_3 (Heymont et al., 2000). Conserved amino acid residues that form positive charges at the catalytic site (Fl1 Ptn1 H93, K164 and K167) were all conserved (Mitra et al., 2004). The Q221 residue required for hydrogen bonding to PIP_3 was conserved. The other residue required for hydrogen bonding to PIP3, S217, differed to threonine found at this position in related sequences. However, threonine and serine have similar functional groups, so this may not alter hydrogen bonding to PIP_3 at this position.

6.1.1.3 The *prt3* locus

Sequence similarity to the *E. typhina At1* gene was used to identify the *E. festucae* Fl1 and *N. lolii* Lp19 *At1* homologues (designated as *prt3;* Section 3.1.3). The *prt3* gene of *N. lolii* Lp19 and Lp5 strains had a single nucleotide deletion towards the end of exon 2. This deletion leads to a frame shift in the *prt3* open reading frame, which will result in premature truncation of the Prt3 protein. As the truncated Prt3 protein lacks the conserved catalytic residues required for enzymatic activity, the Prt3 protein in *N. lolii* Lp19 (and Lp5) is expected to be non-functional (Section 3.1.3.2). The deletion in the *N. lolii* Lp19 and Lp5 *prt3* homologues has a similar effect to the minisatellite sequence downstream of the *prt1* gene in *N. lolii* Lp19 (Section 3.1.1), where a stop codon is introduced into the *orf4* gene, resulting in premature truncation of the Orf4 protein. Analysis of gene fragments in the *S. cerevisiae* genome suggests that after gene duplication, the function of many genes is lost by the accumulation of deleterious mutations (Lafontaine et al., 2004).

The inactivation of *prt3* in the Lp19 and Lp5 strains (and premature truncation of *orf4* in Lp19) may be a reflection of the exclusively mutualistic, asexual lifestyle of *N. lolii.* Selection pressure to retain gene function in the asexual *N. lolii* may be reduced in comparison to its sexual ancestor, *E. festucae.* However, the deletion may also be a

consequence of the asexual life cycle of the *N. lolii* strains. These strains will tend to accumulate genetic mutations which are not compensated for by new genetic material introduced during sexual reproduction, which tends to make genomes of asexual organisms unstable (Taylor et al., 1999). It is also possible the *prt3* gene may only be required during the sexual phase of growth, which could mean its function is no longer necessary in the asexual *N. lolii* strains. However, not all asexual *N. lolii* strains contained the single base pair deletion leading to truncation of the Prt3 protein.

Although *prt3* expression is up-regulated *in planta*, the level of expression is still relatively low (Section 3.6). The Prt3 orthologue in *E. typhina,* Atl, is a highly abundant protein in the leaf sheaths of *E. typhina*-infected *P. ampla* (Lindstrom and Belanger, 1994). Using northern analysis, (Reddy et al., 1996) showed that while the *At1* transcript was readily detected in endophyte-infected *Poa* spp. grasses, transcripts of *prt3* in grasses infected with *N. lolii* or *E. festucae* were at much lower levels. The results obtained in this study were consistent with these findings, with *prt3* from *E. festucae* and *N. lolii* expressed at relatively low levels *in planta.* Reddy et al. (1996) suggested the differences in expression for the *E. typhina At1* and *E. festucae* and *N. lolii prt3* genes could be due to differences in gene regulation or to fungal biomass within the plant.

Expression of the *N. lolii* Lp19 and *E. festucae prt3* genes were up-regulated during infection of *L. perenne* cv. Nui compared to conditions in culture (Figure 3.39). These findings were interesting because expression of the *E. typhina At1* gene was not detected in the same host. Although the *N. lolii* Lp19 *prt3* gene produces a truncated product, it is expressed in culture, and as for *E. festucae* Fl1 *prt3*, the *N. lolii* Lp19 *prt3* gene appears to be up-regulated *in planta.*

An interesting finding in this study was that when the *E. typhina* endophyte from *P. ampla* was inoculated into *L. perenne* cv. Nui, *At1* gene expression was not detected in culture or *in planta* by RT-PCR (Figure 3.39). This was despite the biomass levels of the *E. typhina* endophyte in *L. perenne* being higher than that of either *E. festucae* or *N. lolii* in the same host. This was due to an increase in the number of extracellular

hyphae on the leaf surface of *L. perenne* infected with *E. typhina* (Appendix A15), a finding consistent with the results seen for *Poa* sp. infected with a different *E. typhina* strain (M. Christensen, personal communication). This study suggests that *At1* gene expression may be regulated differently in its natural *Poa ampla* host than it is when in an artificial association with *L. perenne*. Potentially, different nutritional environments or specific host factors between the two hosts affect the regulation of gene expression. This may be particularly relevant to researchers attempting to identify novel endophytes for grass pasture species. Often researchers have found that some artificial associations lead to incompatible interactions. Although the association between *E. typhina* PN2311 and perennial ryegrass was compatible, endophyte gene expression is obviously affected by host factors.

The At1 protease is not the only endophyte protein identified at high levels in the association between *E. typhina* and *Poa ampla*. Interestingly, the major protein produced in culture, a chitinase, is also found in apoplastic fluids of infected plants (Amiard et al., 2004). *N*-acetylglucosaminidase and β-1,6-glucanases have also been detected (Li et al., 2005; Moy et al., 2002). The fact that all of these proteins are found at relatively high levels in endophyte-infected *P. ampla* suggests differences in expression may be due to a difference in biomass levels. This difference could be experimentally determined by microscopy, or by using a real-time PCR approach similar to that described by Young (2005).

Analysis of sequence upstream and downstream of *prt3* identified the *ats1* and *gao1* genes (Figure 3.15). These genes are not closely linked to each other or to a *prt3* homologue in the closely related species, *F. graminearum*. The *ats1* gene encodes a putative asparaginyl-tRNA synthetase. The *gao1* gene encodes a putative galactose oxidase, which oxidise primary alcohols and generates hydrogen peroxide (Whittaker, 2003). All of the residues required for catalytic activity are conserved in the *E. festucae* Fl1 Gao1 protein. Like other galactose oxidases, the Gao1 protein contains a putative carbohydrate binding domain (Baumgartner, 1998) and two putative Kelch domains

(Adams et al., 2000). In *Fusarium*, the two Kelch domains form a 7-fold beta propeller structure (Whittaker, 2003).

6.1.1.4 The *prt4* gene

The *prt4* gene was identified by degenerate PCR with primers based on vacuolar proteases from other fungi (Figure 3.19). Fungal vacuolar proteases are involved in the recycling of macromolecules in the vacuole during autophagy (Pinan-Lucarre et al., 2003; Takeshige et al., 1992). The *prt4* gene encodes a putative vacuolar protease belonging to subfamily 3 of proteinase K family. Phylogenetic analysis confirmed that the Prt4 protein was closely related to other fungal vacuolar like proteases (Figure 3.25).

6.1.2 *Kex2* is a member of the kexin family of subtilisin-like proteases

The *E. festucae* Fl1 *kex2* gene was identified by screening of a genomic DNA cosmid library with a *N. lolii* Lp19 *kex2* probe (Section 3.3). *kex2* encodes a putative proprotein convertase of the kexin family of subtilisin-like proteases, with similarities to related sequences from *F. graminearum*, *M. grisea*, *N. crassa* and *Aspergillus* spp. Proteins that pass through the fungal secretory pathway, in particular the *trans* Golgi network, are potentially targets of kexins (Redding et al., 1991). As such, the proteins encoded by some of the genes identified in this study are potential targets of the *E. festucae* Fl1 Kex2 protein. One potential example of kexin processing identified in this study was the Gcn1 protein, which shares a conserved kexin recognition site with related proteins from *Neotyphodium* sp. FCB2002 and *T. harzianum* (Figure 5.2, recognition site KR at residues 39-40; Moy et al., 2002).

6.1.3 Regulation of expression of genes encoding subtilisin-like proteases

The expression of genes encoding subtilisin-like proteases in fungi is commonly regulated by carbon catabolite repression, nitrogen metabolite repression or pH. The global regulatory systems mediated by CreA or AreA/Nit2 prevent expression of enzymes for utilising alternative carbon or nitrogen sources if preferred carbon or

nitrogen sources are available (Strauss et al., 1999; Tao and Marzluf, 1999). pH regulation is mediated by PacC, which activates gene expression of alkaline protease genes under alkaline conditions (Tilburn et al., 1995). Expression of some genes is induced by an external protein source. The regulation of expression of subtilisin-like protease genes is described in Table 6.1.

Expression of the *prl A* gene from the entomopathogenic fungus *M. anisopliae* is repressed in the presence of preferred carbon and/or nitrogen sources (St Leger et al., 1992). *prl A* is also pH regulated, with maximal gene expression at alkaline pH (St Leger et al., 1998). Proteinaceous components of insect cuticle induce *prl A* gene expression (Paterson et al., 1994). Expression of the *prb1* gene from the mycoparasitic

Table 6.1 Regulation of fungal subtilisin-like protease genes

Organism	Gene	Family[a]	Ccr[b]	Nmr[c]	pH	Inducers
M. anisopliae	*pr1A*	ProtK sf 1	√	√	√	Proteinaceous components of insect cuticle
T. harzianum	*Prb1*	ProtK sf 2	√	√	-	Chitin, fungal cell walls (if C and N derepr) Osmotic stress (if N derepr)
A. oligospora	*Pll*	Prot K unk	√	√	?	Exogenous protein
O. piliferum	*Opil1*		X	X	√	Exogenous Protein
O. piceae	*Opic1*		√	√	√	Exogenous protein (if C and N derepr)
A. niger	*pepC*	Prot K vac	X	X	-	X
O. piliferum	*Opil2*	Prot K vac	X	X	X	X
P. brassicae	*Psp2*	ProtK vac	X	X	X	X
C. albicans	*CaPRB1*	Prot K vac	X	√	-	Heat shock GlcNAc (inhibited by glucose)
S. cerevisiae	*PRB1*	Prot K vac	√	√	-	Diauxic phase growth

[a] Family or subfamily of fungal subtilisin like proteases based on (Hu and St Leger, 2004)
[b] carbon catabolite repression, where the presence of glucose represses the expression of genes for utilisation of alternative carbon sources
[c] nitrogen metabolite repression, where the presence of ammonium or glutamine represses gene expression

fungus *T. harzianum* is also repressed in the presence of preferred carbon and nitrogen sources (Geremia et al., 1993; Olmedo-Monfil et al., 2002). If a preferred nitrogen

source is absent, expression of *prb1* can be induced by chitin, fungal cell walls or osmotic stress (Olmedo-Monfil et al., 2002). Expression of the *A. oligospora PII* gene is repressed in the presence of preferred carbon and nitrogen sources, but was induced by an external protein source (Åhman et al., 1996).

The *opi11* and *opic* protease genes from the wood-staining *Ophiostoma* sp. fungi showed different regulation patterns (Hoffman and Breuil, 2004a). *opi11* expression was not subject to carbon or nitrogen repression, but was expressed if the ambient pH was alkaline. The presence of exogenous protein also induced *opi11* gene expression. The *opic* gene was subject to carbon and nitrogen repression, and was regulated by pH. If no preferred carbon or nitrogen source was available, gene expression could be induced by exogenous proteins.

Genes encoding vacuolar subtilisin-like proteases differed in their regulation. Expression of the *pepC* (*Aspergillus niger*), *opi12* (*O. piliferum*) and *psp2* (*P. brassicae*) genes were not repressed in the presence of preferred carbon and nitrogen sources or ambient pH, nor were these genes induced by an exogenous protein source (Hoffman and Breuil, 2004a; Jarai et al., 1994; Keniry et al., 2002). However, expression of the vacuolar protease genes from *S. cerevisiae* and *C. albicans* were regulated in a different manner. Expression of the *C. albicans CaPRB1* gene was not repressed in the presence of glucose, but was repressed in the presence of a preferred nitrogen source (Orozco et al., 2002). CaPRB1 expression was also induced by heat shock and by *N*-acetylglucosamine if glucose was absent. The *S. cerevisiae PRB1* gene was repressed in the presence of preferred carbon and nitrogen sources (Hofman-Bang, 1999; Moehle et al., 1987).

The different regulation patterns observed with the extracellular and vacuolar subtilisin-like protease genes corresponds to their cellular functions. The extracellular subtilisin-like proteases are used by the cell to break down proteins to provide carbon and nitrogen sources to support growth. If preferred carbon and nitrogen sources are present, the fungus will utilise these sources first, and the protease genes will be repressed. When the preferred nutrient sources have been utilised, expression of the fungal protease genes

will be derepressed. Induction by exogenous protein acts to promote protease gene expression in the presence of the protease substrate. Subtilisin-like proteases are generally most active at neutral to alkaline pH. Regulation of gene expression by ambient pH allows the genes to be expressed under conditions where the encoded proteins are most likely to be active. Vacuolar proteases are likely to have a housekeeping function within the cell, by breaking down components of macromolecules within the vacuole. The constitutive expression of vacuolar protease genes in filamentous fungi is consistent with a housekeeping function of vacuolar proteases within the cell (Hoffman and Breuil, 2004a).

Carbon, nitrogen and pH regulation of genes encoding subtilisin-like proteases was correlated with the presence of CreA and AreA binding sites within promoter sequences (Cortes et al., 1998; Screen et al., 1997). On the basis of this, CreA, AreA and PacC consensus binding sites were analysed in the untranslated regions upstream of the *prt1, prt2, prt3, prt4, prt5* and *kex2* open reading frames (Figures 3.6, 3.12, 3.17, 3.24 and 3.29). The regions upstream of the *prt1*, *prt2, prt3, prt4* and *prt5* genes all contain multiple sequence motifs that could potentially be bound by the CreA, AreA and PacC transcription factors. However, the role of potential transcription factor binding sites must be confirmed by experimental procedures such as DNA mobility shift assays. In addition, the effects of preferred carbon and nitrogen sources, pH and exogenous protein on expression of the *prt* and *kex2* genes remain to be experimentally determined.

Recognition site distribution and frequency suggests that the *prt5, prt2, prt3, prt4* and *kex2* genes may be regulated by carbon and nitrogen catabolite repression controlled by orthologues of the *A. nidulans* CreA and AreA proteins. The *prt3* gene may also be regulated in response to ambient pH by an orthologue of the PacC protein. The *prt1* gene may be regulated in response to glucose by a CreA orthologue.

Some genes that are up-regulated *in planta* are also induced by carbon or nitrogen starvation (Snoeijers et al., 1999; Solomon et al., 2005; Talbot et al., 1993). In terms of endophyte growth, it is generally assumed the apoplast where the endophyte grows is

nutrient poor. Studies of different grass-endophyte systems have proved contradictory. A study by Bacon and White (2000) showed that endophyte infection has a significant effect of the host plant's nitrogen metabolism, with the concentration of ammonium doubled in the leaf sheaths of infected plants. This situation is similar to that found by Solomon et al. (2003), who showed that the concentration of nitrogen sources in the leaf increased during compatible infections of tomato by *Cladosporium fulvum*. However, experiments by Johnson and Rasmussen (unpublished) have shown that free amino acids in endophyte-infected grass tissues are significantly reduced compared to uninfected tissues, suggesting that the endophyte may be growing in an environment that is relatively low in available nitrogen. This could have implications for the regulation of subtilisin-like protease genes *in planta* if gene expression is derepressed in the absence of a preferred nitrogen source.

The Seb1 protein is a transcriptional regulator that is involved in, but is not required for, the response to osmotic response in *Trichoderma atroviride* (Seidl et al., 2004). In this study, the distribution of Seb1 was studied in the promoters of the *prt* and *kex2* genes. The distribution patterns of Seb1 binding sites in the *prt5, prt3* and *kex2* genes suggested that these genes could be regulated by the Seb1 transcription factor. However, the significance of these binding sites is unclear, as the function of Seb1 homologues in other fungi has not been determined. In *T. atroviride*, the *seb1* gene was identified by its sequence similarity to the *S. cerevisiae* genes encoding the Msn2p/Msn4p proteins (Peterbauer et al., 2002), which regulate gene expression in response to stress (Schmitt and McEntee, 1996). However, although Seb1 binds to the same sequence as Msn2p/Msn4p, it was not able to functionally complement a Δ*msn2/4* mutant of *S. cerevisiae* (Peterbauer et al., 2002).

MEME analysis (Bailey and Elkan, 1994) also identified some sequence motifs that were present in the regions upstream of the *prt* genes. While several of these motifs are found in multiple copies in the promoters of several *prt* genes, the functional significance of these motifs is unclear. Again, DNA mobility shift assays using DNA fragments from the promoter containing particular MEME motifs and promoter deletion

analysis may provide an insight to any potential function of these motifs. Other motif-finding programs that are purported to be more sensitive than MEME have also been developed, which may be more accurate at finding motifs in the *prt* promoters (Down and Hubbard, 2005; Leung and Chin, 2005).

Whole genome analysis would also provide clues to the abundance of these motifs in the promoters of other genes, potentially providing information about the function of these motifs. Comparative analysis, where the promoters of the *E. festucae* Fl1 *prt* and *kex2* genes are compared with the orthologous sequences from other *Epichloë* or related species, could help distinguish which motifs may be functional. Similar studies have been used to identify potential protein-binding motifs in *S. cerevisiae* and related *Saccharomyces* species (Kellis et al., 2003).

In this study, the expression of the *prt* and *kex2* genes was compared in culture and *in planta* (Section 3.6). Due to biomass differences between the endophyte in culture and *in planta*, it was necessary to normalise the expression levels of a constitutively expressed gene between culture and symbiota samples to allow for this difference in biomass. The endophyte *tub2* gene was selected as a constitutively expressed gene, and cDNA dilutions analysed by RT-PCR were compared for similar levels of *tub2* expression (Figure 3.37).

Analysis in *E. festucae* Fl1 showed that expression of the *prt1, prt3* and *prt4* genes appeared to be up-regulated *in planta* compared to in culture (Figure 3.38). Expression of the *prt5, kex2* and *prt2* genes were below the detection levels of the RT-PCR approach used in this study. The expression of the *gcn1* gene appeared to be unchanged between the two growth conditions. This study also confirmed that expression of the *ltmM* gene is induced during growth *in planta*, but not during growth in culture, a result consistent with previous experiments performed by Young (2005).

Studies using a wider range of plant-endophyte associations confirmed the differential expression of the *prt1* and *prt3* genes in symbiota of *E. festucae* Fl1 with perennial

ryegrass, and in meadow fescue (*Festuca pratensis*) (Figure 3.39). The *prt1* and *prt3* genes were also up-regulated in a symbiotum of *N. lolii* Lp19 and perennial ryegrass. However, the two genes appeared to be regulated quite differently in a symbiotum of an *E. typhina* strain (from *Poa ampla*) with perennial ryegrass. The *prt1* homologue in *E. typhina* was expressed at the same levels in culture and *in planta*, which differs to the increased *prt1* expression *in planta* that was observed for the *N. lolii*/perennial ryegrass, *E. festucae*/perennial ryegrass and *E. festucae*/meadow fescue symbiota. Meanwhile, expression of the *prt3* homologue *At1* in the *E. typhina* strain was not detected either in culture or *in planta*. Expression of the *prt2* gene was not detected in any of these endophyte strains either in culture or *in planta*.

Some inherent limitations are present with this technique. Firstly, it is assumed that expression of the *tub2* gene is truly constitutive, and that expression of the gene does not change when the endophyte grows *in planta*. This may not be true during growth within the plant. Analyses of arbuscular mycorrhizal symbioses have indicated that for these zygomycete fungi, tubulin gene expression is differentially regulated during growth *in planta* (Delp et al., 2003; Rhody et al., 2003).

The expression differences observed between hyphae growing in culture and *in planta* may also be due to differences in nutrient availability. While the mycelia grown in culture are grown under rich conditions in potato dextrose broth, which contains plenty of glucose and amino acids, the hyphae growing *in planta* may have been growing in an environment with less available carbon and nitrogen sources. Experiments analysing the effect of various carbon and nitrogen sources on expression of the *prt* genes still need to be carried out to ensure differences in expression are due to growth within the plant rather than nutritional differences. There is some precedent for the expression of endophyte genes up-regulated *in planta* not being influenced by nutrient availability in culture. Expression of the lolitrem biosynthetic genes, *ltmG*, *ltmM* and *ltmK*, is strong up-regulated *in planta*, but does not appear to be induced by a lack of nutrient availability in culture (Young et al., 2005).

The expression of genes in culture is analysed at a particular stage of growth. Expression of the *prt* and *kex2* genes may vary during development and aging of fungal hyphae in culture. This is particularly important when comparing the expression of genes in various endophyte strains. In this experiment, the *E. typhina* strains were grown for five days, *E. festucae* for seven days, and *N. lolii* for twelve days in an attempt to allow for the different growth rates of the strains and to isolate roughly equivalent amounts of fungal biomass. However, the earlier harvest of the *E. typhina* culture in particular may have meant that expression of some of the genes may not have been induced at this stage. For the *prt3* homologue, Atl, Reddy *et al.* (1996) found that expression levels were higher in older cultures.

6.1.4 Genomic distribution of subtilisin-like proteases in filamentous fungi

The genomes of filamentous fungi contain varying numbers of subtilisin-like proteases (Table 1.2). While saprophytic fungi such as *A. nidulans* and *N. crassa* contain only a few, some phytopathogenic fungi such as *M. grisea* and *F. graminearum* contain large numbers of subtilisin-like proteases (Hu and St Leger, 2004). However, the number of subtilisin-like proteases in a fungal genome does not necessarily correspond with fungal lifestyle, as the phytopathogenic fungi *B. cinerea* and *S. sclerotiorum* contain relatively low numbers of subtilisin-like protease-encoding genes (Table 1.2).

The distribution of subtilisin-like protease genes in fungal genomes suggests these genes have been duplicated and diversified in some lineages, but have been lost in other lineages (Hu and St Leger, 2004). However, genes encoding vacuolar subtilisin-like proteases and kexin-like proprotein convertases are found in all fungal genomes sequenced to date (Table 1.2). This is probably a reflection of the specialised biological functions of the vacuolar and kexin-like proteases in macromolecule recycling in the vacuole and post-translational modification of secreted proteins.

However, the numbers of genes encoding subtilisin-like proteases from the proteinase K family subfamilies 1 and 2 and the pyrolysin family are much more variable (Hu and St

Leger, 2004). It has been suggested that extracellular subtilisin-like proteases from proteinase K subfamily 1 were originally found in Ascomycetes, and subsequent gene duplication and diversification resulted in the evolution of the proteinase K subfamily 2 members based on the presence of subfamily 1 protease-encoding gene in the genome of the yeast *S. cerevisiae.* Alternatively, these genes may be derived from duplication and diversification from the sequences found in the common ancestor of basidiomycetes and ascomycetes, with deletion of the subfamily 2 class in *S. cerevisiae* and deletion of both the subfamily 1 and 2 classes in *S. pombe* (Table 1.2).

Based on the number of proteases present in fungi that are closely related to *E. festucae* Fl1, such as *M. anisopliae* and *F. graminearum* (Hu and St Leger, 2004), it is possible that more subtilisin-like protease-encoding genes are present in the *E. festucae* genome. Classes of particular interest are the proteinase K subfamilies 1 and 2, and the pyrolysin family. The closely related *M. anisopliae*, which like *E. festucae* is a member of the Clavicipitaceae, contains five and four genes respectively from the proteinase K subfamilies 1 and 2 classes respectively. This study identified three subfamily 1 and two subfamily 2 protease-encoding genes from the proteinase K family in *E. festucae.*

Three protease genes each in *F. graminearum* and *M.* anisopliae encode proteins that group closely with the *E. festucae* and *N. lolii* Prt1 proteins (Figure 3.18). The conservation of the three proteins across the two species suggests the *E. festucae* genome may also contain other sequences that are closely related to *prt1.* Previous Southern analysis with *N. lolii* genomic DNA appears to support this hypothesis (data not shown). The *prt6* gene appeared to encode a homologue of the *M. anisopliae* Pr1J protein, which is also a member of subfamily 2 from the proteinase K family. The *prt2* and *prt5* gene products clustered closely with the Pr1I and Pr1K proteins respectively from *M. anisopliae.* However, the *prt3* gene products, while clustering closely with the *E. typhina* At1 protease, did not cluster with a particular *M. anisopliae* or other fungal protein within subfamily 1 of the proteinase K family. However, the conserved intron

structures of the *prt2* and *prt3* genes may suggest these two genes have arisen within subfamily 2 by gene duplication followed by genetic divergence.

Members of the pyrolysin family are common in the filamentous fungal genomes, especially in the genome of the phytopathogenic fungus *M. grisea.* The role of these proteases in fungi is currently unclear. The pyrolysin-like proteases are characterised by the presence of a protease-associated (PA) domain, which may be associated with substrate binding and recognition. To date, the only functionally characterised pyrolysin, PoS1 is from the basidiomycete *P. ostratus*, where it is associated with triggering a proteolytic cascade that regulates degradation of laccase isoenzymes involved in lignin degradation. Two genes encoding pyrolysin-like enzymes were identified in this study: the *prt7* gene (from subfamily 2), and the *prt8* gene (from subfamily 1).

In this study, protease genes were identified in a very specific manner. The *prt1* and *prt2* genes were identified in a previous study, using probes amplified from *N. lolii* Lp19 genomic DNA with primers designed based on the sequence of the At1 gene from *E. typhina* (McGill, 2000). These primers were designed to nucleotide sequences encoding conserved regions of the At1 protein, but the primers were not degenerate. It is unclear why the At1 homologue of *N. lolii* Lp19 (*prt3*) did not amplify using these primers. However, by amplifying *N. lolii* Lp19 genomic DNA using a different primer set based on the *At1* nucleotide sequence rather than on conserved polypeptide sequences, *prt3*, the *At1* homologue was discovered and subsequently characterised in *N. lolii* Lp19 and *E. festucae* Fl1 (Section 3.1.3). The *prt5* gene was only identified because of its proximity to the *prt1* gene in the *E. festucae* Fl1 and *N. lolii* Lp19 genomes (Figures 3.2 and 3.3).

The *prt4* gene was identified by PCR using degenerate primers designed to regions that were conserved in related vacuolar subtilisin-like proteases such as *pr1H* (Section 3.2). However, the peptide sequences to which these degenerate primers were designed were not present in the extracellular subfamilies (1 and 2) of the proteinase K family. This meant only the vacuolar protease gene was likely to be amplified from the *E. festucae*

Fl1 genome using these primers. The *kex2* gene was identified based on an *N. lolii* Lp19 sequence fragment (Section 3.3). For both the *prt4* vacuolar protease and *kex2* kexin-like protease-encoding genes, only a single copy of each gene was expected in the *E. festucae* genome based on the distribution of related genes in other fungal genomes (Table 1.2).

An alternative degenerate PCR strategy was used to identify other subtilisin-like protease genes in the *E. festucae* genome (Section 3.4). Other subtilisin-like protease-encoding genes from *E. festucae* Fl1 were amplified using degenerate primers designed to the most conserved protein regions surrounding the histidine and serine residues required for catalytic activity. Sequencing of some of the products amplified using these degenerate primers revealed the presence of the *prt6, prt7* and *prt8* genes encoding subtilisin-like proteases in the *E. festucae* Fl1 genome. However, some of the products amplified using these degenerate primers have not yet been characterised. At least two products are the size expected for the *prt1* gene and the *prt2, prt3,* and *prt5* genes. Sequencing of these products would confirm if any of the remaining products have been amplified from the subtilisin-like protease encoding genes identified in this study, or if they represent novel subtilisin-like protease-encoding genes.

The chromosomal localisation of the *prt* genes and *kex2* genes differed between the endophyte strains (Section 3.5). As expected due to the proximity of the *prt5* and *prt1* genes, these two genes were found on the same chromosome in all the strains analysed. However, the distribution of the other *prt* genes and *kex2* genes varied between strains. In *E. festucae* Fl1, *prt1, prt5*, *prt2* and *prt3* genes were all on the same chromosome, or on chromosomes that were similar in size. *prt4* and *kex2* were located on different chromosomes to each other and to the chromosome containing the other *prt* genes. However, in *N. lolii*, the *prt2*, *prt3*, *prt4* and *kex2* genes were all located on separate chromosomes to each other, and were not on the chromosome containing the *prt5* and *prt1* genes. In *E. typhina* PN2311, the *prt2*, *prt3* and *prt4* genes all appear to be on the same chromosome or a chromosome of similar size, with the *prt5* and *prt1* genes on one separate chromosome and the *kex2* gene on another separate chromosome.

The chromosomal distribution of the protease-encoding genes is important as it provides an insight into the evolution of the subtilisin-like gene family. Initially, the subtilisin-like protease gene family in fungi probably arose through successive gene duplications, followed by divergence of sequences and/or gene loss in some strains (Hu and St Leger, 2004). Some classes of subtilisin-like protease genes diverged in function at an early time point in evolution. For instance, kexins (proprotein convertases) are common to all eukaryotes, suggesting these genes diverged from other subtilisin-like protease genes early during eukaryote evolution. Other genes may have arisen by more recent duplication and divergence (Hu and St Leger, 2004).

6.2 HETEROLOGOUS EXPRESSION OF *PRT1* AND *PRT2* IN *EPICHLOË FESTUCAE* FL1

Studies in other fungi suggest subtilisin-like proteases play important roles in fungal-host interactions. Based on these results, it was hypothesised that the Prt1 and Prt2 subtilisin-like proteases may affect the interaction of *E. festucae* with its host grass. The *prt1* and *prt2* genes were selected for analysis based on their different patterns of regulation. While *prt1* is expressed in culture and *in planta*, no *prt2* expression has been detected (Section 3.6). This suggests the Prt1 protein may be present in the symbiosis. The presence of the Prt2 protein in the grass-endophyte symbiosis, where it is not normally present, may perturb the fungal-host interaction.

Many strategies have been used to identify the role of hydrolytic enzymes in fungal host interactions (Section 1.7). However, most of these strategies contain some limitations for characterising the role of subtilisin-like proteases in fungal-host interactions. While gene replacement is a commonly used technique to investigate gene function, this method may not be suitable for determining the function of subtilisin-like protease-encoding genes due to gene redundancy in fungal genomes (Table 1.2). In E. festucae, the exact number of subtilisin-like protease genes within the genome is unknown. Sequential replacement of genes is often used to determine gene function where members of a gene family may be partially or fully redundant, as described for the *THI* gene family in *S. cerevisiae* (Wightman and Meacock, 2003).

The creation of strains bearing multiple gene replacements can be both tedious and time-consuming. The primary organism used in this study, *E. festucae* Fl1, grows more slowly in culture than model fungi such as *A. nidulans* and *N. crassa*. Protoplast regeneration after transformation is relatively slow, with hygromycin resistant transformants routinely growing for at least two weeks before becoming visible on plates. The frequency of homologous recombination resulting in gene replacement is relatively low. In addition, *E. festucae* is not genetically well characterised and auxotrophic strains that enable the use of nutritional selectable markers have not yet been developed. Only two selectable markers are in regular use in *E. festucae*, one of which confers hygromycin resistance, the other of which confers geneticin resistance. While replacements in two genes could be constructed, selectable markers would need to be recycled if more gene replacements were to be performed. The Flp and Cre recombinases have both been used to excise selectable markers from fungal genomes so they can be reused to replace other fungal genes (Fickers et al., 2003; Guldener et al., 1996; Iwaki and Takegawa, 2004; Toh-e, 1995). The Flp and Cre recombinases both catalyse the recombining of DNA at particular target sequences, so if the marker is flanked by these target sequences, the recombinases can effectively excise the marker DNA.

Functional analysis of protease-encoding genes by gene replacement has had mixed success in fungi. In the wood rot fungus *O. piliferum*, deletion of the albin gene encoding the major protease activity produced by the fungus resulted in significant loss of protease activity and reduced growth rates on BSA and on wood (Hoffman and Breuil, 2004b). However, in *F. oxysporum*, deletion of the *prt1* gene, which appeared to be expressed constitutively in low levels both in culture and *in planta*, did not result in any detectable changes in proteolytic activity or in pathogenicity, virulence or host colonisation (Di Pietro et al., 2001). The presence of unrelated enzyme activity can also complicate analysis of the phenotype of strains with deletions. Gene replacements in protease-encoding genes from fungi such as *S. nodorum* and *C. carbonum* have shown

that the presence of multiple protease activities complicates study of the phenotype (Carlile et al., 2000; Murphy and Walton, 1996).

As an alternative approach, an RNAi approach could have been used. It is possible to silence two genes simultaneously using chimeric RNA molecules that form hairpin structures in fungi (Fitzgerald et al., 2004). While this method may be useful for determining the function of two genes simultaneously, the RNAi method has the same limitations of the gene replacement in determining gene function in gene families, especially where there are many family members.

A strategy resulting in increased expression of subtilisin-like protease genes has been successful in identifying the function of subtilisin-like proteases in the interactions of the insect pathogenic fungus *M. anisopliae*, the mycoparasitic fungi *T. harzianum* and *T. virens* and the nematode pathogenic fungus *A. oligospora* (Åhman et al., 2002; Flores et al., 1997; Pozo et al., 2004; St Leger et al., 1996c). Over-expression of genes encoding subtilisin-like proteases in these fungi was clearly detrimental to the host for all of these fungi, indicating these proteases play roles in the pathogenesis or virulence of these fungi toward their hosts.

Over-expression has advantages over the gene replacement and RNAi methods because an increase in activity is being studied, rather than a loss of activity. The phenotype from a loss of activity may be difficult to analyse, as it may be masked by the presence of other related activity that may partially or fully compensate for this loss. However, the phenotype resulting from over-expression is not masked by other similar activities that are present. Although this technique has an advantage over gene replacement in terms of detecting a phenotype, there are some disadvantages. Over-expression of a particular protein may be harmful to cells, which can cause defects in growth or even cell death. In addition, over-expressing a gene may result in abnormal distribution of proteins within the cell. Localisation in a particular subcellular compartment may be required for the normal activity of a protein. If the protein is over-expressed, it might also accumulate in other subcellular compartments where activity may change or be lost.

In light of the results obtained in other functional analyses of proteases, the decision was made to analyse the function of *E. festucae* Fl1 *prt1* and *prt2* in symbioses with perennial ryegrass. The *prt1* and *prt2* coding regions (containing introns) were expressed under the control of the *gpdA* promoter from *A. nidulans* or the *ltmM* promoter from *E. festucae* Fl1 (Section 4.1). The *gpdA* promoter was previously shown to drive constitutive expression of the *uidA* reporter gene *in planta* (Saunders, 1997). The *ltmM* promoter controls expression of a lolitrem biosynthetic gene that is induced and highly expressed during growth *in planta*, but is expressed at very low levels, if at all, in culture (Young et al., 2005).

The copy number of the transgenes inserted into the genome of transformants varied markedly between different strains (Section 4.2). As circular DNA was used for transformation, integration into the *E. festucae* Fl1 genome could occur at any point within the vector DNA. A Southern approach was used to determine how many transgenes had inserted into the *E. festucae* Fl1 genome with the *prt1* or *prt2* coding regions were still intact. The copy number for intact *prt1* or *prt2* transgenes varied widely between the strains. While some transformants contained only one intact copy, others contained more than twenty intact copies.

In culture, RT-PCR analysis showed that the *prt1* and *prt2* genes were expressed under the control of the *gpdA* promoter in strains transformed with either the P*gpdA-prt1* or P*gpdA-prt2* transgenes respectively (Figure 4.7). These analyses were particularly useful for *prt2*, where gene expression had not previously been detected either in culture or *in planta*. The fact that the *prt2* transgene was expressed and spliced to create an mRNA that creates a functional protein suggests *prt2* expression has not been detected due to a strong repressible element in the *prt2* promoter or to a lack of a suitable transcription start site. cDNA sequencing also indicated the intron in the 5' untranslated region of the *gpdA* gene that was fused to the *prt2* gene is spliced out during RNA processing in the same manner as in *A. nidulans* (results not shown).

No expression of the *prt1* or *prt2* genes under control of the *ltmM* promoter was detected in culture. This result was expected because the wild type *ltmM* gene is expressed at either undetectable or detected at very low levels in culture (Young, 2005; Young et al., 2005). However, this analysis may need to be repeated, as one of the primers used in this study, lol107, may anneal within the promoter region rather than in the 5' untranslated region of the *ltmM* gene.

As the *prt1* and *prt2* transgenes were expressed under the control of the *gpdA* promoter in all transformed strains containing these constructs in culture, it was expected the expression of these transgenes would also be detected *in planta*, as the *gpdA* promoter is meant to drive constitutive gene expression. However, no expression was detected for the P*gpdA-prt1* transgene *in planta*, and only two strains expressed the P*gpdA-prt2* transgene *in planta* (Figures 4.8 and 4.9). As the *ltmM* gene is strongly induced in culture, it was also expected that the P*ltmM-prt1* or P*ltmM-prt2* transgenes would be strongly expressed in transformants containing these constructs. However, only three of the P*ltmM-prt1* transformants and one of the P*ltmM-prt2* transformants showed evidence of *prt1* or *prt2* transgene expression.

In these experiments, differences between strains that did or did not express the transgenes *in planta* could not be explained by the number of intact copies. Potentially, the lack of transgene expression in some strains could be explained by two means. Firstly, positional effects could suppress the expression of some of these constructs *in planta*. Transgenes may have inserted in genomic regions where the chromosome is maintained as heterochromatin, and is not available for gene expression. Constructs may also have inserted near regions that suppress the endophyte gene expression during growth *in planta*. Secondly, gene silencing may be taking place in some strains. In *N. crassa*, transgenes are silenced during vegetative growth by a reversible post-transcriptional gene silencing phenomenon called "quelling" (Cogoni et al., 1994; Romano and Macino, 1992). A similar mechanism may have silenced expression of the transgenes introduced during this study.

No significant differences were detected between wild type and transformant strains during growth *in planta* (Section 4.4). The transformant hyphae grew between the host cells with infrequent branching in the same manner as wild type hyphae. Epiphytic hyphae also appeared for both wild type and transformant strains. These results were expected as most of the transformants strains did not express the transgenes *in planta*. However, the analysis of fungal growth *in planta* was very limited, with only the leaf sheath tissues studied. Different hyphal phenotypes may be observed in other host tissues such as meristematic zones, developing inflorescences and leaf blades. None of the associations resulted in stunting of the host grass, a phenotype that has been observed in some other associations (Zhang, 2004).

6.3 FUNCTION OF THE *E. FESTUCAE* FL1 *GCN1* GENE

In mycoparastic fungi, β-1,6-glucanases act synergistically with other enzymes to degrade fungal cell walls. However, related β-1,6-glucanases have also been identified in plant pathogenic fungi such as *F. graminearum* and *S. nodorum*, saprophytic fungi such as *A. nidulans* and also in a *Neotyphodium* sp. grass endophyte. While the role of β-1,6-glucanases in the interaction of mycoparasitic fungi with their hosts is obvious, it is unclear what function these glucanases may have in fungi that do not rely on mycoparasitism. In this study, it was hypothesised that the Gcn1 β-1,6-glucanase played a role in the interaction of *E. festucae* Fl1 with its grass host.

The *gcn1* gene was first identified in the DNA located 3' to the end of the *N. lolii* Lp19 *prt2* gene (Section 3.1.2). Sequencing confirmed that *gcn1* was also located directly downstream of the *prt2* gene in the *E. festucae* Fl1 genome. The major difference in the gene arrangement between the two strains was a 406 bp insertion in the *prt2-gcn1* intergenic region in *E. festucae* Fl1 compared to *N. lolii* Lp19 (Figure 5.1).

The *E. festucae* Fl1 and *N. lolii* Lp19 Gcn1 proteins were 99.3% identical to each other, with three amino acid changes at 76 (Fl1 R>Lp19 M), 248 (Fl1 A>Lp19 C) and 373 (Fl1 Q>Lp19 K) (Figure 5.2). The proteins were also very similar to the β-1,6-glucanase

from *Neotyphodium* sp. FCB2002 (Moy et al., 2002). SignalP3.0 analysis showed that the Gcn1 proteins appear to contain signal peptides of 17 amino acid residues. This corresponds with the predicted signal peptides of the *Neotyphodium* sp. β-1,6-glucanase and the *T. harzianum* BGN16.2 protein. Another feature also conserved with the *T. harzianum* BGN16.2 was the presence of a kexin recognition site (KR) at residues 39-40. The Kex2 cleavage site in *T. harzianum* was confirmed by N-terminal sequencing of secreted BGN16.2, which started at residue 41 of the BGN16.2 preproprotein (Lora et al., 1995). Kexins (such as the enzyme encoded by *kex2*) digest proteins on the carboxyl terminal side of a dibasic peptide motif, such as KR, KK or RR (Henrich et al., 2005). Kexin recognition motifs were conserved in BGN16.2, Bgn3 and the three endophyte β-1,6-glucanases, but not in the VfGlu1 protein (Amey et al., 2003; Kim et al., 2002; Lora et al., 1995). Together, this data suggests the Gcn1 proteins are synthesised as preproproteins. The signal peptide would be removed from the preproprotein by signal peptidase in the endoplasmic reticulum, before a second proteolytic processing mediated by Kex2 in the Golgi body.

All three endophyte β-1,6-glucanases contain the conserved I**E**VLN**E**P catalytic signature, where the glutamic acid residues (shown in bold) are probably critical for catalysis (Lora et al., 1995). Phylogenetic analysis showed that the *E. festucae* Fl1 and *N. lolii* Lp19 Gcn1 proteins were members of glycosyl hydrolase family 5 (Figure 5.3). Other members of glycosyl hydrolase family 5 include the endo-β-1,6-glucanases such as the *Trichoderma* spp. BGN16.2 and Bgn3, exo-β-1,3-glucanases and endo-β-1,4-glucanases.

Expression of the *gcn1* gene was detected at approximately the same levels in culture and *in planta* (Figure 3.38). However, much further analysis needs to be conducted to determine factors regulating expression of the *gcn1* gene. In *Neotyphodium* sp. FCB2002, production of β-1,6-glucanase gene was induced by the β-1,6-glucan pustulan. Analysis of the *prt2-gcn1* intergenic region revealed five CreA binding sites and five Nit2/AreA binding sites. Expression of the related *BGN16.2* gene was repressed by glucose in *T. harzianum*, suggesting that *gcn1* expression could be regulated in a

similar manner. However, the degradation of β-1,6-glucan produces glucose. Lora *et al* (1995) suggested degradation of pustulan by β-1,6-glucanases will produce glucose, which may in turn repress gene expression. No PacC motifs were identified in the *prt2-gcn1* intergenic region, suggesting the *gcn1* gene is not subject to PacC-mediated pH regulation. However, the *prt2-gcn1* intergenic region did contain multiple copies of the STRE element CCCCT, associated with expression under stress conditions in yeast (Peterbauer et al., 2002). Based on these findings, it would be interesting to study the expression of *gcn1* in the presence of pustulan, under carbon limitation and stress conditions.

Homologues of the *gcn1* gene in other fungi are associated with mycoparasitism, with the VfGlu1 and BGN16.2 proteins implicated in antifungal activity. The BGN16.2 protein directly degrades *S. cerevisiae* cell walls, and can act synergistically with other cell wall degrading enzymes such as chitinases to degrade the cell walls of filamentous fungi (De la Cruz et al., 1995). The BGN16.2 protein also inhibits growth of *B. cinerea* and *G. fujikuroi*. Deletion of *VfGlu1* reduced *V. fungicola* growth on chitin, and reduced chitinase activity (Amey et al., 2003). It is unclear why deletion of the *VfGlu1*, encoding a putative β-1,6-glucanase, affects growth on chitin, a polymer of β-1,4-linked *N*-acetyl-D-glucosamine. However, the synergistic action of BGN16.2 with chitinase (De la Cruz et al., 1995), may suggest that the VfGlu1 protein could degrade the β-1,6-glucan attached to chitin in the fungal cell wall, thus making the remaining chitin polymer easier to access for chitinases.

This study represents the first attempt to characterise the function of a putative β-1,6-glucanase from a fungus that is not mycoparasitic. In order to characterise the role of the *gcn1* gene in fungal growth in culture and during grass infection, the *gcn1* gene was replaced by an *hph* cassette conferring hygromycin resistance (Section 5.2). The rate of gene replacement by homologous recombination was relatively high, with 10% of transformants screened containing a gene replacement. The use of large 2.8 kb flanking fragments probably contributed to the high efficiency of homologous recombination.

Southern blotting confirmed that two transformants contained one copy of the *gcn1*::*hph* construct that had replaced the wild type *gcn1* gene.

E. festucae Fl1 Δ*gcn1* strains were indistinguishable from wild type and ectopic *gcn1*::*hph* strains when grown on a complex media such as potato dextrose agar (PDA) or on a media containing glucose (Section 5.2.2). However, when grown on plates containing the β-1,6-glucan pustulan, clear differences in growth were seen between the Δ*gcn1* strains and the wild type and ectopic *gcn1*::*hph* strains. Although the Δ*gcn1* colonies were a similar diameter, they lacked the aerial hyphae seen in the wild type and ectopic strains. The submerged hyphae that are present for the Δ*gcn1* strain are sparsely distributed. Deletion of the *gcn1* gene also led to the loss of the major β-1,6-glucanase activity produced during growth on pustulan. Both Δ*gcn1* strains grown on pustulan did not produce the large halo of degraded β-1,6-glucan identified by Congo red staining for the wild type and ectopic strains.

A possible explanation for the lack of aerial hyphae in Δ*gcn1* strains may be that in these colonies, vegetative hyphae could not differentiate to form aerial hyphae due to a lack of available carbon during growth on pustulan. However, in other fungal species, carbon starvation is known to lead to the production of aerial hyphae and conidia. However, the induction of conidiation by carbon starvation in *E. festucae* Fl1 has not been studied. The media used in this study did contain 0.1% yeast extract, which probably provided some carbon to support fungal growth.

Some residual β-1,6-glucanase activity that is unrelated to Gcn1 may still be present in the endophyte. In the fungus *T. harzianum*, three different unrelated β-1,6-glucanase activities have been identified. However, of these three activities, BGN16.2 (the *T. harzianum* homologue of Gcn1) is the most effective at degrading pustulan. The possibility of residual β-1,6-glucanase activity in the Δ*gcn1* strain is supported by the presence of a hydrolytic halo around the Δ*gcn1* strains that have been incubated on pustulan for a prolonged time. The residual β-1,6-glucanase activity may still degrade pustulan to support fungal growth.

Further work is needed to confirm the source of any residual β-1,6-glucanase activity in the Δ*gcn1* strains. Two approaches could be used to determine this: a protein activity approach, or a gene expression approach. If extracellular proteins were collected from the culture supernatant during growth on pustulan and separated using SDS-PAGE, β-1,6-glucanase activity can be determined by incubation with a replica gel containing pustulan following renaturing of the proteins in the polyacrylamide gel (Soler et al., 1999). A more sensitive method to detect activity was also suggested by Soler et al (1999), with the incubation of extracellular proteins separated by isoelectric focusing (IEF) with solubilised pustulan followed by detection of released reduced sugars with 2,3,5-triphenyltetrazolium chloride. These protein-based methods should ensure all β-1,6-glucanases induced during growth on pustulan are detected.

Of the three known β-1,6-glucanases, DNA and protein sequences are currently only available for the *BGN16.2* and for two of the *BGN16.3* (known as P1 and P2 respectively) genes (Lora et al., 1995; Montero et al., 2005). To date, no sequence is available for the BGN16.1 gene, which encodes a basic β-1,6-glucanase (de la Cruz and Llobell, 1999). A degenerate PCR approach based on the BGN16.3-encoding P1 and P2 genes and related genes such as *N. crassa negl* could be used to identify if a related gene is present in the *E. festucae* Fl1 genome. RT-PCR could be used to identify if a gene encoding a glycosyl hydrolase family 30 β-1,6-glucanase was expressed in both the wild type and Δ*gcn1* strains during growth on pustulan.

Complementation of the Δ*gcn1* phenotype by the wild type or ectopic strains was seen in some instances (Section 5.2.2). However, complementation was only detected after prolonged growth when Δ*gcn1* hyphae were grown in very close proximity to the wild type or ectopic strains. Near the interface between the colonies, Δ*gcn1* colonies produced some aerial hyphae, although not at the level of the wild type strain. On the other side of the Δ*gcn1* colony, where hyphae were not in close proximity to wild type or ectopic strains, no complementation of the Δ*gcn1* phenotype was observed.

To confirm the phenotype of the *gcn1* strains was solely due to deletion of the *gcn1* gene, genetic complementation of the MM20.15 Δ*gcn1* strain was performed (Section 5.3). The Δ*gcn1* strain was co-transformed with pMM44, which contains the complete *gcn1* gene and the 5' region of the *cyc1* gene, and pII99, which contains the *nptII* gene that confers geneticin resistance. Transformants were screened by PCR and for complementation of the Δ*gcn1* growth defect on pustulan plates. Co-transformation with pMM44 and pII99 restored β-1,6-glucanase activity and the Δ*gcn1* growth defect on pustulan plates for 19 of the 20 transformants analysed. The phenotype of the geneticin-resistant complemented strains grown on pustulan varied, with phenotypes ranging from small dense colonies with large halos of pustulan degradation to a phenotype that resembled wild type, with only a moderate zone of pustulan degradation. The one geneticin-resistant strain tested that did not degrade pustulan showed a similar phenotype to the Δ*gcn1* strain, with a lack of aerial hyphae and a much larger colony diameter.

The differences seen between the pustulan degrading complemented strains could be due to a number of factors. Firstly, it should be noted that the copy number of the constructs inserted into each strain has not been determined. Therefore, differences in phenotype between the complemented strains could be due to a variation in *gcn1* copy number. However, the integration sites of the pMM44 plasmid in the *E. festucae* genome may affect *gcn1* expression.

Complemented strains where pustulan hydrolysis was detected early (i.e. after 2 days) and that produced large hydrolytic zones tended to produce quite small, dense colonies with many aerial hyphae. Potentially, two explanations could explain this phenotype. Firstly, the overproduction of glucanase may be detrimental to fungal cell wall formation, which could reduce growth rate and colony size. However, the dense and small colonies for these strains were similar to colonies grown in glucose, which could suggest the availability of glucose affects colony morphology of the *E. festucae* Fl1. Strains over expressing glucanases will break down more pustulan into glucose, so the compact colony morphology could be due to increased glucose

availability. In *S. cerevisiae, S. pombe* and *A. nidulans*, glucose activates the cAMP-PKA signalling pathway (Hoffman, 2005; Lafon et al., 2005; Thevelein et al., 2005). Activation of the cAMP signalling pathway by addition of exogenous cAMP in *A. niger* (Oliver et al., 2002) results in a reduction in radial growth that is similar to that observed for strains overproducing Gcn1. This may suggest that when these strains are grown on pustulan, they degrade more pustulan to produce higher glucose levels than wild type strains. These high levels of glucose could increase the levels of cAMP, resulting in activation of the cAMP pathway, which may in turn inhibit radial growth.

Secondly, the phenotype of these strains could be affected by altered expression of the 5' region of the *cyc1* gene. As the Cyc1 protein is thought to be a part of the CTD kinase that affects RNA polymerase, potentially an altered Cyc1 protein could affect the CTD kinase complex, potentially affecting gene expression within the organism.

Strains over expressing the *gcn1* gene may also be more effective at inhibiting the growth of phytopathogenic strains compared to wild type or Δ*gcn1* strains. Although the *gcn1* gene is expressed in culture and *in planta*, higher levels of *gcn1* expression may be induced by the presence of β-1,6-glucan (Moy et al., 2002). This might suggest that in the presence of fungal cell walls containing β-1,6-glucan, the *gcn1* gene could be induced at higher levels in some of the complemented strains than in wild type strains. Growth inhibition studies with strains with high levels of *gcn1* expression could potentially provide an insight into the role of β-1,6-glucanase activity against other fungal species.

The phenotype of endophyte hyphae during grass infection for the Δ*gcn1* strains was compared with that of wild type *E. festucae* Fl1 and the ectopic Δ*gcn1*::*hph* strains. No differences in hyphal growth were observed between the strains. However, the analysis was only conducted in epidermal peels of infected grass leaf sheaths. Phenotypic differences between the Δ*gcn1* and wild type strains may be observed in other infected plant tissues, such as the meristematic zone, leaf blade or developing and mature inflorescences. As no phenotypic differences in colony morphology were observed

between Δ*gcn1* and wild type strains when colonies were grown in PD agar or media containing glucose, perhaps no phenotypic differences should be expected between the Δ*gcn1* and wild type strains during growth *in planta*. In previous studies of the phloem sap of the grass *L. perenne*, the major carbohydrate identified was sucrose (Amiard et al., 2004). The endophyte tends to be at highest concentrations in grass sink tissues *i.e.* where phloem unloading takes place. Based on this, it is expected the endophyte would grow in an environment where sucrose is the major available carbon source. In this environment, the hyphal growth of Δ*gcn1* and wild type strains should be similar.

The phenotype of strains over expressing *gcn1* has not yet been determined *in planta*. However, it may be interesting to determine if these strains still grow normally *in planta*. In culture, strains overproducing the Gcn1 protein did not appear to grow differently in the complex PD agar medium. Based on these results in culture, it may be that no difference is seen in the phenotype of the *gcn1* over expressing strains in planta. However, phenotypic differences between the Δ*gcn1*, wild type and *gcn1* over expressing strains may be observed when symbiota are challenged by phytopathogenic fungi that contain β-1, 6-glucan in their cell walls. One means of assessing the possible induction of *gcn1 in planta* in response to attack of the host by phytopathogenic fungi could be to involve the use of symbiota containing *E. festucae* Fl1 transformed with a P*gcn1-uidA* reporter gene construct.

The *E. festucae* Δ*gcn1* strain created in this study is a valuable tool in assessing the function of β-1,6-glucanases in fungi that are not mycoparasitic. However, further experiments must be carried out to analyse the role of the *gcn1* gene during growth *in planta*. In order to conduct these studies, the phenotype of the Δ*gcn1* endophyte hyphae must be analysed throughout the symbiota life cycle (as described in Figure 1.1). Expression of the *gcn1* gene in different host tissues is currently being analysed in symbiota with fungal transformants containing the P*gcn1-uidA* reporter construct (May and Bryant, unpublished results). The effect of *gcn1* deletion or over-expression on the interaction of the symbiota with other fungi remains to be determined.

APPENDIX

A1: Restriction maps

Appendix A1.1 Vectors for general use

A1.1.1 pFunGus

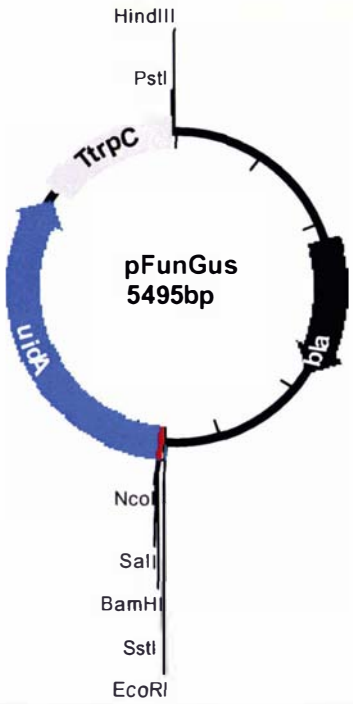

A1.1.2 pAN7-1

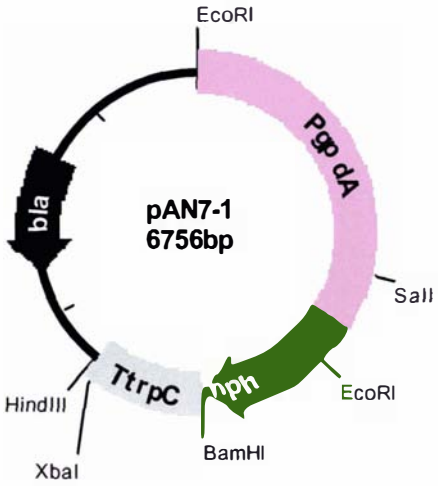

Appendix A1.1 Vectors for general use

A1.1.3 phGFP2

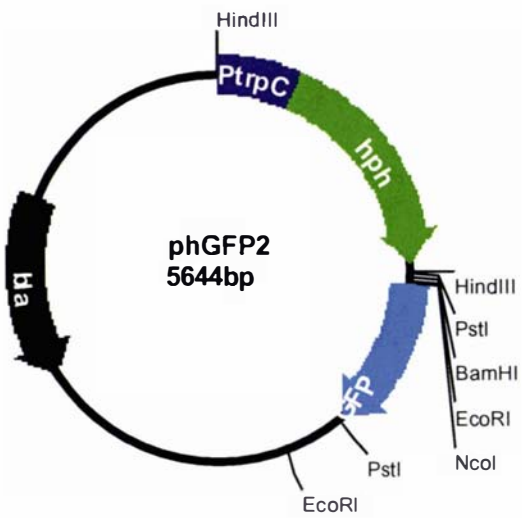

A1.1.4 pII99

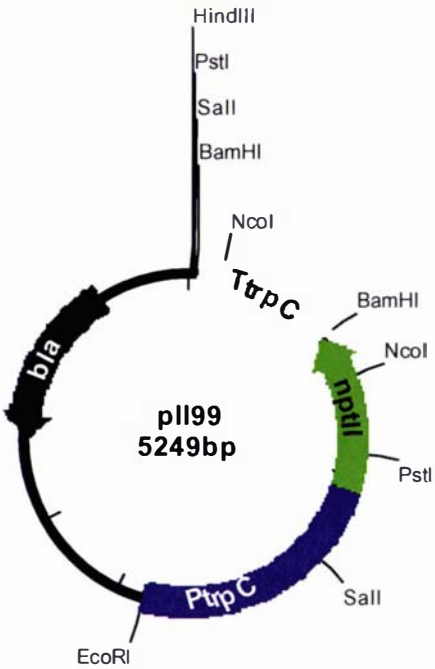

Appendix A1.1 Vectors for general use

A1.1.5 pPN1688

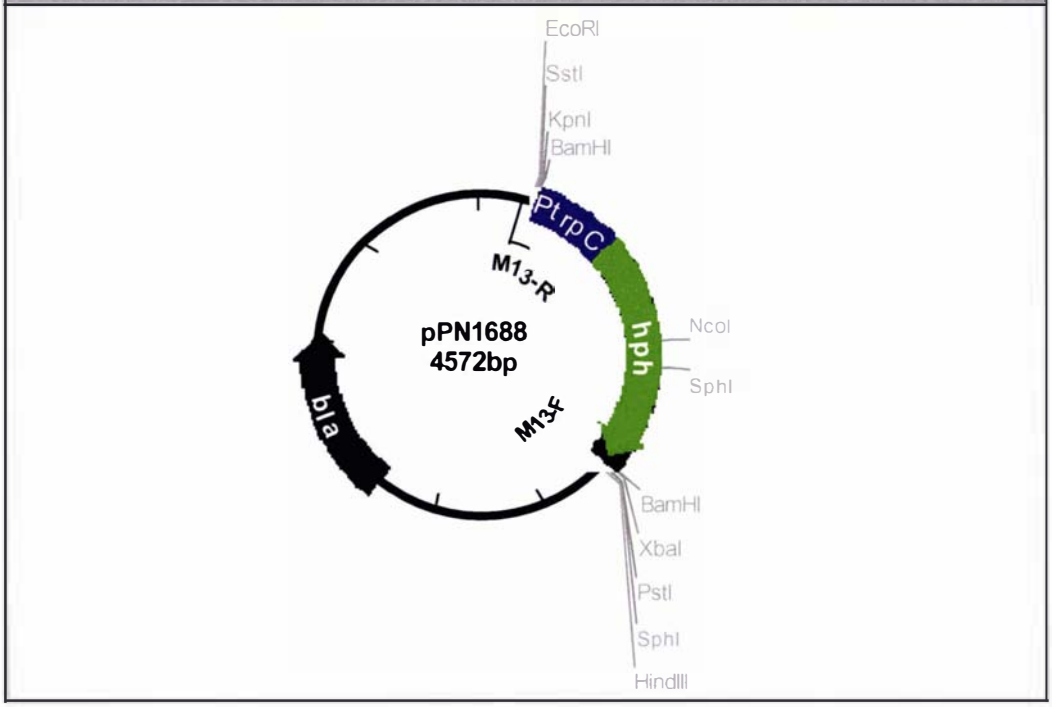

A1.1.6 pUC118

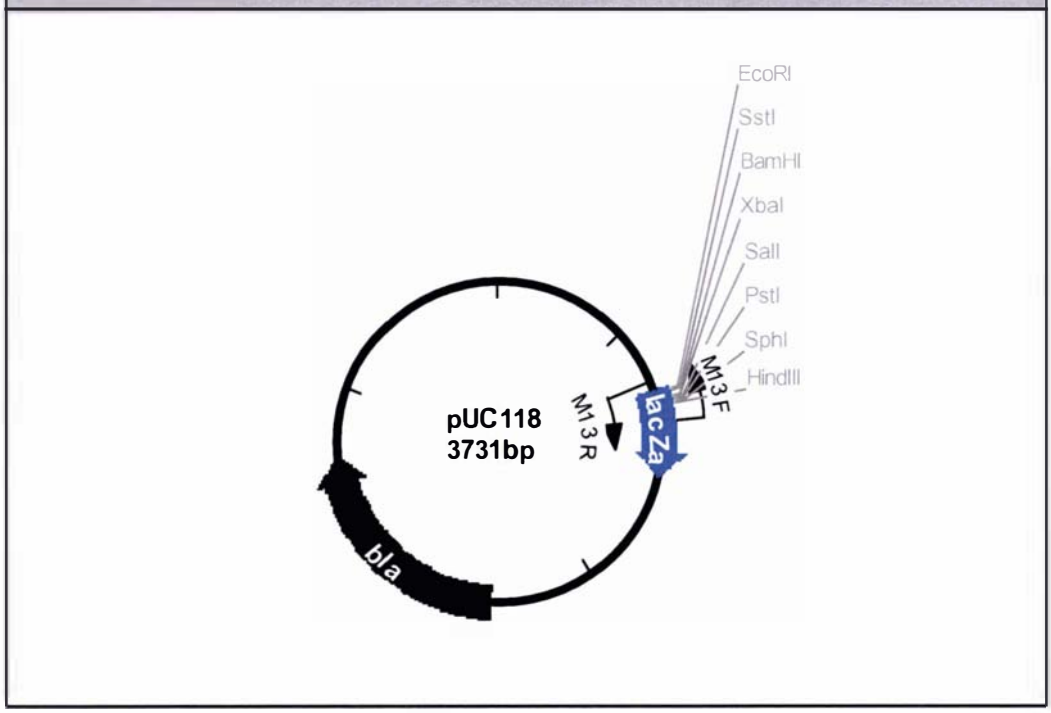

Appendix A1.1 Vectors for general use

A1.1.7 pXZ56

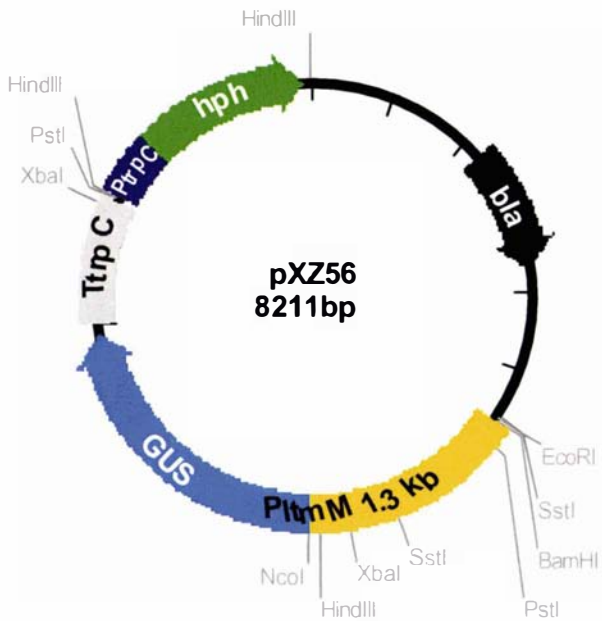

A1.1.8 pGEM-T Easy

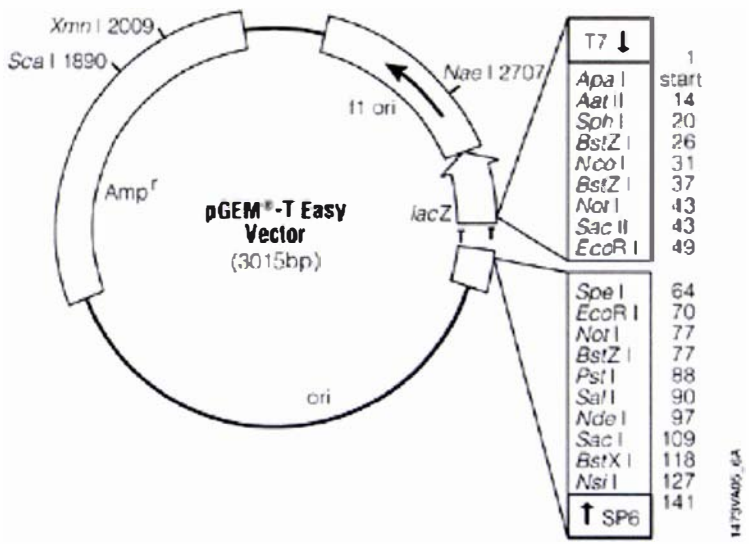

Appendix A1.2 *prt*1 vectors

A1.2.1 pMM2

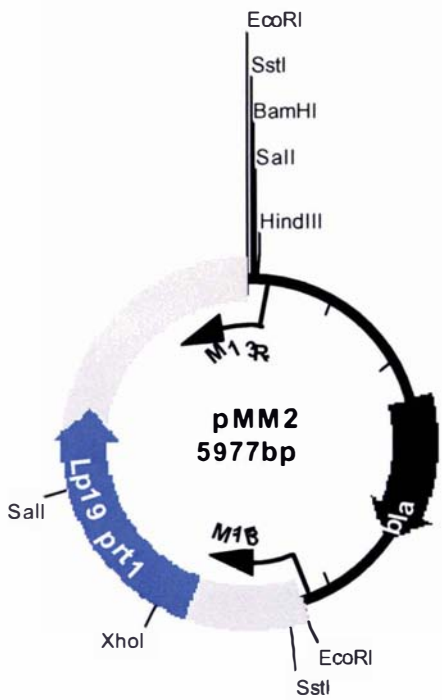

A1.2.2 pMM3

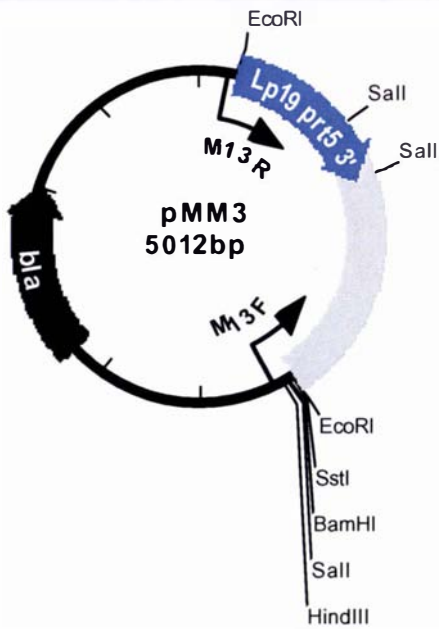

Appendix A1.2 *prt*1 vectors

A1.2.3 pMM4

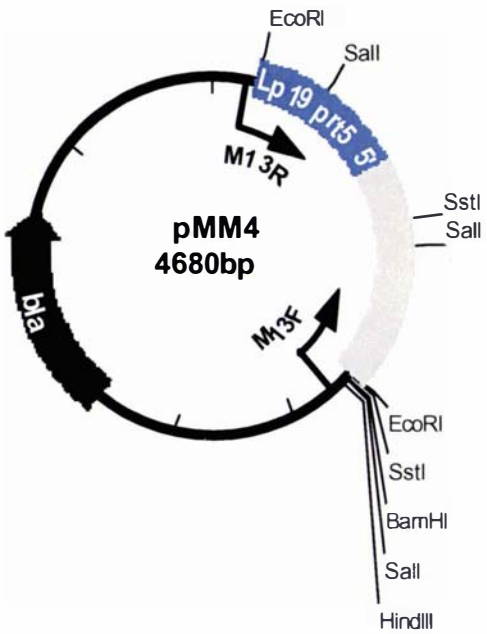

A1.2.4 pMM51

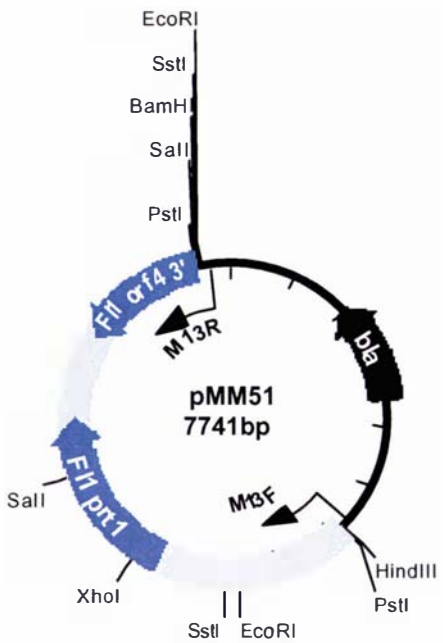

Appendix A1.3 *prt2* vectors

A1.3.1 pMM7

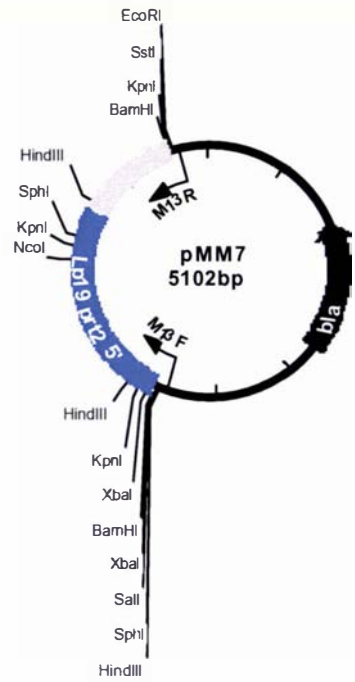

A1.3.2 pMM44

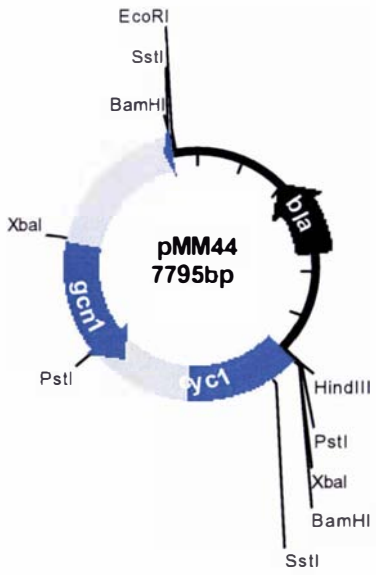

Appendix A1.4 *kex2* vectors

A1.4.1 pMM65

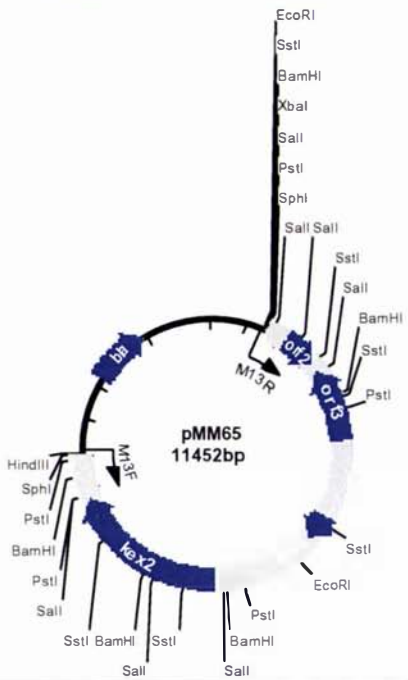

Appendix A1.5 Other genomic sequences

A1.5.1 Ltm cluster 1 from *E. festucae* Fl1

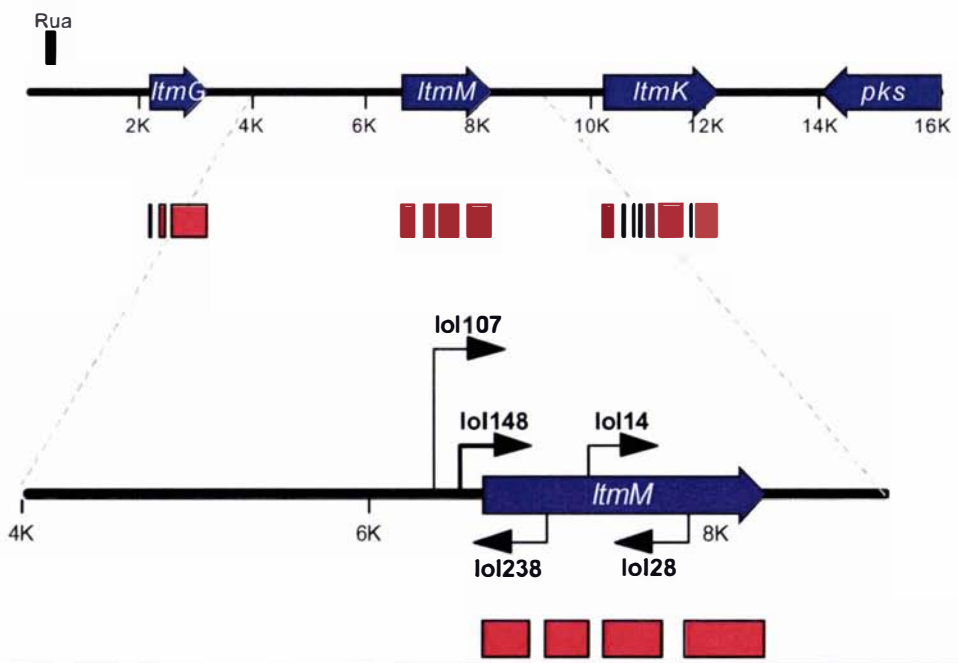

Appendix A1.5 Other genomic sequences

A1.5.2 The *E. festucae* Fl1 *tub2 gene*

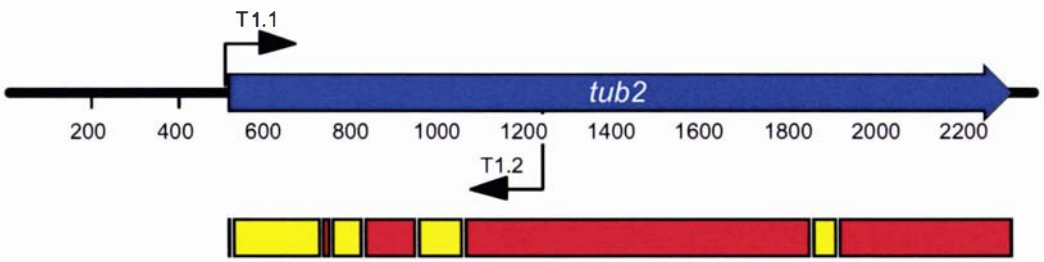

A1.5.3 The *A. nidulans gpdA* gene

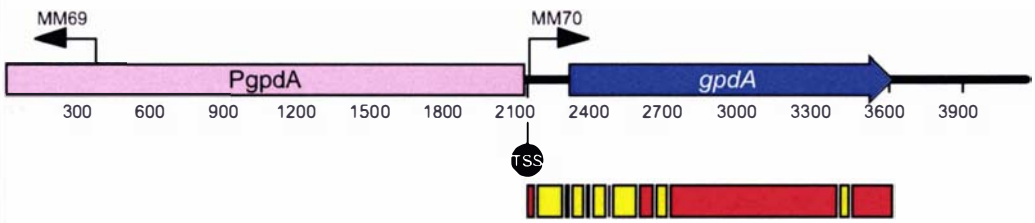

APPENDIX

A2: Comparison of *E. festucae* and *N. lolii* sequences

A2.1 Comparison of the *E. festucae* Fl1 and *N. lolii* Lp19 *prt5* and *prt1* sequences

Alignment of the nucleotide sequences of the *E. festucae* Fl1 and *N. lolii* Lp19 *prt5* and *prt1* sequences. Non-coding sequences such as intergenic sequences and introns are shown in lower case letters. Coding sequences are shown in upper case letters. Identity between *E. festucae* Fl1 and *N. lolii* Lp19 in intergenic sequences, coding sequences and introns is indicated by grey, black and yellow shading respectively. The positions of the translation initiation and termination codons of the genes are identified by green and red boxed arrows respectively. Exons and introns are labelled at the beginning of the relevant sequence by green and yellow boxes respectively. The $(YTT)_4(YA)_{13}$ minisatellite is indicated by dark green shading. The Lp19 minisatellite sequence is indicated by a green border. Red borders indicate direct repeats surrounding the Lp19 minisatellite sequence.

```
Lp19      1  gatctgcaaaaggaggcccgttatcatgaattgcacagccaatcagcaatgcacctttg   59
Fl1     841  cgatctgcaaaaggaggcccgttatcatgaattgcacagccaatcagcaatgcacctttg  900

Lp19     60  gcgctccccaacggcctcggggagtttccgagcttcttcgtgtatcgacttatctattcg  119
Fl1     901  gcgctccccaacggcctcggggagtttccgagcttcttcgtgtatcgacttatctattcg  960

Lp19    120  cagcctgtccaatggcaaattcaatccatcatcgccttgttgcctgccgacaaatcttcc  179
Fl1     961  cagcctgtccaatggcaaattcaatccatcatcgccttgttgcctgccgacaaatcttcc 1020

Lp19    180  atcaactcggcaagcaagcagagtctcgtgaactcgtgagaacaggggataggagacagg  239
Fl1    1021  atcaactcggcaagcaagaagagtctcgtgaactcgtgagaacaggggataggagacagg 1080

Lp19    240  gaacagaacagggaacaggggacagggacaagggacagggtctccgggacctttgacg  299
Fl1    1081  gaacagaacagggaacaggggacagaggacaggggacagggtctccgggacctttgacg 1140

Lp19    300  cggctggttgtccatggcgattgctccctcccctcctgggtctagcctcgtttagggagg  359
Fl1    1141  cggctggttgtcgatggcgattgctccctcccctcctgggtctagcctcgtttagggagg 1200

Lp19    360  taatggtcatccggggccatgttgtaggcaatgtaggcaatcacgcaatgtaggcgacgc  419
Fl1    1201  taatggtcatccggggccatgttgtaggcaatgtaggcaatcacgcaatgtaggcgacgc 1260

Lp19    420  ccccgcgacacggccgagaagaacgcatgttatcgtacgtgtgggtgcacgcggacaaga  479
Fl1    1261  ccccgcgacacggccgagaagaacgcatgttatcgtacgtgtgggtgcacgcggacaaga 1320

Lp19    480  ttgccgttgatctgcgcctaaccgtctggttcagggaggagtccggaggacaacgagatt  539
Fl1    1321  ttgccgttgatctgcgcctaaccgtctggttcagggaggagtccggaggacaacgagatt 1380

Lp19    540  gctggccaaatcacctgccaattgtcgacgaactcgacacggcgccggactgcaatgtaa  599
Fl1    1381  gctggccaaatcacctgccaattgtcgacgaactcgacacggcgccggactgcaatgtaa 1440

Lp19    600  tcttgggtctgggttgccaacttgctagtaacctaccagtaccgacgacggaacggtggg  659
Fl1    1441  tcttgggtctgggttgccaacttgctagtaacctaccagtaccgacgacggaacggtggg 1500

Lp19    660  agctcgacaaagtcaccggcttggaagtcctgctttcgacgaggcacttggcaggcaaac  719
Fl1    1501  agctcgacaaagtcaccggcttggaagtcctgctttcgacgaggcacttggcaggcaaac 1560

Lp19    720  ttggatcaaggccagaaagataaatagattggccttctcccgcccagcatcatggaaaga  779
Fl1    1561  ttggatcaaggccagaaagataaatagattggccttctcccgcccagcatcatggaaaga 1620

Lp19    780  aattggattccaaggcgcttcatccccatcatttttcccatctcgcttatctcgcccatc  839
Fl1    1621  aattggattccaaggcgcttcatccccatcattcttcccatctcgcttatctcgcccatc 1680

Lp19    840  ttgcacacatacacgacccagaacaaggtccagaaacttctttccaagttaccaaatcgc  899
Fl1    1681  ttgcacacatagacgacccagaacaaggtccagaaacttctttccaagttaccaaatcgc 1740

                prt5 exon 1
                Prt5 start
Lp19    900  aaacATGAAGGTCTCGGCTCTTCTCGCTCTTCTCCCCCTTCTCCCCGTGGCCGTGGCCGC  959
Fl1    1741  aaacATGAAGGTCTCGGCTCTTCTCGCTCTTCTCCCCCTTCTCCCCGTGGCCGTGGCCGC 1800
```

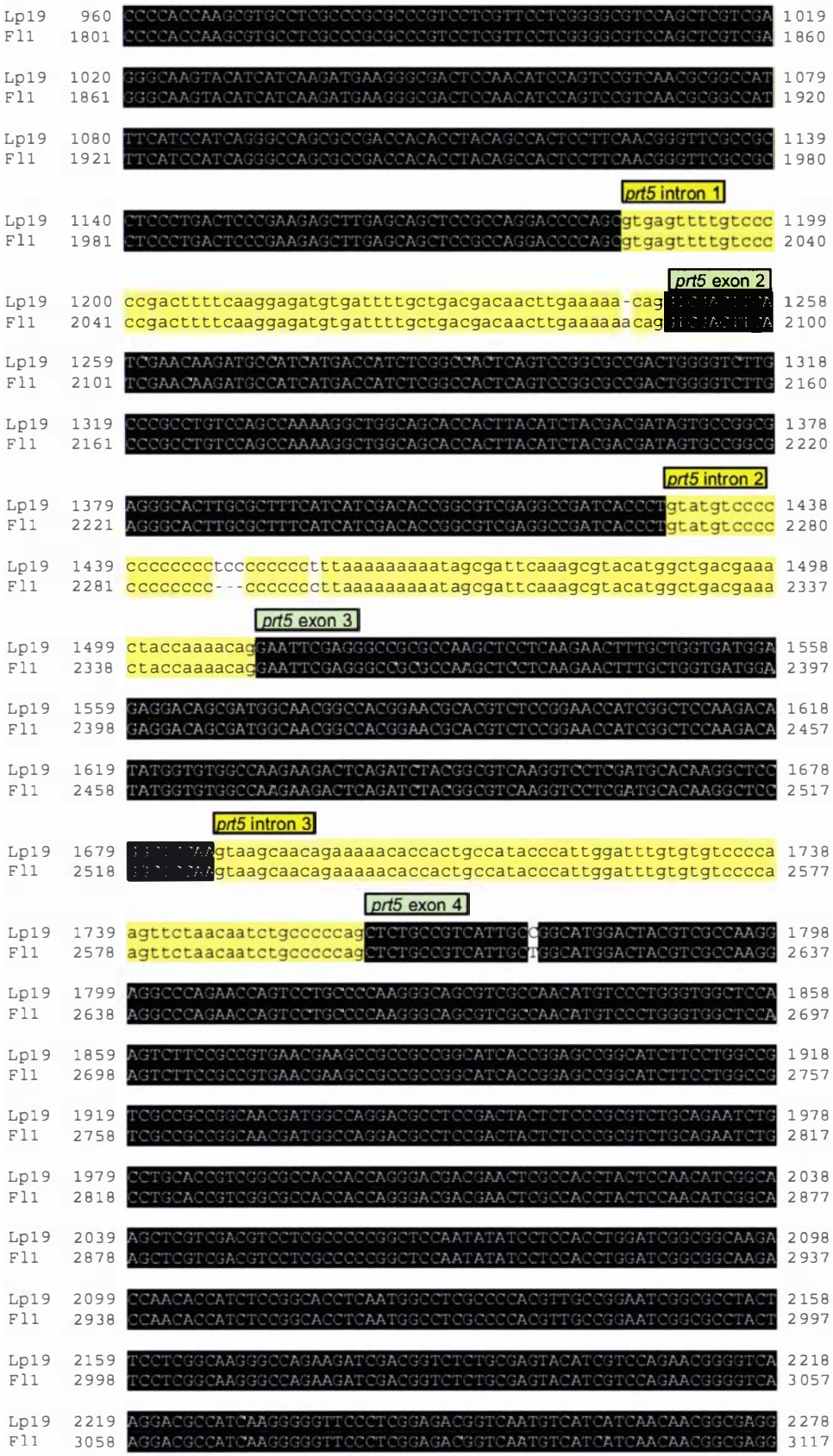
prt5 intron 1
prt5 exon 2
prt5 intron 2
prt5 exon 3
prt5 intron 3
prt5 exon 4

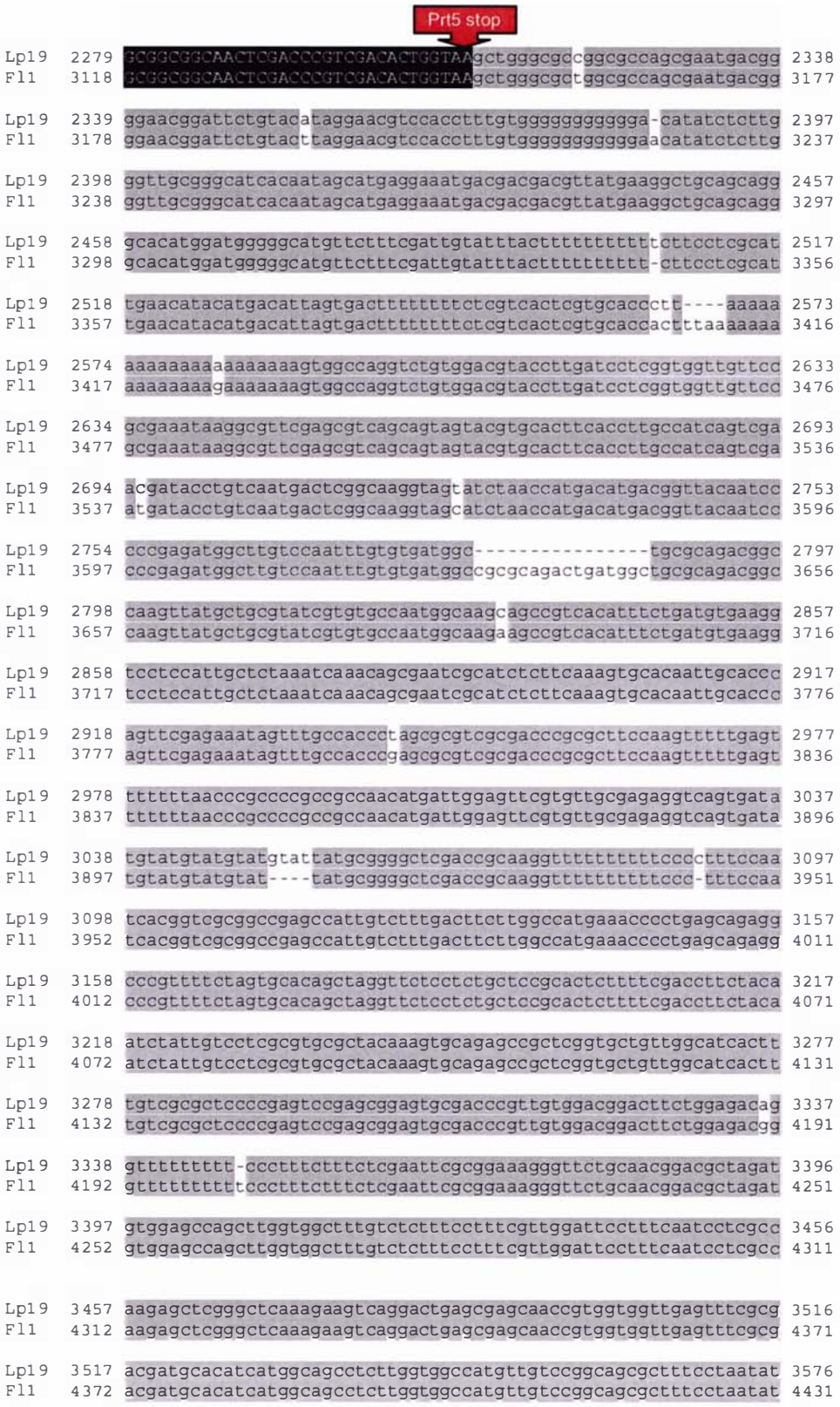
Prt5 stop
Lp19 2279 GCGGCGGCAACTCGACCCGTCGACACTGGTAAgctgggcgccggcgccagcgaatgacgg 2338
Fl1 3118 GCGGCGGCAACTCGACCCGTCGACACTGGTAAgctgggcgctggcgccagcgaatgacgg 3177
Lp19 2339 ggaacggattctgtacataggaacgtccacctttgtgggggggggga-catatctcttg 2397
Fl1 3178 ggaacggattctgtacttaggaacgtccacctttgtgggggggggggaacatatctcttg 3237
Lp19 2398 ggttgcgggcatcacaatagcatgaggaaatgacgacgacgttatgaaggctgcagcagg 2457
Fl1 3238 ggttgcgggcatcacaatagcatgaggaaatgacgacgacgttatgaaggctgcagcagg 3297
Lp19 2458 gcacatggatgggggcatgttctttcgattgtatttacttttttttttcttcctcgcat 2517
Fl1 3298 gcacatggatgggggcatgttctttcgattgtatttacttttttttt-cttcctcgcat 3356
Lp19 2518 tgaacatacatgacattagtgactttttttctcgtcactcgtgcacccctt----aaaaa 2573
Fl1 3357 tgaacatacatgacattagtgactttttttctcgtcactcgtgcaccacttaaaaaaa 3416
Lp19 2574 aaaaaaaaaaaaaaaagtggccaggtctgtggacgtaccttgatcctcggtggttgttcc 2633
Fl1 3417 aaaaaaaaagaaaaaaagtggccaggtctgtggacgtaccttgatcctcggtggttgttcc 3476
Lp19 2634 gcgaaataaggcgttcgagcgtcagcagtagtacgtgcacttcaccttgccatcagtcga 2693
Fl1 3477 gcgaaataaggcgttcgagcgtcagcagtagtacgtgcacttcaccttgccatcagtcga 3536
Lp19 2694 acgatacctgtcaatgactcggcaaggtagtatctaaccatgacatgacggttacaatcc 2753
Fl1 3537 atgatacctgtcaatgactcggcaaggtagcatctaaccatgacatgacggttacaatcc 3596
Lp19 2754 cccgagatggcttgtccaatttgtgtgatggc----------------tgcgcagacggc 2797
Fl1 3597 cccgagatggcttgtccaatttgtgtgatggccgcgcagactgatggctgcgcagacggc 3656
Lp19 2798 caagttatgctgcgtatcgtgtgccaatggcaagcagccgtcacatttctgatgtgaagg 2857
Fl1 3657 caagttatgctgcgtatcgtgtgccaatggcaagaagccgtcacatttctgatgtgaagg 3716
Lp19 2858 tcctccattgctctaaatcaaacagcgaatcgcatctcttcaaagtgcacaattgcaccc 2917
Fl1 3717 tcctccattgctctaaatcaaacagcgaatcgcatctcttcaaagtgcacaattgcaccc 3776
Lp19 2918 agttcgagaaatagtttgccacccgagcgcgtcgcgacccgcgcttccaagtttttgagt 2977
Fl1 3777 agttcgagaaatagtttgccacccgagcgcgtcgcgacccgcgcttccaagtttttgagt 3836
Lp19 2978 ttttttaacccgccccgccgccaacatgattggagttcgtgttgcgagaggtcagtgata 3037
Fl1 3837 ttttttaacccgccccgccgccaacatgattggagttcgtgttgcgagaggtcagtgata 3896
Lp19 3038 tgtatgtatgtatgtattatgcggggctcgaccgcaaggttttttttttcccctttccaa 3097
Fl1 3897 tgtatgtatgtat----tatgcggggctcgaccgcaaggttttttttttccc-tttccaa 3951
Lp19 3098 tcacggtcgcggccgagccattgtctttgacttcttggccatgaaacccctgagcagagg 3157
Fl1 3952 tcacggtcgcggccgagccattgtctttgacttcttggccatgaaacccctgagcagagg 4011
Lp19 3158 cccgttttctagtgcacagctaggttctcctctgctccgcactcttttcgaccttctaca 3217
Fl1 4012 cccgttttctagtgcacagctaggttctcctctgctccgcactcttttcgaccttctaca 4071
Lp19 3218 atctattgtcctcgcgtgcgctacaaagtgcagagccgctcggtgctgttggcatcactt 3277
Fl1 4072 atctattgtcctcgcgtgcgctacaaagtgcagagccgctcggtgctgttggcatcactt 4131
Lp19 3278 tgtcgcgctccccgagtccgagcggagtgcgacccgttgtggacggacttctggagacag 3337
Fl1 4132 tgtcgcgctccccgagtccgagcggagtgcgacccgttgtggacggacttctggagacgg 4191
Lp19 3338 gttttttttt-ccctttctttctcgaattcgcggaaagggttctgcaacggacgctagat 3396
Fl1 4192 gttttttttttccctttctttctcgaattcgcggaaagggttctgcaacggacgctagat 4251
Lp19 3397 gtggagccagcttggtggctttgtctctttcctttcgttggattcctttcaatcctcgcc 3456
Fl1 4252 gtggagccagcttggtggctttgtctctttcctttcgttggattcctttcaatcctcgcc 4311
Lp19 3457 aagagctcgggctcaaagaagtcaggactgagcgagcaaccgtggtggttgagtttcgcg 3516
Fl1 4312 aagagctcgggctcaaagaagtcaggactgagcgagcaaccgtggtggttgagtttcgcg 4371
Lp19 3517 acgatgcacatcatggcagcctcttggtggccatgttgtccggcagcgctttcctaatat 3576
Fl1 4372 acgatgcacatcatggcagcctcttggtggccatgttgtccggcagcgctttcctaatat 4431


prt1 exon 1
Prt1 start
prt1 intron 1
prt1 exon 2

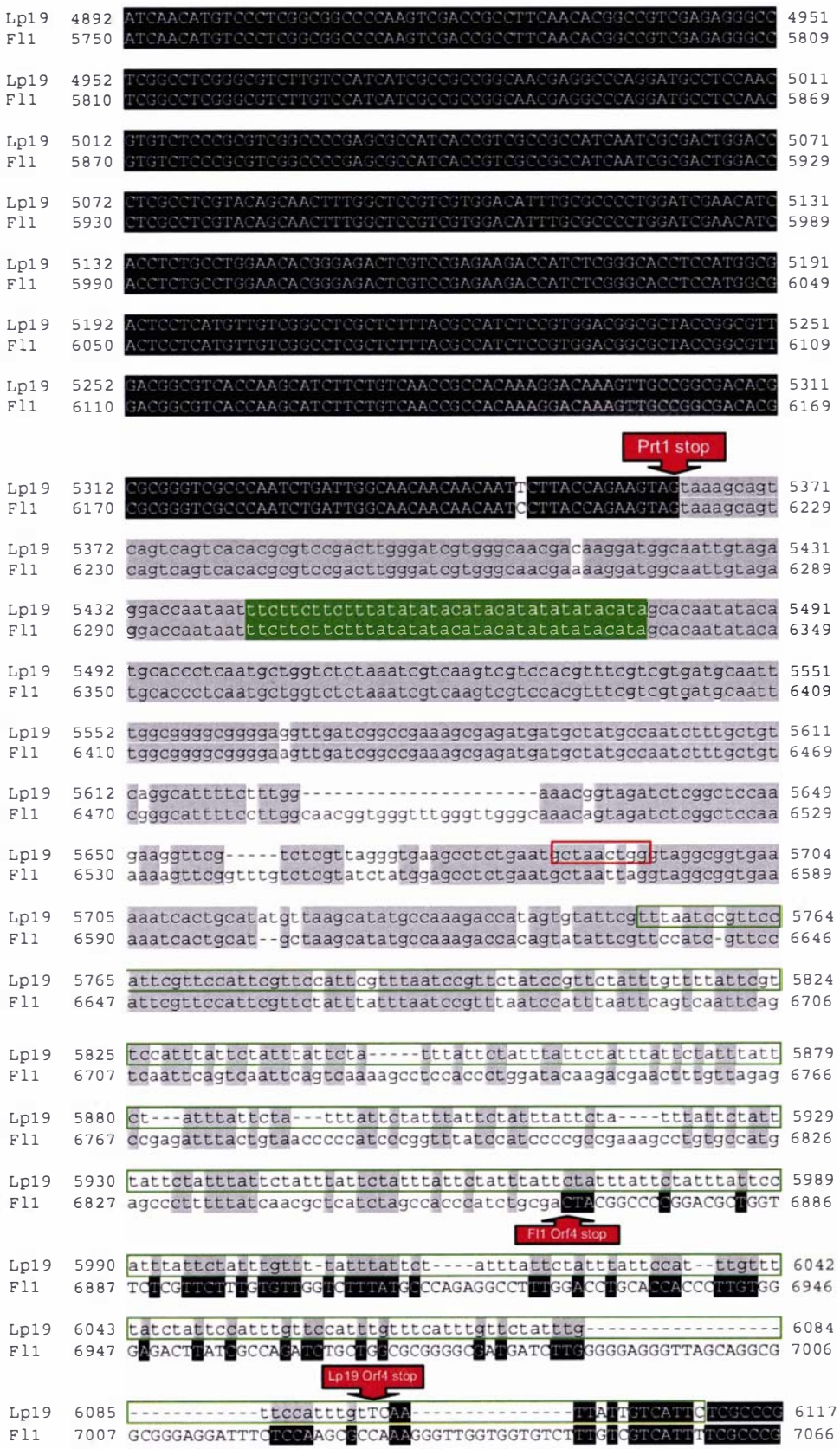
Prt1 stop
Fl1 Orf4 stop
Lp19 Orf4 stop


Lp19 6118 GAGGAACCTGGCCAGTGGGGACCTGTGACACCCACTCCGCAACGCTAACTGGCACTTCTT 6177
Fl1 7067 GAGGAACCTGGCCAGTGGGGACCTGCGACACCCACTCCGCAACGCTAACTGGCACTTCTT 7126
Lp19 6178 GTTGAGCTAAAAGCTGGTCCATTTGGTGGTCATGGCGAGACTCGTCGGTAGGCTCAGCAC 6237
Fl1 7127 GTTGAGCTAAAATTTGGTCCATTTGG---TCATGACGAGACTCGTCGGTAGGCTCAGCAC 7183
Lp19 6238 CGCCAGACATAGCAGCTAGTTGTACTAGAGCCCACTGAATTTTTATGACAGTGATGAATT 6297
Fl1 7184 CGCCTGACATAGCAGCTAGTTGTACCAAAGCCCACTGAAGTTTTATGACAGTGATGAATT 7243
Lp19 6298 TGGGCGCGTCGATTTCATCCAGAGCCACGTCAAAAGTCTGGCCTGATAAGATTGGCCGGT 6357
Fl1 7244 TAGGTGCGTCGATATCATCCAGCGTCACGTCAAAAGTCTGGCCTGATAAGATTGGCCGGT 7303
Lp19 6358 TAGATGGGCACACGTTAGCTGCCACAGCAGGTTGAGGCGCCTCGAATAGCTTAGCTCGGA 6417
Fl1 7304 TAGATGGGCACATGTTGGCTGCCACAGCAGGTTGAGGCGCCTCGAATAGCTTAGCTCGGA 7363
Lp19 6418 AACCATGCTGCTGTTGCTGATTGAGAGTATCGGTCGCCTTGGAGTGCTTGTTCTGCTTCA 6477
Fl1 7364 AATCATGCTGCTGTTGCTGATTGAGAGTGTCGGTCGCCTTGGAGTGCTGTTCTGCTTCA 7423
Lp19 6478 GCCAGCGAAATTCGAGCGTGACGATTACCTTAATCTGAGCGTTATCAGACTGAAAGGCA 6537
Fl1 7424 GCCAGCGAAATTCGAGTGTAACTGTTACCTTGCTCTGAGCGTTATTAGACTCAGAAGGCA 7483
Lp19 6538 TTGAGCCCAGATATTTTAGGCCAAAGTAGGCCTTGCCCCACCACGTATGAAGCGATGCGC 6597
Fl1 7484 TTGAGCCTAGATATTTGAGGCCAAAGTAGGCCTTGCCCCACCACGTATGAAGCGATGGGC 7543
Lp19 6598 TCAGACAAATCATATTCCATGACTTATCCAAATTGCCAGATACAAAACCGGCGCGAATTC 6657
Fl1 7544 TCAGACAAATCATATTCCATGACTTATCCGAATTGCCAGACATCAATTCGACTCGTATGT 7603

A2.2 Comparison of the *E. festucae* Fl1 and *N. lolii* Lp19 *prt2* and *gcn1* sequences

Alignment of the nucleotide sequences of the *E. festucae* Fl1 and *N. lolii* Lp19 *prt2* and *gcn1* sequences. Non-coding sequences such as intergenic sequences and introns are shown in lower case letters. Coding sequences are shown in upper case letters. Identity between *E. festucae* Fl1 and *N. lolii* Lp19 in intergenic sequences, coding sequences and introns is indicated by grey, black and yellow shading respectively. The positions of the translation initiation and termination codons of the genes are identified by green and red arrows respectively. Exons and introns are labelled at the beginning of the relevant sequence by green and yellow boxes respectively. The insertion in the *E. festucae* Fl1 *prt2-gcn1* intergenic region relative to the same region in *N. lolii* Lp19 is indicated by purple shading.

```
Lp19     1 ggatccgtatttatggtagcttgtgcgcattctgtgcgcaggccgcatccgcatagccct    60
Fl1      1                                                          t     1

Lp19    61 aacctacatgtacatgtagctgcacacaatccgcatccttactggacccggacttgaccc   120
Fl1      2 aacctacatgtacatgtagctgcacacaatccgcatccttactggacccgga-ttgaccc    60

Lp19   121 ggacttgacccggacttgacctaagcttatctcgattccatgacgacgtgtcacggcttt   180
Fl1     61 ga----------gacttgacctaagcttatctcgattccatgacgacgtgtcacggcttt   110

Lp19   181 cggcctagatgatgaaaacagagtcaaggctgagatacgccgtcgctgctagatgatgtt   240
Fl1    111 cggcctagatgatgaaaacagagtcaaggctgagatacgccgtcgctgctagatgatgtt   170

Lp19   241 cttctgccaagaaaaccaaggggtgggttacacagcgtcggcacgtcgttcactgctgtg   300
Fl1    171 cttctgccaagaaaaccaaggggtgggttacacagcgtcggcacgtcgttcactgctgtg   230

Lp19   301 gtccgtctgctcaacttcggtcacagagagcagttgtactccgtagagttggggtcaata   360
Fl1    231 gtccgtctgttcaacttcggtcacagagagcagttgtactccgtagagttggg-----ta   285

Lp19   361 ttgatgcgtcatggaaacacccaccacaagtcattgttctatccgctgcatccgccatat   420
Fl1    286 ttgatgcgtcatggaaacacccaccacaagtcattgttctatccgctgcatccgccatat   345

Lp19   421 gcgattgacctgcctagaagcattcattgcatcaaaattcggtgagcgtgcgcataagcc   480
Fl1    346 gcgattgacctgcctagaagcattcattgcatcaaaattcggtgagcgtgcgcataagcc   405

Lp19   481 cgatagtccgcagatttatttcccgacaatcatttttttcggccttctggctcgaggatga   540
Fl1    406 cgatagtccgcagatttatttcccgacaatcatttttttcggccttctggctcgaggatga   465

Lp19   541 ctgcttctttgcaagttggggacggttacgctctcatgcatgcgcccagaccatgcccaa   600
Fl1    466 ctgcttctttgcaagttggggacggttacgctctcatgcatgcgcccagaccatgcccaa   525

Lp19   601 acgctgaaagtaatcgacccatgccatgtgatgatgatgatgacatgtgttggatatcgc   660
Fl1    526 acgctgaaagtaatcgacccatgccatgtg---------atgacatgtgttggatatcgc   576

Lp19   661 agcctcctatatcgcgtttgtcatcgtgacccgtgctatgctttgtttgttaatctattc   720
Fl1    577 agcctcctatatcgcgtttgtcatcgtgacccgtgctatgctctgtttgttaatctattc   636

Lp19   721 caagaccttgctttgtttgtgaa-ccagagacgaacaagatgtatggcctttggatgttc   779
Fl1    637 caagaccttgctttgtttgtgaaaccagagacgaacaagatgtatggccattggatgttc   696

Lp19   780 aatcgcgcggcaaaggctctcaggactccaggagggtcatgtctgcattttgaaactctt   839
Fl1    697 aatcgcgcggcaaaggctctcaggactccaggagggtcatgtctgcattttgaaactctt   756

Lp19   840 gatacctggcattctcgaccaagacttcagcatttccatgctgcaaagaactcatccttc   899
Fl1    757 gatacctggcattctcgaccaagacttcagcatttccatgctgcaaagaactcatccttc   816

Lp19   900 gtcctagcagccgttttgaaatttgggggtttccagttcttgaatctcagggttagggtt   959
Fl1    817 gtcctagcagccgtttcgaaatttgggggtttccagttcttgaatctcagggttagggtt   876
```

```
Lp19   960 gtccaacgtctttcacggcgcaattagcagacttgtcgactcaaaagcgggaagaaagaa 1019
Fl1    877 gtccaacgtctttcacggcgcaattagcagacttgtcgactcaaaagcgggaagaaagaa  936

Lp19  1020 ctatgcctggcgagtccggcagctctcatggcggcatgggacttttccccgggtacaggg 1079
Fl1    937 ctatgcctggcgagtccggcagctctcatggcggcatgggacttttccccgggtacaggg  996

Lp19  1080 gcgcccgggcccggggccgggatggaatatcatgtggtgccagctatcgcgcataatttg 1139
Fl1    997 gcgcccgggcccggggccgggatggaatatcatgtggtgccagctatcgcgcataatttg 1056

Lp19  1140 agtgacattttgtttcatgcacatgcaaatcgggaaggtgtctccgtgcgtctcccagtg 1199
Fl1   1057 agtgacattttgtttcatgcacatgcaaatcgggaaggtgtctccgtgcgtctcccagtg 1116

Lp19  1200 ccatctccggtatatatatatatccgatgctgggggttctctcggcagcacaatcgttc 1259
Fl1   1117 ccatctccggtatatatatatatccgatgctgggggttctctcggcagcacgctcgttc 1176

Lp19  1260 ttgattgggaaagtatggaaataaatggtcacaacttctcccgcgccatgcatagaagct 1319
Fl1   1177 ttgattgggaaagtatggaaataaatggtcacaacttctcccgcgccatgcatagaagct 1236

Lp19  1320 caaggtccgcgaagtaaagtttccaagcatgctcctgccgcagtttgtgtgagatttcag 1379
Fl1   1237 caaggtccgcgaagtaaagtttccaagcatgctcctgccgcagtttgtgtgagatttcag 1296

Lp19  1380 ggaattgataaatggcggcgcccaacaaggccgcggccgtgagtcgtgagccgtcacggc 1439
Fl1   1297 ggaattgataaatggcggcgcccaacaaggccgcggccgtgagtcgtgagccgtcacggc 1356

Lp19  1440 ttcttcctgtcggccatgttccgagtctaggacggccatgtacacggatgtgtacgattg 1499
Fl1   1357 ttcttcctgtcggccatgttccgagtctaggacggccatgtacacggatgtgtacgattg 1416

Lp19  1500 aatggcatcacttggtggctccatgactttgttcttcagatggccgtgaatcagtccgtc 1559
Fl1   1417 aatggcatcacctggtggctccatgactttgttcttcagatggccgtgaatcagtccgtc 1476

Lp19  1560 ccaccgactcaaaagccggcggtcaccacagcagggcctcccgatcagttgggtaacggg 1619
Fl1   1477 ccaccgactcaaaagccggcggtcaccacagcagggcctcccgatcagttgggtaacggg 1536

Lp19  1620 ttgctgctggaaatcgaggagtcgcgtctccctcggccatgcatcaagtgagcaactgca 1679
Fl1   1537 ttgctgctggaaatcgaggagtcgcgtctccctcggccatgcatcaagtgagcaactgca 1596

Lp19  1680 ggcatggtggcacaccgcgtttcctaatccttttcccggcgacatgtcaacagcggagggg 1739
Fl1   1597 ggcatggtggcacaccgcgtttcctaatccttttcccggcgacatgtcaacaacggagggg 1656

Lp19  1740 agggggggagccacgaaaacgaatcaatggtgcggcggccgccgaccgtgatccgcgagc 1799
Fl1   1657 agggggggagccacgaaaacgaatcaatggtgcggcggccgccgaccgtgatccgcgagc 1716

Lp19  1800 cacatgccaaatcgttggcggctgcggccctcgtgcgacgcccgtgatcaaagtcttaca 1859
Fl1   1717 cacatgccaaatcgttggcggctgcggccctcgtgcgacgcccgtgatcaaagtcttaca 1776

Lp19  1860 ttggcatcggcatctcatcttgtgcgtaacgtgacgtccgaatgacaccgatcatggcag 1919
Fl1   1777 ttggcatcggcatctcatcttgtgcgtaacgtgatgtccgaatgacaccgatcatggcag 1836

Lp19  1920 aacaccttcttgtcgaaaccttcctctttgggcgaatccgcgcgggagctgccagccttg 1979
Fl1   1837 aacaccttcttgtcgaaaccttcctctttgggcgaatccgcgcgggagctgccagccttg 1896

Lp19  1980 gtgccctatcatccgcccgcggagtattgttttttttatttttcgggtggtggaaccgaca 2039
Fl1   1897 gtgccctatcatccgcccgcggagtattgttttttttatttttcgggtggtggaaccgaca 1956

Lp19  2040 cggcaggacactgcttatgctggaccagcataacgaatgtcatcttcagacagagcctgc 2099
Fl1   1957 cggcaggacactgcttatgctggaccaggataacgaatgtcatcttcagacagagcctgc 2016

Lp19  2100 atggttcgacaaaaacgaactccaaggttcgaaagacgtcttcgtcttgcgcaagagatc 2159
Fl1   2017 atggttcgacaaaaacgaactccaaggttcgaaagacgtcttcgtcttgcgcaagggatc 2076

Lp19  2160 gagccatccgccacgccaaacagggtcgtttccgcaaagaaccgttacaccaagtttgta 2219
Fl1   2077 gagccatccgccacgccaaacagggtcgtttccgcaaagaaccgttacaccaagtttgta 2136
```


Lp19 2220 tacctcgcatggttggaaggtagatcatggcaaaagcgcagtaagtatggtgatgatgtc 2279
Fl1 2137 tacctcgcatggttggaaggtagatcatggcaaaagcgcagtaagtatggtgatgatgtc 2196
Lp19 2280 tcttgatccaaacttgtagatataaaaggggggcaagacatgtctccagatatccagctct 2339
Fl1 2197 tcttgatccaaacttgtagatataaaaggggggcaagacatgtctccagatatccagctct 2256
Lp19 2340 cctctgagagactcaaaagtcctctgattcccaagcttcaggtgtcaacagtagatacca 2399
Fl1 2257 cctctgagagactcaaaagtcctctgattcccaagcttcaggtgtcaacagtagatacca 2316
prt2 exon 1
Prt2 start
Lp19 2400 gtatcctgacgggagccagccacgATGCGTCCTGGTCTTCTATTCCTCCAGCTGCTCCCG 2459
Fl1 2317 gtatcctgacgggagccagccacgATGCGTCCTGGTCTTCTATTCCTCCAGCTGCTCCCG 2376
Lp19 2460 CTAGCTCTTGCAGCTCCCGGAGCAAGGCGATCGGAGCCAGCCCCGATCCTCGCTCCACGT 2519
Fl1 2377 CTAGCTCTTGCAGCTCCCGGAGCAAGGCGATCGGAGCCAGCCCCGATCCTCGCTCCACGT 2436
Lp19 2520 GGGGCCGTGATCGAGAACAAGTACATTGTTAAATACAAAAAGACATTTTCTATTGCCTCA 2579
Fl1 2437 GGGGCCGTGATCGAGAACAAGTACATTGTTAAATACAAAAAGACATTTTCTATTGCCTCA 2496
Lp19 2580 GCCGATCACACTTTAAAGGCATGCAGCGCTGGTGCCGACAGAGTGTACTCCAACATCTTC 2639
Fl1 2497 GCCGATCACACTTTAAAGGCATGCAGCGCTGGTGCCGACAGAGTGTACTCCAACATCTTC 2556
Lp19 2640 CACGGATTTTCTGGTACCTTGAACGAGAGCGCCATTGAGCAGCTTCGTCACCACCCTGAT 2699
Fl1 2557 CACGGATTTTCTGGTACCTTGAACGAGAGCGCCATTGAGCAGCTTCGTCACCACCCTGAT 2616
prt2 intron 1
Lp19 2700 gtgagacttggccaagtagtggacactggacatggccatggcaaattactaactttgtgc 2759
Fl1 2617 gtgagacttggccaagtagtggacactggacatggccatggcaaattactaactttgtgc 2676
prt2 exon 2
Lp19 2760 tccccaaaacagGTTGACTACATCGAGAAGGATGCCATCTTCAAGATGAACACTTTTGTT 2819
Fl1 2677 tccccaaaacagGTTGACTACATCGAGAAGGATGCCATCTTCAAGATGAACACTTTTGTT 2736
Lp19 2820 GAGCAGCGCGATGCTCCTCGGGGATTGAGACGTGTTTCTCACCGCCAGGGTGACATTGGT 2879
Fl1 2737 GAGCAGCGCGATGCTCCTCGGGGATTGAGACGTGTTTCTCACCGCAAGGGTGACATTGGT 2796
Lp19 2880 GGCTACGTTTATCATGCGAGTGCCGGCGAGGGCACATGCTCCTACATTATTGACACTGGA 2939
Fl1 2797 GGCTACGTTTATCACGAGAGTGCCGGCGAGGGCACGTGCTCCTACATTATTGACACTGGA 2856
prt2 intron 2
Lp19 2940 GTTGACGACTCCCACCCTgtatgtcatttcgtccaagtcgatcccgatgtgcccaggttc 2999
Fl1 2857 GTTGACGACTCCCACCCTgtatgtcatttcgtccaagtcgatcccgatgtgcccaggttc 2916
prt2 exon 3
Lp19 3000 tcgctggcaaggcggacatcccaactaacccggagtcgcagGAGTTCGAGGGTCGCGCTC 3059
Fl1 2917 tcgctggcaaggcggacatcccaactaacccggagtcgcagGAGTTCGAGGGTCGCGCTC 2976
Lp19 3060 AGCTCGTCACATCCTTTGTCGATGGGGAGGATGCCGACGGCCACGGTCACGGCACTCACG 3119
Fl1 2977 AGCTCGTCACATCCTTTGTCGATGGGGAGGATGCCGATGGCCACGGTCACGGCACTCACG 3036
Lp19 3120 TCGCTGGCACCATCGGTAGCCGTAGCTACGGCATCGCCAAGAAGACTCAGCTGCTTGGCA 3179
Fl1 3037 TCGCTGGCACCATCGGTAGCCGCAGCTACGGCATCGCCAAGAAGACTCAGCTGCTTGGCA 3096
Lp19 3180 TCAAGGTACTCAGCGACCAGGGATCTGGAAACAATTCCGCCATTATCGCGGGCATGGACT 3239
Fl1 3097 TCAAGGTACTCAGCGACCAGGGATCTGGAAACAATTCCGCCATCATCGCGGGCATGGACT 3156
Lp19 3240 TTGCCGTCCAGGACGCCAGGCAACGAAGCTGCGCCAAGGGTGTTCTCGCCAACATGAGTC 3299
Fl1 3157 TTGCCGTCCAGGACGCCAGGCAACGAAGCTGCGCCAAGGGTGTTCTCGCCAACATGAGTC 3216

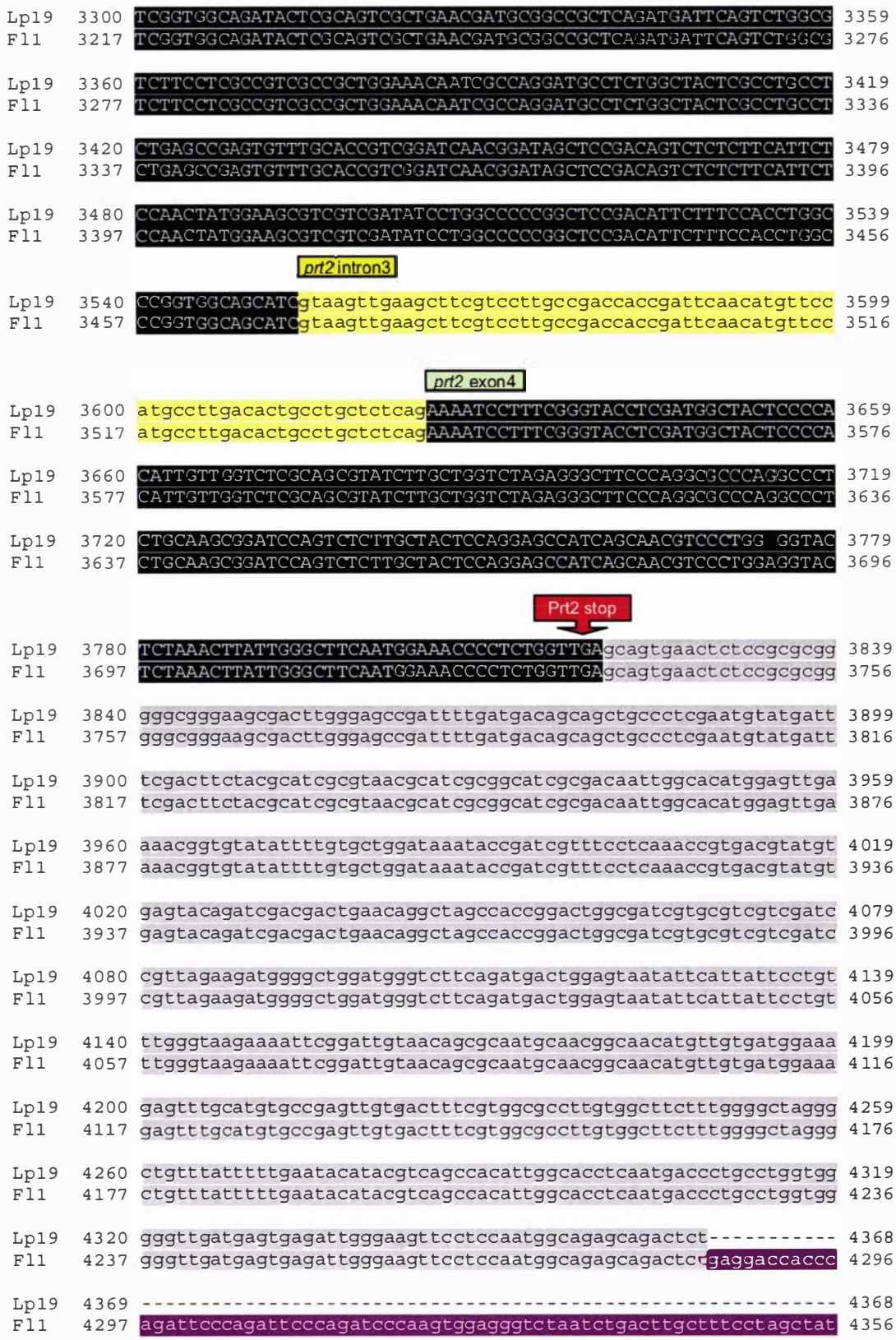
prt2 intron3
prt2 exon4
Prt2 stop

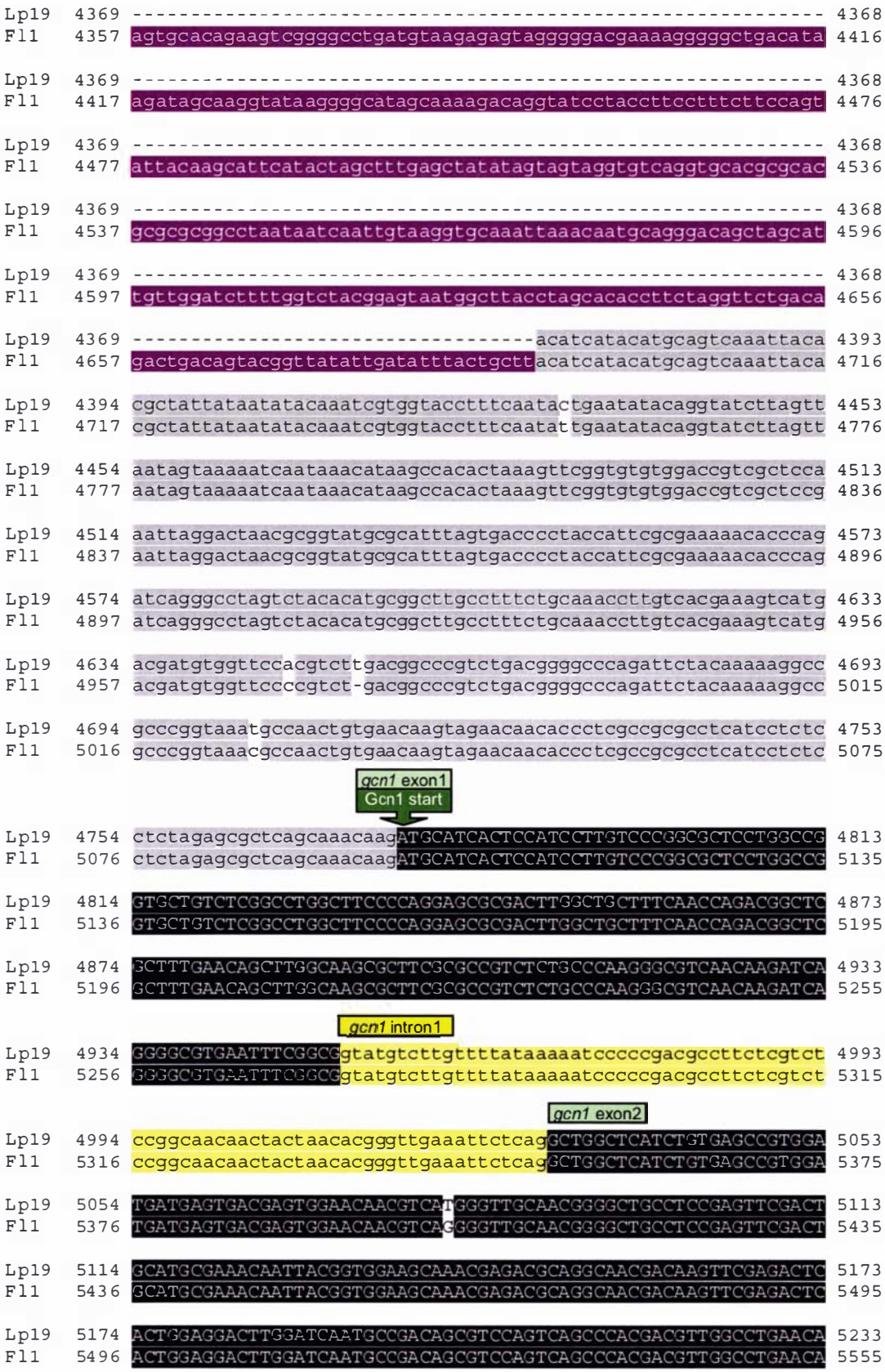
Lp19 4369 ---------- 4368
Fl1 4357 agtgcacagaagtcggggcctgatgtaagagagtaggggacgaaaaggggctgacata 4416
Lp19 4369 ---------- 4368
Fl1 4417 agatagcaaggtataaggggcatagcaaaagacaggtatcctaccttcctttcttccagt 4476
Lp19 4369 ---------- 4368
Fl1 4477 attacaagcattcatactagctttgagctatatagtagtaggtgtcaggtgcacgcgcac 4536
Lp19 4369 ---------- 4368
Fl1 4537 gcgcgcggcctaataatcaattgtaaggtgcaaattaaacaatgcagggacagctagcat 4596
Lp19 4369 ---------- 4368
Fl1 4597 tgttggatcttttggtctacggagtaatggcttacctagcacaccttctaggttctgaca 4656
Lp19 4369 ----------acatcatacatgcagtcaaattaca 4393
Fl1 4657 gactgacagtacggttatattgatatttactgcttacatcatacatgcagtcaaattaca 4716
Lp19 4394 cgctattataatatacaaatcgtggtacctttcaatactgaatatacaggtatcttagtt 4453
Fl1 4717 cgctattataatatacaaatcgtggtacctttcaatattgaatatacaggtatcttagtt 4776
Lp19 4454 aatagtaaaaatcaataaacataagccacactaaagttcggtgtgtggaccgtcgctcca 4513
Fl1 4777 aatagtaaaaatcaataaacataagccacactaaagttcggtgtgtggaccgtcgctccg 4836
Lp19 4514 aattaggactaacgcggtatgcgcatttagtgacccctaccattcgcgaaaaacacccag 4573
Fl1 4837 aattaggactaacgcggtatgcgcatttagtgacccctaccattcgcgaaaaacacccag 4896
Lp19 4574 atcagggcctagtctacacatgcggcttgcctttctgcaaaccttgtcacgaaagtcatg 4633
Fl1 4897 atcagggcctagtctacacatgcggcttgcctttctgcaaaccttgtcacgaaagtcatg 4956
Lp19 4634 acgatgtggttccacgtcttgacggcccgtctgacggggcccagattctacaaaaaggcc 4693
Fl1 4957 acgatgtggttccccgtct-gacggcccgtctgacggggcccagattctacaaaaaggcc 5015
Lp19 4694 gcccggtaaatgccaactgtgaacaagtagaacaacaccctcgccgcgcctcatcctctc 4753
Fl1 5016 gcccggtaaacgccaactgtgaacaagtagaacaacaccctcgccgcgcctcatcctctc 5075
gcn1 exon1
Gcn1 start
Lp19 4754 ctctagagcgctcagcaaacaagATGCATCACTCCATCCTTGTCCCGGCGCTCCTGGCCG 4813
Fl1 5076 ctctagagcgctcagcaaacaagATGCATCACTCCATCCTTGTCCCGGCGCTCCTGGCCG 5135
Lp19 4814 GTGCTGTCTCGGCCTGGCTTCCCCAGGAGCGCGACTTGGCTGCTTTCAACCAGACGGCTC 4873
Fl1 5136 GTGCTGTCTCGGCCTGGCTTCCCCAGGAGCGCGACTTGGCTGCTTTCAACCAGACGGCTC 5195
Lp19 4874 GCTTTGAACAGCTTGGCAAGCGCTTCGCGCCGTCTCTGCCCAAGGGCGTCAACAAGATCA 4933
Fl1 5196 GCTTTGAACAGCTTGGCAAGCGCTTCGCGCCGTCTCTGCCCAAGGGCGTCAACAAGATCA 5255
gcn1 intron1
Lp19 4934 GGGGCGTGAATTTCGGCGgtatgtcttgttttataaaaatcccccgacgccttctcgtct 4993
Fl1 5256 GGGGCGTGAATTTCGGCGgtatgtcttgttttataaaaatcccccgacgccttctcgtct 5315
gcn1 exon2
Lp19 4994 ccggcaacaactactaacacgggttgaaattctcagGCTGGCTCATCTGTGAGCCGTGGA 5053
Fl1 5316 ccggcaacaactactaacacgggttgaaattctcagGCTGGCTCATCTGTGAGCCGTGGA 5375
Lp19 5054 TGATGAGTGACGAGTGGAACAACGTCATGGGTTGCAACGGGGCTGCCTCCGAGTTCGACT 5113
Fl1 5376 TGATGAGTGACGAGTGGAACAACGTCAGGGGTTGCAACGGGGCTGCCTCCGAGTTCGACT 5435
Lp19 5114 GCATGCGAAACAATTACGGTGGAAGCAAACGAGACGCAGGCAACGACAAGTTCGAGACTC 5173
Fl1 5436 GCATGCGAAACAATTACGGTGGAAGCAAACGAGACGCAGGCAACGACAAGTTCGAGACTC 5495
Lp19 5174 ACTGGAGGACTTGGATCAATGCCGACAGCGTCCAGTCAGCCCACGACGTTGGCCTGAACA 5233
Fl1 5496 ACTGGAGGACTTGGATCAATGCCGACAGCGTCCAGTCAGCCCACGACGTTGGCCTGAACA 5555

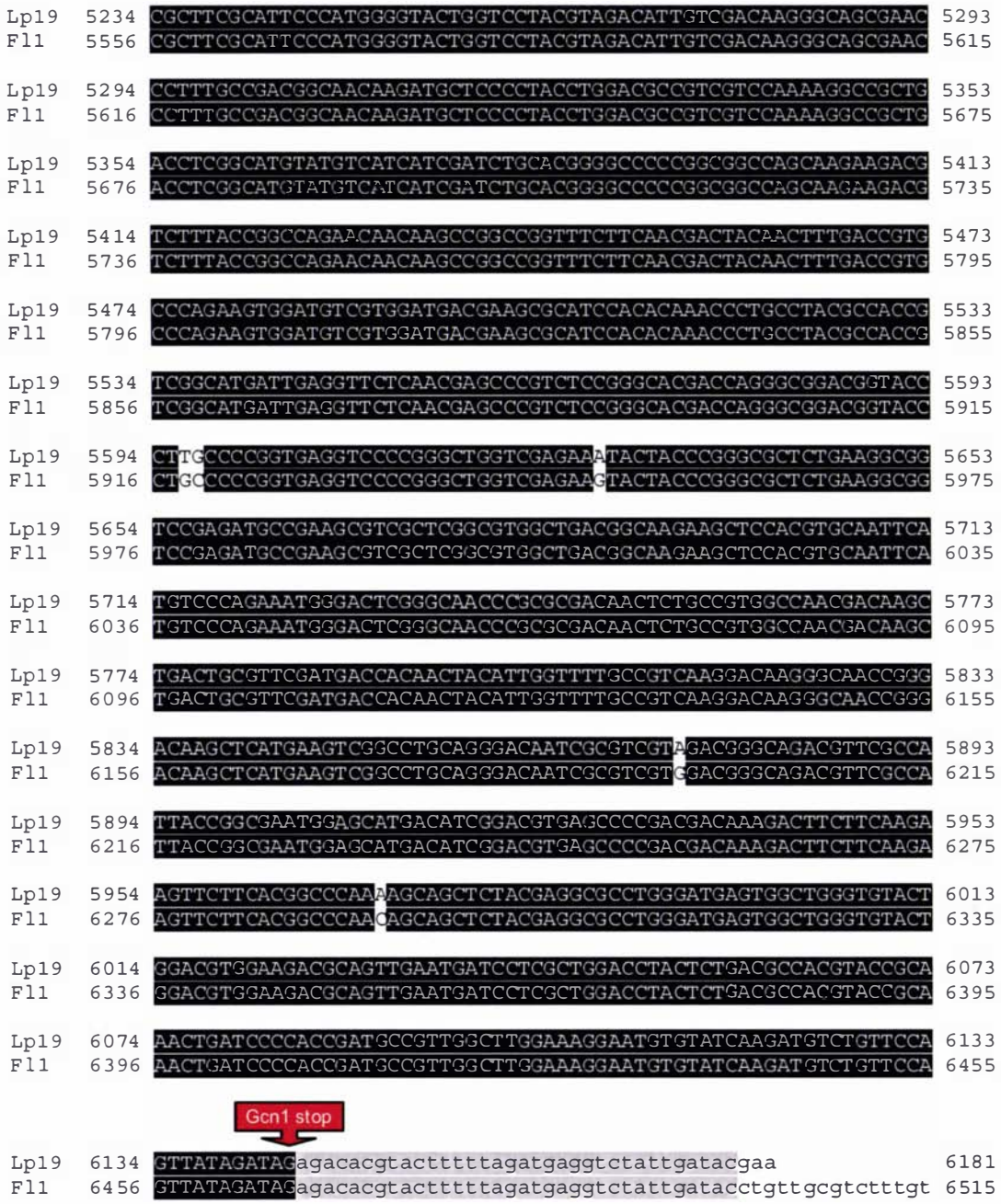
Lp19 5234 CGCTTCGCATTCCCATGGGGTACTGGTCCTACGTAGACATTGTCGACAAGGGCAGCGAAC 5293
Fl1 5556 CGCTTCGCATTCCCATGGGGTACTGGTCCTACGTAGACATTGTCGACAAGGGCAGCGAAC 5615
Lp19 5294 CCTTTGCCGACGGCAACAAGATGCTCCCCTACCTGGACGCCGTCGTCCAAAAGGCCGCTG 5353
Fl1 5616 CCTTTGCCGACGGCAACAAGATGCTCCCCTACCTGGACGCCGTCGTCCAAAAGGCCGCTG 5675
Lp19 5354 ACCTCGGCATGTATGTCATCATCGATCTGCACGGGGCCCCCGGCGGCCAGCAAGAAGACG 5413
Fl1 5676 ACCTCGGCATGTATGTCATCATCGATCTGCACGGGGCCCCCGGCGGCCAGCAAGAAGACG 5735
Lp19 5414 TCTTTACCGGCCAGAACAACAAGCCGGCCGGTTTCTTCAACGACTACAACTTTGACCGTG 5473
Fl1 5736 TCTTTACCGGCCAGAACAACAAGCCGGCCGGTTTCTTCAACGACTACAACTTTGACCGTG 5795
Lp19 5474 CCCAGAAGTGGATGTCGTGGATGACGAAGCGCATCCACACAAACCCTGCCTACGCCACCG 5533
Fl1 5796 CCCAGAAGTGGATGTCGTGGATGACGAAGCGCATCCACACAAACCCTGCCTACGCCACCG 5855
Lp19 5534 TCGGCATGATTGAGGTTCTCAACGAGCCCGTCTCCGGGCACGACCAGGGCGGACGGTACC 5593
Fl1 5856 TCGGCATGATTGAGGTTCTCAACGAGCCCGTCTCCGGGCACGACCAGGGCGGACGGTACC 5915
Lp19 5594 CTTGCCCCGGTGAGGTCCCCGGGCTGGTCGAGAAATACTACCCGGGCGCTCTGAAGGCGG 5653
Fl1 5916 CTGCCCCCGGTGAGGTCCCCGGGCTGGTCGAGAAGTACTACCCGGGCGCTCTGAAGGCGG 5975
Lp19 5654 TCCGAGATGCCGAAGCGTCGCTCGGCGTGGCTGACGGCAAGAAGCTCCACGTGCAATTCA 5713
Fl1 5976 TCCGAGATGCCGAAGCGTCGCTCGGCGTGGCTGACGGCAAGAAGCTCCACGTGCAATTCA 6035
Lp19 5714 TGTCCCAGAAATGGGACTCGGGCAACCCGCGCGACAACTCTGCCGTGGCCAACGACAAGC 5773
Fl1 6036 TGTCCCAGAAATGGGACTCGGGCAACCCGCGCGACAACTCTGCCGTGGCCAACGACAAGC 6095
Lp19 5774 TGACTGCGTTCGATGACCACAACTACATTGGTTTTGCCGTCAAGGACAAGGGCAACCGGG 5833
Fl1 6096 TGACTGCGTTCGATGACCACAACTACATTGGTTTTGCCGTCAAGGACAAGGGCAACCGGG 6155
Lp19 5834 ACAAGCTCATGAAGTCGGCCTGCAGGGACAATCGCGTCGTAGACGGGCAGACGTTCGCCA 5893
Fl1 6156 ACAAGCTCATGAAGTCGGCCTGCAGGGACAATCGCGTCGTGGACGGGCAGACGTTCGCCA 6215
Lp19 5894 TTACCGGCGAATGGAGCATGACATCGGACGTGAGCCCCGACGACAAAGACTTCTTCAAGA 5953
Fl1 6216 TTACCGGCGAATGGAGCATGACATCGGACGTGAGCCCCGACGACAAAGACTTCTTCAAGA 6275
Lp19 5954 AGTTCTTCACGGCCCAAAAGCAGCTCTACGAGGCGCCTGGGATGAGTGGCTGGGTGTACT 6013
Fl1 6276 AGTTCTTCACGGCCCAACAGCAGCTCTACGAGGCGCCTGGGATGAGTGGCTGGGTGTACT 6335
Lp19 6014 GGACGTGGAAGACGCAGTTGAATGATCCTCGCTGGACCTACTCTGACGCCACGTACCGCA 6073
Fl1 6336 GGACGTGGAAGACGCAGTTGAATGATCCTCGCTGGACCTACTCTGACGCCACGTACCGCA 6395
Lp19 6074 AACTGATCCCCACCGATGCCGTTGGCTTGGAAAGGAATGTGTATCAAGATGTCTGTTCCA 6133
Fl1 6396 AACTGATCCCCACCGATGCCGTTGGCTTGGAAAGGAATGTGTATCAAGATGTCTGTTCCA 6455
Gcn1 stop
Lp19 6134 GTTATAGATAGagacacgtacttttttagatgaggtctattgatacgaa 6181
Fl1 6456 GTTATAGATAGagacacgtacttttttagatgaggtctattgatacctgttgcgtctttgt 6515

A2.3 Comparison of the endophyte sequences homologous to *prt3*

Alignment of the nucleotide sequences of the *prt3* homologues from *E. typhina* (At1), *E. festucae* (Fl1 and Fr1) and *N. lolii* (Lp19, Lp5 and AR1) strains. Non-coding intron sequences are shown in lower case letters. Coding sequences are shown in upper case letters. Identity between the *prt3* sequences is indicated for coding sequences and introns by black or yellow shading respectively. Positions of the translation initiation and termination codons of the genes are identified by green and red arrows respectively. Exons and introns are labelled at the beginning of the relevant sequence by green and yellow boxes respectively. The position of the deletion in exon 2 in *N. lolii* Lp19 and Lp5 is indicated by a red box.

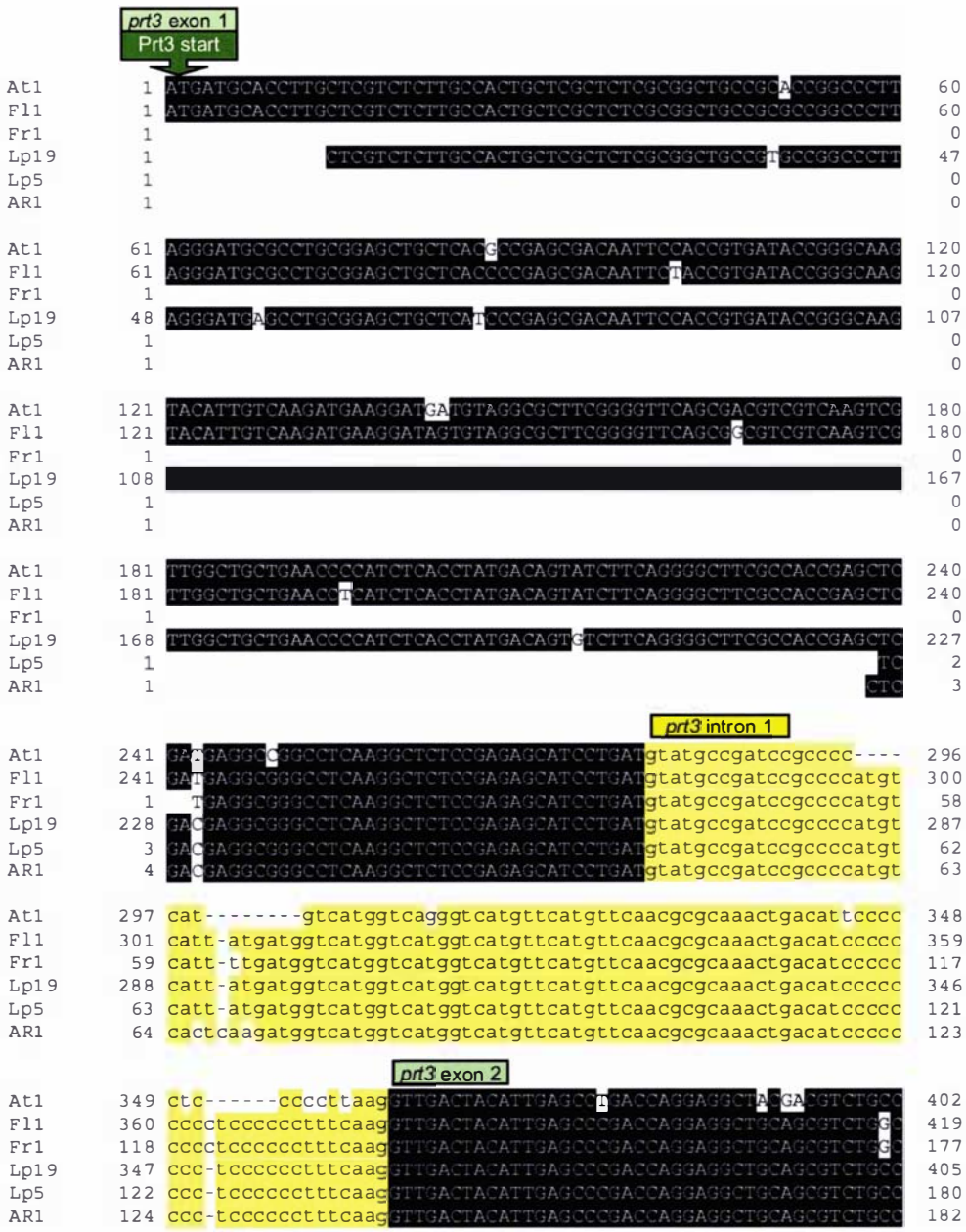

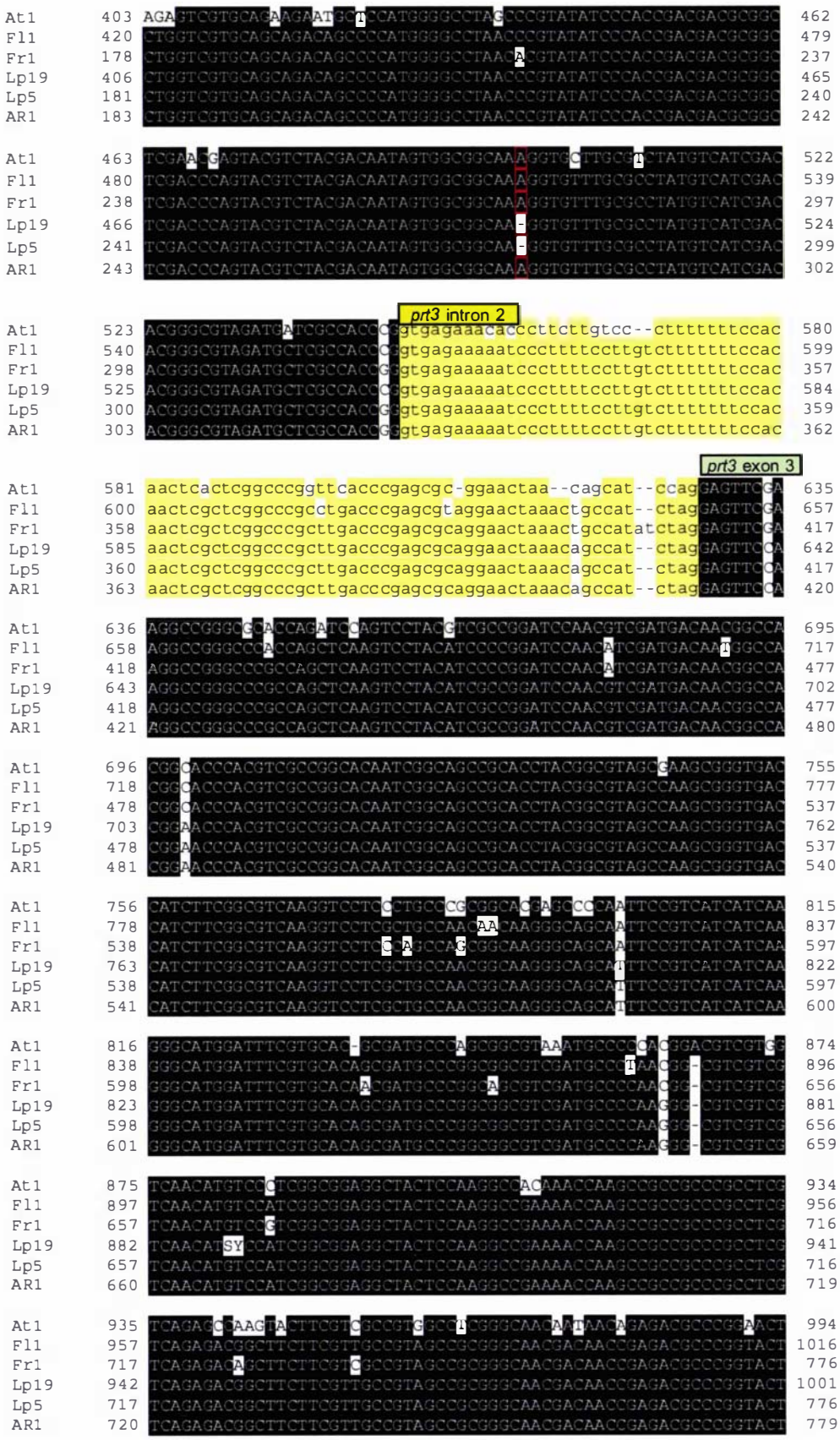
prt3 intron 2
prt3 exon 3
At1
Fl1
Fr1
Lp19
Lp5
AR1


prt3 intron 3
prt3 exon 4
Prt3 stop

APPENDIX

A3: Analysis of Orf4

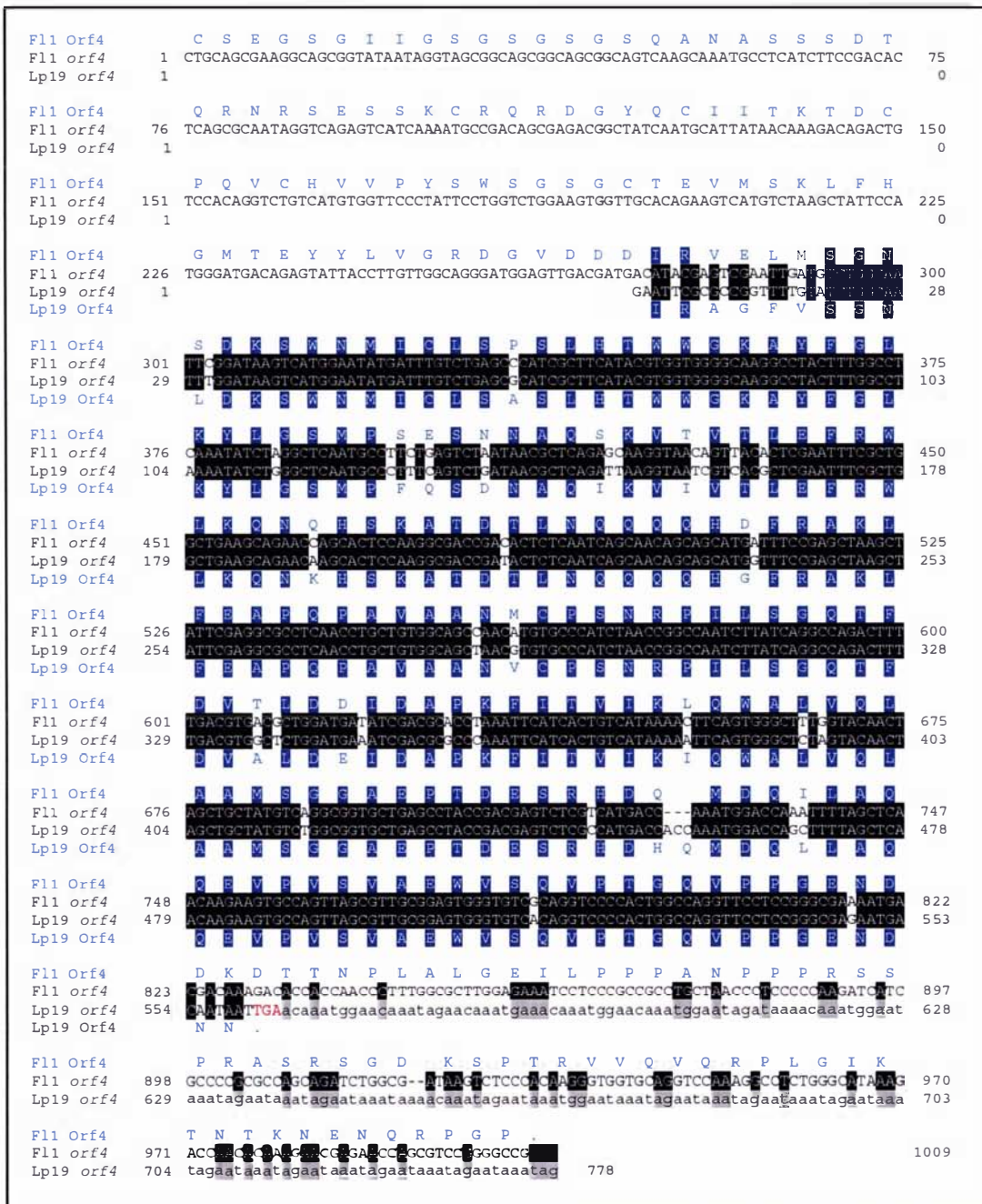

Appendix A3 Comparison of the *E. festucae* Fl1 and *N. lolii* Lp19 *orf4* sequences

Alignment of the nucleotide sequences of the *E. festucae* Fl1 and *N. lolii* Lp19 *orf4* genes along with the encoded Orf4 polypeptide sequences. Protein-coding sequences are shown in uppercase letters, and non-coding sequences are shown in lowercase letters. Homology between sequences at the nucleotide level is indicated by black or grey shading for coding or non-coding sequences respectively. The stop codons are indicated in red text. The polypeptide sequences are indicated in blue text, with identity at the amino acid level indicated by blue shading.

APPENDIX

A4: Analysis of Cyc1

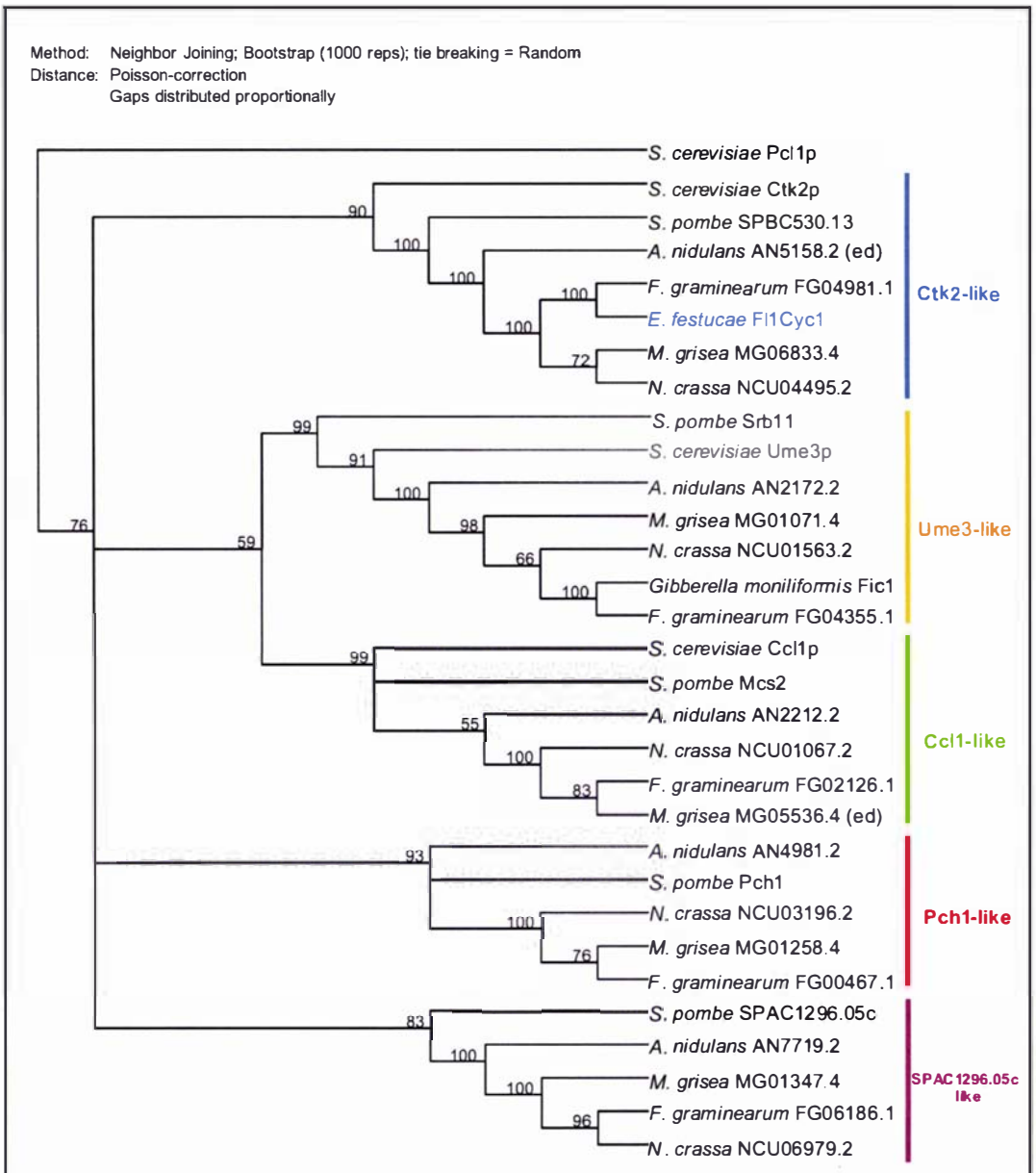

Appendix A4 Phylogenetic relationship of Cyc1 to other fungal C-type cyclins

Phylogenetic relationship of the *E. festucae* Fl1 Cyc1 protein with other related fungal cyclins. The phylogenetic tree in this figure was prepared in the MacVector 7.2.3 program, using Neighbour joining and bootstrapping (1000 replicates) of sequences aligned using the ClustalW module of MacVector. For details of the sequences used in this alignment, see Appendix A13.6. In this phylogenetic tree, the Fl1 Cyc1 protein name is shown in blue text, with all other protein names in black text. C-type and A/B-type cyclins are indicated by red and blue lines respectively. Ctk2, Ume3, Ccl1, Pch1 and SPAC1296.05c-like cyclins are indicated by blue, orange, green, red and purple lines respectively.

APPENDIX

A5: Analysis of Ptn1

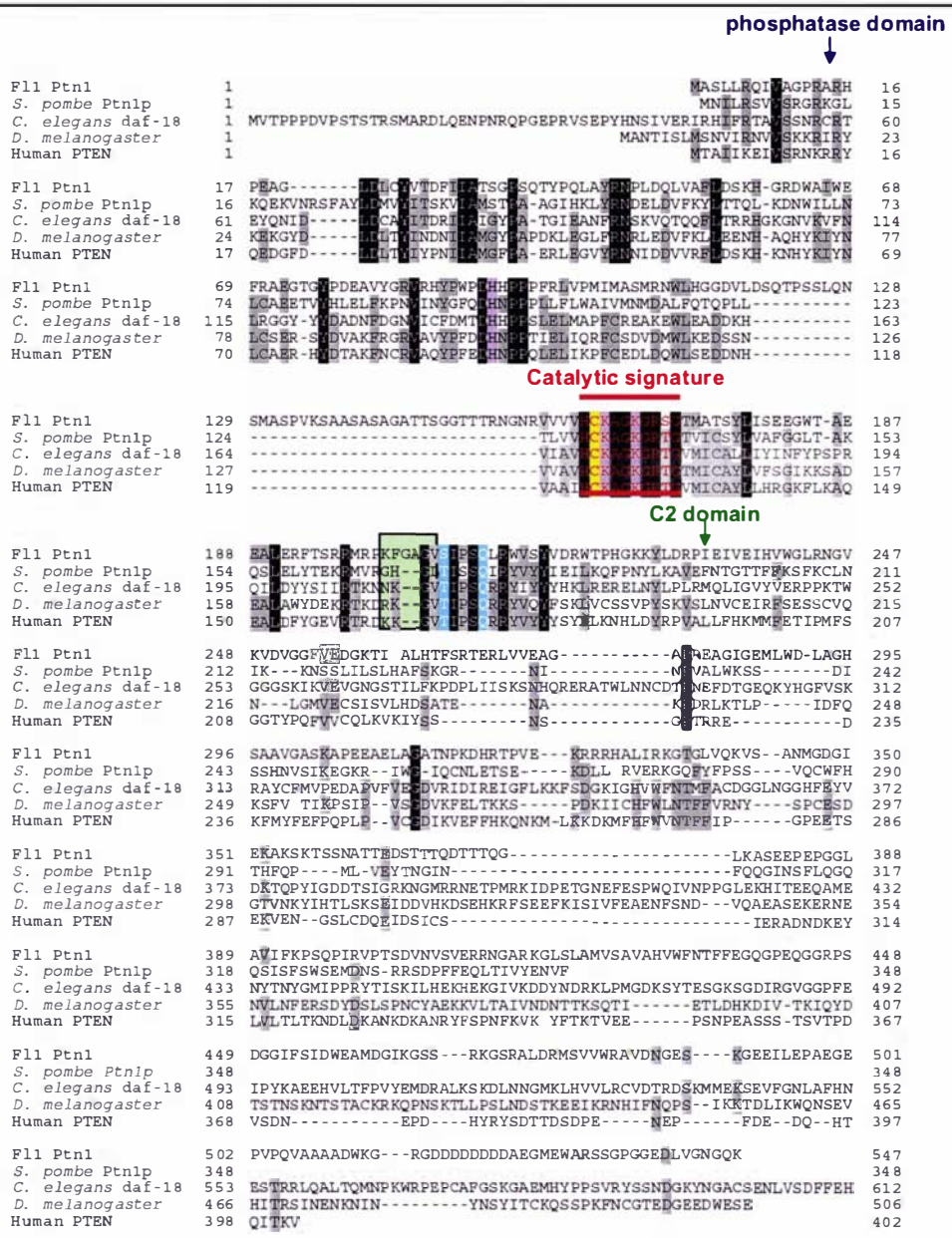

APPENDIX A5.1 Alignment of the *E. festucae* Fl1 Ptn1 protein with phosphoinositide 3-phosphatase sequences

Alignment of the deduced Fl1 Ptn1 protein with known phosphoinositide 3-phosphatases from other organisms. Included are *Schizosaccharomyces pombe* Ptn1p (also known as SPBC609.02, accession number CAA22831.1) (Mitra et al 2004), *Caenorhabditis elegans* daf-18 (Mihaylova et al 1999; accession number T51924), *Drosophila melanogaster* PTEN (Smith et al 1999; accession number AAF23236.1) and human PTEN (Li et al 1997; accession number NP_000305.2). Residues conserved between all sequences are shown in black shading, while residues conserved between most (but not all) sequences are shown in grey shading. Residues shown in red text are important in catalysis. The residues shaded in yellow are absolutely required for catalysis. Residues shown in blue hydrogen bond with PIP_3. Residues shown in purple shading have positive charges important in the catalytic site. The green box indicates an insertion in PTEN homologues that is not present in dual specificity phosphatases.

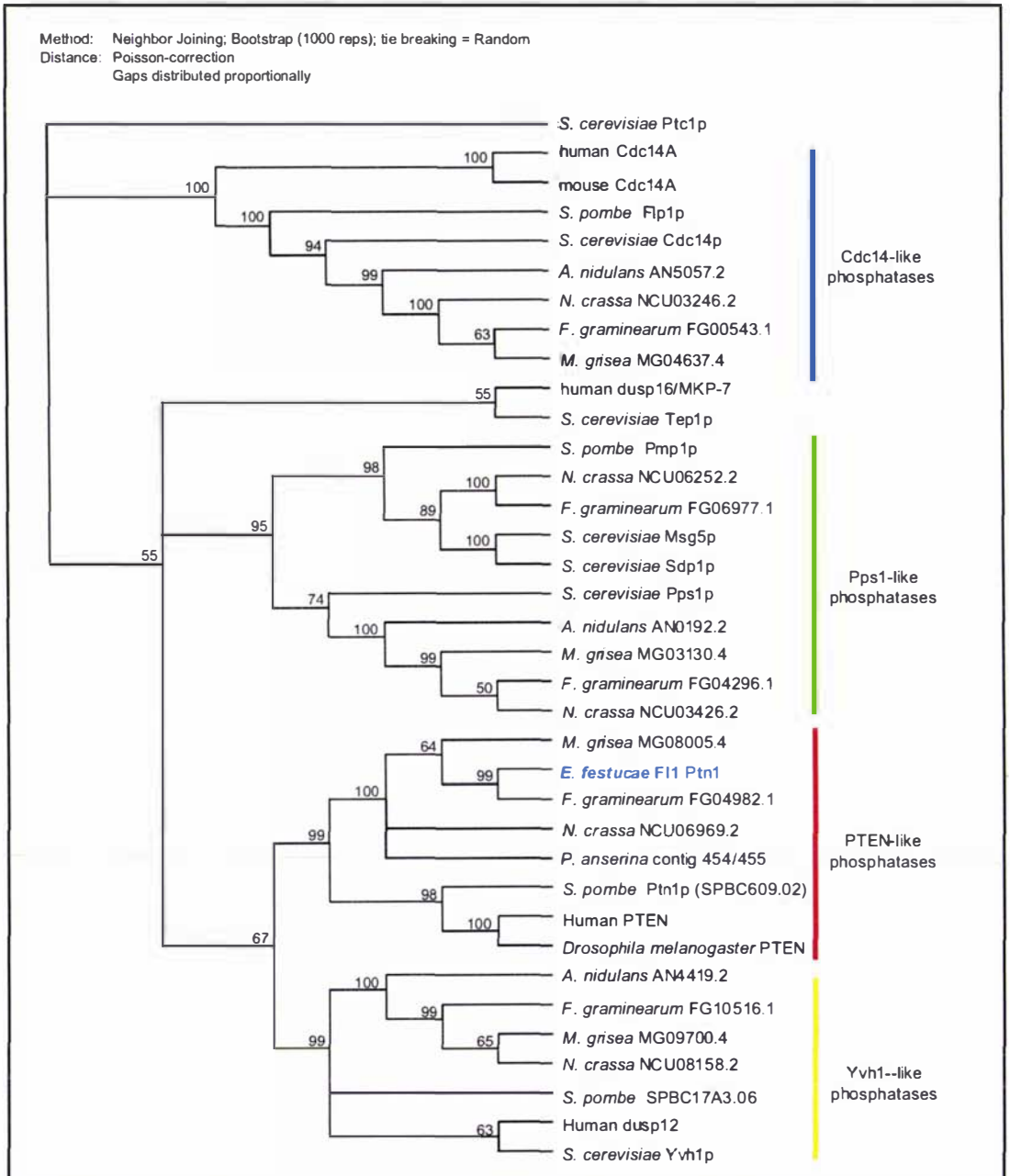

Appendix A5.2 Phylogenetic relationship of Ptn1 to fungal PTEN-like phosphatases

Phylogenetic relationships of the *E. festucae* Fl1 Ptn1 protein with other related fungal peptide sequences. The phylogenetic tree in this figure was prepared in the MacVector 7.2.3 program, using Neighbour joining and bootstrapping (1000 replicates) of sequences aligned using the ClustalW module of MacVector to form the tree. For details of the sequences used in this alignment, see Appendix A13.7. In this phylogenetic tree, the Fl1 Ptn1 protein name is shown in blue text, with all other protein names in black text. Cdc14, Pps1, PTEN and Yvh1-like phosphatase groups are indicated by blue, green, red and yellow lines respectively.

APPENDIX

A6: Analysis of Gao1

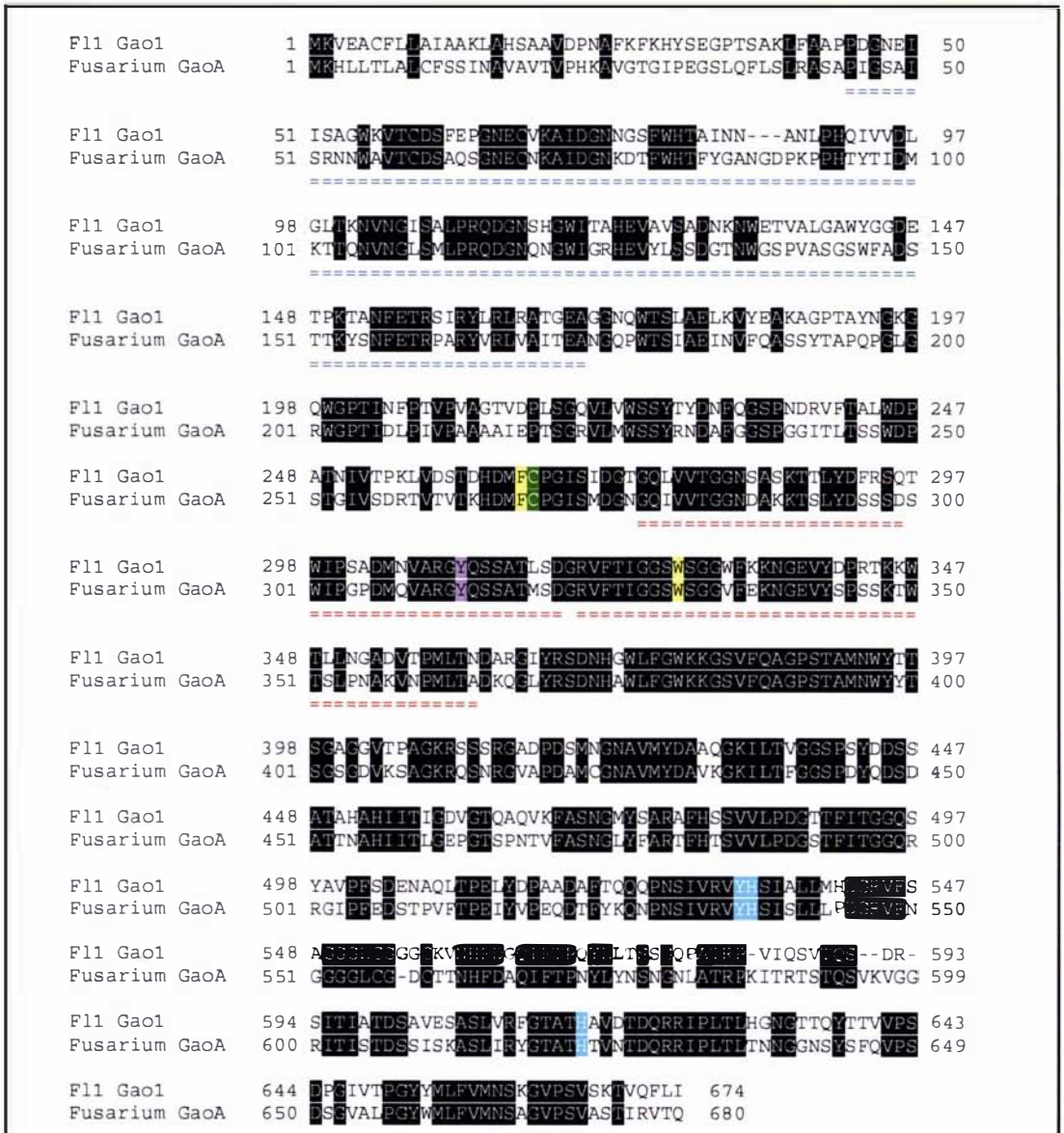

Appendix 6.1 Alignment of Gao1 with GaoA from *Fusarium* sp.

Alignment of the *E. festucae* Fl1 galactose oxidase precursor protein with the related peptide sequence from *Fusarium* sp. (accession number Q01745). Residues conserved between the two proteins are shown by white text in black boxes. Tyrosine 313 (shown in whtie text in a purple box) and cysteine 269 (shown in green) form an unusual covalent bond critical for enzyme activity. Tyrosine 536, Histidine 537, and Histidine 623 (shown in white text in a blue box) together with Tyrosine 313 bind the copper co-factor critical for enzyme activity. Also shown are residues phenyalanine 268 and tryptophan 333, which both interact with amino acid residues in the active site.

Conserved domains are indicated by underscoring below the alignment. Blue underscoring represents a putative sugar binding domain, with two Kelch domains shown in red underscoring.

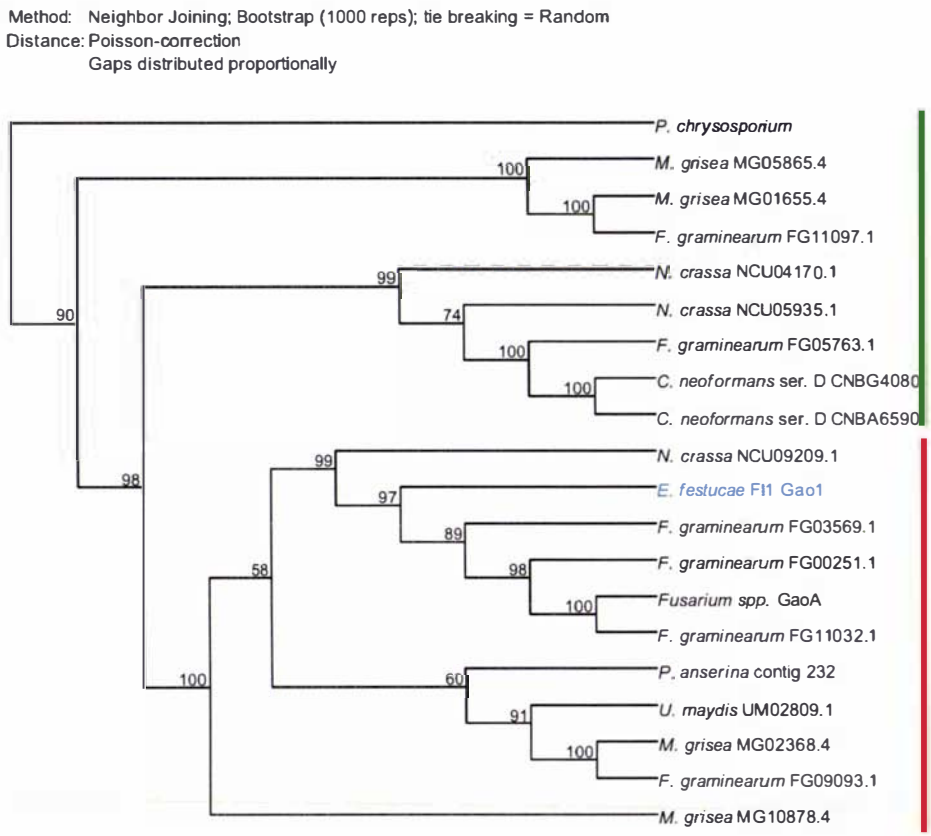

APPENDIX 6.2 Phylogenetic analysis of the *E. festucae* FI1 Gao1 protein with D-galactose oxidases

Alignment of the deduced *E. festucae* FI1 Gao1 protein with galactose and glyoxal oxidases from other organisms. The phylogenetic tree in this figure was prepared in the MacVector 7.2.3 program, using Neighbour joining and bootstrapping (1000 replicates) of sequences aligned using the ClustalW module of MacVector to form the tree. For details of the sequences used in this alignment, see Appendix A13.8. In this phylogenetic tree, the *E. festucae* FI1 Gao1 protein name is shown in blue text, with all other protein names in black text. Glyoxal and galactose oxidases are indicated by green and red lines respectively.

APPENDIX

A7: Design of degenerate primers

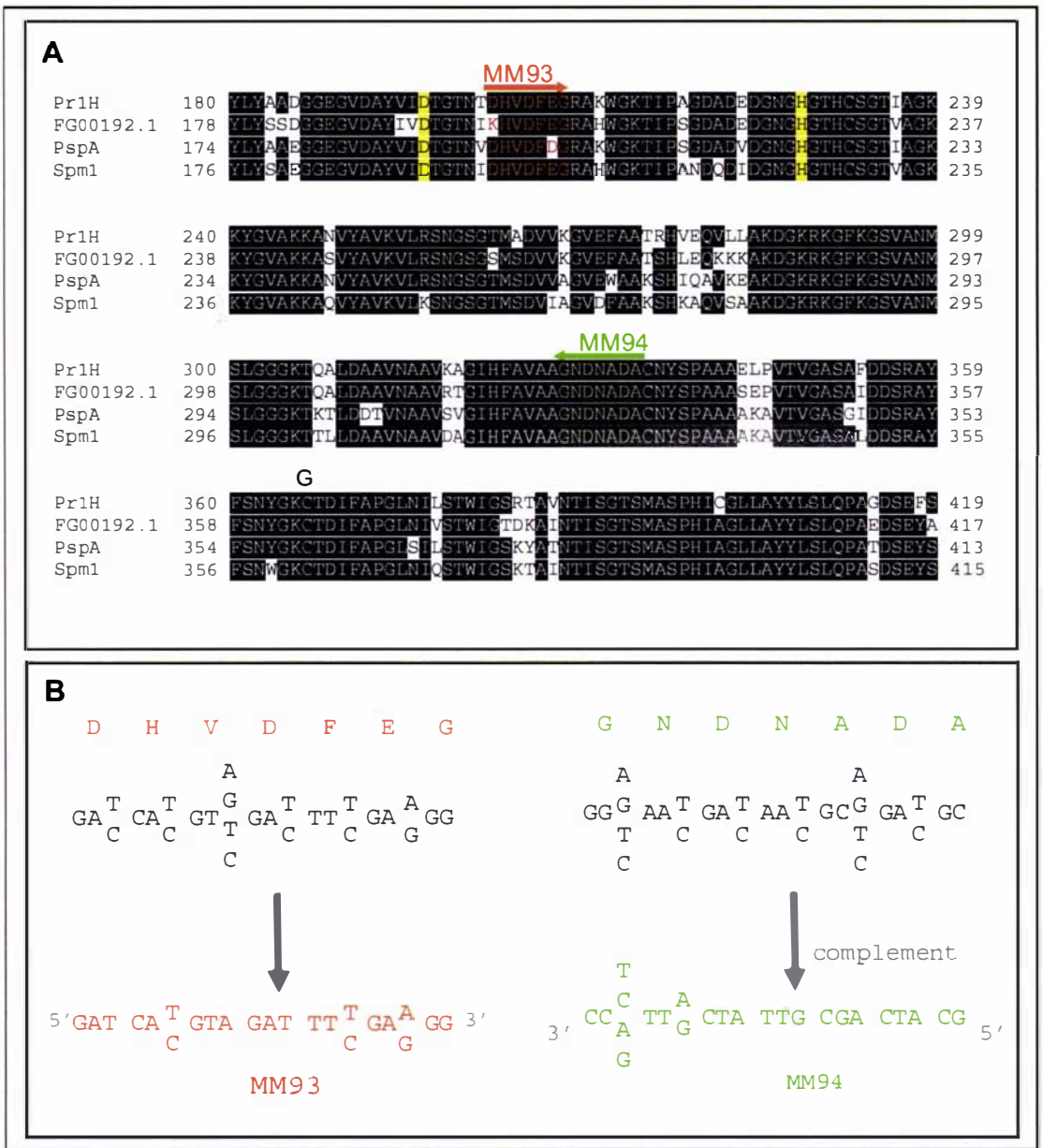

Appendix A7.1 Design of degenerate PCR primers used to amplify the vacuolar protease encoding gene *prt4*

(A) Partial alignment of peptide sequences corresponding to homologues of the *S. cerevisiae* Prb1 protein from the fungi *M. anisopliae* (Pr1H), *F. graminearum* (FG00192.1), *P. anserina* (PspA) and *M. grisea* (Spm1). Identity between the peptide sequences is shown by black shading with white text. The position where the primers were designed are indicated by black shading with either orange (MM93) or green (MM94) text respectively, together with an arrow of the same colour showing the direction of amplification. Conserved residues required for catalytic activity of the enzyme are indicated by black text with yellow shading. **(B)** The peptide sequences to which the MM93 and MM94 sequences were designed are shown in orange and green respectively. The nucleotide sequence that codes for this sequence is shown beneath the peptide sequence in black text, with multiple letters at positions where more than one codon specifies the same amino acid. The sequence of the the derived MM93 and MM94 primers is shown below in orange and green text respectively.

Appendix A7.2 Design of degenerate primers for *prt* isolation

Gene	Organism	Class	H site	S site
FG09156.1	*F. graminearum*	Kexin	RHGTRCA	GTSAAAP
MG03742.4	*M. grisea*	Kexin	RHGTRCA	GTSAAAP
NCU03219.2	*N. crassa*	Kexin	KHGTRCA	GTSAAAP
FG02956.1	*F. graminearum*	Other	GHGTHVG	GTSMAAP
FG03331.1	*F. graminearum*	Other	GHGTHVA	GSSMSSQ
FG04375.1	*F. graminearum*	Other	GHGTHIA	GTSVSTP
FG04506.1	*F. graminearum*	Other	GHGTHCA	GTSCAAP
FG09115.1	*F. graminearum*	Other	GHGTAVA	GSSFACP
FG11223.1	*F. graminearum*	Other	GHGTHVC	GTSMSTP
MG04939.4	*M. grisea*	Other	GHGTFVT	GTSFATP
FG02976.1	*F. graminearum*	protK sf1	GHGTHVA	GTSMASP
FG03315.1	*F. graminearum*	protK sf1	GHGTHVA	GTSMACP
MG08966.4	*M. grisea*	protK sf1	GHGTHVA	GTSMASP
MG10449.4	*M. grisea*	protK sf1	GHGTHVA	GTSMATP
NCU07159.2	*N. crassa*	protK sf1	GHGTHVA	GTSMATP
Pr1A	*M. anisopliae*	protK sf1	GHGTHCA	GTSMATP
Pr1B	*M. anisopliae*	protK sf1	GHGTHLA	GSSMSAA
Pr1G	*M. anisopliae*	protK sf1	LHGTHVA	GTSMAAP
Pr1I	*M. anisopliae*	protK sf1	GHGTHVA	GTSMATP
Pr1K	*M. anisopliae*	protK sf1	GHGTHVA	GTSMASP
FG00806.1	*F. graminearum*	protK sf2	GHGTHVA	GTSMATP
FG08012.1	*F. graminearum*	protK sf2	GHGTHCA	GTSMATP
FG08464.1	*F. graminearum*	protK sf2	GHGTHVA	GTSMACP
FG09382.1	*F. graminearum*	protK sf2	GHGSHVA	GTSMASP
FG10525.1	*F. graminearum*	protK sf2	GHGTHCA	GTSMACP
FG10595.1	*F. graminearum*	protK sf2	QHGTLVA	GTSEAAP
FG10712.1	*F. graminearum*	protK sf2	QHGTLVA	GTSEASP
FG11405.1	*F. graminearum*	protK sf2	GHGTHVA	GTSMAAP
MG02863.4	*M. grisea*	protK sf2	GHGTHVA	GTSSATP
MG06558.4	*M. grisea*	protK sf2	GHGTHVA	GTSMATP
MG07965.4	*M. grisea*	protK sf2	GHGSHVA	GTSMATP
NCU06055.2	*N. crassa*	protK sf2	GHGSHVA	GTSMASP
NCU06949.2	*N. crassa*	protK sf2	GHGTHVT	GTSMASP
Pr1D	*M. anisopliae*	protK sf2	GHGTHVA	GTSMASP
Pr1E	*M. anisopliae*	protK sf2	IHGDHGT	GSSFATP
Pr1F	*M. anisopliae*	protK sf2	GHGTHVA	GTSMAAP
Pr1J	*M. anisopliae*	protK sf2	GHGTHVA	GTSQAAP
FG06572.1	*F. graminearum*	pyrolysin sf1	GHGTHVA	GTSMASP
FG11472.1	*F. graminearum*	pyrolysin sf1	GHGTHVA	GTSMACP
MG00282.4	*M. grisea*	pyrolysin sf1	IHGTHVLG	GTSMATP
MG03316.4	*M. grisea*	pyrolysin sf1	GHGTHVT	GTSMACP
MG03870.4	*M. grisea*	pyrolysin sf1	GHGTHVA	GTSMACP
MG07358.4	*M. grisea*	pyrolysin sf1	AHGTHVS	GTSMAAP
MG08415.4	*M. grisea*	pyrolysin sf1	GHGTHVA	GTSMAAP
MG10445.4	*M. grisea*	pyrolysin sf1	GHGTHVA	GTSMATP
NCU00263.2	*N. crassa*	pyrolysin sf1	GHGSHVL	GTSMACP
Pr1C	*M. anisopliae*	pyrolysin sf1	GHGSHVA	GTSMSCP
FG06332.1	*F. graminearum*	pyrolysin sf2	GHGTHVA	GTSMSAP
MG02531.4	*M. grisea*	pyrolysin sf2	GHGTHVA	GTSMACP
MG02649.4	*M. grisea*	pyrolysin sf2	GHGTHVA	GTSMATP
MG04733.4	*M. grisea*	pyrolysin sf2	GHGTHVA	GTSMATP
MG08429.4	*M. grisea*	pyrolysin sf2	GHGTHVA	GTSMATP
MG08436.4	*M. grisea*	pyrolysin sf2	GHGTHVA	GTSMATP
MG09352.4	*M. grisea*	pyrolysin sf2	GHGTHVA	GTSQATP
MG09817.4	*M. grisea*	pyrolysin sf2	GHGTHVA	GTSMATP
MG09990.4	*M. grisea*	pyrolysin sf2	GHGTHVA	GTSMATP
FG00192.1	*F. graminearum*	Vacuolar	GHGTHCS	GTSMASP
MG03670.4	*M. grisea*	Vacuolar	GHGTHCS	GTSMASP
NCU00673.2	*N. crassa*	Vacuolar	GHGTHCS	GTSMASP
Pr1H	*M. anisopliae*	vacuolar	GHGTHCS	GTSMASP

protK sf1 and protK sf2 stand for proteinase K subfamily 1 and proteinase K subfamily 2 respectively
pyrolysin sf1 and pyrolysin sf2 stand for pyrolysin subfamily 1 and pyrolysin subfamily 2 respectively
The MM149 primer was designed to the H site and the MM150 primer was designed to the S site

APPENDIX

A8: Analysis of Orf2

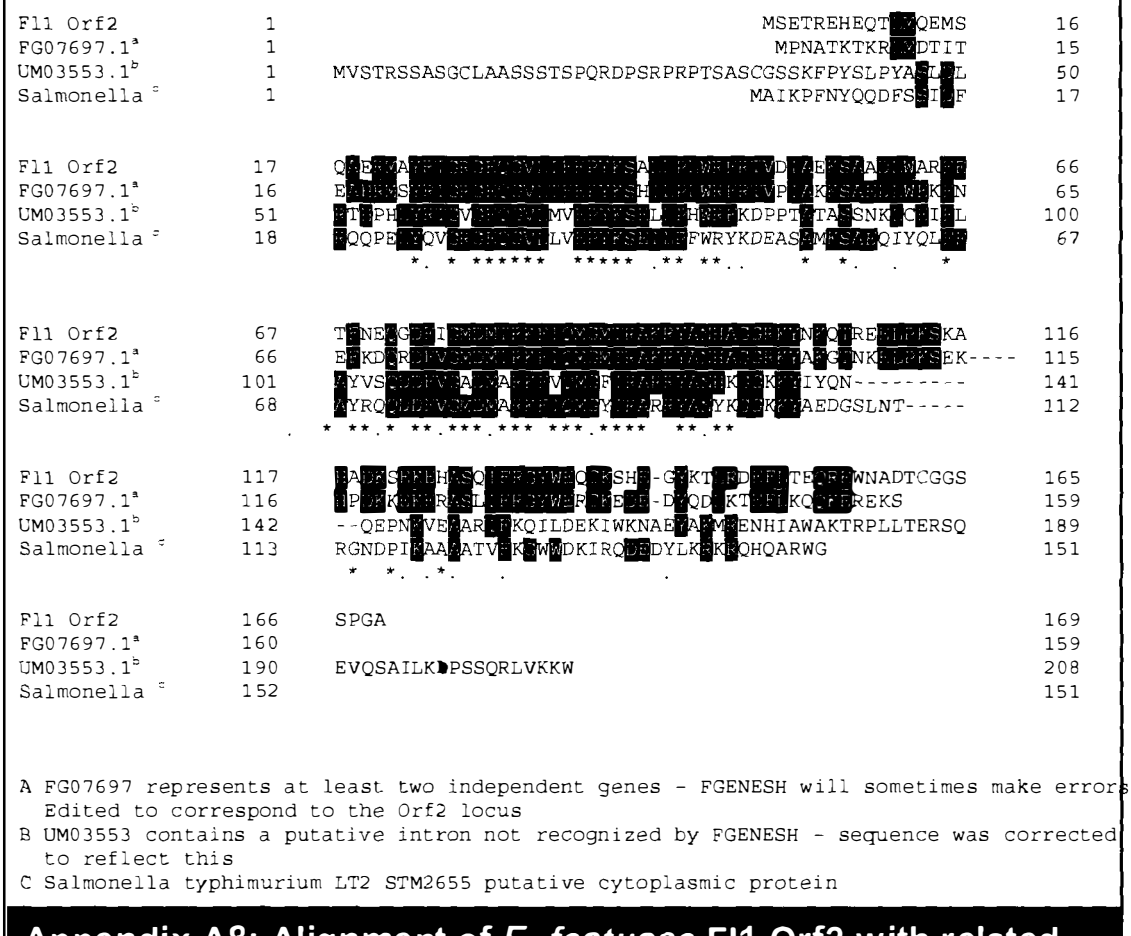

A FG07697 represents at least two independent genes - FGENESH will sometimes make errors Edited to correspond to the Orf2 locus

B UM03553 contains a putative intron not recognized by FGENESH - sequence was corrected to reflect this

C Salmonella typhimurium LT2 STM2655 putative cytoplasmic protein

Appendix A8: Alignment of *E. festucae* Fl1 Orf2 with related fungal and bacterial sequences

Alignment of the *E. festucae* Fl1 Orf2 protein with related sequences from *F. graminearum* (FG07697.1), *U. maydis* (UM03553.1) and *Salmonella typhimurim*. Identity between the sequences is indicated by black shading.

APPENDIX

A9: Analysis of Orf3

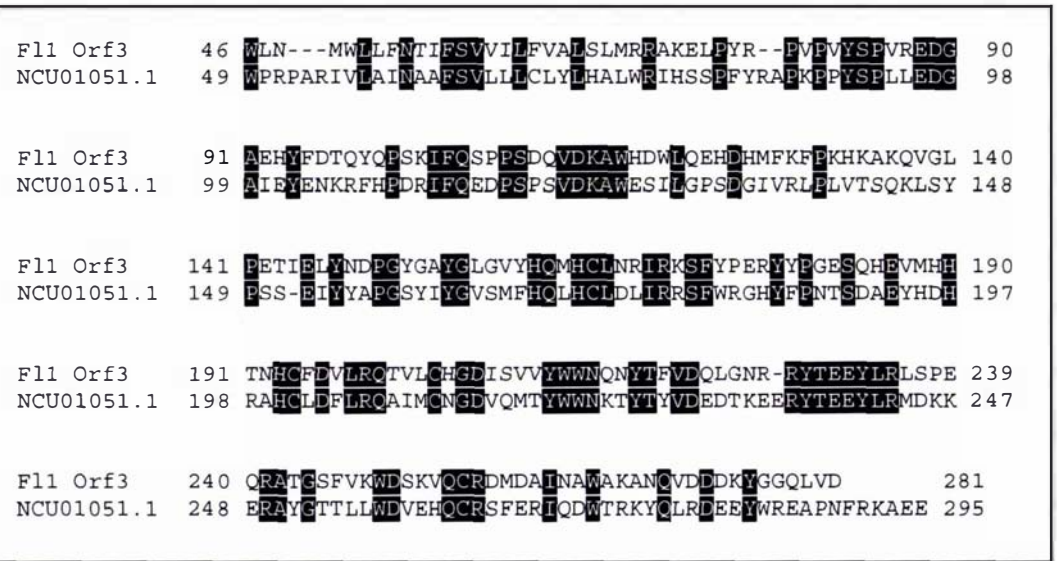

Appendix A9: Alignment of *E. festucae* Fl1 Orf3 with the NCU01051.1 sequence

Alignment of the *E. festucae* Fl1 Orf3 polypeptide with NCU01051.1. Identity between the sequences is indicated by black shading.

APPENDIX

A10: Analysis of Nc25

Appendix A10: Alignment of *E. festucae* Fl1 Nc25 with related *Neotyphodium* sequences

Alignment of the *E. festucae* Fl1 Nc25 polypeptide with the homologous sequences from *N. lolii* and *N. coenophialum*. Identity between the sequences is indicated by black shading. The *E. festucae* Fl1 Nc25 protein is 88% identical to the *N. coenophialum* Nc25 protein, and 54% identical to the *N. lolii* Nc25 protein.

APPENDIX

A11: MEME analysis for *prt* promoters

Appendix 11.1: MEME analysis of *E. festucae* Fl1 *prt* promoters

MEME (Multiple Excitation Maximisation for Motif Elicitation) analysis of the *E. festucae* Fl1 *prt* promoters was performed at the website http://meme.sdsc.edu/meme/website/meme.html (Bailey and Elkan, 1994). MEME analysis using an algorithm to recognise motifs (defined as a sequence pattern that occurs repeatedly in a group of DNA sequences) from a given subset of sequences.

The promoter regions from the *prt1, prt2, prt3, prt4* and *prt5* genes were submitted for MEME analysis. The distribution of motifs within the sequence was set as "any number of repetitions", with a maximum number of 25 motifs searched for. The minimum motif size was set to 5bp, and the maximum size to 50 bp.

The 25 motifs discovered are indicated on the promoter sequences as shown in Figures 3.6, 3.12, 3.17, 3.24 and 3.29. Motif numbers were entered, with common motifs having a particular colour to differentiate them from other motifs. Less common motifs were left uncoloured. A list and alignment of the motif sequences is shown in Appendix 11.2. The sequence alignments of the motifs are shown on the next four pages.

Appendix 11.2 MEME motifs

MOTIF 1:

Multilevel consensus sequence: AAAAAAAAAAAAGAAAAAAA

NAME	STRAND	START	P-VALUE	SITES
prt1	+	264	3.74e-13	CCACTTTAAA AAAAAAAAAAAAGAAAAAAA GTGGCCAGGT
prt3	-	961	1.12e-12	GCGAGTCAAA AAAAAAAAAAAAAAAAAAAA GGCAAGGTTT
prt1	-	1044	4.97e-10	CGAATTCGAG AAAGAAAGGGAAAAAAAAAA CCCGTCTCCA
prt1	-	179	9.06e-10	AATGCGAGGA AGAAAAAAAAAAAGTAAATAC AATCGAAAGA
prt3	+	1730	2.36e-09	GCGTCGACGC AAAAAAGAAGAAGAAGAAAA CCAGCATCTT
prt1	+	1562	2.70e-09	TCTTGTTGGG AGAAAAAAAAAAGTACTTAA GGGCCCATGA
prt1	-	223	1.57e-08	GCACGAGTGA CGAGAAAAAAAAGTCACTAA TGTCATGTAT
prt2	-	1921	2.02e-08	TTCCACCACC CGAAAATAAAAAAAACAATA CTCCGCGGGC
prt1	-	1122	2.89e-08	AAAGGAATCC AACGAAAGGAAAGAGACAAA GCCACCAAGC
prt1	-	783	7.34e-08	GCGACCGTGA TTGGAAAGGGAAAAAAAAAA CCTTGCGGTC

MOTIF 2:

Multilevel consensus sequence: GCTCCCTACCCTCCATGCATGCCATGACG

NAME	STRAND	START	P-VALUE	SITES
prt3	+	765	9.32e-17	ACGGGGAGTT GCTCCCTTCCCTCGATGCATGCCATGACG GAACCGGGCC
prt3	+	708	7.78e-15	TTACTACTTT GCTCCGTTTCCTCGATGCATGCCATGACG AAACCGGCCT
prt2	-	1635	4.93e-12	TTCGTGGCTC CCCCCCTCCCCTCCGTTGTTGACATGTCG CCGGGAAAGG
prt5	+	1637	1.11e-10	ATTCCAAGGC GCTTCATCCCCATCATTCTTCCCATCTCG CTTATCTCGC
prt1	+	409	2.15e-10	CAATGACTCG GCAAGGTAGCATCTAACCATGACATGACG GTTACAATCC
prt3	+	1463	2.71e-10	GGCAGTCTTG GCTCTCTACTTTCCGAGGTAGCCAAGACA ATTCGAAAGA

MOTIF 3:

Multilevel consensus sequence: GGCCTTGTTGGGTGCGGCGA

NAME	STRAND	START	P-VALUE	SITES
prt3	+	800	1.22e-10	GACGGAACCG GGCCTCGTTGGGTACGGGGA GTACGAGCCG
prt3	+	742	8.39e-10	TGACGAAACC GGCCTCATTGGGTACGGGGA GTTGCTCCCT
prt2	-	1309	1.13e-09	TCACGGCCGC GGCCTTGTTGGGCGCCGCCA TTTATCAATT
prt5	+	993	2.44e-09	AATCCATCAT CGCCTTGTTGCCTGCCGACA AATCTTCCAT
prt4	+	1296	8.05e-09	GTTGGCCGGG CGCATTGATGGCTGCGGCCA TTGGCCTCAC
prt3	+	1770	1.07e-08	GTCGCTGAGC GGGCATCTTGGCTGCGGCGA AAGCCAATAT
prt4	-	1148	2.88e-08	AGTACACGCG GCCCTCTTTGCGTGCGGAGG AGTGCACTGG

Appendix 11.2 MEME motifs

MOTIF 4:

Multilevel consensus sequence: CCTGGACCCTGTTCTC

NAME	STRAND	START	P-VALUE	SITES
prt3	-	1700	7.06e-09	CGACGCCATG TCTTGACTTTGTTCTC GTAATATTTT
prt2	-	124	9.06e-09	CGTATCTCAG CCTTGACTCTGTTTTC ATCATCTAGG
prt5	-	1699	4.62e-08	GAAAGAAGTT TCTGGACCTTGTTCTG GGTCGTCTAT
prt5	-	1058	7.65e-08	TTCCCTGTCT CCTATCCCCTGTTCTC ACGAGTTCAC
prt5	-	1084	1.32e-07	TCCTCTGTCC CCTGTTCCCTGTTCTG TTCCCTGTCT
prt5	-	1105	2.12e-07	TCCCGGAGAC CCTGTCCCCTGTCCTC TGTCCCCTGT
prt2	+	1437	2.30e-07	CCTGGTGGCT CCATGACTTTGTTCTT CAGATGGCCG
prt5	+	326	9.03e-07	GTCTCTCGTT CCTCGGATTTGTTTTC CGACACGAAT

MOTIF 5:

Multilevel consensus sequence: ATATATACATATA

NAME	STRAND	START	P-VALUE	SITES
prt3	+	1903	7.85e-09	CTCTCTGTAT ATATATATATATA TTCATCCATC
prt2	-	1127	7.85e-09	CCAGCATCGG ATATATATATATA CCGGAGATGG
prt5	+	747	7.10e-08	CTCCCCGCAC ATATATACACATA CGGCCGAGAG
prt1	-	744	1.31e-07	CGCATAATAC ATACATACATATC ACTGACCTCT

MOTIF 6:

Multilevel consensus sequence: GGCTTGCCGAGCTGC

NAME	STRAND	START	P-VALUE	SITES
prt5	+	834	4.78e-09	ATCAATGGGC GGCTTGCCGATCTGC AAAAGGAGGC
prt5	+	265	2.51e-08	CCATCCGTAC GGCTTGCCGATTTGC ACGCACGGCA
prt4	-	262	5.31e-07	GTTCCATATC GCCATGCCGATCTTC CCTCTGTCAT
prt5	+	1451	5.31e-07	TCTTGGGTCT GGGTTGCCAACTTGC TAGTAACCTA
prt4	-	1330	1.13e-06	AGGTAGATAA GGCAAGCCAAGCTGC CAACGTGAGG
prt2	+	2281	1.13e-06	AAAAGTCCTC TGATTCCCAAGCTTC AGGTGTCAAC
prt5	-	160	1.32e-06	GATCAGGCCA GGCTTCCCATCCTTC CTTCCCCGCG
prt3	-	834	1.43e-06	ACGATCAATC GCGTACCCGAGCTTC CCGGCGGCTC
prt2	-	1081	1.80e-06	GCACGGAGAC ACCTTCCCGATTTGC ATGTGCATGA
prt5	+	922	1.80e-06	CGGCCTCGGG GAGTTTCCGAGCTTC TTCGTGTATC
prt5	-	1022	2.26e-06	AGACTCTTCT TGCTTGCCGAGTTGA TGGAAGATTT
prt2	+	786	3.16e-06	CAAGACTTCA GCATTTCCATGCTGC AAAGAACTCA

MOTIF 7:

Multilevel consensus sequence: ATCGGCATCGACATC

NAME	STRAND	START	P-VALUE	SITES
prt3	-	1500	6.74e-09	CACATGAAGA ATGGGCATCGACATC TTTCGAATTG
prt4	+	1600	1.35e-08	AACTACCGGC ATCGGCATCATCATC ATCATCATCA
prt2	+	1776	2.62e-08	AAAGTCTTAC ATTGGCATCGGCATC TCATCTTGTG
prt3	+	452	7.18e-08	TTTGTTGGGG CTCAGCATCGACATC CAACACGTCG
prt5	-	1147	7.18e-08	GGAGGGAGCA ATCGCCATCGACAAC CAGCCGCGTC
prt3	-	853	3.25e-07	ACAACAGGCG AGCGGCATCACGATC AATCGCGTAC

MOTIF 8:

Multilevel consensus sequence: GTATCAATTCGCAGACATGTC

NAME	STRAND	START	P-VALUE	SITES
prt4	+	53	6.32e-11	ATAAGCACAA GTCTCAATTTGCAGACCTTTC TGGCGGTAAG
Prt2	-	1287	2.15e-09	GCGCCGCCAT TTATCAATTCCCTGAAATCTC ACACAAACTG
prt3	-	928	8.47e-09	CAAGGTTTGG GAATCAATTTGCTTGCATCTC ATCCCCCGCA
prt5	+	950	2.36e-08	GTGTATCGAC TTATCTATTCGCAGCCTGTCC AATGGCAAAT
Prt2	+	893	4.07e-08	CGTCTTTCAC GGCGCAATTAGCAGACTTGTC GACTCAAAAG
prt2	+	627	5.03e-08	CTCTGTTTGT TAATCTATTCCAAGACCTTGC TTTGTTTGTG
prt4	-	733	6.65e-08	CTGCCATCAT TTATCATTTCACACGCAGGTC GTCACTACAT
prt2	-	732	7.14e-08	GGTATCAAGA GTTTCAAAATGCAGACATGAC CCTCCTGGAG

Appendix 11.2 MEME motifs

MOTIF 9:

Multilevel consensus sequence: TTTTCGAGTATTTTTA

NAME	STRAND	START	P-VALUE	SITES
prt1	+	679	2.57e-10	CGCTTCCAAG TTTTTGAGTTTTTTTA ACCCGCCCCG
prt4	+	5	5.39e-10	AAGC TTTTCGAGTATTTTTA TCGGGATTTC

MOTIF 10:

Multilevel consensus sequence: TTCTTTCCATG

NAME	STRAND	START	P-VALUE	SITES
prt5	-	1611	4.07e-07	GGAATCCAAT TTCTTTCCATG ATGCTGGGCG
prt4	-	95	8.15e-07	CGTTGCAACT TTGTTTCCATG TCAAATACCA
prt2	+	470	1.63e-06	GGATGACTGC TTCTTTGCAAG TTGGGGACGG
prt5	+	1718	1.63e-06	GTCCAGAAAC TTCTTTCCAAG TTACCAAATC
prt3	-	1622	2.44e-06	GCAGTCAGCG TTGTTTGCATC GAGGGTGTAA
prt2	-	1223	3.26e-06	GACCTTGAGC TTCTATGCATG GCGCGGGAGA
prt2	-	295	5.38e-06	CTTGTGGTGG GTGTTTCCATG ACGCATCAAT
prt2	+	368	7.42e-06	CCTAGAAGCA TTCATTGCATC AAAATTCGGT

MOTIF 11:

Multilevel consensus sequence: AATCATTTTAT

NAME	STRAND	START	P-VALUE	SITES
prt4	-	218	3.05e-07	TGAATAAGCT AATCATTTTAT CCTTCATGCA
prt2	+	433	3.05e-07	ATTTCCCGAC AATCATTTTTT CGGCCTTCTG

MOTIF 12:

Multilevel consensus sequence: TTGGCAATGCAACACATGAGCA

NAME	STRAND	START	P-VALUE	SITES
prt1	+	837	1.90e-10	CTTTGACTTC TTGGCCATGAAACCCCTGAGCA GAGGCCCGTT
prt2	+	1569	3.14e-10	CGCGTCTCCC TCGGCCATGCATCAAGTGAGCA ACTGCAGGCA
prt3	-	1515	1.24e-09	AGGCTGTCCA TTGGCAATCGACCACATGAAGA ATGGGCATCG
prt4	-	428	1.37e-09	AGTACTTCTG TTGGCTGTCCAACAACTCATCA CAAGGGAGAA
prt5	-	862	2.46e-09	GCATTGCTGA TTGGCTGTGCAATTCATGATAA CGGGCCTCCT
prt3	+	1243	1.24e-08	TGCTGATGTC TCGGCAATTGACCTCGAGAGCT TTGTCGACAG

MOTIF 13:

Multilevel consensus sequence: AAATATTGAGAG

NAME	STRAND	START	P-VALUE	SITES
prt1	-	1538	8.81e-08	CAACAAGAGC AAATATTGTGAG ATCGGGCCGC
prt3	+	235	8.81e-08	AACAGAATGA AAATATTGAGAG TAAGTGAGTG

MOTIF 14:

Multilevel consensus sequence: TAAAACTTACCATAAG

NAME	STRAND	START	P-VALUE	SITES
prt3	+	372	1.13e-09	ACGCCACAGA TAATACTTATCATAAG GTGCTTCTTA
prt3	+	1579	2.37e-09	TCGGTATTAG TATAAGTTACCATAAG CCCATGTTTC

Appendix 11.2 MEME motifs

MOTIF 15:

Multilevel consensus sequence: TTGTACTCCGTACT

NAME	STRAND	START	P-VALUE	SITES
prt4	+	1171	7.23e-08	AGAGGGCCGC GTGTACTCCGTACT CGCCACCGGA
prt2	+	264	1.09e-07	CAGAGAGCAG TTGTACTCCGTAGA GTTGGGTATT
prt4	+	565	1.43e-07	ATTTGGCCAT TTTTACTCCGTCCT TCGCAGGCCT
prt3	-	1357	1.85e-07	AATCCTATCG TAGTATTCCGTAAT GGCTTTCGAA
prt4	+	1059	3.04e-07	TGGCCGGCTA TTGTGCTCCGTCGT CGGTTGCATT
prt5	-	1360	5.00e-07	AGCAATCTCG TTGTCCTCCGGACT CCTCCCTGAA
prt5	+	241	1.06e-06	AAGTAGTTGC TACTAGTCCGTAAT CCATCCGTAC

MOTIF 16:

Multilevel consensus sequence: ACTCAAAA

NAME	STRAND	START	P-VALUE	SITES
prt2	+	2267	1.25e-05	CCTCTGAGAG ACTCAAAA GTCCTCTGAT
prt2	+	1483	1.25e-05	CGTCCCACCG ACTCAAAA GCCGGCGGTC

MOTIF 17:

Multilevel consensus sequence: AATGTAGT

NAME	STRAND	START	P-VALUE	SITES
prt4	+	722	1.25e-05	TCATACTTAC AATGTAGT GACGACCTGC
prt3	+	63	1.25e-05	ACGTGTAGTC AATGTAGT TAGTGCATGG

MOTIF 18:

Multilevel consensus sequence: ACGCAATGTAGG

NAME	STRAND	START	P-VALUE	SITES
prt5	+	1243	5.88e-08	GTAGGCAATC ACGCAATGTAGG CGACGCCCCC
prt4	+	113	1.18e-07	CAAAGTTGCA ACGCTATGTAGG TGGCTATCGA
prt5	+	1226	4.01e-07	GCCATGTTGT AGGCAATGTAGG CAATCACGCA
prt2	-	582	1.03e-06	ACGATGACAA ACGCGATATAGG AGGCTGCGAT
prt3	+	1193	1.85e-06	CAAGTCGGTC TCGCAATGTATG TCTCATGACA
prt1	+	127	2.65e-06	AATGACGACG ACGTTATGAAGG CTGCAGCAGG

MOTIF 19:

Multilevel consensus sequence: AAAAGAA

NAME	STRAND	START	P-VALUE	SITES
prt3	-	880	4.76e-05	TCTCCGCGAG AAAAGAA CAACAACAGG
prt5	+	122	4.76e-05	CGGTGATGTC AAAAGAA TGGTTGGGGT

MOTIF 20:

Multilevel consensus sequence: AATAGAT

NAME	STRAND	START	P-VALUE	SITES
prt4	+	496	4.76e-05	TTGCGAAGAG AATAGAT GGCAGCAGGC
prt1	-	923	4.76e-05	ACGCGAGGAC AATAGAT TGTAGAAGGT

MOTIF 21:

Multilevel consensus sequence: ACTTGTACATACAA

NAME	STRAND	START	P-VALUE	SITES
prt3	+	1384	1.45e-08	TAGGATTTGC ACTTTTACATACAA CAGAGTGAGC
prt2	+	2208	1.45e-08	CTTGATCCAA ACTTGTAGATATAA AAGGGGGCAA

Appendix 11.2 MEME motifs

MOTIF 22:

Multilevel consensus sequence: ACATGTTGTTGCATGC

NAME	STRAND	START	P-VALUE	SITES
prt2	+	1061	3.42e-10	AATTTGAGTG ACATTTTGTTTCATGC ACATGCAAAT
prt3	+	1034	1.51e-09	ACACACTTAC ACTTGTTGTTGCATGC TTTCGCCGAA

MOTIF 23:

Multilevel consensus sequence: TTTCACAAACAA

NAME	STRAND	START	P-VALUE	SITES
prt2	-	649	8.81e-08	TCGTCTCTGG TTTCACAAACAA AGCAAGGTCT
prt2	-	1177	1.85e-07	ATTTCCATAC TTTCCCAATCAA GAACGAGCGT

MOTIF 24:

Multilevel consensus sequence: ATGTTCAAT

NAME	STRAND	START	P-VALUE	SITES
prt1	-	206	2.97e-06	AATGTCATGT ATGTTCAAT GCGAGGAAGA
prt2	+	691	2.97e-06	TGGCCATTGG ATGTTCAAT CGCGCGGCAA

MOTIF 25:

Multilevel consensus sequence: TCGAATACTTTC

NAME	STRAND	START	P-VALUE	SITES
prt2	-	531	9.70e-08	ATGGCATGGG TCGATTACTTTC AGCGTTTGGG
prt5	+	293	9.70e-08	CACGGCACGC TCGAATACTTTC GACTGGGGTC

APPENDIX

A12: Raw data for assessing transgene copy number

APPENDIX A12.1 Raw data for copy number analysis in pMM32 transformants

NO[a]	SAMPLE[b]	PSL[c]	PSL-BG[d]	Ratio[e]	% of lane[f]	Dist (mm)[g]	RF[h]	INF[i]
1	MM19.1	2738.69	2082.97	100.00	100.00	1.55	0.04	S
1	MM8.1	5595.23	4470.03	100.00	28.96	2.80	0.08	S
2	MM8.1	14667.61	10966.03	245.32	71.04	27.85	0.77	I
1	MM8.2	7267.67	6864.90	100.00	1.65	2.60	0.07	S
2	MM8.2	7236.34	6512.71	94.87	1.56	7.40	0.21	
3	MM8.2	4085.45	3676.91	53.56	0.88	16.60	0.46	
4	MM8.2	13627.25	12264.53	178.66	2.94	18.95	0.53	
5	MM8.2	430756.80	387681.12	5647.29	92.97	27.90	0.77	I
1	MM8.3	7933.08	6849.97	100.00	13.55	2.45	0.07	S
2	MM8.3	46850.13	43700.95	637.97	86.45	27.90	0.77	I
1	MM8.4	6751.29	5345.20	100.00	20.65	2.30	0.06	S
2	MM8.4	22772.52	20544.19	384.35	79.35	27.80	0.77	I
1	MM8.5	8560.83	7079.73	100.00	2.47	1.95	0.04	S
2	MM8.5	3809.34	3144.14	44.41	1.10	7.10	0.20	
3	MM8.5	282870.45	276420.59	3904.40	96.43	27.50	0.76	I
1	MM8.6	10297.86	3135.04	100.00	2.61	1.70	0.05	S
2	MM8.6	10588.08	8968.74	286.08	7.47	7.15	0.20	
3	MM8.6	15946.16	8870.72	282.95	7.39	12.30	0.34	
4	MM8.6	9837.91	7702.58	245.69	6.42	17.50	0.49	
5	MM8.6	100428.22	91329.26	2913.18	76.10	27.25	0.76	I
1	MM8.7	7943.11	4794.47	100.00	12.36	1.40	0.04	S
2	MM8.7	7059.57	4621.49	96.39	11.91	3.00	0.08	
3	MM8.7	34066.25	28128.04	586.68	72.49	26.50	0.74	I
4	MM8.7	4750.83	1256.81	26.21	3.24	34.50	0.96	
1	MM8.8	9384.19	6422.66	100.00	20.81	1.50	0.04	S
2	MM8.8	17706.01	16267.79	253.29	52.72	27.30	0.76	I
3	MM8.8	9503.11	8165.95	127.14	26.46	30.25	0.84	

Samples shaded in yellow were selected for artificial inoculations into plants

[a] identifier for the detected band for this sample
[b] sample refers to the transformant strains analysed. The MM19.1 strain is wild type *E. festucae* Fl1 regenerated after protoplasting
[c] PSL refers to the measurement scale used to measure signal intensity
[d] PSL-BG is the PSL reading minus background signal
[e] Ratio is the ratio of the PSL-BG signal for a particular band compared to the standard (in this case, the PSL-BG signal obtained for the wild type *prt1* band)
[f] % of lane refers to the % of the total signal for a lane that the signal for a particular band represents
[g] Dist (mm) refers to the distance (in mm) that a particular DNA fragment is located at from a common start point
[h] RF shows the relative distance from the start point for a particular DNA fragment (where the whole length of the \blot is set to 1)
[i] This lane gives information about whether a particular band is at the wild-type genomic size (S, used as the standard) or at the expected size of the copies containing intact P*gpdA-prt1* coding regions (I).

APPENDIX A12.2 Raw data for copy number analysis in pMM33 transformants								
NO[a]	SAMPLE[b]	PSL[c]	PSL-BG[d]	Ratio[e]	% of lane[f]	Dist (mm)[g]	RF[h]	INF[i]
1	MM19.1	1633.43	1131.01	100.00	100.00	2.70	0.09	S
1	MM9.1	4020.07	3089.55	100.00	48.53	2.95	0.10	S
2	MM9.1	4067.52	3276.90	106.06	51.47	25.25	0.85	I
1	MM9.2	5852.21	5220.62	100.00	15.24	4.40	0.13	S
2	MM9.2	31663.08	29043.36	556.32	84.76	26.65	0.81	I
1	MM9.3	6331.07	1924.78	389.50	1.98	1.15	0.04	
2	MM9.3	3552.04	494.17	100.00	0.51	3.95	0.12	S
3	MM9.3	3953.15	962.63	194.80	0.99	5.65	0.17	
4	MM9.3	3034.90	1176.79	238.14	1.21	9.30	0.29	
5	MM9.3	6324.55	1967.49	398.14	2.02	13.20	0.41	
6	MM9.3	5337.01	1565.36	316.77	1.61	16.05	0.50	
7	MM9.3	98162.64	89174.92	18046.00	91.68	26.25	0.81	I
1	MM9.4	7106.24	5004.88	100.00	22.54	4.95	0.14	S
2	MM9.4	19938.80	17203.97	343.74	77.46	27.50	0.76	I
1	MM9.5	5292.78	1307.06	100.00	0.34	4.05	0.11	S
2	MM9.5	4586.46	682.01	52.18	0.18	5.55	0.15	
3	MM9.5	9158.46	2786.66	213.20	0.73	12.20	0.33	
4	MM9.5	9814.34	6300.06	482.00	1.64	20.05	0.54	
5	MM9.5	431885.00	361460.21	27654.00	94.30	28.60	0.77	I
6	MM9.5	44593.50	10773.52	824.26	2.81	33.50	0.90	

Samples shaded in yellow were selected for artificial inoculations into plants

[a] identifier for the detected band for this sample
[b] sample refers to the transformant strains analysed. The MM19.1 strain is wild type *E. festucae* Fl1 regenerated after protoplasting
[c] PSL refers to the measurement scale used to measure signal intensity
[d] PSL-BG is the PSL reading minus background signal
[e] Ratio is the ratio of the PSL-BG signal for a particular band compared to the standard (in this case, the PSL-BG signal obtained for the wild type *prt1* band)
[f] % of lane refers to the % of the total signal for a lane that the signal for a particular band represents
[g] Dist (mm) refers to the distance (in mm) that a particular DNA fragment is located at from a common start point
[h] RF shows the relative distance from the start point for a particular DNA fragment (where the whole length of the \blot is set to 1)
[i] This lane gives information about whether a particular band is at the wild-type genomic size (S, used as the standard) or at the expected size of the copies containing intact P*ltmM-prt1* coding regions (I).

APPENDIX A12.3 Raw data for copy number analysis in pMM26 transformants								
NO[a]	SAMPLE[b]	LAU[c]	LAU-BG[d]	Ratio[e]	% of lane[f]	Dist (mm)[g]	RF[h]	INF[i]
1	MM19.1	71641.39	46079.37	100.00	100	2.7	0.05	S
1	MM4.1	81286.82	49095.36	100.00	49.52	2.45	0.05	S
2	MM4.1	76364.81	50048.34	101.94	50.48	21.05	0.41	
1	MM4.2	72264.74	42927.13	100.00	33.81	2.70	0.05	S
2	MM4.2	114120.41	84056.43	195.81	66.19	33.80	0.65	I
1	MM4.3	31764.57	14352.35	100.00	6.12	2.95	0.06	S
2	MM4.3	254209.42	220329.67	1535.15	93.88	34.15	0.66	I
1	MM4.4	49175.82	28516.01	100.00	8.19	2.55	0.05	S
2	MM4.4	38420.98	20948.73	73.46	6.02	7.60	0.15	
3	MM4.4	69773.41	42408.48	148.72	12.18	18.10	0.35	
4	MM4.4	293234.05	256230.49	898.55	73.61	33.60	0.65	I
1	MM4.5	53306.30	29923.71	100.00	18.30	2.00	0.04	S
2	MM4.5	162482.24	133601.26	446.47	81.70	33.25	0.64	I
1	MM4.6	48414.79	25985.77	100.00	28.41	2.05	0.04	S
2	MM4.6	60797.67	31433.57	120.96	34.37	27.65	0.53	
3	MM4.6	66250.62	34047.33	131.02	37.22	33.00	0.64	I
1	MM4.7	26705.31	12175.74	100.00	1.39	1.95	0.04	S
2	MM4.7	39696.74	18020.88	148.01	2.06	8.10	0.16	
3	MM4.7	20591.48	9106.06	74.79	1.04	16.95	0.33	
4	MM4.7	40873.15	23351.81	191.79	2.67	19.55	0.38	
5	MM4.7	920917.45	788906.96	6479.34	90.16	32.75	0.63	I
6	MM4.7	55034.43				38.90	0.75	
7	MM4.7	55075.28	23475.15	192.80	2.68	47.90	0.92	
1	MM4.8	33164.53	15213.53	100.00	0.89	1.85	0.04	S
2	MM4.8	29105.34	16123.91	105.98	0.95	9.60	0.18	
3	MM4.8	46853.40	22614.86	148.65	1.33	18.75	0.36	
4	MM4.8	29395.23	6588.47	43.31	0.39	21.80	0.42	
5	MM4.8	57665.81	20380.83	133.97	1.20	25.15	0.48	
6	MM4.8	1690506.92	1599824.50	10515.80	93.95	32.80	0.63	I
7	MM4.8	70751.80	22064.28	145.03	1.30	41.40	0.80	
1	MM4.9	36863.78	11780.62	100.00	17.61	1.70	0.03	S
2	MM4.9	40553.15	12184.82	103.43	18.22	24.05	0.46	
3	MM4.9	72780.32	42917.37	364.30	64.17	32.60	0.63	I
1	MM4.10	83518.08	52974.81	100.00	25.51	1.45	0.03	S
2	MM4.10	187524.51	154692.47	292.01	74.79	32.35	0.62	I
1	MM4.11	41372.19	17149.21	100.00	3.09	1.40	0.03	S
2	MM4.11	65924.88	41417.60	241.51	7.46	13.40	0.26	
3	MM4.11	545480.92	496940.33	2897.74	89.46	32.75	0.63	I
1	MM4.12	92766.19	61266.13	100.00	76.57	2.30	0.04	S
2	MM4.12	39417.22	18747.91	30.60	23.43	32.90	0.63	I

Samples shaded in yellow were selected for artificial inoculations into plants

[a] identifier for the detected band for this sample
[b] sample refers to the transformant strains analysed. The MM19.1 strain is wild type *E. festucae* Fl1 regenerated after protoplasting
[c] LAU refers to the measurement scale used to measure signal intensity
[d] LAU-BG is the PSL reading minus background signal
[e] Ratio is the ratio of the LAU-BG signal for a particular band compared to the standard (in this case, the LAU-BG signal obtained for the wild type *prt2* band)
[f] % of lane refers to the % of the total signal for a lane that the signal for a particular band represents
[g] Dist (mm) refers to the distance (in mm) that a particular DNA fragment is located at from a common start point
[h] RF shows the relative distance from the start point for a particular DNA fragment (where the whole length of the \blot is set to 1)
[i] This lane gives information about whether a particular band is at the wild-type genomic size (S, used as the standard) or at the expected size of the copies containing intact P*gpdA-prt2* coding regions (I).

APPENDIX A12.4 Raw data for copy number analysis in pMM27 transformants								
NO[a]	SAMPLE[b]	LAU[c]	LAU-BG[d]	Ratio[e]	% of lane[f]	Dist (mm)[g]	RF[h]	INF[i]
1	MM19.1	35775.02	21029.98	100.00	100.00	4.15	0.06	S
1	MM5.1	37767.88	14277.20	100.00	17.61	2.60	0.04	S
2	MM5.1	96483.78	66809.73	467.95	82.39	32.50	0.50	I
1	MM5.2	36919.86	7340.12	100.00	11.53	3.10	0.05	S
2	MM5.2	92351.92	56346.56	767.65	88.47	32.90	0.50	I
1	MM5.3	32089.13	9342.02	100.00	12.25	2.65	0.04	S
2	MM5.3	24879.46	9526.07	101.97	12.49	7.50	0.12	
3	MM5.3	93225.29	57380.00	614.21	75.25	32.95	0.51	I
1	MM5.4	27141.75	9219.90	100.00	3.29	2.55	0.04	S
2	MM5.4	41656.85	14289.57	153.79	5.06	16.20	0.25	
3	MM5.4	308941.79	258958.39	2786.93	91.65	32.60	0.50	I
1	MM5.5	28154.68	9845.46	100.00	9.97	2.30	0.04	S
2	MM5.5	49582.38	20893.25	212.21	21.16	25.90	0.40	
3	MM5.5	81989.17	50463.30	512.55	51.11	32.25	0.50	I
4	MM5.5	40371.80	17523.75	177.99	17.75	49.50	0.76	
1	MM5.6	12354.38	2008.70	100.00	0.92	2.15	0.03	S
2	MM5.6	321181.89	216589.70	10782.58	99.08	32.40	0.50	I
1	MM5.7	32878.32	7390.24	100.68	27.08	2.60	0.04	S
2	MM5.7	45523.63	19897.46	271.07	72.92	32.95	0.51	I
1	MM5.8	27856.62	7743.58	100.00	2.18	3.20	0.05	S
2	MM5.8	432433.68	347796.23	4491.41	97.82	32.90	0.50	I
1	MM5.9	48396.29	22649.65	100.00	36.76	3.05	0.05	S
2	MM5.9	63269.92	38963.40	172.03	63.24	32.00	0.50	I
1	MM5.10	45667.15	28316.19	100.00	4.42	3.35	0.05	S
2	MM5.10	32503.63	15110.16	53.36	2.36	0.50	0.13	
3	MM5.10	76477.15	42249.94	147.21	6.60	18.50	0.28	
4	MM5.10	16969.38	6100.71	21.54	0.95	26.10	0.40	
5	MM5.10	606697.58	548769.26	1938.01	85.67	33.55	0.51	I
1	MM5.11	46145.04	24329.97	100.00	15.91	3.90	0.06	S
2	MM5.11	38848.39	6867.87	28.23	4.49	17.10	0.26	
3	MM5.11	152669.92	109958.07	451.94	71.91	34.10	0.52	I
4	MM5.11	38548.87	11759.19	48.33	7.69	41.30	0.63	
1	MM5.12	45268.79	25590.08	100.00	5.28	4.25	0.07	S
2	MM5.12	45268.79	14548.17	56.85	3.00	7.20	0.11	
3	MM5.12	488369.29	444442.31	1736.78	91.72	34.25	0.53	I

Samples shaded in yellow were selected for artificial inoculations into plants

[a] identifier for the detected band for this sample
[b] sample refers to the transformant strains analysed. The MM19.1 strain is wild type *E. festucae* Fl1 regenerated after protoplasting
[c] LAU refers to the measurement scale used to measure signal intensity
[d] LAU-BG is the LAU reading minus background signal
[e] Ratio is the ratio of the LAU-BG signal for a particular band compared to the standard (in this case, the LAU-BG signal obtained for the wild type *prt2* band)
[f] % of lane refers to the % of the total signal for a lane that the signal for a particular band represents
[g] Dist (mm) refers to the distance (in mm) that a particular DNA fragment is located at from a common start point
[h] RF shows the relative distance from the start point for a particular DNA fragment (where the whole length of the \blot is set to 1)
[i] This lane gives information about whether a particular band is at the wild-type genomic size (S, used as the standard) or at the expected size of the copies containing intact P*ltmM-prt2* coding regions (I).

APPENDIX

A13: Sequences used in phylogenetic analysis

APPENDIX A13.1 Nucleotide sequences used in rRNA phylogenetic analysis

SPECIES	PHYLUM	CLASS	ORDER	FAMILY	ACCESSION
Rhizopus oryzae	Zygomycota				AY213685
Cryptococcus neoformans	Basidiomycota	Heterobasidiomycetes	Tremellales	Tremellaceae	AJ876598
Pseudohydnum gelatinosum	Basidiomycota	Heterobasidiomycetes	Auriculariales	Hyaloriaceae	AF384861
Pleurotus ostreatus	Basidiomycota	Homobasidiomycetes	Agaricales	Pleurotaceae	AY540332
Coprinus cinereus	Basidiomycota	Homobasidiomycetes	Agaricales	Agaricaceae	AB097562
Phanerochaete chrysosporium	Basidiomycota	Homobasidiomycetes	Agaricales	Agaricaceae	
Ustilago maydis	Basidiomycota	Ustilaginomycetes	Ustilaginales	Ustilaginaceae	AY854090
Tilletiopsis albescens	Basidiomycota	Ustilaginomycetes	-	-	AB025697
Saccharomyces cerevisiae	Ascomycota	Saccharomycetes	Saccharomycetales	Saccharomycetaceae	SCE275936
Yarrowia lipolytica	Ascomycota	Saccharomycetes	Saccharomycetales	Dipodascaceae	DQ249205
Hyaloria brevisipitis	Ascomycota	Orbiliomycetes	Orbiliales	Orbiliaceae	AY514636
Arthrobotrys oligospora	Ascomycota	Orbiliomycetes	Orbiliales	Orbiliaceae	AY773462
Monacrosporium leptospermum	Ascomycota	Orbiliomycetes	Orbiliales	Orbiliaceae	AY773466
Verticillium dahliae	Ascomycota	Sordariomycetes	Phyllachorales	mitosporic Phyllachorales	DQ282123
Ophiostoma piliferum	Ascomycota	Sordariomycetes	Ophiostomatales	Ophiostomataceae	AY934516
Leptographium truncatum	Ascomycota	Sordariomycetes	Ophiostomatales	mitosporic Ophiostomaceae	AY935625
Trichoderma asperellum	Ascomycota	Sordariomycetes	Hypocreales	Hypocreaceae	AY667149
Trichoderma reesei	Ascomycota	Sordariomycetes	Hypocreales	Hypocreaceae	scaffold 862
Trichoderma harzianum	Ascomycota	Sordariomycetes	Hypocreales	Hypocreaceae	AF278793
Trichoderma virens	Ascomycota	Sordariomycetes	Hypocreales	Hypocreaceae	DQ083023
Atkinsonella hypoxylon	Ascomycota	Sordariomycetes	Hypocreales	Clavicipitaceae	AHU57405
Epichloe festucae	Ascomycota	Sordariomycetes	Hypocreales	Clavicipitaceae	L07139
Epichloe typhina	Ascomycota	Sordariomycetes	Hypocreales	Clavicipitaceae	L07132
Claviceps purpurea	Ascomycota	Sordariomycetes	Hypocreales	Clavicipitaceae	DQ119114
Verticillium chlamydosporium	Ascomycota	Sordariomycetes	Hypocreales	Clavicipitaceae	AJ291800
Metarhizium anisopliae	Ascomycota	Sordariomycetes	Hypocreales	Clavicipitaceae	AB027383
Verticillium fungicola	Ascomycota	Sordariomycetes	Hypocreales	Clavicipitaceae	AB107135
Cordyceps bassiana	Ascomycota	Sordariomycetes	Hypocreales	Clavicipitaceae	DQ364698
Fusarium graminearum	Ascomycota	Sordariomycetes	Hypocreales	Nectriaceae	G578P60193PB7.T0
Magnaporthe grisea	Ascomycota	Sordariomycetes	Sordariomycetes incertae sedis	Magnaporthaceae	AM180561
Gauemannomyces graminis	Ascomycota	Sordariomycetes	Sordariomycetes incertae sedis	Magnaporthaceae	AJ010034
Neurospora crassa	Ascomycota	Sordariomycetes	Sordariales	Sordariaceae	M13906
Podospora anserina	Ascomycota	Sordariomycetes	Sordariales	Lasiosphaeriaceae	from genome
Chaetomium globosum	Ascomycota	Sordariomycetes	Sordariales	Chaetomiaceae	DQ266046
Stagonospora nodorum	Ascomycota	Dothideomycetes	Pleosporales	Phaesphaeriaceae	G707P6863FD10.T0
Cochliobolus carbonum	Ascomycota	Dothideomycetes	Pleosporales	Pleosporaceae	AF071326
Leptosphaeria maculans	Ascomycota	Dothideomycetes	Pleosporales	Leptosphaeriaceae	DQ133891
Coccidioides immits	Ascomycota	Eurotiomycetes	Onygenales	mitosporic Onygenales	AB232891
Aspergillus nidulans	Ascomycota	Eurotiomycetes	Eurotiales	Trichocomaceae	AF138289
Aspergillus fumigatus	Ascomycota	Eurotiomycetes	Eurotiales	Trichocomaceae	DQ325450
Penicillium paxilli	Ascomycota	Eurotiomycetes	Eurotiales	Trichocomaceae	AF033426
Pyrenopeziza brassicae	Ascomycota	Leotiomycetes	Helotiales	Dermateaceae	AJ305236
Sclerotinia sclerotiorum	Ascomycota	Leotiomycetes	Helotiales	Sclerotiniaceae	DQ117969
Botrytis cinerea	Ascomycota	Leotiomycetes	Helotiales	Sclerotiniaceae	Z73765

APPENDIX A13.2 Polypeptide sequences used in Prt1, Prt2, Prt3 and Prt5 phylogenetic analysis				
Species	**Protein name**	**Accession number**	**Contig?**	**Reference**
C. cinereus	-	-	1.277B	Hu and St Leger (2004)
C. cinereus	-	-	1.277A	Hu and St Leger (2004)
C. cinereus	-	-	1.62	Hu and St Leger (2004)
C. cinereus	-	-	1.39B	Hu and St Leger (2004)
M. grisea	MG10449.4	XP_366230	2.2008	Hu and St Leger (2004)
F. graminearum	FG08012.1	XP_388188	1.323	Hu and St Leger (2004)
A. chrysogenum	CahB	CAB87194	-	Velasco et al. (2001)
F. graminearum	FG02976.1	XP_383152	1.144	Hu and St Leger (2004)
F. oxysporum	Prt1	AAC27316	-	Di Pietro et al. (2001)
T. album	Proteinase T	P20015	-	Samal et al. (1989)
M. anisopliae	Pr1K	CAC07219	-	Bagga et al. (2004)
E. festucae Fl1	Prt5	-	-	This study
N. lolii Lp19	Prt5	-	-	This study
M. anisopliae	Pr1G	CAD24291	-	Bagga et al. (2004)
P. anserina	-	-	2663	http://podospora.igmors.u-psud.fr/index.html
M. grisea	MG08966.4	XP_364121	2.1683	Hu and St Leger (2004)
N. crassa	NCU07159.1	XP_327445	3.416	Galagan et al. (2003); Hu and St Leger (2004)
P. anserina	-	-	508	http://podospora.igmors.u-psud.fr/index.html
P. anserina	-	-	151	http://podospora.igmors.u-psud.fr/index.html
M. anisopliae	Pr1B	CAC95044	-	Bagga et al. (2004)
E. festucae Fl1	Prt3	-	-	This study
N. lolii Lp19	Prt3	-	-	This study
E. typhina	At1	AAB62277	-	Reddy et al. (1996)
M. anisopliae	Pr1I	CAC95043	-	Bagga et al. (2004)
N. lolii Lp19	Prt2	-	-	This study
E. festucae Fl1	Prt2	-	-	This study
M. anisopliae	Pr1A (Pr1)	P29138	-	Bagga et al. (2004); St Leger et al. (1992)
T. album	Proteinase R	P23653	-	Samal et al. (1990)
T. album	Proteinase K	P06873	-	Gunkel and Gassen (1989)
F. graminearum	FG10712.1	XP_390888	1.446	Hu and St Leger (2004)
F. graminearum	FG10595.1	XP_390771	1.444	(Hu and St Leger, 2004)
S. cerevisiae	YCR045c		-	Hu and St Leger (2004)
M. grisea	MG06558.4	XP_370043	2.1218	Hu and St Leger (2004)
M. grisea	MG02863.4	XP_366787	2.583	Hu and St Leger (2004)
M. grisea	MG07965.4	XP_368061	2.1479	Hu and St Leger (2004)
F. graminearum	FG03315.1	XP_383491	1.151	Hu and St Leger (2004)
T. virens	Tvsp1	AAO63588	-	Pozo et al. (2004)
T. harzianum	Prb1	Q03420	-	Geremia et al. (1993)
A. chrysogenum	Alp	P29118	-	Isogai et al. (1991)
A. nidulans	AN5558.2	XP_409695	1.95	Hu and St Leger (2004)
A. fumigatus	Serine proteinase	P28296	-	Kolattukudy et al. (1993)
M. anisopliae	Pr1J	CAC95041	-	Bagga et al. (2004)
N. crassa	NCU06949.1	XP_327235	3.404	Galagan et al. (2003); Hu and St Leger (2004)
F. graminearum	FG10525.1	XP_390701	1.441	Hu and St Leger (2004)
P. anserina	-	-	742	http://podospora.igmors.u-psud.fr/index.html
M. anisopliae	Pr1D	CAC98215	-	Bagga et al. (2004)
F. graminearum	FG00806.1	XP_380982	1.35	Hu and St Leger (2004)
F. graminearum	FG11405.1	XP_391581	1.467	Hu and St Leger (2004)
F. graminearum	FG08464.1	XP_388640	1.34	Hu and St Leger (2004)
M. anisopliae	Pr1F	CAD68050	-	Bagga et al. (2004)
M. anisopliae	Pr1E	CAD68049	-	Bagga et al. (2004)
N. lolii Lp19	Prt1	-	-	This study
E. festucae Fl1	Prt1	-	-	This study
P. anserina	-	-	2229	http://podospora.igmors.u-psud.fr/index.html
A. oligospora	PII	CAA63841	-	Åhman et al. (1996)
A. oligospora	Aoz1	AAM93666	-	Zhao et al. (2004)
F. graminearum	FG09382.1	XP_389558	1.383	Hu and St Leger (2004)
N. crassa	NCU06055.1	XP_325910	3.351	Galagan et al. (2003); Hu and St Leger (2004)
P. anserina	-	-	1086	http://podospora.igmors.u-psud.fr/index.html

APPENDIX 13.3 Polypeptide sequences used in Prt4 phylogenetic analysis				
Species	**Protein name**	**Accession number**	**Contig?**	**Reference**
S. pombe	ISP6	P40903	-	Sato et al. (1994)
P. chrysosporium	-	-	Scaffold 13	-
C. cinereus	-	-	1.39A	Hu and St Leger (2004)
U. maydis	UM04400.1	XP_402015		http://www.broad.mit.edu/annotation/fungi/ustilago_maydis/
C. neoformans serotype A	-		1.94	Hu and St Leger (2004)
S. pombe	Psp3 SPAC1006.01	Q9UTS0	-	Wood et al. (2002)
S. cerevisiae	Prb1	NP_010854	-	Moehle et al. (1987); Takeshige et al. (1992)
S. cerevisiae	Ysp3	P25036	-	Sterky et al. (1996)
P. oxalicum	Pen o 18	AAG44478	-	Shen et al. (2001)
A. nidulans	AN0238.2	XP_404375	1.5	-
A. fumigatus	ALP2	CAB45520	-	Reichard et al. (2000)
A. niger	PepC	P33295	-	Frederick et al. (1993)
M. grisea	Spm1 (MG03670.4)	P58371	2.715	Fukiya et al. (2002)
P. anserina	PspA	AAC03564	1035	Paoletti et al. (2001); Pinan-Lucarre et al. (2003)
N. crassa	NCU00673.1	XP_324853	3.23	Galagan et al. (2003)
F. graminearum	FG00192.1	XP_380368	1.8	Hu and St Leger (2004)
M. anisopliae	Pr1H	CAD13274	-	Bagga et al. (2004)
E. festucae Fl1	Prt4	-	-	This study
P. brassicae	Psp2	CAC85639	-	Keniry et al. (2002)
O. piliferum	-	AAL08510	-	Hoffman and Breuil (2002)

APPENDIX 13. 4 Polypeptide sequences used in Kex2 phylogenetic analysis				
Species	**Protein name**	**Accession number**	**Contig?**	**Reference**
U. maydis	UM02843.1	EAK84001		http://www.broad.mit.edu/annotation/fungi/ustilago_maydis/
C. neoformans	CNBL1060	EAL17844	-	-
C. cinereus	-	-	1.52	Hu and St Leger (2004)
C. cinereus	-	-	1.118	Hu and St Leger (2004)
C. cinereus	-	-	1.104	Hu and St Leger (2004)
P. chrysosporium	-	-	Scaffold 3	-
S. cerevisiae	Kex2	P13134		Mizuno et al. (1988)
C. albicans	Kex2			Newpo t and Agabian (1997); Newport et al. (2003)
S. pombe	Krp1	CAA93896		Davey et al. (1994)
P. carinii f. sp carinii	Kex1	AAB66701		Lugli et al. (1997)
E. festucae Fl1	Kex2	-	-	This study
F. graminearum	FG09156.1	EAA78206		Hu and St Leger (2004)
M. grisea	MG03742.4	EAA52147		Hu and St Leger (2004)
P. anserina	-	-	503	http://podospora.igmors.u-psud.fr/index.html
N. crassa	NCU03219.1	XP_330655		Galagan et al. (2003)
C. globosum	-	-	1.1	-
P. anserina	-	-	503	http://podospora.igmors.u-psud.fr/index.html
C. immitis	-	-	1.9	-
A. nidulans	AN3583.2	EAA59791		Kwon et al. (2001)
A. niger	kexin	CAB4692.1	-	Jalving et al. (2000)

APPENDIX 13. 5 Polypeptide sequences used in Gcn1 phylogenetic analysis

Species	Protein name	Accession number	Contig	Reference
T. harzianum	AGN13.1	CAC80493	-	Ait-Lahsen et al. (2001)
U. maydis	UM04357.1	XP_760504	1.154	http://www.broad.mit.edu/annotation/fungi/ustilago_maydis/
T. harzianum	P1	CAC80490	-	Montero et al. (2005)
M. grisea	MG02126.4	XP_365424	-	http://www.broad.mit.edu/annotation/fungi/magnaporthe/
N. crassa	Neg1 (NCU04935.1)		-	Oyama et al. (2002)
A. fumigatus	Afu8g07120	XP_747510	-	-
T. harzianum	P2	CAC80492	-	Montero et al. (2005)
S. nodorum	SNU10661.1	-	1.17	http://www.broad.mit.edu/annotation/fungi/stagonospora_nodorum/
M. grisea	MG07846.4	XP_367942	2.1455	http://www.broad.mit.edu/annotation/fungi/magnaporthe/
F. graminearum	FG03918.1	XP_384094	1.168	http://www.broad.mit.edu/annotation/fungi/fusarium/
F. graminearum	FG07617.1	XP_387793	1.315	http://www.broad.mit.edu/annotation/fungi/fusarium/
A. fumigatus	Afu7g05610	XP_748948	-	-
M. grisea	MG09433.4	XP_364493	2.1808	http://www.broad.mit.edu/annotation/fungi/magnaporthe/
S. nodorum	SNU06608.1	-	1.9	http://www.broad.mit.edu/annotation/fungi/stagonospora_nodorum/
S. nodorum	SNU14269.1	-	1.3	http://www.broad.mit.edu/annotation/fungi/stagonospora_nodorum/
C. carbonum	Exg2	AAF65310	-	Kim et al. (2002)
S. nodorum	SNU00606.1	-	1.1	http://www.broad.mit.edu/annotation/fungi/stagonospora_nodorum/
A. nidulans	AN4052.2	XP_408189	1.65	http://www.broad.mit.edu/annotation/fungi/aspergillus/
A. oryzae	HGT-BG	CAD97460	-	-
F. graminearum	FG01596.1	XP_381772	1.84	http://www.broad.mit.edu/annotation/fungi/fusarium/
A. fumigatus	Afu2g09350	XP_755269	-	-
A. nidulans	AN3777.2	XP_407914	1.61	http://www.broad.mit.edu/annotation/fungi/aspergillus/
S. nodorum	SNU12534.1	-		http://www.broad.mit.edu/annotation/fungi/stagonospora_nodorum/
V. fungicola	VfGlu1	AAO63562	-	Amey et al. (2003)
Acremonium sp. OXF C13	Bgn6.1	AAT97707	-	-
T. virens	Bgn3	AAL84696	-	Kim et al. (2002)
T. harzianum	BGN16.1	CAA55789	-	Lora et al. (1995)
F. graminearum	FG08265.1	XP_388441	1.348	http://www.broad.mit.edu/annotation/fungi/fusarium/
Neotyphodium sp. FCB2002	beta-1,6-glucanase	AAN04103	-	Moy et al. (2002)
N. lolii Lp19	Gcn1	-	-	This study
E. festucae Fl1	Gcn1	-	-	This study

APPENDIX 13. 6 Polypeptide sequences used in Cyc1 phylogenetic analysis				
Species	**Protein name**	**Accession number**	**Contig?**	**Reference**
S. cerevisiae	Pcl1p	NP_014110	-	Espinoza et al. (1994)
S. cerevisiae	Ctk2p	NP_012528	-	Sterner et al. (1995)
S. pombe	SPBC530.13	NP_595326	-	http://www.genedb.org/genedb/pombe/index.jsp
A. nidulans	AN5158.2*	-	1.88	http://www.broad.mit.edu/annotation/fungi/aspergillus/
F. graminearum	FG04981.1	XP_385157	1.200	http://www.broad.mit.edu/annotation/fungi/fusarium/
E. festucae Fl1	Cyc1	-	-	This study
M. grisea	MG06833.4	XP_370336	2.1272	http://www.broad.mit.edu/annotation/fungi/magnaporthe/
N. crassa	NCU04495.2	XP_323848	7.2	Galagan et al. (2003)
S. pombe	Srb11	CAA22680	-	Balciunas and Ronne (1999)
S. cerevisiae	Ume3p	NP_014373	-	Cooper et al. (1997)
A. nidulans	AN2172.2	XP_406309	1.34	http://www.broad.mit.edu/annotation/fungi/aspergillus/
M. grisea	MG01071.4	XP_368173	2.189	http://www.broad.mit.edu/annotation/fungi/magnaporthe/
N. crassa	NCU01563.2	XP_328002	7.5	Galagan et al. (2003)
G. moniliformis	Fic1	AAK30047	-	Shim and Woloshuk (2001)
F. graminearum	FG04355.1	XP_384531	1.189	http://www.broad.mit.edu/annotation/fungi/fusarium/
S. cerevisiae	Ccl1p	NP_015350	-	Svejstrup et al. (1996)
S. pombe	Mcs2	NP_595776	-	Damagnez et al. (1995)
A. nidulans	AN2212.2	XP_406349	1.35	http://www.broad.mit.edu/annotation/fungi/aspergillus/
N. crassa	NCU01067.2	XP_326560	7.15	Galagan et al. (2003)
F. graminearum	FG02126.1	XP_382302	1.111	http://www.broad.mit.edu/annotation/fungi/fusarium/
M. grisea	MG05536.4*	-	2.1019	http://www.broad.mit.edu/annotation/fungi/magnaporthe/
A. nidulans	AN4981.2	XP_409118	1.84	http://www.broad.mit.edu/annotation/fungi/aspergillus/
S. pombe	Pch1	CAA19367	-	Furnari et al. (1997)
N. crassa	NCU03196.2	XP_330632	7.9	Galagan et al. (2003)
M. grisea	MG01258.4	XP_363332	2.228	http://www.broad.mit.edu/annotation/fungi/magnaporthe/
F. graminearum	FG00467.1	XP_380643	1.19	http://www.broad.mit.edu/annotation/fungi/fusarium/
S. pombe	SPAC1296.05c	NP_593045	-	http://www.genedb.org/genedb/pombe/index.jsp
A. nidulans	AN7719.2	XP_411856	1.131	http://www.broad.mit.edu/annotation/fungi/aspergillus/
M. grisea	MG01347.4	XP_363421	2.244	http://www.broad.mit.edu/annotation/fungi/magnaporthe/
F. graminearum	FG06186.1	XP_386362	1.247	http://www.broad.mit.edu/annotation/fungi/fusarium/
N. crassa	NCU06979.2	XP_327265	7.35	Galagan et al. (2003)
* These sequences were edited compared to the protein sequences encoded by genes identified by FGENESH genome analysis. These putative genes appeared to contain exons from more than one gene, so the protein sequences were edited so they only contained sequence from the cyclin domains				

APPENDIX 13. 7 Polypeptide sequences used in Ptn1 phylogenetic analysis				
Species	**Protein name**	**Accession number**	**Contig?**	**Reference**
S. cerevisiae	Ptc1p	S41854	-	Maeda et al. (1993)
Homo sapiens sapiens	Cdc14A	Q9UNH5	-	Wong et al. (1999)
Mus musculus	Cdc14A	AAH72644	-	Strausberg et al. (2002)
S. pombe	Flp1	Q9P7H1	-	Cueille et al. (2001)
S. cerevisiae	Cdc14p	NP_116684	-	Taylor et al. (1997)
A. nidulans	AN5057.2	XP_409194	1.85	http://www.broad.mit.edu/annotation/fungi/aspergillus/
N. crassa	NCU03246.2	XP_330682	7.9	Galagan et al. (2003)
F. graminearum	FG00543.1	XP_380179	1.22	http://www.broad.mit.edu/annotation/fungi/fusarium/
M. grisea	MG04637.4	XP_362192	2.870	http://www.broad.mit.edu/annotation/fungi/magnaporthe/
Homo sapiens sapiens	Dusp16/MKP-7	AAH42101	-	Masuda et al. (2001)
S. cerevisiae	Tep1p	NP_014271	-	Heymont et al. (2000)
S. pombe	Pmp1p	013453	-	Sugiura et al. (1998)
N. crassa	NCU06252.2	XP_326107	7.25	Galagan et al. (2003)
F. graminearum	FG06977.1	XP_387153	1.287	http://www.broad.mit.edu/annotation/fungi/fusarium/
S. cerevisiae	Msg5p	BAA04485	-	Doi et al. (1994)
S. cerevisiae	Sdp1p	NP_012153	-	Hahn and Thiele (2002)
S. cerevisiae	Pps1p	NP_009835	-	Emsting and Dixon (1997)
A. nidulans	AN0192.2	XP_404266	1.5	http://www.broad.mit.edu/annotation/fungi/aspergillus/
M. grisea	MG03130.4	XP_360587	2.625	http://www.broad.mit.edu/annotation/fungi/magnaporthe/
F. graminearum	FG04296.1	XP_384472	1.185	http://www.broad.mit.edu/annotation/fungi/fusarium/
N. crassa	NCU03426.2	XP_322684	7.8	Galagan et al. (2003)
M. grisea	MG08005.4	XP_362422	2.1485	http://www.broad.mit.edu/annotation/fungi/magnaporthe/
E. festucae Fl1	Ptn1	-	-	This study
F. graminearum	FG04982.1	XP_385158	1.200	http://www.broad.mit.edu/annotation/fungi/fusarium/
N. crassa	NCU06969.2	XP_327255	7.35	Galagan et al. (2003)
P. anserina	-	-	454/455	http://podospora.igmors.u-psud.fr/index.html
S. pombe	Ptn1p	CAA22831	-	Mitra et al. (2004)
Homo sapiens sapiens	PTEN	NP_000305	-	Li et al. (1997)
D. melanogaster	PTEN	AAF23236	-	Smith et al. (1999)
A. nidulans	AN4419.2	XP_408556	1.76	http://www.broad.mit.edu/annotation/fungi/aspergillus/
F. graminearum	FG10516.1	XP_390692	1.441	http://www.broad.mit.edu/annotation/fungi/fusarium/
M. grisea	MG09700.4	XP_364855	2.1685	http://www.broad.mit.edu/annotation/fungi/magnaporthe/
N. crassa	NCU08158.1	XP_328864	7.52	Galagan et al. (2003)
S. pombe	SPBC17A3.06	NP_595588	-	Wood et al. (2002)
Homo sapiens sapiens	Dusp12	CAH74153	-	Martell et al. (1998)
S. cerevisiae	Yvh1p	NP_012292	-	Park et al. (1996)

APPENDIX 13. 8 Polypeptide sequences used in Gao1 phylogenetic analysis

Species	Protein name	Accession number	Contig?	Reference
P. chrysosporium	glyoxal oxidase precursor	A48296	scaffold 52	Kersten and Cullen (1993)
M. grisea	MG05865.4	XP_369599	2.1106	http://www.broad.mit.edu/annotation/fungi/magnaporthe/
M. grisea	MG01655.4	XP_363729	2.307	http://www.broad.mit.edu/annotation/fungi/magnaporthe/
F. graminearum	FG11097.1	XP_391273	1.459	http://www.broad.mit.edu/annotation/fungi/fusarium/
N. crassa	NCU04170.1	XP_323510	7.13	Galagan et al. (2003)
N. crassa	NCU05935.1	XP_325790	7.4	Galagan et al. (2003)
F. graminearum	FG05763.1	XP_385939	1.233	http://www.broad.mit.edu/annotation/fungi/fusarium/
C. neoformans (serotype D)	CNBG4080	EAL19461	-	Fung et al (unpublished)
C. neoformans (serotype D)	CNBA6590	EAL22890	-	Fung et al (unpublished)
N. crassa	NCU09209.1	XP_331601	7.65	Galagan et al. (2003)
E. festucae Fl1	Gao1	-	-	This study
F. graminearum	FG03569.1*	-	1.160	http://www.broad.mit.edu/annotation/fungi/fusarium/
F. graminearum	FG00251.1*	-	1.10	http://www.broad.mit.edu/annotation/fungi/fusarium/
Fusarium spp.	GaoA	Q01745	-	McPherson et al (1992); Ogel et al (1994)
F. graminearum	FG11032.1	XP_391208	1.458	http://www.broad.mit.edu/annotation/fungi/fusarium/
P. anserina	-	-	232	http://podospora.igmors.u-psud.fr/index.html
U. maydis	UM02809.1	XP_400424	1.94	http://www.broad.mit.edu/annotation/fungi/ustilago_maydis/
M. grisea	MG02368.4	XP_365666	2.473	http://www.broad.mit.edu/annotation/fungi/magnaporthe/
F. graminearum	FG09093.1	XP_389269	1.370	http://www.broad.mit.edu/annotation/fungi/fusarium/
M. grisea	MG10878.4	XP_360566	2.2099	http://www.broad.mit.edu/annotation/fungi/magnaporthe/

* These sequences were edited compared to the protein sequences encoded by genes identified by FGENESH genome analysis. These putative genes appeared to contain exons from more than one gene, so the protein sequences were edited so they only contained sequence from the cyclin domains

APPENDIX

A14: Intron conservation

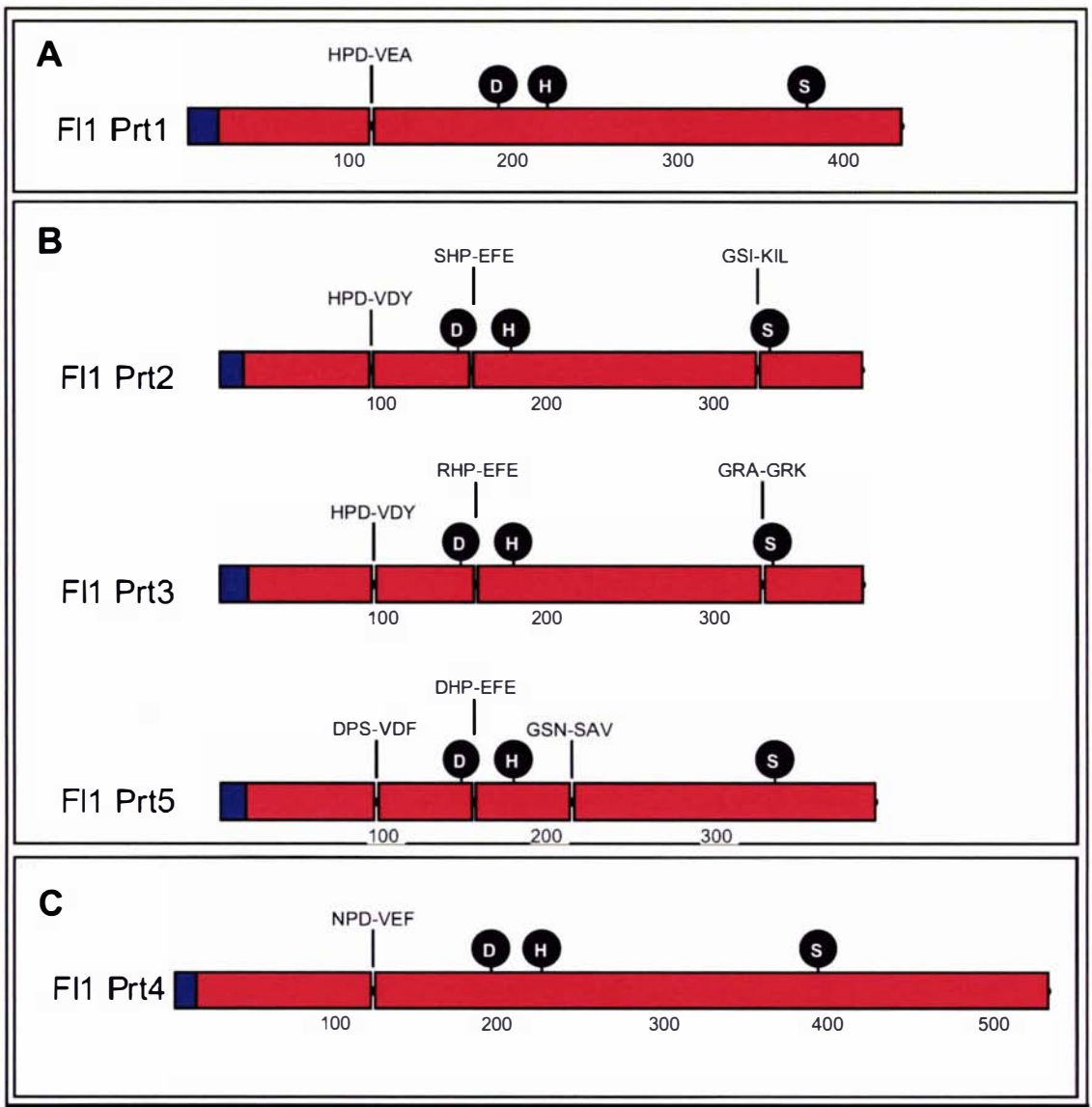

Appendix 14.1 Conservation of intron position in *prt* genes

Structural features of the *prt* coding regions and corresponding proteins in *E. festucae* Fl1. Regions of proteins corresponding to exons in gene are indicated by discrete red blocks, with the surrounding protein sequence indicated in black text above. The putative signal peptides (identified by the SignalP 3.0 algorithm) are indicated by blue boxes. The position of onserved active site residues required for protease activity are indicated by white text in black circles. **(A)** Proteinase K family subfamily 1 member, Fl1 Prt1. **(B)** Proteinase K family subfamily 2 members Fl1 Prt2, Prt3 and Prt5. **(C)** Proteinase K family subfamily 3 member (vacuolar protease) Fl1 Prt4.

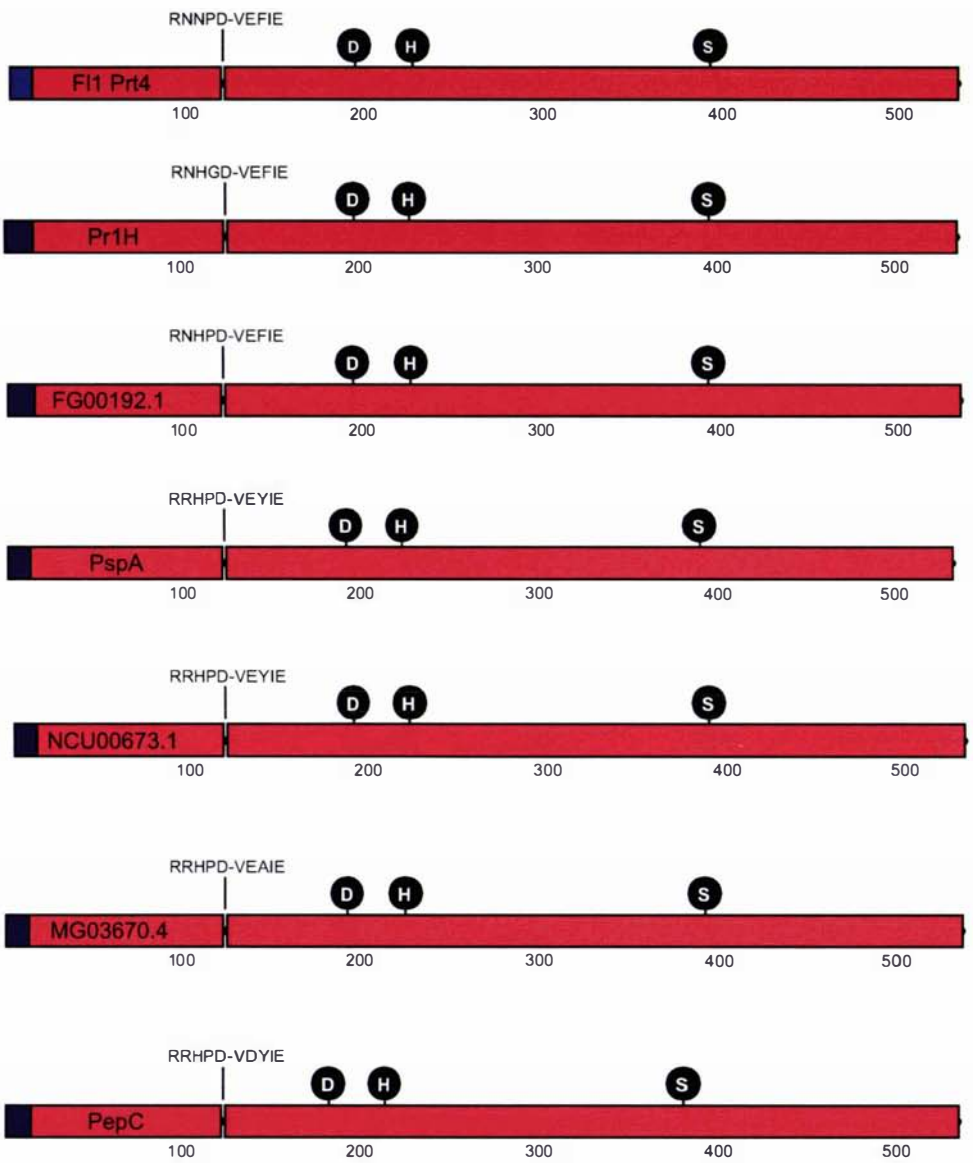

Appendix 14.2 Conservation of intron position in Fl1 *prt4*

Conservation of introns in genes encoding vacuolar protease genes. The coding sequence of the gene is shown as a schematic of the encoded protein. Each exom is shown as a red box, with the encoded protein sequence surrounding the intron shown above the intron position. The putative signal peptide for the protein (determined by SignalP 3.0 analysis) is shown in blue. Conserved active site residues required for catalytic activity are shown in black circles.

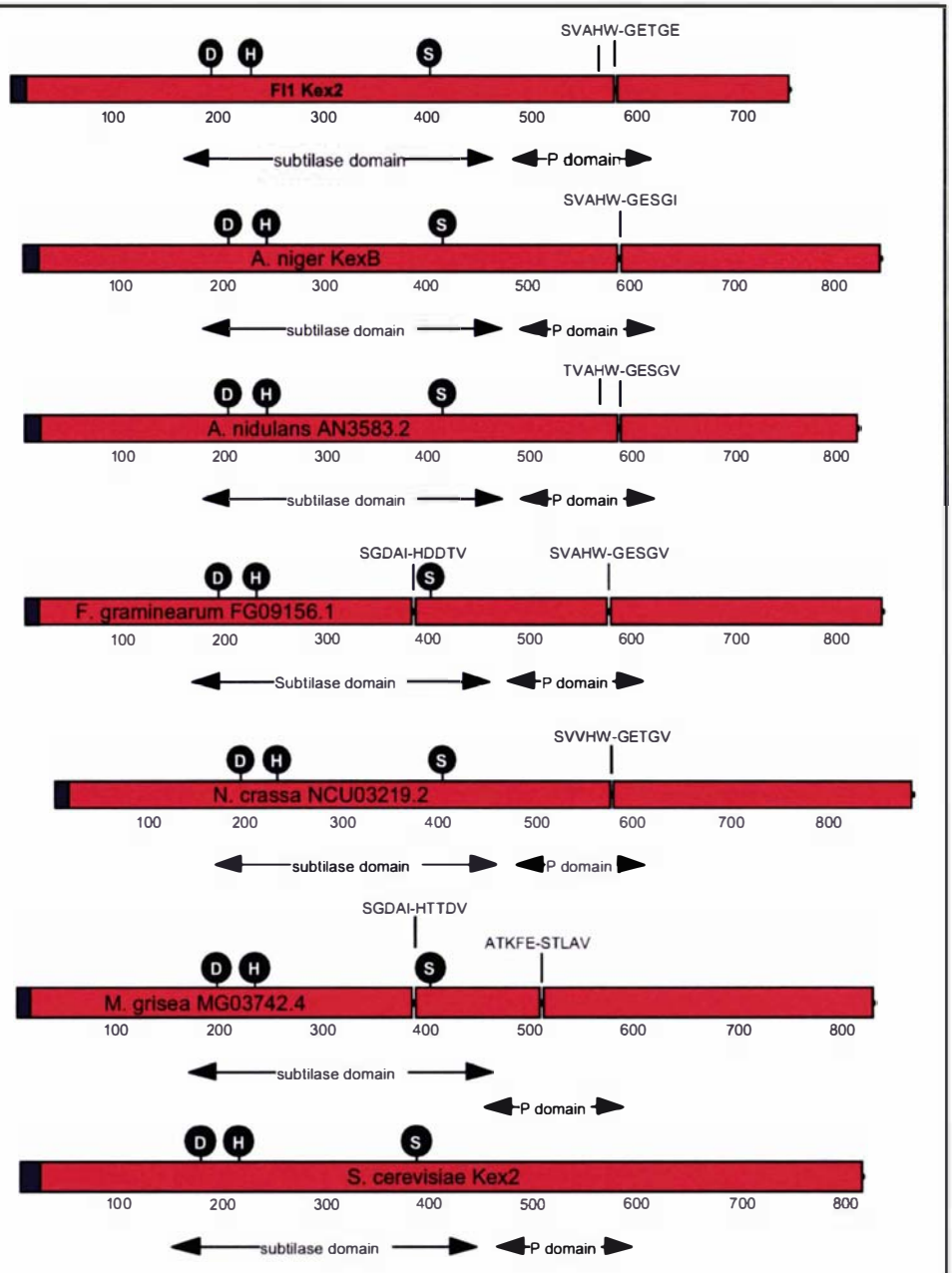

Appendix 14.3: Intron conservation in kexin-encoding genes

Conservation of introns in genes encoding vacuolar protease genes. The coding sequence of the gene is shown as a schematic of the encoded protein. Each exom is shown as a red box, with the encoded protein sequence surrounding the intron shown above the intron position. The putative signal peptide for the protein (determined by SignalP 3.0 analysis) is shown in blue. Conserved active site residues required for catalytic activity are shown in black circles. Conserved subtilase and P domains are indicated below the coding sequences by double-ended arrows.

APPENDIX

A15: Growth of *E. typhina* PN2311 *in planta*

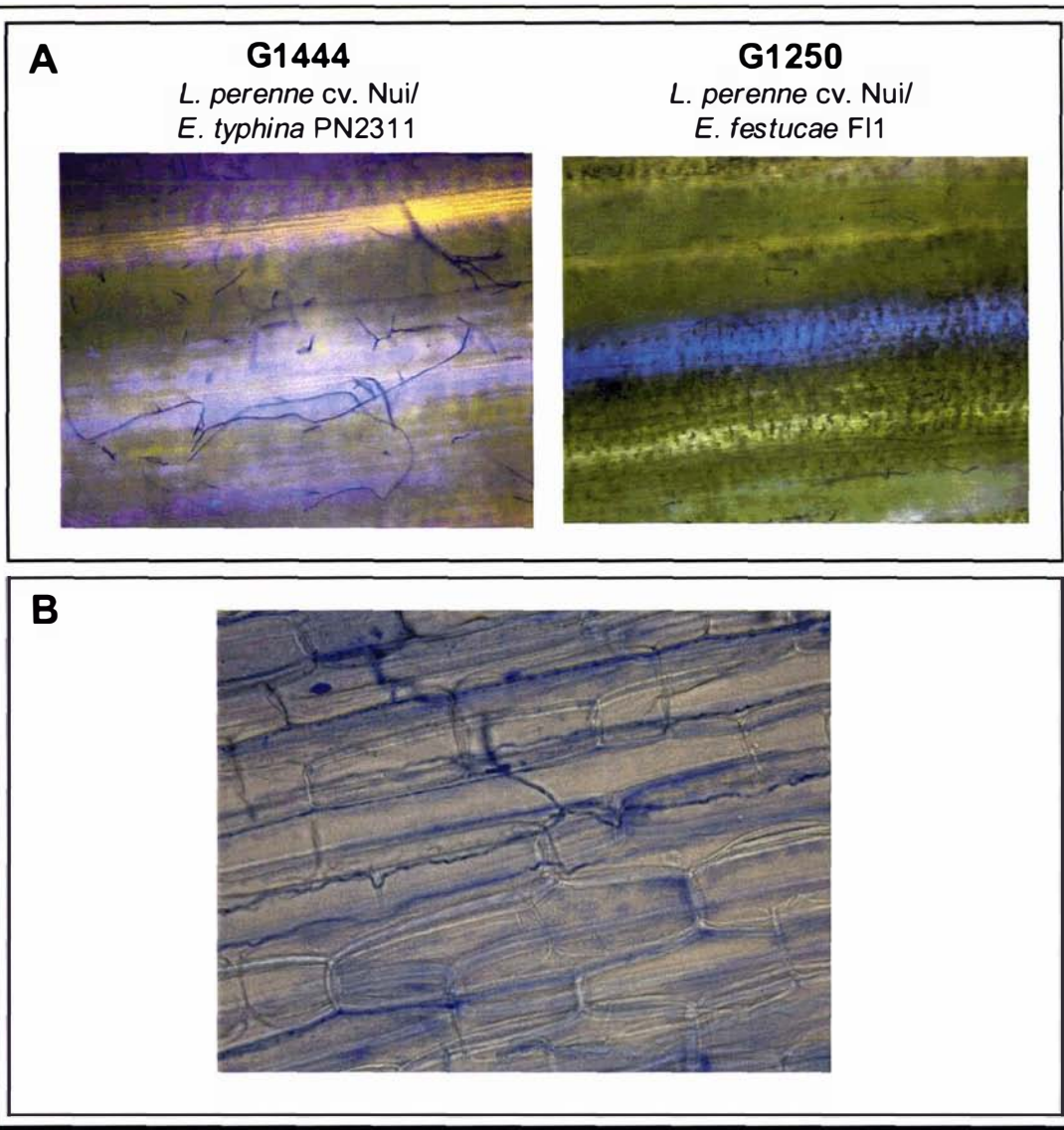

Appendix A15: Growth of *E. typhina* PN2311 in perennial ryegrass (*L. perenne* cv. Nui)

Hyphal growth in the G1444 symbiota between *E. typhina* PN2311 and *L. perenne* cv. Nui as analysed by aniline blue staining. (A) Epiphytic hyphae growing on the leaf surface of the G1444 and G1250 symbiota. (B) Growth of E. typhina PN2311 hyphae in an older leaf sheath of the G1444 symbiota.

Epiphytic hyphae growing on the leaf sheath are much more prevalent in theG1444 compared to the G1250 symbiota, which suggests that the *E. typhina* PN2311 could represent a higher percentage of the biomass in the G1444 symbiosis than *E. festucae* FI1 does in the G1250 symbiosis. Within the leaf tissue, *E. typhina* PN2311 grows in a similar manner to *E. festucae* FI1 (Figures 4.10, 4.11, 4.12 and 4.13), growing within the intercellular spaces.

APPENDIX

A16: Gene features

Appendix A16.1 *E. festucae* Fl1 gene features

Gene	Function	Kozak sequence	Introns						Stop codon	Top BlastX hit	Species	E Value
			#	Phase	Size (bp)	5' splice	Lariat consensus	3' splice				
prt5	subtilisin-like protease	CAAACATGAA	1	0	64	GTGAGT	TGCTGACA	CAG	TAA	Pr1K (accession CAC07219)	*Metarhizium anisopliae* var anisopliae	e-60
			2	0	79	GTATGT	GGCTGACG	CAG				
			3	2	74	GTAAGC	TTCTAACA	CAG				
prt1	subtilisin-like protease	CCAGAATGTT	1	0	78	GTTAGT	TGCTAACA	CAG	TAG	FG00806.1 (accession XP_380982)	*Fusarium graminearum (Gibberella zeae)*	e-112
*orf4**	unknown	?	-	-	-	-	-	-	TGA	FG10456.1 (accession XP_390632)	*Fusarium graminearum (Gibberella zeae)*	e-12
prt2	subtilisin-like protease	CCACGATGCG	1	0	72	GTGAGA	TACTAACT	CAG	TGA	Pr1I (accession CAB64346)	*Metarhizium anisopliae* var anisopliae	e-59
			2	0	83	GTATGT	AACTAACC	CAG				
			3	0	71	GTAAGT	CCTTGACA	CAG				
gcn1	beta-1,6-glucanase	ACAAGATGCA	1	1	78	GTATGT	TACTAACA	CAG	TAG	b-1,6-glucanase (accession AAN04103)	*Neotyphodium* sp. FCB2002	0.0
cyc1	C- type cyclin	CTCGAATGGC	1	2	113	GTATGT	TTCTAACC	TAG	TGA	FG04981.1 (accession XP_385157)	*Fusarium graminearum (Gibberella zeae)*	e-121
ptn1	phosphoinositide 3-phosphatase	CAGGCATGGC	1	2	154	GTGCGT	AACTAACT	CAG	TAA	FG04982.1 (accession XP_385157)	*Fusarium graminearum (Gibberella zeae)*	e-168
*ats1**	asparaginyl-tRNA synthetase	-	?	2	98	GTAAGG	ATCAAACA	CAG	TGA	AN7479.2 (accession XP_680748)	*Aspergillus nidulans*	e-32
prt3	subtilisin-like protease	TCGCCATGAT	1	0	98	GTATGC	AACTGACA	AAG	TAG	At1 (accession AAB62277)	*Epichloë typhina*	e-86
			2	0	86	GTGAGA	GGCTGACC	TAG				
			3	0	78	GTATGT	AACTGACC	CAG				
gao1	galactose oxidase	TCGAGATGAA	0	-	-	-	-	-	TAA	GaoA (FG11032.1; accession XP_391208)	*Fusarium graminearum (Gibberella zeae)*	0
prt4	subtilisin-like protease	TCACCATGAA	1	0	91	GTAAGT	CGCTGACT	CAG	TAA	Pr1H (accession CAB63913)	*Metarhizium anisopliae* var anisopliae	e-177
orf2	unknown	TCAACATGTC	0	-	-	-	-	-	TGA	FG07697.1 (accession XP_387873)	*Fusarium graminearum (Gibberella zeae)*	e-57
orf3	unknown	CCACCATGAG	1	1	61	GTAAGC	TACTAACA	CAG	TAG	NCU01051.1 (XP_326544)	*Neurospora crassa*	e-18
			2	1	65	GTGAGA	AGCTAACG	AAG				
			3	1	59	GTAGGT	TGCTGACA	AAG				
Nc25	unknown	TCACCATGCA	0	-	-	-	-	-	TAA	Nc25 (accession AAO92021)	*Neotyphodium coenophialum*	e-59
kex2	subtilisin-like protease	CCATCATGCA	1	2	79	GTAGGT	TGTTGTCT	CAG	TGA	KexB (accession CAB64692)	*Aspergillus niger*	0
*prt6**	subtilisin-like protease	?	?	1	127	GTATGT	CGCTAACA	CAG	?	Pr1J (accession CAC95041)	*Metarhizium anisopliae* var anisopliae	e-29
*prt7**	subtilisin-like protease	?	a	2	66	GCAAGA	CACTAACA	AAG	?	FG06332.1 (accession XP_386508)	*Fusarium graminearum (Gibberella zeae)*	e-37
			b	0	62	GTATGT	CTTATACG	CAG				
			c	0	51	GTAAGT	GAGTATCA	CAG				
*prt8**	subtilisin-like protease	?	-	-	-	-	-	-	?	Pr1C (accession CAD11898)	*Metarhizium anisopliae* var anisopliae	e-66
*orf5**	WD40 domain protein	?	-	-	-	-	-	-	?	FG09135.1 (accession XP_389311.1	*Fusarium graminearum (Gibberella zeae)*	e-37

Blast X was analysed using the maximum available coding sequence (and introns contained within this sequence)
* marks sequences where the full coding sequence was not available. In these cases, the available sequence was used for BlastX analysis
Sequences where a feature is not present are marked with dashes
Features that are not present in incomplete sequences are marked with a question mark.
The introns in the *prt7* sequence are marked a, b, c etc. because other introns may be present within upstream sequences.

APPENDIX

A17: SignalP analysis

	SignalP-NN prediction					SignalP-HMM prediction
Fl1 prt5	MEASURE	POSITION	VALUE	CUTOFF	SIG PEPTIDE	
	max. C	19	0.959	0.32	YES	Most likely cleavage site between pos. 18 and 19: AVA-AP
	max. Y	19	0.887	0.33	YES	Prediction: signal peptide
	max. S	13	0.993	0.87	YES	Signal peptide probability: 1.000
	mean S	1-18	0.961	0.48	YES	Signal anchor probability: 0.000
	D	1-18	0.924	0.43	YES	Max cleavage site probability: 0.973 between pos. 18 and 19
	SignalP-NN prediction					SignalP-HMM prediction
Fl1 prt1	MEASURE	POSITION	VALUE	CUTOFF	SIG PEPTIDE	
	max. C	22	0.507	0.32	YES	Most likely cleavage site between pos. 21 and 22: AIA-AP
	max. Y	22	0.598	0.33	YES	Prediction: signal peptide
	max. S	9	0.933	0.87	YES	Signal peptide probability: 1.000
	mean S	1-21	0.759	0.48	YES	Signal anchor probability: 0.000
	D	1-21	0.679	0.43	YES	Max cleavage site probability: 0.962 between pos. 21 and 22
	SignalP-NN prediction					SignalP-HMM prediction
Fl1 prt2	MEASURE	POSITION	VALUE	CUTOFF	SIG PEPTIDE	
	max. C	17	0.810	0.32	YES	Most likely cleavage site between pos. 16 and 17: ALA-AP
	max. Y	17	0.786	0.33	YES	Prediction: signal peptide
	max. S	13	0.982	0.87	YES	Signal peptide probability: 1.000
	mean S	1-16	0.946	0.48	YES	Signal anchor probability: 0.000
	D	1-16	0.866	0.43	YES	Max cleavage site probability: 0.620 between pos. 16 and 17
	SignalP-NN prediction					SignalP-HMM prediction
Fl1 gcn1	MEASURE	POSITION	VALUE	CUTOFF	SIG PEPTIDE	
	max. C	18	0.724	0.32	YES	Most likely cleavage site between pos. 17 and 18: VSA-WL
	max. Y	18	0.713	0.33	YES	Prediction: signal peptide
	max. S	13	0.928	0.87	YES	Signal peptide probability: 0.997
	mean S	1-17	0.806	0.48	YES	Signal anchor probability: 0.000
	D	1-17	0.760	0.43	YES	Max cleavage site probability: 0.793 between pos. 17 and 18
	SignalP-NN prediction					SignalP-HMM prediction
Fl1 cyc1	MEASURE	POSITION	VALUE	CUTOFF	SIG PEPTIDE	
	max. C	21	0.029	0.32	NO	-
	max. Y	21	0.021	0.33	NO	Prediction: non-secretory protein
	max. S	1	0.084	0.87	NO	Signal peptide probability: 0.001
	mean S	1-20	0.040	0.48	NO	Signal anchor probability: 0.000
	D	1-20	0.030	0.43	NO	Max cleavage site probability: 0.000 between pos. 20 and 21
	SignalP-NN prediction					SignalP-HMM prediction
Fl1 ptm1	MEASURE	POSITION	VALUE	CUTOFF	SIG PEPTIDE	
	max. C	18	0.112	0.32	NO	-
	max. Y	18	0.086	0.33	NO	Prediction: non-secretory protein
	max. S	13	0.414	0.87	NO	Signal peptide probability: 0.008
	mean S	1-17	0.263	0.48	NO	Signal anchor probability: 0.007
	D	1-17	0.175	0.43	NO	Max cleavage site probability: 0.002 between pos. 14 and 15
	SignalP-NN prediction					SignalP-HMM prediction
Fl1 prt3	MEASURE	POSITION	VALUE	CUTOFF	SIG PEPTIDE	
	max. C	17	0.257	0.32	NO	Most likely cleavage site between pos. 16 and 17: AAA-AP
	max. Y	17	0.428	0.33	YES	Prediction: signal peptide
	max. S	13	0.992	0.87	YES	Signal peptide probability: 0.999
	mean S	1-16	0.970	0.48	YES	Signal anchor probability: 0.000
	D	1-16	0.699	0.43	YES	Max cleavage site probability: 0.460 between pos. 19 and 20
	SignalP-NN prediction					SignalP-HMM prediction
Fl1 gao1	MEASURE	POSITION	VALUE	CUTOFF	SIG PEPTIDE	
	max. C	19	0.485	0.32	YES	Most likely cleavage site between pos. 18 and 19: AHS-AA
	max. Y	19	0.587	0.33	YES	Prediction: signal peptide
	max. S	13	0.942	0.87	YES	Signal peptide probability: 0.996
	mean S	1-18	0.769	0.48	YES	Signal anchor probability: 0.000
	D	1-18	0.678	0.43	YES	Max cleavage site probability: 0.878 between pos. 18 and 19
	SignalP-NN prediction					SignalP-HMM prediction
Fl1 prt4	MEASURE	POSITION	VALUE	CUTOFF	SIG PEPTIDE	
	max. C	16	0.405	0.32	YES	Most likely cleavage site between pos. 15 and 16: AQA-AF
	max. Y	16	0.547	0.33	YES	Prediction: signal peptide
	max. S	6	0.937	0.87	YES	Signal peptide probability: 0.999
	mean S	1-15	0.819	0.48	YES	Signal anchor probability: 0.000
	D	1-15	0.683	0.43	YES	Max cleavage site probability: 0.519 between pos. 15 and 16

	SignalP-NN prediction					SignalP-HMM prediction
Fl1 orf2	MEASURE	POSITION	VALUE	CUTOFF	SIG PEPTIDE	
	max. C	29	0.155	0.32	NO	-
	max. Y	35	0.020	0.33	NO	Prediction: non-secretory protein
	max. S	34	0.071	0.87	NO	Signal peptide probability: 0.000
	mean S	1-34	0.023	0.48	NO	Signal anchor probability: 0.000
	D	1-34	0.022	0.43	NO	Max cleavage site probability: 0.000 between pos. -1 and 0
	SignalP-NN prediction					SignalP-HMM prediction
Fl1 orf3	MEASURE	POSITION	VALUE	CUTOFF	SIG PEPTIDE	
	max. C	59	0.072	0.32	NO	-
	max. Y	59	0.144	0.33	NO	Prediction: signal anchor
	max. S	55	0.843	0.87	NO	Signal peptide probability: 0.000
	mean S	1-58	0.174	0.48	NO	Signal anchor probability: 0.501
	D	1-58	0.159	0.43	NO	Max cleavage site probability: 0.000 between pos. -1 and 0
	SignalP-NN prediction					SignalP-HMM prediction
Fl1 Nc25	MEASURE	POSITION	VALUE	CUTOFF	SIG PEPTIDE	
	max. C	19	0.881	0.32	YES	Most likely cleavage site between pos. 18 and 19: GLA-AP
	max. Y	19	0.846	0.33	YES	Prediction: signal peptide
	max. S	6	0.976	0.87	YES	Signal peptide probability: 0.998
	mean S	1-18	0.926	0.48	YES	Signal anchor probability: 0.001
	D	1-18	0.886	0.43	YES	Max cleavage site probability: 0.830 between pos. 18 and 19
	SignalP-NN prediction					SignalP-HMM prediction
Fl1 Kex2	MEASURE	POSITION	VALUE	CUTOFF	SIG PEPTIDE	
	max. C	20	0.608	0.32	YES	Most likely cleavage site between pos. 19 and 20: GIG-IG
	max. Y	20	0.656	0.33	YES	Prediction: signal peptide
	max. S	13	0.970	0.87	YES	Signal peptide probability: 0.991
	mean S	1-19	0.831	0.48	YES	Signal anchor probability: 0.007
	D	1-19	0.743	0.43	YES	Max cleavage site probability: 0.493 between pos. 19 and 20

BIBLIOGRAPHY

Adams, J., Kelso, R. and Cooley, L. (2000). The kelch repeat superfamily of proteins: propellers of cell function. Trends in Cell Biology *10*, 17-24.

Åhman, J., Ek, B., Rask, L. and Tunlid, A. (1996). Sequence analysis and regulation of a gene encoding a cuticle-degrading serine protease from the nematophagous fungus *Arthrobotrys oligospora*. Microbiology (Reading, England) *142*, 1605-1616.

Åhman, J., Johansson, T., Olsson, M., Punt, P. J., van den Hondel, C. A. M. J. J. and Tunlid, A. (2002). Improving the pathogenicity of a nematode-trapping fungus by genetic engineering of a subtilisin with nematotoxic activity. Applied and Environmental Microbiology *68*, 3408-3415.

Ait-Lahsen, H., Soler, A., Rey, M., de la Cruz, J., Monte, E. and Llobell, A. (2001). An antifungal exo-alpha-1,3-glucanase (AGN13.1) from the biocontrol fungus *Trichoderma harzianum*. Applied and Environmental Microbiology *67*, 5833-5839.

Albrecht, A., Felk, A., Pichova, I., Naglik, J. R., Schaller, M., de Groot, P., Maccallum, D., Odds, F. C., Schafer, W., Klis, F. et al. (2006). Glycosylphosphatidylinositol-anchored proteases of *Candida albicans* target proteins necessary for both cellular processes and host-pathogen interactions. Journal of Biological Chemistry *281*, 688-694.

Allard, G. and Nelson, C. J. (1991). Photosynthate partitioning in basal zones of tall fescue leaf blades. Plant Physiology *95*, 663-668.

Al-Samarrai, T. H. and Schmid, J. (2000). A simple method for extraction of fungal genomic DNA. Letters in Applied Microbiology *30*, 53-56.

Altschul, S. F., Madden, T. L., Schaffer, A. A., Zhang, J., Zhang, Z., Miller, W. and Lipman, D. J. (1997). Gapped BLAST and PSI-BLAST: a new generation of protein database search programs. Nucleic Acids Research *25*, 3389-3402.

Amey, R. C., Mills, P. R., Bailey, A. and Foster, G. D. (2003). Investigating the role of a *Verticillium fungicola* beta-1,6-glucanase during infection of *Agaricus bisporus* using targeted gene disruption. Fungal Genetics and Biology *39*, 264-275.

Amiard, V., Morvan-Bertrand, A., Cliquet, J.-B., Billard, J.-P., Huault, C., Sandström, J. P. and Prud'homme, M.-P. (2004). Carbohydrate and amino acid composition in phloem sap of *Lolium perenne* L. before and after defoliation. Canadian Journal of Botany *82*, 1594-1601.

Bacon, C. W. and White, J. F. J. (2000). Physiological adaptions in the evolution of endophytism in the Clavicipitaceae. In *Microbial Endophytes*, eds. C. W. Bacon and J. F. J. White), pp. 237-261. New York: Marcel Dekker, Inc.

Bader, O., Schaller, M., Klein, S., Kukula, J., Haack, K., Muhlschlegel, F., Korting, H. C., Schafer, W. and Hube, B. (2001). The *KEX2* gene of *Candida glabrata* is required for cell surface integrity. Molecular Microbiology *41*, 1431-1444.

Bagga, S., Hu, G., Screen, S. E. and St Leger, R. J. (2004). Reconstructing the diversification of subtilisins in the pathogenic fungus *Metarhizium anisopliae*. Gene *324*, 159-169.

Bailey, T. L. and Elkan, C. (1994). Fitting a mixture model by expectation maximization to discover motifs in biopolymers. In *Proceedings of the Second International Conference on Intelligent Systems for Molecular Biology*, pp. 28-36: AAAI Press.

Balciunas, D. and Ronne, H. (1999). Yeast genes *GIS1-4*: multicopy suppressors of the Gal⁻ phenotype of *snf1 mig1 srb8/10/11* cells. Molecular and General Genetics *262*, 589-599.

Baumgartner, S., Hofmann, K., Chiquet-Ehrismann, R. and Bucher, P. (1998). The discoidin domain family revisited: new members from prokaryotes and a homology-based fold prediction. Protein Science *7*, 1626-1631.

Bendtsen, J. D., Nielsen, H., von Heijne, G. and Brunak, S. (2004). Improved prediction of signal peptides: SignalP 3.0. Journal of Molecular Biology *340*, 783-795.

Bindschedler, L. V., Sanchez, P., Dunn, S., Mikan, J., Thangavelu, M., Clarkson, J. M. and Cooper, R. M. (2003). Deletion of the SNP1 trypsin protease from *Stagonospora nodorum* reveals another major protease expressed during infection. Fungal Genetics and Biology *38*, 43-53.

Blankenship, J. D., Spiering, M. J., Wilkinson, H. H., Fannin, F. F., Bush, L. P. and Schardl, C. L. (2001). Production of loline alkaloids by the grass endophyte, *Neotyphodium uncinatum*, in defined media. Phytochemistry *58*, 395-401.

Bonants, P. J. M., Fitters, P. F. L., Thijs, H., de Belder, E., Waalwijk, C. and Henfling, J. D. W. M. (1995). A basic serine protease from *Paecilomyces lilacinus* with biological activity against *Meloiogyne hapla* eggs. Microbiology (Reading, England) *141*, 775-784.

Bouchoux, C., Hautbergue, G., Grenetier, S., Carles, C., Riva, M. and Goguel, V. (2004). CTD kinase I is involved in RNA polymerase I transcription. Nucleic Acids Research *32*, 5851-5860.

Broekaert, W. F., Cammue, B. P. A., De Bolle, M. F. C., Thevissen, K., De Samblanx, G. and Osborn, R. W. (1997). Antimicrobial peptides from plants. Critical Reviews in Plant Science *16*, 297-323.

Brouta, F., Descamps, F., Monod, M., Vermout, S., Losson, B. and Mignon, B. (2002). Secreted metalloprotease gene family of *Microsporum canis*. Infection and Immunity *70*, 5676-5683.

Brul, S., King, A., vanderVaart, J. M., Chapman, J., Klis, F. and Verrips, C. T. (1997). The incorporation of mannoproteins in the cell wall of *S. cerevisiae* and filamentous Ascomycetes. Antonie Van Leeuwenhoek International Journal of General and Molecular Microbiology *72*, 229-237.

Bullock, W. O., Fernandez, J. M. and Short, J. M. (1987). XL1-Blue: a high efficiency plasmid transforming *rec*A *Escherichia coli* strain with beta-galactosidase selection. Biotechniques *5*, 376-378.

Bultman, T. L., White, J. F., Jr., Bowdish, T. I. and Welch, A. M. (1998). A new kind of mutualism between fungi and insects. Mycological Research *102*, 235-238.

Buscot, F., Munch, J. C., Charcosset, J. Y., Gardes, M., Nehls, U. and Hampp, R. (2000). Recent advances in exploring physiology and biodiversity of ectomycorrhizas highlight the functioning of these symbioses in ecosystems. FEMS Microbiology Reviews *24*, 601-614.

Bush, L. P., Fannin, F. F., Siegel, M. R., Dahlman, D. L. and Burton, H. R. (1993). Chemistry, occurrence and biological effects of saturated pyrrolizidine alkaloids associated with endophyte-grass interactions. Agriculture Ecosystems & Environment *44*, 1-4.

Bush, L. P., Wilkinson, H. H. and Schardl, C. L. (1997). Bioprotective alkaloids of grass-fungal endophyte symbioses. Plant Physiology *114*, 1-7.

Carlile, A. J., Bindschedler, L. V., Baile, A. M., Bowyer, P., Clarkson, J. M. and Cooper, R. M. (2000). Characterization of SNP1, a cell wall-degrading trypsin, produced during infection by *Stagonospora nodorum*. Molecular Plant-Microbe Interactions *13*, 538-550.

Carroll, G. (1988). Fungal endophytes in stems and leaves: from latent pathogen to mutualistic symbiont. Ecology *69*, 2-9.

Christensen, M. J. (1995). Variation in the ability of *Acremonium* endophytes of *Lolium perenne*, *Festuca arundinacea* and *F. pratensis* to form compatible associations in the three grasses. Mycological Research *99*, 446-470.

Christensen, M. J., Ball, O. J. P., Bennett, R. J. and Schardl, C. L. (1997). Fungal and host genotype effects on compatibility and vascular colonization by *Epichloë festucae*. Mycological Research *101*, 493-501.

Christensen, M. J., Leuchtmann, A., Rowan, D. D. and Tapper, B. A. (1993). Taxonomy of *Acremonium* endophytes of tall fescue (*Festuca arundinacea*), meadow fescue (*F. pratensis*) and perennial ryegrass (*Lolium perenne*). Mycological Research *97*, 1083-1092.

Chung, K.-R., Hollin, W., Siegel, M. R. and Schardl, C. L. (1997). Genetics of host specifictiy in *Epichloë typhina*. Phytopathology *87*, 599-605.

Chung, K.-R. and Schardl, C. L. (1997). Vegetative compatibility between and within *Epichloë* species. Mycologia *89*, 558-565.

Clay, K. (1988). Fungal endophytes of grasses: a defensive mutualism between plant and fungi. Ecology *69*, 10-16.

Cogoni, C., Romano, N. and Macino, G. (1994). Suppression of gene expression by homologous transgenes. Antonie Van Leeuwenhoek International Journal of General and Molecular Microbiology *65*, 205-209.

Conesa, A., Punt, P. J., van Lujik, N. and van den Hodnel, C. A. M. J. J. (2001). The secretion pathway in filamentous fungi: a biotechnological view. Fungal Genetics and Biology *33*, 155-171.

Cooper, K. F., Mallory, M. J., Smith, J. B. and Strich, R. (1997). Stress and developmental regulation of the yeast C-type cyclin Ume3p (Srb11p/Ssn8p). EMBO Journal *16*, 4665-4675.

Cortes, C., Gutierrez, A., Olmedo, V., Inbar, J., Chet, I. and Herrera-Estrella, A. (1998). The expression of genes involved in parasitism by *Trichoderma harzianum* is triggered by a diffusible factor. Molecular and General Genetics *260*, 218-225.

Cueille, N., Salimova, E., Esteban, V., Blanco, M., Moreno, S., Bueno, A. and Simanis, V. (2001). *Flp1*, a fission yeast orthologue of the *S. cerevisiae CDC14* gene, is not required for cyclin degradation or rum1p stabilisation at the end of mitosis. Journal of Cell Science *114*, 2649-2664.

da Silva, M. V., Santi, L., Staats, C. C., da Costa, A. M., Colodel, E. M., Driemeier, D., Vainstein, M. H. and Schrank, A. (2005). Cuticle-induced endo/exoacting chitinase CHIT30 from *Metarhizium anisopliae* is encoded by an ortholog of the *chi3* gene. Research in Microbiology *156*, 382-392.

Damagnez, V., Makela, T. P. and Cottarel, G. (1995). *Schizosaccharomyces pombe* Mop1-Mcs2 is related to mammalian CAK. EMBO Journal *14*, 6164-6172.

Davey, J., Davis, K., Imai, Y., Yamamoto, M. and Matthews, G. (1994). Isolation and characterization of Krp, a dibasic endopeptidase required for cell viability in the fission yeast *Schizosaccharomyces pombe*. EMBO Journal *13*, 5910-5921.

de la Cruz, J. and Llobell, A. (1999). Purification and properties of a basic endo-β-1,6-glucanase (BGN16.1) from the antagonistic fungus *Trichoderma harzianum*. European Journal of Biochemistry *265*, 145-151.

De la Cruz, J., Pintor-Toro, J. A., Benítez, T. and Llobell, A. (1995). Purification and characterization of an endo-β-1,6-glucanase from *Trichoderma harzianum* that is related to its mycoparasitism. Journal of Bacteriology *177*, 1864-1871.

Delp, G., Timonen, S., Rosewarne, G. M., Barker, S. J. and Smith, S. (2003). Differential expression of *Glomus intraradices* genes in external mycelium and mycorrhizal roots of tomato and barley. Mycological Research *107*, 1083-1093.

Descamps, F., Brouta, F., Monod, M., Zaugg, C., Baar, D., Losson, B. and Mignon, B. (2002). Isolation of a *Microsporum canis* gene family encoding three subtilisin-like proteases expressed *in vivo*. Journal of Investigative Dermatology *119*, 830-835.

Di Pietro, A., Huertas-González, M. D., Gutierrez-Corona, J. F., Martinéz-Cadena, G., Méglecz, E. and Roncero, M. I. G. (2001). Molecular characterization of a subtilase from the vascular wilt fungus *Fusarium oxysporum*. Molecular Plant-Microbe Interactions *14*, 653-662.

Dobinson, K. F., Grant, S. J. and Kang, S. (2004). Cloning and targeted disruption, via Agrobacterium tumefaciens-mediated transformation, of a trypsin protease gene from the vascular wilt fungus *Verticillium dahliae*. Current Genetics *45*, 104-110.

Doi, K., Gartner, A., Ammerer, G., Errede, B., Shinkawa, H., Sugimoto, K. and Matsumoto, K. (1994). Msg5, a novel protein phosphatase promotes adaptation to pheromone response in *Saccharomyces cerevisiae*. EMBO Journal *13*, 61-70.

Down, T. A. and Hubbard, T. J. P. (2005). NestedMICA: sensitive inference of over-represented motifs in nucleic acid sequence. Nucleic Acids Research *33*, 1445-1453.

Downes, C. P., Bennett, D., McConnachie, G., Leslie, N. R., Pass, I., MacPhee, C., Patel, L. and Gray, A. (2001). Antagonism of PI 3-kinase-dependent signalling pathways by the tumour suppressor protein, PTEN. Biochemical Society Transactions *29*, 846-851.

Dymock, J. J., Prestidge, R. A. and Rowan, D. D. (1989). The effects of lolitrem B on Argentine stem weevil larvae. In *Proceedings of the 42nd NZ weed and pest control conference*. New Plymouth: Swiftprint.

Easton, H. S., Latch, G. C. M., Tapper, B. A. and Ball, O. J.-P. (2002). Ryegrass host genetic control of concentrations of endophyte-derived alkaloids. Crop Science *42*, 51-57.

Ebeling, W., Hennrich, N., Klockow, M., Metz, H., Orth, H. D. and Lang, H. (1974). Proteinase K from *Tritirachium album* Limber. European Journal of Biochemistry *47*, 91-97.

El-Katatny, M. H., Gudelj, M., Robra, K. H., Elnaghy, M. A. and Gubitz, G. M. (2001). Characterization of a chitinase and an endo-β-1,3-glucanase from *Trichoderma harzianum* Rifai T24 involved in control of the phytopathogen *Sclerotium rolfsii*. Applied Microbiology and Biotechnology *56*, 137-143.

Enderlin, C. S. and Ogrydziak, D. M. (1994). Cloning, nucleotide sequence and functions of *xpr6*, which codes for a dibasic processing endoprotease from the yeast *Yarrowia lipolytica*. Yeast *10*, 67-79.

Ernsting, B. R. and Dixon, J. E. (1997). The *PPS1* gene of *Saccharomyces cerevisiae* codes for a dual specificity protein phosphatase with a role in the DNA synthesis phase of the cell cycle. Journal of Biological Chemistry *272*, 9332-9343.

Espinoza, F. H., Ogas, J., Herskowitz, I. and Morgan, D. O. (1994). Cell-Cycle Control by a Complex of the Cyclin Hcs26 (Pcl1) and the Kinase Pho85. Science *266*, 1388-1391.

Faraco, V., Palmieri, G., Festa, G., Monti, M., Sannia, G. and Giardina, P. (2005). A new subfamily of fungal subtilases: structural and functional analysis of a *Pleurotus ostreatus* member. Microbiology-Sgm *151*, 457-466.

Felk, A., Kretschmar, M., Albrecht, A., Schaller, M., Beinhauer, S., Nichterlein, T., Sanglard, D., Korting, H. C., Schafer, W. and Hube, B. (2002). *Candida albicans* hyphal formation and the expression of the Efg1-regulated proteinases SAP4 to SAP6 are required for the invasion of parenchymal organs. Infection and Immunity *70*, 3689-3700.

Fickers, P., Le Dall, M. T., Gaillardin, C., Thonart, P. and Nicaud, J. M. (2003). New disruption cassettes for rapid gene disruption and marker rescue in the yeast *Yarrowia lipolytica*. Journal of Microbiological Methods *55*, 727-737.

Fitzgerald, A., van Kan, J. A. L. and Plummer, K. M. (2004). Simultaneous silencing of multiple genes in the apple scab fungus, *Venturia inaequalis*, by expression of RNA with chimeric inverted repeats. Fungal Genetics and Biology *41*, 963-971.

Flores, A., Chet, J. and Herrera-Estrella, A. (1997). Improved biocontrol activity of *Trichoderma harzianum* by over-expression of the proteinase-encoding gene *prb1*. Current Genetics *31*, 30-37.

Fraissinet-Tachet, L., Reymond-Cotton, P. and Fevre, M. (1995). Characterization of a multigene family encoding an endopolygalacturonase in *Sclerotinia sclerotiorum*. Current Genetics *29*, 96-99.

Frederick, G. D., Rombouts, P. and Buxton, F. P. (1993). Cloning and characterisation of *pepC*, a gene encoding a serine protease from *Aspergillus niger*. Gene *125*, 57-64.

Freimoser, F. M., Screen, S., Bagga, S., Hu, G. and St Leger, R. J. (2003). Expressed sequence tag (EST) analysis of two subspecies of *Metarhizium anisopliae* reveals a plethora of secreted proteins with potential activity in insect hosts. Microbiology (SGM) *149*, 239-247.

Freimoser, F. M., Hu, G. and St Leger, R. J. (2005). Variation in gene expression patterns as the insect pathogen *Metarhizium anisopliae* adapts to different host cuticles or nutrient deprivation in vitro. Microbiology-Sgm *151*, 361-371.

Frobius, A. C., Kanost, M. R., Gotz, P. and Vilcinskas, A. (2000). Isolation and characterization of novel inducible serine protease inhibitors from larval hemolymph of the greater wax moth *Galleria mellonella*. European Journal of Biochemistry *267*, 2046-2053.

Fukiya, S., Kuge, T., Tanishima, T., Sone, T., Kamakura, T., Yamaguchi, I. and Tomita, F. (2002). Identification of a putative vacuolar serine protease gene in the rice blast fungus, *Magnaporthe grisea*. Bioscience Biotechnology and Biochemistry *66*, 663-666.

Fuller, R. S., Brake, A. and Thorner, J. (1989). Yeast prohormone processing enzyme (*KEX2* gene product) is a Ca^{2+}-dependent serine protease. Proceedings of the National Academy of Sciences of the United States of America *86*, 1434-1438.

Furnari, B. A., Russell, P. and Leatherwood, J. (1997). *pch1*$^{+}$, a second essential C-type cyclin gene in *Schizosaccharomyces pombe*. Journal of Biological Chemistry *272*, 12100-12106.

Galagan, J. E., Calvo, S. E., Borkovich, K. A., Selker, E. U., Read, N. D., Jaffe, D., FitzHugh, W., Ma, L. J., Smirnov, S., Purcell, S. et al. (2003). The genome sequence of the filamentous fungus *Neurospora crassa*. Nature *422*, 859-868.

Geremia, R. A., Goldman, G. H., Jacobs, D., Ardiles, W., Vila, S. B., Van Montagu, M. and Herrera-Estrella, A. (1993). Molecular characterisation of the proteinase-encoding gene, *prb1*, related to mycoparasitism by *Trichoderma harzianum*. Molecular Microbiology *8*, 603-613.

Giraud, T., Fortini, D., Levis, C. and Brygoo, Y. (1998). The minisatellite MSB1, in the fungus Botrytis cinerea, probably mutates by slippage. Molecular Biology and Evolution *15*, 1524-1531.

Glenn, A. E., Bacon, C. W., Price, R. and Hanlin, R. T. (1996). Molecular phlogeny of *Acremonium* and its taxonomic implications. Mycologia *88*, 369-383.

Goettel, M. S., St Leger, R. J., Rizzo, N. W., Staples, R. C. and Roberts, D. W. (1989). Ultrastructural localization of a cuticle-degrading protease produced by the entomopathogenic fungus *Metarhizium anisopliae* during penetration of host (*Manduca sexta*) cuticle. Journal of General Microbiology *135*, 2233-2239.

Govrin, E. M. and Levine, A. (2002). Infection of *Arabidopsis* with a necrotrophic pathogen, *Botrytis cinerea*, elicits various defense responses but does not induce systemic acquired resistance (SAR). Plant Molecular Biology *48*, 267-276.

Griesch, J. (1998). Proteases released by entomopathogenic fungi impair phagocytic activity, attachment and spreading of plasmatocytes isolated from haemolymph of the greater wax moth *Galleria mellonella*. Biocontrol Science and Technology *8*, 517-531.

Gron, H. and Breddam, K. (1992). Interdependency of the binding subsites in subtilisin. Biochemistry *31*, 8967-8971.

Guldener, U., Heck, S., Fiedler, T., Beinhauer, J. and Hegemann, J. H. (1996). A new efficient gene disruption cassette for repeated use in budding yeast. Nucleic Acids Research *24*, 2519-2524.

Gunkel, F. A. and Gassen, H. G. (1989). Proteinase K from *Tritirachium album* Limber. Characterization of the chromosomal gene and expression of the cDNA in *Escherichia coli*. European Journal of Biochemistry *179*, 185-194.

Gwinn, K. D., Collins-Shepard, M. H. and Reddick, B. B. (1991). Tissue print-immunoblot, an accurate method for the detection of *Acremonium coenophialum* in tall fescue. Phytopathology. *81*, 747–748.

Haber, J. E. and Louis, E. J. (1998). Minisatellite origins in yeast and humans. Genomics *48*, 132-135.

Hahn, J. S. and Thiele, D. J. (2002). Regulation of the *Saccharomyces cerevisiae* Slt2 kinase pathway by the stress-inducible Sdp1 dual specificity phosphatase. Journal of Biological Chemistry *277*, 21278-21284.

Harman, G. E., Howell, C. R., Viterbo, A., Chet, I. and Lorito, M. (2004). *Trichoderma* species - opportunistic, avirulent plant symbionts. Nature Reviews Microbiology *2*, 43-56.

Hautbergue, G. and Goguel, V. (2001). Activation of the cyclin-dependent kinase CTDK-I requires the heterodimerization of two unstable subunits. Journal of Biological Chemistry *276*, 8005-8013.

Henrich, S., Lindberg, I., Bode, W. and Than, M. E. (2005). Proprotein convertase models based on the crystal structures of furin and kexin: Explanation of their specificity. Journal of Molecular Biology *345*, 211-227.

Heymont, J., Berenfeld, L., Collins, J., Kaganovich, A., Maynes, B., Moulin, A., Ratskovskaya, I., Poon, P. P., Johnston, G. C., Kamenetsky, M. et al. (2000). *TEP1*, the yeast homolog of the human tumor suppressor gene PTEN/MMAC1/TEP1, is linked to the phosphatidylinositol pathway and plays a role in the developmental process of sporulation. Proceedings of the National Academy of Sciences of the United States of America *97*, 12672-12677.

Hoffman, B. and Breuil, C. (2002). Cloning and genetic analysis of subtilases in sapstaining fungi. Current Genetics *41*, 168-175.

Hoffman, B. and Breuil, C. (2004a). Analysis of the distribution and regulation of three representative subtilase genes in sapstaining fungi. Fungal Genetics and Biology *41*, 274-283.

Hoffman, B. and Breuil, C. (2004b). Disruption of the subtilase gene, *albin1*, in *Ophiostoma piliferum*. Applied and Environmental Microbiology *70*, 3898-3903.

Hoffman, C. S. (2005). Glucose sensing via the protein kinase A pathway in *Schizosaccharomyces pombe*. Biochemical Society Transactions *33*, 257-260.

Hofman-Bang, J. (1999). Nitrogen catabolite repression in *Saccharomyces cerevisiae*. Molecular Biotechnology *12*, 35-73.

Holmes, D. S. and Quigley, M. (1981). A rapid boiling method for the preparation of bacterial plasmids. Analytical Biochemistry *114*, 193-197.

Hu, G. and St Leger, R. J. (2004). A phylogenomic approach to reconstructing the diversification of serine proteases in fungi. Journal of Evolutionary Biology *17*, 1204-14.

Hube, B., Sanglard, D., Odds, F. C., Hess, D., Monod, M., Schafer, W., Brown, A. J. P. and Gow, N. A. R. (1997). Disruption of each of the secreted aspartyl proteinase genes *SAP1*, *SAP2*, and *SAP3* of *Candida albicans* attenuates virulence. Infection and Immunity *65*, 3529-3538.

Isogai, T., Fukugawa, M., Kojo, H., Kohsaka, M., Aoki, H. and Imanaka, H. (1991). Cloning and nucleotide sequences of the complementary and genomic DNAs for the alkaline protease from *Acremonium chrysogenum*. Agricultural and Biological Chemistry *55*, 471-477.

Iwaki, T. and Takegawa, K. (2004). A set of *loxP* marker cassettes for cre-mediated multiple gene disruption in *Schizosaccharomyces pombe*. Bioscience Biotechnology and Biochemistry *68*, 545-550.

Jalving, R. (2005). Proteolytic processing in the secretory pathway of *Aspergillus niger*, pp. 116. Wageningen: Wageningen University.

Jalving, R., van de Vondervoort, P. J. I., Visser, J. and Schaap, P. J. (2000). Characterization of the kexin-like maturase of *Aspergillus niger*. Applied and Environmental Microbiology *66*, 363-368.

Jarai, G., van den Hombergh, H. and Buxton, F. P. (1994). Cloning and characterization of the *pepE* gene of *Aspergillus niger* encoding a new aspartic protease and regulation of *pepE* and *pepC*. Gene *145*, 171-178.

Jennings, D. H. (1995). The Physiology of Fungal Nutrition. Cambridge: Cambridge University Press.

Johnson, L. J., Johnson, R. D., Schardl, C. L. and Panaccione, D. G. (2003). Identification of differentially expressed genes in the mutualistic association of tall fescue with *Neotyphodium coenophialum*. Physiological and Molecular Plant Pathology *63*, 305-317.

Joshi, L. and St Leger, R. J. (1999). Cloning, expression, and substrate specificity of MeCPA, a zinc carboxypeptidase that is secreted into infected tissues by the fungal entomopathogen *Metarhizium anisopliae*. Journal of Biological Chemistry *274*, 9803-9811.

Joshi, L., St Leger, R. J. and Roberts, D. W. (1997). Isolation of a cDNA encoding a novel subtilisin-like protease (Prl B) from the entomopathogenic fungus, *Metarhizium anisopliae* using differential display-RT-PCR. Gene *197*, 1-8.

Jousson, O., Lechenne, B., Bontems, O., Capoccia, S., Mignon, B., Barblan, J., Quadroni, M. and Monod, M. (2004a). Multiplication of an ancestral gene encoding secreted fungalysin preceded species differentiation in the dermatophytes *Trichophyton* and *Microsporum*. Microbiology (Reading, England) *150*, 301-10.

Jousson, O., Lechenne, B., Bontems, O., Mignon, B., Reichard, U., Barblan, J., Quadroni, M. and Monod, M. (2004b). Secreted subtilisin gene family in *Trichophyton rubrum*. Gene *339*, 79-88.

Kapteyn, J. C., Van Den Ende, H. and Klis, F. M. (1999). The contribution of cell wall proteins to the organization of the yeast cell wall. Biochimica et Biophysica Acta (General Subjects) *1426*, 373-383.

Kasza, Z., Vagvolgyi, C., Fevre, M. and Cotton, P. (2004). Molecular characterization and in planta detection of *Sclerotinia sclerotiorum* endopolygalacturonase genes. Current Microbiology *48*, 208-213.

Kellis, M., Patterson, N., Endrizzi, M., Birren, B. and Lander, E. S. (2003). Sequencing and comparison of yeast species to identify genes and regulatory elements. Nature *423*, 241-254.

Keniry, C. A., Li, D. H. and Ashby, A. M. (2002). Cloning and expression studies during vegetative growth and sexual development of Psp2, a serine protease gene from *Pyrenopeziza brassicae*. Biochimica et Biophysica Acta (Gene Structure and Expression) *1577*, 159-163.

Kersten, P. J. and Cullen, D. (1993). Cloning and characterization of a cDNA-encoding glyoxal oxidase, a H_2O_2-producing enzyme from the lignin-degrading basidiomycete *Phanerochaete chrysosporium*. Proceedings of the National Academy of Sciences of the United States of America *90*, 7411-7413.

Kim, D. J., Baek, J. M., Uribe, P., Kenerley, C. M. and Cook, D. R. (2002). Cloning and characterization of multiple glycosyl hydrolase genes from *Trichoderma virens*. Current Genetics *40*, 374-384.

Koga, H., Christensen, M. J. and Bennett, R. J. (1993). Incompatibility of some grass-*Acremonium* endophyte associations. Mycological Research *97*, 1237-1244.

Kolattukudy, P. E., Lee, J. D., Rogers, L. M., Zimmerman, P., Ceselski, S., Fox, B., Stein, B. and Copelan, E. A. (1993). Evidence for possible involvement of an elastolytic serine protease in aspergillosis. Infection and Immunity *61*, 2357-2368.

Kollar, R., Reinhold, B. B., Petrakova, E., Yeh, H. J. C., Ashwell, G., Drgonova, J., Kapteyn, J. C., Klis, F. M. and Cabib, E. (1997). Architecture of the yeast cell wall - β(1->6)-glucan interconnects mannoprotein, β(1-3)-glucan, and chitin. Journal of Biological Chemistry *272*, 17762-17775.

Komano, H. and Fuller, R. S. (1995). Shared Functions *in vivo* of a glycosyl-phosphatidylinositol-linked aspartyl protease, Mkc7, and the proprotein processing protease Kex2 in yeast. Proceedings of the National Academy of Sciences of the United States of America *92*, 10752-10756.

Kretschmar, M., Felk, A., Staib, P., Schaller, M., Hess, D., Callapina, M., Morschhauser, J., Schafer, W., Korting, H. C., Hof, H. et al. (2002). Individual acid aspartic proteinases (Saps) 1-6 of *Candida albicans* are not essential for invasion and colonization of the gastrointestinal tract in mice. Microbial Pathogenesis *32*, 61-70.

Krysan, D. J., Ting, E. L., Abeijon, C., Kroos, L. and Fuller, R. S. (2005). Yapsins are a family of aspartyl proteases required for cell wall integrity in *Saccharomyces cerevisiae*. Eukaryotic Cell *4*, 1364-1374.

Kulkarni, R. K. and Nielsen, B. D. (1986). Nutritional requirements for growth of a fungus endophyte of tall fescue grass. Mycologia *78*, 781-786.

Kwon, B. K., Han, K. H., Han, K. Y., Ju, S. M., Hwang, S. G., Jeon, B. H., Han, D. M. and Kim, W. S. (2001). Molecular cloning of *kpcA* gene encoding a Kex2p-like endoprotease from *Aspergillus nidulans*. Molecules and Cells *12*, 142-147.

Lafon, A., Seo, J. A., Han, K. H., Yu, J. H. and d'Enfert, C. (2005). The heterotrimeric G-protein GanBα-SfaDβ-GpgAγ is a carbon source sensor involved in early cAMP-dependent germination in *Aspergillus nidulans*. Genetics *171*, 71-80.

Lafontaine, I., Fischer, G., Talla, E. and Dujon, B. (2004). Gene relics in the genome of the yeast *Saccharomyces cerevisiae*. Gene *335*, 1-17.

Lam, C. K., Belanger, F. C., White, J. F. and Daie, J. (1995). Invertase activity in *Epichloë-Acremonium* fungal endophytes and its possible role in choke disease. Mycological Research *99*, 867-873.

Lane, G. A., Christensen, M. J. and Miles, C. O. (2000). Coevolution of fungal endophytes with grasses: the significance of secondary metabolites. In *Microbial Endophytes*, eds. C. W. Bacon and J. F. J. White), pp. 341-388. New York: Marcel Dekker.

Leibowitz, M. J. and Wickner, R. B. (1976). Chromosomal gene required for killer plasmid expression, mating, and spore maturation in *Saccharomyces cerevisiae*. Proceedings of the National Academy of Sciences of the United States of America *73*, 2061-2065.

Leuchtmann, A. and Clay, K. (1990). Isozyme variation in the *Acremonium/Epichloë* fungal endophyte complex. Phytopathology *80*, 1133-1139.

Leung, H. C. M. and Chin, F. Y. L. (2005). Finding exact optimal motifs in matrix representation by partitioning. Bioinformatics *21*, 86-92.

Levin, D. E. (2005). Cell wall integrity signaling in *Saccharomyces cerevisiae*. Microbiology and Molecular Biology Reviews *69*, 262-291.

Li, H. M., Crouch, J. A. and Belanger, F. C. (2005). Fungal endophyte *N*-acetylglucosaminidase expression in the infected host grass. Mycological Research *109*, 363-373.

Li, H. M., Sullivan, R., Moy, M., Kobayashi, D. Y. and Belanger, F. C. (2004). Expression of a novel chitinase by the fungal endophyte in *Poa ampla*. Mycologia *96*, 526-536.

Li, J., Yen, C., Liaw, D., Podsypanina, K., Bose, S., Wang, S. I., Puc, J., Miliaresis, C., Rodgers, L., McCombie, R. et al. (1997). PTEN, a putative protein tyrosine phosphatase gene mutated in human brain, breast, and prostate cancer. Science *275*, 1943-1947.

Lim, H. A., Raku, T. and Tokiwa, Y. (2005). Hydrolysis of polyesters by serine proteases. Biotechnology Letters *27*, 459-64.

Lindstrom, J. T. and Belanger, F. C. (1994). Purification and characterisation of an endophytic fungal proteinase that is abundantly expressed in the infected host grass. Plant Physiology *106*, 7-16.

Lindstrom, J. T., Sun, S. and Belanger, F. C. (1993). A novel fungal protease expressed in endophytic infection of *Poa* species. Plant Physiology *102*, 645-660.

Lora, J. M., De la Cruz, J., Llobell, A., Benítez, T. and Pintor-Toro, J. A. (1995). Molecular characterization and heterologous expression of an endo-β-1,6-glucanase gene from the mycoparasitic fungus *Trichoderma harzianum*. Molecular and General Genetics *247*, 639-645.

Lu, Z. X., Tombolini, R., Woo, S., Zeilinger, S., Lorito, M. and Jansson, J. K. (2004). *In vivo* study of *Trichoderma*-pathogen-plant interactions, using constitutive and inducible green fluorescent protein reporter systems. Applied and Environmental Microbiology *70*, 3073-3081.

Lugli, E. B., Allen, A. G. and Wakefield, A. E. (1997). A *Pneumocystis carinii* multi-gene family with homology to subtilisin-like serine proteases. Microbiology (Reading, UK) *143*, 2223-2236.

Machado, L. C. H. and Kemmelmeier, C. (2001). Identification of deoxynivalenol, 3-acetyldeoxynivalenol and zearalenone in the galactose oxidase-producing fungus *Dactylium dendroides*. Mycopathologia *149*, 79-85.

Maeda, T., Tsai, A. Y. M. and Saito, H. (1993). Mutations in a protein-tyrosine-phosphatase gene (*PTP2*) and a protein-serine threonine phosphatase gene (*PTC1*) cause a synthetic growth defect in *Saccharomyces cerevisiae*. Molecular and Cellular Biology *13*, 5408-5417.

Maehama, T., Taylor, G. S. and Dixon, J. E. (2001). PTEN and myotubularin: Novel phosphoinositide phosphatases. Annual Review of Biochemistry *70*, 247-279.

Mahon, P. and Bateman, A. (2000). The PA domain: a protease-associated domain. Protein Science *9*, 1930-1934.

Majewska-Sawka, A. and Nakashima, H. (2004). Endophyte transmission via seeds of *Lolium perenne* L.: immunodetection of fungal antigens. Fungal Genetics and Biology *41*, 534-541.

Maor, R. and Shirasu, K. (2005). The arms race continues: battle strategies between plants and fungal pathogens. Current Opinion in Microbiology *8*, 399-404.

Martell, K. J., Angelotti, T. and Ullrich, A. (1998). The "VH1-like" dual-specificity protein tyrosine phosphatases. Molecules and Cells *8*, 2-11.

Masuda, K., Shima, H., Watanabe, M. and Kikuchi, K. (2001). MKP-7, a novel mitogen-activated protein kinase phosphatase, functions as a shuttle protein. Journal of Biological Chemistry *276*, 39002-39011.

McGill, M. K. (2000). Cloning and characterisation of two subtilisin-like protease genes from *Neotyphodium lolii*. In *Institute of Molecular Biosciences*, pp. 161. Palmerston North: Massey University.

McGowan, T. L. (1996). Construction of a novel fungal gus expression plasmid, and its evaluation in *Aspergillus nidulans*. In *Department of Microbiology and Genetics*, pp. 122 leaves. Palmerston North: Massey University.

McPherson, M. J., Ogel, Z. B., Stevens, C., Yadav, K. D. S., Keen, J. N. and Knowles, P. F. (1992). Galactose oxidase of *Dactylium dendroides* - gene cloning and sequence analysis. Journal of Biological Chemistry *267*, 8146-8152.

Mitra, P., Zhang, Y. J., Rameh, L. E., Ivshina, M. P., McCollum, D., Nunnari, J. J., Hendricks, G. M., Kerr, M. L., Field, S. J., Cantley, L. C. et al. (2004). A novel phosphatidylinositol(3,4,5)P-3 pathway in fission yeast. Journal of Cell Biology *166*, 205-211.

Mizuno, K., Nakamura, T., Ohshima, T., Tanaka, S. and Matsuo, H. (1988). Yeast *KEX2* gene encodes an endopeptidase homologous to subtilisin-like serine proteases. Biochemical and Biophysical Research Communications *156*, 246-254.

Mizutani, O., Nojima, A., Yamamoto, M., Furukawa, K., Fujioka, T., Yamagata, Y., Abe, K. and Nakajima, T. (2004). Disordered cell integrity signaling caused by disruption of the *kexB* gene in *Aspergillus oryzae*. Eukaryotic Cell *3*, 1036-1048.

Moehle, C. M., Aynardi, M. W., Kolodny, M. R., Park, F. J. and Jones, E. W. (1987). Protease B of *Saccharomyces cerevisiae* -isolation and regulation of the *PRB1* structural gene. Genetics *115*, 255-263.

Moller, E. M., Bahnweg, G., Sandermann, H. and Geiger, H. H. (1992). A simple and efficient protocol for isolation of high molecular weight DNA from filamentous fungi, fruit bodies, and infected plant tissues. Nucleic Acids Research *20*, 6115-6116.

Monod, M., Lechenne, B., Jousson, O., Grand, D., Zaugg, C., Stocklin, R. and Grouzmann, E. (2005). Aminopeptidases and dipeptidyl-peptidases secreted by the dermatophyte *Trichophyton rubrum*. Microbiology (Reading, England) *151*, 145-55.

Montero, M., Sanz, L., Rey, M., Monte, E. and Llobell, A. (2005). BGN16.3, a novel acidic β-1,6-glucanase from mycoparasitic fungus *Trichoderma harzianum* CECT 2413. Febs Journal *272*, 3441-3448.

Moon, C. D., Craven, K. D., Leuchtmann, A., Clement, S. L. and Schardl, C. L. (2004). Prevalence of interspecific hybrids amongst asexual fungal endophytes of grasses. Molecular Ecology *13*, 1455-1467.

Moon, C. D., Scott, B., Schardl, C. L. and Christensen, M. J. (2000). The evolutionary origins of *Epichloë* endophytes from annual ryegrasses. Mycologia *92*, 1103-1118.

Movahedi, S. and Heale, J. B. (1990). The roles of aspartic proteinase and endo-pectin lyase enzymes in the primary stages of infection and pathogenesis of various host tissues by different isolates of *Botrytis cinerea* Pers Ex Pers. Physiological and Molecular Plant Pathology *36*, 303-324.

Moy, M., Li, H. J. M., Sullivan, R., White, J. F. and Belanger, F. C. (2002). Endophytic fungal beta-1,6-glucanase expression in the infected host grass. Plant Physiology *130*, 1298-1308.

Murphy, J. M. and Walton, J. D. (1996). Three extracellular proteases from *Cochliobolus carbonum*: cloning and targeted disruption of *ALP1*. Molecular Plant-Microbe Interactions *9*, 290-297.

Naffaa, W., Ravel, C. and Guillaumin, J.-J. (1998). Nutritional requirements for growth of fungal endophytes of grasses. Canadian Journal of Microbiology *44*, 231-237.

Naglik, J., Albrecht, A., Bader, O. and Hube, B. (2004). *Candida albicans* proteinases and host/pathogen interactions. Cellular Microbiology *6*, 915-926.

Naglik, J. R., Challacombe, S. J. and Hube, B. (2003). *Candida albicans* secreted aspartyl proteinases in virulence and pathogenesis. Microbiology and Molecular Biology Reviews *67*, 400-428.

Namiki, F., Matsunaga, M., Okuda, M., Inoue, I., Nishi, K., Fujita, Y. and Tsuge, T. (2001). Mutation of an argnine biosynthesis gene causes reduced pathogenicity in *Fusarium oxysporum* f. sp. *melonis*. Molecular Plant-Microbe Interactions *14*, 580-584.

Nash III, T. H. (1996). Lichen Biology. Cambridge: Cambridge University Press.

Neill, J. C. (1940). The endophyte of rye-grass (*Lolium perenne*). New Zealand Journal of Science and Technology *Feb 1940*, 280A-291A.

Neumann, M. J. and Dobinson, K. F. (2003). Sequence tag analysis of gene expression during pathogenic growth and microsclerotia development in the vascular wilt pathogen *Verticillium dahliae*. Fungal Genetics and Biology *38*, 54-62.

Newport, G. and Agabian, N. (1997). *KEX2* influences *Candida albicans* proteinase secretion and hyphal formation. Journal of Biological Chemistry *272*, 28954-28961.

Newport, G., Kuo, A., Flattery, A., Gill, C., Blake, J. J., Kurtz, M. B., Abruzzo, G. K. and Agabian, N. (2003). Inactivation of Kex2p diminishes the virulence of *Candida albicans*. Journal of Biological Chemistry *278*, 1713-1720.

Odds, F. C., Brown, A. J. P. and Gow, N. A. R. (2003). Antifungal agents: mechanisms of action. Trends in Microbiology *11*, 272-279.

Ögel, Z. B., Brayford, D. and Mcpherson, M. J. (1994). Cellulose-triggered sporulation in the galactose oxidase-producing fungus *Cladobotryum* (*Dactylium*) *dendroides* Nrrl-2903 and its reidentification as a species of *Fusarium*. Mycological Research *98*, 474-480.

Oliver, B. G., Panepinto, J. C., Askew, D. S. and Rhodes, J. C. (2002). cAMP alteration of growth rate of *Aspergillus fumigatus* and *Aspergillus niger* is carbon-source dependent. Microbiology (SGM) *148*, 2627-2633.

Olivieri, F., Zanetti, M. E., Oliva, C. R., Covarrubias, A. A. and Casalongue, C. A. (2002). Characterization of an extracellular serine protease of *Fusarium eumartii* and its action on pathogenesis related proteins. European Journal of Plant Pathology *108*, 63-72.

Olmedo-Monfil, V., Mendoza-Mendoza, A., Gomez, I., Cortes, C. and Herrera-Estrella, A. (2002). Multiple environmental signals determine the transcriptional activation of the mycoparasitism related gene *prb1* in *Trichoderma atroviride*. Molecular Genetics and Genomics *267*, 703-712.

Orozco, I., Ortiz, L., Elorza, M. V., Ruiz-Herrera, J. and Sentandreu, R. (2002). Cloning and characterization of PRB1, a *Candida albicans* gene encoding a putative novel endoprotease B and factors affecting its expression. Research in Microbiology *153*, 611-620.

Osbourn, A. E. (1995). Saponin detoxification by plant pathogenic fungi. Abstracts of Papers of the American Chemical Society *210*, 206-Agfd.

Ostapenko, D. and Solomon, M. J. (2005). Phosphorylation by Cak1 regulates the C-terminal domain kinase Ctk1 in *Saccharomyces cerevisiae*. Molecular and Cellular Biology *25*, 3906-3913.

Oyama, S., Yamagata, Y., Abe, K. and Nakajima, T. (2002). Cloning and expression of an endo-1,6- β-D-glucanase gene (negl) from *Neurospora crassa*. Bioscience Biotechnology and Biochemistry *66*, 1378-1381.

Panaccione, D. G., Wang, J., Young, C. A., Schardl, C. L., Scott, B. and Damrongkool, P. (2001). Elimination of ergovaline from a grass-*Neotyphodium* endophyte symbiosis by genetic modification of the endophyte. Proceedings of the National Academy of Sciences (U. S. A.) *in press*.

Paoletti, M., Castroviejo, M., Begueret, J. and Clave, C. (2001). Identification and characterization of a gene encoding a subtilisin-like serine protease induced during the vegetative incompatibility reaction in *Podospora anserina*. Current Genetics *39*, 244-252.

Park, G., Bruno, K. S., Staiger, C. J., Talbot, N. J. and Xu, J. R. (2004). Independent genetic mechanisms mediate turgor generation and penetration peg formation during plant infection in the rice blast fungus. Molecular Microbiology *53*, 1695-707.

Park, H. D., Beeser, A. E., Clancy, M. J. and Cooper, T. G. (1996). The *S. cerevisiae* nitrogen starvation-induced Yvh1p and Ptp2p phosphatases play a role in control of sporulation. Yeast *12*, 1135-1151.

Paterson, I. C., Charnley, A. K., Cooper, R. M. and Clarkson, J. M. (1994). Partial characterization of specific inducers of a cuticle-degrading protease from the insect pathogenic fungus *Metarhizium anisopliae*. Microbiology (Reading, UK) *140*, 3153-3159.

Peterbauer, C. K., Litscher, D. and Kubicek, C. P. (2002). The *Trichoderma atroviride seb1* (stress response element binding) gene encodes an AGGGG-binding protein which is involved in the response to high osmolarity stress. Molecular Genetics and Genomics *268*, 223-231.

Philipson, M. N. and Christey, M. C. (1986). The relationship of host and endophyte during flowering, seed formation, and germination on *Lolium perenne*. New Zealand Journal of Botany *24*, 125-134.

Pinan-Lucarre, R., Paoletti, M., Dementhon, K., Coulary-Salin, B. and Clave, C. (2003). Autophagy is induced during cell death by incompatibility and is essential for differentiation in the filamentous fungus *Podospora anserina*. Molecular Microbiology *47*, 321-333.

Plummer, K. M., Clark, S. J., Ellis, L. M., Loganathan, A., Al-Samarrai, T. H., Rikkerink, E. H. A., Sullivan, P. A., Templeton, M. D. and Farley, P. C. (2004). Analysis of a secreted aspartic peptidase disruption mutant of *Glomerella cingulata*. European Journal of Plant Pathology *110*, 265-274.

Poussereau, N., Creton, S., Billon-Grand, G., Rascle, C. and Fevre, M. (2001a). Regulation of *acp1*, encoding a non-aspartyl acid protease expressed during pathogenesis of *Sclerotinia sclerotiorum*. Microbiology (Reading, UK) *147*, 717-726.

Poussereau, N., Gente, S., Rascle, C., Billon-Grand, G. and Fevre, M. (2001b). *aspS* encoding an unusual aspartyl protease from *Sclerotinia sclerotiorum* is expressed during phytopathogenesis. FEMS Microbiology Letters *194*, 27-32.

Pozo, M. J., Baek, J. M., Garcia, J. M. and Kenerley, C. M. (2004). Functional analysis of *tvsp1*, a serine protease-encoding gene in the biocontrol agent *Trichoderma virens*. Fungal Genetics and Biology *41*, 336-348.

Punt, P. J., Oliver, R. P., Dingemanse, M. A., Pouwels, P. H. and van den Hondel, C. A. (1987). Transformation of *Aspergillus* based on the hygromycin B resistance marker from *Escherichia coli*. Gene *56*, 117-124.

Rawlings, N. D., Tolle, D. P. and Barrett, A. J. (2004). Evolutionary families of peptidase inhibitors. Biochemical Journal *378*, 705-716.

Redding, K., Holcomb, C. and Fuller, R. S. (1991). Immunolocalization of Kex2 protease identifies a putative late golgi compartment in the yeast *Saccharomyces cerevisiae*. Journal of Cell Biology *113*, 527-538.

Reddy, P. V., Lam, C. K. and Belanger, F. C. (1996). Mutualistic fungal endophytes express a proteinase that is homologous to proteases suspected to be important in fungal pathogenicity. Plant Physiology *111*, 1209-1218.

Reichard, U., Cole, G. T., Hill, T. W., Rüchel, R. and Monod, M. (2000). Molecular characterization and influence on fungal development of ALP2, a novel serine proteinase from *Aspergillus fumigatus*. International Journal of Medical Microbiology *290*, 549-558

Rhody, D., Stommel, M., Roeder, C., Mann, P. and Franken, P. (2003). Differential RNA accumulation of two β-tubulin genes in arbuscular mycorrhizal fungi. Mycorrhiza *13*, 137-42.

Richardson, M. D., Chapman, G. W. J., Hoveland, C. S. and Bacon, C. W. (1992). Sugar alcohols in endophyte infected tall fescue under drought. Crop Science *32*, 1060-1061.

Roelants, F. M., Torrance, P. D., Bezman, N. and Thorner, J. (2002). Pkh1 and Pkh2 differentially phosphorylate and activate Ypk1 and Ykr2 and define protein kinase modules required for maintenance of cell wall integrity. Molecular Biology of the Cell *13*, 3005-3028.

Romano, N. and Macino, G. (1992). Quelling - transient inactivation of gene expression in *Neurospora crassa* by transformation with homologous sequences. Molecular Microbiology *6*, 3343-3353.

Rowan, D. D. and Gaynor, D. L. (1986). Isolation of feeding deterrents against Argentine stem weevil from ryegrass infected with the endophyte *Acremonium loliae*. Journal of Chemical Ecology *12*, 647-658.

Salamov, A. A. and Solovyev, V. V. (2000). Ab initio gene finding in *Drosophila* genomic DNA. Genome Research *10*, 516-22.

Samal, B. B., Karan, B., Boone, T. C., Chen, K. K., Rohde, M. F. and Stabinsky, Y. (1989). Cloning and expression of the gene encoding a novel proteinase from *Tritirachium album* limber. Gene *85*, 329-333.

Samal, B. B., Karan, B., Boone, T. C., Osslund, T. D., Chen, K. K. and Stabinsky, Y. (1990). Isolation and characterisation of the gene encoding a novel, thermostable serine proteinase from the mould *Tritirachium album Limber*. Molecular Microbiology *4*, 1789-1792.

Samuels, R. I. and Reynolds, S. E. (2000). Proteinase inhibitors from the molting fluid of the pharate adult tobacco hornworm, *Manduca sexta.* Archives of Insect Biochemistry and Physiology *43*, 33-43.

Sanger, F., Nicklen, S. and Coulson, A. R. (1977). DNA sequencing with chain-terminating inhibitors. Proceedings of the National Academy of Sciences (U. S. A.) *74*, 5463-5467.

Sanglard, D., Hube, B., Monod, M., Odds, F. C. and Gow, N. A. R. (1997). A triple deletion of the secreted aspartyl proteinase genes SAP4, SAP5, and SAP6 of *Candida albicans* causes attenuated virulence. Infection and Immunity *65*, 3539-3546.

Sato, S., Suzuki, H., Widyastuti, U., Hotta, Y. and Tabata, S. (1994). Identification and characterization of genes induced during sexual differentiation in *Schizosaccharomyces pombe.* Current Genetics *26*, 31-37.

Saunders, K. (1997). Development of the β-glucuronidase reporter gene system to study *Acremonium* endophyte interactions with perennial ryegrass. In *Department of Microbiology and Genetics.* Palmerston North: Massey University.

Schardl, C. L. (2001). *Epichloë festucae* and related mutualistic symbionts of grasses. Fungal Genetics and Biology *33*, 69-82.

Schardl, C. L., Leuchtmann, A. and Spiering, M. J. (2004). Symbioses of grasses with seedborne fungal endophytes. Annual Review of Plant Biology *55*, 315-340.

Schardl, C. L., Leuchtmann, A., Tsai, H.-F., Collett, M. A., Watt, D. M. and Scott, D. B. (1994). Origin of a fungal symbiont of perennial ryegrass by interspecific hybridisation of a mutualist with the ryegrass choke pathogen, *Epichloë typhina.* Genetics *136*, 1307-1317.

Schardl, C. L., Liu, J.-S., White, J. F., Jr., Finkel, R. A., An, Z.-Q. and Siegel, M. R. (1991). Molecular phylogenetic relationships of nonpathogenic grass mycosymbionts and clavicipitaceous plant pathogens. Plant Systematics and Evolution *178*, 27-41.

Schmitt, A. P. and McEntee, K. (1996). Msn2p, a zinc finger DNA-binding protein, is the transcriptional activator of the multistress response in *Saccharomyces cerevisiae.* Proceedings of the National Academy of Sciences of the United States of America *93*, 5777-5782.

Schoffelmeer, E. A. M., Klis, F. M., Sietsma, J. H. and Cornelissen, B. J. C. (1999). The cell wall of *Fusarium oxysporum.* Fungal Genetics and Biology *27*, 275-282.

Schulze-Lefert, P. and Panstruga, R. (2003). Establishment of biotrophy by parasitic fungi and reprogramming of host cells for disease resistance. Annual Review of Phytopathology *41*, 641-667.

Scott, J. H. and Schekman, R. (1980). Lyticase - endoglucanase and protease activities that act together in yeast cell lysis. Journal of Bacteriology *142*, 414-423.

Screen, S., Bailey, A., Charnley, K., Cooper, R. and Clarkson, J. (1997). Carbon regulation of the cuticle-degrading enzyme PR1 from *Metarhizium anisopliae* may involve a trans-acting DNA-binding protein CRR1, a functional equivalent of the *Aspergillus nidulans* CREA protein. Current Genetics *31*, 511-8.

Segers, R., Butt, T. M., Kerry, B. R. and Peberdy, J. F. (1994). The nematophagous fungus *Verticillium chlamydosporium* produces a chymoelastase-like protease which hydrolyses host nematode proteins *in situ.* Microbiology (Reading, UK) *140*, 2715-2723.

Seidl, V., Seiboth, B., Karaffa, L. and Kubicek, C. P. (2004). The fungal STRE-element-binding protein Seb1 is involved but not essential for glycerol dehydrogenase (*gld1*) gene expression and glycerol accumulation in *Trichoderma atroviride* during osmotic stress. Fungal Genetics and Biology *41*, 1132-1140.

Sharon, E., Bar-Eyal, M., Chet, I., Herrera-Estrella, A., Kleifeld, O. and Spiegel, Y. (2001). Biological control of the root-knot nematode *Meloidogyne javanica* by *Trichoderma harzianum*. Phytopathology *91*, 687-693.

Shen, H. D., Wang, C. W., Lin, W. L., Lai, H. Y., Tam, M. F., Chou, H., Wang, S. R. and Han, S. H. (2001). cDNA cloning and immunologic characterization of Pen o 18, the vacuolar serine protease major allergen of *Penicillium oxalicum*. Journal of Laboratory and Clinical Medicine *137*, 115-124.

Shim, W. B. and Woloshuk, C. P. (2001). Regulation of fumonisin B-1 biosynthesis and conidiation in *Fusarium verticillioides* by a cyclin-like (C-type) gene, *FCC1*. Applied and Environmental Microbiology *67*, 1607-1612.

Siegel, M. R. and Bush, L. P. (1997). Toxin production in grass/endophyte associations. In *Plant Relationships*, vol. V Part A eds. G. C. Carroll and P. Tudzynski, pp. 185-207. Berlin: Springer-Verlag.

Siegel, M. R. and Schardl, C. L. (1991). Fungal endophytes of grasses: detrimental and benefical associations. In *Microbial Ecology of Leaves*, eds. J. H. Andrew and S. S. Hirano), pp. 198-221. Berlin: Springer Verlag.

Small, C. L. and Bidochka, M. J. (2005). Up-regulation of Pr1, a subtilisin-like protease, during conidiation in the insect pathogen *Metarhizium anisopliae*. Mycological Research *109*, 307-313.

Smith, A., Smith, A., Alrubaie, S., Coehlo, C., Leevers, S. J. and Ashworth, A. (1999). Alternative splicing of the *Drosophila* PTEN gene. Biochimica et Biophysica Acta (Gene Structure and Expression) *1447*, 313-317.

Snoeijers, S. S., Vossen, P., Goosen, T., van den Broek, H. W. J. and De Wit, P. J. G. M. (1999). Transcription of the avirulence gene *Avr9* of the fungal tomato pathogen *Cladosporium fulvum* is regulated by a GATA-type transcription factor in *Aspergillus nidulans*. Molecular and General Genetics *261*, 653-659.

Soler, A., de la Cruz, J. and Llobell, A. (1999). Detection of β-1,6-glucanase isozymes from *Trichoderma* strains in sodium dodecyl sulphate polyacrylamide gel electrophoresis and isoelectrofocusing gels. Journal of Microbiological Methods *35*, 245-251.

Solomon, P. S., Tan, K. C. and Oliver, R. P. (2003). The nutrient supply of pathogenic fungi; a fertile field for study. Molecular Plant Pathology *4*, 203-210.

Solomon, P. S., Waters, O. D. C., Simmonds, J., Cooper, R. M. and Oliver, R. P. (2005). The Mak2 MAP kinase signal transduction pathway is required for pathogenicity in *Stagonospora nodorum*. Current Genetics *48*, 60-68.

Spiering, M. J. (1999). Distribution of *Neotyphodium lolii* endophyte metabolic activity in perennial ryegrass (*Lolium perenne*, L.) and its implications for alkaloid distribution and photosynthesis. In *Institute of Molecular Biosciences*, pp. 208. Palmerston North: Massey University.

Spiering, M. J., Moon, C. D., Wilkinson, H. H. and Schardl, C. L. (2005). Gene clusters for insecticidal loline alkaloids in the grass-endophytic fungus *Neotyphodium uncinatum*. Genetics *169*, 1403-1414.

Sreedhar, L., Kobayashi, D. Y., Bunting, T. E., Hillman, B. I. and Belanger, F. C. (1999). Fungal proteinase expression in the interaction of the plant pathogen *Magnaporthe poae* with its host. Gene *235*, 121-129.

St Leger, R. J., Charnley, A. K. and Cooper, R. M. (1987). Characterization of cuticle-degrading proteases produced by the entomopathogen *Metarhizium anisopliae.* Archives of Biochemistry and Biophysics *253*, 221-232.

St Leger, R. J., Frank, D. C., Roberts, D. W. and Staples, R. C. (1992). Molecular cloning and regulatory analysis of the cuticle-degrading-protease structural gene from the entomopathogenic fungus *Metarhizium anisopliae.* European Journal of Biochemistry *15*, 991-1001.

St Leger, R. J., Bidochka, M. J. and Roberts, D. W. (1994). Characterization of a novel carboxypeptidase produced by the entomopathogenic fungus *Metarhizium anisopliae.* Archives of Biochemistry and Biophysics *314*, 392-398.

St Leger, R. J., Joshi, L., Bidochka, M. J., Rizzo, N. W. and Roberts, D. W. (1996a). Biochemical characterization and ultrastructural localization of two extracellular trypsins produced by *Metarhizium anisopliae* in infected insect cuticles. Applied & Environmental Microbiology *62*, 1257-1264.

St Leger, R. J., Joshi, L., Bidochka, M. J., Rizzo, N. W. and Roberts, D. W. (1996b). Characterization and ultrastructural localization of chitinases from *Metarhizium anisopliae*, *M. flavoviride*, and *Beauveria bassiana* during fungal invasion of host (*Manduca sexta*) cuticle. Applied and Environmental Microbiology *62*, 907-912.

St Leger, R. J., Joshi, L., Bidochka, M. J. and Roberts, D. W. (1996c). Construction of an improved mycoinsecticide overexpressing a toxic protease. Proceedings of the National Academy of Sciences (U. S. A.) *93*, 6349-6354.

St Leger, R. J., Joshi, L. and Roberts, D. (1998). Ambient pH is a major determinant in the expression of cuticle-degrading enzymes and hydrophobin by *Metarhizium anisopliae.* Applied and Environmental Microbiology *64*, 709-713.

Staib, P., Kretschmar, M., Nichterlein, T., Hof, H. and Morschhauser, J. (2000). Differential activation of a *Candida albicans* virulence gene family during infection. Proceedings of the National Academy of Sciences of the United States of America *97*, 6102-6107.

Sterky, F., Holmberg, A., Pettersson, B. and Uhlen, M. (1996). The sequence of a 30 kb fragment on the left arm of chromosome XV from *Saccharomyces cerevisiae* reveals 15 open reading frames, five of which correspond to previously identified genes. Yeast *12*, 1091-1095.

Sterner, D. E., Lee, J. M., Hardin, S. E. and Greenleaf, A. L. (1995). The yeast carboxyl-terminal repeat domain kinase Ctdk-I is a divergent cyclin-cyclin-dependent kinase complex. Molecular and Cellular Biology *15*, 5716-5724.

Strausberg, R. L., Feingold, E. A., Grouse, L. H., Derge, J. G., Klausner, R. D., Collins, F. S., Wagner, L., Shenmen, C. M., Schuler, G. D., Altschul, S. F. et al. (2002). Generation and initial analysis of more than 15,000 full-length human and mouse cDNA sequences. Proceedings of the National Academy of Sciences (U. S. A.) *99*, 16899-16903.

Strauss, J., Horvath, H. K., Abdallah, B. M., Kindermann, J., Mach, R. L. and Kubicek, C. P. (1999). The function of CreA, the carbon catabolite repressor of

Aspergillus nidulans, is regulated at the transcriptional and post-transcriptional level. Molecular Microbiology *32*, 169-178.

Strickland, J. R., Oliver, J. W. and Cross, D. L. (1993). Fescue toxicosis and its impact on animal agriculture. Veterinary and Human Toxicology *35*, 454-464.

Suarez, B., Rey, M., Castillo, P., Monte, E. and Llobell, A. (2004). Isolation and characterization of PRA1, a trypsin-like protease from the biocontrol agent *Trichoderma harzianum* CECT 2413 displaying nematicidal activity. Applied Microbiology and Biotechnology *65*, 46-55.

Suarez, M. B., Sanz, L., Chamorro, M. I., Rey, M., Gonzalez, F. J., Llobell, A. and Monte, E. (2005). Proteomic analysis of secreted proteins from *Trichoderma harzianum*: identification of a fungal cell wall-induced aspartic protease. Fungal Genetics and Biology *42*, 924-934.

Sugiura, R., Toda, T., Shuntoh, H., Yanagida, M. and Kuno, T. (1998). *pmp1*$^{+}$, a suppressor of calcineurin deficiency, encodes a novel MAP kinase phosphatase in fission yeast. EMBO Journal *17*, 140-148.

Svejstrup, J. Q., Feaver, W. J. and Kornberg, R. D. (1996). Subunits of yeast RNA polymerase II transcription factor TFIIH encoded by the *CCL1* gene. Journal of Biological Chemistry *271*, 643-645.

Takeshige, K., Baba, M., Tsuboi, S., Noda, T. and Ohsumi, Y. (1992). Autophagy in yeast demonstrated with proteinase-deficient mutants and conditions for its induction. Journal of Cell Biology *119*, 301-311.

Talbot, N. J., Ebbole, D. J. and Hamer, J. E. (1993). Identification and characterisation of *MPG1*, a gene involved in pathogenicity from the rice blast fungus *Magnaporthe grisea*. Plant Cell *5*, 1575-1590.

Tanaka, A., Tapper, B. A., Popay, A., Parker, E. J. and Scott, B. (2005). A symbiosis expressed non-ribosomal peptide synthetase from a mutualistic fungal endophyte of perennial ryegrass confers protection to the symbiotum from insect herbivory. Molecular Microbiology *57*, 1036-1050.

Tao, Y. and Marzluf, G. A. (1999). The NIT2 nitrogen regulatory protein of *Neurospora*: expression and stability of *nit2* mRNA and protein. Current Genetics *36*, 153-158.

Taylor, G. S., Liu, Y., Baskerville, C. and Charbonneau, H. (1997). The activity of Cdc14p, an oligomeric dual specificity protein phosphatase from *Saccharomyces cerevisiae*, is required for cell cycle progression. Journal of Biological Chemistry *272*, 24054-24063.

Taylor, J. W., Jacobson, D. J. and Fisher, M. C. (1999). The evolution of asexual fungi: reproduction, speciation and classification. Annual Review of Phytopathology *37*, 197-246.

ten Have, A., Dekkers, E., Kay, J., Phylip, L. H. and van Kan, J. A. L. (2004). An aspartic proteinase gene family in the filamentous fungus *Botrytis cinerea* contains members with novel features. Microbiology-Sgm *150*, 2475-2489.

Thevelein, J. M., Gelade, R., Holsbeeks, I., Lagatie, O., Popova, Y., Rolland, F., Stolz, F., Van de Velde, S., Van Dijck, P., Vandormael, P. et al. (2005). Nutrient sensing systems for rapid activation of the protein kinase A pathway in yeast. Biochemical Society Transactions *33*, 253-256.

Thuring, R. W., Sanders, P. M. and Borst, P. (1975). A freeze squeeze method for recovering DNA from agarose gels. Analytical Biochemistry *66*, 213-220.

Tikhonov, V. E., Lopez-Llorca, L. V., Salinas, J. and Jansson, H. B. (2002). Purification and characterization of chitinases from the nematophagous fungi *Verticillium chlamydosporium* and *V. suchlasporium*. Fungal Genetics and Biology *35*, 67-78.

Tilburn, J., Sarkar, S., Widdick, D. A., Espeso, E. A., Orejas, M., Mungroo, J., Penalva, M. A. and Arst, H. N. J. (1995). The *Aspergillus* PacC zinc finger transcription factor mediates regulation of both acid- and alkaline-expressed genes by ambient pH. EMBO Journal *14*, 779-790.

Toh-e, A. (1995). Construction of a marker gene cassette which is repeatedly usable for gene disruption in yeast. Current Genetics *27*, 293-297.

Tsai, H.-F., Liu, J.-S., Staben, C., Christensen, M. J., Latch, G. C. M., Siegel, M. R. and Schardl, C. L. (1994). Evolutionary diversification of fungal endophytes of tall fescue grass by hybridisation with *Epichloë* species. Proceedings of the National Academy of Sciences (U. S. A.) *91*, 2542-2546.

Tunlid, A. and Jansson, S. (1991). Proteases and their involvement in the infection and immobilization of nematodes by the nematophagous fungus *Arthrobotrys oligospora*. Applied and Environmental Microbiology *57*, 2868-2872.

Velasco, J., Gutierrez, S., Casqueiro, J., Fierro, F., Campoy, S. and Martin, J. F. (2001). Cloning and characterization of the gene cahB encoding a cephalosporin C acetylhydrolase from *Acremonium chrysogenum*. Applied Microbiology and Biotechnology *57*, 350-356.

Viani, F. C., Dos Santos, J. I., Paula, C. R., Larson, C. E. and Gambale, W. (2001). Production of extracellular enzymes by *Microsporum canis* and their role in its virulence. Medical Mycology *39*, 463-468.

Vieira, J. and Messing, J. (1987). Production of single-stranded plasmid DNA. Methods in Enzymology *153*, 3-11.

Viterbo, A., Harel, M. and Chet, I. (2004). Isolation of two aspartyl proteases from *Trichoderma asperellum* expressed during colonization of cucumber roots. FEMS Microbiology Letters *238*, 151-158.

Wang, C. S., Hu, G. and St Leger, R. J. (2005). Differential gene expression by *Metarhizium anisopliae* growing in root exudate and host (*Manduca sexta*) cuticle or hemolymph reveals mechanisms of physiological adaptation. Fungal Genetics and Biology *42*, 704-718.

Wang, C. W. and Klionsky, D. J. (2003). The molecular mechanism of autophagy. Molecular Medicine *9*, 65-76.

Wang, J. H., Machado, C., Panaccione, D. G., Tsai, H. F. and Schardl, C. L. (2004a). The determinant step in ergot alkaloid biosynthesis by an endophyte of perennial ryegrass. Fungal Genetics and Biology *41*, 189-198.

Wang, J. Y., Cai, Y., Gou, J. Y., Mao, Y. B., Xu, Y. H., Jiang, W. H. and Chen, X. Y. (2004b). VdNEP, an elicitor from *Verticillium dahliae*, induces cotton plant wilting. Applied and Environmental Microbiology *70*, 4989-4995.

Weber, R. W. S., Wakley, G. E., Thines, E. and Talbot, N. J. (2001). The vacuole as central element of the lytic system and sink for lipid droplets in maturing appressoria of *Magnaporthe grisea*. Protoplasma *216*, 101-112.

Weitzman, I. and Summerbell, R. C. (1995). The dermatophytes. Clinical Microbiology Reviews *8*, 240-259.

White, S., McIntyre, M., Berry, D. R. and McNeil, B. (2002). The autolysis of industrial filamentous fungi. Critical Reviews in Biotechnology *22*, 1-14.

Whittaker, J. W. (2003). Free radical catalysis by galactose oxidase. Chemical Reviews *103*, 2347-2363.

Wightman, R. and Meacock, P. A. (2003). The TH15 gene family of *Saccharomyces cerevisiae*: distribution of homologues among the hemiascomycetes and functional redundancy in the aerobic biosynthesis of thiamin from pyridoxine. Microbiology (SGM) *149*, 1447-1460.

Wilcox, C. A., Redding, K., Wright, R. and Fuller, R. S. (1992). Mutation of a tyrosine localization signal in the cytosolic tail of yeast Kex2 protease disrupts Golgi retention and results in default transport to the vacuole. Molecular Biology of the Cell *3*, 1353-1371.

Wilkinson, H. H., Bush, L. P., Burton, H. R., Siegel, M. R. and Schardl, C. (1997). Lolines are fungal metabolites. In *International Neotyphodium/Grass Interactions Symposium.* Athens, Georgia, U. S. A.

Wong, A. K., Chen, Y., Lian, L., Ha, P. C., Petersen, K., Laity, K., Carillo, A., Emerson, M., Heichman, K., Gupte, J. et al. (1999). Genomic structure, chromosomal location, and mutation analysis of the human CDC14A gene. Genomics *59*, 248-251.

Wood, V. Gwilliam, R. Rajandream, M. A. Lyne, M. Lyne, R. Stewart, A. Sgouros, J. Peat, N. Hayles, J. Baker, S. et al. (2002). The genome sequence of *Schizosaccharomyces pombe.* Nature *415*, 871-880.

Woodfolk, J. A., Wheatley, L. M., Piyasena, R. V., Benjamin, D. C. and Platts-Mills, T. A. E. (1998). Trichophyton antigens associated with IgE antibodies and delayed type hypersensitivity - Sequence homology to two families of serine proteinases. Journal of Biological Chemistry *273*, 29489-29496.

Young, C. A. (2005). The indole-diterpene gene cluster from the ryegrass endophyte, *Neotyphodium lolii*, is required for the biosynthesis of lolitrem B, a bioprotective alkaloid. In *Institute of Molecular Biosciences*, pp. 270. Palmerston North: Massey University.

Young, C. A., Bryant, M. K., Christensen, M. J., Tapper, B. A., Bryan, G. T. and Scott, B. (2005). Molecular cloning and genetic analysis of a symbiosis-expressed gene cluster for lolitrem biosynthesis from a mutualistic endophyte of perennial ryegrass. Molecular Genetics and Genomics *274*, 13-29.

Zhang, X. (2004). Functional analysis of a thiamine biosynthetic gene in the interaction of *Epichloë typhina* with perennial ryegrass. In *Institute of Molecular Biosciences*, pp. 336. Palmerston North: Massey University.

Zhao, M. L., Mo, M. H. and Zhang, K. Q. (2004). Characterization of a neutral serine protease and its full-length cDNA from the nematode-trapping fungus *Arthrobotrys oligospora.* Mycologia *96*, 16-22.

Zubenko, G. S. and Jones, E. W. (1981). Protein degradation, meiosis and sporulation in proteinase-deficient mutants of *Saccharomyces cerevisiae.* Genetics *97*, 45-64.

Zubenko, G. S., Mitchell, A. P. and Jones, E. W. (1979). Septum formation, cell division, and sporulation in mutants of yeast deficient in proteinase B. Proceedings of the National Academy of Sciences (U. S. A.) *76*, 2395-2399.

Zubenko, G. S., Mitchell, A. P. and Jones, E. W. (1980). Mapping of the proteinase b structural gene *PRB1*, in *Saccharomyces cerevisiae* and identification of nonsense alleles within the locus. Genetics *96*, 137-146.